

University of Southampton Research Repository ePrints Soton

Copyright © and Moral Rights for this thesis are retained by the author and/or other copyright owners. A copy can be downloaded for personal non-commercial research or study, without prior permission or charge. This thesis cannot be reproduced or quoted extensively from without first obtaining permission in writing from the copyright holder/s. The content must not be changed in any way or sold commercially in any format or medium without the formal permission of the copyright holders.

When referring to this work, full bibliographic details including the author, title, awarding institution and date of the thesis must be given e.g.

AUTHOR (year of submission) "Full thesis title", University of Southampton, name of the University School or Department, PhD Thesis, pagination

UNIVERSITY OF SOUTHAMPTON

FACULTY OF MEDICINE CANCER SCIENCES

RETARGETING NON-COGNATE CYTOTOXIC T CELLS TO TUMOUR ANTIGENS USING [PEPTIDE-MHC x FAB'] CONJUGATES

by

ANGELA DIANE HAMBLIN

Thesis for the degree of Doctor of Philosophy

March 2012

UNIVERSITY OF SOUTHAMPTON

ABSTRACT

FACULTY OF MEDICINE CANCER SCIENCES

Doctor of Philosophy

RETARGETING NON-COGNATE CYTOTOXIC T CELLS TO TUMOUR ANTIGENS USING [PEPTIDE-MHC x FAB'] CONJUGATES

By Angela Diane Hamblin

Attempts to generate robust anti-tumour cytotoxic T lymphocyte (CTL) responses using immunotherapy are frequently thwarted by CTL tolerance of tumour-associated antigens. One strategy to circumvent this is retargeting efficacious populations of CTLs against non-cognate tumour cell antigens. This can be achieved using a bivalent molecule specific for both tumour antigen (via an antibody fragment e.g. Fab') and a selected population of CTLs (e.g. those specific for a single antigenic viral peptide) through peptide presented by conjugated recombinant MHC class I (pMHC). As proof of concept, human (h)CD20⁺ lymphoblasts were coated in a two-step process with streptavidin-conjugated anti-hCD20 scFv and biotinylated HLA-A2/CMV peptide (*NLVPMVATV*)-containing monomer. Coated cells could be lysed by retargeted *NLVPMVATV*-specific CTLs at effector:target ratios ≤ 5:1.

Attempts were made to refine this retargeting strategy and produce a single molecule consisting of pMHC chemically conjugated to Fab': Various bacterial and mammalian expression systems for production of pMHC have been investigated including expression of NLVPMVATV- β_2 microglobulin-HLA- $A2\alpha_1$ - α_3 as a single fusion protein; single chain trimer (SCT). However, difficulties with poor mammalian protein yield and inefficient bacterial protein refolding hindered further evaluation of this approach. Instead the in vitro and in vivo performances of murine CTL (OT-1) retargeting conjugates consisting of anti-hCD20 Fab' fragment(s) chemically conjugated to K^b/OVA peptide (SIINFEKL) SCT in Fab':pMHC ratios of 1:1 or 2:1 (F2 & F3) have been evaluated. In vitro both constructs can redirect OT-1 CTLs to lyse hCD20⁺ cells, and in the presence of hCD20 induce proliferation of naïve OT-1 cells. In an in vivo hCD20 transgenic mouse model, single doses of 1 nmole F3 and 2 nmole F2 caused respectively up to 95% and 85% B cell depletion at day 7. Inflammatory cytokine release produced by F3-mediated B cell depletion is lower than that measured when a similarly efficacious dose of anti-mCD3-containing bispecific F(ab')₂ is administered. Initial in vitro evaluations of a pharmaceutically-produced K^bSIINFEKL SCT x (anti-hCD20 Fab)₂ construct conjugated using 'Dock and Lock' technology shows equivalent efficacy to the F3 construct and may provide an avenue for taking this retargeting strategy forward.

Table of Contents

Title Page	i
Abstract	iii
Table of Contents	v
List of Tables.	xi
List of Figures	xiii
Declaration of Authorship	xvii
Acknowledgements	xix
Abbreviations	xxi
Confidentiality Agreement	. xxvii
Chapter 1: Introduction 1.1 Background 1.2 The Immune System and Cancer 1.2.1 Tumour immunosurveillance 1.2.1.1 Murine evidence 1.2.1.2 Human evidence 1.2.1.3 Cancer immunoediting 1.2.2 Inflammation and cancer 1.2.2.1 The role of T _H cells in determining the immune response to a tumour	3 5 5 5 9 10
1.2.2.2 The role of macrophages in determining the immune response to a tumour	20
1.3.1 T cell receptor structure. 1.3.2 MHC restriction of TCR antigen recognition. 1.3.2.1 Antigen presentation by MHC class I. 1.3.2.2 Antigen presentation by MHC class II.	21 23 25
1.3.2.3 Cross-presentation. 1.3.3 T cell development. 1.3.3.1 Gene rearrangement: αβ versus γδ lineage commitment. 1.3.3.2 Positive and negative selection of αβ T cells.	29 30
1.3.4 T cell activation. 1.3.4.1 Migration. 1.3.4.2 Role of dendritic cells. 1.3.4.3 Costimulation. 1.3.4.4 TCR signal transduction.	35 36 37
1.3.5 CTL effector mechanisms 1.3.5.1 Granule dependent exocytosis 1.3.5.2 Fas:FasL engagement 1.3.6 T cell memory	40 40 41 41
1.4 T Cell Immunotherapy 1.4.1 Vaccination 1.4.2 Adoptive T cell transfer 1.4.3 Adoptive transfer of genetically modified T cells	45 47

52
52
53
55
56
63
63
65
68
70
. 73
75
77
77
77
77
78
78
78
81
81
81
85
86
86
o o I-
87
88
88
90
91
91
92 95
95
95
99
99
100
100
T
101
ıg
102
ıg
102
102
102
102
103
104
104

2.3.3 Protein characterization	
2.3.3.1 Bradford assay	
2.3.3.1 SDS-PAGE analysis	106
2.3.3.2 Enzyme-linked Immunosorbent Assay	
2.3.3.3 Tetramer formation.	
2.4 Bacterial Construct Production and Characterisation (Murine)	109
2.4.1 Production of murine <i>SIINFEKL</i> -β ₂ microglobulin-K ^b -biotin-AviTag	100
(mSCT-B) protein.	
2.4.1.1 SIINFEKL-β ₂ microglobulin-K ^b -biotin-AviTag construct design	
2.4.1.2 SIINFEKL-β ₂ microglobulin-K ^b -biotin-AviTag protein production	109
2.4.1.3 SIINFEKL-β ₂ microglobulin-K ^b -biotin-AviTag protein	400
characterisation	109
2.4.2 Production of murine <i>SIINFEKL</i> -β ₂ microglobulin-K ^b -biotin-AviTag	
(mSCT-B) x anti-hCD20 (AT80) Fab' conjugates	
2.4.2.1 Digestion of anti-hCD20 IgG to anti-hCD20 F(ab)' ₂	
2.4.2.2 Purification of anti-hCD20 F(ab') ₂ using anti-mouse Fc column	
2.4.2.3 Conjugation of mSCT-B to anti-hCD20 Fab' using SMCC	
2.4.3 Production of anti-hCD20 x anti-mCD3 F(ab') ₂ conjugate	112
2.4.4 <i>In vitro</i> functional characterisation of mSCT-B x anti-hCD20 Fab'	111
conjugates	114
2.4.4.1 Binding of mSCT-B x anti-hCD20 Fab' conjugates to hCD20 ⁺	111
cells	
2.4.4.2 Labelling of 25D1 with fluorescein isothiocyanate (FITC)	
2.4.4.3 Cytotoxicity assay using mSCT-B x anti-hCD20 Fab' conjugates 2.4.4.4 OT-1 proliferation assays	
2.4.5 <i>In vivo</i> functional characterisation of mSCT-B x anti-hCD20 Fab'	110
conjugates	117
2.4.5.1 B cell depletion assay	
2.4.5.1 Meso Scale Discovery cytokine assay	
2.5 Characterisation of Dock and Lock Construct (Murine)	
2.0 Characterisation of Dock and Book Constituet (Marine)	11/
Chapter 3: Results - Human Retargeting Constructs	121
3.1 CTL Generation and Characterisation	123
3.1.1 Flow cytometric analysis of <i>NLVPMVATV</i> -specific CTL lines	123
3.1.2 Two-stage retargeting cytotoxicity assay	
3.2 Mammalian Protein Expression	
3.2.1 Construct design	127
3.2.2. Production of genetic constructs	
3.2.3 Characterisation of proteins expressed in mammalian cells	
3.2.3.1 Western blotting of proteins expressed in mammalian cells	131
3.2.3.2 ELISA analysis of proteins produced in mammalian cells	133
3.3 Bacterial Protein Expression	139
3.3.1 Construct design.	139
3.3.2. Production of genetic constructs	. 140
3.3.2.1 pET21a-CMV-β ₂ microglobulin-HLA-A2-human IgG ₁ hinge	
(SCT-3xCys)	141
3.3.2.2 pET21a-CMV-β ₂ microglobulin-HLA-A2-human IgG ₁ hinge	
single cysteine (SCT-Cys-I, SCT-Cys-II & SCT-Cys-III)	
3.3.2.3 pET21a-CMV-β ₂ microglobulin-HLA-A2-Cysteine (SCT-C)	142
3.3.2.4 pET21a-CMV-β ₂ microglobulin-HLA-A2 (SCT-X)	143
3.3.2.5 pET21a-CMV-β ₂ microglobulin-HLA-A2-biotin-AviTag (SCT-B)	143
$3.3.2.6$ pET21a-CMV-short-linker- β_2 microglobulin-HLA-A2-cysteine	
(SCT-SL-C)	143
3.3.2.7 pET21a-CMV-short linker-β ₂ microglobulin-HLA-A2-biotin-	

AviTag (SCT-SL-B)	144
3.3.2.8 pET21a-CMV-short linker-β ₂ microglobulin-HLA-A2-biotin-	
AviTag disulfide trap (SCT-SL-B DST)	144
3.3.3 Expression of bacterial SCT proteins	
3.3.4 Purification of inclusion bodies.	
3.3.5 Refolding of denatured SCT proteins	
3.3.6 Purification of refolded SCT proteins	
3.3.6.1 Purification using immunoaffinity chromatography	
3.3.6.2 Purification using size exclusion chromatography	
3.3.7 SCT protein characterisation	
3.3.7.1 Characterisation of protein purified using immunoaffinity	10 .
chromatography	154
3.3.7.2 Characterisation of protein purified using size exclusion	
chromatography	159
Cin on account of a physical control of the control	10)
Chapter 4: Discussion (1) Human Constructs	169
4.1 Summary of Human Construct Data	
4.2 Potential Future Studies: Human Construct	
4.3 Future Studies: Murine Construct	
The I detail of the control of the c	1,0
Chapter 5: Results - Murine Retargeting Constructs	175
5.1 Production of Murine SIINFEKL-β ₂ microglobulin-K ^b -biotin-AviTag	
(mSCT-B) Protein	175
5.2 Functional Characterisation of SIINFEKL-β ₂ microglobulin-K ^b -biotin-	
AviTag mSCT-B) Protein	179
5.3 Production of mSCT-B x anti-hCD20 Fab' Conjugates	
5.4 Production of anti-hCD20 x anti-mCD3 F(ab') ₂ Conjugate: BsAb	
5.5 In Vitro Functional Characterisation of mSCT-B x anti-hCD20 Fab'	105
Conjugates	186
5.5.1 Staining hCD20 ⁺ cells.	
5.5.2 <i>In vitro</i> cytotoxicity assay	
5.5.3 <i>In vitro</i> proliferation assays	
5.6 In Vivo Functional Characterisation of mSCT-B x anti-hCD20 Fab'	170
Conjugates	104
5.6.1 B cell depletion assay.	
5.6.2 Measurement of cytokine release accompanying B cell depletion	100
5.6.2 Measurement of cytokine release accompanying B cen depletion	199
Chapter 6: Results - 'Dock and Lock' Construct	207
6.1 Introduction	
6.2 Evaluation of [mSCT x (anti-hCD20 Fab) ₂] DnL	
6.2.1 Staining hCD20 ⁺ cells.	
6.2.2 <i>In vitro</i> cytotoxicity assay.	
6.2.3 <i>In vitro</i> proliferation assays	
0.2.5 In varo promeration assays	414
Chapter 7: Discussion (2) Murine Constructs	217
7.1 Summary of Mouse Construct Data.	
7.2. Principles of a Retargeting Strategy	
7.3 Current Retargeting Strategies.	
7.4 Developing the pMHC x Fab ^(*) Retargeting Strategy	
7.4 Developing the pittle A rab Retarguing buategy	222
Appendices	227
Appendix 1: Reagent recipes	
Appendix 2: Supplementary Data	
Appendix 3: Sequences	

erences.	277
Δ r Δn <i>r</i> Δς	7.11
CI CHCC3	# / /

List of Tables

Table 1.1: Summary of evidence for the role of the immune system in reducing tumour	
susceptibility	. 7
Table 1.2: Tumour antigen classification	.12
Table 1.3: Mechanisms mediating immune escape	15
Table 1.4: Anti-CD3-containing bispecific antibodies used <i>in vitro</i> or <i>in vivo</i> to retarget	
CTLs to tumour cells	.57
Table 2.1: 293F transient transfections performed	89
Table 2.2: CHO-K1 stable transfections performed.	.90
Table 2.3: Antibodies used for Western Blotting.	92
Table 2.4: Antibodies and standards used for mammalian protein ELISAs	.93
Table 2.5: Antibodies used for bacterial protein ELISAs.	. 106
Table 2.6: Retargeting constructs used in B cell depletions.	. 118

List of Figures

Figure 1.1: Polarization of the immune response during tumour development	18
Figure 1.2: The structure of the TCR/CD3 complex	22
Figure 1.3: Schematic diagram of the structure of MHC class I & II	25
Figure 1.4: Schematic representation of MHC class I antigen processing	26
Figure 1.5: Schematic representation of MHC class II antigen processing	28
Figure 1.6: Schematic representation of T cell development in the thymus	30
Figure 1.7: Schematic diagram of the kinetic segregation theory of TCR triggering	39
Figure 1.8: Schematic diagram of signalling pathways activated by TCR engagement	ıt 40
Figure 1.9: Structure of a chimeric antigen receptor	51
Figure 1.10: Alternative structures of bispecific antibodies.	54
Figure 1.11: Retargeting Fcγ receptor-bearing cells	56
Figure 1.12: Retargeting CTLs	60
Figure 1.13: Different retargeting system designs	66
Figure 1.14: Various single-step retargeting molecule designs (Reiter et al)	68
Figure 2.1: Design of genetic constructs for mammalian expression	82
Figure 2.2: Design of genetic constructs for bacterial expression	96
Figure 2.3: Design of genetic construct for SIINFEKL- β_2 microglobulin- K^b -biotin-A	viTag
(mSCT-B)	109
Figure 3.1: Flow cytometry profiles of unstimulated PBMCs	123
Figure 3.2: Flow cytometry profiles of non-peptide and peptide stimulated PBMCs.	124
Figure 3.3: Specific lysis of coated Daudi cells by NLVPMVATV-specific CTLs	125
Figure 3.4: Design of one-step retargeting molecules to be produced in mammalian	
cells	128
Figure 3.5: Schematic representation of (co-)transfections undertaken to produce M	HC
component of retargeting protein in mammalian cells	131
Figure 3.6: Western blot analysis of mammalian construct protein production from t	ransient
transfections of 293F cells	132
Figure 3.7: ELISA analysis of HLA-A2-human hinge-Fc/β ₂ m protein secretion from	ı 293F
(co-)transfections; capturing with W6/32, BB7.2 or anti-hFc & detecting with	h anti-
β_2 m-HRP	135
Figure 3.8: ELISA analysis of <i>NLVPMVATV</i> -β ₂ m-HLA-A2 protein secretion from S	Signal
pIg plus-CMV-short linker-β ₂ m-HLA-A2-biotin-AviTag transfected 293F co	ells;
capturing with W6/32 and detecting with anti- β_2 m antibodies	136
Figure 3.9: SCT construct design	141

Academic Thesis: Declaration Of Authorship

I, <u>Angela Diane Hamblin</u> declare that this thesis and the work presented in it are my own and has been generated by me as the result of my own original research.

RETARGETING NON-COGNATE CYTOTOXIC T CELLS TO TUMOUR ANTIGENS USING [PEPTIDE-MHC x FAB'] CONJUGATES

I confirm that:

- 1. This work was done wholly or mainly while in candidature for a research degree at this University;
- 2. Where any part of this thesis has previously been submitted for a degree or any other qualification at this University or any other institution, this has been clearly stated;
- 3. Where I have consulted the published work of others, this is always clearly attributed;
- 4. Where I have quoted from the work of others, the source is always given. With the exception of such quotations, this thesis is entirely my own work;
- 5. I have acknowledged all main sources of help;
- 6. Where the thesis is based on work done by myself jointly with others, I have made clear exactly what was done by others and what I have contributed myself;
- 7. Parts of this work have been published as:

Hamblin, A., et al., *Non-Cognate Cytotoxic T Cells Can Be Retargeted Against CD20 Positive Tumour Cells Using [Fab' x MHC Class I/Peptide] Conjugates.* Blood (ASH Annual Meeting Abstracts), 2010. 116(21): 2838.

Signed:	 	 	 	 	 	.
Ü						
Date:	 	 	 	 	 	

Acknowledgements

I would like to gratefully acknowledge the following people:

Professor Martin Glennie & Professor Peter Johnson for overall supervision of the project. Dr Ruth French for support and advice with both experimental work and preparation of this thesis.

Dr Ben King for generously imparting all his knowledge regarding the production of retargeting constructs.

Cancer Research UK for providing funding for this project.

Dr Claude Chan, Alison Tutt, Chris Penfold, Professor Mark Cragg, Dr Steve Beers, Dr Ann White, Dr Weng Leong, Snita Bansal, BRF staff & everyone in the Tenovus laboratory for their unstinting help and support with this project. Mr Leon Douglas & Dr Patrick Duriez in the Protein Core Facility, Cancer Sciences Division, University of Southampton for their help and advice with protein purification.

Professor Ted Hansen (Washington University) for the kind gift of the *SIINFEKL*- β_2 microglobulin- K^b single chain trimer DNA construct.

Dr Phil Savage for providing the B9E9-SA fusion protein and the $[mSCT \ x \ (anti-hCD20 \ Fab)_2]$ DnL construct.

Finally I would like to thank my parents and husband Stuart for all their support and patience during this project.

Abbreviations

 $(G_xS)_x$ glycine serine linker

2-ME 2-mercaptoethanol

Ab antibody

ABC ATP-binding cassette

ACT adoptive cell transfer

AD anchoring domain

ADCC antibody dependent cell-mediated cytotoxicity

Ag antigen

AIRE autoimmune regulator

Alb albumin

AML acute myeloid leukaemia

APC allophycocyanin

APC antigen presenting cells

B biotin

BCCP biotin carboxyl carrier protein

BCR B cell receptor

Bcr-abl breakpoint cluster region: Abl1 fusion protein

BirA biotin holoenzyme synthetase

BiTE Bispecific T cell Engaging

BSA bovine serum albumin

BsAb bispecific antibody

C cysteine

C terminus carboxy terminus

CAR chimeric antigen receptor

CCL CC chemokine ligand

CCR CC chemokine receptor

CD20 antigen found on B cells

CD3 antigen found on T cells

CD4 helper T cell antigen

CD40L CD40 ligand

CD8 cytotoxic T cell antigen

cDNA complementary deoxyribonucleic acid

CDR complementarity determining region

CEA carcinoembryonic antigen

CFSE Carboxyfluorescein succinimidyl ester

C_{Hx} heavy chain constant domains

CHO Chinese Hamster Ovary

C_L light chain constant domain

CLIP class II-associated invariant chain peptide

CLL chronic lymphocytic leukaemia

CML chronic myeloid leukaemia

CMV cytomegalovirus

CO₂ carbon dioxide

Cre Cre recombinase

cTEC cortical thymic epithelial cell

CTL cytotoxic T lymphocyte

Cys cysteine

D day

D diversity

DC dendritic cell

DDD dimerisation docking domain

DLI donor lymphocyte infusion

DMBA/TPA 7,12-dimethylbenz[a]anthracene/12-0-tetradecanyolphorbol-13-acetate

DMF dimethylformamide

DMSO dimethyl sulfoxide

DN double negative

DNA deoxyribonucleic acid

DnL dock and lock

DP double positive

DST disulfide trap

DTT dithiothreitol

EBV Epstein Barr virus

EDTA ethylenediaminetetraacetic acid

EGFR epidermal growth factor receptor

EGP-2 epithelium-associated glycoprotein

ELISA Enzyme Linked Immunosorbent Assay

ELISPOT Enzyme Linked Immunosorbent Spot assay

EpCAM epithelial cell adhesion molecule

ER endoplasmic reticulum

ERAAP endoplasmic reticulum amino-peptidase

F(ab')₂ fragment, antibody binding, including hinge region (both arms)

F2 [mSCT-B x anti-hCD20 Fab']

F3 [mSCT-B x (anti-hCD20 Fab')₂]

Fab' fragment, antibody binding, including hinge region (one arm)

Fab fragment, antibody binding, excluding hinge region (one arm)

FACS fluorescence activated cell sorting

FADD Fas-associated death domain

Fc fragment, crystallisable (constant region of antibody)

FcR receptor for antibody fragment, crystallisable

FcRn neonatal receptor for antibody fragment, crystallisable

FCS foetal calf serum

FITC fluorescein isothiocyanate

flu influenza

FOXP3 forkhead box P3

FSC forward scatter

G0-G1 cell cycle gap 0 gap 1

G-CSF granulocyte-colony stimulating factor

GFP green fluorescent protein

GILT Gamma-interferon-inducible lysosomal thiolreductase

GM-CSF granulocyte macrophage colony-stimulating factor

GVHD graft versus host disease

GVL graft versus leukaemia

h human

H₂O water

H₂SO₄ sulfuric acid

HCl hydrochloric acid

HEK human embryonic kidney

HEPES 4-(2-hydroxyethyl)-1-piperazineethanesulfonic acid

HER2 human epidermal growth factor receptor 2

HEV high endothelial venule

HHD H-2D^{b-/-} β_2 m^{-/-} double knockout, human β_2 m /HLA-A2 $\alpha_1\alpha_2$ -mouse H-2D^b α_3 transgenic mice

HHV8 human herpes virus 8

hi high

HIV human immunodeficiency virus

HLA human leukocyte antigen

HPLC high performance liquid chromatography

HPV human papillomavirus

HRP horse radish peroxidase

HSCT haematopoietic stem cell transplantation

ICOS inducible T cell costimulator

IFN interferon

IgG immunoglobulin class G

IL interleukin

IPTG isopropyl β-D-thiogalactopyranoside

ITAM immunoreceptor tyrosine-based activation motif

J joining

LAK lymphokine activated killer

LAT linker for the activation of T cells

LB Luria-Bertani

LCMV Lymphocytic Choriomeningitis Virus

Letal lymphocyte effector cell toxicity-activating ligand

LMP latent membrane protein

lo low

LoxP locus of crossover P1

m mouse

mAb monoclonal antibody

MACS magnetic-activated cell sorting

MAGE melanoma antigen gene

MART-1 Melanoma-associated antigen recognised by T cells

MCA 3'-methylcholanthrene

MCSP melanoma chondroitin sulfate proteoglycan

MDSC myeloid derived suppressor cell

MFI mean fluorescence intensity

MGUS monoclonal gammopathy of undetermined significance

MHC major histocompatibility complex

MICA/B MHC class I chain-related proteins A & B

MM multiple myeloma

mRNA messenger ribonucleic acid

mSCT SIINFEKL-β₂microglobulin-K^b expressed as a single fusion protein

mSCT-B SIINFEKL-β₂microglobulin-K^b-biotin-AviTag expressed as a single fusion protein

MTD maximum tolerated dose

mTEC medullary cortical epithelial cell

MUC1 mucin 1, cell surface associated

MW molecular weight

MWCO molecular weight cut-off

NF-κB nuclear factor kappa-light-chain-enhancer of activated B cells

NHS N-hydroxysuccinimide

NK natural killer cell

NKT natural killer T cell

NMR nuclear magnetic resonance

NP40 nonyl phenoxypolyethoxylethanol

NY-ESO-1 New York esophageal squamous cell carcinoma 1

OD optical density

o-PDM *N,N'-(o-Phenylene)*dimaleimide

OT-1 mouse with transgenic TCR specific for K^bSIINFEKL

OVA ovalbumin

PBMCs peripheral blood mononuclear cells

PBS phosphate buffered saline

PCR polymerase chain reaction

PD-1 programmed cell death-1

PE phycoerythrin

PGE₂ prostaglandin E2

pMHC peptide: major histocompatibility complex

PMSF phenylmethylsulfonyl fluoride

PNAd peripheral node addressin

PRR pattern recognition receptor

PSA prostate specific antigen

PSMA prostate specific membrane antigen

PTK protein tyrosine kinases

R receptor

RAG recombination activating gene

RET rearranged during transfection

RNA ribonucleic acid

RSS recombination signal sequence

RT room temperature

s/n supernatant

SA streptavidin

SARS severe acute respiratory syndrome

scFv single chain variable fragment

SCT single chain trimer

SD standard deviation

SDS-PAGE sodium dodecyl sulfate polyacrylamide gel electrophoresis

SEM standard error of the mean

SH sulfhydryl residue

SL short linker

SLP-76 SH2 domain-containing leukocyte phosphoprotein

SMCC Succinimidyl-4-(*N*-maleimidomethyl)cyclohexane-1-carboxylate

SOC super optimal broth with catabolite repression

SOE splicing by overlap extension

SP single positive

S-S disulfide bond

SSC side scatter

STAT Signal Transducer and Activator of Transcription

SV40 T-Ag Simian vacuolating virus 40 large T antigen

TAE tris acetate ethylenediaminetetraacetic acid

Tag large T antigen of SV40

TAP transporter associated with antigen processing

TBS/T tris buffered saline/tween-20

TCM T cell medium

TCR T cell receptor

TdT terminal deoxynucleotidyl transferase

TE tris ethylenediaminetetraacetic acid

TERT telomerase reverse transcriptase

Tg transgenic

TGF transforming growth factor

 T_H helper T cell

TIL tumour-infiltrating lymphocytes

TLR Toll-like receptor

TNF tumour necrosis factor

TNFR tumour necrosis factor receptor

TPPII Tripeptidyl-peptidase II

TRAIL Tumour necrosis factor-related apoptosis-inducing ligand

 T_{reg} regulatory T cell

ULBPs UL16 binding proteins

 $\begin{array}{c} \textbf{UV} \ \ \textbf{ultraviolet} \\ \textbf{V} \ \ \textbf{variability} \\ \textbf{VEGF} \ \ \textbf{vascular} \ \ \textbf{endothelial} \ \ \textbf{growth} \ \ \textbf{factor} \\ \textbf{V}_{\textbf{H}} \ \ \textbf{heavy} \ \ \textbf{chain} \ \ \textbf{variable} \ \ \textbf{domain} \\ \textbf{V}_{\textbf{L}} \ \ \textbf{light} \ \ \textbf{chain} \ \ \textbf{variable} \ \ \textbf{domain} \\ \textbf{WB} \ \ \textbf{Western} \ \ \textbf{blot} \\ \textbf{WT} \ \ \textbf{wild} \ \ \textbf{type} \\ \textbf{\beta}_{2} \textbf{m} \ \ \textbf{beta}_{2} \textbf{microglobulin} \\ \end{array}$

Confidentiality Agreement

All data obtained using the [mSCT x (anti-hCD20 Fab)₂] DnL construct and discussions pertaining to these results are governed by a confidentiality agreement with Immunomedics, New Jersey, USA, who kindly provided the reagent.

Chapter 1: Introduction

1.1 Background

Amongst 58 million deaths worldwide in 2008, 7.6 million (13%) were from cancer.¹ Although there have been significant improvements in cancer survival in Europe since the early 1990s with better use of conventional treatments,² globally the annual cancer mortality rate is expected to rise to over 13.1 million by 2030.¹ With continuing improvements in the treatment of infectious diseases in developing countries and better cardiovascular disease prevention, cancer is likely to become responsible for a greater proportion of all mortality making the search for new and innovative treatments a high priority.

Cancer can be defined as, 'the rapid creation of abnormal cells growing beyond their usual boundaries which can invade adjoining parts of the body and spread to other organs, a process referred to as metastasis.' Successful anti-cancer treatment to date has largely consisted of a combination of surgery, chemotherapy and radiotherapy. Although surgery can be curative in early localised disease, it is inappropriate for many tumour types due to their diffuse spread or close apposition to vital structures. Radiotherapy and chemotherapy can have more of an effect on disseminated tumours, but the collateral damage caused to other cells either anatomically close to the tumour in the case of radiotherapy, or those rapidly dividing in the case of chemotherapy means the toxic dose of either treatment for the tumour often exceeds the fatal dose for the body as a whole.

An alternative method of eliminating tumours is to try and use the body's own immune system to destroy tumour cells. The immune system is a collection of specialised cells and organs whose role is to recognise and normally eliminate or contain foreign pathogens; an ability which relies on the discrimination of self from non-self. Being derived from self tissues, tumours often escape recognition by the immune system allowing them to grow unchecked. Immunotherapy aims to circumvent this normal tolerance of tumours and utilise components of the immune system in the destruction of malignant cells.

Immunotherapy involves any treatment that manipulates, augments or suppresses the immune system and can be divided into active and passive therapies. Active immunotherapy involves administering agents to promote the immune response to a particular antigen (Ag) *in vivo* such as a vaccine or cytokine. Passive immunotherapy involves administering an immune response developed *in vitro* such as a specific monoclonal antibody (mAb) or adoptively transferring *ex vivo* expanded autologous T cells. Although there have been some very efficacious mAbs developed in the last few years, with both herceptin in breast cancer³ and rituximab in CD20⁺ B cell tumours causing a significant improvement in survival⁴ there are now efforts to try and improve the success of (cytotoxic) T cell immunotherapy.

The subsequent introduction will consider current ideas regarding the endogenous immune response to tumours before focussing on T cell biology (particularly that of cytotoxic T cells), and the immunotherapeutic strategies being pursued to try and improve anti-tumour T cell responses.

1.2 The Immune System and Cancer

1.2.1 Tumour immunosurveillance

The sometimes controversial concept that the immune system has an active role in the detection and elimination of tumours dates back as far as Ehlrich who in 1909 suggested that 'the immune system could repress a potentially overwhelming frequency of carcinomas.' The theory was first formalised with the cancer immunosurveillance hypothesis of Burnet and Thomas which proposed that, given the frequency of somatic mutations in long-lived warmblooded vertebrates with the potential to move a cell along the pathway to malignancy, it was an evolutionary necessity to have a mechanism to detect and eliminate such mutated cells. They suggested that these mutations produced new 'antigenic potentialities' within the cells which provoked an immunological reaction which they believed was mediated by lymphocytes. Their evidence for this concept came from the observation that inbred mice could be immunised against syngeneic tumours induced through chemical carcinogenesis or viral infection, suggesting the presence of tumour-specific Ags that could be recognised as 'foreign' by the immune system.

1.2.1.1 Murine evidence

Following this initial observation much effort was expended trying to demonstrate that immunosuppressed mice had a higher rate of either spontaneously arising or chemically induced carcinogenesis. However, although early studies revealed an increased incidence of virally-induced tumours and lymphomas in mice with induced immunosuppression, no increase in chemically induced carcinomas or sporadic tumours could be demonstrated in these or genetically immunosuppressed 'nude' mice and interest in the concept waned.

It was not until the more accurate definition of the immunological deficiency of *nude* mice and the development of a number of gene knock out mice that more supportive evidence for the concept of cancer immunosurveillance could be obtained. The discovery that *nude* mice, although possessing decreased numbers of T cells, still have NK cells and even small numbers of functional αβ T cells¹¹ provides some explanation for the lack of increased chemical carcinogenesis observed in these animals. In contrast, similar experiments in RAG (recombination activating gene) knock out mice which are unable to rearrange the genes required for a functioning lymphocyte Ag receptor and thus lack B, T and NKT cells¹² did show an increase in both chemically-induced and sporadic tumours.¹³ Similarly, repeating these experiments in mice deficient in perforin, a key component of the cytotoxic granules found in both T and NK cells, demonstrated similar results.¹⁴

Table 1.1 shows that through the development of gene knock out mice and the use of depleting antibodies, a role in tumour elimination has been suggested for all the cellular components of the adaptive immune system as well as several cytokines and proteins which have a role in Ag processing and presentation to cytotoxic T cells.

However, the concept of cancer immunosurveillance is still somewhat controversial: Studies by Blankenstein *et al* suggest that the difference in susceptibility to chemically-induced tumours seen between gene knock-out mice and wild-type controls is a function of IFNγ levels rather than individual immune component deficiencies.¹⁵ In many studies, wild-type controls are purchased from outside institutions rather than bred in-house, as is usually the case with immunodeficient mice. Blankenstein *et al* argue that the resulting change in flora, food, air and water is likely to provide an 'immune stimulus' resulting in the release of IFNγ which subsequently produces a non-specific anti-tumour effect.¹⁵ Their most recent work suggest there is no role for T/NKT cells or their effector molecules in preventing carcinogenesis, but rather B cells and IL-4 actively promote 3′-methylcholanthrene (MCA) tumorigenesis.¹⁶

However in turn, other investigators suggest the dose of the chemical MCA used by Blankenstein *et al* to induce tumours is sufficiently large to overwhelm the protective effects of any immune response, even in immunocompetent mice. ¹⁷ At present data from chemically-induced carcinogenesis models remains conflicting with both exponents and detractors of tumour immunosurveillance using data obtained from this model to support their theory. ¹⁸ The variation between the different experiments in terms of dose, route of administration, mouse background and origin of controls means it is very difficult to perform any meaningful comparison of results from one investigator to another. However, it would seem unlikely that all of the results listed in Table 1.1 supporting the theory of immunosurveillance can be attributed to deficits in the experimental method.

Mouse strain	Treatment	Deficiency	Tumour susceptibility	Reference
nude (athymic) Nil		T cells	Increased incidence B cell lymphoma compared to heterozygous littermates	19
` '	Anti-μ		Increased incidence B cell lymphoma compared to heterozygous littermates	
RAG-2 ^{-/-}	Nil	T, B & NKT cells	Increased incidence spontaneous intestinal neoplasia	13
	MCA		Increased incidence MCA-induced sarcomas	
RAG-2 ^{-/-} x	Nil	T, B & NKT cells & IFNγ and	Increased incidence of spontaneous mammary and intestinal neoplasia	13
STAT1 ^{-/-}	MCA	IFNα/β receptor mediated signalling	Increased incidence MCA-induced sarcomas	
RAG-1 ^{-/-}	MCA	T, B & NKT cells	Increased incidence MCA-induced sarcomas	20
scid	MCA	T, B & NKT cells	Increased incidence MCA-induced sarcomas	20
TCRβ ^{-/-}	MCA	αβT cells	Increased incidence MCA-induced sarcomas	21
TCRδ ^{-/-}	MCA DMBA/TPA	γδT cells	Increased incidence MCA-induced sarcomas Increased incidence DMBA/TPA skin tumours	21
$TCR\beta^{-/-}\delta^{-/-}$	DMBA/TPA	αβT cells & γδT cells	Increased incidence DMBA/TPA skin tumours	22
Jα281 ^{-/-}	MCA	Vα14 TCR ⁺ NKT cells	Increased incidence MCA-induced sarcomas	23
B6 / Balb/c WT	Anti-asialo GM1 Ab & MCA	NK cells	Increased incidence MCA-induced sarcomas	20
B6 WT	Anti-NK1.1 Ab & MCA	NK cells	Increased incidence MCA-induced sarcomas	23
B6 WT	Anti-Thy1 Ab & MCA	T cells	Increased incidence MCA-induced sarcomas	23
Balb/c WT	Anti-CD25 Ab & MCA	CD4 ⁺ CD25 ⁺ T _{reg} cells	Decreased susceptibility to MCA-induced sarcomas	24
IFNGR ^{-/-}	MCA	IFNγR α chain: therefore insensitive to IFNγ	Increased incidence MCA-induced sarcomas	25
IFNγR ^{-/-} x p53 ^{-/-}	Nil	IFNγR α chain: therefore insensitive to IFNγ & p53 deficient	Faster development of spontaneous tumours affecting a wider variety of tissues compared to IFNγ sensitive p53 ^{-/-} mice	25
IFNγ ^{-/-}	MCA Nil (C57BL/6) Nil (Balb/c)	IFNγ production	Increased incidence MCA-induced sarcomas Increased incidence spontaneous disseminated lymphoma compared to WT Increased incidence spontaneous lung adenocarcinoma compared to WT	26 27
IFNγ ^{-/-} x Tax ⁺	Nil	IFNγ production	Accelerated tumour (resembles adult T cell lymphoma) onset and progression compared to Tax ⁺ mice	28

IFNAR1 ^{-/-}	MCA	IFNα/β receptor 1: therefore insensitive to IFNα/β	Increased incidence MCA-induced sarcomas	29
WT DBA/2, C57BL/6 & BALB/c	Anti-IFNα/β Ab & administration of syngeneic tumour	IFNα/β	Enhanced transplantability of syngeneic tumours compared to controls	30
STAT-/-	MCA	IFNγ and IFNα/β mediated signal	Increased incidence MCA-induced sarcomas	25
STAT ^{-/-} x p53 ^{-/-}	Nil	IFNγ and IFNα/β mediated signal AND p53 deficient	Faster development of spontaneous tumours affecting a wider variety of tissues compared to p53 ^{-/-} mice	25
Perforin ^{-/-}	MCA Nil	Perforin-mediated cytotoxicity	Increased incidence MCA-induced sarcomas Increased incidence of spontaneous disseminated lymphomas	14 31
Perforin ^{-/-} x IFNγ ^{-/-}	MCA Nil	Perforin-mediated cytotoxicity & IFNγ production	Increased incidence MCA-induced sarcomas Increased incidence of spontaneous disseminated lymphomas	26 27
TRAIL-/-	MCA	TRAIL-mediated cytotoxicity	Increased incidence MCA-induced sarcomas	32
B6 WT	Anti-TRAIL Ab & MCA	TRAIL-mediated cytotoxicity	Increased incidence MCA-induced sarcomas	33
p53 ^{+/-}	Anti-TRAIL Ab	TRAIL-mediated cytotoxicity	Increased incidence spontaneous sarcomas and disseminated lymphomas	33
IL-12 p40 ^{-/-}	MCA	IL-12p40 subunit (component of IL-12 and IL-23)	Increased incidence MCA-induced sarcomas	23
LMP2 ^{-/-}	Nil	IFNγ-inducible low molecular mass polypeptide-2 (LMP2) subunit	Increased incidence of spontaneous uterine neoplasias	34

Table 1.1: Summary of evidence for the role of the immune system in reducing tumour susceptibility *Unless otherwise stated all differences in tumour development described are in comparison to untreated or wild-type animals. Table adapted from Smyth et al. Adv Immunol. 2006; 90:1*³⁵

1.2.1.2 Human evidence

Evidence for the concept of tumour immunosurveillance in humans was first provided by examining the incidence of tumour formation in those who are immunosuppressed. The hereditary Chediak Higashi syndrome (results in impaired NK cell cytotoxicity) is associated with a 200-fold increased risk of malignancy³⁶. Several transplant registries demonstrate the significant increase of both virus-associated tumours such as non-Hodgkin's lymphoma (EBV-associated), Kaposi's sarcoma (HHV8-associated) and genitourinary / anal carcinomas (HPV-associated), ³⁷ as well as tumours not known to have a viral origin such as colon, kidney, thyroid and melanoma. ³⁸

Further evidence for tumour immunosurveillance in humans comes from studies on tumour infiltrating lymphocytes (TILs). Initial studies demonstrated that a higher number of TILs correlated with a better prognosis: In 1989, a study of over 500 stage I cutaneous melanomas demonstrated that the level of infiltrating lymphocytes was an independent prognostic factor for 8 year survival with an odds ratio of 11.4, second only to mitotic index. A similar phenomenon was observed in several other malignancies including colorectal tumours.

As methods for identifying types of lymphocytes improved attempts were made to characterise tumour infiltrates. One study in colorectal adenocarcinoma demonstrated that prognosis was related to the CD4/CD8 ratio of the infiltrating T cells: A low CD4/CD8 ratio was associated with better 5 year survival. A more recent investigation of colorectal tumour lymphocyte infiltrates has shown that up-regulation of T_H1 type' genes (e.g. IFNγ, CD8, granzyme B) associated with a cytotoxic T cell response correlates better with a good prognosis than the standard tumour-node-metastasis staging system conventionally used. A correlation between improved prognosis and CD8+ T cell infiltration has also been seen in several other tumours including melanoma, and oesophageal carcinoma.

One possible explanation for the poor outcome associated with a high CD4/CD8 ratio is a suppressive effect of CD4⁺ T cells on tumour immunity. The discovery of CD4⁺/CD25^{hi}/FOXP3⁺ regulatory T cells (T_{reg}) provides a mechanism through which CD4⁺ T cells can suppress host tumour immunity. T_{regs} can suppress immune responses by a number of mechanisms including production of inhibitory cytokines (e.g. TGFβ and IL-10), direct cytolysis, metabolic disruption and targeting dendritic cells. ⁴⁶ Subsequent studies have shown that heavy T_{reg} tumour infiltration is associated with a poor prognosis in several different tumour types including ovarian, ⁴⁷ pancreatic ductal ⁴⁸ and hepatocellular carcinomas. ⁴⁹ Examination of resected colonic carcinomas has also shown an increased frequency of T_{regs} within tumours compared to adjacent normal mucosa which following purification are able to

inhibit the proliferation of CD25 $^{-}$ tumour infiltrating T cells. ⁵⁰ However, a recent study correlating tumour T_{reg} infiltration with prognosis in colorectal cancer has suggested that a high tumour:normal tissue ratio of infiltrating T_{regs} is paradoxically associated with an improved prognosis. ⁵¹ This observation is not limited to colorectal carcinomas with improved survival being seen with high levels of T_{reg} infiltration in Hodgkin's lymphoma, ⁵² follicular lymphoma ⁵³ head and neck carcinomas. ⁵⁴

A number of explanations have been proposed for these contradictory observations including the suggestion that it is not absolute numbers of T_{regs} which determines outcome, rather the ratio of T_{regs} :CD8⁺ effectors. In addition the significance of T_{regs} may vary with stage: Although in the overall population of ovarian carcinoma patients infiltrating T_{regs} correlate with a poor prognosis, ⁴⁷ in advanced or metastatic disease heavy infiltration of T_{regs} was shown to be an independent factor for longer disease-specific survival.

In haematological and head and neck malignancies where T_{reg} infiltration has been correlated with improved survival, the tumours are normally heavily infiltrated with cells from the innate immune system (e.g. macrophages and neutrophils) which produce inflammatory cytokines, growth factors and pro-angiogenic factors, all of which can promote tumour growth. It is proposed that T_{reg} suppression of innate immune cells will reduce this inflammatory protumour environment impeding tumour growth. Furthermore, in the above studies T_{regs} were identified phenotypically by their expression of FOXP3, rather than by their immunosuppressive function: Some investigators have found that FOXP3 expression is not limited to T cells with a regulatory function.

Although less frequently investigated than CD4⁺ T_{regs}, FOXP3⁺ CD8⁺ T cells with an immunosuppressive function *in vitro* have also been described. These have also been shown to be present in significant numbers in some tumours,⁵⁷ although less information is available about the correlation between their frequency and disease prognosis. Taken as a whole, the data relating prognosis to tumour infiltration by various subsets of lymphocytes suggests a role for the immune system in the control of tumours.

1.2.1.3 Cancer immunoediting

In light of the above evidence, the theory of tumour immunosurveillance has been refined into the cancer immunoediting concept.⁵⁸ This suggests that the immunogenicity of a tumour is shaped by the immunological environment in which it develops. This theory divides the interaction between a tumour and the immune system into three phases; elimination, equilibrium and escape. Evidence for the elimination phase comes largely from the studies

outlined above, showing increased tumour incidence in the immunosuppressed and a better prognosis associated with effector cell infiltration of tumours.

Elimination

The spectrum of immunodeficient mouse models in which there is an increased susceptibility to tumour development indicates the range of immune system components which are thought to be involved in the elimination phase. The authors of this theory suggest that initially cells of the innate immune system (e.g. macrophages, DCs, NK and NKT cells) are attracted to the site of an early tumour due to the release of proinflammatory cytokines, chemokines and markers of cellular stress such as heat shock proteins⁵⁹ (and other Toll-like receptor ligands) and uric acid. These are either produced by the tumour itself or result from the disruption of surrounding normal tissue by its growth. In addition to initiating an innate immune response to the tumour, some of the proinflammatory cytokines (e.g. $TNF\alpha$ and $IFN\gamma$) are able to present a danger signal to DCs allowing their maturation and differentiation, ultimately resulting in specific tumour Ag presentation to cells of the adaptive immune system.

Once recruited to the tumour site, NK cells and $\gamma\delta$ T cells are able to interact with tumour cells via their NKG2D activating receptor. This recognises MHC class I chain-related proteins A and B (MICA/B) which have been reported as being expressed on carcinomas from a number of different tissues. Other NKG2D ligands such as UL16 binding proteins (ULBPs) and lymphocyte effector cell toxicity-activating ligand (Letal) have also been found expressed on human tumours. Recent work has shown that NKG2D ligands can be upregulated in response to genotoxic stress and stalled DNA replication, events likely to occur during the process of tumour development. Once the NKG2D receptor is engaged by an appropriate ligand the effector cell is able to initiate perforin-mediated cytotoxicity which can result in the elimination of the tumour cell.

These early events are thought to result in IFN γ secretion which, in addition to recruiting more immune effectors, has anti-proliferative, ⁶⁵ pro-apoptotic ⁶⁶ and angiostatic ⁶⁷ effects. IFN γ can also activate macrophages which express reactive oxygen ⁶⁸ and nitrogen ⁶⁹ species which can have a tumoricidal effect. Another early event is postulated to be the activation of NKT cells by CD1d:glycolipid Ag allowing them to have an anti-tumour effect. Studies have shown that NKT cells are able to lyse several tumour lines in vitro and in selected tumours their infiltration has been associated with an improved prognosis. ⁷⁰

The net effect of these early tumoricidal events is the release of tumour cell Ags in the context of innate 'danger' signals which allows the development of Ag specific adaptive immune responses (i.e. B, CD4⁺ T and CD8⁺ T cell responses). Originally tumour Ags were classified as either tumour specific (i.e. expression limited to the tumour cell alone) or tumour associated (usually reflecting ectopic or over-expression of a normal tissue Ag). More recently advances in determining tissue expression of any particular protein have led to these Ags being classified on the basis of their genetic structure. Table 1.2 lists the different categories of tumour Ags along with examples of each type for which confirmed CD8⁺ antitumour responses have been demonstrated either *in vitro* or *in vivo*.

Antigen Classification	Examples	Tumour	Reference
Differentiation	CEA Melan-A/MART-	Gastrointestinal tract Melanoma	71 72
Mutational	Bcr-abl p53 mutants	CML Head and neck squamous carcinoma	73 74
Overexpressed	HER2/neu MUC1	Breast (and others) Lung (and others)	75 76
Cancer-testis	MAGE NY-ESO-1	Melanoma (and others) Melanoma (and others)	77 78
Viral	EBV HPV	Nasopharyngeal (and others) Cervical	79 80

Table 1.2: Tumour antigen classification

Differentiation Ags are expressed in the tissue of tumour origin in addition to the tumour itself. Mutational Ags are 'new' Ags expressed only in the tumour as a result of a genetic alteration; the examples listed are ones which have been observed to occur in many different patients, but often a mutational tumour Ag is unique to a single patient making it an unsuitable target for immunotherapy. Overexpressed Ags are found in a number of normal tissues in addition to the tumour. Cancer-testis Ags are expressed in tumours from many different tissues, but the only significant expression in the absence of a tumour is on placental trophoblasts and testicular germ cells. Viral Ags are derived from viruses which have a consistent association with a particular tumour type. All the references relate to MHC class I restricted peptides (mostly HLA-A2), however more recently MHC class II restricted peptides are beginning to be described for recognised tumour Ags.

Equilibrium

The above evidence provides a persuasive argument for the ability of the immune system to eliminate tumours. However, providing evidence for the next component of the theory, equilibrium, is a little more problematic as it is much harder to demonstrate control of a tumour by the immune system in a living subject. However, there can often be a large lag phase between exposure to a known carcinogen and development of a clinically evident tumour for example as occurs with asbestos exposure and mesothelioma. This led to the concept of tumour dormancy; defined as a population of transformed cells that is not increasing in size. Several theories have been put forward to explain this observation including cellular dormancy where cells enter a G0-G1 arrest, angiogenic dormancy where

the failure of tumour cells to develop their own blood supply limits further growth, or immune dormancy where components of the immune system prevent unregulated proliferation of malignant cells. This latter explanation of tumour dormancy correlates with the equilibrium stage of cancer immunoediting.

An additional observation consistent with immunoediting is that many patients enter a clinical remission after treatment of an initial primary lesion only to relapse many years later with widespread disease. Eurthermore, recent studies have identified circulating 'tumour' cells in breast cancer patients post-mastectomy, who have been in clinical remission for more than 20 years. However, although all these observations provide evidence for tumour dormancy, they do not provide any information on the mechanism responsible for this phenomenon.

More mechanistic evidence is provided by studies examining relapse in the context of immunosuppression: In one case series of 6 patients, recurrences of non-small cell lung cancer were reported 7-14 years after clinical remission and in each case relapse was associated with immunosuppressive treatment. A There have also been cases of donor-transmitted tumours arising after transplantation into immunosuppressed hosts. This could be explained by outgrowth of a tumour, previously kept in equilibrium by the donor's immune system, once it is exposed to an immunosuppressive environment. However it is possible that other explanations such as fluctuating expression of oncogenes could be responsible.

Further clinical evidence comes from anti-tumour responses detected in haematological malignancies: In one study of paediatric AML patients who achieved complete remission following chemotherapy +/- autologous stem cell transplantation, relapse was significantly associated with the absence of anti-tumour CTLs after induction chemotherapy.⁸⁷ Similarly in the pre-neoplastic plasma cell disorder monoclonal gammopathy of undetermined significance (MGUS) a vigorous CTL response against these cells can be detected, a response absent in the neoplastic plasma cell disorder multiple myeloma (MM). Although the plasma cells in MGUS have many of the genetic changes seen in MM, many patients remain stable without evidence of progression, suggesting a role of the immune system in controlling the potentially malignant clone.⁸⁸

Experimental mouse models have provided further evidence of an equilibrium period mediated, at least in part, via the immune system. In one model wild type BALB/c mice were immunized using an idiotype vaccine against the murine B cell lymphoma line BCL₁ before receiving a tumour challenge. Although 30% of mice rapidly developed splenomegaly in a

similar timescale to non-immunized control mice, the remaining animals remained tumour free at day 60 (historically considered to be the time point at which dormancy has been achieved). Long term follow-up of these animals demonstrated that circulating BCL_1 cells could be detected and splenomegaly was subsequently observed up to >610 days post initial tumour inoculation. The time required for splenomegaly development was significantly reduced by administration of a neutralizing anti-IFN γ Ab suggesting a role for immune effector mechanisms mediated via this cytokine in prolonging tumour dormancy.⁸⁹

A more recent investigation has perhaps provided the most convincing evidence for the equilibrium phase of immunoediting: Amongst wild-type C57BL/6 and 129SvEv mice exposed to a small dose of the carcinogen MCA 70% failed to develop a progressive sarcoma despite monitoring for >200 days. When tumour-free mice were treated weekly with a mixture of depleting anti-CD4 and anti CD8 antibodies and a neutralizing anti-IFN γ Ab about half quickly developed rapidly progressive sarcomas.

Examination of the injection site in MCA-treated mice revealed a collection of atypical cells with immune cell infiltrate. These cells formed a palpable stable mass which showed decreased proliferation and increased apoptosis in comparison to out-growing sarcomas. Moreover, when cells from these stable masses were transplanted into immunodeficient RAG2^{-/-} mice they were able to form rapidly growing sarcomas. Taken as a whole these experiments suggest that in certain situations malignant cells can be maintained in an equilibrium phase by elements of the immune system. This ensures that proliferation does not exceed apoptosis resulting in a stable lesion. ⁹⁰

Escape

An extension of these experiments also provides evidence for the final phase of the immunoediting theory; escape. A small number of MCA-treated wild type mice developed progressively growing sarcomas at a very late stage. When these were transplanted into either RAG2^{-/-} or wild type mice they showed no immunogenicity, growing progressively with similar kinetics to sarcomas appearing early in MCA-treated wild type mice. In contrast sarcomas developing post-MCA treatment in RAG2^{-/-} mice or post-depleting Ab administration in wild type mice, although able to grow progressively in immunodeficient mice were rejected in 51% and 31% of wild type mice respectively, suggesting the tumour is highly immunogenic.⁹⁰

These results suggest the concept of editing i.e. the immunogenicity of the tumour is determined by the immune environment in which it develops. Thus tumours that develop in an immunodeficient environment are not subject to any immunological pressure. Consequently there is no selective elimination of immunogenic cells so that the tumour remains unedited and retains its immunogenicity. In contrast a tumour which arises in an immunocompetent host is subject to immunological pressure potentially allowing the elimination of immunogenic cells. The cells which remain are those which lack immunogenicity and are 'unseen' by the immune system. The tumour is therefore edited resulting in the perverse situation where the immune system which aimed to eliminate an emerging malignancy has actually selected a more aggressive phenotype, resistant to immune attack.

The molecular and cellular mechanisms believed to mediate this escape include those specific to the tumour which reduce its ability to be accessed or recognized by the immune system, and those pertaining to the immune system where an element of its function has been subverted. Table 1.3 lists some of these mechanisms.

Mechanism	Reference
Danner detica of MIC along Hands and a	91
Downregulation of MHC class II molecules	92
Downregulation of costimulatory molecules	-
Downregulation of MHC class I molecules	93
Downregulation of proteins involved in Ag processing	94
e.g. TAP, LMP	
Loss of expression of tumour-associated Ags	95
Insensitivity to IFNs	96
Inaccessibility of tumour Ags to cells of immune system	97
Ignorance of tumour Ags	98
Tolerance of tumour Ags secondary to anergy	99
T cell suppression secondary to tumour-derived factors	100
e.g. TGFβ	
Tumour secretion of soluble ligands to block	101
lymphocyte activation e.g. MICA	
Impaired maturation of APCs	102
Myeloid-derived suppressor cells	103
Regulatory T cells	104

Table 1.3: Mechanisms mediating immune escape

However the concept of cancer immunoediting is not universally accepted. In particular Blankenstein *et al* have developed a murine model of spontaneous tumour development which they argue disputes the theory. In their model the dormant oncogene SV40 T-Ag is separated from a ubiquitously active promoter (chimeric β -actin/ β -globin) by a stop codon (LoxP-Tag mice). Owing to rare stochastic events, this oncogene is expressed in individual cells which

once transformed can develop into tumours affecting a variety of different tissues (e.g. kidney, liver, spleen) which express the T Ag (Tag). 105

They have demonstrated that LoxP-Tag mice spontaneously develop tumours within 6-14 months which, despite expressing the Tag, are not eliminated by detectable anti-Tag Ab and CTL responses. Young LoxP-Tag mice immunized against Tag are protected from subsequent spontaneous development of these tumours indicating that they are not tolerant of Tag from birth and are capable of producing functional CTLs against the Ag. When transplanted into immunodeficient hosts, tumours arising in LoxP-Tag mice are able to grow progressively, whereas in wild-type or young LoxP-Tag mice they are rejected suggesting they retain their immunogenicity. The observation that these tumours are able to grow in LoxP-Tag x Alb-Cre mice (that constitutively express Tag under the control of the albumin promoter and are therefore tolerant of Tag) provides experimental evidence that Tag is the rejection Ag. ¹⁰⁵

Further work with this model has shown that once low levels of anti-Tag IgG are detectable (assumed to correspond with first expression of Tag), mice are tolerant of Tag (unable to eliminate splenocytes loaded with an appropriately restricted Tag-derived peptide). Clinically this stage corresponds to tiny lesions (~1 mm diameter) which are positive for both Tag and the proliferation marker Ki67. The authors have termed this early tumour stage 'premalignant' as there is often a 1-2 year delay before the appearance of macroscopic tumour. They argue that the demonstration of Tag tolerance at this stage provides evidence against the immune-system mediated equilibrium stage of the tumour immunosurveillance theory.

However, other studies have shown that mice with highly immunogenic Tag positive tumours become unable to mount CTL responses against other Ags. In contrast mice with a high load of a non-immunogenic tumour (Tag positive tumour in LoxP-Tag x Alb-Cre mice which are Tag tolerant) do not demonstrate this general CTL non-responsiveness. Although the mechanism for this difference between the two model systems is as yet unclear, one suggested factor is the TGF- β 1 level. This inhibitory cytokine is elevated in tumour-bearing LoxP-Tag mice (i.e. have immunogenic tumour) whilst remains at normal levels in LoxP-Tag x Alb-Cre mice (i.e. have non-immunogenic tumour).

Although Blankenstein *et al* suggest evidence generated from this model disproves elements of the immunosurveillance hypothesis, (equilibrium and editing), Schreiber *et al* suggest these results actually support their theory by providing evidence of a tumour extrinsic mechanism of tumour escape.³⁵ Recent work by Schreiber's group has suggested a role for CD8⁺ T cells in the immunoediting process; using MCA-induced sarcoma cell lines they demonstrated that

mice could mount a CTL response to peptides derived from mutant spectrin- β_2 . On occasion this led to outgrowth of cell lines which had down-regulated the mutant spectrin- β_2 and therefore escaped this mechanism of immune control.¹⁰⁷

1.2.2 Inflammation and cancer

While most investigators now accept that the immune system does play a role in the elimination of tumours, conversely there is also evidence that the immune system can promote tumour formation and growth. The link between inflammation and cancer was first suggested by Virchow in 1863 when he noticed that not only were neoplasms often found at sites of chronic inflammation but, when examined histologically, they contained leukocyte infiltrates. ¹⁰⁸

Further support comes from the association of a number of malignancies with infectious agents (for example bladder cancer with schistosomiasis and gastric carcinoma with H. pylori-induced gastritis) or areas of chronic inflammation (for example oesophageal carcinoma with Barrett's metaplasia and colorectal carcinoma with ulcerative colitis). In addition non-steroidal anti-inflammatory drugs are able to prevent some cancers¹⁰⁹ while the overexpression of inflammatory cytokines can promote tumour progression. Mechanisms via which inflammation can predispose to cancer development include the production of toxic reactive oxygen species which can cause DNA damage and genetic instability leading to cellular transformation, production of pro-angiogenic factors such as VEGF, and production of matrix metalloproteinases which can facilitate invasion. Using the K14-HPV16 mouse model Coussens *et al* have demonstrated a role for immune complexes and activatory FcγR receptors on myeloid cells squamous carcinogenesis.

In addition to this extrinsic pathway where chronic inflammation predisposes a previously 'normal' tissue to become malignant, there is also evidence that an intrinsic pathway exists whereby activation of an oncogene can enable a tumour to induce inflammation itself via the secretion of chemokines, cytokines and prostaglandins. Such a situation is seen in human papillary carcinoma of the thyroid where activation of the RET oncogene (a protein tyrosine kinase) results in production of a number of inflammatory mediators such as IL-1 β , cyclooxygenase 2, CCL2 and IL-8 which can recruit inflammatory cells and promote angiogenesis.¹¹⁵

1.2.2.1 The role of T_H cells in determining the immune response to a tumour

The observation that the immune system is apparently able to both promote and restrict a tumour's growth raises the question as to what determines this variable response. Figure 1.1 demonstrates the different components of the adaptive immune system which have a role in skewing the immune response and illustrates the centrality of $CD4^+$ T_H subsets in orchestrating this decision. Depending on the nature of the inflammatory milieu within which the T_H cell encounters Ag presented by a mature Ag presenting cell (APC) it can differentiate to possess various effector functions which either promote tumour elimination (a T_H1 phenotype) or tumour growth (T_H2 , T_H17 or T_{reg}).

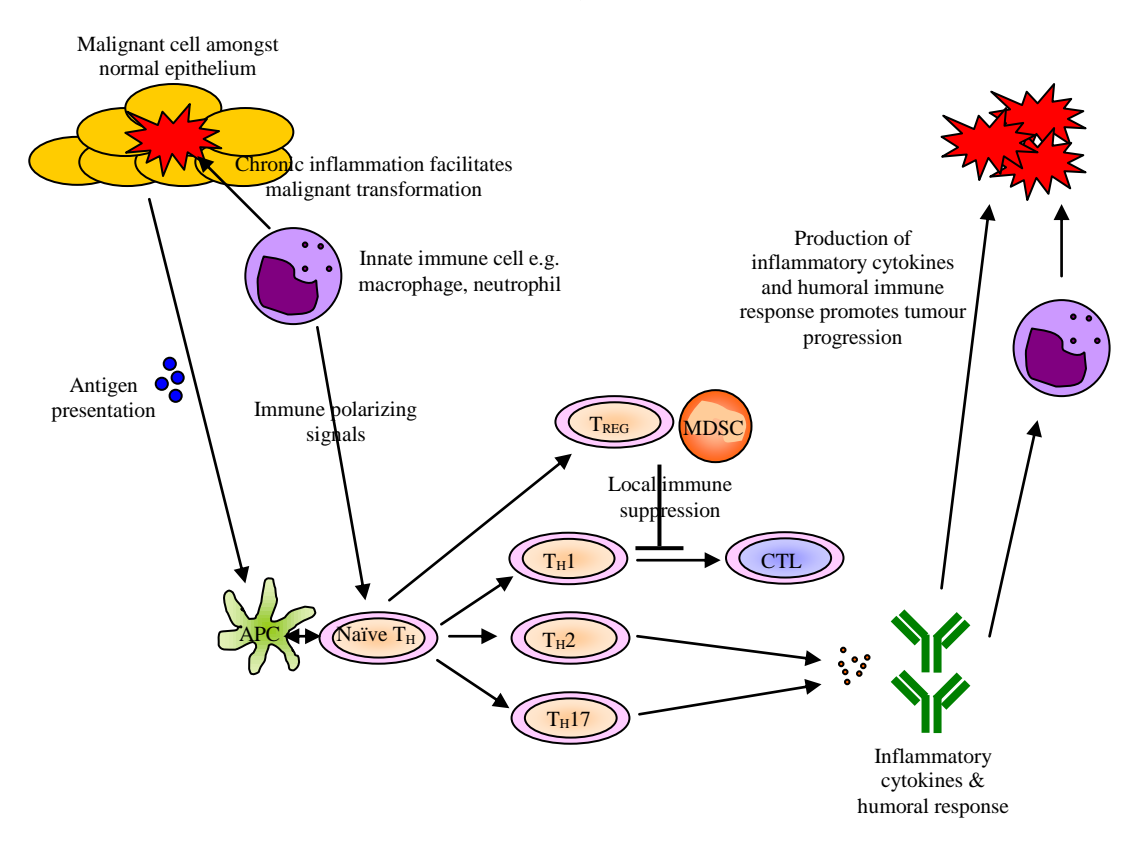


Figure 1.1 Polarization of the immune response during tumour development Chronic inflammation itself can encourage malignant transformation which then elicits an immune response. Depending on the polarizing signals received by naïve T_H cells this can either be a potentially useful CTL response (i.e. involves T_H1) or a less helpful inflammatory response involving the release of antibodies and inflammatory cytokines (involves T_H2 , T_H17 and T_{reg}). By induction of T_{reg} and MDSC a potentially useful CTL response can also be inhibited. Figure adapted from Johansson et al Immunol Rev. 2008; 222:145. 116

T_H activation requires both engagement of the T cell receptor (TCR) with peptide-MHC class II (pMHCII) on the APC and co-stimulatory molecule interactions (e.g. CD40:CD40L and CD28:CD80/CD86).¹¹⁷ However, in order for the APC to orchestrate an immune response it has to be activated itself by 'danger' signals usually detected through pattern recognition receptors (PRRs). The best studied group of PRRs are the Toll-like receptors (TLRs).¹¹⁸ TLRs engage a wide variety of ligands including microbial components and, perhaps more relevant

to cancer, components of host cells such as heat shock proteins, fibrinogen and hyaluronic acid fragments. Once TLRs are engaged by a ligand they dimerise, undergo a conformational change and recruit one of four adapter molecules (e.g. MyD88) to initiate downstream activation events. 119

Different immune responses to a tumour can, in part, be explained by the skewing of the induced T_H response. One determinant of this skewing is the identity of the TLRs engaged and their downstream adapter proteins. TLR3, TLR4, TLR7 and TLR9 engagement produces a T_H1 response mediated via either a MyD88 dependent¹²⁰ or independent¹²¹ pathway. This leads to both IFN secretion and the production of specific CTLs. In contrast engagement of other TLRs can elicit a pro-inflammatory, pro-tumour T_H2 response usually mediated via a MyD88 dependent pathway.¹²² Cytokines implicated in this pathway include IL-6.¹²³ The skewing of CD4⁺ T cells to a T_H2 phenotype also promotes development of tumour specific B cells and subsequent Ab production, in part through the production of the cytokines IL-4, IL-5 and IL-13. ¹²⁴ Despite the success of some monoclonal antibodies in clinical practice, the endogenous production of antibodies specific for tumour-associated Ags such as HER2/neu and p53 does not appear to provide any protection but instead correlates with a poor prognosis.¹²⁵

Inflammatory cytokines within the tumour microenvironment also participate in the skewing of the T_H response: IL-6 and TGF- β can stimulate the development of T_H17 cells¹²⁶ that produce IL-23 and IL-17 and are associated with tumorigenesis.¹²⁷ Adaptive T_{reg} are formed in peripheral tissues in response to IL-2 and TGF- β ¹²⁸ and are able to suppress CTL responses via the release of soluble mediators such as IL-10 and TGF- β .¹²⁹

1.2.2.2 The role of macrophages in determining the immune response to a tumour

In addition to T_H cell polarization, more recently tumour-associated macrophage (TAM) polarization has been reported. This has been described as a continuum of phenotypes: At one extreme is the M1 anti-tumour macrophage which develops in response to IFN γ , produces IL-12 and TNF α , and retains effector functions such as tumour cytotoxicity. At the other extreme is the M2 pro-tumour macrophage which develops in response to IL-4 and IL-10, secretes IL-10 and TGF- β and is involved in matrix remodelling and tumour promotion. There has been some suggestion that progression from a useful M1 phenotype to an inhibitory M2 phenotype correlates with movement through immunoediting from elimination to escape and may be mediated by changes in NF- κ B expression, a transcription factor that regulates various components of the immune response.

1.2.2.3 Myeloid-derived suppressor cells

One further type of immune cell that has been shown to have a role in the inhibition of antitumour responses is the myeloid-derived suppressor cell (MDSC). 132 MDSCs are immature myeloid cells which are precursors of dendritic cells, macrophages or granulocytes, and have been noted to accumulate in both humans 133 and mice 134 with cancer. They accumulate and become activated in response to a number of soluble factors associated with inflammation including IL-1 β , IL- 6135 and prostaglandin E2 (PGE₂) 136 and use a variety of different mechanisms to suppress immune responses including arginase production, 137 nitration of the TCR, 138 induction of T_{regs} and changes in the local cytokine milieu. 140

In summary, the relationship between cancer and the immune system is an extremely complex one: The context in which different components of the immune system encounter a developing tumour determines whether it is able to exert a level of control or contribute to its progression. The obvious interaction between cancer cells and parts of the immune system have led to a raft of different strategies to try and influence the outcome of this interaction, either by promoting a tumoricidal or blocking a tumour-promoting response. Although a full review of these different approaches is outside the scope of this introduction, different strategies used to develop or promote an anti-tumour CTL response are considered below.

1.3 T Cell Biology

A key cell implicated in the endogenous immune response to tumours is the T cell. T cells are a component of the adaptive immune system, meaning each is able to recognise a specific Ag. They are usually identified by the presence of a membrane Ag receptor (T cell receptor: TCR) in association with CD3,¹⁴¹ a membrane spanning polypeptide which has a role in signal transduction following engagement of the TCR. They are further subdivided by function and phenotype into CD8⁺ cytotoxic, CD4⁺ helper, CD4⁺CD25⁺FOXP3⁺ regulatory and more recently T_H17 and T_H22 T cell subsets. The following sections briefly describe the TCR structure and mechanism of Ag recognition, Ag processing, T cell development and education, activation and function, particularly focusing on the role of cytotoxic T lymphocytes (CTLs).

1.3.1 T cell receptor structure

The TCR is a membrane bound heterodimer; either $\alpha\beta$ or $\gamma\delta$ which confers on a T cell the ability to recognise Ag. Each chain has two extracellular domains (one variable, one constant showing structural homology to the immunoglobulin domains) a transmembrane element and a cytoplasmic tail (see Figure 1.2). The majority of T cells have $\alpha\beta$ rather than $\gamma\delta$ TCRs; the latter thought to recognise Ag in a different manner and being more poorly understood. Generally, each T cell expresses only one phenotype (idiotype) of TCR, but the sequence and hence antigenic specificity of TCRs amongst different T cells varies considerably.

TCR variability is partially a product of the recombination of a number of gene segments to form the functional gene: α and γ chains are formed by joining V (variability) and J (joining) segments to a constant region ^{142,143} whereas β and δ chains require the rearrangement of V, D (diversity) and J segments before joining to a constant region. ^{144,145} Humans carry between one (constant regions of α and δ chains) ^{146,147} and 67 (V region of β chain) ¹⁴⁸ different copies of each of these gene segments (some of which are non-functional or pseudogenes) providing multiple potential combinations for each mature chain. Recombination is catalysed by recombination activating genes (RAG-1 & RAG-2), deficiency of which results in no mature T (or B cell) due to lack of functional Ag receptors. ¹⁴⁹

Further variability is added via the mechanism through which RAG-1 and RAG-2 function: They recognise conserved heptamer and nonamer recombination signal sequences (RSS) flanking the gene segment and after bringing two gene segments into close proximity produce a single strand DNA break allowing hairpin formation. Random cleavage of the hairpin structure allows addition of a few nucleotides in a palindromic sequence (p-nucleotides).¹⁵⁰

Further nucleotides can be added to the free ends of the DNA strands via the action of terminal deoxynucleotidyl transferase (TdT) resulting in n-(non-templated) nucleotides. ¹⁵¹ This addition of nucleotides is followed by pairing of the DNA strands, exonuclease trimming of non-complementary bases, DNA synthesis and finally ligation of the DNA breaks to form continuous gene segments. Unlike the B cell receptor (BCR), TCR genes do not undergo somatic mutation.

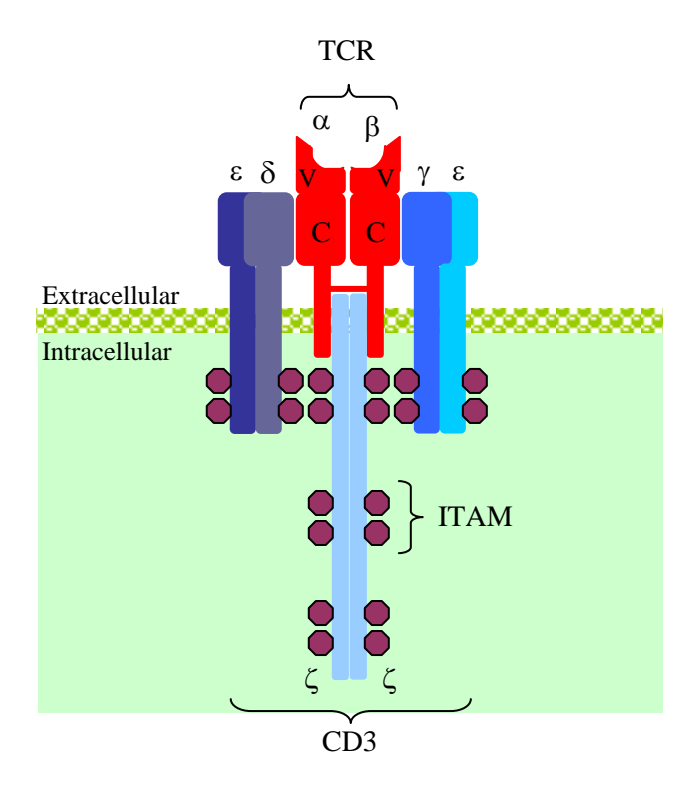


Figure 1.2: The structure of the TCR/CD3 complex

The α and β chains (each composed of a variable; ν and constant; ν domain) form the TCR. CD3 is formed of three dimers; $\delta \varepsilon$, $\gamma \varepsilon$ and $\zeta \zeta$. Each of these chains is associated with ITAMs which play an important role in signal transduction. Figure adapted from Immunity: The Immune Response in Infectious and Inflammatory Disease, De Franco et al. Published Oxford University Press.

Although the ability to add extra nucleotides contributes to the diversity of the TCR, it also reduces the probability of a successful recombination event due to an abortive frame shift, or via the introduction of amino acids into the expressed protein which prevent successful synthesis, folding or trafficking to the cell membrane. The probability of a successful rearrangement is however enhanced by the presence of two copies of each of the gene clusters in each cell (one on each of the chromosomes) and by the distribution of the DJC β gene segments into two distinct clusters on chromosome 7, allowing two separate attempts at rearrangement. Rearrangement of the TCR gene segments occurs at particular stages of T cell development and in a specific temporal order; this is considered further in section 1.3.3 and Figure 1.6.

Although the TCR heterodimer is able to recognise and bind appropriately presented Ag, it does not contain the necessary intracellular signalling machinery to transmit this signal downstream. Instead, this is done by CD3 which forms part of the TCR complex. In $\alpha\beta$ T cells CD3 is composed of 6 chains; $\gamma\epsilon$ heterodimer, $\delta\epsilon$ heterodimer and a $\zeta\zeta$ homodimer, whereas in $\gamma\delta$ T cells, at least in mice, there is evidence that most CD3 complexes contain two $\gamma\epsilon$ heterodimers and no δ delta chain. The δ , γ and ϵ chains resemble Ig α and Ig β with extracellular immunoglobulin domains and an intracellular immunoreceptor tyrosine-based activation motif (ITAM), while the ζ chains have a very short extracellular domain and three intracellular ITAMs. Engagement of the TCR by Ag results in tyrosine residue phosphorylation within the ITAMs, initiating an intracellular signalling cascade which is described in more detail in section 1.3.4.4.

1.3.2 MHC restriction of TCR antigen recognition

Unlike B cells, T cells do not recognise entire protein Ags in their native conformation. Instead, TCRs usually recognise Ag which has been processed to a small peptide and is presented by major histocompatibility complex molecules (MHC) so called because of their initial discovery as molecules involved in the acceptance or rejection of allogeneic tissue transplants. The classic experiments of Zinkernagel and Doherty demonstrated that CTL recognition of Ag showed MHC restriction; CTLs from LCMV infected mice could only lyse LCMV infected target cells *in vitro* if they had an identical H-2 haplotype. ¹⁵⁴

The MHC genes found on chromosome 6 in humans are divided into three groups; the classical MHC class I and class II genes which encode transmembrane glycoproteins on the cell surface that present Ag to T cells, and the more variable class III group which encode a number of secreted proteins used within the immune system such as TNF- α and complement proteins. The class I and II gene loci are highly polymorphic with several hundred allelic variants identified. However, proximity to one another means they are generally inherited in haplotypes with meiotic crossover events only having a frequency of 0.5%. Class I molecules consist of a variable 45 kDa α chain which complexes with the invariant 12 kDa β_2 microglobulin chain (encoded on chromosome 15) whilst class II molecules consist of a variable 33 kDa α chain complexed with a variable 28 kDa β chain. The alleles are codominantly expressed with an individual expressing up to 6 different class I alleles (two each at loci A, B & C) and 12 class II alleles (two different α chains can complex with two different β chains giving a possibility of four different alleles at loci DR, DP, DQ).

Figure 1.3 illustrates the structure of MHC class I and II molecules. Sequence variability is concentrated in the α_1 and α_2 chains in the class I molecule and in the α_1 and β_1 chains of the class II molecules corresponding to the location of the peptide binding groove. The remainder of the molecule is more conserved as this interacts with the conserved regions of both the TCR and its co-receptors CD4 and CD8. The peptide binding groove of both molecules consists of a floor of 8 β -pleated sheets and walls of α -helices. The class I peptide binding groove is closed at both ends, accommodating 8-10 amino acid peptides which are anchored at both ends but arch away from the cleft in the centre. In contrast the class II binding groove is open at both ends, accommodating peptides of 13-18 amino acids and having anchor residues distributed along the length of the cleft meaning the peptide is held at a constant level above the groove. The nature of the interaction between the amino acids of the peptide and the binding cleft mean binding is promiscuous; many different peptides can be accommodated in one groove.

For $\alpha\beta$ TCRs the distribution of polymorphic residues within the TCR correlates with the nature of the interaction between it and peptide-MHC (pMHC): Within all TCRs polymorphism is concentrated in 3 complementarity determining regions (CDR1-3), with CDR3 being the most variable. X-ray crystallographic data has shown that residues from CDR3 interact with the centre of the MHC-bound peptide, CDR1 residues contact the ends of the peptide whilst CDR2 residues interact with MHC residues which form the α -helical walls of the peptide cleft. This arrangement ensures the most polymorphic areas of both the TCR and MHC molecules are in contact with one another, maximising the chance of Ag recognition.

In addition to presenting peptides of contrasting lengths, MHC class I and II molecules have varying cellular expression, derive their antigenic peptides from alternative sources and interact with the TCRs on different subsets of T cells by virtue of their co-receptors. Class I molecules are found on virtually all nucleated cells, albeit at different levels, usually (but not always) present endogenous Ag and interact with the TCR on CD8⁺ CTLs. In contrast the expression of class II molecules is restricted to Ag presenting cells (APCs; dendritic cells, macrophages and B cells), where they present exogenously derived Ag and interact with CD4⁺ T cells.

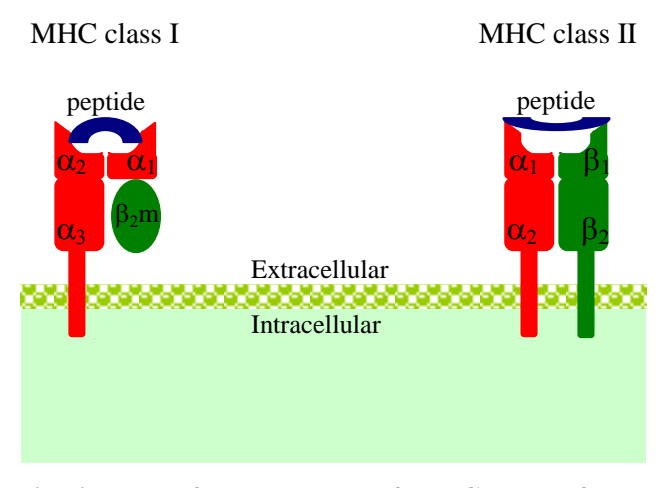


Figure 1.3: Schematic diagram of the structure of MHC class I & II

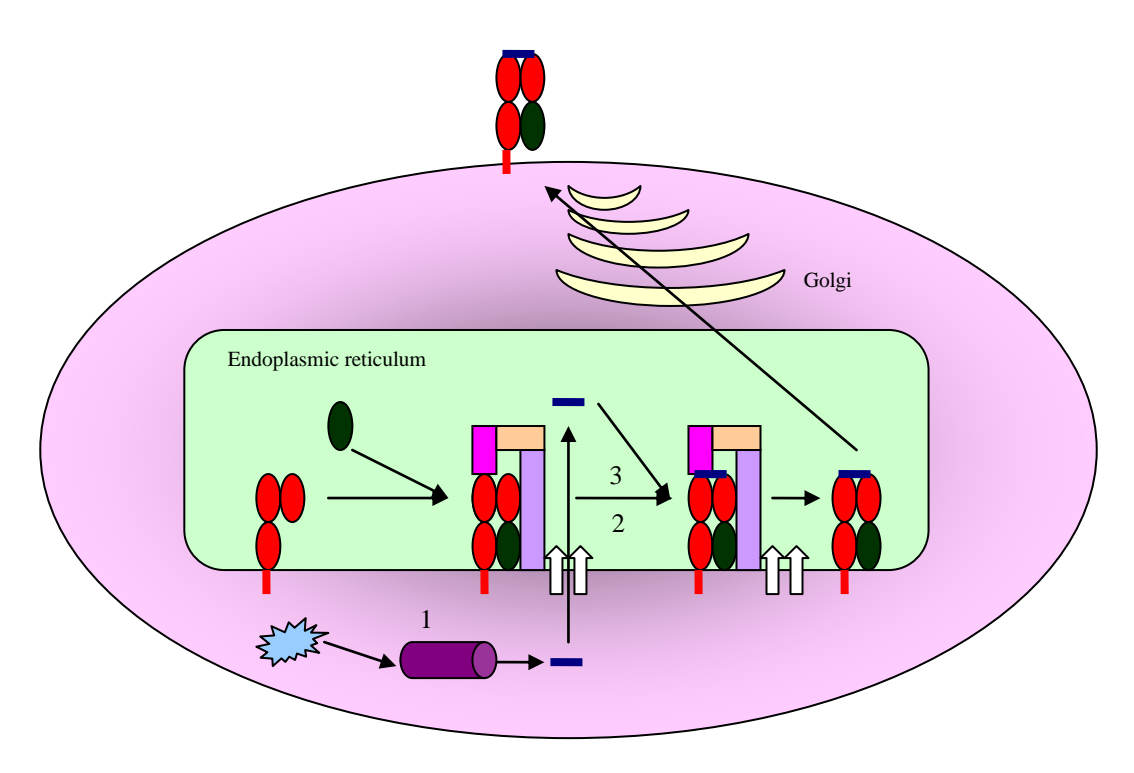
1.3.2.1 Antigen presentation by MHC class I

In order to present Ags derived from different sources (exogenous or endogenous proteins) two distinct pathways of Ag processing and presentation have arisen. Figure 1.4 is a schematic representation of the class I pathway. After synthesis of the heavy chain in the endoplasmic reticulum (ER) it is initially stabilised with the chaperone protein calnexin which helps mediate its assembly with β_2 microglobulin. In the absence of a suitable peptide the heavy chain- β_2 microglobulin complex is unstable meaning after release from calnexin it associates with the peptide-loading complex; a multi-protein complex which includes the soluble chaperone calreticulin, ERp57, tapasin and the transporter associated with Ag processing (TAP).

Meanwhile endogenously derived proteins (usually either viral proteins or tumour Ags) are processed in the cytoplasm into short peptides (2-25 amino acids)¹⁵⁶ via the action of the proteasome complex and other cytoplasmic peptidases. A few of these peptides avoid cytoplasmic degradation and are actively transported into the ER lumen via the action of TAP, an ATP-binding cassette (ABC) transporter. It is thought the proteasome generates the final carboxy-terminal residues of successfully bound peptides, whilst the amino terminal is subject to further trimming. Although the cytoplasmic peptidase Tripeptidyl-peptidase II (TPPII) is able to trim amino residues from peptides more than 15 residues in length, ¹⁵⁷ it is the endoplasmic reticulum amino-peptidase (ERAAP) which is responsible for final amino-residue trimming to render peptides suitable for presentation. ¹⁵⁸

Once in the ER lumen, the peptide-loading complex mediates the association of peptides with the heavy chain- β_2 microglobulin complex to form a complete stable MHC class I molecule which can be transported via the Golgi apparatus to the cell membrane. The peptide loading

process is not fully understood but is thought to involve peptide exchange and editing in order to ensure only the most stable complexes are presented at the cell surface.



- 1. Cytoplasmic proteasome and peptidase generation of peptides from endogenous proteins.
- 2. Peptide loading and exchange via peptide-loading complex.
- 3. Peptide trimming by ERAAP.

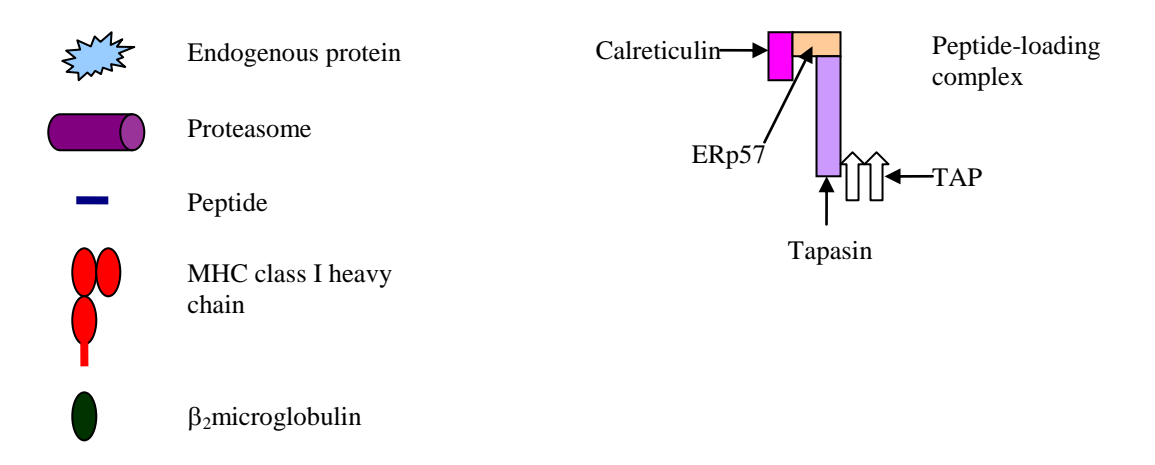


Figure 1.4: Schematic representation of MHC class I antigen processing

Studies have shown that tapasin is critical for the selection of stable pMHC complexes.¹⁵⁹ The role of ERp57 is less clear, but it is thought to be necessary for the proper function of tapasin under physiological conditions, perhaps through maintaining its correct conformation.¹⁶⁰ A further molecule associated with the peptide-binding complex is protein disulfide isomerase

(PDI). It has been suggested to be critical in regulating the redox state of a disulfide bond in the α_2 domain which is located in the peptide-binding groove, and thus has implications for peptide binding.¹⁶¹

1.3.2.2 Antigen presentation by MHC class II

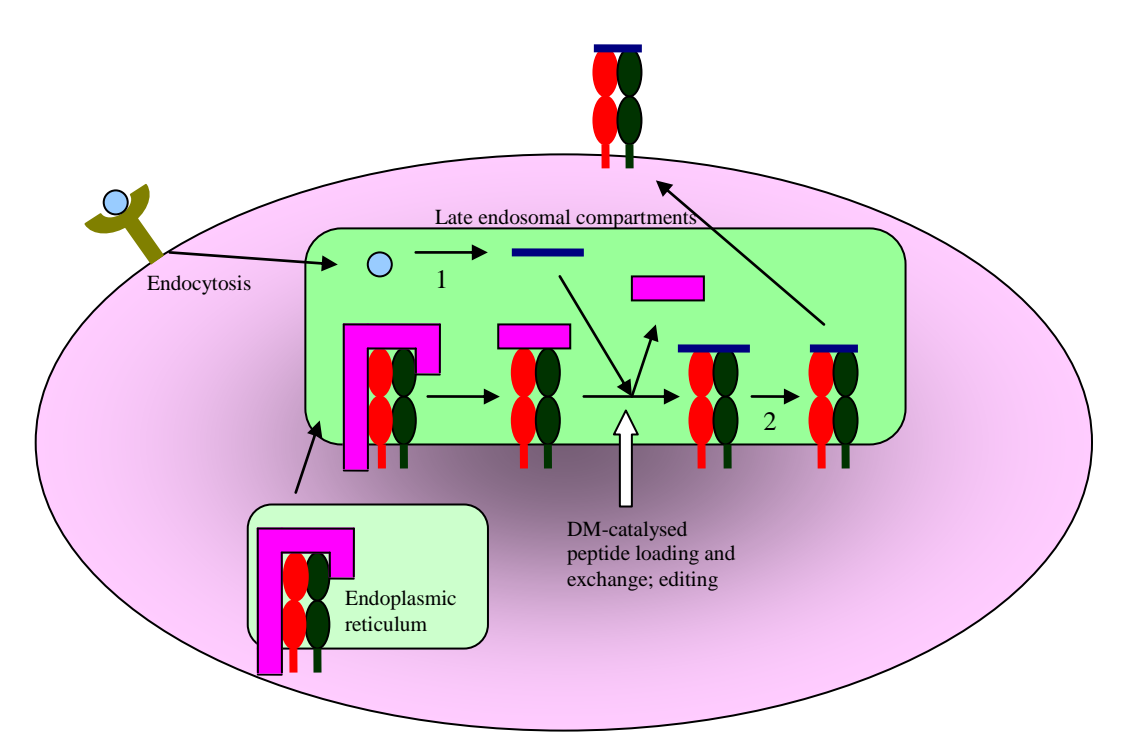
The exogenous Ag processing and presentation pathway is illustrated in Figure 1.5. MHC class II molecules are also initially synthesised in the endoplasmic reticulum and due to their instability without a bound peptide immediately complex with the invariant chain (Ii). This is a specialised type II membrane protein which has a segment able to fit into the class II binding groove (behaving as a surrogate peptide and stabilising the molecule) and also contains a cytoplasmic endosomal sorting and retention signal. ¹⁶²

Once in the late endosomal compartments the invariant chain is progressively cleaved by proteases (including cathepsin S) from the carboxy terminus to leave only a short peptide bound to the peptide binding groove. This MHC class II-associated invariant chain peptide (CLIP) is protected form further protease degradation due its position within the peptide-binding groove. CLIP must be replaced with an antigenic peptide before translocation of the class II molecule to the cell membrane. This process is catalysed by the catalyst-chaperone protein HLA-DM, a non-classical non-polymorphic class II heterodimer of α and β chains found predominantly in the endosomal compartment. The mechanism of action of HLA-DM is not yet fully elucidated but it is thought to interfere with some of the conserved hydrogen bonds between the peptide and MHC molecule, allowing dissociation and skewing the repertoire of successfully presented peptides towards those with greater kinetic stability. 163

The role of HLA-DM appears to be modified by another non-classical non-polymorphic class II molecule HLA-DO. The function of this molecule remains unclear, but is thought to modify peptide exchange mediated via HLA-DM. HLA-DO complexes with HLA-DM and was initially found to inhibit its function. ¹⁶⁴ Later work suggested that its inhibitory abilities were reduced in the increasingly acidic lysosomal compartments of B cells which would therefore promote presentation of peptides derived from proteins ingested via the BCR. ¹⁶⁵ However, the recent discovery of HLA-DO expression in subsets of DCs ¹⁶⁶ suggests its role is rather more widespread in modulating the loading of antigenic peptides.

Peptides for loading on class II are generated via the action of the lysosomal thiol reductase GILT (Gamma-interferon-inducible lysosomal thiolreductase) and endosomal proteases found within the late endosomal compartments. Proteins obtained via a number of endocytic

processes including pinocytosis, scavenger receptors, mannose receptors and autophagy (provides a mechanism of targeting peptides derived from endogenous proteins to class II¹⁶⁷) are targeted to the late endosomal compartments where they are unfolded and cleaved. The exact degree of unfolding and cleavage necessary for initial binding to class II remains undecided.



 $1. \ Unfolding \ and \ digestion \ of \ exogenous \ proteins \ catalysed \ by \ lysosomal \ proteases \ and \ disulfide \ reductase \ GILT$

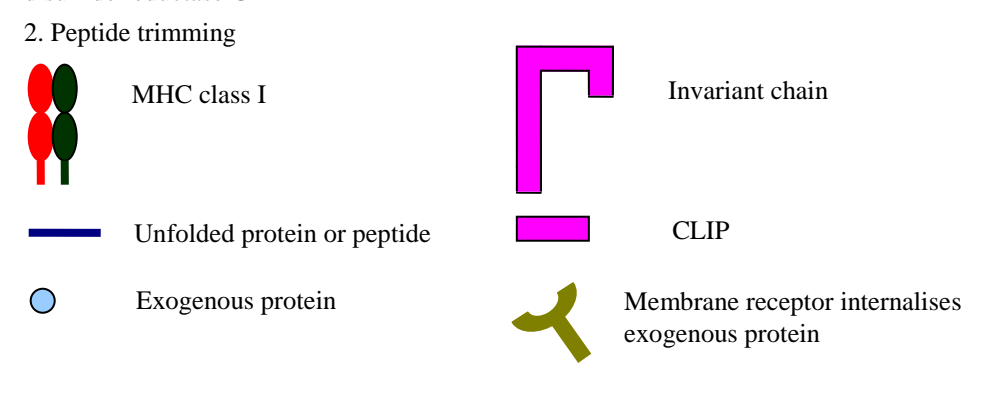


Figure 1.5: Schematic representation of MHC class II antigen processing

Classically it was thought that peptides are substantially trimmed to between 12 & 26 amino acids in length before binding to the peptide groove after which there may be a small degree of further refinement. However, further studies revealed that a significant proportion of the elutable peptide fraction is much longer suggesting that it is possible for partially unfolded and cleaved peptides to bind to class II before more extensive trimming takes place.

Furthermore studies suggest that Ags do not have to be completely denatured to bind and a degree of secondary structure can be accommodated when binding to MHC class II. 170

1.3.2.3 Cross-presentation

Although class I and class II were initially described as presenting endogenously and exogenously derived peptides respectively, the ability of class II to present endogenously derived Ags via autophagy shows this division is not absolute. Cross-presentation of exogenously derived peptides on class I molecules has been extensively studied and was conclusively demonstrated when splenocytes from $H2^b$ and $H2^d$ mice were injected into F_1 $H2^bH2^d$ mice of a different genetic background: A proportion of the CD8⁺ T cells were restricted to an H2 allele from the F_1 cells (not present on the donor cells) presenting a peptide derived from a minor histocompatibility Ag on the donor cells.¹⁷¹

Macrophages and DCs are both able to present exogenously derived Ags on class I and in mice, at least, the CD8⁺ DCs appear specialised for this task. There are several mechanisms through which cross-presentation is thought to happen. In a TAP-dependent mechanism, Ag can be transferred from phagosomes into the cytoplasm from where it can enter the normal MHC class I processing pathway. Alternatively in a TAP-independent process peptides can be generated directly in the ER-phagosome through protease (including cathepsin S) digestion, ¹⁷² before being loaded directly onto newly synthesised MHC class I. It is thought that mechanism of ingestion by the cell determines the likelihood of an Ag being cross-presented: Ag internalised via the mannose receptor is targeted to early endosomes and thus can be cross-presented whereas Ag ingested via the scavenger receptor or pinocytosis is targeted to lysosomes from where it enters the class II processing pathway. ¹⁷³

The particular cells involved with Ag presentation to cytotoxic T cells and the cellular signals involved in subsequent T cell activation are discussed in section 1.3.4.

1.3.3 T cell development

A schematic outline of T cell development in a mouse is given in Figure 1.6. Pluripotent lymphoid progenitor cells, produced initially in the foetal liver and then the bone marrow, enter the thymus where they can undergo differentiation into T cells. The process has a very high rate of attrition with less than 5% of progenitor cells entering the thymus emerging as functional T cells. Thymic stroma has a critical role in the differentiation process demonstrated by the results of reciprocal thymus and bone marrow grafts between *scid*

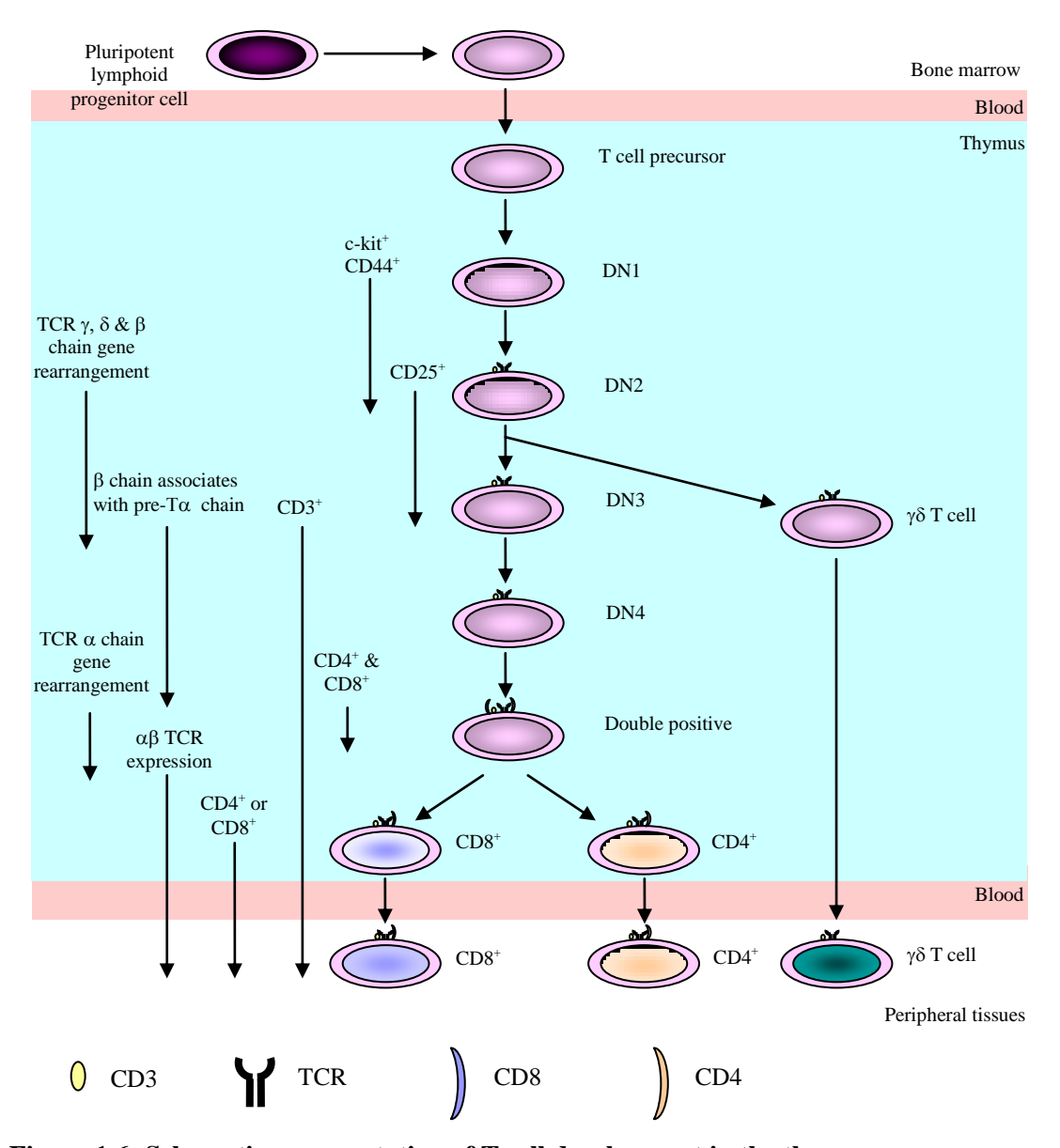


Figure 1.6: Schematic representation of T cell development in the thymus

(defective in TCR gene-rearrangement) and *nude* (lack differentiated thymic epithelia) mice, neither of which have mature T cells. *nude* bone marrow precursors can develop into normal T cells in *scid* mice, and transplanting a *scid* thymus into *nude* mice allows endogenous *nude* T cell precursors to develop normally. In contrast *scid* bone marrow precursors cannot develop into mature T cells in any thymus.¹⁷⁵

1.3.3.1 Gene rearrangement: αβ versus γδ lineage commitment

The different stages of T cell differentiation can be identified by the expression of various cell surface proteins, by gene rearrangement and finally by the expression of the TCR. Early T cell precursors do not express either of the co-receptors CD4 or CD8 so are known as double negative (DN). They initially traffic to the subcapsular zone of the thymus where they

undergo early differentiation. The DN stage is further subdivided into stages 1-4 based on the expression of CD44 (adhesion molecule), CD25 (α chain of the IL-2 receptor) and c-kit (receptor for stem cell factor). Although at the early stages of DN1 there is some evidence that the progenitor cells retain some plasticity and can differentiate into NK and myeloid cells, ¹⁷⁶ from DN2 when somatic rearrangement of the β , γ and δ chains starts they are committed to a T cell lineage.

Proteins of the notch family of signalling proteins are critical in the decision to commit to a T cell lineage; Notch1-deficient bone marrow precursors differentiate into B cells even in the thymus, ¹⁷⁷ whereas if engineered to express a constitutively active Notch1 signalling domain, bone marrow precursors differentiate into early T cells even in the bone marrow. ¹⁷⁸ Gene rearrangement continues into DN3 until a $\gamma\delta$ TCR or pre-TCR is expressed in association with CD3 on the cell membrane, or if no successful gene rearrangement occurs, the cell dies by apoptosis. In the case of $\alpha\beta$ T cells this is known as β -selection. ¹⁷⁹

It was thought that at the DN2/DN3 stage $\alpha\beta$ or $\gamma\delta$ lineage commitment occurs essentially based on which chains successfully rearranged first; if a functional γ and δ chain were produced the cell expressed this at its surface and became committed to the $\gamma\delta$ lineage whereas if, as is more common, a β chain was successfully rearranged this combined with the invariant surrogate α chain to form a pre-T-cell receptor and committed the cell to the $\alpha\beta$ lineage. However, analysis of gene rearrangements in functional T cells demonstrates that a number of mature T cells have potentially functional rearrangements of all three loci, although in frame rearrangements of the β chain in $\gamma\delta$ T cells are much more common than in frame rearrangements of the γ^{181} or δ^{182} chain in $\alpha\beta$ T cells.

This has led to the idea that lineage commitment is a function of the TCR, in particular the strength of the signal delivered, rather than a predetermined fate which TCR expression merely confirms. Single cell studies with bipotent TCR $\gamma\delta^+$ DN3 cells have shown that a strong TCR signal produces $\gamma\delta$ -expressing progeny whereas a weak TCR signal produces $\alpha\beta$ -expressing progeny. Notch appears to have a role to play in T cell differentiation and lineage commitment, although conflicting data has arisen from mice and men: In murine T cell cultures $\alpha\beta$ rather than $\gamma\delta$ T cell development is more dependent on notch signalling, whereas in humans high intensity notch signalling promotes $\gamma\delta$ rather than $\alpha\beta$ T cell differentiation. 185

Once a cell expresses the pre-TCR, RAG-2 undergoes degradation, preventing further β chain gene rearrangement (allelic exclusion at the β locus)¹⁸⁶. The cell then proliferates extensively to produce a clone of cells with a particular β chain gene rearrangement, and expresses the CD4 and CD8 co-receptor molecules (double positive: DP). Evidence suggests that signalling via the pre-TCR is ligand independent (signalling continues in the absence of MHC class I and II) and instead involves a multimerisation process, although the exact structural details of this have yet to be determined. ¹⁸⁷ Once the proliferative phase has terminated, RAG-1 & 2 are upregulated and α chain gene rearrangement occurs in these DP cells, which if successful allows the expression of a mature $\alpha\beta$ TCR. At the DP stage, developing T cells migrate further into the thymic cortex, mediated by the differential expression of chemokine receptors on the developing thymocytes and chemokine ligands on the thymic stromal cells. ¹⁸⁹

1.3.3.2 Positive and negative selection of $\alpha\beta$ T cells

The developing T cell then undergoes the process of positive selection, first demonstrated by the classic bone marrow chimera experiments of Bevan $et~al.^{190}$ If the expressed TCR is able to bind to a self-pMHC located on the surface of cortical thymic epithelial cells (cTECs) with sufficient avidity, the cell receives a survival signal. Owing to the generally low avidity of the interaction between pMHC and the TCR, binding is critically dependent on the CD4/CD8 coreceptor which stabilises the strength of the interaction. If the first expressed TCR fails positive selection, the existence of multiple V_{α} and J_{α} gene segments allows each cell to have many attempts at rearranging the α chain gene segments to produce a functional $\alpha\beta$ TCR. If however, after 3-4 days no $\alpha\beta$ TCR able to bind to self pMHC with sufficient avidity has been produced, in the absence of a survival signal the developing T cell undergoes apoptosis; so-called 'death-by-neglect'. Multiple attempts at α chain gene segment rearrangement coupled with the immediately preceding proliferation maximises the chance of the production of a useful $\alpha\beta$ TCR for any given β chain gene rearrangement.

Owing to α chain gene rearrangement occurring independently on both chromosomes, it is possible for two different TCRs to be expressed in a single cell, a phenomenon observed in both normal human donors¹⁹¹ and murine transgenic studies.¹⁹² This raises the possibility that a TCR is selected via only one of its TCRs allowing a potentially autoreactive receptor to persist, resulting in autoimmune disease.¹⁹³ However, the requirement for self-MHC restriction and peripheral mechanisms of tolerance are likely to counteract some of this risk.

The process of positive selection ensures that there is almost perfect correlation between coreceptor expression and class of MHC restriction, achieved by the CD8 and CD4 co-receptor

molecules binding to invariant residues on MHC class I and II respectively. How the differential binding of co-receptor to MHC class translates into lineage commitment has been hotly debated and theories of stochastic selection, strength-of-signal and duration-of-signal instructional models have all been proposed and then negated experimentally. ¹⁹⁴ An alternative theory is the kinetic signalling model which proposes that duration of TCR signalling, as detected by IL-7, determines lineage: ¹⁹⁵ Briefly it proposes that after TCR engagement, all thymocytes down regulate CD8 expression. Signalling via a class II restricted TCR will be unaffected by CD8 down regulation, and the persisting signal prevents IL-7 mediated signalling, ¹⁹⁶ allowing the cell to differentiate into a mature CD4⁺ T cell. In contrast signalling via a class I restricted TCR will be terminated via CD8 down regulation allowing IL-7-mediated signalling to prevail causing co-receptor reversal and maturation into a mature CD8⁺ T cell. ¹⁹⁷ Unlike other proposed mechanisms of CD4/CD8 lineage commitment, this theory suggests positive selection precedes lineage commitment rather than occurring simultaneously.

Once a T cell has undergone positive selection and become co-receptor single positive (SP) it migrates to the cortical medulla where it undergoes the process of negative selection. Although T cells destined for release into the peripheral tissues need to be able to see Ag in the context of self MHC, if the interaction with self pMHC is too strong there is the risk of uncontrolled autoimmunity with potentially fatal results. Negative selection provides a mechanism for deleting strongly self-reactive T cells from the repertoire creating self tolerance to avoid this situation. SP T cells interact with pMHC on the surface of medullary cortical epithelial cells (mTECs) and medullary DCs. It is thought that if the T cell is able to bind with high affinity, as determined by the intensity of TCR signal strength, it receives an apoptotic signal and dies. Evidential support for this idea comes from increased negative selection in mice deficient in Cbl family proteins which negatively regulate TCR signalling. ¹⁹⁸

Therefore, both positive and negative selection are determined by the strength of the interaction between the TCR and self-pMHC, resulting in the death of cells either unrestricted to self-MHC or strongly reactive against self-pMHC. The exact mechanism which allows two distinct signals to be delivered via one interaction remains uncertain. A recent model proposed suggests discrimination of high and low affinity TCR-ligand interactions is achieved via the duration of the interaction which results in differential leucine zippering between the TCR and co-receptor. ¹⁹⁹ A high affinity interaction results in a dwell time of greater than 4 seconds allowing stable zippering between the TCR and co-receptor. This causes the signal-initiating tyrosine kinase Lck to stably associate with CD3, resulting in full ITAM phosphorylation and subsequent negative selection. ²⁰⁰ In contrast lower affinity interactions

result in a sub-4 second dwell time and therefore only partial TCR:co-receptor zippering. This results in transient Lck association with CD3 and only partial ITAM phosphorylation resulting in positive selection.

The selection of self peptides presented by cTECs, mTECs and medullary DCs is critical in shaping the repertoire of T cells which finally emerges from positive and negative selection. Until recently it was thought that the self peptides presented during both positive and negative selection were all generated via conventional Ag processing pathways as described in sections 1.3.3 and 1.3.4. However, the recent discovery of a novel proteasome β-type subunit exclusively expressed in cTECs²⁰¹ suggests that these cells are able to generate a unique repertoire of self peptides presented by MHC class I for the process of positive selection. The 'thymoproteasome' is thought to be able to generate a repertoire of self-peptides enabling a low affinity TCR:pMHC interaction. An analogous mechanism has been suggested for class II peptide generation involving the lysosomal cysteine protease cathepsin L; few CD4⁺ T cells emerge from positive selection in cathepsin L knock out mice suggesting a non-redundant function in generating the repertoire of class II restricted self peptides necessary for positive selection.

Unlike cTECs, mTECs and medullary DCs do use classical Ag presentation pathways to generate peptides for negative selection. During negative selection developing thymocytes need to be exposed to as many self-peptides as possible in order to reduce the possibility of autoreactive T cells. mTECs and medullary DCs will automatically present peptides derived from ubiquitously expressed Ags naturally found in the thymus, but there needs to be some mechanism by which T cells specific for tissue-specific Ags are deleted or inactivated. Although part of this tolerance process is achieved in the peripheral tissues (either through presentation of Ag in the absence of appropriate costimulatory signals or through the action of T_{regs}), promiscuous expression of tissue-specific self Ags, at least partly under the transcriptional control of the autoimmune regulator (AIRE) protein, provides a central mechanism for deleting autoreactive T cells. Mutations abrogating AIRE function result in significant tissue-specific autoimmunity in both humans 204 and mice. 205

The development of $\gamma\delta$ T cells does not follow the same pathway as that described for $\alpha\beta$ T cells; they do not appear to go through either a DP stage²⁰⁶ or an MHC-mediated mechanism of selection.²⁰⁷ However, further discussion of the development of these cells or their function which on occasion bridges the innate and adaptive immune system is beyond the scope of this introduction. ²⁰⁸

1.3.4 T cell activation

Once a developing T cell has survived positive and negative selection it emerges from the thymus and enters the circulation. In order to become activated it must encounter its specific Ag in the correct context; presented by a professional APC which has been appropriately primed. Given that the number of naïve T cells with any particular antigenic specificity is estimated to only be in the hundreds, ²⁰⁹ ensuring these manage to interact with their specific Ag wherever it might occur in the body is potentially problematic. This challenge is overcome by secondary lymphoid organs (lymph nodes, Peyer's patches, tonsils and spleen) which provide a specialised environment in which APCs and T cells can interact.

1.3.4.1 Migration

Naïve T cells continuously recirculate through the blood and lymph pausing in either the spleen or lymph nodes en route. Once in the lymph nodes, a proportion of the naïve T cells transmigrate through the high endothelial venule (HEV) in order to reach the paracortical area of the node where they can encounter APCs. Movement of T cells through the lymph node can be divided into four stages; rolling, activation, firm adhesion and transmigration. L-selectin (CD62L) expressed on the naïve T cell is engaged by peripheral node addressin (PNAd) expressed on the HEV resulting in weak tethering which encourages rolling. ²¹⁰ This promotes the interaction of CCR7 on the naïve T cell with CCL19 or CCL21 on the HEV which results in G-coupled protein-mediated activation of integrins and subsequent firm adhesion to the vascular endothelium. The integrin $\alpha L\beta 2$ which interacts with HEV-expressed ICAM-1 is particularly important in mediating this adhesion. ²¹² Finally naïve T cells transmigrate either between or through endothelial cells into the T cell zone of the lymph node in a poorly understood process which is thought to involve VE-cadherin, several junctional adhesion molecules and ICAM-1 and 2. ²¹³

Once in the T cell zone of the lymph node naïve cells migrate around a conduit system formed by collagen fibrils surrounded by extracellular matrix proteins, produced by fibroblastic reticular cells. Although this migration was originally thought to be random, experimental evidence is starting to emerge which suggests otherwise. ²¹⁴ DCs, although forming a more stationary network, can also migrate along the same 'pathways' scanning the local area for T cells with their dendrites. Ag-bearing DCs particularly congregate around the HEVs which form an entry point for T cells, ²¹⁵ therefore maximising the probability that an Ag-bearing DC will find a T cell with a cognate receptor.

1.3.4.2 Role of dendritic cells

Within the T cell zone of the secondary lymphoid organ, a naïve T cell may encounter Ag presented by a DC. The maturation and activation state of the DC on which the naïve T cell encounters its cognate Ag is central in determining the nature of the resulting immune response. As discussed in section 1.2.2.1 DCs require engagement of their TLRs in order to mature and become activated. Immature DCs are very sensitive to inflammatory chemokines and have a high rate of phagocytosis and endocytosis but are relatively insensitive to homeostatic chemokines, perform little Ag processing and have low expression levels of MHC class II and co-stimulatory molecules. This phenotype ensures they are attracted to sites of inflammation where they ingest Ag.

After TLR engagement their phenotype reverses (levels of phagocytosis and endocytosis drop, sensitivity to homeostatic chemokines increases, sensitivity to inflammatory chemokines decreases and cell surface expression of MHC class II and co-stimulatory molecules increases) resulting in their trafficking to sites of naïve T cells to whom they can present Ag. Although some investigators have suggested exposure to inflammatory cytokines can replace TLR engagement, there is evidence that this produces a mature but inactivated DC which is incapable of producing an effective T cell response. Indirect activation of DCs with inflammatory cytokines has also been shown to be associated with expansion of T_{regs} which are usually (though not universally) felt to be unhelpful in the antitumour immune response.

A fully mature and activated DC is able to produce three signals which are now thought to be required for T cell activation. Signal 1 is the specific Ag presented by MHC, signal 2 are costimulatory molecules such as CD80 and CD86 which interact with CD28 on the T cells and signal 3 are mediators which promote T cell differentiation into an effector phenotype (for example the $T_{\rm H}1$ polarising cytokine IL-12). If a DC presents Ag in the absence of signal 2 or signal 3, 219 tolerance often ensues.

DC Licensing

The CD8⁺ T cell response to a number of Ags is critically dependent on CD4⁺ T cell 'help': The initial explanation of this theory was that both an Ag specific T_H cell and CTL must encounter their cognate Ag on a single APC simultaneously.²²⁰ However, given how rare a T cell with any particular Ag specificity is, the probability of both the appropriate T_H and CTL encountering the APC together is extremely low. The observation that CD4⁺ T cell deficient mice could have their ability to mount a CTL response restored by the administration of an agonistic CD40 Ab while CTL responses were abolished in wild type mice who received a

blocking anti-CD40 Ab suggested that the interaction between CD40 on DCs and CD40 ligand (CD40L) on T_H cells was critical.²²¹

These results have led to the concept of DC licensing: 222 The interaction of a T_H cell with its cognate pMHC class II expressed on the surface of an APC allows engagement of CD40 on the APC by CD40L (CD154) on the T_H cell which provides an activatory signal to the DC causing upregulation of pMHC class I and costimulatory molecules. This allows Ag presentation to a CTL in the appropriate context to elicit an effective response even after the T_H cell has dissociated from the DC. 223 This model reconciles the fact that not all CTL responses are T_H dependent by suggesting that if an Ag is encountered in a context which allows TLR engagement and subsequent inflammatory cytokine production by the DC, the CD40:CD40L interaction is unnecessary for DC activation and maturation.

1.3.4.3 Costimulation

Seminal experiments by Jenkins *et al* demonstrated if CTLs were activated by immobilized anti-CD3 Ab in the absence of any accessory cells it produced long lasting proliferative-unresponsiveness²²⁴ (anergy), suggesting the importance of costimulatory molecules. The pathways involved fall into two receptor families; the immunoglobulin superfamily and the tumour necrosis factor (TNF)/TNFR family. The immunoglobulin superfamily includes the B7-1 (CD80)/B7-2 (CD86): CD28/CTLA-4 pathway, the best characterized pathway of costimulation. CD28 is expressed on naïve T cells and is able to engage B7-1 and B7-2 on DCs, both of which are upregulated following activation of the APC. Engagement of CD28 by DCs allows the molecules to cluster with TCRs within the 'immunological synapse' resulting in the recruitment of protein kinase Cθ and the initial signals required for T cell activation.²²⁵

Once a T cell is activated it upregulates expression of CTLA-4, an inhibitory regulator of T cell activation which competes with CD28 for engagement with B7-1 and B7-2. The higher affinity of B7-1 for CTLA-4 compared to CD28²²⁶ prevents exponential expansion of an immune response and the development of unwanted toxicity associated with immune stimulation. In addition to physically preventing CD28 engagement, CTLA-4 inhibits activatory signalling within the T cell, induces motility reducing the APC:T cell contact and can promote survival of anergic cells.²²⁷ Other receptor:ligand pairs in this family include inducible T cell costimulator (ICOS):ICOS-L which has a role in fine tuning effector cell function and programmed cell death-1 (PD-1):PD-L1/PD-L2 which has a role in the induction and maintenance of peripheral T cell tolerance.²²⁸

Members of the receptor:ligand pairs of the TNF:TNFR superfamily include CD40:CD40L (discussed above), CD27:CD70, 4-1BB:4-1BBL and OX40:OX40L. Other than CD27 which is constitutively expressed on T cells these are all upregulated in response to T cell activation and have a role in regulating effector and memory responses. The CD27:CD70 interaction has been shown to have a role in the proliferation of activated T cells and the development of memory responses; mice deficient in CD70 have both reduced numbers of T cells and very poor memory responses. The timing of this activatory signal is also very important as continuous signalling via this pathway has been suggested to be associated with the development of immune pathology (autoimmunity or tissue destruction associated with chronic viral infection). 230

4-1BB, which is upregulated in response to TCR engagement, is generally described as having a role in the survival of activated T cells and the development of a memory response, particularly in CTLs. However, in addition to these central functions it also appears to have a role in the suppression of humoral immune responses and autoimmunity as it is expressed on T_{regs} where its ligation causes their proliferation.²³¹ OX40 is also upregulated in response to TCR engagement where upon ligation with OX40L it performs a similar function to 4-1BB promoting the division and survival of particularly CD4⁺ T cells. However, it suppresses the differentiation and activation of T_{regs} which enhances the immune response.²³²

1.3.4.4 TCR signal transduction

Once a T cell has undergone TCR engagement by its cognate pMHC (and ligation of appropriate co-stimulatory molecules) in order for an effector function to become apparent this signal must be transduced into the cell, a feat accomplished by CD3 which is coexpressed with the TCR. The first step of this signal transduction pathway is phosphorylation of ITAMs within CD3 (see Figure 1.2) by the Src-family protein tyrosine kinases (PTK) Lck and Fyn. How TCR ligation is converted into this first signal remains unclear but is suggested to involve TCR aggregation and conformational change of the CD3/TCR complex upon cognate Ag binding.

A number of models have been proposed for the mechanism of the conformational change including piston-like movement of the T cell and APC towards each other, receptor deformation, permissive geometry, pseudodimer formation and kinetic segregation.²³⁴ This latter theory is particularly attractive as it provides a model which incorporates immunological synapse formation and the role of CD45. It suggests that close contact zones between an APC and a T cell are produced by the interaction of adhesion molecules with short extracellular domains (e.g. CD2). pMHC and TCR molecules are able to diffuse into

and out of these contact zones, becoming trapped if they interact with their cognate molecule. A feature of these regions is the exclusion of cell surface molecules with large extracellular domains such as CD45 and CD148.

Under physiological conditions Src kinases oscillate between activated and inhibited states due to dephosphorylation and rephosphorylation of their regulatory kinases respectively. This results in a proportion of CD3-associated ITAMs being phosphorylated at any one time irrespective of TCR engagement. However, the phosphatase activity of CD148 and CD45 counteracts ITAM phosphorylation meaning in the absence of TCR ligation net phosphorylation is too low for T cell activation. However, when TCR:pMHC complexes become trapped in these close contact zones their CD3 ITAM phosphorylation is unopposed due to the exclusion of CD45 and CD148. This results in the threshold for recruitment of downstream signalling molecules being reached and the cell being activated. Support for this model comes from the observation that if inhibitory molecules are engineered to have shorter extracellular domains or adhesion molecules altered to have longer extracellular domains, signalling via the TCR is significantly reduced.

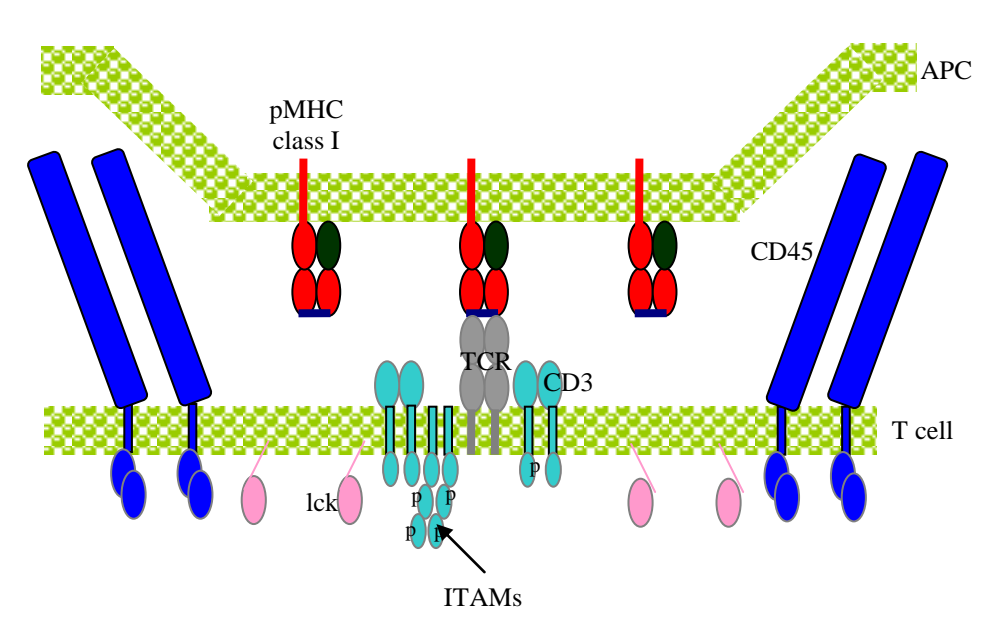


Figure 1.7: Schematic diagram of the kinetic segregation theory of TCR triggering *Figure adapted from Burroughs N & van der Merwe P. Immunol Rev* 2007; 216:69²³⁷

Phosphorylation of the CD3-associated ITAMs, particularly on the ζ chain results in the recruitment of the Syk kinase family phosphoprotein ZAP-70. There follows a cascade of phosphorylation events which results in the assembly of an adapter protein nucleated multimolecular signalling complex which mediates a range of downstream events. Two important targets of ZAP-70 are LAT (linker for the activation of T cells) and SLP-76 (SH2

domain-containing leukocyte phosphoprotein) which subsequently activate Ras, PK θ , NF- κ B and Ca²⁺ signalling pathways.²³⁴

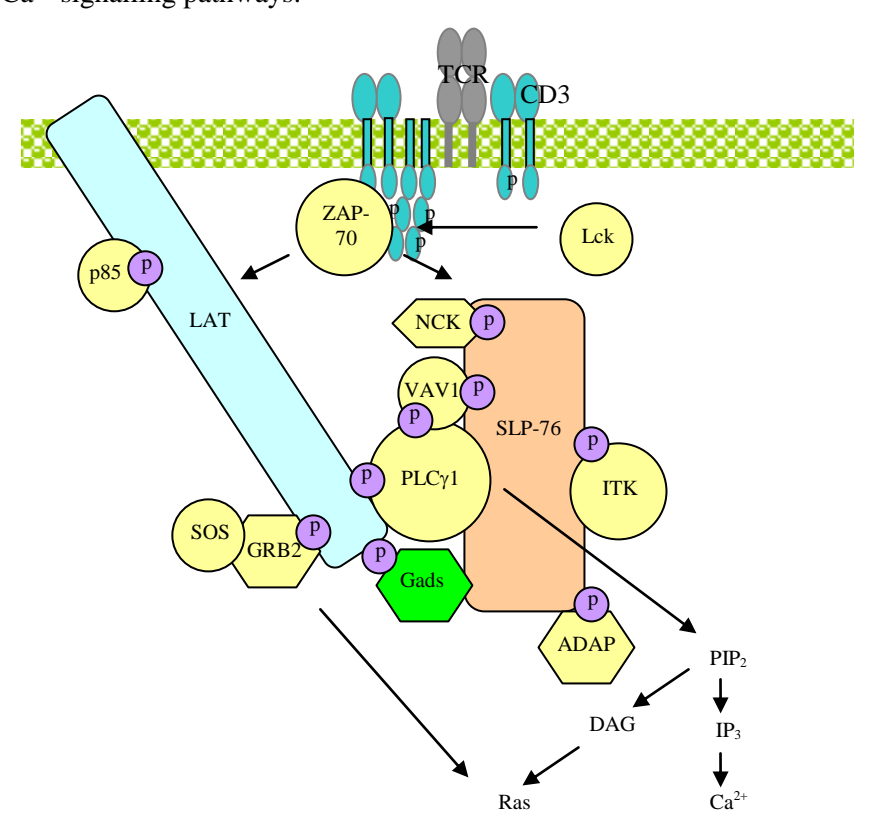


Figure 1.8: Schematic diagram of signalling pathways activated by TCR engagement *Lck-mediated phosphorylation of ITAMs on CD3 causes ZAP-70 recruitment which activates further signalling via its interaction with LAT and SLP-76. Circles represent proteins containing SH2 domains while hexagons represent adapter proteins, Overlaps represent SH3 domains. Adapted from Smith-Garvin et al. Annu Rev Immunol.* 2009; 27:591-619²³⁴

1.3.5 CTL effector mechanisms

Once activated, CTLs are able to fulfil their primary function; the elimination of infected or transformed cells in a controlled manner. This is accomplished by two major pathways which induce apoptosis; granule-dependent exocytosis and Fas:FasL engagement.

1.3.5.1 Granule dependent exocytosis

CTLs have been shown to contain electron-dense storage granules which contain perforin, granzymes and granulysin. Perforin has classically been described as the mechanism by which the granules traverse the target cell membrane to allow release of granzyme and granulysin into the cell: After CTL:target cell interaction it is released by exocytosis²³⁸ and in the presence of Ca²⁺ polymerises to form cylindrical pores.²³⁹ However, little experimental evidence has been generated to support this hypothesis and in the absence of perforin other granule components (granzyme-B) have been shown to be able to enter the cell via a mannose-6-phosphate receptor.²⁴⁰ Other investigators have suggested that adherence of

perforin to the target cell membrane and subsequent pore formation causes an influx of calcium which activates the target cell and induces internalisation of the perforin (along with attached granzymes) in an attempt to 'mend' the pore. However, although the exact mechanism via which perforin produces cytotoxicity is uncertain its contribution to the process is not in doubt as patients with familial haematophagocytic lymphohistiocytosis which involves mutations in the perforin gene are unable to mount an effective immune response to intracellular pathogens. However, although the exact

Granzymes are soluble serine proteases which are able to induce apoptosis in the target cell via both caspase dependent and independent pathways. Granzyme A induces caspase-independent apoptosis by promoting cleavage of single stranded DNA and hydrolysing proteins containing basic amino acids (arginine or lysine). Granzyme B can directly activate caspase 3 (results in DNA fragmentation and membrane and cytoskeleton disruption) and can promote permeability in the outer mitochondrial membrane and cleave Bid. This releases cytochrome C from the mitochondria which in turn activates caspase 9 and ultimately causes cell death. Studies in cathepsin-C knock out mice have shown that granzyme-B is able to function in a cathepsin-C independent manner.

Granulysin is a member of the saposin-like protein family which is thought to produce cell membrane damage resulting in the release of cytochrome C, decrease of mitochondrial function and subsequent apoptosis.²⁴⁵ Its lytic activity is augmented by the presence of perforin.²⁴⁶ It is also able to induce cell death via caspase 3 activation.²⁴⁶

1.3.5.2 Fas:FasL engagement

The other pathway of CTL-mediated cytotoxicity is mediated via Fas:FasL interaction. Upon activation CTLs express FasL which can recognise Fas, a member of the tumour necrosis receptor (TNFR)-1 type family. Engagement of Fas on the target cell with FasL causes trimerisation and recruitment of Fas-associated death domain (FADD) proteins. These recruit procaspases 8 and 10 which, via proteolysis, become activated and form a death-inducing signalling complex. This activates further caspases which cleave DNA and produce damage to the mitochondrial outer membrane thus triggering cytochrome C release and causing the cell to undergo apoptosis. 244

1.3.6 T cell memory

A defining characteristic of the adaptive immune system is the ability to rapidly 'recall' a specific immune response against a previously encountered Ag in order to provide life-long protection from a pathogen. This requires the generation and maintenance of a population of

specialised 'memory' T cells which are able to be rapidly activated in response to Ag and produce an effector response. Compared to naïve cells, memory T cells have much less stringent requirements for activation being able to respond to low doses of Ag²⁴⁷ presented by a wider range of APCs.²⁴⁸ This allows the generation of a functional response within hours rather than days.²⁴⁹

Two types of memory cell have been described based on their phenotypic profile; effector memory cells are $CD62L^{lo}$, $IFN\gamma^+$ and have variable expression of granzyme B and IL- $7R\alpha$. In contrast central memory cells are $CD62L^{hi}$, $IFN\gamma^+$, IL- $7R\alpha^+$ but do not express granzyme B. ²⁵⁰ Both central and effector memory cells are able to proliferate in response to antigenic stimulation although there is some controversy as to whether central memory cells are able to retain a cytotoxic phenotype (as effector memory cells do). ²⁵¹

Two models for the generation of memory cells from an initial primed naïve T cell have been proposed; linear progression or asymmetric division. In the former theory, a proportion of the effector cells survive and acquire a memory phenotype (e.g.CD44 $^+$, CD11c $^+$) after the initial phase of the immune response (seen with the immune response to lymphocytic choriomeningitis in mice). It has been suggested that naïve T cells differentiate along a pathway from naïve > effector T cell > effector memory T cell (CD62L lo) > central memory T cell (CD62L lo) with massive attrition in numbers between the effector and effector memory stages.

The alternative explanation of T cell memory is asymmetrical division of primed cells; upon initial Ag stimulation some T cells are destined to become effectors while others are programmed to become memory cells. A recent study by Chang *et al* suggested that a dividing CD8⁺ T cell was able to have unequal segregation of mRNA and proteins following a prolonged interaction with an APC in an immunological synapse: The resulting daughter cells exhibited either an effector (CD62L^{lo}, CD25⁺, IFN γ ⁺, granzyme B⁺) or memory (CD62L^{hi}, IL-7R α ⁺) phenotype. However, studies have also shown that cells with an effector phenotype (granzyme B⁺) can retain their ability to proliferate and descendants of the cells involved in the primary response can be involved in the secondary response, evidence which refutes the theory of asymmetrical cellular division. ²⁵⁵

Bannard *et al* have suggested a further model of memory cell development which is an adaptation of the linear progression model. They suggest that naïve cells go through a central memory phenotype on their way to functional effectors and a proportion of cells remain at

this stage to produce the memory pool. However as yet there is little experimental evidence to support this theory. ²⁵⁶ The signals required during priming to produce a successful memory response remain unclear. CD4⁺ T cell help²⁵⁷ and IL-2²⁵⁸ appear necessary and it is suggested the costimulatory molecules 4-1BB and OX40 have a role in establishing memory. The cytokines IL-7 and IL-15 are important for the maintenance of CTL memory cells. ²⁵⁹ Therefore, although the generation of memory is one of the hallmarks of a successful CTL response, how this occurs is still not fully understood.

1.4 T Cell Immunotherapy

Given the specialized cytotoxic abilities of CTLs and the experimental evidence that they can have a significant role in the elimination of tumours, increasingly efforts have been focused on trying to generate an anti-tumour CD8⁺ T cell response. These approaches can broadly be classified as either active where a patient receives a vaccine to try and generate anti-tumour CTLs *in vivo*, or passive where the cytotoxic T cell response is developed *in vitro* before being adoptively transferred. The following section outlines some of the strategies pursued with a particular reference to malignant melanoma which due to its apparent intrinsic immunogenicity (several reports describe spontaneous regression of metastatic malignant melanoma²⁶⁰ which correlates with its expression of several differentiation and cancer testis Ags) has been the subject of many clinical trials.

1.4.1 Vaccination

In the context of T cell immunotherapy, tumour vaccines all have the aim of presenting an Ag derived from a tumour cell in such a context that it stimulates an effective cytotoxic antitumour T cell response. As discussed in section 1.2.2.1 this requires the Ag to be presented by a DC which receives appropriate TLR-ligand and cytokine cues to skew the immune system towards a T_H1 -mediated response. The manner in which the tumour Ag is administered to the patient and its accompanying adjuvant(s) are therefore critical in determining the outcome of the vaccination.

Early melanoma tumour vaccines consisted of either irradiated autologous or allogeneic whole tumour cells²⁶¹ or cell lysates, ²⁶² with or without adjuvant. The use of such polyvalent vaccines maximizes the probability any particular patient will respond as it provides a number of different Ags likely to yield peptides restricted to a variety of HLA alleles. In addition to generating detectable 'anti-melanoma' CTLs, some limited clinical success was seen with such vaccines including occasional complete remissions. However, these were usually short-lived and larger scale trials, particularly in the adjuvant setting of high risk fully resected melanoma, have failed to show any long-term benefit.²⁶³

The identification of tumour-specific and tumour-associated Ags has allowed vaccines to develop from whole cells to protein and, with the discovery of the immunogenic epitopes, peptides. Administration of melanoma-derived proteins (including MART1/Melan A and MAGE-3) with either alum or IL-2 liposomes to patients with high risk fully resected melanoma was able to generate MART1/Melan A or MAGE-3-specific CTLs in some patients, who subsequently had an increased length of recurrence free survival. ²⁶⁴ Similarly administration of either native ²⁶⁵ or modified ²⁶⁶ tumour Ag-derived class I-restricted peptides

has been associated with both the production of specific CTLs and objective clinical responses. Ideally peptide vaccines are composed of a mixture of peptides restricted to different HLA alleles as this increases the patient population for whom the vaccine may be appropriate.

Melanoma Ag-derived peptides have been administered with a variety of cytokines (IFN α , IL-2, IL-12 and GM-CSF) and adjuvants (incomplete Freund's adjuvant and QS21)²⁶⁷ as well as MHC class II-restricted T_H epitopes²⁶⁵ in order to try and provide the necessary inflammatory signals and TLR stimulation to initiate a protective immune response rather than induce tolerance. However, although these vaccines frequently produce melanoma Agspecific CTLs and across all phase I-II trials produce a clinical response in 10-30% patients, ²⁶⁷ these remissions are often short-lived and production of specific CTLs is not well correlated with clinical response. ²⁶⁸

In tumours other than melanoma, administration of class I restricted peptides, even with an immunostimulatory adjuvant, has a propensity to induce tolerance rather than an effective CTL response. To avoid tolerance some investigators are immunizing with long peptides which consist of both a class I-restricted antigenic peptide and a class II-restricted helper epitope which is able to activate T_H cells and skew the immune response towards the generation of effective CTLs. Early studies using a vaccine of this design have shown some promising clinical results in HPV-associated malignancies (i.e. cervical and vulval carcinoma).²⁶⁹

An alternative vaccination strategy is the administration of DNA encoding a tumour Ag which upon expression provides a ready source of tumour Ag for DCs (either by direct transfection of DCs or via cross-presentation) to process and present to CD8⁺ T cells. Tumour Ag DNA can either be given 'naked', incorporated into a standard expression vector²⁷⁰ or inserted into an attenuated virus²⁷¹ (e.g. vaccinia virus) or a recombinant replication-incompetent viral vector (e.g. adenovirus). Viral vectors have the advantage of providing multiple immunogenic 'helper' epitopes. DNA encoding costimulatory molecules has been incorporated into some vectors²⁷² to try and enhance the immune response and avoid tolerance, and different vectors can be used to first prime, and then boost a response.²⁷³

In order to bypass the difficulty of giving tumour Ag in a suitable format for effective presentation by DCs, some investigators have created DC vaccines where Ag is loaded directly onto Ag presenting cells *ex vivo*. DCs can be generated *in vitro* from either monocytes or CD34⁺ blood stem cells by exposure to GM-CSF and TNFα.²⁷⁴ These can then

be loaded with tumour Ags either exogenously in the form of synthetic peptides, proteins, cell lysates or apoptotic debris, or endogenously via transfection with DNA or mRNA. Exposure to varying cocktails of cytokines and TLRs can mature the DCs and optimize them for Ag presentation to CTLs.²⁷⁵ The tumour Ag-bearing DCs can then be administered intradermally or intranodally with or without an adjuvant (e.g. IL-2) in order to elicit a CTL response. Many clinical trials have been undertaken in melanoma using DCs at different stages of maturation, different sources of Ag, different routes of administration and different adjuvants: These have shown that although specific CTLs can be generated this is not universally associated with a clinical response.²⁷⁶

A comparative analysis of 35 different vaccine trials in melanoma undertaken by Rosenberg *et al* calculated an overall objective response rate of just 3.8% suggesting that although there are individual successes with melanoma vaccines, none of the current approaches are consistently able to produce a response.²⁷⁷ Anti-tumour CTLs often fail to correlate with clinical regression, presumably due to either the generation of anergic T cells or the presence of immunosuppressive factors (e.g. T_{regs} and MDSCs) in the vicinity of the tumour which prevent CTL-medicated cytotoxicity. Additionally most trials measure anti-tumour CTLs in the peripheral blood rather than at the tumour site (their desired site of localisation). Paradoxically absence of anti-tumour CTLs in the peripheral blood may be a promising sign as it suggests (if present) the CTLs have localised to the tumour where they can eliminate their target cells. Investigation of this hypothesis would require serial tumour sampling which is beyond the ethical scope of most solid tumour trials.

1.4.2 Adoptive T cell transfer

Despite the range of vaccine strategies discussed above, objective responses to anti-tumour vaccines are disappointingly rare and therefore many investigators have pursued an adoptive cell transfer (ACT) approach. This involves identification of autologous or allogeneic lymphocytes with anti-tumour activity *ex vivo*, expansion and / or enhancement of their specificity if required, and finally administration to the patient with appropriate cytokines and growth factors to improve function and survival. As with tumour vaccines, malignant melanoma has been a particular focus of ACT therapy, not least because its immunogenicity means CTLs specific for peptides derived from tumour Ags can be identified.

Autologous CTLs specific for immunogenic peptides derived from melanoma Ags can be identified both in the peripheral blood and infiltrating the tumour in many melanoma patients. These can be induced to proliferate via successive rounds of stimulation with melanoma Agloaded autologous APCs in the presence of IL-2. They can then be cloned and evaluated *in*

vitro for effector phenotype before expansion and infusion into the patient.²⁷⁸ Initial studies using this approach were encouraging with up to 30% of patients showing some clinical response even though CTLs were not evaluated for lytic abilities prior to infusion and *in vivo* persistence was extremely short lived with less than 0.01% of transferred cells being detectable in the peripheral circulation at a week despite the co-administration of high dose IL-2.²⁷⁹

The persistence of adoptively transferred CTLs can be enhanced by using non-myeloablative lymphodepleting preconditioning (e.g. cyclophosphamide and fludarabine) prior to adoptive transfer: 280 In addition to depleting immunosuppressive T_{regs} , 281 by reducing the host endogenous lymphocyte pool, transferred CTLs have greater access (due to less competition) to growth promoting cytokines such as IL-7 and IL-15 which allows the transferred lymphocytes to maintain function and rapidly expand and replenish the normally tightly regulated T cell pool. 282

It has also become increasingly apparent that the differentiation state of the transferred CTLs has an impact on persistence and therefore anti-tumour effect. In response to increasing stimulatory signal strength CD8 $^+$ T cells differentiate from naïve cells through early, intermediate and late stages. As they move along this pathway (i.e. through central memory to effector memory to effector T cells) they down-regulate costimulatory and lymph node homing molecules (CD62L, CCR7, β 7-integrin and CD27), lose their ability to produce IL-2, shorten their centromeres which restricts proliferative potential and ultimately enter replicative senescence and undergo apoptosis.

However, they also acquire full cytolytic effector function (upregulate CD44, CD69, CD25, granzyme B and perforin) and produce higher levels of IFNγ. Although more differentiated CTLs produce higher levels of tumour cell lysis *in vitro*, *in vivo* this phenotype is associated with an inability to cause tumour regression.²⁸³ Previously human adoptive transfer studies have used effector T cells (a consequence of selecting clones for transfer on the basis of their ability to lyse tumour cells *in vitro*), but in a recent study in primates effector T cells derived from central but not effector memory cells were able to reacquire a memory cell phenotype and persist long term.²⁸⁴ A recent study of MART-1 specific CTLs in patients with advanced stage melanoma by Hirano *et al* has shown that if CTLs for adoptive transfer are manipulated *in vitro* by an artificial APC system they can be educated to acquire effector and central memory phenotypes which upon transfer can persist for long periods without the need for concurrent administration of cytokines or myeloablative lymphodepleting preconditioning.²⁸⁵

Adoptive cell therapy has also been used with some success in the treatment of Epstein Barr Virus (EBV) associated malignancies (post-solid organ transplant lymphoproliferative disease, ²⁸⁶ Hodgkin's disease ²⁸⁷ and nasopharyngeal carcinoma). ²⁸⁸ In these trials the transferred CTLs are specific for peptides derived from latent EBV Ags expressed by the tumour and clinical responses could be seen in malignancies which express only the very limited range of Ags seen in type II latency (LMP1 and LMP2). ²⁸⁹ Owing to difficulties generating sufficient tumour-specific CTLs from heavily pre-treated patients and the time such an approach requires, some investigators have adoptively transferred partially HLA-matched allogeneic EBV-Ag specific CTLs to treat Hodgkin's disease: although some clinical improvement was seen, co-administration with fludarabine made it difficult to differentiate the contribution of the CTLs. ²⁹⁰

Perhaps, the most successful example of adoptive immunotherapy is the graft versus leukaemia (GVL) effect seen with haematopoietic stem cell transplantation (HSCT): Host DCs are able to activate donor CTLs (putative Ags are minor histocompatibility and tumourderived Ags) to eliminate leukaemic (or other malignant) cells (e.g. in chronic myeloid leukaemia). Although potentially beneficial, this response can itself be fatal if manifest as graft versus host disease (GVHD). Attempts have been made to maximize the beneficial GVL effect by reducing the intensity of conditioning, reducing the initial suppression of GVHD, using stem cells derived from the peripheral blood rather than bone marrow, administration of cytokines (e.g. IL-2) and giving donor lymphocyte infusions (DLI) once chimerism and tolerance have developed. Following the success of this approach in haematological malignancies HSCT has been used in a number of solid organ malignancies including renal, breast, colorectal, ovarian and pancreatic with responses observed in some patients.

Other than HSCT and DLI, the above examples refer to the adoptive transfer of CD8⁺ T cells. However, interest is now growing in the concept of transferring CD4⁺ T cells, not least because of the central role they have in coordinating the immune response. Lack of progress in this area can in part be explained by the paucity of well defined class II restricted peptides derived from tumour Ags and difficulties generating large numbers of T_H cells *in vitro*. However, a recent case report describing a spectacular remission in malignant melanoma following the adoptive transfer of a CD4⁺ clone specific for an NY-ESO-1 class II restricted peptide without the need for either preceding lymphodepletion or subsequent cytokine support, with subsequent evidence of epitope spreading amongst the CD8⁺ T cell response²⁹⁴ suggests there may be some merit in this approach.

1.4.3 Adoptive transfer of genetically modified T cells

Despite the success seen with adoptive cell transfer of expanded, naturally occurring CTLs in melanoma, this is the only malignancy where potentially effective autologous CTLs can be reliably isolated. In order to expand the strategy to include other malignancies it is necessary to artificially confer tumour-specificity on the transferred CTLs. This can be done by introducing a transgenic TCR or chimeric Ag receptor into autologous CTLs specific for non-tumour Ags, therefore artificially creating a population of CTLs specific for tumour Ags.

The genes encoding the α and β chains of a TCR from a rare tumour-Ag specific CTL (either isolated from a patient, a phage display library, or tumour-Ag immunized transgenic mouse) are cloned into a retroviral vector, if necessary after gene optimization to increase expression of the transgene. This is then used to transfect a non-tumour Ag-specific CD8⁺ T cell where it confers anti-tumour specificity on the cell. In vivo murine studies have shown that such gene-modified T cells are able to produce very effective cytotoxic T cell responses against cells expressing the cognate Ag, even if the endogenous T cell repertoire is tolerant of the Ag. 297

Although there is the theoretical risk of unwanted autoimmunity either due to the specificity of the endogenous TCR or cross-reactivity of the transgenic TCR with a non-tumour host Ag, endogenous deletion of strongly self-reactive CTLs and pre-infusion screening should reduce this risk. A more significant risk is the production of mixed TCR dimers where an endogenous α chain pairs with a transgenic β chain (and vice versa) producing a TCR with a new specificity. During *in vivo* studies this has on occasion been associated with a GVHD-like pathology. The risk of chimeric TCRs can however be reduced by genetic modification such as the introduction of an additional disulfide bond between the chains.

Adoptive transfer of CTLs with transgenic TCRs specific for HLA-A2-restricted melanoma peptides derived from MART-1 or gp100 into patients with metastatic melanoma has recently been evaluated in clinical trials. Although some objective responses were seen, several patients developed autoimmune toxicities due to the destruction of melanocytes in the skin, ear and eye (a phenomenon not generally observed with the adoptive transfer of wild-type MART-1 or gp100-specific CTLs) illustrating the potential risk of infusing CTLs with high affinity TCRs for Ags expressed on tissues other than the tumour. These rather unexpected toxicities suggest that Ags whose expression was thought to be sufficiently tumour-restricted to be a suitable target may in fact be associated with unacceptable levels of toxicity.

Adoptive transfer, as discussed above, using CTLs which recognize Ag via their TCR is only going to be useful for tumours which have retained the ability to process and present peptide Ag in the context of MHC class I. Any tumour which down-regulates class I or develops an impairment of Ag processing and presentation will be able to avoid detection and elimination with this therapy. An alternative strategy for tumour recognition which negates this escape mechanism is to transfect CTLs for adoptive transfer with chimeric Ag receptors (CARs) whose structure is shown in Figure 1.9: Instead of possessing a TCR which recognizes pMHC, CARs contain the variable regions from an Ab and are therefore able to recognize native cell surface Ags in a manner similar to their parental Ab. The Ab variable region is fused to the signalling domain (zeta chain) of the TCR/CD3 receptor so that upon engagement of the Ag binding region the T cell is activated via its normal signalling pathways. 303

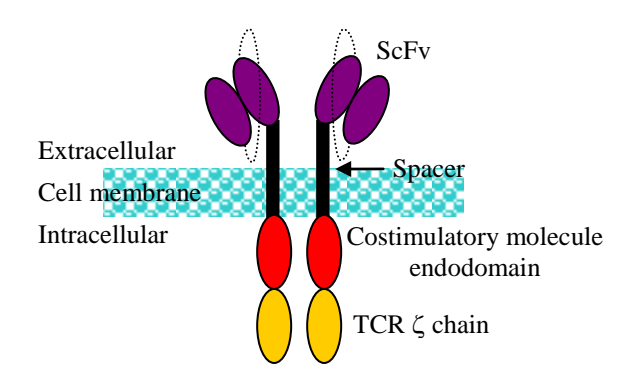


Figure 1.9: Structure of a chimeric antigen receptor

The CAR illustrated as an optional costimulatory signalling molecule endodomain which is intended to enhance activation of the CAR-transfected CTLs following engagement of the Ag recognition domain (scFv).

Several CARs have been generated against a variety of cell surface tumour Ags (e.g. GD2, 304 CD30305 and CEA306 expressed in neuroblastoma, Hodgkin's disease and colorectal carcinoma respectively) which, when expressed in non-tumour specific CTLs, are able to effect recognition and lysis of tumour cells *in vitro* expressing the cognate Ag. To avoid the potential problem of tolerance induction due to signalling via the TCR-zeta chain in the absence of a second costimulatory signal, CARs have subsequently been produced which incorporate one or several endodomains from a costimulatory molecule (e.g. CD28, CD137, 41BB or OX40):307 The provision of a second stimulatory signal within the receptor is associated with improved activation, proliferation and cytotoxicity.308

An alternative strategy to improve the activation and persistence of CAR-expressing CTLs is to transfect populations of CTLs which, due to the Ag specificity of their native TCR, are likely to receive ongoing stimulation to maintain longevity: Such CTLs include those specific for viruses which produce lifelong latency; e.g. EBV. Studies have shown that adoptively

transferred EBV-specific CTLs can persist *in vivo* long term³⁰⁹ through regular encounter with EBV-infected B cells which both present Ag to the native TCR and provide costimulatory signals. A recent study in which EBV-specific and polyclonally activated CTLs were both transfected with the same CAR (specific for the neuroblastoma surface Ag GD2) demonstrated that after infusion of both cell types into the same subjects, the EBV-specific CTLs persisted in higher numbers initially and could be stimulated to proliferate 6 months after adoptive transfer. This trial also demonstrated the efficacy of adoptively transferred CAR-expressing CTLs as a therapy as 50% of patients had a clinical response.³¹⁰

1.4.4 Antibody and cytokine therapy

Attempts have been made to non-specifically stimulate an endogenous anti-tumour CTL response through the administration of either a stimulatory cytokine (i.e. IFN α or IL-2) or an Ab which reduces negative regulation of the CTL response (i.e. anti-CTLA-4 Ab; ipilimumab). Both IL-2³¹¹ and IFN α^{312} have had low rates of success in melanoma, although these have to be considered in the context of significant toxicities. Ab blockade of the inhibitory receptor CTLA-4 found on CTLs not only prevents the cell from receiving an inhibitory signal, but also results in CTLA-4's natural ligands being free to interact with CD28 and further activate T cells (CD80 and CD86 bind with higher affinity to CTLA-4 than CD28). Clinically, administration of ipilimumab alone in melanoma is associated with modest response rates. ³¹³ Improved clinical responses can be seen if the Ab is co-administered with a peptide vaccine, but this is associated with higher rates of autoimmunity. ³¹⁴ More recently a study of ipilimumab in combination with dacarbazine improved overall survival in previously untreated patients with metastatic melanoma but with significant autoimmune toxicity (particularly autoimmune hepatitis). ³¹⁵

In summary, although there have been some individual impressive remissions through the use of T cell immunotherapy, particularly in melanoma, as yet no therapy has been associated with consistent clinical responses. In addition many of these approaches, particularly those which require the development of a personalised cell product are both costly and time consuming making them harder to implement outside of very specialised centres. In order for the strategies described above to become more widely utilised not only will their efficacy have to improve, but they will need to be less individualised and more 'off the shelf'.

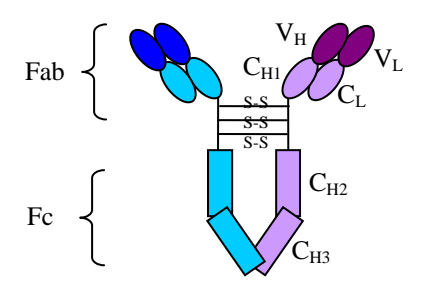
1.5 Retargeting Immune Effector Cells with Bispecific Antibodies

In light of the difficulty in generating an effective anti-tumour CTL response, one strategy being revisited is bispecific antibodies. These are heterodimeric proteins consisting of two arms, each containing at least the variable regions of two antibodies with different specificities. They are able to target immune effector cells to tumour cells by having one arm specific for an effector cell surface protein, and the other for a tumour cell surface Ag.

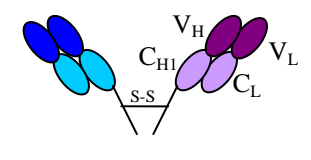
Bispecific antibodies have concentrated on targeting two groups of effector cells; either Fc receptor (FcR) bearing cells of the innate immune system (e.g. NK cells and macrophages), or the specialized 'killer' cells of the adaptive immune system; cytotoxic T cells. FcR-bearing cells are targeted via constructs containing Ab moieties specific for one of the FcRs (usually FcRI i.e. CD64 or FcRIII i.e. CD16). T cells are retargeted using a bispecific (BsAb) containing a moiety specific for the universal T cell Ag CD3 which is able to bypass the MHC restriction normally required for the activation of T cells. The ubiquitous expression of CD3 on all T cells means subtypes other than CD8⁺ CTLs are also susceptible to engagement by anti-CD3-containing bispecific antibodies, although in many clinical trial protocols attempts are made to counteract this by the use of a PBMC pre-activation regime which preferentially activates CTLs.

Figure 1.10 illustrates how the design for bispecific antibodies has evolved from quadromas and the chemical fusion of two Fab' fragments (fragment Ab binding; i.e. the variable regions of the Ab heavy and light chains), to smaller tandem scFvs (single-chain variable fragment; i.e. the fusion of the variable regions of the Ab heavy and light chains) in an effort to improve efficacy and limit toxicity.

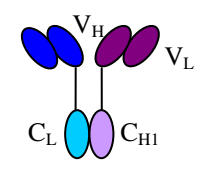
A: Quadroma-derived



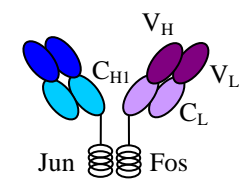
B: F(ab')₂



C: Heterodimeric scFv



D: Heterodimeric Fab



E: Diabody



F: Tandem scFv

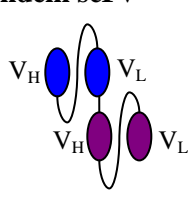


Figure 1.10: Alternative structures of bispecific antibodies

A indicates a quadroma-derived BsAb (formed by the fusion of two hybridomas) which has a similar size and structure to normal IgG. B-D are intermediate sized bispecific formats: B illustrates bispecific F(ab')₂ formed either by enzymatic digestion of a quadroma-derived BsAb or chemical conjugation of two different Fab's. C shows a heterodimeric scFv which exploits the natural ability of C_L to associate with C_{HI} ; complementary constant domains are fused genetically to V_H of each of the parental antibodies and then expressed in E. coli allowing production of two different scFvs which naturally associate via the constant regions. 316 **D** indicates a heterodimeric Fab', produced in E. coli, which uses the natural association of the leucine zipper domains of Jun and Fos to effect conjugation of the two Fab's. 317 E & F indicate minimally sized bispecific formats: E illustrates a diabody (produced in E. coli) where the V_H region of one Ab is joined to the V_L of the other and vice versa by a very short flexible polypeptide linker (3-9 amino acids) preventing interaction of non-cognate V regions. 318 \boldsymbol{F} shows a tandem scFv, produced in mammalian cells where the variable regions are linked by a flexible polypeptide linker sufficiently short to prevent non-cognate pairing. 319 The design of the tandem scFv confers more flexibility in the orientation of the Ag binding sites on the molecule than that observed for a diabody, meaning there may be enhanced retargeting of cells if the availability of one of the target Ags is restricted. Abbreviations; Fab' – fragment Ag binding, Fc – constant region, V_H - heavy chain variable domain, V_L –light chain variable domain, C_{HI-3} - heavy chain constant domains, C_L – light chain constant domain, S-S - disulfide bond. The use of blue and purple is to indicate domains derived from the two different parental antibodies. Figure adapted from Kufer et al, Trends Biotechnol. 2004; 22:238³²⁰

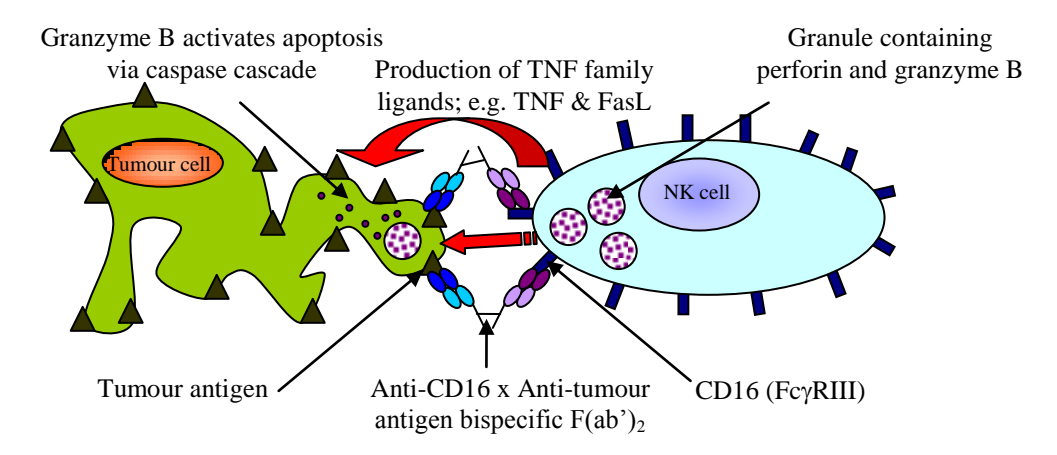
1.5.1 Retargeting FcyR-bearing cells

An early attempt to retarget FcγR-bearing cells was performed by Titus *et al* who cross-linked an anti-CD16 Fab' (i.e. directed against the activatory FcγRIII found on macrophages, neutrophils and natural killer cells) with Fab' fragments derived from antibodies specific for melanoma, lung and ovarian tumour Ags. ³²¹ *In vitro* these bispecific antibodies were able to redirect 'killer' and natural killer cells obtained from peripheral blood to specifically lyse tumour cells bearing the target Ag while *in vivo* they were able to prevent tumour growth. Some moderate success was seen in early clinical trials of an anti-CD16 x anti-CD30 bispecific F(ab)₂ in refractory Hodgkin's disease, ^{322,323} but few clinical trials using anti-CD16-containing bispecific antibodies have been undertaken.

Bispecific constructs containing Fab' fragments specific for the higher affinity³²⁴ FcγRI receptor (CD64) have also been produced:³²⁵ The bispecific antibodies MDX-447 and MDX-H210, which consist of anti-CD64 Fab' fragments chemically conjugated to anti-epidermal growth factor receptor (EGFR) and anti-HER2/neu Fab's respectively, have been clinically evaluated in a range of EGFR and HER2/neu positive tumours in phase I trials where they were reasonably well tolerated and appeared to have modest effects in selected patients.³²⁶ However, follow up studies during which these bispecific antibodies were co-administered with granulocyte-colony stimulating factor (G-CSF) in order to increase the availability of FcγR-bearing cells for retargeting did not confirm these early observations.^{327,328} In addition, co-administration of G-CSF with MDX-447 increased the toxicity of the therapy, reducing the maximum tolerated dose (MTD).³²⁸

However, with the development of novel bispecific formats brought about by advances in genetic engineering, retargeting FcR-bearing cells is being re-visited as a possible immunotherapy strategy: A 'single chain Fv triple body' consisting of two distal anti-CD19 scFvs and a central anti-CD16 scFv has recently been described which is able to efficiently lyse both leukaemic cell lines and primary leukaemia / lymphoma cells *in vitro*, ³²⁹ as has a 'bispecific single chain Fv' consisting of an anti-CD64 scFv genetically fused to an anti-CD30 scFv which is able to lyse Hodgkin's lymphoma cells *in vitro*. ³³⁰ Figure 1.11 illustrates the postulated immunological mechanisms utilized to kill tumour cells when retargeting Fcγ receptor-bearing cells using bispecific antibodies.

A: Retargeting CD16⁺ cells



B: Retargeting CD64⁺ cells

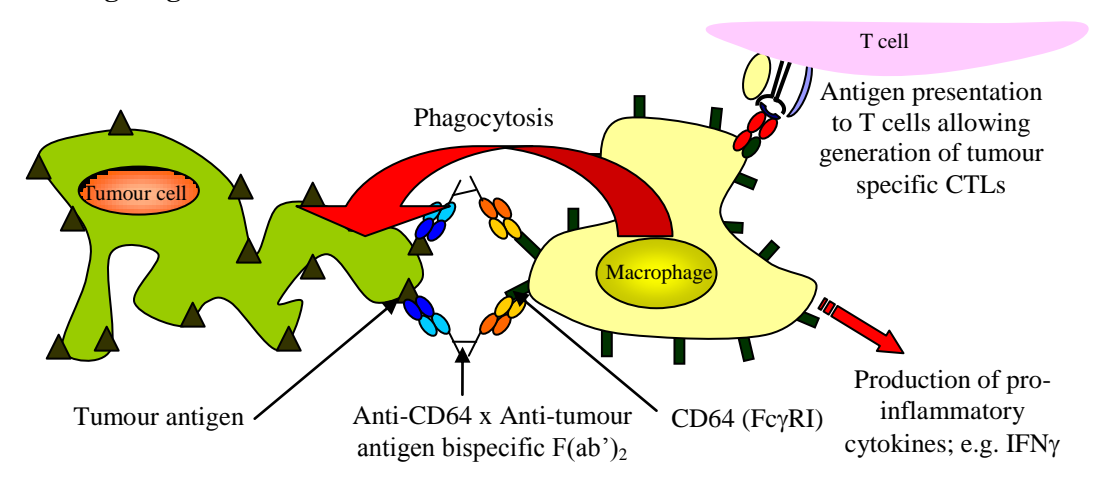


Figure 1.11: Retargeting Fcy receptor-bearing cells

A demonstrates the proposed cytotoxic mechanisms involved when retargeting NK cells via ligation of CD16. When CD16 is ligated on macrophages and monocytes the mechanisms shown in \boldsymbol{B} for CD64 ligation apply. \boldsymbol{B} demonstrates the proposed cytotoxic mechanisms involved when retargeting macrophages and monocytes via ligation of CD64. If CD64 engagement causes phagocytosis of tumour cells, monocytes and macrophages are able to act as professional APCs and present tumour Ags to T cells generating a specific anti-tumour response from the cellular components of the adaptive immune system. Production of inflammatory cytokines such as IFN γ can increase the immunogenicity of tumours by upregulating pMHC expression on the tumour cell surface. 331

1.5.2 Retargeting CD3 positive cells

Many attempts have also been made to retarget cytotoxic T cells, the specialized killer cells of the adaptive immune system: These use bispecific antibodies containing an anti-CD3 moiety which is able to bypass the MHC restriction normally required for the activation of T cells. The first published example of retargeting CD3⁺ T cells involved cross-linking Fab' fragments from an anti-CD3 Ab with those derived from antibodies specific for 'xenogenic tumour Ags' and chicken red blood cells. Human T cells were then able to lyse cells bearing these Ags.³³²

Anti-CD3 antibodies have subsequently been combined with a range of anti-tumour antibodies as shown in Table 1.4. This list is by no means exhaustive but aims to illustrate the breadth of tumour Ags which have been targeted both *in vitro* and subsequently *in vivo*. The earlier references listed relied on quadroma technology or chemical conjugation of Fab's to produce the bispecific antibodies investigated, whilst the agents used for the later studies benefit from some of the advances in genetic engineering which allow production of the structures shown in Figure 1.10 **E** & **F**.

Antigenic target of mAb	Tumour expression	Pre-clinical studies	Clinical Trials	Reference
tenascin	glioma	Yes	No	333
glioma-associated Ag	glioma	Yes	Yes	334,335
CD13	AML	Yes	No	336
MUC-1	carcinoma of the bile duct	Yes	No	337
epithelial cell adhesion molecule (EpCAM)	adenocarcinomas	Yes	Yes	338,339,340, 341,342,343
folate-binding protein	ovarian carcinoma	Yes	Yes	344,345
renal cell carcinoma Ag	renal cell carcinoma	Yes	No	346,347
Transferrin receptor	overexpressed in many different malignancies ³⁴⁸	Yes	No	349
Epithelium-associated glycoprotein (EGP-2)	pancarcinoma	Yes	Yes	350,351
CD19	malignant B cells	Yes	Yes	352,353,354
Carcinoembryonic Ag (CEA)	particularly on colorectal tumours, but also some pancreas, stomach, breast, lung, thyroid and ovarian cancers	Yes	No	355,356
HER2/neu	breast, renal and colon carcinomas	Yes	Yes	357,358
CD30	Hodgkin's lymphoma	Yes	No	359
PSA	prostate carcinoma	Yes	No	360
CA19.9	adenocarcinomas	Yes	No	361
Epidermal Growth Factor Receptor (EGFR)	many tumour types including gliomas, colorectal, ovarian and lung carcinomas	Yes	No	362
PSMA	Prostate carcinoma	Yes	No	363
CD20	Malignant B cells	Yes	Yes	364,365,366

Table 1.4: Anti-CD3-containing bispecific antibodies used *in vitro* or *in vivo* to retarget CTLs to tumour cells

Although all the bispecific antibodies listed in the above table were able to cause T cell-mediated lysis of target tumour cells *in vitro*, the responses seen *in vivo* in subsequent clinical trials were much more variable. Initial trials involved administering the BsAb simultaneously with activated lymphocytes, usually locally into the tumour. This approach has the potential advantages of ensuring activated T cells are available in the vicinity of the tumour to be

retargeted, BsAb is in the appropriate location to perform the retargeting and the systemic distribution (and accompanying toxicity) of cytokines released by the activation of T cells (a phenomenon observed with the administration of the anti-CD3 Ab OKT3³⁶⁷) should be limited. An early trial by Nitta *et al*, which using this approach with the intratumoral administration of lymphokine activated killer (LAK) cells with an anti-CD3 x anti-glioma Ag bispecific F(ab')₂, produced several significant tumour regressions in contrast to the near universal progression observed amongst patients who received LAK cells alone.³³⁵

A more comprehensive multi-centre clinical trial employing this approach involved giving an anti-CD3 x anti-folate receptor bispecific Fab' intraperitoneally to patients with ovarian carcinoma along with *in vitro* activated (i.e. with IL-2 and phytohemagglutin) autologous T cells derived from the peripheral blood: Several promising clinical results were seen including complete remissions. Administration of the BsAb-armed T cells directly into the peritoneal cavity was associated only with minor toxicity limited to mild fevers, nausea and vomiting, so consistent with later studies which show that T cells recovered from the systemic circulation are only weakly coated in the BsAb and not able to lyse folate receptor-expressing cells. In contrast, when this Ab was administered intravenously, although preferentially localizing to ovarian tumours, it was associated with significant toxicity and elevations in IL-2, IFN γ and TNF α , supporting the theory that localized administration of a BsAb limits systemic toxicity.

However, intratumoral administration is not always possible due to the disseminated nature of certain malignancies and therefore systemic intravenous delivery is required. Some of the earliest trials of intravenous bispecific antibodies were not accompanied by the coadministration of activated T cells, presumably due to the ready availability of circulating lymphocytes. However, such trials tended to be associated with the appearance of systemic toxicity before a clinical effect was observed. One such early trial involved intravenous administration of a bispecific anti-CD3 x anti-CD19 IgG (derived from a quadroma) to patients with non-Hodgkin's lymphoma. Despite the presence of fevers, rigors and mild thrombocytopenia, no clinical response was observed. More recently $ex\ vivo$ opsonisation of T cells with bispecific antibodies has been used as a mechanism to 'wash out' the cytokines produced by T cell activation (IFN γ and TNF α) prior to intravenous administration in order to limit systemic toxicity. 341

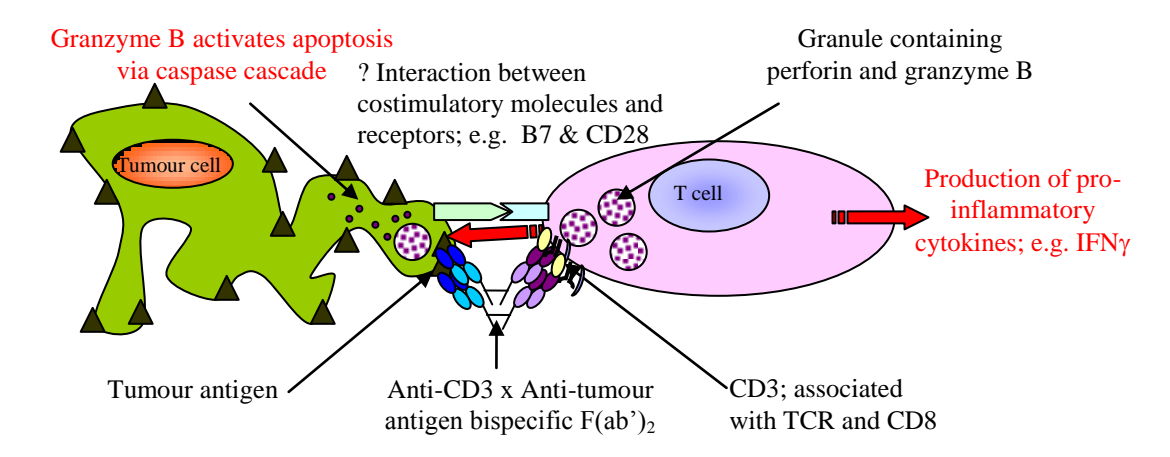
The dose limiting toxicity seen in a number of early BsAb trials led to investigations as to whether the presence of an Fc region increased toxicity. Work by Link *et al* with IgG and

F(ab')₂ formats of the same anti-CD3 x anti-HLA-DR BsAb (1D10) demonstrated that in contrast to the F(ab')₂ format, the Fc-containing version was able to activate T cells in the absence of target Ag-expressing cells.³⁷¹ This was proposed to occur via engagement of FcR-bearing cells which provided costimulatory signals to T cells to complement CD3 engagement, hence producing activation. It was therefore thought that Fc-containing bispecific antibodies were more likely to be associated with toxicity due to indiscriminate activation of T cells even in the absence of tumour Ag.

Although Fc-containing bispecific formats were avoided for a period of time, more recently they have become popular and the additional reactivity with FcR-bearing effector cells has been seen as a virtue as recognized in their classification as tri-functional antibodies. Their ability to activate T cells *in vivo* without the need for pre- or co-stimulation is seen as an advantage and promising results have been seen with an anti-CD3 x anti-EpCAM tri-functional Ab following intraperitoneal and intrapleural administration with reductions in malignant ascites³³⁹ and pleural effusions³⁴² respectively, with relatively limited toxicities. Intravenous administration of an anti-CD3 x anti-HER2/neu tri-functional Ab, although associated with more severe toxicity has also produced several clinical responses including the complete remission of target lesions in patients with metastatic breast cancer. ³⁵⁸ Figure 1.12 demonstrates the postulated immunological mechanisms utilized to kill tumour cells when retargeting T cells using bispecific antibodies containing an anti-CD3 moiety, with or without an Fc domain.

Perhaps the most exciting development in the field of bispecific antibodies has been the emergence of the 'BiTE' or Bispecific T cell Engaging antibodies which are composed of tandem scFvs; one specific for CD3, the other for a tumour Ag. The two most studied BiTE antibodies are specific for CD19³⁷² and EpCAM.³⁷³ *In vitro* studies have shown that these are able to cause cell lysis at concentrations several orders of magnitude lower than other bispecific antibodies and at very low effector:target ratios.³⁷⁴ This is postulated to be due to their ability to polyclonally activate T cells without the need for co-administration of co-stimulatory agents, which in turn is suggested to be as a result of their ability to efficiently form large numbers of immunological synapses which resemble those formed when a T cell is activated via its TCR by engagement with a cognate pMHC complex.³⁷⁵

A: Retargeting CD3⁺ cells using a bispecific construct lacking an Fc domain



B: Retargeting CD3⁺ cells using a bispecific construct lacking an Fc domain

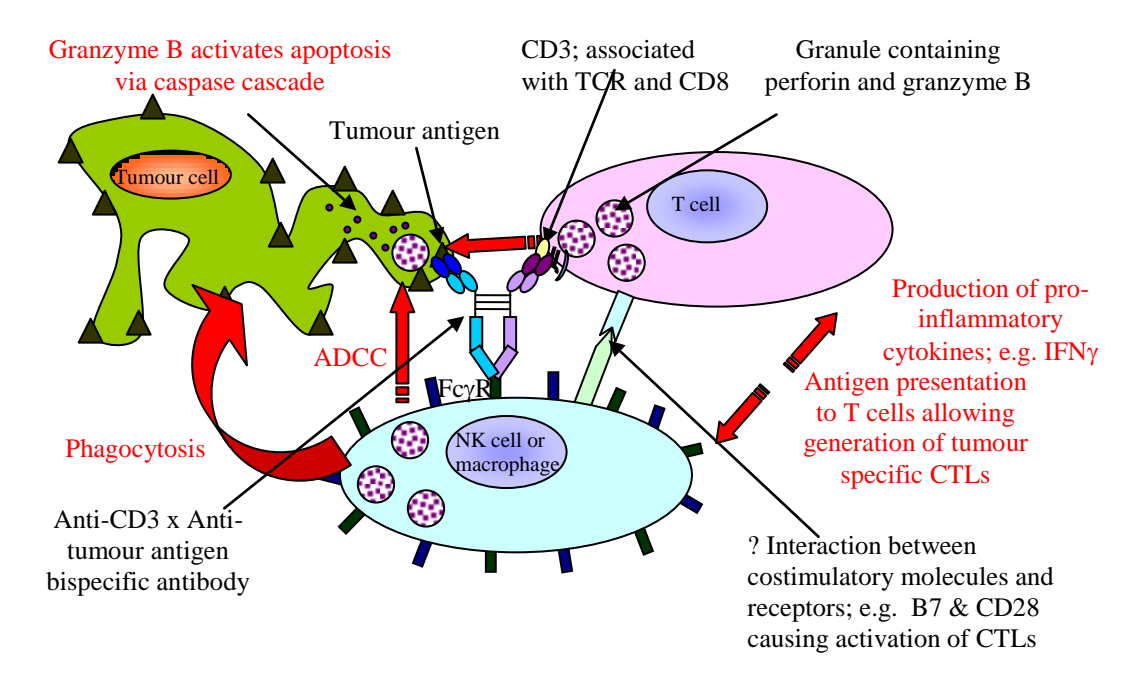


Figure 1.12: Retargeting CTLs

Postulated cytotoxicity mechanisms utilized when retargeting $CD3^+$ cells using bispecific constructs with (\mathbf{B}) and without (\mathbf{A}) an Fc domain. It is suggested that in addition to the mechanisms indicated that T cell killing also takes place via Fas: FasL interactions. However, this mechanism is speculative and it is of note that it appears that this pathway makes a negligible contribution to the cytotoxicity of BiTe antibodies which retarget CTLs. 376

The ease with which they can apparently form functional immunological synapses is proposed to be a function of their small size which allows close apposition of the T cell and target cell membrane possibly excluding negative regulatory proteins from the synapse such as CD45, and their flexibility allowing interaction of the two target Ags. Tudies have suggested that T cells retargeted by BiTE antibodies predominantly used the perforin/granzyme B rather than

the Fas/FasL pathway to effect lysis of the tumour cell as there is proteolytic cleavage of caspases 3 and 7 and lysis is prevented by administration of a calcium chelator *in vitro*.³⁷⁶

Although polyclonal T cell activation without the need for co-stimulation or pre-activation regimes is not unique to BiTE antibodies (Fc-containing tri-functional antibodies are able to activate and retarget resting T cells and the toxicity seen with some bispecific $F(ab')_2s$ even in the absence of clinical efficacy suggests they are able to activate at least a proportion of the circulating T cells), pre-clinical data suggests they are able to produce much more efficient activation of a larger proportion of T cells: If translated in to clinical performance this should mean smaller and hence cheaper amounts of the BsAb are able to produce a clinical effect.

A recent phase I trial of the anti-CD3 x anti-CD19 BiTE Ab in relapsed indolent non-Hodgkin's lymphoma (predominantly mantle cell and follicular lymphomas) has shown a number of partial and complete tumour remissions at doses which range from 0.015 - 0.06 mg/m²/day (for comparison the standard dose of rituximab is 375 mg/m² per treatment cycle; varies from 1-3 weeks). A number of toxicities were observed in treated patients despite pre-medication with methylprednisolone including sepsis (fatal in one patient), renal acidosis and neurological deficits (all reversible on discontinuation of treatment), although no patient demonstrated the clinical features of a cytokine-release syndrome. The significant toxicities observed in this trial demonstrate the potential risk of activating very large numbers of T cells although this is in the context of extremely promising clinical results. Through a combination of extremely low doses given as a continuous infusion with prophylactic corticosteroids, the toxicity profile of this construct is tolerable for the majority of patients.

Further studies of the anti-CD3 x anti-CD19 BiTE Ab are being undertaken in acute lymphoblastic leukaemia while the anti-CD3-anti-EpCAM Ab is being evaluated clinically in patients with adenocarcinoma as described in chapter 7.

1.6 Retargeting Specific Populations of T Cells

Owing to the potential ability of anti-CD3 moiety-containing bispecific antibodies to activate all T cells with the associated toxicity, the concept of T cell retargeting has been refined to try and activate and retarget only a specific population of cytotoxic (CD8⁺) T cells. Populations of CTLs can be defined by the pMHC specificity of the TCR through which they are activated: This mechanism of activation can be exploited to retarget a specific population by designing a bivalent molecule which contains a recombinant MHC class I molecule presenting a specific peptide, and an Ab fragment specific for a cell surface tumour Ag. Using this mechanism, CTLs specific for the pMHC component of the retargeting molecule can be redirected to kill a tumour cell expressing a non-cognate Ag i.e. the Ag targeted by the Ab component of the retargeting construct.

The most well-defined Ag-specific populations of CTLs are those directed against peptides derived from the common viruses highly prevalent throughout the population. There exists a growing body of literature describing 'immunodominant' peptides for the almost ubiquitous herpes viruses EBV and CMV³⁷⁸ (and other common viruses such as influenza³⁷⁹) presented by different MHC class I alleles. Of relevance to retargeting, the herpes viruses produce lifelong latent infection (in the absence of immunosuppression) and maintain a detectable circulating population of either CD8⁺ memory³⁸⁰ or effector T cells.³⁸¹ Populations of virus-specific CD8⁺ T cells have therefore been a starting point for many retargeting strategies owing to their widespread prevalence against a relatively restricted repertoire of peptides.

1.6.1 Multi-step T cell retargeting

The earliest report of retargeting viral peptide-specific CTLs to tumour cells was by Ogg *et al*:³⁸² Human (h) CD20⁺ (MHC class Γ) tumour cells were coated with a biotinylated anti-hCD20 mAb which was linked via an avidin bridge to biotinylated HLA-A2 monomers presenting an HIV gag-derived peptide. This three step labelling process (illustrated in Figure 1.13 **A**) subsequently allowed CTLs with a TCR specific for the HLA-A2 restricted HIV gag protein-derived peptide to lyse hCD20⁺ cells. The use of an MHC class Γ target cell line prevented transfer of gag peptide from the monomer directly onto the tumour cell which would also result in target cell lysis.

This unwieldy three-step labelling process was refined by the same investigators to a two-step method by using a tetrameric complex consisting of four anti-hCD20 scFv molecules genetically fused to streptavidin (B9E9-SA).³⁸³ This can then combine directly with biotinylated pMHC (demonstrated in Figure 1.13 **B**). Both viral (e.g. EBV and influenza) and

tumour Ag (e.g. MART-1/Melan-A) derived HLA-A2-restricted peptides have been presented using this system and are able to mediate lysis of hCD20⁺ target cells by CTLs specific for the particular peptide presented. A similar two-step retargeting method was developed by Robert *et al*: Fab' molecules specific for CEA, ErbB-2 receptor and hCD20 were chemically conjugated to streptavidin and then complexed with biotinylated HLA-A2-flu peptide monomer. CTLs specific for this pMHC were subsequently able to lyse malignant bowel, breast and B cells. Because of the presented of the presented of the particular peptides are subsequently able to lyse malignant bowel,

Mous *et al* have used this two-step retargeting system in a pre-clinical model for chronic lymphocytic leukaemia (CLL): They demonstrated that a patient's own CMV-peptide specific CTLs can be expanded and then redirected against their malignant hCD20⁺ B cells using a retargeting complex consisting of B9E9-SA and an appropriate pMHC for their haplotype³⁸⁶. The data suggest that lysis via the retargeting complex is as efficient as that seen when CMV peptide is loaded directly onto the surface of B-CLL cells and thus presented by autologous HLA molecules.

The two-step retargeting system has also been evaluated in several *in vivo* models: *scid* mice injected intraperitoneally with Daudi cells (hCD20⁺, MHC Class Γ lymphoma cell line) precoated with B9E9-SA and biotinylated pMHC were protected from developing tumour if simultaneously inoculated intraperitoneally with human CTLs specific for the pMHC coating the tumour.³⁸⁷ In a separate model, wild type C57BL/6 mice were adoptively transferred with OT-1 CTLs (transgenic TCR clone with specificity for H2K^b presenting *SIINFEKL*, a peptide derived from the model Ag OVA) which were then activated by OVA / anti-CD40 mAb immunization. B16 melanoma cells stably transfected with hCD20 (B16hCD20), pre-coated with B9E9-SA and either pMHC presenting *SIINFEKL* or an irrelevant peptide, were then administered intravenously to the mice. Mice who received B16hCD20 cells coated with an irrelevant peptide went on to develop multiple pulmonary metastases whereas those who received tumour coated with pMHC presenting *SIINFEKL* developed only occasional pulmonary metastases illustrating the potential of this system to retarget endogenous CTLs³⁸⁸ (albeit initially derived from adoptive transfer).

While certainly proving proof-of-principle that CTLs can be retargeted to malignant cells expressing non-cognate Ags, this two-step retargeting system has some limitations: It involves a large multivalent molecule which may have suboptimal tissue penetrance compared to a smaller single molecule. However in a recent phase I clinical trial of B9E9-SA in combination with biotinylated ⁹⁰yttrium as treatment for non-Hodgkin's lymphoma tissue penetrance of the radioactive moiety appeared reasonable. ³⁸⁹ Of greater concern is the

immunogenicity of the biotin / streptavidin complex: Trials of a streptavidin-conjugated Ab / biotin-labelled ⁹⁰yttrium system in metastatic colon cancer have shown that development of antibodies against the various components is almost inevitable, ³⁹⁰ (providing the patient is not too immunosuppressed to mount an immune response) which would limit the scope for retreatment.

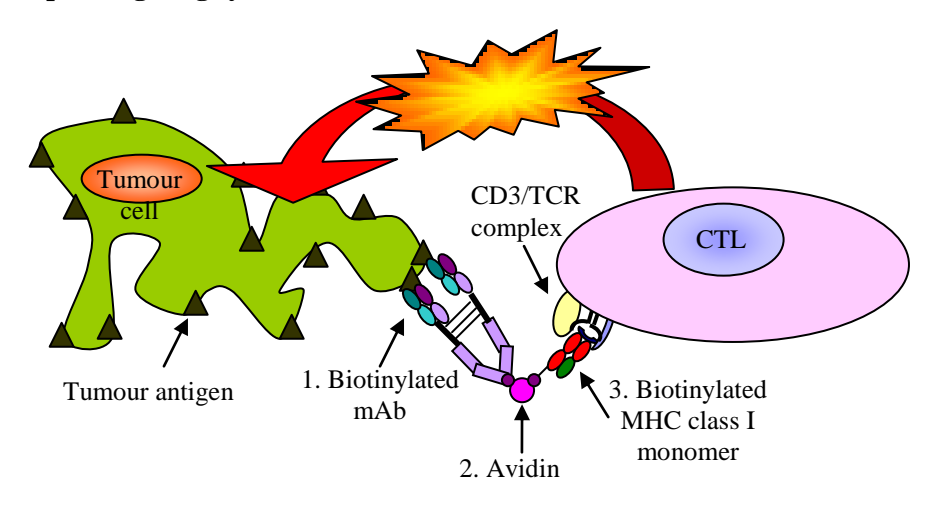
1.6.2 One step T cell retargeting

To circumvent some of the problems associated with a multi-step retargeting system Robert *et al* have refined their system into a single molecule consisting of a Fab' fragment conjugated to a pMHC monomer via a bismaleimide linker, ³⁹¹ (illustrated in Figure 1.13 C). This 95 kDa molecule was able to redirect CTLs specific for an HLA-A2-flu peptide to lyse tumour cells expressing either hCD20, ErbB-2 or CEA *in vitro*, providing the HLA-A2-flu pMHC monomer was conjugated to the appropriate Fab'.

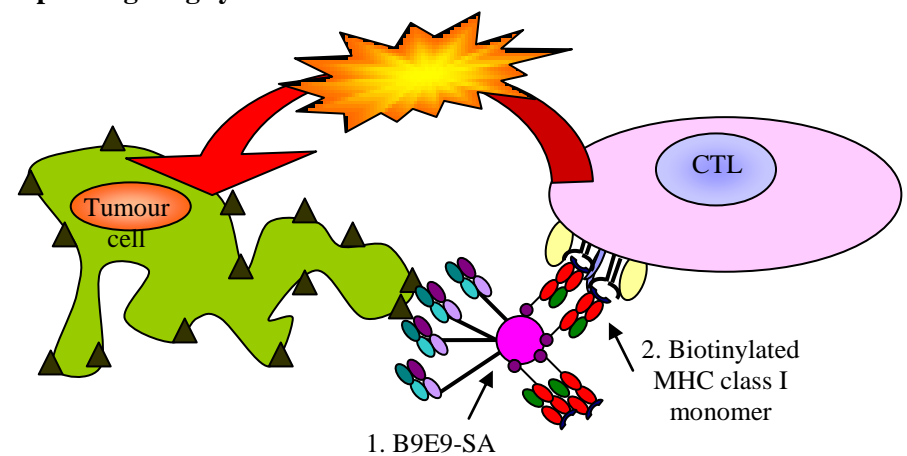
This construct has also been evaluated *in vivo*: H2K^b/SIINFEKL has been conjugated to a high affinity anti-CEA Fab' and injected into OT-1 transgenic mice grafted subcutaneously with syngeneic MC38-CEA⁺ colon carcinoma cells. Mice receiving pMHC/Fab' injections demonstrated significant inhibition of tumour growth compared to mice who received unconjugated anti-CEA Fab', with some of the treated mice remaining tumour free for 30 days. ³⁹²

In a separate model, C57BL/6 mice were adoptively transferred with OT-1 cells which were then activated: Once the peak of the primary immune response had receded (in order to exclude a non-specific cytokine-mediated anti-tumour response) the mice were grafted subcutaneously with MC38-CEA⁺ colon carcinoma cells. Treatment with anti-CEA Fab' x H2K^b/SIINFEKL started once nodules of the tumour were palpable (~8 days after engraftment). Again, mice which received the pMHC/Fab' conjugate showed inhibition of tumour growth compared to those that received only the anti-CEA Fab', even though treatment was delayed until the tumour was established.³⁹² The ability of this construct to retarget a diminishing CTL response suggests the conjugate has some ability to activate CTLs *in vivo* which as discussed later is of clinical significance (section 7.2).

A 3-step retargeting system



B 2-step retargeting system



C Single retargeting molecule

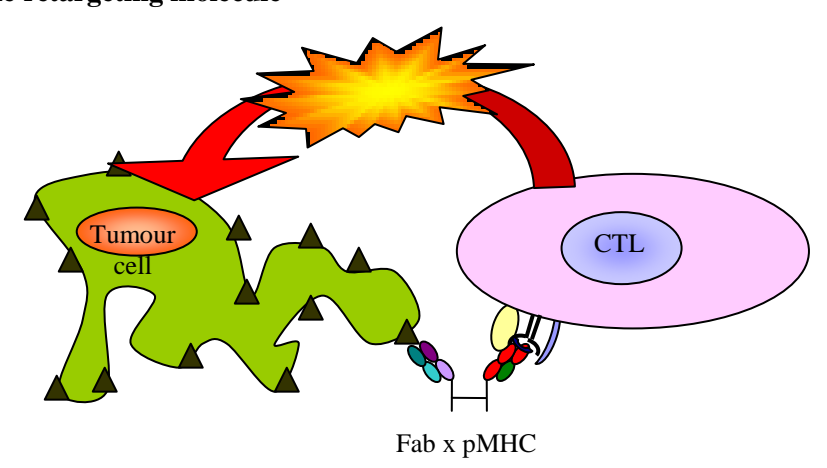


Figure 1.13: Different retargeting system designs

 ${\bf A}$ shows the three-step system used by ${\bf Ogg}$ et al, ${\bf B}$ the two-step system of Savage et al and ${\bf C}$ the single retargeting molecule of Robert et al. Further details of each system are given in the text.

Studies have also shown that endogenously generated anti-viral peptide-specific CTLs can be retargeted to tumour cells *in vivo*: B6 mice infected with lymphochoriomeningitis virus (LCMV) generate a significant population of CTLs specific for the H2D^b restricted peptide GP33-41. Infected mice grafted with MC38-CEA⁺ colon carcinoma cells coated with anti-CEA Fab' x H2D^b/GP33-41 peptide are able to eliminate a majority of the tumours whereas grafts coated with anti-CEA Fab' alone invariably grow.³⁹³ A similar anti-tumour response was seen in experiments using influenza-infected B6 mice, B16-HER2⁺ melanoma cells, and an anti-HER2 Fab' x H2D^b/flu peptide retargeting molecule: Infected mice which received tumour coated with the retargeting molecule developed far fewer lung metastases than those who received tumour coated with the anti- HER2 Fab'.³⁹³

In a slightly more physiological model LCMV infected mice received uncoated MC38-CEA⁺ colon carcinoma grafts on the flank and one day later received a course of injections of the H2D^b/GP33-41 retargeting molecule or anti-CEA Fab'. Mice which received the anti-CEA Fab' all went on to develop palpable tumours whereas most of those receiving the retargeting molecule remained tumour free. ³⁹³ Of note is the fact that the GP33-41 peptide presented by the MHC class I molecule was photo-cross-linked to H2D^b, thus preventing its dissociation and replacement by another peptide *in vivo*: Covalent attachment of the peptide to MHC class I will be discussed later when considering optimal design of the retargeting molecule.

A one-step T cell retargeting process has also been pursued by Reiter *et al*, although rather than linking pMHC to a Fab' via chemical means they have used various levels of genetic fusion to join the components. They initially produced a fusion protein containing the V_L domain of an anti-CD25 Ab, the extracellular domains of HLA-A2 and β₂microglobulin linked via glycine/serine linkers. This was refolded under reducing conditions in the presence of the anti-CD25 V_H region and HLA-A2 restricted peptides derived from the melanoma Ag gp100.³⁹⁴ Owing to the presence of engineered cysteine residues in the Ab V_H and V_L regions the two chains became covalently linked via a disulfide bond creating the complete retargeting molecule. This molecule was able to redirect human CTLs specific for the HLA-A2 restricted gp100 derived peptides and cause lysis of CD25⁺ cells both *in vitro* and *in vivo* in a tumour model involving human xenografts in *nude* mice.³⁹⁴

A later derivative of this construct consisted of an anti-CD25 scFv genetically linked to HLA-A2 and β_2 microglobulin and refolded in presence of either gp100 or EBV derived peptides, which was able to retarget CTLs of appropriate specificity to lyse CD25⁺ positive tumour cells both *in vitro* and *in vivo*.³⁹⁵ A retargeting construct of similar structure but containing a

scFv derived from the anti-EGFR mAb cetuximab has also been produced³⁹⁶ which is able to mediate *in vitro* and *in vivo* elimination of EGFR-expressing tumour cells by CTLs specific for the peptide presented by the retargeting molecule.

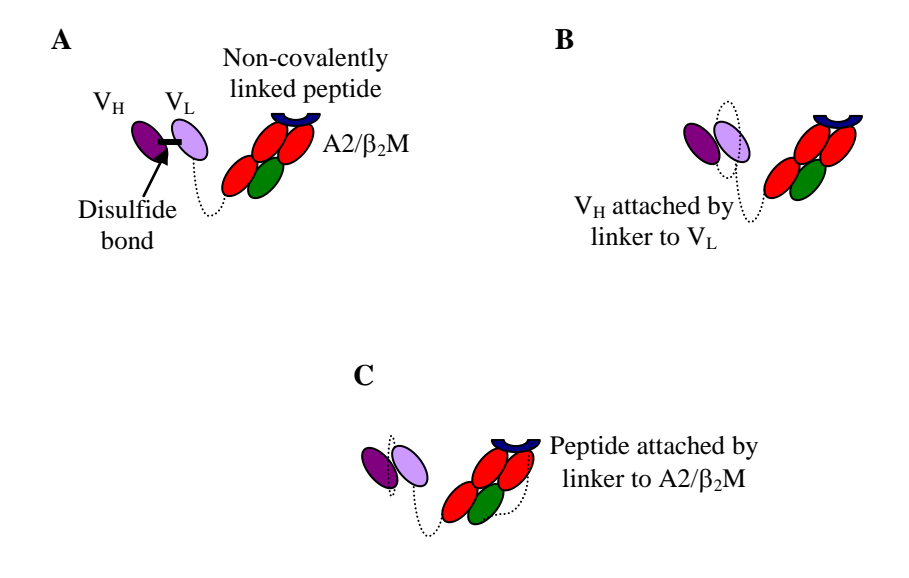


Figure 1.14: Various single-step retargeting molecule designs (Reiter et al) In A the peptide is non-covalently attached and the V_H domain is linker via a disulfide bond. In B V_H is genetically fused to V_L via a flexible linker. In C the peptide is covalently attached to the $A2/\beta_2M$ complex via a flexible linker.

A further variant of this construct involves peptide (either derived from EBV or the melanoma differentiation Ags gp100 or MART1) being genetically fused to the above molecule so all elements of the construct are covalently linked.³⁹⁷ Figure 1.14 demonstrates the evolving structure of these retargeting molecules. *In vitro* experiments with this molecule has shown efficient lysis of CD25⁺ tumour cells by CTLs specific for the peptide presented by the retargeting molecule.³⁹⁷

1.6.2.1 Covalent versus non-covalent linkage of peptide

The above descriptions demonstrate that there are three main areas in which the retargeting complexes produced thus far differ; the structure of the Ab component (Fab' versus scFv), the mechanism of joining the Ab and MHC class I components (genetic fusion versus maleimide linkage) and the linkage status of the peptide (covalent or non-covalent linkage). The structure chosen for the Ab component needs to both allow binding of the target Ag *in vivo* with sufficient affinity to allow retargeting and not itself be immunogenic. Likewise, the mechanism of linking the two components must be non-immunogenic and permanent. As yet little work has been done comparing the relative efficacies of different Ab moiety structures and linkage methods. Although producing the two arms of the molecule separately

and then linking them via chemical means, is a more efficient method of expression (it allows a 'mix and match' approach to the pairing of MHC and Ab derivative arms), it may be that a more flexible molecule produced by genetic linkage has greater efficacy (as observed with the BiTE BsAb format)³⁷⁷ due to closer apposition of the CTL and target cell.

The method of peptide linkage (covalent versus non-covalent) however, does have some wider implications: If the MHC class I arm of the molecule is produced without a covalently attached peptide it is clearly more versatile as it can be refolded around any suitably restricted peptide and therefore a single construct has the potential to retarget many different populations of CTLs. However, if the peptide is non-covalently attached it has the potential to dissociate and be replaced by another peptide, thus removing its ability to retarget the intended population of CTLs. In addition, there is evidence that the dissociated peptide can be transferred to MHC class I on CTLs which mean they can present peptide to naïve CD8⁺ T cells causing their activation.

This transfer phenomenon was first suggested by investigations into whether monomeric pMHC was sufficient to activate CTLs. The murine 2C TCR recognizes both the allogeneic pMHC QL9-L^d and the autologous pMHC SIY-K^b. Although tetramers of both pMHCs can activate 2C-expressing CTLs, only monomeric pMHC expressing the same MHC class I as the CTLs (pMHC SIY-K^b) can activate the CTLs, consistent with peptide transfer to the CTL's K^b being necessary for activation. ³⁹⁸ This suggestion was supported by the finding that K^b negative CTLs expressing the OT-1 TCR could not be activated by pMHC K^bSIINFEKL. ³⁹⁹ In a further experiment green fluorescent protein (GFP) expressing 2C CTLs were incubated with pMHC SIY-K^b. These cells were then washed to remove the pMHC SIY-K^b and subsequently incubated with GFP 2C CTLs. The GFP 2C CTLs became activated despite never being directly exposed to the appropriate pMHC, suggesting the transfer of peptide from pMHC to CTLs. ³⁹⁸

Although the activation of CTLs by pMHC *in vivo* by whatever mechanism could be seen as an advantageous function of the retargeting molecule, the presence of target peptide on a CTL's surface can also render it a target for elimination by other CTLs; so-called fratricide. This has been reported when peptide is loaded directly onto a CTL's MHC class I, 400 albeit at very high concentrations of peptide, far higher than those likely to be generated by peptide dissociating from the retargeting molecule. Mechanistic experiments have shown that this cytolysis is dependent on the perforin-mediated killing pathway rather than Fas:FasL interactions. 401

Given the potential problems of peptide dissociation, covalent linkage of the peptide to the MHC class I molecule has been favoured by a number of investigators: One method involves refolding the MHC class I molecule with an altered photo-reactive amino acid residue which on exposure to UV (ultraviolet) irradiation is photo-crosslinked into the peptide-binding groove. Another mechanism involves genetically fusing the peptide to β_2 microglobulin and the MHC class I heavy chain via flexible linkers as favoured by Reiter. This peptide- β_2 microglobulin-heavy chain complex is known as a single-chain trimer (SCT) and has been used by other investigators both for CTL activation and as a vaccine to generate peptide specific CTLs as described below.

1.6.2.2 Single chain trimer design and applications

The earliest description of any type of SCT complex was by Mottez *et al* who, in contrast to Reiter's approach, joined the components in the order peptide-*heavy chain*-β₂microglobulin. They produced a soluble Cw3 peptide-K^d-β₂microglobulin molecule which was able to activate a T cell hybridoma specific for the Cw3 peptide *in vitro*. The first studies of the more extensively investigated peptide-β₂microglobulin-heavy chain SCT format were by Vest Hansen *et al*: They expressed an SCT molecule on the surface of filamentous phage that although the complexes could be recognized by conformation-specific monoclonal antibodies with 'TCR-like' specificity, it was impossible to show interaction with specific T cells using either labelling or stimulation techniques. The authors felt this finding may be related to lack of expression of sufficiently high numbers of correctly folded complexes on any one phage.

The first description of a functionally active SCT of this format was by the group of T Hansen who produced an SCT of the OVA-derived peptide SIINFEKL linked to murine β_2 microglobulin and the mature K^b heavy chain via flexible glycine/serine linkers. They demonstrated using flow cytometry that following transfection it was expressed at the cell surface and rendered the cells susceptible to lysis by CTLs specific for the expressed peptide (OT-1 cells). They also demonstrated that SCT-expressing cells could act as APCs to stimulate specific CTL responses *in vitro* and vaccination of mice with a plasmid encoding the SCT resulted in production of antibodies specific for the protein complex, indicating it can be expressed *in vivo*.

This group has gone on to express several different murine and human SCTs and has refined the design to improve the stability of the complex. The linker length between the three components has been optimized to achieve the best recognition by specific CTLs.⁴⁰⁴ The

interaction of the antigenic peptide with the binding groove has been examined as unlike the MHC class II peptide-binding site which has an open conformation at both ends, the class I site is closed at both ends. This makes accommodation of the linker potentially problematic as it destroys some of the conserved interactions of the heavy chain with the C terminus of the peptide. However, peptide displacement experiments have suggested that due to the tethering effect of the linker the peptide is able to continuously dissociate and then rebind, ⁴⁰⁵ a phenomenon which compensates for the abolition of these interactions.

In the murine SCT, substitution of an alanine for a tyrosine residue at position 84 in the heavy chain (forms part of the F pocket of the peptide binding groove) improves recognition by specific CTLs (crystal structures suggests the tyrosine side group obstructs the glycine/serine linker), although this modification appears to make no difference in the human HLA-A2 SCTs evaluated. To enhance retention of the peptide within the binding groove, disulfide trapping has been utilised which involves mutating this tyrosine residue to a cysteine, in combination with substituting the second glycine in the peptide β_2 microglobulin linker for a cysteine. This allows the two substituted cysteines to form a disulfide bond, effectively trapping the peptide in the binding groove, preventing dissociation and subsequent reoccupation by an exogenous peptide. 406

Direct comparison of these three 'generations' of *SIINFEKL*- K^b SCT constructs reveals the 'disulfide-trap' version is 1000 times more resistant to exogenous peptide binding compared to the earlier molecules whilst all three are recognized in a similar fashion by OT-1 cells. 407 Similar resistance to exogenous peptide binding, whilst maintaining function, has been demonstrated for human SCTs which employ a disulfide-trap. 408 In addition to being used to stain specific CTLs, generate anti-MHC/peptide antibodies *in vivo* and stimulate specific CTLs *in vitro*, the major application of SCTs described in the literature is as vaccines. The first description involved vaccinating HLA-A2/hCD8 double transgenic mice with a plasmid encoding a human HLA-A2/mammaglobin A (breast cancer Ag) peptide SCT. 409 This produced significant expansion of specific CTLs (as determined by ELISPOT assay) which were able to produce specific lysis of HLA-A2+/mammaglobin A+ breast cancer cell lines *in vitro*.

In another model, mice were vaccinated with a plasmid encoding a murine K^b SCT expressing a peptide derived from the E6 Ag of HPV type 16. ⁴¹⁰ This produced higher frequencies of E6 peptide-specific CTLs compared to vaccination with a plasmid containing the full length E6 Ag and provided protection when mice were challenged with TC-1 cells (HPV-16 E6-expressing murine tumour line). Vaccination with this construct also caused a reduction in the

size of established TC-1 tumours. Similar protection was seen with a plasmid encoding an HLA-A2 SCT expressing a peptide from human mesothelin (expressed on over 95% of ovarian tumours);⁴¹¹ when mice were challenged with TC-1 cells transfected with HLA-A2 and mesothelin. The SCT format is also being investigated for its potential in viral vaccines and has been used to produce specific CTLs *in vivo* in mice against peptides derived from hepatitis B,⁴¹² influenza⁴¹³ and coronavirus⁴¹⁴ (cause of severe acute respiratory syndrome; SARS).

Therefore over the last decade retargeting CTLs against non-cognate (tumour) Ags has gradually been investigated as a concept and the process has evolved from unwieldy multistep systems to a single molecule. In addition to *in vitro* data demonstrating that populations of peptide-specific CTLs can be retargeted to lyse tumour cells expressing non-cognate Ags, there is evidence that murine CTLs (either adoptively transferred of generated endogenously) can be retargeted *in vivo* to suppress tumour growth. Therefore further investigation of this therapeutic strategy which exploits the cytotoxic potential of CTLs whilst circumventing the problem of tumour Ag-specific tolerance is warranted.

1.7 The Current Study

The published *in vivo* data pertaining to peptide-specific CTL retargeting presently falls into two categories; experiments where human peptide-specific CTLs are retargeted against human tumours in immunodeficient mice³⁹⁴ and studies where murine peptide-specific CTLs (either adoptively transferred or generated endogenously) are redirected against murine tumours usually ectopically expressing human tumour Ags.³⁹² The development of HLA-A2 transgenic mice (e.g. HHD mice; H-2D^{b-/-} β_2 m^{-/-} double knockout, human β_2 m /HLA-A2 $\alpha_1\alpha_2$ -mouse H-2D^b α_3 transgenic)⁴¹⁵ allows the possibility of generating an endogenous CTL response within a mouse specific for peptides restricted to human HLA-A2.⁴¹⁶ This 'human' CTL response can then be retargeted *in vivo* in a more immunologically intact organism than the *scid* mice currently used.

The focus of this study was to produce a retargeting construct capable of redirecting a population of 'human CTLs' to kill tumour cells which ultimately could be evaluated in human class I transgenic mice in which an appropriate endogenous CTL response had been generated. The availability of HLA-A2 transgenic mice and the frequency of this allele within the Caucasian population⁴¹⁷ meant this was chosen as the class I allele for the retargeting construct. The high prevalence of CMV immunity⁴¹⁸ coupled with the observation that significant numbers of virus-specific CTLs can be detected particularly in the elderly⁴¹⁹ meant the HLA-A2 restricted immunodominant CMV pp65 (virion tegument protein) -derived peptide *NLVPMVATV* was considered a suitable peptide for inclusion in a retargeting molecule.

This peptide is also the target Ag of an experimental vaccine being developed within the division that potentially could provide a suitable method by which to generate an endogenous *NLVPMVATV*-specific CTL response for retargeting within HHD mice. As yet no *in vivo* studies have been published within the literature using a retargeting construct containing this peptide despite its immunodominance and the high frequency of *NLVPMVATV*-specific CTLs amongst HLA-A2⁺ CMV⁺ individuals. However, some pre-clinical *in vitro* work has been undertaken by Mous *et al*³⁸⁶ to retarget CTLs of this specificity to lyse B-CLL cells using the two-step system of Savage.³⁸⁴

The tumour Ag chosen for initial experiments was hCD20, a transmembrane protein⁴²⁰ found on both normal and malignant B cells (i.e. in Non Hodgkin's lymphoma and chronic lymphocytic leukaemia) which regulates calcium flux across the cell membrane. The targeting of this Ag by mAb is the focus of much work in our laboratory; therefore many anti-hCD20

mAbs and hCD20⁺ tumours were available for use in the retargeting molecule and its evaluation respectively. The choice of this Ag also allows comparison of the efficacy of retargeting CTLs with mAbs (e.g. rituximab) which at present is the gold-standard of immunotherapy in hCD20⁺ malignancies. Although the need for new therapeutic approaches is arguably greater in solid tumours rather than hCD20⁺ malignancies, changing the tumour Ag specificity of the retargeting construct will not be difficult as it is to be made by the chemical conjugation of pMHC and Fab' components.

As proof of principle we planned to first generate *NLVPMVATV*-specific CTL lines *in vitro* and confirm their cytotoxic phenotype by redirecting these to lyse hCD20⁺ tumour cells using the two-step retargeting system of Savage.³⁸⁴ We then planned to investigate the design and production of the retargeting construct including expression of the recombinant MHC molecule in mammalian cells to allow the inclusion of an Fc region; this should increase half-life of the retargeting construct by allowing recycling via the neonatal FcR.⁴²¹ We also intended to investigate production of the pMHC component in an SCT format within bacterial cells and the subsequent refolding and purification steps necessary using this approach.

Once sufficient quantities of the pMHC arm of the retargeting construct was produced we planned to conjugate it chemically to an anti-hCD20 Fab' and then evaluate the efficacy of the construct first *in vitro* and then *in vivo* using a variety of tumour protection and therapy models in HHD transgenic mice in which an endogenous anti-*NLVPMVATV* CTL response had been generated. If successful retargeting could be seen we planned to go on to investigate whether it was possible to retarget a memory CTL response and whether the retargeting construct itself was able to induce proliferation of *NLVPMVATV*-specific CTLs *in vivo*.

In the event that expression and production of the HLA-A2-*NLVPMVATV* pMHC construct was problematic it was decided that further evaluation of murine K^bSIINFEKL x hCD20 Fab' (available within our laboratory) would be undertaken.

Chapter 2: Materials & Methods

2.1 CTL Generation and Characterisation

2.1.1 Generating CTL lines

Cytotoxic T cells were grown in 'T cell medium' (TCM) consisting of RPMI 1640 medium containing 25 mM HEPES (Invitrogen, UK), further supplemented with 2 mM L-glutamine, 1 mM pyruvate, 100 U/ml penicillin, 100 μ g/ml streptomycin (all Invitrogen, UK), 50 U/ml amphotericin B (Squibb & Sons, UK) and 10% human AB serum (Sigma, UK) at 37 °C in 5% CO_2 in a Hera Cell 240 Incubator.

2.1.1.1 Isolation of peripheral blood mononuclear cells (PBMCs)

CMV and HLA status of donors was confirmed by local microbiology and tissue typing laboratories respectively. After obtaining informed consent, 60 ml of blood from CMV⁺ HLA-A2⁺ donors was collected via peripheral venesection into preservative-free heparin. Heparinised blood was layered in a 1:1 ratio onto the density gradient separation medium Lymphoprep (Axis Shield, UK) and centrifuged for 10 min at 2,000 rpm in a Sorval RT7 Plus centrifuge with the brake off, allowing collection of PBMCs from the Lymphoprep: serum interface. PBMCs were washed in sterile phosphate buffered saline (PBS, Lonza, UK), resuspended and counted using a Coulter Industrial D Cell Counter (Coulter Electronics, UK) and either used immediately to generate *NLVPMVATV*-peptide specific CTL lines, or frozen at -80 °C (cells frozen in L-glutamine-containing RPMI 1640 medium supplemented with 15% human AB serum and 10% dimethyl sulfoxide (DMSO)) for later use.

2.1.1.2 *NLVPMVATV* peptide stimulation of PBMCs

The method used to generate CTL lines specific for the HLA-A2 restricted peptide *NLVPMVATV*, derived from the CMV tegument protein pp65, was adapted from that of Ghei *et al*⁴²² and Lee *et al*⁴²³. PBMCs were suspended in TCM at a concentration of 3x10⁶/ml and 2 ml added per well to a 24 well plate. 3 μg/ml *NLVPMVATV* peptide (Protein Peptide Research, UK; dissolved in DMSO to a stock concentration of 5 mg/ml) was added (i.e. 1 μg/10⁶ cells) at culture initiation. After 3 days (and thereafter twice weekly) cultures were supplemented with 25 U/ml IL-2 (VWR, UK). Every 14 days CTLs were restimulated with *NLVPMVATV* peptide and irradiated (60 Gy) autologous PBMCs at a 1:1 ratio to *NLVPMVATV*-specific CTL. The absolute number per culture of *NLVPMVATV*-specific CTL was calculated using the following formula;

Once the number of *NLVPMVATV*-specific CTLs per culture had been determined, half the medium was removed and replaced with fresh TCM containing an equal number of irradiated autologous PBMCs in addition to *NLVPMVATV* peptide and IL-2 to give a final concentration of 3 µg/ml and 25 U/ml respectively.

2.1.2 CTL characterisation

2.1.2.1 Flow cytometry

The generation of *NLVPMVATV*-specific CTL lines was monitored using flow cytometric analysis by staining with anti-hCD8 allophycocyanin (APC)-conjugated Ab (BD Biosciences, UK) and phycoerythrin (PE)-conjugated HLA-A2-*NLVPMVATV* tetramer (Beckman Coulter, UK). The generic method for staining cells for flow cytometric analysis is as follows; ~1x10⁶ cells were suspended in 100 µl PBS in a 5 ml polystyrene round-bottomed tube (BD Biosciences) and staining Ab/ tetramer was added as per manufacturer's recommended concentrations (usually 10 µg/ml). After a 15 min incubation at room temperature (RT) or 4 °C (temperature dependent on both cell and Ab identity), cells were washed with PBS/BSA/Azide (PBS containing 1% w/v Bovine Serum Albumin fraction V (Wilfred Smith Ltd, UK) and 20 mM sodium azide). Flow cytometry was performed on a FacsCalibur (BD Biosciences) and data was analysed using Cell Quest Pro software.

2.1.2.2 Cytotoxicity assay using a two-step retargeting system

The cytotoxic potential of *NLVPMVATV*-specific CTL lines was examined using a two-step retargeting system as demonstrated in Figure 1.13 **B**. Cells of the human lymphoblastoid CD20⁺ MHC class Γ Daudi cell line (maintained in RPMI 1640 supplemented with L-glutamine, pyruvate and 10% foetal calf serum (FCS, Lonza)) were used as targets. 10⁷ growing Daudi cells were pelleted, had all supernatant removed and were resuspended in 100 μl ⁵¹Chromium (dissolved in sterile saline, GE Life Sciences, UK) and incubated at 37 °C in a water bath for 1 h. After being washed twice in PBS they were labelled with B9E9-SA (a tetrameric anti-hCD20 scFv/streptavidin complex, kind gift of P Savage, Imperial College, London, UK) by resuspending in 0.5 ml PBS containing 5 μg/ml B9E9-SA. Following a 30 min incubation at RT, target cells were washed with PBS to remove unbound B9E9-SA.

B9E9-SA-coated targets were then resuspended in either PBS or 0.5 μg/ml *NLVPMVATV* or *SLYNTVATL* (derived from HIV gag protein) peptide-containing biotinylated HLA-A2 monomer (Sanquin, Netherlands) diluted in PBS. After a 30 min incubation at RT, coated Daudi cells were washed to remove unbound monomer and resuspended in TCM. Cells were counted using a neubauer haemocytometer and trypan blue exclusion. The concentration of

viable Daudi cells was adjusted to $5x10^4$ /ml and 100 μ l was added per well (i.e. 5000 targets per well) to a round-bottomed 96 well plate (Nunc, Denmark).

The percentage of 'effector' *NLVPMVATV*-peptide specific CTLs was determined using flow cytometry (see section 2.1.2.1), and used to determine the absolute number of cells required to be added per well to give effector: target ratios of 0.5-5:1. Effectors were added in 100 μ l TCM per well. To determine spontaneous target cell lysis TCM alone was added to some wells. Plates were centrifuged at 800 rpm for 2 min to ensure mixing of targets and effectors and then incubated at 37 °C / 5% CO₂ for 4 h. Target cells in positive control wells (lack effectors) were then completely lysed by the addition of 100 μ l NP40. Plates were centrifuged at 1,500 rpm for 5 min and 100 μ l of the supernatant harvested and transferred to flat-bottomed polytubes (Thermo Scientific, UK) for analysis on a Wizard 1470 Automatic Gamma counter (Perkin Elmer, UK). The percentage of target cell lysis per well was calculated using the following formula:

Percentage target cell lysis per well	=	Counts per well	Counts per negative control well (spontaneous lysis)	x 100
		Counts per positive control well (total lysis)	Counts per negative - control well (spontaneous lysis)	

2.2 Mammalian Construct Production and Characterisation (Human)

2.2.1 Genetic engineering of constructs

The designs of the different mammalian constructs produced are shown in Figure 2.1.

2.2.1.1 pcDNA3.1-HLA-A2-human IgG₁ hinge-Fc

The DNA sequence encoding the signal peptide and three extracellular domains (α_1 - α_3) of HLA-A2 was amplified by polymerase chain reaction (PCR) from cDNA synthesised from mRNA extracted from PBMCs from the blood of an individual known to express the HLA-A2 MHC class I allele.

Isolation of mRNA from blood

Blood was collected into heparin via peripheral venesection of an HLA-A2 positive donor after informed consent. mRNA was isolated from the PBMCs using the Aqua Pure RNA blood kit (Bio-Rad, UK) as per manufacturer's instructions and resuspended in RNA rehydration solution (20 μ l per pellet). After rehydrating on ice for 30 min, mRNA was reprecipitated by mixing with 10 μ l 3M sodium acetate, 10 μ l glycogen and 300 μ l 100% ethanol and incubating at -80 °C for 30 min. mRNA was pelleted by centrifugation at 16,000 g for 5 min before being resuspended in 20 μ l RNase free H₂O.

Synthesis of cDNA

cDNA synthesis was performed using the First-Strand cDNA synthesis kit (GE Life Sciences) as per instructions: 20 µl mRNA, 11 µl bulk 1st strand reaction mix, 1 µl primer solution and 1 µl DTT solution were mixed and incubated at 37 °C for 1 hr.

Polymerase Chain Reaction (PCR) amplification of DNA encoding HLA-A2 $\alpha_1\text{-}\alpha_3$ domains from cDNA

DNA encoding HLA-A2 α_1 - α_3 domains was amplified (with the insertion of flanking HindIII and SpeI restriction enzyme sites) using the above cDNA as template and the following primers (all primers throughout methods from Invitrogen, UK). Restriction enzyme sites are underlined. The PCR reaction was performed using the standard procedure with annealing temperature at 66 $^{\circ}$ C.

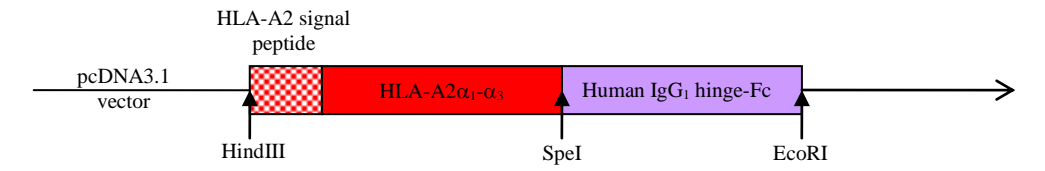
Sense 5' TTA AGC TTA TGG CCG TCA TGG CGC CCC GAA CCC T 3'

Hind III

Antisense 5' TGA CTA GTA TGG GGA TGG TGG GCT GGG AAG A 3'

SpeI

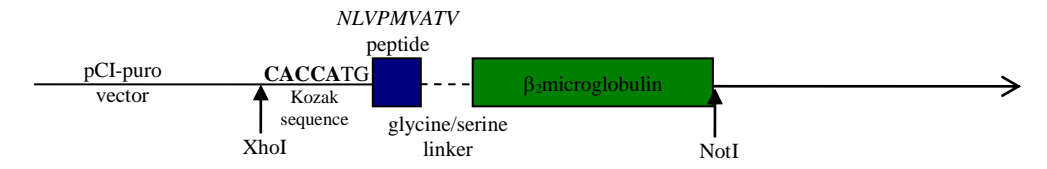
A: pcDNA3.1-HLA-A2-human IgG₁ hinge-Fc



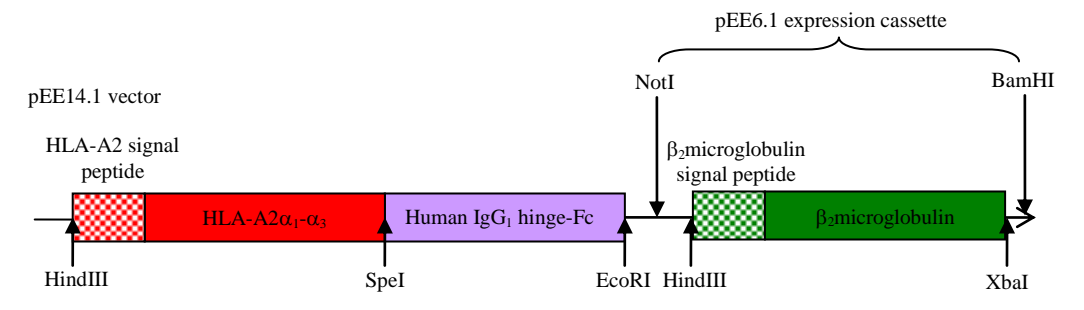
B: pCI-puro-β₂microglobulin



C: pCI-puro-CMV-(G₄S)₄-β₂microglobulin



D: pEE14.1-HLA-A2-human IgG₁ hinge-Fc/pEE6.1-β₂microglobulin



$E: Signal\ pIg\ plus-CMV-short\ linker-\beta_2 microglobulin-HLA-A2-biotin-AviTag$

Signal pIg plus vector

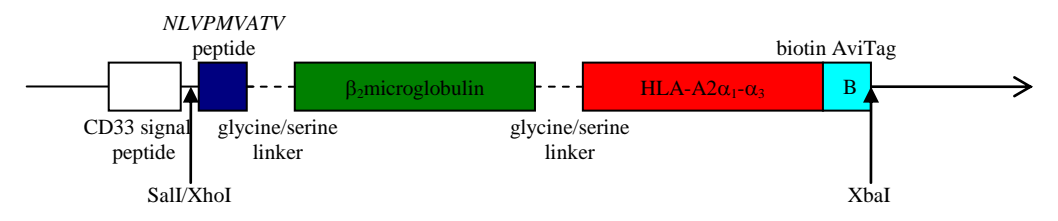


Figure 2.1: Design of genetic constructs for mammalian expression

Schematic representation of genetic constructs used for mammalian expression. Restriction enzyme sites used for sub-cloning into the various vectors are indicated.

Purification of HLA-A2 PCR product

Amplification of the appropriate PCR product was verified using electrophoresis on a 0.7% tris acetate EDTA (TAE; recipe in appendix 1) agarose gel containing ethidium bromide (0.5 μ g/ml) or gel red (Biotium, US) (1/20,000) to allow visualisation of DNA under UV light. PCR products were mixed with 6x Orange DNA Loading Dye (Fermentas, UK) in a 5:1 ratio prior to loading. PCR product size was determined via comparison to DNA markers (O'GeneRuler 1 kb DNA ladder, Fermentas). The PCR product was extracted from the agarose gel using the QIAEX II gel extraction kit (Qiagen, UK) as per the manufacturer's instructions and suspended in 20 μ l tris/EDTA (TE) buffer.

Ligation of HLA-A2 PCR product into pCR-Blunt II-TOPO vector

The extracted HLA-A2 PCR product was cloned into pCR-Blunt II-TOPO vector using the Zero Blunt TOPO PCR Cloning kit (Invitrogen). 4 μ l of purified PCR product was mixed with 1 μ l open vector and 1 μ l salt solution in a 15 ml round-bottomed Falcon tube (Becton Dickinson, UK) and incubated at RT for 5 min.

Transformation of TOP10 cells by pCR-Blunt II-TOPO-HLA-A2

TOP10 *E. coli* cells (Invitrogen) were pipetted over the above ligation reaction and incubated on ice for 30 min. Bacteria were heat-shocked by immersion in a water bath at 42 °C for 45 s before a 2 min incubation on ice. 500 μl of super optimal broth with catabolite repression (SOC) medium was added to the cells before growing for 1 hr at 37 °C Successfully transformed bacteria were selected by plating out cells on a kanamycin (50 μg/ml) -containing Luria-Bertani broth (LB) agar plate and grown overnight at 37 °C. Colonies were used to seed 10 ml cultures in LB/kanamycin (50 μg/ml) which were grown overnight at 37 °C in an orbital incubator.

Miniprep of pCR-Blunt II-TOPO-HLA-A2 plasmid

Bacterial cells from 10 ml overnight cultures were pelleted by centrifugation at 3,000 rpm for 5 minutes in a Mistral 3000i centrifuge and plasmids extracted into 50 µl of elution buffer using the QIAprep Spin Miniprep Kit (QIAGEN) as per manufacturer's instructions.

Restriction enzyme digestion of pCR-Blunt II-TOPO-HLA-A2

To confirm the plasmid contained the HLA-A2 gene insert a restriction enzyme digest was performed using HindIII and SpeI (all restriction enzymes obtained from Promega, UK). The standard digestion reaction used throughout the methods consists of 10 U of each restriction enzyme, 0.5-1.5 µg (i.e. 8-16 µl) of miniprep plasmid, 2 µl of 10x enzyme compatible buffer

and RNase free H_2O to give a final reaction volume of 20 μ l. The reaction was incubated at 37 °C for 1 hr before being analysed by gel electrophoresis on a 0.7% agarose gel.

Sequencing of pCR-Blunt II-TOPO-HLA-A2

Plasmids which upon HindIII/SpeI restriction enzyme digestion contained the appropriately sized insert underwent confirmatory sequencing using the BigDye Terminator v3.1 Cycle sequencing kit (Applied Biosystems, UK) and the following primers:

T7 5' TAA TAC GAC TCA CTA TAG GG 3' Sp6 5' ATT TAG GTG ACA CTA TAG 3'

Sequencing reactions were precipitated by mixing with 1 μ l 3M sodium acetate and 25 μ l 100% ethanol and incubating on ice for 10 min, before centrifugation at 16,000 g for 30 min at 4 °C. DNA was washed with 125 μ l 70% ethanol then resuspended in 10 μ l formamide. Sequencing was performed on a 3130x/ Genetic Analyzer (Applied Biosystems). Data was analysed using the SeqMan application of the DNASTAR Lasergene 6 software package. The sequence of HLA-A2 α_1 - α_3 domains was aligned against the HLA-A*0201 allele; AY365426 gene locus.

Sub-cloning of HLA-A2 extracellular domains' DNA into TOPO-human IgG_1 hinge-Fc vector

Human IgG_1 hinge-Fc was added to the C terminus of the HLA-A2 extracellular domains by sub-cloning these via HindIII/SpeI restriction sites into TOPO-human IgG_1 hinge-Fc vector; in house vector derived from TOPO vector (Invitrogen))which contains the human IgG_1 hinge Fc sequence (i.e. hinge, C_H2 and C_H3 domains) which aligns to the BC073782 gene locus,.

Transformation of JM109 *E. coli* cells with TOPO-HLA-A2-human IgG₁ hinge-Fc ligation reaction

The above ligation reaction was used to transform JM109 *E. coli* cells (Promega). Selection of successfully transformed bacteria was performed as before using kanamycin and insertion of the desired DNA confirmed Hind III/SpeI digestion.of plasmids.

Sub-cloning of HLA-A2-human IgG₁ hinge-Fc into pcDNA3.1 vector

1 μg of TOPO HLA-A2-human IgG₁ hinge-Fc plasmid and pcDNA3.1 vector plasmid (Invitrogen) underwent a Hind III/EcoR1 digest with the resulting DNA products being ligated and used to transform JM109 *E. coli*. Successfully transformed bacteria were selected

using LB-ampicillin plates (100 μg/ml), expanded and after plasmid extraction, insertion of the HLA-A2-human IgG₁ hinge-Fc fusion gene confirmed by Hind III/EcoRI digest.

Sequencing of pcDNA3.1-HLA-A2-human IgG₁ hinge-Fc

Plasmids which contained an appropriately sized insert upon Hind III/EcoR1 digestion were sequenced using the following primers:

T7 & Sp6 as before
A2 new I 5'
Hu hinge 5'
Fc I 5'
A2 new I 3'
A2 new I rev 3'
Hu hinge 3'
S' GAT ACC TGG AGA ACG GGA AG 3'
5' CTT CTG GAC AGG AGC AGA GA 3'
5' AGC AGT ACA ACA GCA CGT AC 3'
5' TAA TCC TTG CCG TCG TAG GC 3'
5' ATG GGG ATG GTG GGC TGG GA 3'
5' TGC ACT TGT ACT CCT TGC CA 3'

Maxiprep of pcDNA3.1-HLA-A2-human IgG₁ hinge

A bacterial culture shown by DNA plasmid sequencing to contain the correct fusion gene was expanded to 100 ml and grown for 24 h in an orbital incubator at 37 $^{\circ}$ C. Plasmid DNA was then extracted as per manufacturer's instructions using a HiSpeed plasmid maxi kit (Qiagen). Plasmid DNA was eluted in 500 μ l TE buffer. The concentration of DNA was determined using a nanodrop ND-1000 spectrophotometer (Thermo Scientific).

2.2.1.2 pCI-puro-β₂microglobulin

The β_2 microglobulin gene was amplified by PCR from cDNA synthesised from mRNA extracted from the human lymphoblastoid B cell line Bristol 8 (ECACC, UK).

Extraction of mRNA from Bristol 8 cells

mRNA extraction was performed using the QuickPrep mRNA purification kit (GE Life Sciences) as per manufacturer's instructions. Extracted mRNA was precipitated and then used for cDNA synthesis as described in section 2.2.1.1.

PCR amplification of β_2 microglobulin gene from cDNA

DNA encoding the β_2 microglobulin gene was amplified using the cDNA generated above with the following primers, and an annealing temperature of 62 °C.

Sense 5' TCC TCG AGC TGA CAG CAT TCG GGC CGA GAT GTC 3'
XhoI
Antisense 5' ATG CGG CCG CTT CAA ACC TCC ATG ATG CTG CTT 3'
NotI

Sub-cloning of β₂microglobulin into pCI-puro vector

The above 419 bp PCR product was verified and subcloned into pCI-puro (in house vector composed of pCI-neo (Promega) with neomycin resistance gene replaced with puromycin resistance gene) via Xho I and Not I sites (method as in section 2.2.1.1). Successfully transformed bacteria were selected on LB-ampicillin agar plates, underwent a test XhoI/NotI digest and confirmatory sequencing with the following primers:

 β_2 M new I 5' 5' AGC TGT GCT CGC GCT ACT CT 3' β_2 M new I 3' 5' TAA CTA TCT TGG GCT GTG AC 3'

2.2.1.3 pCI-puro-CMV-(G₄S)₄-β₂microglobulin

DNA encoding the CMV peptide *NLVPMVATV* connected to β_2 microglobulin via a glycineserine linker was amplified, with the insertion of flanking XhoI and NotI restriction enzyme sites and a 5' Kozak site for initiation, from the bacterial construct pET21a-CMV- β_2 microglobulin-HLA-A2-Hu-hinge (see section 2.3.1.1) using an annealing temperature of 60 °C and the following primers:

Sense 5' AT<u>C TCG AG</u>C ACC ATG AAC CTG GTG CCC ATG GTT GCT A 3'

XhoI Kozak

Antisense 5' ATG CGG CCG CTT ACA TGT CTC GAT CCC ACT TAA C 3'

NotI

The 397 bp PCR product was purified by agarose gel electrophoresis, it was ligated into pCR-Blunt II-TOPO vector and then sub-cloned into pCI-puro as described in section 2.2.1.2.

2.2.1.4 pEE14.1-HLA-A2-human IgG_1 hinge-Fc/pEE6.1- β_2 microglobulin Sub-cloning HLA-A2-human IgG_1 hinge-Fc into pEE14.1

The HLA-A2-human IgG₁ hinge-Fc fusion gene from TOPO HLA-A2-human IgG₁ hinge-Fc vector was sub-cloned into the pEE14.1 vector (Lonza,) via HindIII/EcoRI restriction enzyme sites. Successfully transformed JM109 *E. coli* were selected on LB-ampicillin agar plates.

PCR mutation of β_2 microglobulin gene to introduce flanking HindIII and XbaI restriction enzyme sites

HindIII and XbaI restriction enzyme sites flanking the β_2 microglobulin gene were introduced via a PCR using pCI-puro- β_2 microglobulin as the DNA template and the following primers and an annealing temperature of 57 °C.

Sense 5' TGA AGC TTA CAG CAT TCG GGC CGA GAT GTC 3'

HindIII

Antisense 5' CTT CTA GAT GCT GCT TAC ATG TCT CGA TCC 3'

XbaI

Sub-cloning β₂microglobulin gene into pEE6.1

The above purified PCR product was first cloned into pCR-Blunt II-TOPO where its sequence was confirmed using T7 and Sp6 primers before being sub-cloned into the pEE6.1 vector (Lonza) using HindIII/XbaI restriction enzyme sites. Successfully transformed JM109 *E. coli* was selected on LB-ampicillin agar plates.

Sub-cloning pEE6.1-β₂microglobulin into pEE14.1-HLA-A2-human IgG₁ hinge-Fc

The pEE6.1- β_2 microglobulin expression cassette was sub-cloned into the pEE14.1-HLA-A2-human IgG₁ hinge-Fc vector via NotI/BamHI restriction enzyme sites Digestion, ligation, transformation and selection of successfully transformed JM109 *E. coli* on LB-ampicillin plates were performed as above. Successfully transformed colonies were expanded, underwent miniprep plasmid extraction and digestion with both HindIII/EcoRI and HindIII/XbaI to demonstrate the insertion of the HLA-A2-human IgG₁ hinge-Fc fusion and β_2 microglobulin genes respectively. Correctly digesting plasmids underwent confirmatory DNA sequencing using the primers A2 new I 5', Hu hinge 5', Fc I 5', A2 new I 3', A2 new I rev 3', Hu hinge 3', β_2 M new I 5' and β_2 M new I 3'.

Megaprep of pEE14.1-HLA-A2-human IgG₁ hinge-Fc/pEE6.1-β₂microglobulin

A culture shown by sequencing to contain a DNA plasmid with the correct sequence underwent expansion to 1 l before extraction of the DNA plasmid using the QIAfilter plasmid mega kit (Qiagen), as per manufacturer's instructions. Plasmid DNA was resuspended in 1 ml TE buffer and concentration determined using a nanodrop.

2.2.1.5 Signal pIg plus-CMV-short linker-β₂microglobulin-HLA-A2-biotin-AviTag

To produce Signal pIg plus-CMV-short linker- β_2 microglobulin-HLA-A2-biotin-AviTag (a single chain trimer fusion gene with the biotin AviTag peptide attached to the carboxy terminus) site-directed mutagenesis was first performed on the pCR-Blunt II-TOPO-CMV-short linker- β_2 microglobulin-HLA-A2-biotin-AviTag construct (generated in section 2.3.1.1). This introduced appropriate flanking restriction enzyme sites to allow incorporation into the Signal pIg plus vector (R&D Systems, UK) which contains the CD33 signal peptide.

Site-directed mutagenesis to introduce SalI and XBaI restriction enzyme sites flanking the CMV-short linker-β₂microglobulin-HLA-A2-biotin AviTag fusion gene

The QuikChange Multi Site-Directed Mutagenesis Kit (Stratagene, UK) was used to introduce flanking SalI and XbaI restriction enzyme sites in the pCR-Blunt II-TOPO- CMV-short linker-β₂microglobulin-HLA-A2-biotin-AviTag construct. Two mutagenic primers were used:

T7-5'-SalI mutation

5' CTG CAG AAT TCG CCC TTA TT<u>G TCG AC</u>A ACC TGG TGC CCA TGG TT 3'
SalI

Sp6-3'-XbaI mutation

5' CAG CAC ACT GGC GGC CGT T<u>TC TAG A</u>GG ATC CGA GCT CCG G 3' XbaI

These primers were used in a PCR according to the manufacturer's instruction and the PCR product underwent DpnI digestion to remove the methylated parental template DNA.

Transformation of XL10-Gold *E. coli* cells with mutagenic PCR products

The DpnI digested PCR product was used to transform XL10-Gold ultracompetent *E. coli* cells. Selection of successfully transformed bacteria was performed on LB/kanamycin agar plates. Incorporation of the appropriate mutations was confirmed first via individual XbaI and SalI digestions, and then via sequencing with T7, A2 5', β₂M 3' and Sp6 primers.

Sub-cloning CMV-short linker- β_2 microglobulin-HLA-A2-biotin AviTag fusion gene into Signal pIg plus vector

The CMV-short linker-β₂microglobulin-HLA-A2-biotin AviTag fusion gene was sub-cloned into the Signal pIg plus vector via XhoI and XbaI restriction enzyme sites. (Insert was generated via a SalI/XbaI digest; a SalI digestion product is compatible with a XhoI restriction enzyme site.) Successfully transformed JM109 *E. coli* underwent selection on LB-ampicillin agar plates, followed by expansion, DNA extraction and test HindIII digestion (should yield a 1300 bp fragment). Correctly digested plasmids underwent confirmatory sequencing with the following primers:

T7, A2 new I 5', A2 new I 3' A2 new I 3' as before

A2 5' 5' GGA GGT GGT GGA TCC GGT GGT GGA GGT AGT GGC TCT CAC TCC

ATG AGG TAT TTC TTC ACA 3'

 β_2 M 3' 5' GGA TCC ACC ACC TCC GGA ACC GCC TCC ACC GGA ACC ACC ACC

GCC ACT GTC TCG ATC CCA 3'

2.2.2 Protein production

Transient and stable transfections of mammalian cells were performed with the above constructs to obtain secretion of the desired proteins.

2.2.2.1 Transfection of HEK 293F cells

The genetic constructs produced in section 2.2.1 were used to produce transient transfections of the human embryonic kidney (HEK) cell line 293F (Invitrogen) using the FreeStyle 293 Expression System (Invitrogen). The generic method used for transfection involved $3x10^7$ 293F cells being suspended in 28 ml FreeStyle Medium in a 125 ml conical flask. 30 µg DNA

for transfection and 40 µl 293fectin (a cationic lipid transfection reagent) were suspended separately in 1 ml Opti-MEM solution each, and allowed to incubate at RT for 5 min. The DNA-Opti-MEM and 293fectin-Opti-MEM solutions were then mixed together and allowed to incubate at RT for a further 30-45 min before being added dropwise to the 293F cells. These were then grown for 72 h in an Infors Multitron shaker incubator at 37 °C, 8% CO₂. After 72 h of growth cells were pelleted by centrifugation at 3,000 rpm for 10 min and the supernatant recovered for analysis of protein production.

Table 2.1 shows the various transfections undertaken. Where co-transfections were performed (to provide a source of both HLA-A2 α_1 - α_3 and β_2 microglobulin) equimolar quantities of DNA were used. Empty vector transfections were performed alongside the HLA-A2/ β_2 microglobulin transfections as a negative control. The pFUSE-irrelevant vector contains a non-functional (frame-shifted) HLA-A2-Fc fusion gene and is used to investigate whether a non-endogenous (HEK cells normally express HLA-A2, B7 and Cw7 on their surface in association with β_2 microglobulin)⁴²⁴ functional source of heavy chain is required for β_2 microglobulin secretion by transfected cells. On occasion larger volume transfections were performed where all amounts were scaled up appropriately to maintain concentrations and ratios.

DNA Species 1	DNA Species 2	Species 1 : Species 2 DNA weights to give equimolar amounts
pcDNA3.1 empty vector	pCI-puro empty vector	15 μg : 15 μg
pcDNA3.1-HLA-A2-human IgG ₁ hinge-Fc	None	not applicable
pcDNA3.1-HLA-A2-human IgG ₁ hinge-Fc	pCI-puro-β ₂ microglobulin	16.7 µg : 13.3 µg
pcDNA3.1-HLA-A2-human IgG ₁ hinge-Fc	pCI-puro-CMV- $(G_4S)_4$ - β_2 microglobulin	16.7 μg : 13.3 μg
pEE14.1 empty vector	pEE6.1 empty vector	20 μg : 10 μg
pEE14.1-HLA-A2-human IgG_1 hinge-Fc/pEE6.1- β_2 microglobulin	None	not Applicable
pFUSE empty vector	pCI-puro empty vector	13.1 μg: 16.9 μg
pFUSE-irrelevant	pCI-puro-β ₂ microglobulin	15.9 μg: 14.1 μg
Signal pIg plus empty vector	None	not Applicable
Signal pIg plus-CMV-short linker-β ₂ microglobulin-HLA- A2-biotin-AviTag	None	not Applicable

Table 2.1: 293F transient transfections performed

2.2.2.2 Transfection of CHO-K1 cells

Genetic constructs which resulted in protein production from transient transfections in 293F cells were used to produce stable transfections of Chinese Hamster Ovary (CHO-K1) cells (ATCC, USA). Adherent CHO-K1 cells were maintained in RPMI 1640 medium supplemented with L-glutamine, pyruvate, penicillin streptomycin, amphotericin B and 10% FCS at 37 °C in 5% CO₂ and routinely passaged using 0.05% trypsin/EDTA (Invitrogen). 24 h prior to transfection, CHO-K1 cells were removed from their growing surface with trypsin/EDTA and seeded at a concentration of $5 \times 10^5 - 1 \times 10^6$ cells per well on 6 well plates. For each well of cells to be transfected, 2 µg DNA and 10 µl genePORTER (Genlantis, USA) were separately suspended in 500 µl RPMI 1640 medium supplemented with only L-glutamine and pyruvate, then mixed together and incubated at RT for 30 min. FCS-containing medium was aspirated from the CHO-K1 cells and replaced with 1 ml of DNA/genePORTER-containing medium. Cells were then incubated at 37 °C for 5 h before the addition of 1 ml RPMI 1640 medium supplemented with L-glutamine, pyruvate and 20% FCS.

After a further 72 h transfected CHO-K1 cells were removed from the 6 well plates using trypsin/EDTA, washed and resuspended in RPMI 1640 medium supplemented with L-glutamine, pyruvate, penicillin, streptomycin, amphotericin B, 10% FCS and appropriate selecting antibiotic. Cells were transferred to a 96 well plate (200 μ l per well) and grown in selection medium. Section 2.2.3 describes how protein production was analysed. Wells containing cells producing the desired protein product were expanded up to medium flasks before, if protein production was maintained, cloning on a 96 well plate by limiting-dilution. Table 2.2 lists the stable transfections performed and the antibiotic used for selection in each case. CHO-K1 cells used for pEE14.1-HLA-A2-human IgG1 hinge-Fc/pEE6.1- β_2 microglobulin transfection were maintained in L-glutamine-free GMEM-S medium (First Link, UK), supplemented with penicillin, streptomycin, amphotericin and 10% dialysed FCS (First Link). The method of transfection was otherwise similar.

Genetic Construct	Selection Antibiotic	Antibiotic Concentration	
pcDNA3.1-HLA-A2-human IgG ₁	Geneticin (Invitrogen) and	Geneticin 1 mg/ml	
hinge-Fc & pCI-puro-β ₂ microglobulin	Puromycin (Clontech, UK)	Puromycin 10 μg/ml	
pEE14.1-HLA-A2-human IgG ₁ hinge-	Methionine sulphoximine	25 μg/ml	
Fc/pEE6.1-β ₂ microglobulin	(Sigma)		
Signal pIg plus-CMV-short linker-	Geneticin	1 mg/ml	
β ₂ microglobulin-HLA-A2-biotin-			
AviTag			

Table 2.2: CHO-K1 stable transfections performed

2.2.3 Protein characterisation

Production of the desired protein species by the above transient and stable transfections was determined qualitatively by Western blotting, and where possible, more quantitatively by Enzyme-linked Immunosorbent Assay (ELISA). Analysis was performed on either neat or concentrated cell supernatants (degree of concentration is indicated in results in section 3.2.3). Where concentrated supernatants were used these were obtained by centrifugation using 4 or 15 ml Amicon ultra centrifugal filter devices with a molecular weight cut-off of 10,000 Da (Millipore, France) at 3,000 rpm.

2.2.3.1 Western blotting

SDS-PAGE

Protein was initially separated and analysed using sodium dodecyl sulfate polyacrylamide gel electrophoresis (SDS-PAGE) with 12.5% resolving gels and 3% stacking gels (see appendix 1). The resolving gel was poured between two glass plates separated by 1.5 mm spacers and once set, the stacking gel mixed and poured. Samples were prepared by mixing with either reducing or non-reducing loading buffer in a 2:1 ratio. Reduced samples were heated to 95 °C for 10 min in a Techne DB-2A dri block. Protein samples were loaded into the lanes of the gel adjacent to High-Range Rainbow Molecular Weight Markers (GE Life Sciences) and gels were run in electrode buffer in a BioRad Mini-Protean 3 gel tank. Gels were run at 100 V for 30-40 min until samples were through the stacking gel, and then at 200 V for a further 40 min to ensure maximum separation of proteins.

Protein transfer to nitrocellulose membrane

Transfer of protein from an SDS gel to nitrocellulose membrane was performed using a cooled TE series Transphor transfer unit (Hoefer Scientific Instruments, USA). Nitrocellulose membrane (Millipore) was activated before use by immersion in methanol for 30 s. Transfer was carried out at 400 mA for 1 h using 4 parts transfer buffer to 1 part methanol. After transfer the membrane was blocked by incubating in 5% Marvel (non-fat powdered milk) w/v TBS/0.05% Tween-20 (TBS/T) at 4 °C overnight on a roller, before being washed 4 times by incubating in TBS/T (each wash consisted of a 5 min incubation on a rocker).

Probing nitrocellulose membranes

The Ab combinations and concentrations used to probe the mammalian constructs are shown in Table 2.3. The membrane was incubated in the primary Ab (diluted in 5% Marvel w/v TBS/T) for 1 h at RT on a roller. It was then washed 4 times in TBS/T as above, before incubation in the secondary Ab (diluted in 5% Marvel w/v TBS/T) for 1 h at RT on a roller. After 4 washes the membrane was incubated in Super Signal West Pico Chemiluminescent

HRP substrate (Perbio, UK) for 5 min at RT. Excess substrate was removed and the membrane was used to expose Hyperfilm (GE Life Sciences) which was developed using a Compact X4 film processor (Xograph Imaging Systems, UK).

Primary Antibody	Concentration of 1° Antibody used	Secondary Antibody	Concentration of 2° Antibody used
Rabbit anti-hMHC class I (ab52922, Abcam, UK)	1/10,000	Anti-rabbit IgG-HRP (GE Life Sciences,)	1/5,000
Rabbit anti-hβ ₂ microglobulin (ab6608, Abcam)	1/25,000	Anti-rabbit IgG-HRP	1/5,000
Rabbit Anti-human Fc (inhouse)	0.5 μg/ml	Anti-rabbit IgG-HRP	1/5,000

Table 2.3: Antibodies used for Western Blotting

Stripping nitrocellulose membranes

In order to allow probing of a single membrane with more than one Ab, on occasion blots were stripped. The membrane was incubated in stripping buffer (65 mM TrisHCl, 2% SDS, 100 mM mercaptoethanol, pH 6.7) for 30 min at 50 °C before undergoing 4 TBS/T washes. It was then blocked with 5% Marvel w/v TBS/T as before and probed as before.

2.2.3.2 Enzyme-linked Immunosorbent Assay

Specific Ab combinations and concentrations used are indicated in Table 2.4. The generic ELISA method involved primary Ab being diluted in coating buffer (recipe in appendix 1) and 100 μl/well added to Maxisorb 96 well plates (Nunc) for a 1 h incubation at 37 °C. Unbound Ab was removed and unoccupied binding sites blocked by the application of 150 μl/well 1% w/v BSA in PBS. After a 1 h incubation at 37 °C the blocking solution was removed and the plate washed 5 times with PBS/0.05% Tween-20 (used for all washes) using a Skan Washer 300 version B ELISA plate washer (Skatron Instruments, Norway). 100 μl/well of protein sample diluted in PBS/BSA (all used for all dilutions) was then applied, and the plate underwent another 1 h incubation at 37 °C.

After a further 5 washes 100 μ l/well diluted secondary Ab (where available HRP-conjugated) was added and incubated at 37 °C for 1 h. If a non HRP-conjugated secondary Ab was used an additional step was required; after a further 5 washes an appropriate anti-xenotype-IgG HRP-conjugated Ab was applied and incubated at 37 °C for 1 h. After a final 5 washes 100 μ l/well o-Phenylenediamine free base (Sigma) containing phospho-buffered citrate ELISA substrate was added and the plate incubated in the dark at 37 °C for 15-30 min, until developed. The

reaction was terminated by the addition of 50 μ l/well 5M H₂SO₄, and the plate read at 490 nm on an automatic spectrophotometer (Dynatec MR4000, Dynatec, UK). Where available protein standards were used as a positive control to generate calibration curves.

Transfection(s)	Primary Antibody	Secondary Antibody/Antibodies	Standard
293F: pcDNA3.1-HLA-A2- human IgG ₁ hinge-Fc & pCI- puro-β ₂ microglobulin	1 μg/ml anti-hFc (in- house) 1 μg/ml W6/32 (anti-	1/40000 rabbit anti- hIgG-HRP (in-house) 1/10000 Anti-	Human IgG (in-house)
	HLA-A,B,C; kind gift Prof Elliott) 1 μg/ml BB7.2 (anti-	hβ ₂ microglobulin-HRP (ab20576, Abcam, UK) 1/10000 Anti-	None
	HLA-A2; available inhouse)	hβ ₂ microglobulin-HRP 1/10000 Anti-	None
	1 μg/ml anti-hFc	hβ ₂ microglobulin-HRP	None
293F: pcDNA3.1-HLA-A2- human IgG_1 hinge-Fc & pCI- puro-CMV- $(G_4S)_4$ - β_2 microglobulin	As above	As above	As above
293F: pEE14.1-HLA-A2- human IgG ₁ hinge- Fc/pEE6.1-β ₂ microglobulin	As above	As above	As above
293F: Signal pIg plus-CMV- short linker-β ₂ microglobulin-	5 μg/ml W6/32	1/5000 Anti- hβ ₂ microglobulin	HLA-A2/β ₂ M monomer
HLA-A2-biotin-AviTag		(ab6608, Abcam, UK) & anti-rabbit IgG-HRP (GE Life Sciences, UK)	(Orpegen)
CHO-K1: pcDNA3.1-HLA- A2-human IgG ₁ hinge-Fc & pCI-puro-β ₂ microglobulin	1 μg/ml anti-hFc	1/40000 rabbit anti-h IgG-HRP	Human Fc
CHO-K1: pEE14.1-HLA-A2- human IgG ₁ hinge- Fc/pEE6.1-β ₂ microglobulin	1 μg/ml anti-hFc	1/40000 rabbit anti-h IgG-HRP	Human Fc
CHO-K1: Signal pIg plus- CMV-short linker- β ₂ microglobulin-HLA-A2- biotin-AviTag	10 μg/ml W6/32	1/5000 Anti- hβ ₂ microglobulin & anti-rabbit IgG-HRP	HLA-A2/β ₂ M monomer

Table 2.4: Antibodies and standards used for mammalian protein ELISAs

Rabbit anti-hIgG-HRP is known to react with the Fc region of h IgG so therefore should react with the Fc region in HLA-A2-human hinge-Fc fusion proteins. Anti-h β_2 microglobulin-HRP (ab20576, Abcam, UK) became unavailable during this project and no suitable HRP-conjugated anti-h β_2 microglobulin Ab could be sourced necessitating the use of an unconjugated anti-h β_2 microglobulin secondary Ab, itself detected with an HRP-conjugated anti-xenotype Ab.

2.3 Bacterial Construct Production and Characterisation (Human)

2.3.1 Genetic engineering of constructs

The designs of the different bacterial constructs produced are indicated in Figure 2.2. The human IgG₁ hinge consists of the upper and middle regions of the hinge.⁴²⁵

To make the CMV- β_2 microglobulin-HLA-A2-human Ig G_1 hinge fusion gene (single chain trimer: SCT), three separate PCR reactions followed by a final two-step PCR splicing by overlap extension (SOE) reaction were required.

PCR 1: Addition of G_4S linkers to 5' and 3' termini of β_2 microglobulin gene

Glycine-serine linkers were introduced to flank the β_2 microglobulin gene in a PCR reaction using pEE6.1- β_2 microglobulin (see section 2.2.1.4) as template DNA and the following primers with an annealing temperature of 56 °C:

Sense	5' GGA GGA GGT GCT AGC GGT GGT GGT AGC GGA GGT GGA GGC
	AGC ATC CAG CGT ACT CCA 3'
Antisense	5' GGA TCC ACC ACC TCC GGA ACC GCC TCC ACC GGA ACC ACC ACC
	GCC ACT GTC TCG ATC CCA 3'

The 399 bp PCR product was purified by agarose gel electrophoresis and DNA was extracted from the gel band. 4µl of this DNA was used as the template in PCR 2.

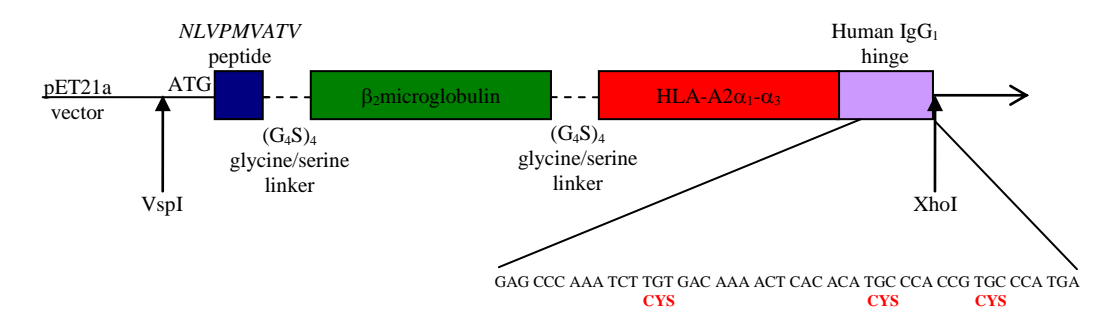
PCR 2: Addition of CMV peptide DNA to 5' terminus of β_2 microglobulin gene

DNA encoding the CMV pp65 HLA-A2-restricted peptide *NLVPMVATV* was added to the glycine-serine linker flanked β_2 microglobulin gene in a PCR reaction using the following primers with an annealing temperature of 65 °C:

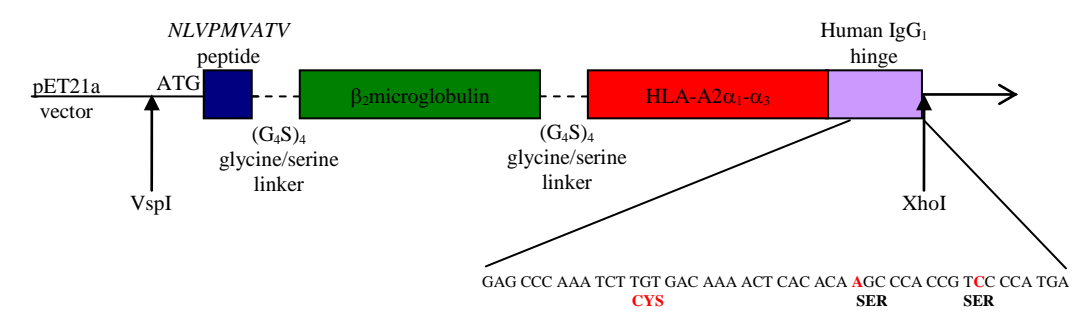
Sense *	5' <u>ATT AAT</u> ATG AAC CTG GTG CCC ATG GTT GCT ACG GTT GGA GGA	1
	VspI M N L V P M V A T V	
	GGT GCT AGC GGT GGT GGT 3'	
Antisense	5' GGA TCC ACC ACC TCC GGA ACC GCC TCC ACC GGA ACC ACC ACC	\mathbb{C}
	GCC ACT GTC TCG ATC CCA 3'	

The 435 bp PCR product was purified by agarose gel electrophoresis and DNA extracted in order to provide one of the DNA templates for the PCR SOE reaction.

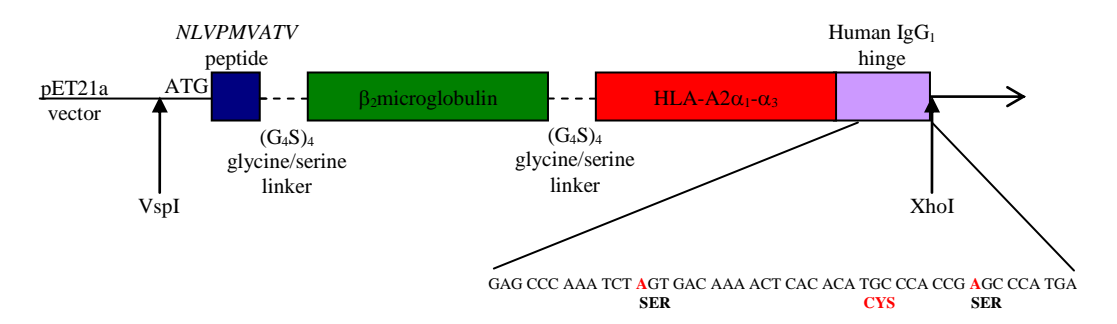
A: pET21a-CMV-β₂microglobulin-HLA-A2-human IgG₁ hinge (SCT-3xCys)



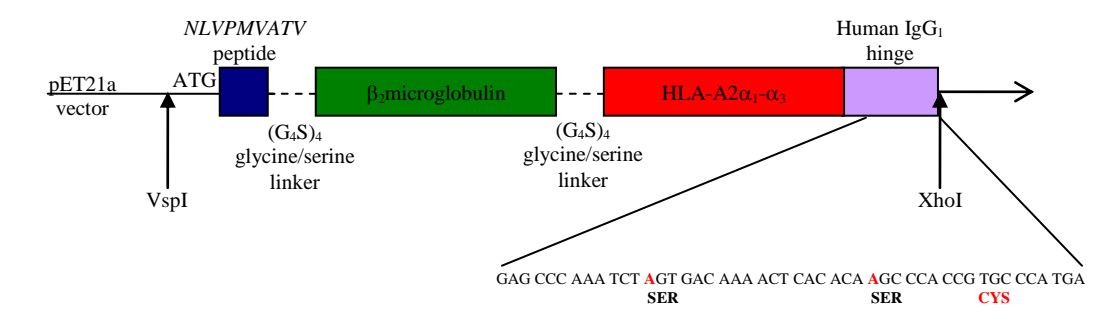
B: pET21a-CMV- β_2 microglobulin-HLA-A2-human Ig G_1 hinge single cysteines SCT-Cys-I



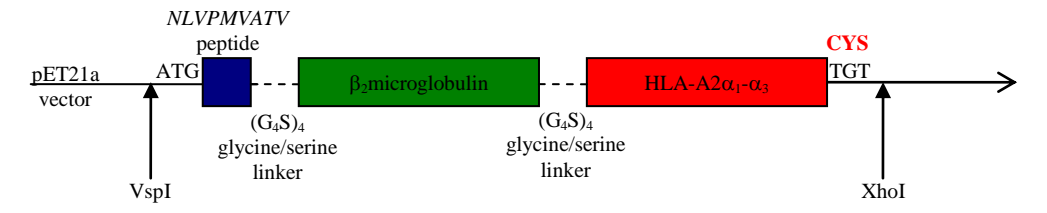
SCT-Cys-II



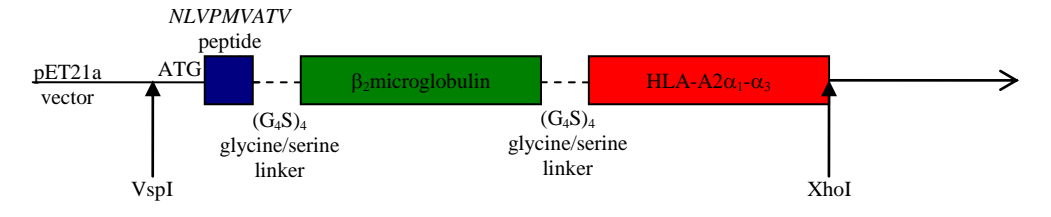
SCT-Cys-III



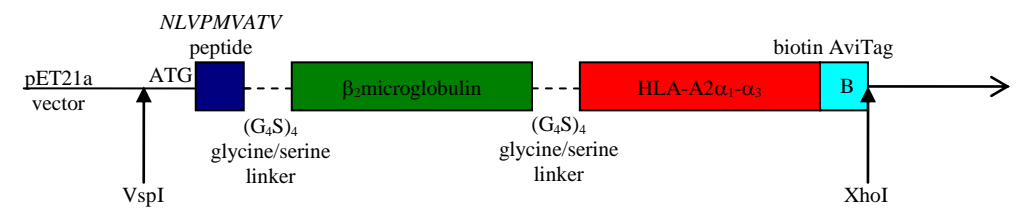
C: pET21a-CMV-β₂microglobulin-HLA-A2-Cysteine (SCT-C)



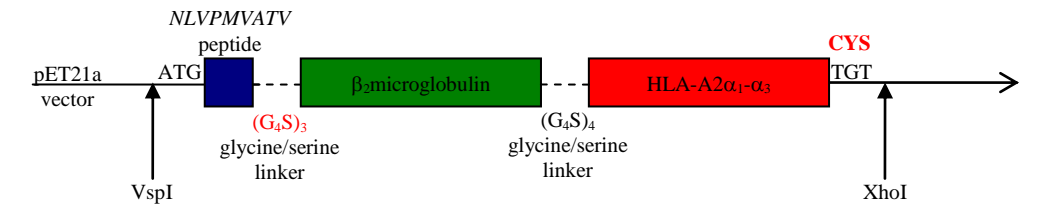
D: pET21a-CMV-β₂microglobulin-HLA-A2 (SCT-X)



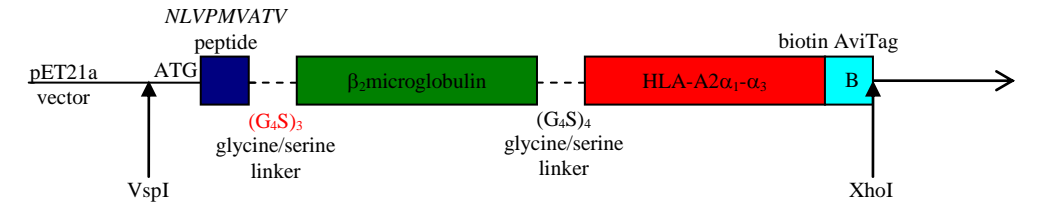
E: pET21a-CMV-β₂microglobulin-HLA-A2-biotin-AviTag (SCT-B)



F: pET21a-CMV-short-linker-β₂microglobulin-HLA-A2-cysteine (SCT-SL-C)



G: pET21a-CMV-short linker- β_2 microglobulin-HLA-A2-biotin-AviTag (SCT-SL-B)



H: pET21a-CMV-short linker- β_2 microglobulin-HLA-A2-biotin-AviTag disulfide trap (SCT-SL-B DST)

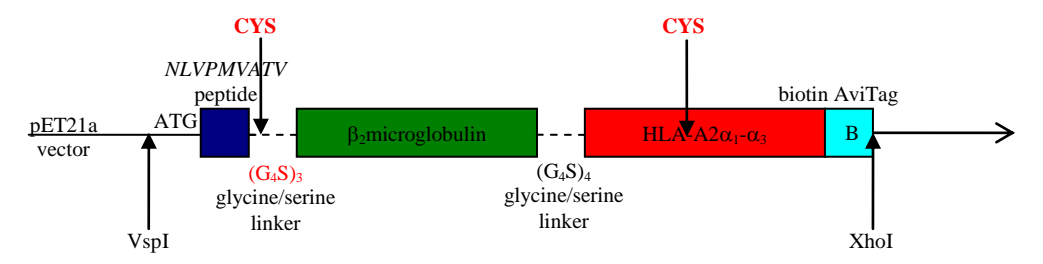


Figure 2.2: Design of genetic constructs for bacterial expression

PCR 3: Addition of G_4S linker to 5' terminus and XhoI site to 3' terminus of HLA-A2-human IgG_1 hinge DNA

A glycine-serine linker and a XhoI restriction enzyme site were added to the 5' and 3' termini of HLA-A2-human IgG_1 hinge DNA in a PCR reaction using TOPO HLA-A2-human IgG_1 hinge-Fc (see section 2.2.1.1) as template DNA and the following primers:

Sense 5' GGA GGT GGA TCC GGT GGT GGA GGT AGT GGC TCT CAC TCC

ATG AGG TAT TTC TTC ACA 3'

Antisense * 5' GA<u>C TCG AG</u>G TCA TGG GCA CGG TGG GCA TGT 3'

XhoI

The PCR was performed with an annealing temperature of 66 °C. The 963 bp PCR product was purified by agarose gel electrophoresis and DNA extracted in order to provide the second DNA template for the PCR SOE reaction.

PCR SOE: Fusion of CMV- β_2 microglobulin with HLA-A2-human Ig G_1 hinge DNA

A two-step PCR SOE reaction was performed using the purified PCR products from reactions 2 and 3:

Step 1 Reagents: 2.5 µl 10x buffer

 $0.5~\mu l~dNTPs$

5 μl purified PCR 2 reaction product 2 μl purified PCR 3 reaction product

1 μl pFU polymerase 14 μl DEPC-treated H₂O

Step 1 Programme: Step 1 Initial denaturation 95 °C 5 min

Step 2 Denaturation94 °C 30 sStep 3 Annealing65 °C 1 minStep 4 Elongation72 °C 2 minStep 5 return to step 2 for total of 20 cycles

After 20 cycles, step 2 reagents were added to the above reaction and the step 2 PCR programme completed.

Step 2 Reagents: 2.5 µl 10x buffer

 $0.5~\mu l~dNTPs$

2 μl sense primer (from PCR 2; indicated with *) 2 μl antisense primer (from PCR 3; indicated with *)

 $1~\mu l~pFU~polymerase$ $17~\mu l~DEPC$ -treated H_2O

Step 2 Programme: Step 1 Denaturation 94 °C 30 s

Sub-cloning CMV- β_2 microglobulin-HLA-A2-human Ig G_1 hinge fusion gene into pET21a vector

Purification of the above 1368 bp CMV- β_2 microglobulin-HLA-A2-human IgG₁ hinge fusion gene PCR product, ligation into pCR-Blunt II-TOPO vector and transformation of TOP10 *E. coli* cells were all carried out as before. A confirmatory VspI/XhoI digest was performed and appropriately digested plasmids were sequenced using T7, A2 5', β_2 M 3' and Sp6 primers. The CMV- β_2 microglobulin-HLA-A2-human IgG₁ hinge fusion gene was then sub-cloned into the pET21a vector (Novagen, USA) using NdeI and XhoI restriction enzyme sites. (Insert was generated via a VspI/XhoI digest; a VspI digestion product is compatible with an NdeI restriction enzyme site.) Successfully transformed JM109 *E. coli* underwent selection on LB-ampicillin agar plates, followed by expansion, DNA extraction and test XhoI/KpnI digestion; should yield 575 bp fragment. Correctly digested plasmids underwent confirmatory sequencing with the following primers;

```
T7, A25' and \beta_2M 3' as before pET21a rev 5' GCT AGT TAT TGC TCA GCG TG 3'
```

A culture shown to contain the correct plasmid was then expanded to 100 ml and a maxiprep performed as before to extract plasmid DNA.

2.3.1.2 pET21a-CMV- β_2 microglobulin-HLA-A2-human Ig G_1 hinge single cysteine (SCT-Cys-I, SCT-Cys-II & SCT-Cys-III)

Site-directed mutagenesis was used to remove two of the cysteine residues from the hinge region of pET21a-CMV- β_2 microglobulin-HLA-A2-human IgG $_1$ hinge, so that each construct contained only one hinge region cysteine residue. Three mutagenic primers were used (Cys-I to produce SCT-Cys-I, Cys-II to produce SCT-Cys-III and Cys-III to produce SCT-Cys-III), each in a different mutagenic PCR reaction to remove a different pair of cysteine residues thus leaving one intact: These primers were used in the reaction described in section 2.2.1.5 with pET21a-CMV- β_2 microglobulin-HLA-A2-human IgG $_1$ hinge as template DNA and an elongation time of 14 min per cycle.

Cys I	5' GAC AAA ACT CAC ACA AGC CCA CCG TCC CCA TGA CCT CGA GTC 3'
Cys II	5' GCC CAA ATC TAG TGA CAA AAC TCA CAC ATG CCC ACC GAG CCC 3'
Cys III	5' GCC CAA ATC TAG TGA CAA AAC TCA CAC AAG CCC ACC GTG CCC 3'

2.3.1.3 pET21a-CMV-β₂microglobulin-HLA-A2-Cysteine (SCT-C)

The hinge region of the CMV- β_2 microglobulin-HLA-A2-human IgG₁ hinge fusion gene was replaced by a C-terminal cysteine residue followed by a stop codon and XhoI restriction enzyme site by PCR using the following primers and an annealing temperature of 65 °C:

Sense 5' <u>ATT AAT</u> ATG AAC CTG GTG CCC ATG GTT GCT ACG GTT GGA GGA

VspI

GGT GCT AGC GGT GGT GGT 3'

Antisense 5' CTC TCG AGC TCA ACA GGG GAT GGT GGG CTG GGA AGA 3'

XhoI

The resulting CMV- β_2 microglobulin-HLA-A2 fusion gene PCR product was sub-cloned into the pET21a vector as in section 2.3.1.1.

2.3.1.4 pET21a-CMV-β₂microglobulin-HLA-A2 (SCT-X)

The hinge region of the CMV- β_2 microglobulin-HLA-A2-human IgG₁ hinge fusion gene was replaced by a stop codon flanked by a XhoI restriction enzyme site by a PCR reaction using the following primers and an annealing temperature of 64 °C:

Sense 5' <u>ATT AAT</u> ATG AAC CTG GTG CCC ATG GTT GCT ACG GTT GGA GGA

VspI

GGT GCT AGC GGT GGT GGT 3'

Antisense 5' CTC TCG AGC TCA GGG GAT GGT GGG CTG GGA AGA 3'

Xho]

The resulting CMV- β_2 microglobulin-HLA-A2 fusion gene PCR product was sub-cloned into the pET21a vector as in section 2.3.1.1.

2.3.1.5 pET21a-CMV-β₂microglobulin-HLA-A2-biotin-AviTag (SCT-B)

The pET21a-CMV- β_2 microglobulin-HLA-A2-biotin-AviTag construct contains a 5' biotin AviTag peptide which can be biotinylated enzymatically by BirA. Production of this construct involved first sub-cloning the CMV- β_2 microglobulin-HLA-A2 fusion gene into the biotin AviTag-containing vector pAC-4 (Avidity, USA), before amplifying the resulting CMV- β_2 microglobulin-HLA-A2-biotin-AviTag fusion gene by PCR and sub-cloning into the pET21a vector.

PCR mutation of CMV- β_2 microglobulin-HLA-A2 fusion gene to introduce flanking XhoI and HindIII restriction enzyme sites

XhoI and HindIII restriction enzyme sites flanking the CMV- $β_2$ microglobulin-HLA-A2 fusion gene were introduced via a PCR using the following primers and an annealing temperature of 65 °C:

Sense 5' CAC TCG AGA ACC TGG TGC CCA TGG TTG CTA 3'

XhoI

Antisense 5' CAA AGC TTG GGA TGG TGG GCT GGG AAG ACG 3'

HindIII

Sub-cloning CMV-β₂microglobulin-HLA-A2 fusion gene into pAC-4 vector

Ligation of the above purified PCR product into pCR-Blunt II-TOPO vector and transformation of TOP10 $E.\ coli$ cells were carried out as before. The CMV- β_2 microglobulin-HLA-A2 fusion gene was verified by restriction digest and sequencing and then sub-cloned into the pAC-4 vector via its XhoI/HindIII sites. Successfully transformed JM109 $E.\ coli$ was selected on LB-ampicillin agar plates, and verified by XhoI/HindIII digestion and sequencing with the following primers:

A25' and β_2M 3' as before pAC-4 5' 5' GCT CAA GGC GCA CTC CCG TTC 3' pAC-4 3' 5' CCC CAC ACT ACC ATC GGC GCT 3'

PCR amplification of CMV-β₂microglobulin-HLA-A2-biotin-AviTag fusion gene

DNA encoding the CMV-β₂microglobulin-HLA-A2-biotin-AviTag fusion gene was amplified (with the insertion of flanking VspI and XhoI restriction enzyme sites) using the above construct as template DNA, the following primers, and an annealing temperature of 65 °C:

Sense 5' ATT AAT ATG AAC CTG GTG CCC ATG GTT GCT ACG GTT GGA GGA

VspI

GGT GCT AGC GGT GGT GGT 3'

Antisense 5' ATT CTC GAG ATG AAT TAT TCG TGC CAT TCG ATT TTC 3'

XhoI

The above CMV- β_2 microglobulin-HLA-A2-biotin-AviTag fusion gene PCR product was subcloned into the pET21a vector as in section 2.3.1.1.

2.3.1.6 pET21a-CMV-short-linker-β₂microglobulin-HLA-A2-cysteine (SCT-SL-C)

To produce the pET21a-CMV-short-linker- β_2 microglobulin-HLA-A2-cysteine construct, which is identical to SCT-C except for the presence of a shorter linker ((G_4S)₃ rather than (G_4S)₄) between the CMV peptide and β_2 microglobulin DNA segments, a very similar method was employed as for the production of pET21a- CMV- β_2 microglobulin-HLA-A2-human Ig G_1 hinge. Similar PCR reactions were used as described in section 2.3.1.1, the only differences being the use of pET21a-CMV- β_2 microglobulin-HLA-A2-Cysteine as the DNA template and the antisense primer used for PCR 3 and step 2 of the PCR SOE, which was as follows:

Antisense 5' CTC TCG AGC TCA ACA GGG GAT GGT GGG CTG GGA AGA 3' XhoI

The resulting PCR product was manipulated as described in section 2.3.1.1 and a fusion gene containing the correct sequence with the shorter $(G_4S)_3$ linker between the CMV peptide and

 β_2 microglobulin DNA segments sub-cloned into the pET21a vector. Confirmatory sequencing was performed using the T7, A2 5', β_2 M 3' and pET21a rev primers.

2.3.1.7 pET21a-CMV-short linker-β₂microglobulin-HLA-A2-biotin-AviTag (SCT-SL-B)

The method used to produce this construct was that described in section 2.3.1.5 for the production of pET21a-CMV- β_2 microglobulin-HLA-A2-biotin-AviTag: The only difference was the starting DNA template of pET21a-CMV-short-linker- β_2 microglobulin-HLA-A2-cysteine.

2.3.1.8 pET21a-CMV-short linker- β_2 microglobulin-HLA-A2-biotin-AviTag disulfide trap (SCT-SL-B DST)

In pET21a-CMV-short linker- β_2 microglobulin-HLA-A2-biotin-AviTag disulfide trap, additional cysteine residues were introduced at the second position of the linker joining the *NLVPMVATV* peptide with β_2 microglobulin, and at position 84 in the HLA-A2 α_1 – α_3 domains via site-directed mutagenesis using the method described in section 2.2.1.5. The mutagenic primers used were as follows:

```
SCT-SL-B-linker-Cys
5' GGT TGC TAC GGT TGG A<u>TG T</u>GG TGC TAG CGG TGG TGG 3'
Cys
SCT-SL-B-A284-Cys
5' GGG GAC CCT GCG CGG C<u>TG C</u>TA CAA CCA GAG CGA GGC 3'
Cys
```

The mutagenic PCR was performed as before, but used both the above primers in a single reaction. The resulting PCR product was manipulated as described in section 2.2.1.5.

2.3.2 Protein production

2.3.2.1 Transformation of KRX E. coli cells

KRX *E. coli* cells (Promega) were used for the expression of protein encoded by the above bacterial constructs within insoluble inclusion bodies. Typically ~0.1-0.5μg DNA was used to transform KRX cells using standard transformation procedure.

2.3.2.2 Growth and induction of transformed KRX cells

Several bacterial colonies resulting from overnight antibiotic selection were picked and used to inoculate 4 ml LB-ampicillin (100 μ g/ml) and grown at 37 °C until the optical density (OD) at 600 nm was 0.6-0.8 as measured on a CE 1021 spectrophotometer (Cecil, UK). Once cultures reached this density they were split into two 2 ml aliquots; in one sample protein

expression was induced by the addition of 1 mM isopropyl β-D-thiogalactopyranoside (IPTG; Bioline, UK) and 0.1% w/v L-rhamnose monohydrate (Sigma), whilst to the other 8 ml of LB-ampicillin was added. Both cultures were then grown for a further 3 ½ h at 37 °C in an orbital incubator. Uninduced cultures were stored at 4 °C over night. To assess protein production in these small scale inductions, each pair of induced and uninduced cultures was analysed by SDS PAGE on a 12.5% gel run under reducing conditions. Gels were run as described in section 2.2.3.1 then stained with Coomassie Blue-containing stain (see appendix 1 for recipe) for ~3 h at RT on a rocker before being destained in destain buffer overnight.

Stored uninduced bacteria which were shown by SDS-PAGE to have good levels of protein production upon induction were used to inoculate 1 l of LB-ampicillin for larger scale inductions. A similar method was used as for the small scale inductions. Uninduced and induced samples were saved for SDS-PAGE analysis. After 3 ½ h of growth, bacteria from induced cultures were recovered by centrifuging at 3,700 g for 30 min (brake off) in 500 ml buckets in a Sorvall RT 6000D centrifuge. The bacterial pellet was weighed and then stored at -20 °C until required for inclusion body extraction.

2.3.2.3 Inclusion body purification

Bacterial cells were disrupted using sonication in order to extract the inclusion bodies. Cell pellets were thawed on ice then resuspended in pre-chilled sonication buffer (10 ml/g bacteria; see appendix 1 for recipe). Bacteria were then sonicated on ice using a Misonix 3000 probe sonicator until a non-viscous liquid was produced. A sample of sonicated cells was retained for SDS-PAGE analysis. Inclusion bodies were recovered by centrifuging at 10,500 rpm for 20 min at 4 °C in 35 ml polycarbonate tubes using a MS60 ultracentrifuge (Sanyo, UK) with a TFT 55.38 rotor. A sample of the discarded supernatant was retained for SDS-PAGE analysis.

The inclusion bodies were washed 4 times (3 times with Wash Buffer 1, once with Wash Buffer 2) by resuspending the pellet in 10 ml chilled buffer and centrifuging for 15 min at 10,500 rpm as before. After the final wash the inclusion bodies were solubilised in either Urea solubilisation buffer or Guanidine solubilisation buffer (choice depends on refolding buffer used) by rotating at 4 °C for 24 h. 10 ml of solubilisation buffer was used per litre of starting bacterial culture. Once inclusion bodies were fully solubilised their concentration was determined using a nanodrop, and they were stored at -80 °C until refolded. The extinction coefficients used to determine the concentration of each different SCT species were calculated using the ProtParam tool, ⁴²⁶ and correction for nucleic acid contamination was done using the

Warburg-Christian equation. 427 Sonicated bacterial cell pellet, discarded sonicated pellet supernatant and solubilised inclusion bodies were examined by SDS-PAGE.

2.3.2.4 Protein refolding

The solubilised inclusion bodies were refolded by dilution using the redox-shuffling refolding buffers described by Lybarger *et al*⁴⁰⁵ (100 mM Tris, 400 mM L-arginine, 2 mM EDTA, 5 mM reduced glutathione, 0.5 mM oxidised glutathione, 0.1 mM PMSF pH 8) or Oved *et al* ³⁹⁷ (100 mM Tris, 500 mM -Larginine, 0.09 mM oxidised glutathione, pH 10). 50 mg (1 µM) of unfolded SCT protein was added slowly in 10 mg aliquots over 24-48 h to 1 l of continuously stirred refolding buffer kept at 4 °C. After 48-72 h the refolding mixture was filtered through Whatmann grade 54 filter paper (GE Life Sciences) to remove macroscopic aggregates and then concentrated using a 400 ml Stirred Cell Series 8000 Concentrator fitted with a 10,000 Da molecular weight cut-off Biomax polyethersulfone membrane ultrafiltration disc (all Millipore).

The concentrated refolded protein was dialysed against 20 mM/Tris 0.1 M NaCl buffer pH 8 at 4° C using 10,000 Da MW cut-off (used for all dialysis unless otherwise stated) dialysis tubing (Medicell, London;), before being filtered through a 0.22 μ m filter (GE Life Sciences). The unpurified refolded SCT protein was analysed at this stage by high performance liquid chromatography (HPLC) using a Zorbax GF-250 column (Hichrom Limited, UK) running in 0.2 M phosphate/ 1 M DMF/ pH 7 buffer using a 280nm detector.

2.3.2.5 Protein purification

SCT protein was purified by either size exclusion chromatography or immunoaffinity chromatography using columns composed of W6/32 or BB7.2 monoclonal Ab conjugated to Sepharose beads.

Immunoaffinity column construction

25 mg of monoclonal Ab (either W6/32 or BB7.2; both available in-house) at a concentration of 2.5 mg/ml was dialysed against 0.2M citrate buffer (see appendix 1 for recipe). 1.5 g CnBr Activated Sepharose 4B beads (GE Life Sciences) were soaked in 200 ml 10 mM HCl then poured onto a sintered glass filter and washed with 300 ml 10mM HCl. The beads were then washed with 500 ml 0.2M citrate buffer, before being transferred to a universal containing the dialysed Ab. The beads were incubated with the Ab overnight on a rotator at 4 °C. The following day the beads were returned to the sintered glass filter and buffer was removed by vacuum pump; the OD of the filtrate at 280 nm was checked (against a 0.2M citrate buffer

blank) to ensure all of the Ab was coupled to the beads. The beads were then incubated with 10 ml 1 M ethanolamine. HCl pH 9.5 on a rotator at RT for 1 h. They were then washed on the sintered glass filter with 200 ml 0.1 M Tris/0.5 M NaCl buffer pH 8, 200 ml ammonium thiocyanate (aqueous solution of 2M ammonia and 1M potassium thiocyanate) and a further 200 ml 0.1 M Tris/0.5 M NaCl buffer pH 8 before being resuspended in 10 ml of 40 mM Tris/0.2 NaCl buffer pH 8.

To construct the column the plunger was removed from a 20 ml syringe and the outlet overlaid with glass wool. The Ab-coupled beads were then added to the column and overlaid with 2 glass paper discs. The top of the column was sealed with a rubber bung (containing inlet tube) and the column equilibrated in 40 mM Tris/0.2M NaCl buffer pH 8 column running buffer.

Immunoaffinity chromatography purification of refolded SCT

Immunoaffinity columns were connected to a Uvicord SII spectrophotometer (absorbance at 280 nm, LKB, Sweden), and concentrated, dialysed, refolded SCT protein applied. SCT protein was eluted using a half column volume of ammonium thiocyanate and immediately dialysed against first 40 mM Tris/0.2M NaCl buffer pH 8 then 20 mM Tris/0.1M NaCl buffer pH 8. SCT protein was then analysed in the first instance by HPLC.

Size exclusion chromatography purification of refolded SCT

Two in series 94.3 x 1.6 cm Superdex 200 (GE Life Sciences) columns running in TE8 buffer (see appendix 1 for recipe) were used for size exclusion chromatography purification of refolded SCT. Concentrated, dialysed, refolded SCT protein was applied to the column (attached to a Uvicord SII spectrophotometer) and multiple fractions (15 min) were collected over 24 h. Collected fractions corresponding to distinct protein peaks as detected by the spectrophotometer were combined, concentrated using Amicon ultra centrifugal filter devices and analysed by HPLC.

2.3.3 Protein characterization

Purified refolded protein was initially analysed using a combination of HPLC (as described above), SDS-PAGE analysis and ELISA. However the ultimate test of conformationally correct refolding is whether the SCT protein is recognised by an appropriate TCR. Therefore SCT protein was used to make fluorescence-labelled tetramers to see if these could stain appropriate CTL.

2.3.3.1 Bradford assay

In order to load similar concentrations of protein during ELISA, SDS-PAGE and Western blot procedures it was necessary to determine the total concentration of protein within various SCT solutions. This was done using a Coomassie (Bradford) protein assay kit (Pierce, UK) as per manufacturer's instructions. Reactions were performed in duplicate on a 96-well plate (Nunc) using bovine serum albumin as the protein standard and was read at 590 nm using an automatic spectrophotometer (Dynatec MR4000). A blank-corrected standard curve was prepared from the absorbances obtained from the BSA dilutions and used to determine the total concentration of protein within the SCT protein samples.

2.3.3.1 SDS-PAGE analysis

Confirmation of the approximate size of the purified refolded SCT was performed using SDS-PAGE as described in section 2.3.2.2, with protein species size being determined by comparison with high range molecular weight markers (12-225 kDa).

2.3.3.2 Enzyme-linked Immunosorbent Assay

ELISAs were performed as described in section 2.2.3.2 coating with either W6/32 or BB7.2 and detecting with anti-hβ₂microglobulin-HRP as before. Standard curves were generated using a commercially available *NLVPMVATV*-containing HLA-A2/β₂microglobulin monomer (Orpegen, Germany). SCT proteins purified using immunoaffinity chromatography were analysed using a slightly different ELISA method: SCT proteins were diluted in coating buffer to a concentration of 400 ng/ml and then applied directly to the plate in a doubling dilution in duplicate. After a1 h incubation at 37 °C, plates were blocked then washed as before. Plates were probed with a primary Ab (see Table 2.5) diluted in PBS/BSA and incubated at 37 °C for 90 min before being washed and probed with a secondary Ab (see Table 2.5) diluted in PBS/BSA for 90 min at 37 °C. After washing, plates were developed as before and read at 490 nm on an automatic spectrophotometer.

Primary Antibody	Concentration of 1° Antibody used	Secondary Antibody	Concentration of 2° Antibody used
W6/32	2 μg/ml	Anti-mouse IgG-HRP (The Jackson Laboratory, Maine, USA)	1/1,000
BB7.2	1 μg/ml	Anti-mouse IgG-HRP	1/1,000
Rabbit anti-hβ ₂ microglobulin (ab6608, Abcam, UK)	1/50,000	Anti-rabbit IgG-HRP (GE Life Sciences, UK)	1/5,000

Table 2.5: Antibodies used for bacterial protein ELISAs

2.3.3.3 Tetramer formation

Enzymatic biotinylation of biotin-AviTag peptide-containing constructs

Refolded proteins containing the biotin-AviTag peptide were biotinylated enzymatically using a Bir A enzyme containing kit (Avidity) as per manufacturer's instructions. Briefly 1-2 mg of protein at a concentration of 1-2 mg/ml was dialysed against 10 mM TrisHCl using a Slide-a-lyzer 10,000 Da MWCO dialysis cassette (Thermo Scientific). 8 parts of protein substrate was then mixed with 1 part biomix A, 1 part biomix B and 2.5 µg Bir A enzyme. The biotinylation reaction was incubated at RT for 4-12 h (time necessary for completion depended on both concentration and total mass of protein to be biotinylated). Biotinylated protein was purified on a 20 x 1.6 cm Sephadex G25 fine column (GE Life Sciences) running in PBS, and then analysed using HPLC. Biotinylation was confirmed by Western blot analysis (see section 2.2.3.1 for method) probing with HRP-conjugated streptavidin (1/5,000). NB Blots to be probed with streptavidin-HRP were blocked with 5% BSA w/v TBS/T.

Chemical biotinylation of free sulfhydryl group-containing constructs

Refolded proteins containing a free sulfhydryl group were biotinylated using Pierce Maleimide-PEG2-Biotin. 1-2 mg of protein at a concentration of 1-2 mg/ml in TE8 buffer was reduced by adding 15 mM reduced glutathione and incubating at RT for 1 h. Reduced protein was separated from reduced glutathione on a cooled Sephadex G25 column (as above) and collected on ice under nitrogen gas to prevent re-oxidisation before being concentrated to > 1 mg/ml in an Amicon ultra centrifugal filter device. Maleimide-PEG2-Biotin was resuspended in PBS and the volume required for a 30 molar excess calculated as per manufacturer's instructions. This was added to the reduced SCT protein and incubated at RT for 3 h. Biotinylated protein was then purified from unconjugated free Maleimide-PEG2-Biotin on a G25 column as before. Biotinylated protein was concentrated and analysed by Western blot as above.

Tetramerisation reaction

Biotinylated monomeric SCT protein was used to make fluorescence-labelled tetramers by adding streptavidin-fluorescein isothiocyanate (SA-FITC) or streptavidin-PE (both Biotium) in a monomer: streptavidin ratio of 1:4. This was added in 10 aliquots to ensure SCT monomer was always in excess and therefore favoured complete tetramer formation. Tetramer formation using SA-FITC was monitored using HPLC (the larger size of PE made HPLC monitoring of tetramers formed using SA-PE more problematic). Tetramers were used to stain *NLVPMVATV*-peptide specific CTL (for generation see section 2.1.1.2) which were analysed by flow cytometry as described in section 2.1.2.1.

2.4 Bacterial Construct Production and Characterisation (Murine)

In order to evaluate the one-step pMHC x anti-hCD20 Fab' CTL retargeting strategy in an animal model, a murine pMHC SCT molecule was produced consisting of *SIINFEKL* peptide (derived from the model Ag ovalbumin (OVA) found in egg white) presented by murine K^b.

2.4.1.1 SIINFEKL-β₂microglobulin-K^b-biotin-AviTag construct design

The pET21a plasmid containing the DNA construct for *SIINFEKL*- β_2 microglobulin-K^b-biotin-AviTag was a kind gift from T Hansen (Washington University School of Medicine, St Louis, MO, USA). This was mutated in-house by B King to include the tyrosine \rightarrow alanine substitution at position 84 of the K^b heavy chain which enhances peptide binding within the F pocket of the peptide binding groove. Figure 2.3 illustrates the design of the DNA construct.

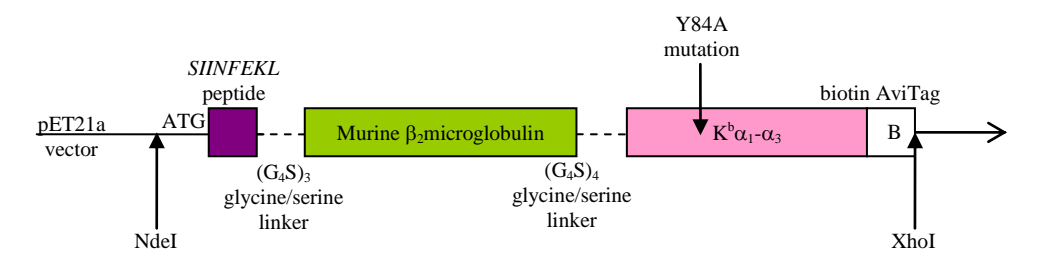


Figure 2.3: Design of genetic construct for SIINFEKL- β_2 microglobulin- K^b -biotin-AviTag (mSCT-B)

2.4.1.2 SIINFEKL-β₂microglobulin-K^b-biotin-AviTag protein production

KRX *E. coli* cells were used for the expression of protein encoded by *SIINFEKL*-β₂microglobulin-K^b-biotin-AviTag using the methods described in sections 2.3.2.1 and 2.3.2.2. Once sufficient bacterial pellet was collected (~20 g), inclusion bodies were purified using the method described in section 2.3.2.3. Solubilised inclusion bodies were then refolded using the method of Lybarger *et al*,⁴⁰⁵ concentrated using Stirred Cell concentrators, dialysed against 20 mM/Tris 0.1 M NaCl buffer pH 8 and filtered as outlined in section 2.3.2.4. The concentrated refolded mSCT-B protein was then purified using size exclusion chromatography as described in section 2.3.2.5. The concentration of purified mSCT-B was determined using a nanodrop in conjunction with the extinction coefficient (1.95 absorbance units per mg/ml) calculated using the ProtParam tool.⁴²⁶

2.4.1.3 SIINFEKL-β₂microglobulin-K^b-biotin-AviTag protein characterisation

An assessment of the size and apparent purity of the purified, refolded mSCT-B was made using a combination of SDS-PAGE (see section 2.3.2.2) and HPLC. An assessment of conformational integrity of the refolded mSCT-B protein was made by enzymatically

biotinylating the protein and using it for tetramer generation (see section 2.3.3.3) which can be used to stain CTLs with the cognate TCRs. Successful biotinylation was confirmed by Western blot probing with HRP-conjugated streptavidin. Successful tetramerisation was confirmed using either HPLC (possible when streptavidin-FITC was used) or via a dot blot (see below for method).

Dot blot

 $2~\mu l$ samples of the tetramerisation reaction were removed immediately before the addition of each streptavidin-fluorochrome aliquot and 10 min after the addition of the last aliquot (by which point the tetramerisation reaction should be complete), and dotted onto a nitrocellulose membrane. The membrane was air-dried and blocked for 1 h with 5% BSA / TBS/T before being probed with streptavidin-HRP (1/5000) for 30 min. It was then washed and developed as a standard Western blot (see section 2.2.3.1).

Staining splenocytes from OT-1 mice with mSCT-B tetramers

6-10 week old OT-1 mice (C57BL/6 background (H2^b) mouse with transgenic TCR Vα2 specific for H2K^bSIINFEKL, bred in-house but originally obtained from Dr M Merkenschlager, Imperial College, London, UK)⁴²⁸ were culled using a schedule 1 method and their spleens removed. These were disaggregated by being passed through a 100 μm cell sieve, washed, suspended in PBS and the concentration of nucleated cells determined using a Coulter Industrial D Cell Counter (red cells lysed prior to counting via the addition of Zapoglobin, Beckman Coulter). The concentration of splenocytes was adjusted to 1 x 10⁷/ml and 100 μl of cells were stained for flow cytometry (see section 2.1.2.1) with 10 μg/ml anti-mouse CD8-APC (eBiosciences, UK) and either 5 μg/ml commercially available K^bSIINFEKL-PE tetramer (Beckman Coulter) or 5 μg/ml mSCT-B-PE tetramer produced as described above. As a negative control splenocytes isolated in an identical fashion from age-matched wild type C57BL/6 mice (bred in-house) were stained.

2.4.2 Production of murine SIINFEKL- β_2 microglobulin- K^b -biotin-AviTag (mSCT-B) x anti-hCD20 (AT80) Fab' conjugates

2.4.2.1 Digestion of anti-hCD20 IgG to anti-hCD20 F(ab')2

A mouse anti-hCD20 Ig G_1 Ab produced in-house (AT80) underwent pepsin digestion to produce a F(ab')₂ which could subsequently be reduced to Fab', suitable for chemical conjugation to mSCT-B. Whole IgG was dialysed against 20 mM/Tris 0.1 M NaCl buffer pH 8 using a Slide-a-lyzer 10,000 Da MWCO dialysis cassette and then concentrated using an Amicon Ultra centrifugal filter device to a concentration of > 10 mg/ml (determined using a

nanodrop in conjunction with an extinction coefficient of 1.45 absorbance units per mg/ml). The pH of the IgG was adjusted to 4.1 using 2M sodium acetate (pH 3.7) and pepsin (Sigma) was added at a 3% w:v ratio for murine IgG (as a 1 mg/ml solution in 2M sodium acetate).

The digestion reaction was incubated in a water bath at 37 $^{\circ}$ C and progress was monitored by analysing 20 μ l aliquots by HPLC approximately every hour. Once >50% of the IgG had been digested to F(ab')₂ the reaction was stopped by increasing the pH to 8 using 1M Tris base. The digested Ab was concentrated using a centrifugal filter device to a concentration of >10 mg of protein per ml and the species were separated using size exclusion chromatography. Two in series 94.3 x 2.6 cm Superdex 200 columns running in TE8 buffer were used as described in section 2.3.2.5 to effect the separation of F(ab')₂ from the undigested IgG. The purity of resulting F(ab')₂ was assessed using SDS-PAGE and HPLC.

2.4.2.2 Purification of anti-hCD20 F(ab')2 using anti-mouse Fc column

To remove any contaminating IgG from the anti-hCD20 $F(ab')_2$, after being purified using size exclusion chromatography, the $F(ab')_2$ was passed down an anti-mouse Fc column which retains any Fc-containing protein (i.e. IgG) allowing the $F(ab')_2$ to pass through the column and be collected in the first unretarded fraction. This process is essentially immunoaffinity purification with the unwanted species being retained by the column. The method is as described in section 2.3.2.5: The column was equilibrated with 40 mM Tris/0.2M NaCl buffer pH 8 column running buffer before the $F(ab')_2$ was applied and the unretarded protein collected. Fc-containing IgG was eluted from the column with 2.5 ml ammonium thiocyanate and discarded. The unretarded $F(ab')_2$ was concentrated and reapplied to the column until no further IgG could be eluted. The purity of the $F(ab')_2$ post anti-mouse Fc column was confirmed by HPLC.

2.4.2.3 Conjugation of mSCT-B to anti-hCD20 Fab' using SMCC

The heterobifunctional cross-linker Succinimidyl-4-(*N*-maleimidomethyl) cyclohexane-1-carboxylate (SMCC) (Pierce, Thermo Fisher Scientific, UK) was used to conjugate equal molar quantities of Fab' to mSCT-B. Initially, F(ab')₂ in TE8 buffer was reduced by incubation with 20 mM 2-mercaptoethanol in a water bath at 30 °C for 30 min. The resulting Fab' was separated from the reducing agent by passing through a 1.6 x 25 cm Sephadex G25 column (GE Healthcare Life Sciences, UK) chilled to 4 °C and run with chilled, degassed PBS. Fab' was collected into a glass tube on ice, under nitrogen gas and stored briefly (~15 min) at 4 °C until required for the conjugation reaction. A 25 μl sample from the peak of the eluted Fab' was collected, mixed with 5 μl 250 mM iodoacetamide (Pierce) to alkylate the

free sulfhydryl groups in the Fab' hinge region via the covalent addition of a carbamidomethyl group thus preventing subsequent oxidation, and analysed using HPLC to assess the completeness of the reduction reaction.

While the $F(ab')_2$ was undergoing reduction, mSCT-B in PBS at a concentration of > 2 mg/ml was incubated with a 20 molar excess of SMCC (dissolved in a minimal volume of dimethylformamide (Sigma)) in a water bath at 30 °C for 30 min to produce mSCT-B_{mal} which is capable of reacting with reduced Fab'. The excess SMCC was removed by passing the reaction through a Sephedex G25 column as described above and the desired protein was collected in a similar fashion. Again a 25 μ l sample from the peak of the eluted protein was collected and analysed by HPLC.

Eluted mSCT_{mal} was immediately mixed with the reduced Fab' in a chilled vivaspin 20 (10,000 Da MWCO, (Sartorius, UK)) and spun at 3000 rpm in a Sorvall RT 6000D centrifuge chilled to 4 °C, until the total volume was < 5 ml. The conjugation reaction was then transferred to a screw top glass vessel which was topped up with nitrogen, sealed with parafilm 'M' and incubated overnight at 4 °C. Once the conjugation reaction was complete, reformed $F(ab')_2$ homodimers were removed by reducing the reaction with 20 mM 2-mercaptoethanol in a water bath at 30 °C for 30 min and then alkylating any free sulfhydryl groups via a 30 min incubation with 10% volume 250 mM iodoacetamide at 30 °C.

Conjugated mSCT-B x Fab' was separated from unconjugated species by passing the reduced, alkylated conjugation reaction through two in series 94.3 x 1.6 cm Superdex 200 columns running in TE8 buffer and collecting 15 min fractions. Fractions equating to the different peaks were pooled, concentrated using centrifugal filter devices and purity analysed using HPLC. The concentration of each protein species was determined using a nanodrop spectrophotometer: an extinction coefficient of 1.95 was used for the mSCT-B component of each construct and 1.45 for the Fab' component (i.e. extinction coefficients of 1.7 and 1.62 for F2 and F3 respectively).

2.4.3 Production of anti-hCD20 x anti-mCD3 F(ab')₂ conjugate

An anti-hCD20 x anti-mCD3 bispecific $F(ab')_2$; [anti-hCD20 x anti-mCD3] BsAb was used as a positive control in both *in vitro* and *in vivo* retargeting experiments. This was composed of Fab' derived from the rat anti-mouse CD3 IgG_{2a} KT3⁴²⁹ (Ab grown in-house, but originally obtained from MRC Clinical Research Centre, Harrow, London, UK) conjugated to mouse anti-hCD20 Fab' (derived from AT80) using N,N'-(o-Phenylene)dimaleimide (o-PDM) crosslinker.⁴³⁰

Equal molar quantities of $F(ab')_2$ (in TE8 buffer at a concentration of 5-12 mg/ml) of both of the species for conjugation were first obtained from the parental IgG via pepsin digestion as described in section 2.4.2.1. Anti-hCD20 $F(ab')_2$ was reduced first by incubation with 20 mM 2-mercaptoethanol in a water bath at 30 °C for 30 min. The resulting Fab' was separated from the reducing agent by passing through a 1.6 x 25 cm Sephadex G25 column chilled to 4 °C and run with chilled, degassed 20 mM HEPES / 5 mM EDTA pH 7.2 buffer . Fab' was collected into a graduated glass tube on ice under nitrogen. To ensure reduction was complete a sample from the peak of the eluted protein was collected, alkylated and analysed by HPLC as described in section 2.4.2.2. While the anti-hCD20 Fab' was passing through the column the anti-mCD3 $F(ab')_2$ reduction was initiated using an identical method as that employed for the anti-hCD20 $F(ab')_2$.

While reduced anti-hCD20 Fab' was eluting from the column o-PDM crosslinker (Sigma) was prepared by dissolving in dimethylformamide (in a glass vessel at RT initially, then in a methylated spirit / ice bath) to a final concentration of 12 mM. A half volume of this was then added to the eluted anti-hCD20 Fab' and incubated at 4 °C for 30 min. The reduced anti-mCD3 Fab' was separated from the reducing agent using the G25 column as described above and collected into a glass tube, on ice, under nitrogen where it was stored briefly (~15 min) until required for conjugation.

Anti-hCD20 Fab'_{mal} was separated from excess o-PDM and DMF using a 2.6 x 20 cm Sephadex G25 column chilled to 4 °C and run with chilled, degassed 20 mM HEPES / 5 mM EDTA pH 7.2 buffer. Eluted Anti-hCD20 Fab'_{mal} was immediately mixed with the reduced anti-mCD3 Fab' in a chilled vivaspin 20 (10,000 Da MWCO) and spun at 3000 rpm in a Sorvall RT 6000D centrifuge chilled to 4 °C, until the total volume was < 5 ml. The conjugation reaction was then transferred to a screw top glass vessel which was topped up with nitrogen, sealed with parafilm 'M' and incubated overnight at 4 °C. Once the conjugation reaction was complete, reformed F(ab')₂ homodimers were removed by reducing the reaction with 20 mM 2-mercaptoethanol in a water bath at 30 °C for 30 min and then alkylating any free sulfhydryl groups via a 30 min incubation with 10% volume 250 mM iodoacetamide at 30 °C. Conjugated bispecific F(ab')₂ was separated from unconjugated species by passing the reduced, alkylated conjugation reaction through two in series 94.3 x 1.6 cm Superdex 200 columns running in TE8 buffer and collecting 15 min fractions. Fractions equating to the different peaks were pooled, concentrated using centrifugal filter devices and purity analysed using HPLC.

The choice of the anti-hCD20 Fab' for initial maleimidation is of significance; Being derived from a parental murine IgG₁ there are three sulfhydryl groups naturally occurring in the hinge region. Although o-PDM is likely to link two adjacent sulfhydryl groups to themselves there is a remaining free sulfhydryl group which can be maleimidated and linked to another molecule. In contrast, the anti-mCD3 Fab' is derived from a parental rat IgG2a which has only two sulfhydryl groups in the hinge region. Once intramolecular crosslinking of adjacent sulfhydryl groups by o-PDM has occurred there are no free remaining sulfhydryl groups to crosslink to another molecule making it an unsuitable choice for initial maleimidation.

2.4.4 In vitro functional characterisation of mSCT-B x anti-hCD20 Fab' conjugates

Initial characterisation of the mSCT-B x anti-hCD20 Fab' conjugates was performed using analytical HPLC and reduced / non-reduced SDS-PAGE (for method see section 2.3.2.2).

2.4.4.1 Binding of mSCT-B x anti-hCD20 Fab' conjugates to hCD20 + cells

Indirect FACS was used to evaluate the structural integrity of both components of the conjugate (i.e. pMHC and Fab'). 1 x 10^6 Daudi cells (see section 2.1.2.2) suspended in $100 \,\mu l$ PBS were incubated with concentrations of mSCT-B x anti-hCD20 Fab' (F2) and mSCT-B x (anti-hCD20 Fab')₂ (F3) varying from 0.5 to 30 $\mu g/m l$ for 15 min at 4 °C. Cells were then washed twice with PBS/BSA/Azide, resuspended in PBS and bound F2 or F3 was detected using the K^bSIINFEKL complex specific Ab $25D1^{431}$ conjugated to FITC: Cells were incubated with 10 $\mu g/m l$ 25D1-FITC (CR UK monoclonal Ab production facility, UK; labelled in-house, see section 2.4.4.2) for 30 min at 4 °C, then washed and analysed on a FacsCalibur.

hCD20 expression on Daudi cells was confirmed by staining with FITC-conjugated rituximab (Ab from Roche, conjugated to FITC in-house, kind gift from M Cragg) and the function of 25D1-FITC was confirmed by staining K^bSIINFEKL-expressing EG7 cells. EG7 is the murine T cell lymphoblastic cell line EL4 stably transfected with OVA. These cells present SIINFEKL peptide in association with surface K^b, and are grown in RPMI 1640 (supplemented as for Daudi cells; section 2.1.2.2) containing 1 mg/ml geneticin (Invitrogen). To demonstrate that the conjugates were binding specifically to hCD20 on Daudi cells, they were pre-incubated with 100 μg/ml anti-CD20 F(ab²)₂ (AT80) for 15 min at 4 °C before being washed and stained with conjugate followed by 25D1-FITC as described above.

2.4.4.2 Labelling of 25D1 with fluorescein isothiocyanate (FITC)

0.5 mg 25D1 IgG was dialysed into PBS overnight and the concentration adjusted to 2 mg/ml. Fluorescein isothiocyanate (FITC) was dissolved in freshly made bicarbonate buffer (see

appendix 1 for recipe) at a concentration of 2 mg/ml. 1/10 volume of FITC was added to 25D1, and incubated in the dark in a water bath at 25 °C for 45 min. Meanwhile a PD-10 desalting column (GE Healthcare Life Sciences) was equilibrated with 25 ml phosphate buffer (see appendix 1 for recipe). The 25D1/FITC labelling mixture was applied to the column and the first eluted coloured peak was collected. The concentration of FITC-labelled Ab recovered was calculated using the following equation in conjunction with the nanodrop measured absorbance at 278 nm (A_{278}) and 495 nm (A_{495}):

[Ab-FITC] =
$$\underline{\mathbf{A}_{278} - (0.26 \times \mathbf{A}_{495})}$$

1.45

2.4.4.3 Cytotoxicity assay using mSCT-B x anti-hCD20 Fab' conjugates Generation of effector cells

Activated OT-1 cells were used as effector cells in cytotoxicity assays. These were generated by the adoptive transfer of splenocytes obtained from OT-1 mice containing a total of 1 x 10⁶ OT-1 cells into wild type C57BL/6 mice (avoiding male into female transfers). Splenocytes were isolated as described in section 2.4.1.3, red cells were lysed via a 2 min incubation with red cell lysis buffer (150 mM NH₄Cl 10 mM KHCO₃ pH 7.3), and the percentage of OT-1 cells within the splenocytes determined by flow cytometry, staining with anti-mouse CD8-APC and K^bSIINFEKL-PE tetramer. The splenocytes were resuspended in PBS so the final concentration of OT-1 cells was 5 x 10⁶/ml, and 200 μl (i.e. 1 x 10⁶ OT-1 cells) was injected via the tail vein into the recipient mouse (D-1).

OT-1 cells were activated one day after adoptive transfer (D0) via intravenous administration of 5 mg OVA (Sigma) and 0.5 mg of the agonistic anti-CD40 Ab $3/23^{432}$ (Ab grown in-house, but originally obtained from National Institute for Medical Research, London, UK) in a total volume of 200 μ l PBS. Activated OT-1 cells were harvested as described above on D5 after administration of OVA and 3/23 and the percentage of OT-1 cells amongst the splenocytes determined as before. The concentration of splenocytes was adjusted to give a final OT-1 cell concentration of 5 x $10^5/m$ l and the cells were resuspended in RPMI 1640 supplemented with 2 mM L-glutamine, 1 mM pyruvate, 50 μ M 2-mercaptoethanol and 10% foetal calf serum. As a negative control, splenocytes from C57BL/6 littermates of the OT-1 splenocyte recipient mice were prepared in an identical fashion and the final concentration of CD8⁺ T cells adjusted to 5 x $10^5/m$ l.

Target cell preparation

Daudi cells were used as target cells and labelled with ⁵¹Cr as described in section 2.1.2.2. EG7 cells were used as a positive control and labelled in an identical fashion. After labelling,

target cells were resuspended in RPMI 1640 supplemented as above to give a final concentration of 5×10^4 cells/ml.

Assay conditions

Target cells were plated out as described in section 2.1.2.2 (i.e. 5 x 10^3 targets per well in 100 µl medium). Effectors were then added at an effector target ration of 10:1 (i.e. 5 x 10^4 effector cells per well in 100 µl medium). The retargeting constructs F2, F3 or the positive control [anti-hCD20 x anti-mCD3] BsAb (all in PBS) were added at concentrations ranging from 0.001 µg/ml to 1 µg/ml (in a volume 2 µl). As a negative control diluent alone (i.e. PBS) was added to some wells. Once all the constituents of the assay were added to the wells the plates were spun, incubated, harvested and data analysed as for the two-step retargeting cytotoxicity assay in section 2.1.2.2. In some experiments after the addition of the target cells either anti-hCD20 F(ab')₂ or 25D1 IgG at a final concentration of 100 µg/ml (in a volume of 2 µl) was added and incubated at RT for 30 min before the addition of effectors and retargeting constructs as described above.

2.4.4.4 OT-1 proliferation assays

The ability of the retargeting constructs to cause proliferation of effector OT-1 cells was assessed using ³H-thymidine incorporation and CFSE dilution assays.

MACS-column purification of OT-1 cells

The mouse CD8a⁺ T cell Isolation Kit (Miltenyi Biotec, Germany) was used to isolate OT-1 cells by negative selection according to the manufacturer's instructions and purity was determined by flow cytometry labelling with anti-mouse CD8-APC and K^bSIINFEKL-PE tetramer.

³H-thymidine incorporation assay

Purified OT-1 cells (or C57BL/6 CD8⁺ T cells) were resuspended in RPMI 1640 supplemented as described in section 2.4.4.3 and 100 μ l (5 x 10⁴ cells) were seeded into wells on a 96 well u-bottomed tissue culture plate. The retargeting constructs F2 and F3 or the positive control [anti-hCD20 x anti-mCD3] BsAb were added at a final concentration of 1 μ g/ml in the presence or absence of 'hi' (1 x 10⁵/well) or 'lo' (1 x 10⁴/well) concentrations of irradiated Daudi cells (60 Gy). Control wells included OT-1 (C57BL/6) alone, *SIINFEKL* peptide (1 μ g/ml), and 'hi' and 'lo' concentrations of irradiated EG7 cells and EL4 cells¹ (both 200 Gy). Points were in triplicate. Plates were incubated at 37° C / 5% CO₂ for 72 h. 18

-

¹ murine T cell lymphoblastic cell line

h before the end of each incubation, 1µ Ci ³H-thymidine (GE Healthcare Life Sciences) was added per well. The plate was harvested using a FilterMate cell harvester and the amount of incorporated ³H-thymidine measured using a Topcount scintillation counter (all PerkinElmer).

Carboxy fluorescein succinimidyl ester (CFSE) dilution assay

MACS-column purified OT-1 cells (or CD8 $^+$ T cells from C57BL/6 mice) were washed twice in PBS to remove all protein and resuspended in PBS at a concentration of 1 x 10 6 cells/ml. CFSE (eBiosciences) was added to give a final concentration of 2 μ M and the reaction was incubated at RT for 8 min in the dark to prevent bleaching of the dye. After 8 min, FCS at a final concentration of 2% was added to stop the reaction and the cells were washed in 2% FCS/PBS twice to remove excess CFSE. CFSE labelled T cells were then used to set up assays identical to those described in section 2.4.4.4 but without the addition of 3 H-thymidine. After 48, 72 or 96 hours the cells were stained with anti-mouse CD8-APC, washed and CFSE dilution in CD8 $^+$ cells was determined by flow cytometry.

2.4.5 *In vivo* functional characterisation of mSCT-B x anti-hCD20 Fab' conjugates 2.4.5.1 B cell depletion assay

The ability of mSCT-B x anti-hCD20 Fab' conjugates to retarget non-cognate CTLs *in vivo* was evaluated using a hCD20 transgenic (Tg) mouse (C57BL/6 background) model⁴³³ where hCD20 is expressed on mature B cells (i.e. a similar distribution to murine CD20). These hCD20-expressing cells acted as an *in vivo* target cell population for adoptively transferred OT-1 cells to be redirected against using the retargeting conjugates: The efficacy of the retargeting construct can be determined by evaluating the depletion of B cells from the mouse.

The appropriate number of OT-1 cells to transfer and the kinetics of their activation was initially determined by transferring variable numbers of OT-1 cells (between 1 x 10⁴ and 8 x 10⁵ cells) into C57BL/6 wild type and hCD20 transgenic mice and activating them with antimouse CD40 Ab and OVA as described in section 2.4.4.3. In order to determine OT-1 cell expansion, mice were bled daily from D3, red blood cells lysed and the percentage of OT-1 cells amongst the peripheral PBMCs determined by flow cytometry staining with anti-mouse CD8-APC and K^bSIINFEKL-PE tetramer. 1 x 10⁵ OT-1 cells were subsequently adoptively transferred into hCD20 Tg mice on D-1 and activated as before on D0. At the peak of the OT-1 response (D6) mice received retargeting constructs via tail vein injection, diluted in PBS to a total volume of 200 µl as shown in Table 2.6.

Retargeting Construct	Mass (µg)	Dose (nmole)
F2	50	0.5
F2	100	1
F2	200	2
F3	75	0.5
F3	150	1
Positive control: [anti-hCD20 x anti-mCD3] BsAb	50	0.5
Negative control: PBS	-	-

Table 2.6: Retargeting constructs used in B cell depletions

Mice were bled via the tail vein at 0, 2, 8, 24, 72 and 168 h after administration of the retargeting construct. 5 μl of the sample was used to count the number of peripheral lymphocytes (using a Coulter Counter) while the remainder of the sample was stained with anti-mouse B220-PerCP-Cy5.5 and anti-mouse CD19-APC and analysed by flow cytometry in order to determine the percentage of peripheral lymphocytes which were B cells. At each time point, the absolute number of B cells/ml peripheral blood was calculated and plotted as a percentage of the starting number. Control depletions were performed in wild type C57BL/6 mice lacking hCD20 on their B cells and in mice which had not received an adoptive transfer of OT-1 cells. For comparison depletions were set up in non-adoptively transferred hCD20 Tg mice with the parental anti-hCD20 IgG (AT80) and F(ab')₂.

2.4.5.2 Meso Scale Discovery cytokine assay

As a marker of the relative toxicity of the pMHC versus anti-CD3 retargeting strategy, cytokine levels in the mice used in the depletion assays described above was determined using a Meso Scale Discovery Mouse TH1/TH2 9-plex Assay (Meso Scale Discovery, US). The assay was performed as per manufacturer's instructions. Data was analysed using the supplied MSD DISCOVERY WORKBENCH analysis software.

2.5 Characterisation of Dock and Lock Construct (Murine)

Pilot experiments were performed comparing a construct consisting of two anti-hCD20 Fab (i.e. exclude hinge region) fragments conjugated to murine *SIINFEKL*-β₂microglobulin-K^b (mSCT) (produced in mammalian cells) using the dock and lock platform (DnL), ^{434,2} with the F2 and F3 constructs described previously. The construct was a kind gift from Phil Savage, Imperial Hospital, London, UK and was manufactured by Immunomedics Inc, New Jersey, USA. The binding of [mSCT x (anti-hCD20 Fab)₂] DnL to hCD20 expressing cells was evaluated as described in section 2.4.4.1. The ability of [mSCT x (anti-hCD20 Fab)₂] DnL to retarget OT-1 cytotoxic T cells to lyse hCD20-expressing cells was determined using cytotoxicity assays as described in section 2.4.4.3. Finally the efficacy with which [mSCT x (anti-hCD20 Fab)₂] DnL could induce proliferation of appropriately restricted effectors was determined using thymidine incorporation assays as described in section 2.4.4.4.

² The dock and lock platform (DnL) exploits the naturally occurring specific protein:protein interaction between the dimerisation docking domain (DDD) in protein kinase A and the anchoring domain (AD) in a reactive A-kinase anchoring protein.

Chapter 3: Results - Human Retargeting Constructs

3.1 CTL Generation and Characterisation

The initial stage of this investigation was to conduct a proof-of-principle experiment to demonstrate that human CMV peptide-specific CTL lines generated *in vitro* were able to kill tumour cells expressing a non-cognate Ag using the two-step retargeting system of Savage *et al*³⁸⁷ demonstrated in Figure 1.13 B. This involved first generating the CTL lines, and then using these as effectors in a cytotoxicity assay.

3.1.1 Flow cytometric analysis of NLVPMVATV-specific CTL lines

The progress of CTL line generation was monitored by flow cytometric analysis of the percentage of cells within a culture expressing both CD8 and a TCR recognising *NLVPMVATV* peptide in the context of HLA-A2. Figure 3.1 shows the frequency of *NLVPMVATV*-specific CTLs in the donor's peripheral blood while Figure 3.2 shows the percentage of specific CTLs in cultures after three rounds of stimulation with irradiated autologous PBMCs and IL-2, with or without *NLVPMVATV* peptide.

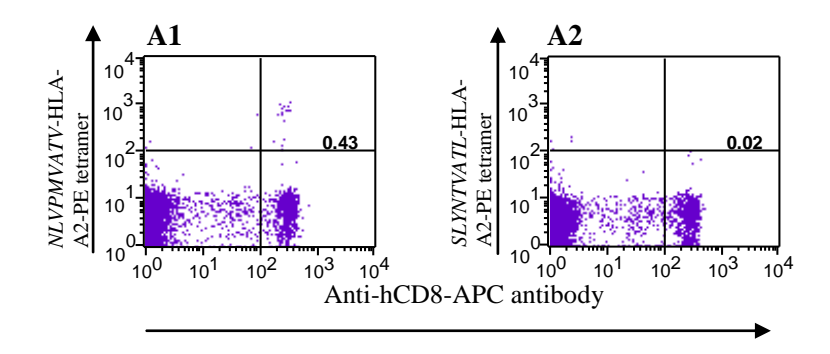
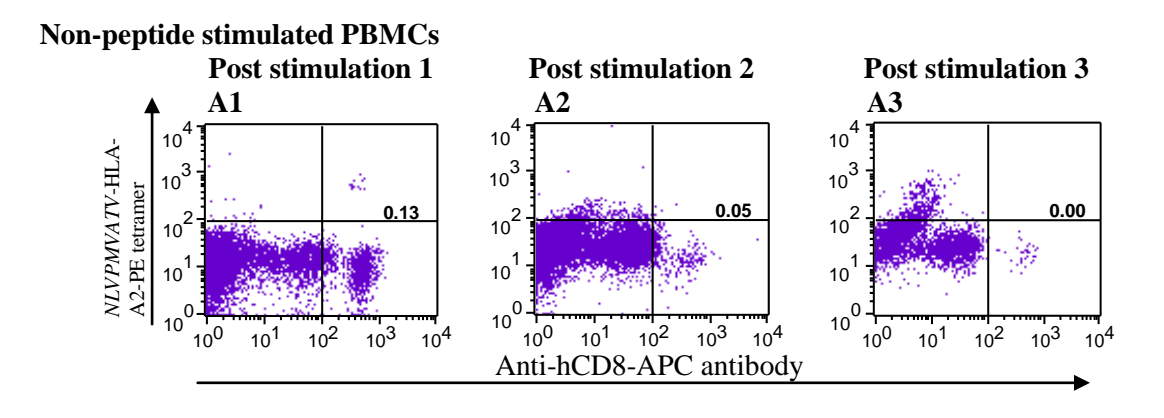


Figure 3.1: Flow cytometry profiles of unstimulated PBMCs
A1 and A2 PBMCs from an HLA-A2⁺/CMV⁺ donor labelled with anti- CD8 APC and NLVPMVATV or SLYNTVATL (irrelevant) tetramers respectively. Two donors were used to generate NLVPMVATV-specific CTL lines, both had similar frequencies of NLVPMVATV-specific CTLs in their PBMCs. Numbers show percentage of tetramer peptide-specific CTL.

Figure 3.2 shows specific peptide is required for the proliferation of *NLVPMVATV*-specific CTLs. The percentage of *NLVPMVATV*-specific CTLs per culture increased over 2-3 cycles stimulation. Although some of this can be accounted for by the death of non-*NLVPMVATV*-specific CTLs, culture cell counts show an increase in the absolute number of peptide-specific CTLS up to a maximum of $\sim 1 \times 10^6$ /ml. After 3 cycles of stimulation there was a dramatic decrease in the absolute number of *NLVPMVATV*-specific CTLs in each culture.



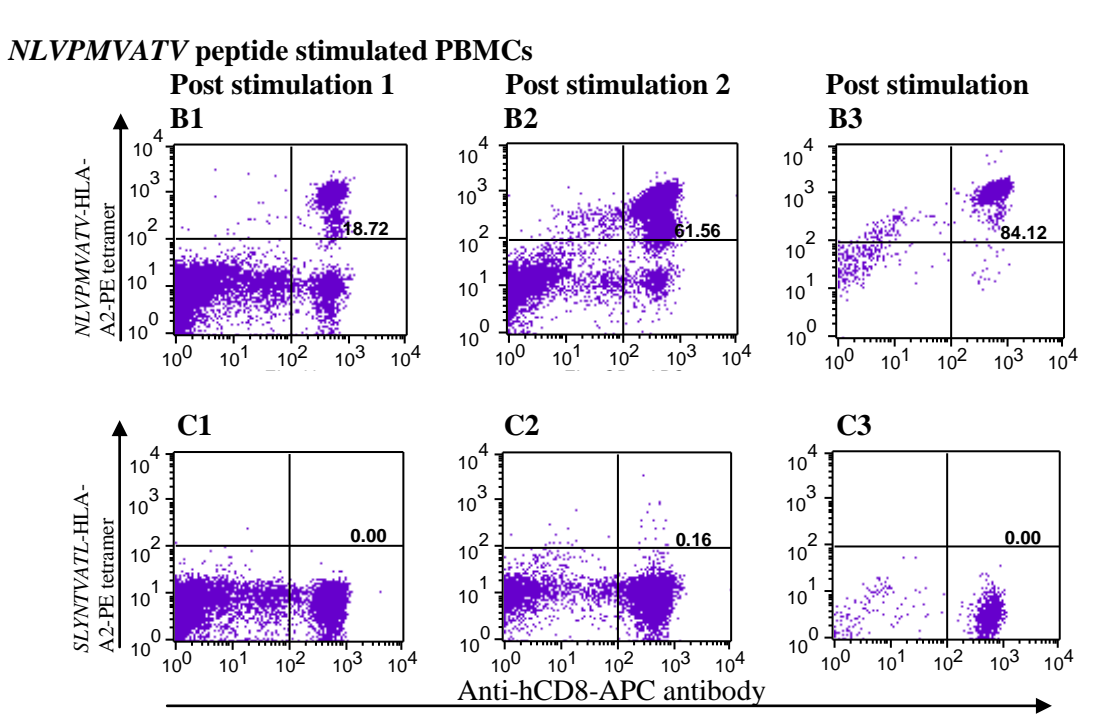


Figure 3.2: Flow cytometry profiles of non-peptide (A) and peptide (B & C) stimulated PBMCs

A1-A3 PBMCs stimulated with IL-2 and autologous irradiated PBMCs (no peptide) labelled with anti-CD8 APC and NLVPMVATV tetramer. B1-C3 show PBMCs repetitively stimulated with NLVPMVATV peptide, IL-2 and autologous irradiated PBMCs stained with anti-hCD8 Ab and NLVPMVATV (B1-B3) or SLYNTVATL (C1-C3) tetramer. The inter-stimulation interval is two weeks. Flow cytometry profiles are from a single culture from one individual. The data shown is representative of multiple cultures from two different donors. Numbers indicate percentage of tetramer peptide-specific CTLs per culture.

Despite initial claims of the existence of 'immortal' T cell cultures (both clones and lines), closer scrutiny has revealed that many of these contain chromosomal abnormalities, particularly trisomy 2, suggesting they have undergone transformation, rather than having 'normal' unlimited proliferative potential. This replicative senescence is likely to be, at least in part, secondary to progressive shortening of the telomeres. Although T cell activation results in the expression of telomerase to maintain telomere length and hence support replication, studies have shown that while the first and second rounds of antigenic

stimulation upregulate telomerase expression, the response to a third round is much reduced and following subsequent stimulations undetectable. Studies have also shown that transfer of the human telomerase reverse transcriptase (TERT) gene into T cells increases their replicative potential allowing more than 170 population doublings.

There is also evidence that the proliferative potential of CTLs is related to donor age; neonates have been shown to have increased numbers of proliferative doublings of their T cells *in vitro* compared to adults, although amongst adults there was no correlation between age of donor and T cell lifespan. Furthermore, given CMV is a chronic infection providing persistent antigenic stress it is possible that amongst older donors CTLs have already gone through a number of divisions (and hence telomere shortenings) *in vivo* 440 before the initiation of the *in vitro* culture, limiting the subsequent replicative potential.

3.1.2 Two-stage retargeting cytotoxicity assay

In order to demonstrate that the *NLVPMVATV*-specific CTLs were functional and capable of causing target cell death when redirected against cells expressing non-cognate Ags, they were used as effectors in a cytotoxicity assay exploiting the two-step retargeting system of Savage *et al.*³⁸⁷ Figure 3.3 demonstrates that up to 80% specific lysis of *NLVPMVATV*-coated Daudi cells can be achieved at an effector: target ratio of 5:1, and even at a ratio of 0.5:1 the *NLVPMVATV*-specific CTLs are able to achieve over 25% specific lysis. The cytotoxicity is peptide specific as no killing of uncoated targets or targets coated with irrelevant peptide is observed.

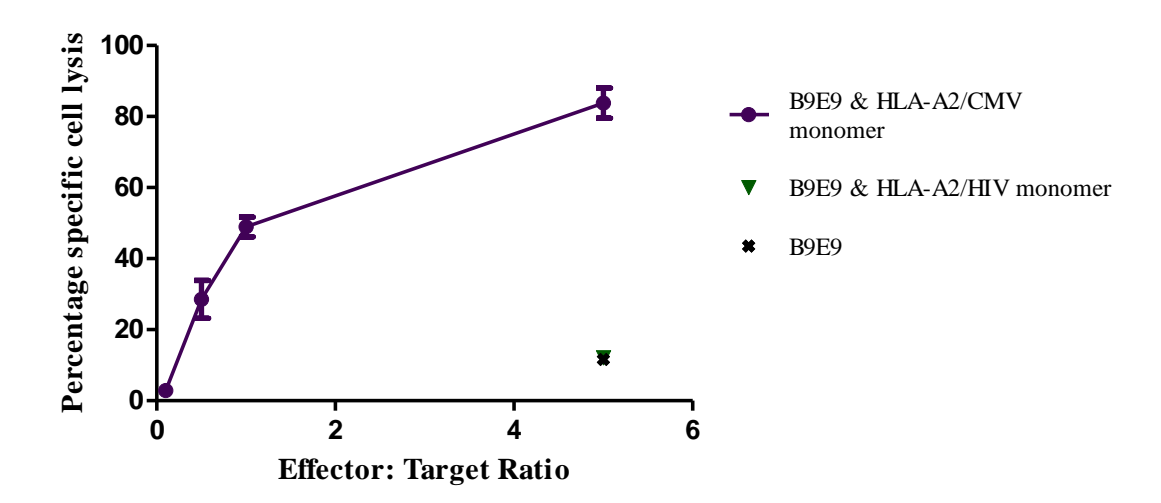


Figure 3.3: Specific lysis of coated Daudi cells by NLVPMVATV-specific CTLs Daudi cells were coated with B9E9-SA alone, B9E9-SA & NLVPMVATV-HLA-A2 monomer or B9E9-SA & SLYNTVATL-HLA-A2 monomer. Specific cell lysis was calculated using the formula in section 2.1.2.2. The culture used had undergone one antigenic stimulation and 42% of the lymphocytes were NLVPMVATV-specific CTLs. Points show mean +/- SEM from at least 3 wells. Data representative of similar experiments.

These experiments demonstrate *NLVPMVATV*-specific CTL lines can be generated *in vitro* from HLA-A2⁺/CMV⁺ donors which are functional as evidenced by their ability to lyse target cells coated in *NLVPMVATV* peptide. The ability of the *NLVPMVATV*-specific CTL lines to be retargeted to cells expressing non-cognate Ags suggests they will be a useful tool for the *in vitro* evaluation of a single bivalent retargeting molecule.

3.2 Mammalian Protein Expression

3.2.1 Construct design

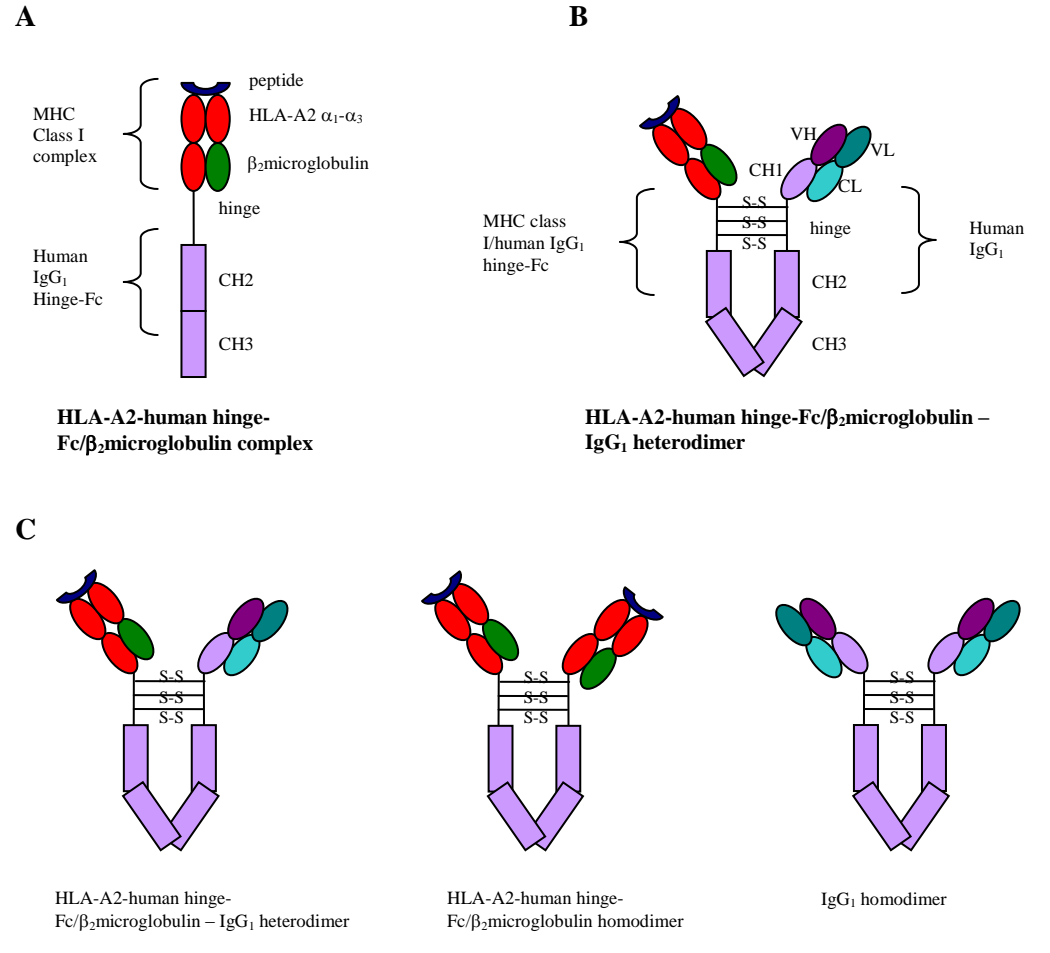
As discussed in the introduction, the T cell retargeting molecule needs to be bivalent with the ability to activate a defined population of cytotoxic T cells (i.e. via an MHC class I/peptide molecule) while exhibiting specificity for a tumour cell surface Ag (i.e. through an Ab moiety). Figure 3.4 demonstrates different designs for a one-step retargeting molecule which avoid the need for streptavidin-biotin linkage of two separate molecules.

The initial design for a one-stage retargeting molecule involved expressing the MHC-component (as separate heavy chain and β_2 microglobulin proteins) in mammalian cells. This is not dissimilar to the approach used in the commercially available DimerX: recombinant soluble dimeric human HLA-A2:Ig Fusion Protein (BD Biosciences, UK). Eukaryotic cells were favoured over bacterial cells, in part, due to their ability to produce folded proteins which do not have to undergo extensive post-expression manipulation in order to obtain a conformationally active structure. Their use also allowed the addition of an immunoglobulin hinge-Fc region to the carboxy terminus of the class I heavy chain (see Figure 3.4) as, in contrast to most prokaryotic cells, mammalian cells are able to glycosylate protein which is necessary for full Fc function.

The addition of an Fc region is expected to improve secretion of the molecule 443 and also provides several sulfhydryl groups on the MHC-component which correspond to those on the Ab arm allowing the formation of heterodimers. It was proposed that the MHC heavy chain-hinge-Fc/ β_2 microglobulin constructs could be expressed in either hybridoma cells or other transfected cells secreting the required immunoglobulin, resulting in the production of a mixture of hetero- and homodimers as shown in Figure 3.4. The presence of an Fc region within the conjugated molecule also has implications for construct half life; an MHC arm lacking a hinge-Fc would need to be conjugated to a Fab' (lacks an Fc region) to preserve symmetry (see Figure 3.4), resulting in a complete molecule the approximate size of F(ab')₂ rather than IgG.

Studies comparing the half- lives of the two molecules have generally shown IgG to have the longer half-life, 444 although there are exceptions. 445 This is likely to be related to the action of the neonatal Fc receptor (FcRn) which is able to prevent IgG from undergoing lysosomal degradation by recycling the molecule to the cell surface after it has undergone endocytosis. 446 It was initially planned to mutate residues within the Fc region in order to enhance its interaction with the FcRn whilst reducing its binding to other Fc receptors. 447 A further

advantage of fusing an Fc region to the MHC class I heavy chain is that the protein can then be purified using a protein A column due to the high affinity of human IgG (particularly IgG₁) for protein A.



Potential range of hetero- and homodimer protein products from hybridoma or other immunoglobulin-producing cell transfected with MHC class I/human IgG_1 hinge Fc construct

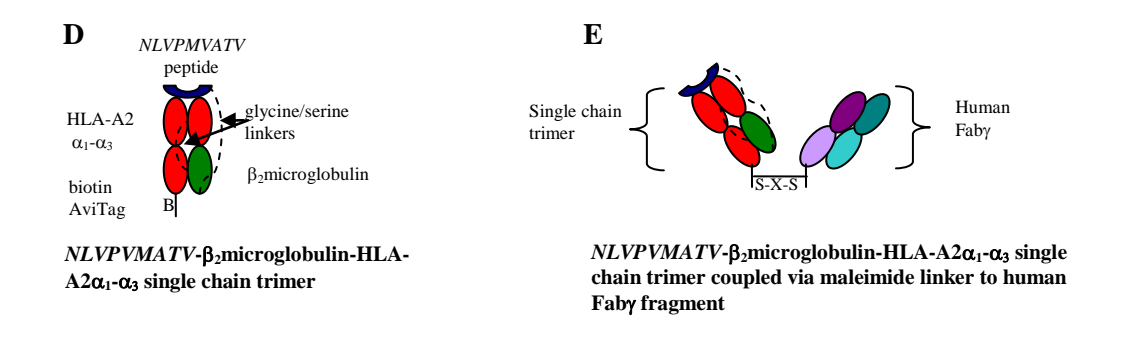


Figure 3.4: Design of one-step retargeting molecules to be produced in mammalian cells A & B: expected structure of the MHC class I/human IgG_1 hinge-Fc construct and its hetero-dimerisation with IgG_1 . C: potential range of hetero- and homodimer products from immunoglobulin-secreting cells transfected with the MHC class I/human IgG_1 hinge-Fc constructs. D & E: expected structure of the single chain trimer protein and its subsequent chemical conjugation to a Fab' fragment. The SCT shown in D would need to have a cysteine inserted at its carboxy terminus in order to provide a sulfhydryl group for conjugation to a Fab' fragment using a maleimide linker.

The expression of xenotypic MHC class I in mammalian cells is not without precedence; there are reports of successful expression of membrane-bound human HLA-A2 in murine C57BL/6 haematopoietic cells using a retroviral vector⁴⁴⁸ and murine β_2 microglobulin in Daudi cells using electroporation.⁴⁴⁹ The incorporation of the transfected gene products into MHC class I complexes at the cell surface suggests they are able to access the endogenous Ag processing and presentation pathway.

3.2.2. Production of genetic constructs

Five different vector constructs for mammalian protein expression were produced (as detailed in section 2.2.1), designed to be transfected alone or in combination. Their structures are shown in Figure 2.1 and the rationale of their individual design is detailed below. The DNA gels illustrating the individual steps in their production and final sequences can be found in appendices 2 & 3 respectively.

pcDNA3.2-HLA-A2-human IgG₁ hinge-Fc (Figure 2.1 **A**) was the first HLA-A2-containing construct produced, designed to be co-transfected with a separate β_2 microglobulin-containing construct to produce the complete MHC class I complex. It does not include any antigenic peptide sequence; the expectation being that the translated protein would enter the normal class I Ag presentation pathway and acquire an endogenously produced antigenic peptide which could be replaced with a peptide of interest using exchange dialysis. It contains exons 1-4 of the HLA-A2 gene which encode the promoter region and the extracellular α_1 - α_3 domains. Its transfection partner pCI-puro- β_2 microglobulin (Figure 2.1 **B**) contains part of exon 1 (encoding the signal peptide and the first two residues of the mature protein) and all of exons 2-4 (encoding the remainder of the mature protein) of the β_2 microglobulin gene.

To ensure lack of appropriately restricted peptide was not limiting the secretion of mature MHC class I complexes, a β_2 microglobulin-containing construct with the HLA-A2-restricted *NLVPMVATV* peptide attached to the 5' terminus via a glycine/serine linker was produced (pCI-puro-CMV-(G₄S)₄- β_2 microglobulin; Figure 2.1 C). This approach has been used previously to increase presentation of a specific peptide by membrane-bound class I, ⁴⁵⁰ and to improve *in vitro* refolding efficiency of bacterially produced MHC class I monomers. ⁴⁵¹ This construct included a Kozak sequence ⁴⁵² rather than the β_2 microglobulin gene signal peptide immediately upstream of the ATG start codon in order to help initiate translation.

The expression of two different recombinant proteins in a single cell requires either cotransfection of two monocistronic vectors (e.g. pcDNA3.2-HLA-A2-human IgG₁ hinge-Fc

and pCI-puro- β_2 microglobulin) or the sub-cloning of both genes into a single bicistronic vector. The latter approach should be more efficient for protein production; whereas cotransfection of two plasmids will result in their integration at different sites (with likely varying transcription rates) a bicistronic vector should result in the integration of both genes at the same site. To investigate whether this was the case for recombinant MHC class I expression the β_2 microglobulin and HLA-A2-human IgG₁ hinge-Fc fusion genes were sub-cloned into the bicistronic vector pEE14.1/pEE6.1 (pEE14.1-HLA-A2-human IgG₁ hinge-Fc/pEE6.1- β_2 microglobulin; Figure 2.1 **D**).

The above constructs all require separately produced heavy chain and β_2 microglobulin proteins to form a complex within the ER Ag processing and presentation pathway before being trafficked to the cell membrane. An alternative approach which has resulted in very successful membrane presentation of class I is to link the peptide, β_2 microglobulin and heavy chain α_1 - α_3 genes together by glycine/serine linkers to produce an SCT which enables the whole complex to be produced as a single protein (see Figure 3.4). 409 Production of soluble complexes using such a construct has been limited to bacterial cells, 405 although the alternative component order of peptide-heavy chain- β_2 microglobulin has been used successfully in CHO cells. 402

To investigate whether expressing the complex as a single protein was more efficient, the fusion gene produced for bacterial expression i.e. NLVPMVATV- β_2 microglobulin-HLA-A2 α_1 - α_3 was sub-cloned into the pIg plus vector in frame with the CD33 signal peptide, thus creating an SCT construct for mammalian expression. The construct included the biotin AviTag at the carboxy terminus of the heavy chain so that complexes could be biotinylated and made into tetramers to investigate their recognition of specific CTLs (Signal pIg plus-CMV-short linker- β_2 microglobulin-HLA-A2-biotin-AviTag; Figure 2.1 **E**).

3.2.3 Characterisation of proteins expressed in mammalian cells

The constructs were used for the transfection of 293F and CHO-K1 cells and expression of the desired protein was confirmed using a combination of western blot analysis and ELISAs. Figure 3.5 illustrates the various (co)transfections undertaken.

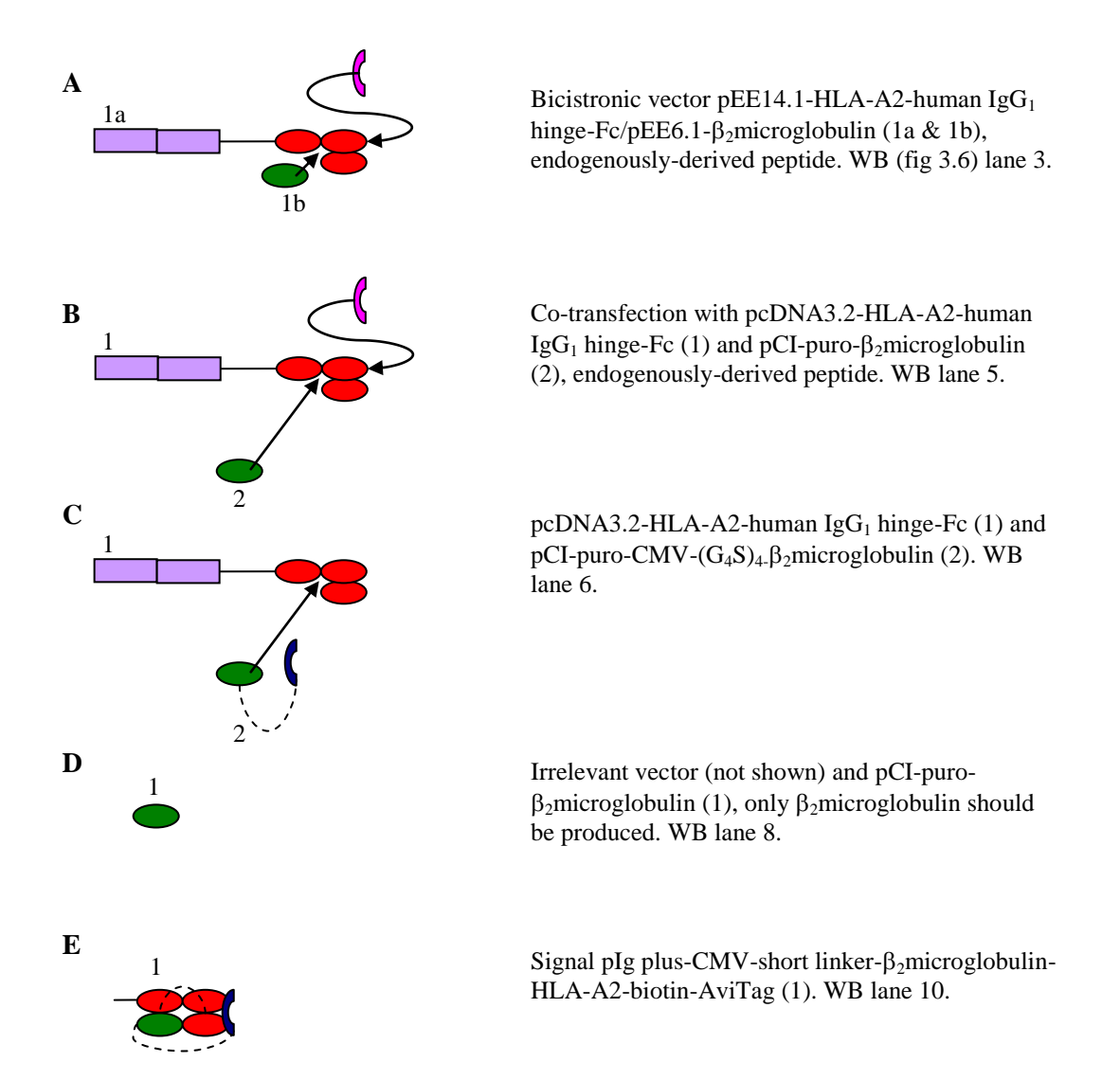
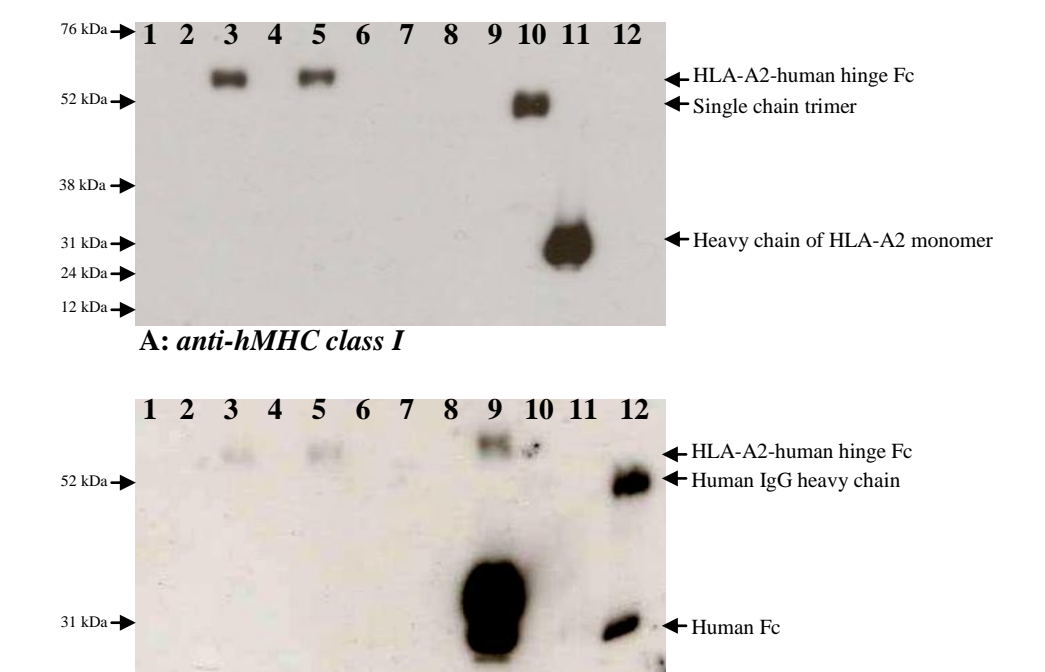


Figure 3.5: Schematic representation of (co-)transfections undertaken to produce MHC component of retargeting protein in mammalian cells

The symbols used represent the same molecular components as shown in Figure 3.4.

3.2.3.1 Western blotting of proteins expressed in mammalian cells

All mammalian cell constructs were initially expressed using a transient transfection of 293F cells and the supernatants (s/n) analysed for the presence of the protein using Western blotting. The blots in Figure 3.6 illustrate the different species secreted as a result of 293F cell transfection. Collectively these blots provide some information about which genetic constructs are able to produce the desired proteins. Transfection with either pEE14.1-HLA-A2-human IgG₁ hinge-Fc/pEE6.1- β_2 microglobulin (lane 3) or pcDNA3.2-HLA-A2-human IgG₁ hinge-Fc *and* pCI-puro- β_2 microglobulin (lane 5) results in the production of two proteins, a larger species (expected size 64.5 kDa) which is recognised by both anti-human MHC class I and anti-human Fc and a smaller ~ 12 kDa species recognised by anti-human β_2 microglobulin.



B: anti-hFc

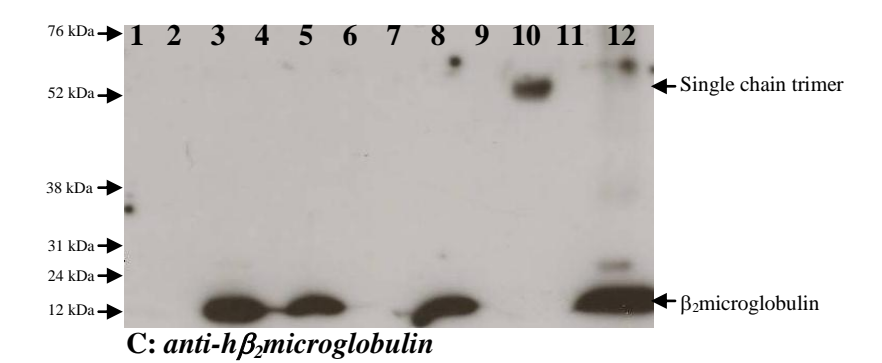


Figure 3.6: Western blot analysis of mammalian construct protein production from transfections of 293F cells

Lane order

- 1. Non-transfected
- 2. pEE14.1/pEE6.1 empty vector transfected
- 3. pEE14.1-HLA-A2- $human IgG_1 hinge$ -Fc/pEE6.1- $\beta_2 m$ (Fig 3.5 A)
- 4. pcDNA3.2/pCI-puro empty vector
- 5. pcDNA3.2-HLA-A2- $human IgG_1 hinge$ -Fc/pCI-puro- $\beta_2 m$ (Fig 3.5 **B**)
- **6.** pcDNA3.2-HLA-A2- $human IgG_1 hinge-Fc/pCI$ -puro-CMV- $(G_4S)_4$ - $\beta_2 m$ (Fig 3.5 C)
- 7. Irrelevant/pCI-puro empty vector
- 8. Irrelevant/pCI-puro- β_2 m (Fig 3.5 **D**)
- 9. Signal plg plus empty vector
- 10. Signal pIg plus-CMV-short linker- β_2 m-HLA-A2-biotin-AviTag (Fig 3.5 E)

Control lane order blots A & B Control lane order blot C

11. HLA-A2 monomer 11. Empty

12. human IgG 12. recombinant human β_2 microglobulin

293F cell supernatants were concentrated and reduced prior to analysis. One blot was probed sequentially with anti-hMHC class I (blot A) and anti-hFc (blot B). Blot C probed with anti-h β_2 microglobulin alone.

In contrast, co-transfection with pcDNA3.2-HLA-A2-human IgG_1 hinge-Fc and pCI-puro-CMV- $(G_4S)_4$ β_2 microglobulin (lane 6) does not result in the production of detectable protein. This suggests that replacement of the β_2 microglobulin signal sequence with a Kozak-antigenic peptide sequence interferes with one or more stages of the β_2 microglobulin production and expression. It is not possible to tell whether any protein is produced and retained within transfected cells. One possibility is that CMV- $(G_4S)_4$ - β_2 microglobulin protein is produced and associates with HLA-A2-human hinge-Fc, but the deviant structure of the complexes prevents their traffic to the cell membrane for secretion, meaning neither species can be detected in the supernatant. Another explanation is that no mature CMV- $(G_4S)_4$ - β_2 microglobulin is produced; either the Kozak-peptide sequence prevents transcription or translation, or the peptide- β_2 microglobulin polypeptide is translated but is unable to fold successfully resulting in its degradation by the proteasome. ⁴⁵⁴

Although there appears to be a requirement for co-transfection of vectors containing functional HLA-A2-human hinge-Fc and β_2 microglobulin for the secretion of any HLA-A2-human hinge-Fc molecules, the reverse does not appear to be true: Co-transfection of an irrelevant vector with pCI-puro- β_2 microglobulin (lane 8) results in the secretion of β_2 microglobulin suggesting it is not necessary to have an additional source of class I heavy chain for its secretion. This is not surprising given β_2 microglobulin is a stably folded molecule in the absence of class I heavy chains, and as part of its normal turnover is shed from the cell membrane into the blood.

Transfection with Signal pIg plus-CMV-short linker- β_2 microglobulin-HLA-A2-biotin-AviTag results in the production of a ~50 kDa species which is recognised by an anti-human MHC class I (lane 10 gel **A**). Gel **C** demonstrates this protein is also recognised by an anti-human- β_2 microglobulin a, as would be expected for an SCT protein. The prominent band in lane 9 resulting from transfection with Signal pIg plus empty vector is human Fc: The empty vector contains the gene for human IgG₁ Fc downstream and in frame with the CD33 signal peptide. This arrangement is destroyed by the insertion of a gene of interest and therefore Fc is not produced after transfection.

3.2.3.2 ELISA analysis of proteins produced in mammalian cells

Production of HLA-A2-human hinge-Fc complexes by transfected 293F cells

The quantity of Fc-containing protein (and therefore HLA-A2 human hinge-Fc) secreted from 293F cells transfected with the various constructs was estimated by ELISA using capture and detection antibodies recognising human Fc, with human IgG used to create a standard curve.

Example results from these ELISAs are shown in appendix 2. This data indicates that all constructs are being produced at levels substantially lower than 1 μ g/ml (pcDNA3.2-HLA-A2-human IgG₁ hinge-Fc/pCI-puro- β_2 m = 31 ng/ml and pEE14.1-HLA-A2-human IgG₁ hinge-Fc/pEE6.1- β_2 m = 46 ng/ml).

Although the Western blots did not detect any pcDNA3.2-HLA-A2-human IgG_1 hinge-Fc/pCI-puro-CMV- $(G_4S)_4$ - β_2m , the ELISA measurements did show a very low level of production at 9 ng/ml. This supports the hypothesis that an additional non-endogenously encoded source of β_2 microglobulin is required for the efficient secretion of HLA-A2-human hinge-Fc fusion. This is further supported by ELISA data showing that transfection with pcDNA3.2-HLA-A2-human IgG_1 hinge-Fc alone does not result in detectable HLA-A2-human hinge-Fc protein.

In order to detect whether the HLA-A2 component is correctly folded, and whether the fusion protein is found in association with β_2 microglobulin, ELISAs were performed with a capture Ab which recognises correctly folded MHC class I heavy chain component (either BB7.2 specific for HLA-A2⁴⁵⁶ or W6/32 specific for HLA-A, -B, -C, -E and -G heavy chains in association with β_2 microglobulin⁴⁵⁷) and a detection Ab specific for h β_2 microglobulin conjugated to HRP. This data is shown in Figure 3.7 ELISA data confirm that pcDNA3.2-HLA-A2-human IgG₁ hinge-Fc/pCI-puro-CMV-(G₄S)₄- β_2 microglobulin transfected cells produce a very low /undetectable level of HLA-A2-human hinge-Fc/ β_2 microglobulin complexes consistent with the western blot data. Transfection with the bicistronic pEE vector construct consistently produces more protein than co-transfection with the separate HLA-A2-human IgG₁ hinge-Fc and β_2 microglobulin vector complexes.

Although these 293F (co-)transfections provided information about which vector constructs could produce the desired protein species, for long-term protein production in adequate quantities for further manipulation (i.e. purification and subsequent conjugation to an Ab moiety) it is necessary to have high-secreting, stably transfected clones. Therefore, those genetic constructs which resulted in detectable levels of protein upon transfection of 293F cells were used to produce stably transfected CHO-K1 cells.

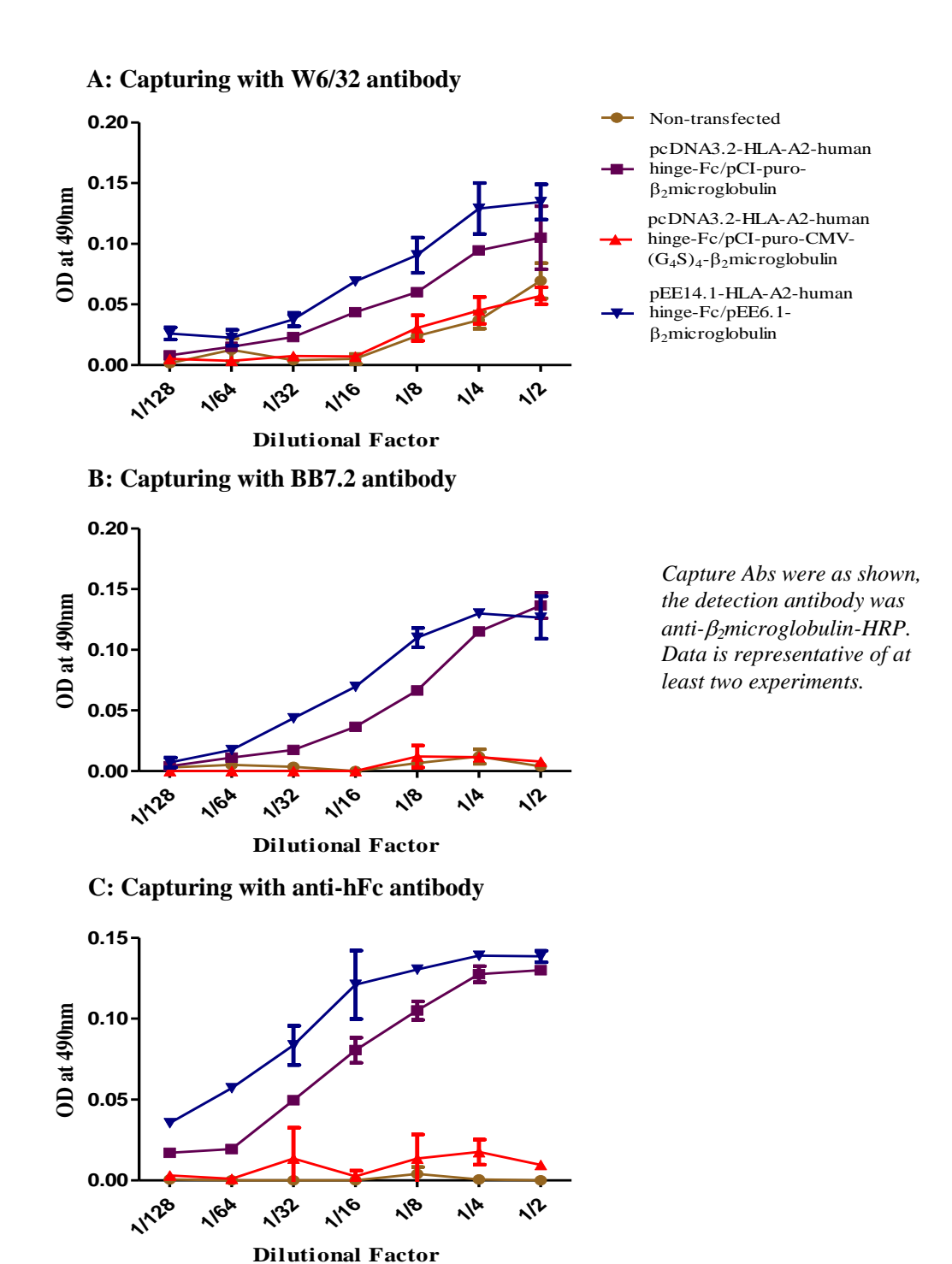


Figure 3.7: ELISA analysis of HLA-A2-human hinge-Fc/ β_2 m protein secretion from 293F (co-)transfections; capturing with W6/32, BB7.2 or anti-hFc & detecting with anti-h β_2 m-HRP

Production of HLA-A2-human hinge-Fc complexes by transfected CHO-K1 cells

pEE14.1-HLA-A2-human IgG₁ hinge-Fc/pEE6.1- β_2 microglobulin and pcDNA3.2-HLA-A2-human IgG₁ hinge-Fc/pCI-puro- β_2 microglobulin vectors were used to transfect CHO-K1 cells in order to produce stable transfectants which were selected with methionine sulphoximine or geneticin & puromycin respectively. Secretion of HLA-A2-human hinge Fc into the

supernatant was analysed using an ELISA as described above. However, HLA-A2-human hinge-Fc fusion protein production by CHO- K1 cells stably transfected with either pEE14.1-HLA-A2-human IgG₁ hinge-Fc/pEE6.1- β_2 microglobulin or pcDNA3.2-HLA-A2-human IgG₁ hinge-Fc/pCI-puro- β_2 microglobulin was very low; 46 ng/ml and 8 ng/ml respectively (data not shown). Therefore an alternative strategy needed to be employed for production of the MHC-component of the single-step retargeting molecule.

Production of NLVPMVATV- β_2 microglobulin-HLA-A2 single chain trimer protein by transfected 293F cells

One such alternative strategy is to produce the MHC arm as an SCT molecule. This requires expression of only a single fusion gene followed by its conformationally correct folding so is potentially easier for a transfected cell to produce. However, the SCT will not have any of the advantages conferred by the presence of an Fc region, discussed in section 3.2.1. An ELISA assay using the pan-class I heavy chain Ab W6/32 for capture and a two-stage detection with anti-human β_2 microglobulin detected with an HRP-conjugated anti-xenotype Ab gave an estimation of the level of SCT protein secretion of ~550 ng/ml, far greater than that observed with the HLA-A2 human hinge-Fc/ β_2 microglobulin complexes shown in Figure 3.7.

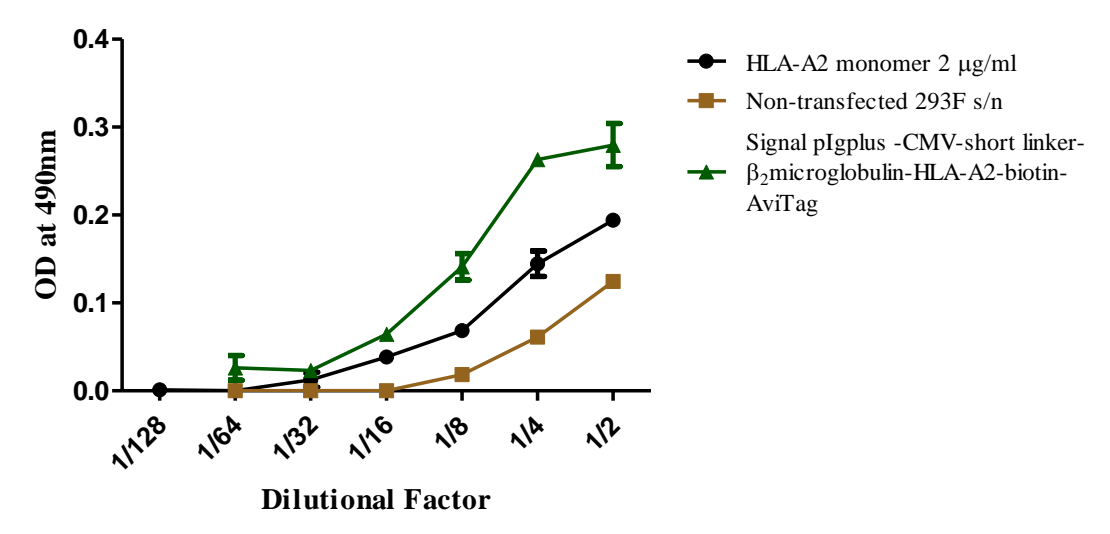


Figure 3.8: ELISA analysis of NLVPMVATV- β_2 m-HLA-A2 protein secretion from Signal pIg plus-CMV-short linker- β_2 m-HLA-A2-biotin-AviTag transfected 293F cells; capturing with W6/32 and detecting with anti-h β_2 m antibodies

7x concentrated transfected 293F cell supernatant was used. Samples were loaded in duplicate and underwent a doubling dilution. Mean values are plotted with error bars demonstrating the range. An HLA-A2 monomer was available as a positive control allowing some quantitative data to be obtained from the ELISA.

Production of NLVPMVATV- β_2 microglobulin-HLA-A2 single chain trimer protein by transfected CHO-K1 cells

Owing to the promising level of SCT protein production by transfected 293F cells, CHO-K1 cells were stably transfected with Signal pIg plus-CMV-short linker- β_2 microglobulin-HLA-A2-biotin-AviTag. Protein secretion was measured by ELISA and showed a level of ~ 1.5 µg/ml. Although this is far below the level considered feasible for immunoglobulin production it is considerably higher than any of the other mammalian expression systems investigated. It is also consistent with the production of 1-3 µg/ml of soluble peptide-heavy chain- β_2 microglobulin fusion protein by CHO cells reported by Mottez *et al.*⁴⁰²

Purification of SCT protein may be problematic as the lack of an Fc region means it will not bind to protein A. It is theoretically possible to purify SCT protein using an immunoaffinity column, although the extreme pH necessary for elution may destroy the tertiary structure of the protein. Alternatively the CMV-short linker- β_2 microglobulin-HLA-A2-biotin-AviTag fusion gene could be linked to a his tag which would allow purification by metal chelate affinity chromatography. These potential problems, together with the low yield led to bacterial expression options being explored to in an attempt to obtain higher levels of protein production.

3.3 Bacterial Protein Expression

3.3.1 Construct design

Owing to the disappointing yield of the MHC class I component of the one-step retargeting molecule from mammalian cells, expression in bacterial cells (*Escherichia coli*) was explored. These prokaryotic cells lack most of the post-translational machinery necessary for the secretion of properly refolded, bioactive recombinant proteins. Instead, many over-expressed recombinant proteins accumulate in the cytoplasm as insoluble misfolded protein aggregates known as inclusion bodies. These have to be extracted, solubilised and denatured before being refolded *in vitro*. Although this process is more labour intensive than purifying a soluble protein from a cellular supernatant, inclusion bodies can provide the recombinant protein with some resistance from protease degradation ⁴⁵⁹ resulting in a purer protein product.

Pursuing bacterial expression meant some alterations were required to the design of the MHC moiety: When expressed in eukaryotic cells the C_{H2} region of human Fc undergoes *N*-glycosylation which influences its ability to bind to both Fc receptors and the complement component C1q, hence affecting effector function. Although *Campylobacter* express PgI proteins which are able to perform *N*-glycosylation *in vivo*, and most bacteria, including *E. coli*, do not possess these enzymes. Therefore the Fc region was omitted from the design of the MHC molecule for bacterial expression.

The use of *E. coli* for the production of soluble MHC class I complexes is an established technology with the production of soluble HLA-A2 monomers first being described in 1992. 462 This involves separate production of the heavy chain α_1 - α_3 domains and β_2 microglobulin as insoluble inclusion bodies in bacteria. These are then extracted and the protein denatured before refolding *in vitro* in the presence of an excess of antigenic peptide. Since the discovery that multimerisation of biotinylated monomers with streptavidin to form tetramers provides a way of enumerating peptide-specific CTL, 463 this method has been widely utilised: The MHC class I component of the one-step retargeting molecule of Robert *et al* 391 is produced using this technique, before being conjugated to a Fab' fragment via a bismaleimide linker.

However, although this method results in a functional, soluble class I molecule, the non-covalent attachment of the antigenic peptide allows for its dissociation which both renders the retargeting molecule ineffective and allows for the possibility of fratricide by cytotoxic T cells³⁹⁹ as discussed in the introduction. To eliminate this possibility the design for the

bacterially produced MHC class I component utilised the SCT arrangement described by both T Hansen *et al* (murine SCT)⁴⁰⁵ and Reiter *et al* (human SCT).³⁹⁷

The absence of an Fc region has implications for both purification and conjugation. Purification will not be possible using a protein A column as the SCT protein has no recognizable region. In order to conjugate the two components of the retargeting molecule with a bismaleimide linker it is necessary for each to possess a free sulfhydryl group. Although these are available in the Fab' fragment, all sulfhydryl groups in the SCT are paired and form critical intra-chain disulfide bonds which help maintain tertiary structure. It is therefore necessary to add a free sulfhydryl group (in the form of a cysteine residue) to the carboxy terminus of the heavy chain in order for this mechanism of conjugation to be used.

Alternatively, another linker, such as succinimidyl-4-(*N*-maleimidomethyl) cyclohexane-1-carboxylate (SMCC) could be used. This contains an amine-reactive *N*-hydroxysuccinimide ester in addition to the sulfhydryl-reactive maleimide group which allows conjugation of the free sulfhydryl group of the Fab' fragment to any primary amine. However, the linkage of the Fab' fragment to a random amine group within the SCT protein means the resulting retargeting molecules are non-uniform (a number of different geometries will be produced depending on the location of the amine residue used) and may include multimers (several Fab' fragments may be conjugated to a single SCT molecule).

Figure 3.9 demonstrates different designs for the MHC component of the retargeting molecule which are suitable for production in bacterial cells. They all utilise the SCT format, but there are some variations in the residues at the carboxy terminus of the molecule, linker length and placement of cysteine residues.

3.3.2. Production of genetic constructs

The appropriate fusion genes encoding the ten different variations of the *NLVPMVATV*- β_2 microglobulin-HLA-A2 α_1 - α_3 single chain trimer construct shown below were all subcloned in the pET21a bacterial expression vector in order to allow IPTG/L-rhamnose induced expression in KRX *E. coli* cells. The constructs' genetic structures are shown in Figure 2.2 and the rationale behind their individual designs is detailed below. The DNA gels illustrating the individual steps required for construct production and final sequences can be found in appendices 2 & 3 respectively.

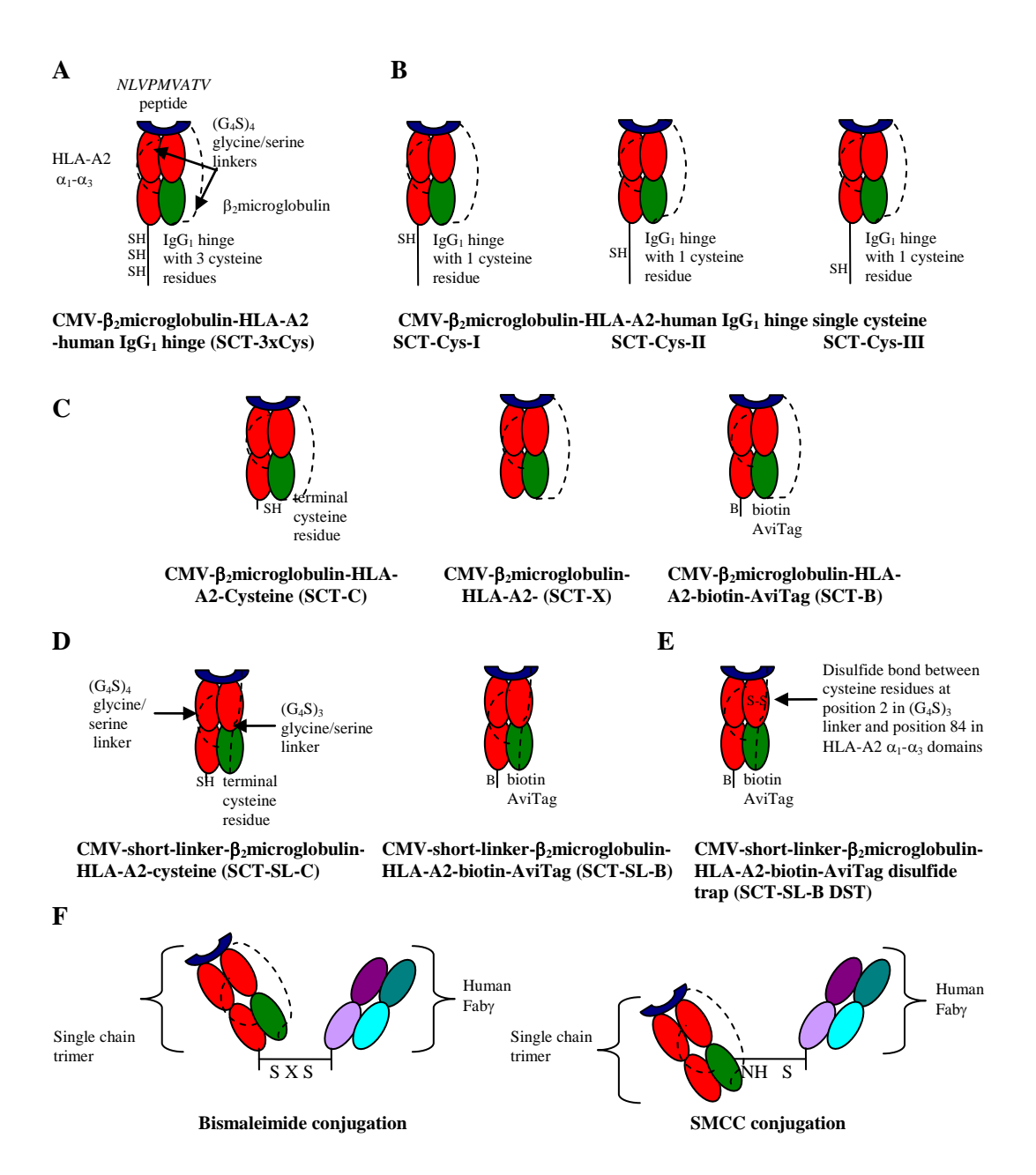


Figure 3.9: SCT construct design

A demonstrates the initial SCT structure which includes the IgG_1 hinge region as a source of cysteine residues and hence free sulfhydryl groups. \mathbf{B} illustrates the single cysteine SCT mutants which retain the IgG_1 hinge. \mathbf{C} shows SCT molecules which lack the IgG_1 hinge and have either nothing, a single cysteine residue or the biotin AviTag motif at the carboxy terminus of the HLA-A2 molecule. \mathbf{D} shows the SCT constructs with the shorter $(G_4S)_3$ linker between the NLVPMVATV peptide and β_2 microglobulin. \mathbf{E} demonstrates the disulfide trap version of the short linker SCT. \mathbf{F} illustrates the two proposed mechanisms of conjugation of the SCT to a Fab' fragment: those with a free cysteine residue and hence sulfhydryl group will be conjugated using a bismaleimide linker whilst those without a free sulfhydryl group will be coupled using an SMCC linker.

3.3.2.1 pET21a-CMV-β₂microglobulin-HLA-A2-human IgG₁ hinge (SCT-3xCys)

By virtue of using the mammalian construct pcDNA3.2-HLA-A2-human IgG_1 hinge-Fc as the template for the HLA-A2 component of the protein, it included the human IgG_1 hinge region at its carboxy terminus providing 3 cysteine residues which could be utilised for conjugation

of the molecule to a Fab' fragment. Aside from this, the structure of the molecule was similar to that used by Hansen *et al* 405 other than a slightly longer linker ([G₄S]₄ versus [G₄S]₃) being present between the antigenic peptide and β_2 microglobulin.

The effect of glycine-serine linker lengths between the peptide and β_2 microglobulin, and β_2 microglobulin and the class I heavy chain was investigated in work by Hansen *et al.*⁴⁰⁴ They generated a murine SCT which consisted of the K^b-restricted OVA-derived peptide *SIINFEKL* linked to murine β_2 microglobulin linked to the full-length K^b protein (results in membrane expression of the SCT protein rather than secretion) with glycine-serine linker lengths between the three components of 10/15, 10/20 and 15/20 amino acids respectively. These were expressed on the surface of mouse fibroblasts and conformational integrity of the constructs was determined by staining with mAb specific for K^b-*SIINFEKL* (25D-1.16) and assessing susceptibility of the transfected cells to lysis by OT-1 cells.

These experiments suggested that the hierarchy of linker lengths for successful *in vivo* protein folding is 15/20 > 10/20 > 10/15. The explanation given for this is that the longer spacers allowed better positioning of the peptide within the peptide-binding groove and reduced steric hindrance of the MHC-TCR interaction. Given these observations, it was thought that the slightly longer $(G_4S)_4$ linker between the peptide and β_2m in SCT-3xCys would not impair folding and ultimately recognition of the SCT construct.

3.3.2.2 pET21a-CMV- β_2 microglobulin-HLA-A2-human Ig G_1 hinge single cysteine (SCT-Cys-I, SCT-Cys-II & SCT-Cys-III)

To investigate whether the presence of three free sulfhydryl groups in the hinge region of SCT-3xCys resulted in high levels of protein aggregation during *in vitro* refolding, therefore reducing the yield of conformationally correct protein, a series of SCT constructs containing only a single cysteine residue in the hinge region were produced. The single hinge-cysteine SCT constructs were produced using site directed mutagenesis of SCT-3xCys (as described in section 2.3.1.2) and the appropriate mutations were verified by sequencing (see appendix 3).

3.3.2.3 pET21a-CMV-β₂microglobulin-HLA-A2-Cysteine (SCT-C)

The two versions of the SCT protein already described in the literature (Hansen *et al*⁴⁰⁵ and Reiter *et al*³⁹⁷) do not contain a hinge region, unlike SCT-3xCys or the single hinge-cysteine SCT proteins described above. Instead, they possess a single cysteine residue inserted at the carboxy terminus of the α_3 domain of the heavy chain. Although the most likely element of the hinge region to impair refolding is the free sulfhydryl group(s) within the non-structural

cysteine residue(s), it is not known whether other residues within the hinge region are able to interfere with refolding, increasing misfolding and protein aggregation. Although the immunoglobulin hinge region can be produced and refolded correctly in *E. coli* in the context of a complete humanised IgG molecule, 465 the location of an IgG₁ hinge region adjacent to the carboxy terminus of an HLA-A2 α_3 domain is non-physiological and could have implications for the refolding of the SCT molecule. Therefore an SCT protein lacking the hinge region but possessing a single cysteine residue at the carboxy terminus was produced; SCT-C.

3.3.2.4 pET21a-CMV-β₂microglobulin-HLA-A2 (SCT-X)

Both SCT proteins described in the literature^{397,405} are engineered to contain a cysteine residue at the carboxy terminus of the heavy chain α_3 domain in order to provide a substrate for conjugation to an Ab fragment using a bismaleimide linker. However, the presence of a free sulfhydryl group has the potential to decrease the yield of correctly folded protein as seen when an additional non-structural cysteine residue is introduced into bovine β -lactoglobulin. Therefore, an SCT protein with nothing attached to the carboxy terminus was produced to investigate whether this improved yield; SCT-X. The absence of a free cysteine residue means it cannot be conjugated to an Ab moiety using a bismaleimide linker.

3.3.2.5 pET21a-CMV-β₂microglobulin-HLA-A2-biotin-AviTag (SCT-B)

Assessment of cognate TCR binding to the SCT protein produced can be performed by making tetramers from the SCT monomers and assessing their ability to recognise appropriately restricted CTLs. This is achieved by biotinylating monomeric SCT protein by conjugation to maleimide-biotin via a free sulfhydryl group, and mixing with fluorochromelabelled streptavidin. Alternatively biotin can be added enzymatically to a 'biotinylation' sequence using the *E. coli* enzyme biotin holoenzyme synthetase (BirA) which catalyses the transfer of biotin to the epsilon amino group of a lysine residue of the biotin carboxyl carrier protein (BCCP) subunit of acetyl-CoA carboxylase. 467 Combinatorial methods and transient kinetic measurements have identified a minimal 14-residue peptide substrate, which although bearing little resemblance to the biotinylated sequence in BCCP is biotinylated by BirA with equivalent efficiency to the natural substrate. 468 Incorporation of this sequence at the carboxy terminus of the SCT construct would allow the resulting protein to be enzymatically biotinylated and then tetramerised using fluorescence-labelled streptavidin.

3.3.2.6 pET21a-CMV-short-linker-β₂microglobulin-HLA-A2-cysteine (SCT-SL-C)

All the SCT constructs described above have glycine/serine linker lengths of 20/20 amino acids; a combination not investigated in the literature. Although it was assumed that the

slightly longer linker length between the peptide and β_2 microglobulin genes would make little difference to folding, and if anything provide greater flexibility for the peptide to sit in its binding groove (as discussed in section 3.3.2.1), this may not be the case. It is thought that within an SCT the peptide is continuously dissociating and rebinding 405 (a phenomenon which compensates for the destruction by the linker of some of the C terminus interactions between residues in the peptide and its binding groove); the longer linker may mean that peptide spends longer dissociated from rather than bound to the peptide-binding groove. Alternatively when the peptide is bound in its groove, the extra linker length may form a bulge which prevents interaction with the cognate TCR due to steric hindrance.

To investigate the significance of the longer linker length pET21a-CMV-short-linker- β_2 microglobulin-HLA-A2-cysteine was generated which had a 15 amino acid glycine-serine linker meaning the construct had linkers of 15/20, identical to those shown to be most successful by Hansen *et al*.

3.3.2.7 pET21a-CMV-short linker-β₂microglobulin-HLA-A2-biotin-AviTag (SCT-SL-B)

The pET21a-CMV-short linker- β_2 microglobulin-HLA-A2-biotin-AviTag construct was generated in order to allow enzymatic biotinylation and subsequent tetramerisation.

3.3.2.8 pET21a-CMV-short linker- β_2 microglobulin-HLA-A2-biotin-AviTag disulfide trap (SCT-SL-B DST)

Further work by Hansen *et al* with both murine⁴⁰⁶ and human⁴⁰⁸ SCTs demonstrated that peptide-binding within the binding groove could be stabilised by introducing cysteine residues into position 2 of the linker between the antigenic peptide and β_2 microglobulin, and position 84 of the heavy chain allowing the creation of a new disulfide bond. This has the effect of more securely anchoring the peptide making it less susceptible to displacement by exogenous peptides. To investigate whether this enhanced recognition of the SCT by its cognate TCR, an SCT was engineered with these amino acid substitutions using site-directed mutagenesis.

3.3.3 Expression of bacterial SCT proteins

The ten different SCT constructs described in section 3.3.2 were all expressed in KRX *E. coli* using IPTG and L-rhamnose induction as described in section 2.3.2.2. Before inclusion bodies were extracted, production of the required species within the bacterial cells was confirmed by SDS-PAGE analysis. Figure 3.10 demonstrates successful production of an appropriately sized (~50 kDa) protein with each of the different SCT constructs.

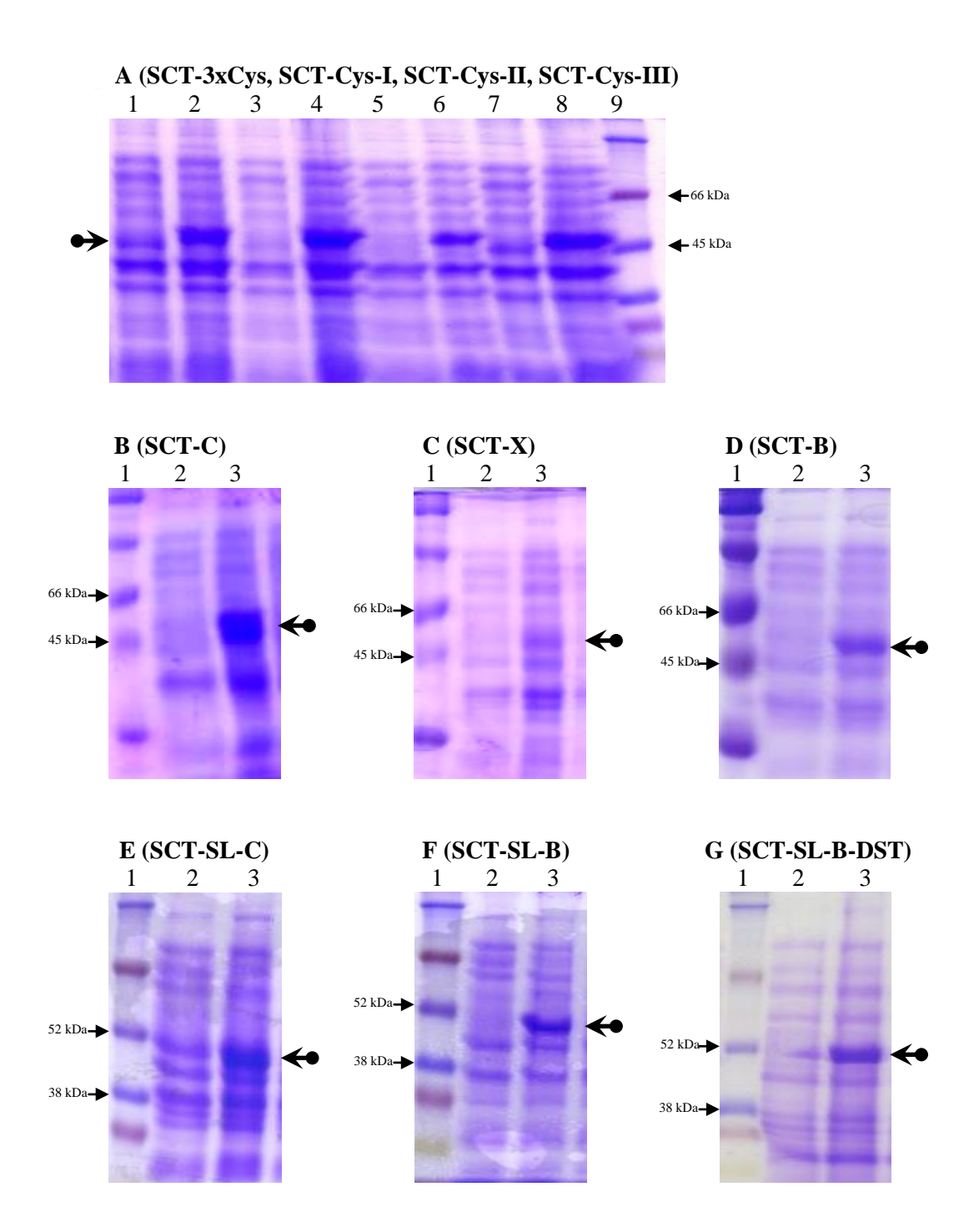


Figure 3.10: SDS-PAGE gels of expression of SCT constructs in KRX *E. coli* cells All gels contain KRX *E. coli* cellular lysates prepared under reducing conditions and run on 12.5% SDS-PAGE gels. Gel **A**: 1 Uninduced SCT-3xCys, 2 Induced SCT-3xCys, 3 Uninduced SCT-Cys-I, 4 Induced SCT-Cys-I, 5 Uninduced SCT-Cys-II, 6 Induced SCT-Cys-II, 7 Uninduced SCT-Cys-III, 8 Induced SCT-Cys-III, 9 markers. Gels **B-G**; 1 marker, 2 Uninduced SCT construct (identity indicated in gel title), 3 Induced SCT construct (identity indicated in gel title). The larger arrow indicates the position of the induced SCT protein.

The mass of inclusion bodies extracted (see section 3.3.4) following induction of equivalent numbers of transformed bacteria was largely uniform across several inductions (~50 mg/l) for each of the SCT species with the exception of the SCT-X construct which consistently resulted in lower levels. This is illustrated by the fainter band with SCT-X.

3.3.4 Purification of inclusion bodies

Transformed *E. Coli* were disrupted using lysozyme and sonication, allowing extraction and purification of the inclusion bodies as described in section 2.3.2.3. In order to monitor the process and ensure the required protein was recovered during washing, samples from several stages of the process were analysed by SDS-PAGE as shown in Figure 3.11. The inclusion bodies were solubilised and denatured in either 8 M urea or 6 M guanidine prior to refolding.

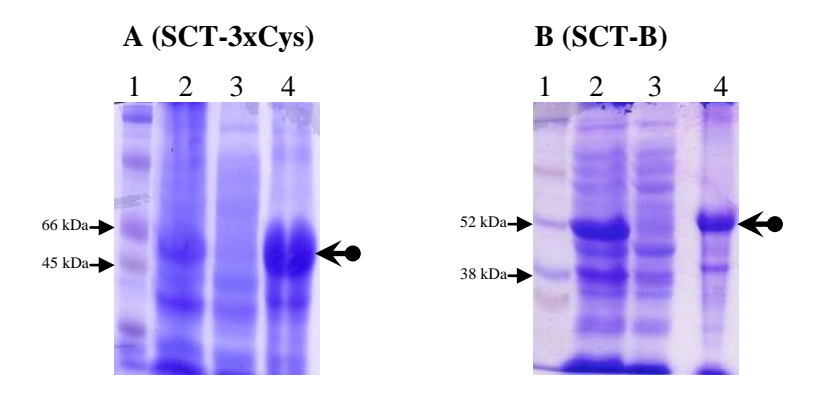


Figure 3.11: SDS-PAGE gels of inclusion body extraction from KRX *E. coli* transformed with SCT constructs

Samples prepared under reducing conditions and run on 12.5% SDS-PAGE gels. Lane order is: 1 Protein marker, 2 Sonicated cell pellet from SCT construct-transformed KRX E. coli cells which had undergone induction of protein production, 3. Supernatant from pelleted inclusion bodies, 4. Denatured solubilised SCT protein-containing purified inclusion bodies. In gel A purified inclusion bodies were denatured with 8 M urea, in gel B purified inclusion bodies were denatured with 6 M guanidine. The smaller arrows indicate relevant protein marker band sizes and the larger arrow indicates the position of the purified SCT-containing inclusion bodies. NB Equal quantities of protein were not loaded on each gel.

These gels demonstrate that appropriately sized protein species (~50 kDa) were extracted from *E. coli* cells for each of the different SCT constructs. The quantity of each species produced was largely equivalent across the various SCT constructs with the exception of SCT-X which consistently produced less. Once extracted from the inclusion bodies, solubilised, denatured protein had to undergo refolding to produce a conformationally correct protein with the appropriate tertiary structure in order to exhibit biological activity.

3.3.5 Refolding of denatured SCT proteins

The underlying principle of protein refolding is to remove the denaturant to allow the protein to assume its native structure. Methods employed include dilution, dialysis, diafiltration, gel filtration and immobilisation onto a solid support. The simplest of these is dilution, ⁴⁶⁹ the approach chosen for this study. Due to the presence of disulfide bonds within the SCT proteins, the refolding buffer chosen must promote disulfide bond formation, best achieved using a redox shuffling system. ⁴⁷⁰ Throughout the literature different additives at varying concentrations have been tried to attempt to increase yields of appropriately refolded proteins.

These include chaotropic agents to prevent aggregation (such as L-arginine),⁴⁷¹ detergents and surfactants⁴⁷² to promote correct disulfide bond formation and chaperones and foldases⁴⁷³ to mimic *in vivo* refolding conditions. In addition to variations in the constituents of the refolding buffer, its pH, temperature and the concentration of denatured protein added can all be adjusted to improve refolding efficiency.

The range of options means there is an almost unlimited number of possible refolding strategies which can be employed. Largely the refolding conditions for any particular protein have to be determined on an empirical basis, often by testing a number of different conditions, starting with those used for a similar protein. The some of the published dilutional refolding methods for monomeric murine MHC class I^{475} and human MHC class I (composed of separate peptide, β_2 microglobulin and heavy chain components) are very similar, the only difference being in the pH of the buffer; pH 7.5 for the murine monomer versus pH 8.0 for the human version. Given that the dilutional refolding method used by Lybarger *et al* 405 to refold their murine SCT protein was identical to that used to refold the human separate component monomers, it was felt that this was a valid method to use when refolding the human SCTs expressed during this study.

After the SCT protein had been refolded as described in section 2.3.2.4, concentrated and dialysed into 20 mM Tris/ 0.1 M NaCl buffer pH 8, initial analysis was performed using high performance liquid chromatography (HPLC) prior to further purification. Although all of the denatured protein which underwent refolding should have been the same size (~50 kDa) it was assumed that only correctly folded material would be able to contribute to a correctly sized peak on HPLC analysis, as unfolded and misfolded protein would aggregate into a much larger protein species. This assumption is supported by the lack of an appropriate peak when denatured human SCT is analysed by HPLC (data not shown).

In order to provide a positive control for the refolding system, an equivalently sized murine SCT (i.e. SIINFEKL- β_2 m- K^b -biotin-AviTag (mSCT-B) derived from the construct initially produced by Lybarger et al) was expressed and refolded using the same method. Figure 3.12 **A** demonstrates the HPLC chromatogram of this protein prior to further purification. Given this protein was able to be purified, biotinylated and made into tetramers which recognised their cognate TCR this provides a useful comparative trace for the human SCT proteins; examples of HPLC traces of the human SCT proteins are shown in Figure 3.12 **B-G.**

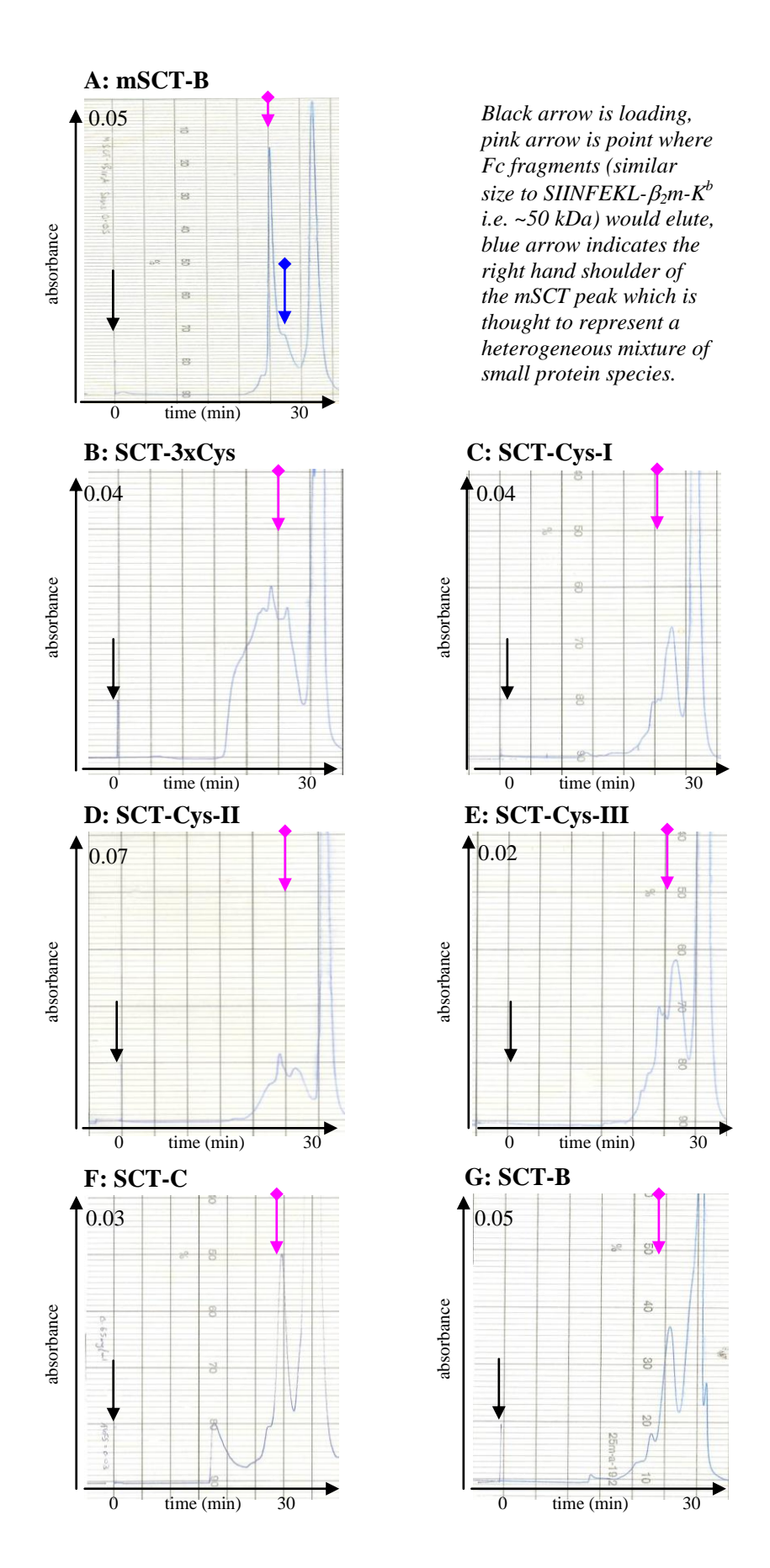


Figure 3.12: HPLC chromatograms of refolded SCT proteins (method of Lybarger)

Comparison of the HPLC profiles suggests that the refolded murine SCT is far purer than any of the human SCT proteins which show a very broad profile suggesting the presence of protein aggregates. This is most marked for SCT-3xCys; a situation not unexpected given the presence of three free sulfhydryl groups in the hinge region. More than one peak can be identified in all the chromatograms suggesting the production of more than one species; this is most marked in the chromatograms of SCT-3xCys and SCT-Cys-II, where there is no predominant peak. Although the remainder of the chromatograms do have a predominant peak, these all elute later than an Fc peak would be expected to, suggesting they represent species smaller than 50 kDa. These analyses showed that although the method described by Lybarger *et al* can successfully refold the murine SCT, it is inadequate for refolding the human SCTs expressed in this study.

As an alternative the dilutional refolding method used by Oved *et al* with their human SCTs was evaluated. This system uses similar principles to that of Lybarger but the buffer contains a slightly higher concentration of arginine (0.5 M versus 0.4 M), is more alkali (pH 10 versus pH 8), and uses a different denaturant and redox pair (6 M guanidine, dithioerythritol and oxidised glutathione versus 8 M urea, reduced and oxidised glutathione).

HPLC analysis showed that compared with the profiles in Figure 3.12 **B-G** more of the product appears to be a single protein, which elutes at a point corresponding to 50 kDa, as would be expected for the SCT proteins. The smaller species which predominates in the chromatograms of proteins refolded using the method of Lybarger *et* al is still present, but is generally less predominant. One explanation may be that when using the buffer of Lybarger the majority of the human SCT protein is misfolded and therefore forms large protein aggregates which either precipitate and are filtered out prior to analysis or are outside the limits of detection . This means that a heterogeneous population of small protein fragments is the predominant species detected as a single peak. In contrast when using the buffer of Oved *et al* less of the protein misfolds and forms aggregates meaning a predominant protein species of the expected size can be detected.

For a given starting amount of denatured SCT protein the refolding method of Oved *et al* results in up to five times the amount of refolded protein being recovered compared with the method of Lybarger *et* al after concentration and filtering through a 0.22 µm filter suggesting less of the protein has formed large aggregates.

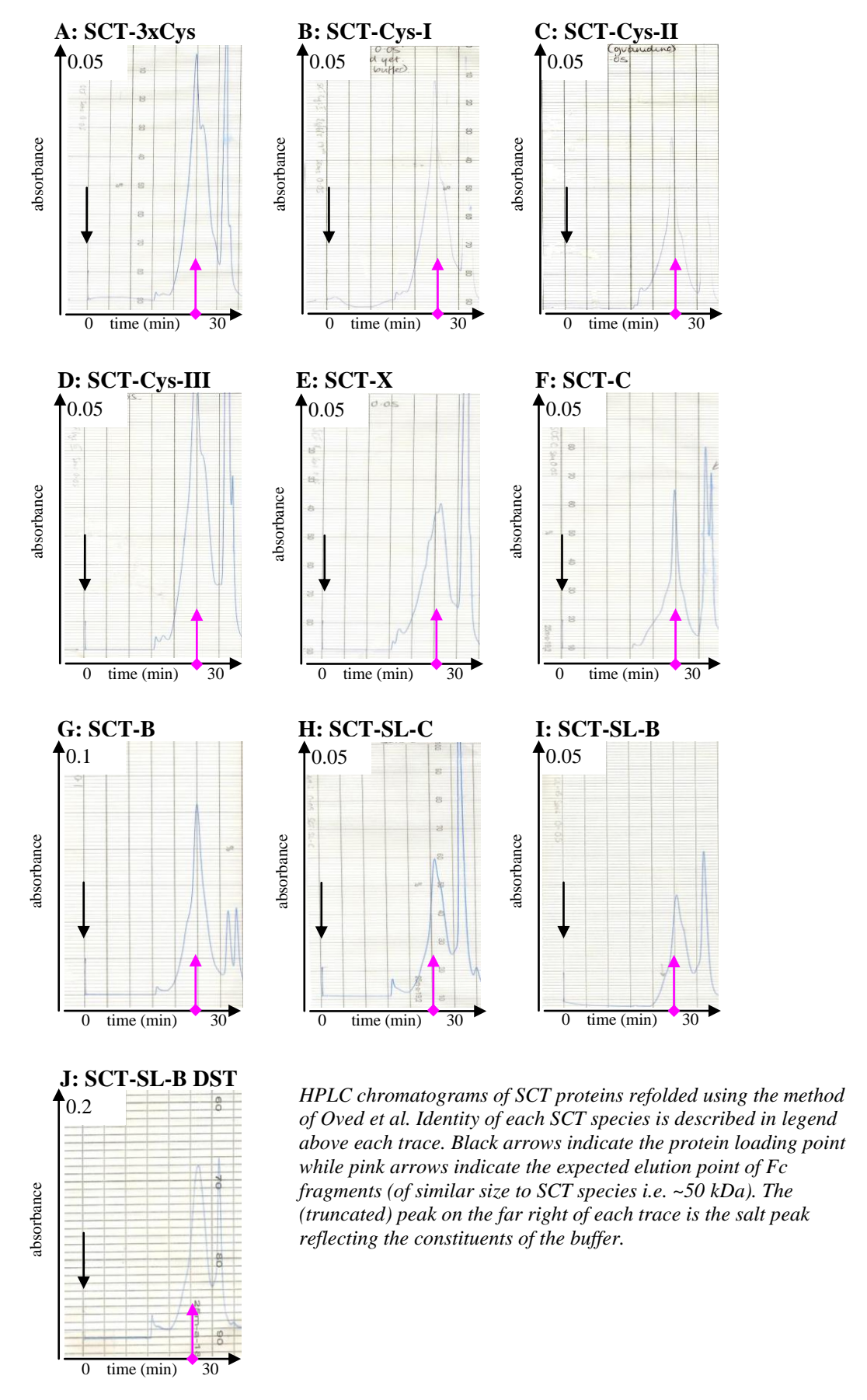


Figure 3.13: HPLC chromatograms of refolded SCT proteins (method of Oved)

3.3.6 Purification of refolded SCT proteins

The HPLC profiles indicate that the refolded SCT proteins need to undergo purification before use in a retargeting molecule. One of the purification strategies used by both Lybarger *et al* and Oved *et al* was size exclusion chromatography. However, the extremely poor yield of protein from refolds performed using the buffer of Lybarger *et al* meant it was difficult to obtain sufficient protein to use with the available size exclusion chromatography system (a minimum of ~10 mg required). Therefore immunoaffinity chromatography with columns coated with anti-MHC class I mAbs was used to try and purify protein refolded using this method.

3.3.6.1 Purification using immunoaffinity chromatography

The antibodies used in this study to construct immunoaffinity columns were W6/32 and BB7.2: W6/32, is a pan-HLA Ab reported as recognising only conformationally correct class I molecules refolded around antigenic peptide with epitopes mapped to both the class I α_2 domain and β_2 microglobulin, meaning it should only capture correctly refolded SCT protein. In contrast BB7.2 recognises only HLA-A2 (and a variant of HLA-A28) via a surface, non peptide-binding-cleft epitope which includes the carboxy terminus of the α_2 domain and a turn on one of the underlying β -strands.

However, immunoaffinity chromatography requires protein elution conditions which are stringent enough to destroy the interaction between the Ab and the protein whilst keeping the latter's conformation intact. Elution is usually performed with a buffer with either a low pH or a chaotropic agent (ammonium thiocyanate). In this case ammonium thiocyanate was used and the eluted protein was collected into a small volume of 40 mM Tris/ 0.2 M NaCl buffer pH 8 in order to reduce the concentration of the chaotrope (and neutralise the alkali pH), and then immediately dialysed against further 40 mM Tris/ 0.2 M NaCl buffer pH 8. Although the time the SCT proteins spent exposed to the chaotropic agent was minimised it is possible it produced a change in their conformation.

Eluted protein was analysed using HPLC. Figure 3.14 shows example HPLC profiles for the SCT proteins SCT-Cys-I, SCT-Cys-II and SCT-Cys-III refolded using the method of Lybarger *et al* and purified using immunoaffinity chromatography columns containing W6/32 and BB7.2 respectively.

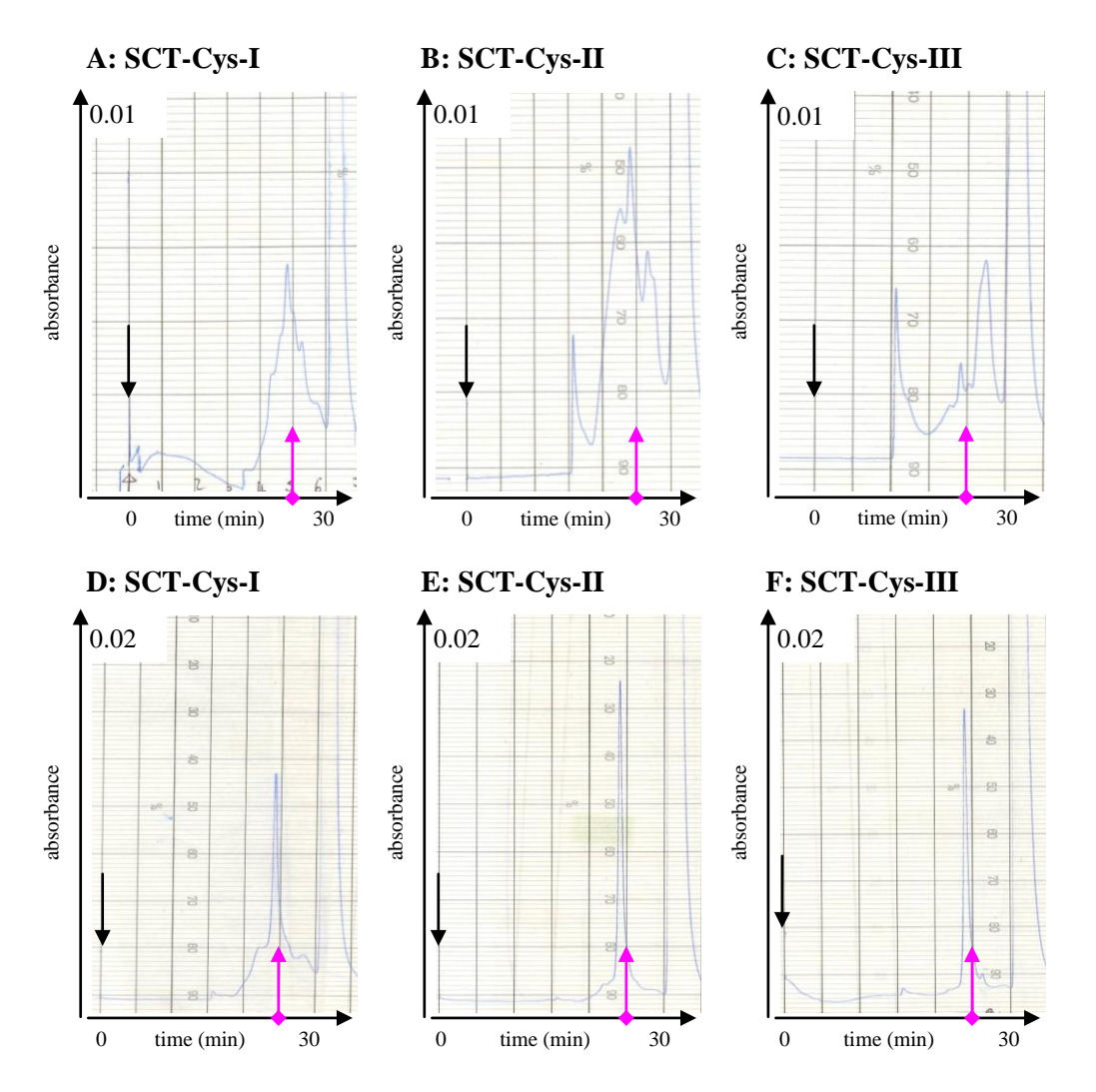


Figure 3.14: HPLC chromatograms of immunoaffinity chromatography purified SCT-Cys-I-III (refolded using method of Lybarger *et al*) using W6/32 and BB7.2-containing columns

A-C W6/32 column, D-F BB7.2 column. Black arrows indicate the protein loading point while pink arrows indicate the expected elution point of SCT proteins.

The protein eluted from the BB7.2 immunoaffinity column appears much purer than that eluted from the W6/32 column. Given that W6/32 recognises a conformational epitope on class-I-peptide- β_2 microglobulin complexes, the elution of such a heterogeneous population of proteins suggests either non-specific binding of misfolded SCT proteins, binding of aggregates, or destruction of the correct SCT tertiary structure by the relatively harsh elution conditions resulting in aggregation. In contrast, the chromatograms of proteins eluted from the BB7.2 column suggest one relatively pure species is eluted. These proteins appear to be of approximately the same size as Fc and apart from SCT-Cys-I are relatively free of contaminating aggregates. The recognition of non-contiguous epitopes in the α_2 chain by BB7.2 suggests it too recognises a conformational rather than linear epitope.

It should be noted that although the protein eluted form the BB7.2 column appears relatively pure, only ~ 0.5 mg of refolded protein was recovered after immunoaffinity purification using this column from a starting quantity of 100 mg purified inclusion bodies. In addition to eluted protein from the W6/32 column being less pure, yields were also significantly lower. Before further manipulation of the purified protein could be considered, protein characterisation was undertaken by ELISA (section 3.3.7.1).

3.3.6.2 Purification using size exclusion chromatography

SCT-C, SCT-SL-C, SCT-B and SCT-SL-B proteins refolded using the method of Oved *et al*, underwent purification using size exclusion chromatography: All these refolded protein species had an Fc-sized protein as their predominant species (expected to be the SCT protein), and appear to be of similar purity. In addition, the yield of unpurified refolded SCT protein from the inclusion bodies extracted from a 3 l bacterial culture was in excess of 10 mg and therefore sufficient for purification using the size exclusion chromatography system available.

Figure 3.15 **B** shows the profile of SCT-SL-C separated by size exclusion chromatography using Superdex 200 columns. The fractions which corresponded to the peaks indicated were combined, concentrated then analysed using HPLC (Figure 3.15 **C-E**). Similar profiles were seen when the other SCT proteins were purified using this method (equivalent data for SCT-SL-B in appendix 2). The profile shown in Figure 3.15 **B** shows that there is incomplete resolution of the different protein species using this method of purification as it shows a number of overlapping peaks. However with careful choice of fractions for combination (i.e. peak D) it is possible to isolate a protein of the expected size, which is considerably purer than the non-purified refolded material. The presence of a ~100 kDa species suggests the formation of SCT dimers upon refolding. This is not unexpected for SCT-SL-C due to the presence of a free sulfhydryl group at the carboxy terminus of each molecule which allows the formation of a disulfide bond.

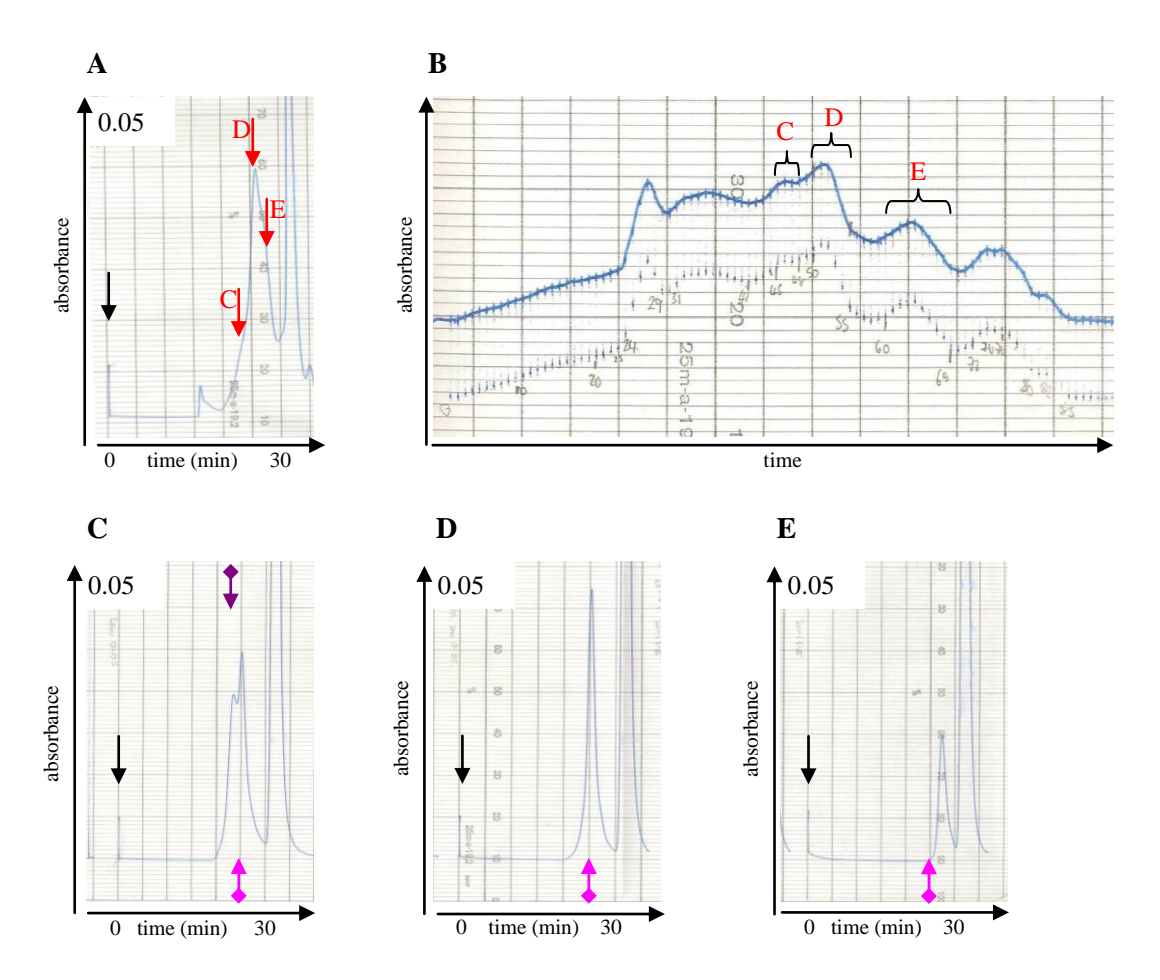


Figure 3.15: Purification of SCT-SL-C using size exclusion chromatography

A HPLC of SCT-SL-C (as shown in Figure 3.13 H) refolded using the method of Oved et al. The black arrow indicates the time point when the protein sample was loaded and the red arrows show the three peaks; C, D & E indicated on the chromatogram in B. B shows the profile obtained when the refolded SCT-SL-C from A was purified by size exclusion chromatography. The fractions containing peaks C, D & E were collected, combined, concentrated and then analysed using HPLC. E, E are the chromatograms obtained when the fractions composing the peaks with the corresponding letter, obtained during size exclusion chromatography, were analysed using HPLC. Black arrows indicate the time point when the protein sample was loaded onto the column, pink arrows indicate the time point when E fragments (of similar size to SCT species i.e. ~50 kDa) would be expected to elute and the purple arrow indicates the time point when E fragments (of similar size to section the salt peak, reflecting the constituents of the buffer.

3.3.7 SCT protein characterisation

3.3.7.1 Characterisation of protein purified using immunoaffinity chromatography

To assess that the protein had been refolded with the correct conformation it was necessary to use methods of analysis which can discriminate between correct and incorrect conformations. The most physiological test of the conformational integrity of refolded SCT protein is whether, when made into tetramers, these can recognise their cognate TCR on CTLs. However, because of the low yields from the immunoaffinity column it was not possible to make tetramers so a modified ELISA was used.

ELISA of refolded SCT proteins purified using immunoaffinity chromatography

Ideally this could be done by using either W6/32 or BB7.2 to coat the plate and detecting with anti- β_2 microglobulin-HRP (i.e. the assay used to analyse MHC class I protein secretion by transfected mammalian cells as shown in Figure 3.7 **A** & **B**). However, at the time of this analysis no anti- β_2 microglobulin-HRP was available meaning a non-conjugated anti- β_2 microglobulin Ab followed by an anti-xenotype HRP-conjugated secondary Ab was used. However, there was significant cross-reactivity between BB7.2 and the anti-xenotype-HRP secondary Ab. The ELISA was therefore modified so protein was coated directly onto the plate and detected separately with W6/32, BB7.2 and anti- β_2 microglobulin antibodies and appropriate HRP-conjugated secondary antibodies. Using both W6/32 and BB7.2 provided an additional check on the structural integrity of the refolded protein as they detect separate conformational epitopes. Unlike W6/32 and BB7.2 which are both monoclonal antibodies, the anti- β_2 microglobulin Ab used was a polyclonal Ab and therefore will react with a variety of epitopes (likely to be both linear and conformational) Figures 3.16a & b illustrate the data obtained from these modified ELISAs.

The ELISA data shows that protein which can be recognised by all three antibodies appears to be purified from each of the refolded SCT constructs by both of the immunoaffinity columns. In addition, the profiles of the graphs obtained for each individual protein species, purified using either column, detected with W6/32 or BB7.2, are similar suggesting that any particular SCT protein molecule which has its W6/32-binding site intact also maintains it BB7.2-binding site. Given that the anti- β_2 microglobulin Ab used is polyclonal and likely to recognise many different epitopes which may be either conformational or linear it follows that this Ab (based on the differences in ODs observed) recognises each of the constructs at a given concentration more equitably than the monoclonal anti-MHC class I. The anti- β_2 microglobulin Ab is likely to be able to recognise unfolded and correctly folded protein as well as any intermediate states. The relative recognition by this Ab of the refolded proteins purified using the W6/32 and BB7.2 columns is SCT-Cys-I > SCT-Cys-II > SCT-Cys-III and SCT-Cys-III > SCT-Cys-III >

In contrast, the results of the other ELISAs are more consistent: SCT-Cys-I purified using the W6/32 or BB7.2-containing immunoaffinity chromatography columns was better recognised by both of the anti-MHC class I than either of the other constructs, suggesting a higher proportion of this protein has refolded successfully. Figure 3.17 suggests one hypothesis which might explain this observation.

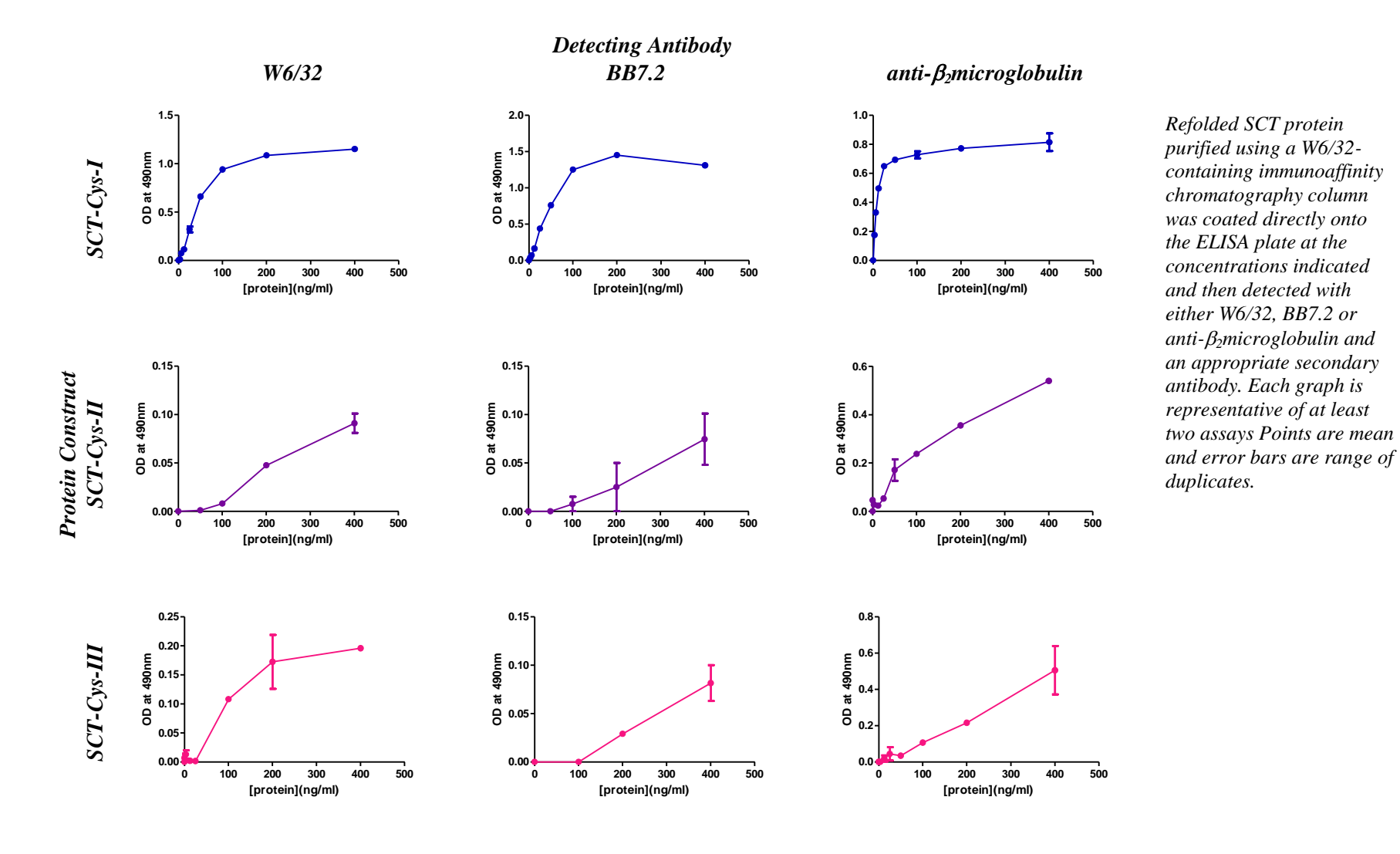


Figure 3.16a: ELISA analysis of refolded SCT-Cys-I-III constructs purified using a W6/32 immunoaffinity chromatography column

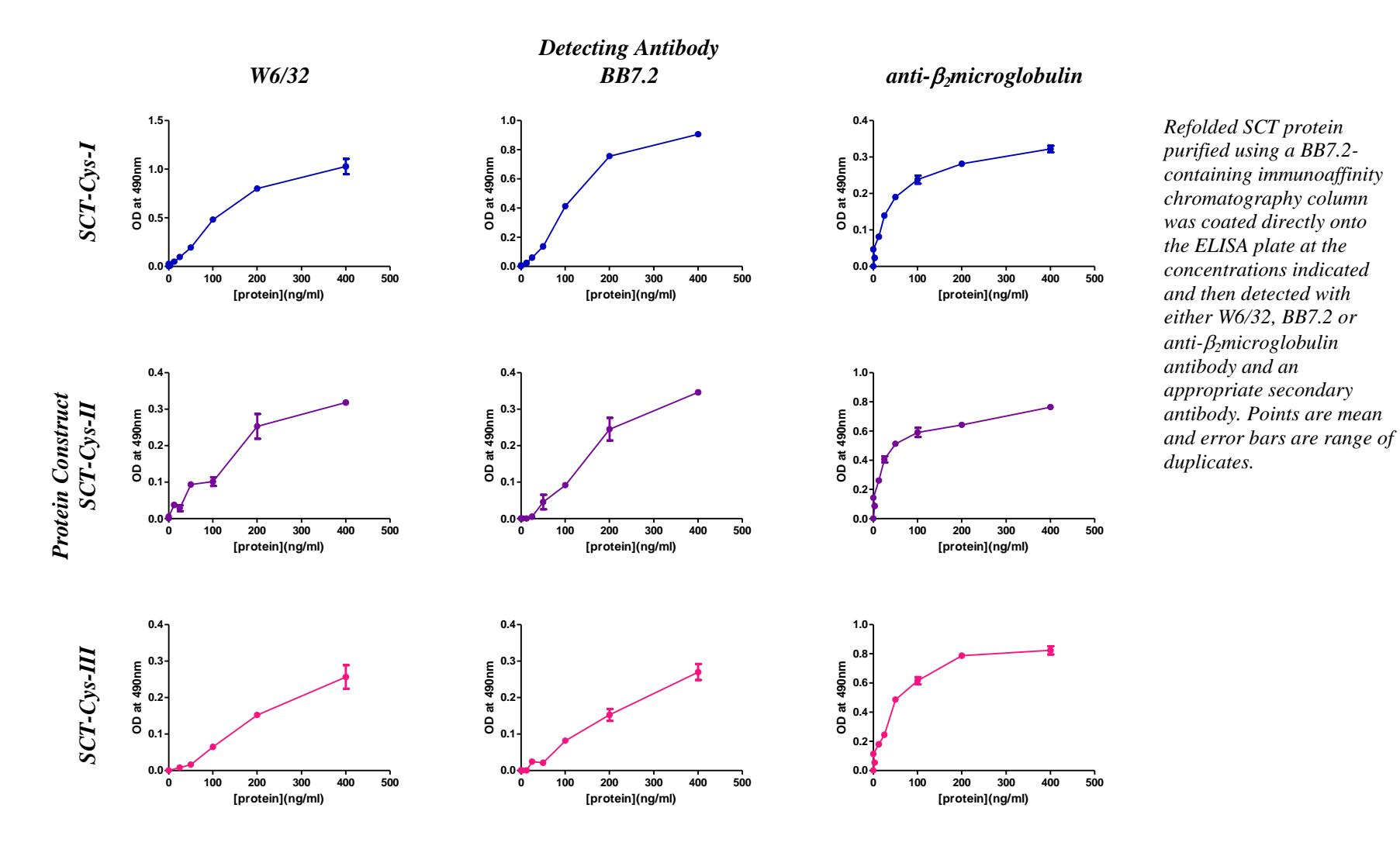
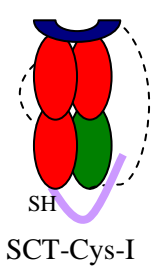
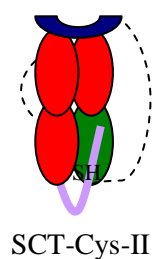


Figure 3.16b: ELISA analysis of refolded SCT-Cys-I-III constructs purified using a BB7.2 immunoaffinity chromatography column





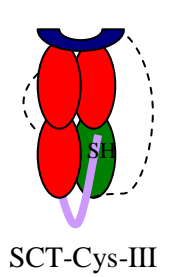


Figure 3.17: Schematic diagram of potential impact of position of cysteine residue in hinge region on refolding

Schematic representation of possible consequences of cysteine → serine substitutions within the hinge region of SCT proteins. The more rigid upper hinge coupled with the more proximal cysteine residue in SCT-Cys-I means the free sulfhydryl group is unlikely to interfere with the formation of intrachain structural disulfide bonds. In contrast the more flexible upper hinge coupled with the more distal cysteine residues in SCT-Cys-II and SCT-Cys-III mean the free sulfhydryl groups in the hinge are more likely to be able to interfere with the formation of intrachain structural disulfide bonds.

An alternative method, other than ELISA, to investigate the conformational integrity of the purified, refolded SCT proteins is circular dichroism as the expected profiles of correctly folded SCT proteins are published. The percentage of correctly folded SCT protein eluted from the immunoaffinity columns could be determined using immunoprecipitation using beads coated with either W6/32 or BB7.2. However, given the very low yields of protein recovered, even for SCT-Cys-I, immunoaffinity chromatography was not felt to be a viable purification option and therefore the method was not investigated any further.

3.3.7.2 Characterisation of protein purified using size exclusion chromatography

After protein was purified by size exclusion chromatography, it underwent a number of processes to try and establish both its purity and the efficacy of the refolding process. Approximate size and the presence of any major contaminating protein species was determined using SDS-PAGE, while the presence of MHC class I heavy chain and β_2 microglobulin within the purified protein, and conformational integrity were confirmed by ELISA as above. Finally, given that the ultimate test of the integrity of refolding of MHC class I molecules is whether they can be recognised by their cognate TCR, SCT molecules were biotinylated, made into tetramers and used to stain hCD8⁺ T cells specific for *NLVPMVATV* peptide presented by HLA-A2.

SDS-PAGE analysis of refolded SCT proteins purified by size exclusion chromatography

The gels in Figure 3.18 demonstrate SDS-PAGE of fractions C-E of SCT-SL-C and SCT-SL-B (as shown in Figures 3.15a & appendix 2), under reducing and non-reducing conditions.

The SDS-PAGE analysis of the different fractions correlates with the HPLC profiles: The double peak seen in the chromatogram of fraction C of SCT-SL-C corresponds to the two major protein species (~50 kDa and ~100 kDa in size) seen on SDS-PAGE when the fraction is analysed under non-reducing conditions. As expected when fraction C is analysed under reducing conditions much of the larger species is destroyed and there is a larger quantity of the smaller species present, consistent with the larger species being a dimer (formed by a disulfide bond at the carboxy termini).

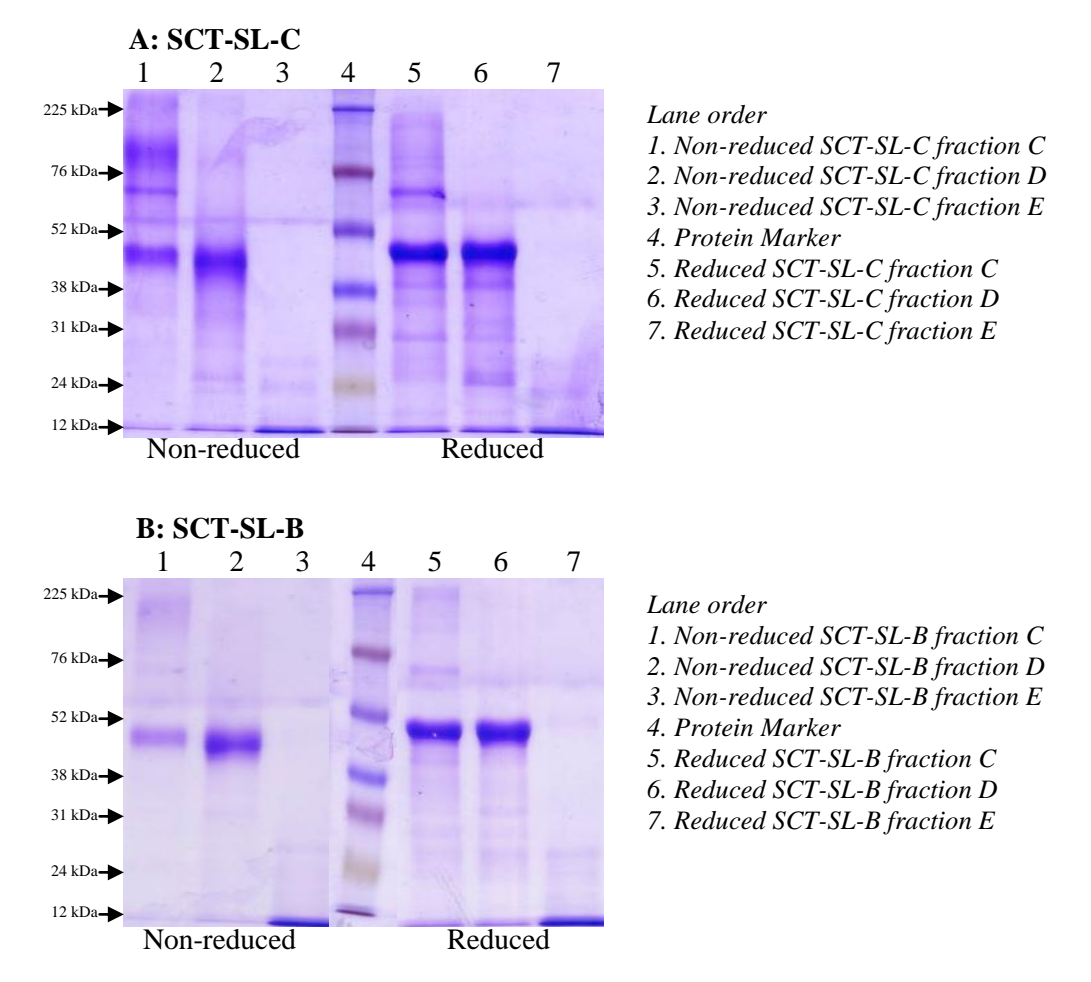


Figure 3.18: SDS-PAGE analysis of SCT-SL-C & SCT-SL-B proteins purified using size exclusion chromatography

Coomassie blue stained 12.5% SDS-PAGE gels of SCT-SL-B and SCT-SL-C fractions separated using size exclusion chromatography. Samples prepared as described in legend. Protein marker sizes indicated on left. 10 µg protein loaded per well (concentration determined by Bradford assay).

The double peak of fraction C of SCT-SL-B (as seen on HPLC) also corresponds to two bands seen on SDS-PAGE when analysed under non-reducing conditions. However, although the expected ~50 kDa band is present, the larger band appears to be more diffuse and represents a larger species than that seen for SCT-SL-C. One explanation could be that the larger SCT-SL-B refold species is a mixture of dimers, trimers and possibly larger multimers

which have refolded together (i.e. the heavy chain of one molecule with the peptide- β_2 microglobulin of another) and are held together by non-covalent interactions (although this is perhaps unlikely given the denaturant properties of SDS, present within the loading buffer). Alternatively some of the structural intrachain disulfide bonds could be occurring between separate SCT molecules, hence the formation of oligomers.

Either explanation would account for both the apparent larger size of the protein species on HPLC and SDS-PAGE analysis, and the 'smeary' appearance of the band on the gel. Interestingly dimer production has been observed when human HLA-A2 SCT proteins, not containing free sulfhydryl groups, are produced as a soluble product from mammalian cells using a retroviral expression system.⁴⁷⁹

Fraction D, as suggested by its HPLC chromatogram is a single species of the expected size for an SCT protein on both gels under reducing and non-reducing conditions. Analysis of fraction E suggests it contains a heterogeneous population of proteins smaller than 50 kDa, with many being smaller than 12 kDa; the lower limit of detection on the gels shown.

ELISA of refolded SCT proteins purified using size exclusion chromatography

Following size exclusion chromatography purification, the SCT-SL-C and SCT-SL-B protein fractions (fraction D), shown by both HPLC analysis and SDS-PAGE to be composed of a single protein species of the expected size, were analysed by ELISA with the SCT protein captured with an anti-MHC class I Ab recognising a conformational epitope (W6/32 or BB7.2) and detected with a polyclonal anti- β_2 microglobulin HRP-conjugated Ab. An HLA-A2 monomer was used as a positive control. This data is shown in Figure 3.19. Similar results were obtained for size exclusion chromatography purified SCT-C and SCT-B (data not shown).

The ELISA data shown in Figure 3.19 suggests that at least some of the purified refolded SCT-SL-C and SCT-SL-B has the desired structure, containing the conformational epitopes necessary for recognition by the capturing antibodies W6/32 and BB7.2. With the exception of SCT-SL-C (**A**) captured with W6/32, the data suggests that neither protein is as well recognised as the HLA-A2 monomer, and that more of the SCT-SL-C protein has the correct structure than the SCT-SL-B

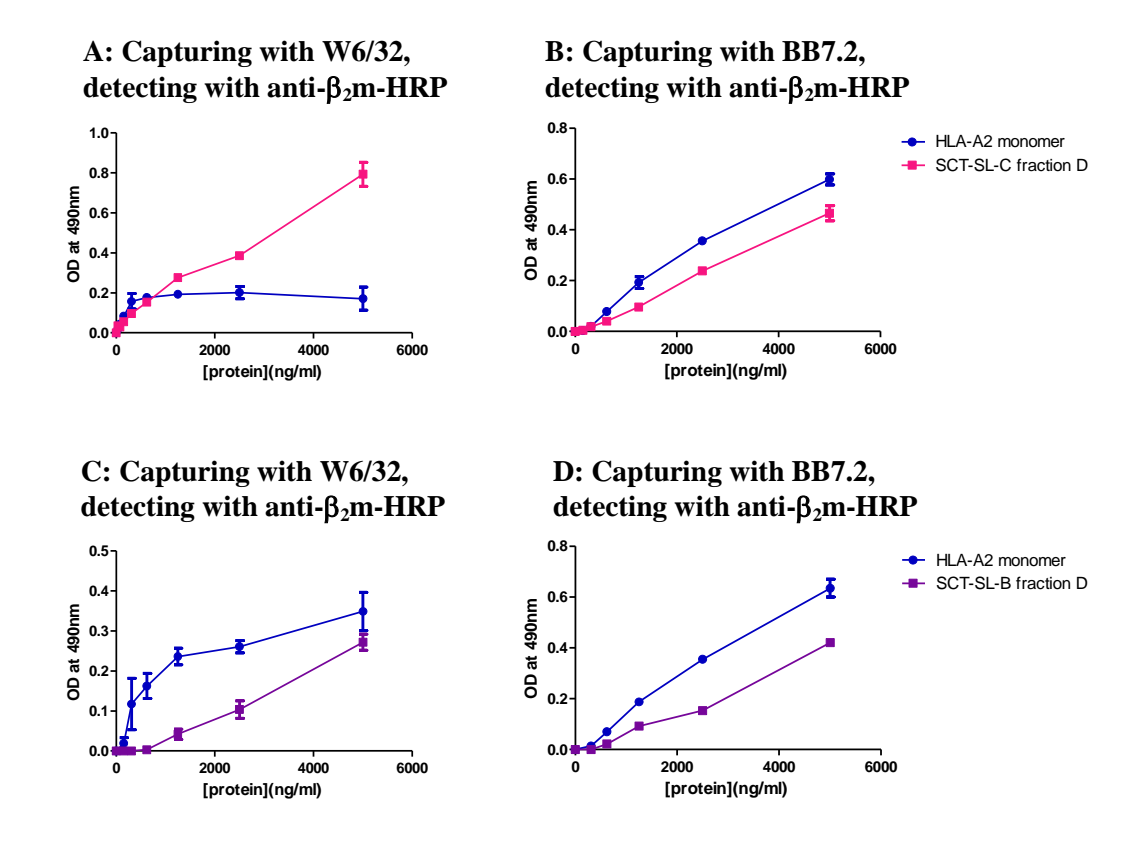
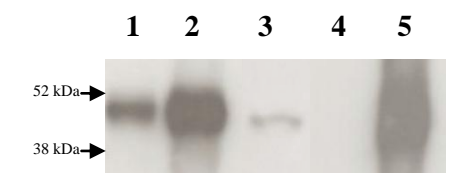


Figure 3.19: ELISA analysis of SCT-SL-C & SCT-SL-B purified using size exclusion chromatography

A commercially available HLA-A2 monomer was used as a positive control. Samples were run in duplicate and data is representative of two assays, Mean values are plotted with bars demonstrating the range.

Construction and analysis of SCT tetramers

Tetramer formation was then used to determine whether the conformational integrity of the molecule was such that it could recognise its cognate TCR. The first stage of tetramer formation was biotinylation of monomeric SCT protein. As discussed, SCT-SL-B contains the AviTag biotinylation sequence which allows the enzyme BirA to transfer biotin to a lysine residue within the sequence under appropriate conditions. SCT-SL-C has no biotinylation site but instead the sulfhydryl group within the unpaired cysteine residue at the carboxy terminus can be reduced and then conjugated to maleimide-biotin. The biotinylation status of the SCT proteins was determined by Western blotting, probing with streptavidin-HRP as shown in Figure 3.20.



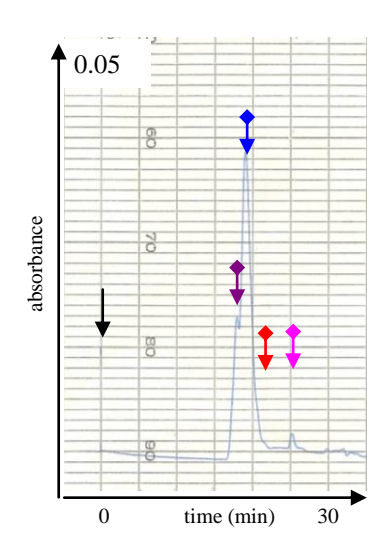
Protein samples prepared under non-reducing conditions and analysed on a 12.5% SDS-PAGE gel. After transfer the membrane was probed with streptavidin-HRP. Lane order: 1. Non-biotinylated SCT-SL-B. 2. Biotinylated SCT-SL-B. 3. Non-biotinylated murine SCT-BirA protein. 4. Non-biotinylated SCT-SL-C. 5. Biotinylated SCT-SL-C.

Figure 3.20: Western blot of biotinylated SCT proteins

This Western blot indicates that both SCT-SL-B and SCT-SL-C were successfully enzymatically or chemically biotinylated respectively, with very strong bands (lanes 2 & 5). Non-biotinylated SCT-SL-C (lane 4) shows no reaction with streptavidin-HRP (suggesting the complete absence of biotin from this molecule) as would be expected. The presence of a much weaker band in lane 1 suggests there is some reaction between non-biotinylated SCT-SL-B and streptavidin-HRP.

Biotinylated monomers were used to make tetramers by the addition of fluorochrome-labelled streptavidin; either streptavidin-FITC (SA-FITC; 50 kDa) or streptavidin-PE (SA-PE; 300 kDa). The success of tetramer formation was initially assessed by HPLC analysis of the reaction; FITC-labelled tetramers should have a molecular weight of 250 kDa whilst PE-labelled tetramers are expected to be larger with a molecular weight of 500 kDa. The greater relative difference in size between streptavidin-FITC and streptavidin-FITC-containing tetramers (50 kDa: 250 kDa) compared to streptavidin-PE and streptavidin-PE-containing tetramers (300 kDa: 500 kDa) means it is easier to monitor the formation of oligomers and tetramers using streptavidin-FITC as the HPLC system has better resolution of smaller protein species. However, it is easier to assess the ability of streptavidin-PE-containing SCT tetramers to bind to cells expressing the cognate TCR, as a commercial PE-conjugated HLA-A2/NLVPMVATV tetramer was available as a positive control.

SCT-SL-C, SCT-B and SCT-SL-B monomers were all biotinylated and used to make fluorochrome labelled tetramers. Figure 3.21 demonstrates HPLC analysis of the tetramerisation reaction involving biotinylated SCT-SL-B and streptavidin-PE.



HPLC chromatogram of SCT-SL-B-PE tetramer. Streptavidin-PE was added in a 1:4 ratio to biotinylated SCT-SL-B monomer. The pink and red arrows indicates the positions where Fc and IgG should elute. The purple and blue arrows indicate the exit of larger proteins species from the column.

Figure 3.21: HPLC chromatogram of SCT-SL-B-PE tetramer

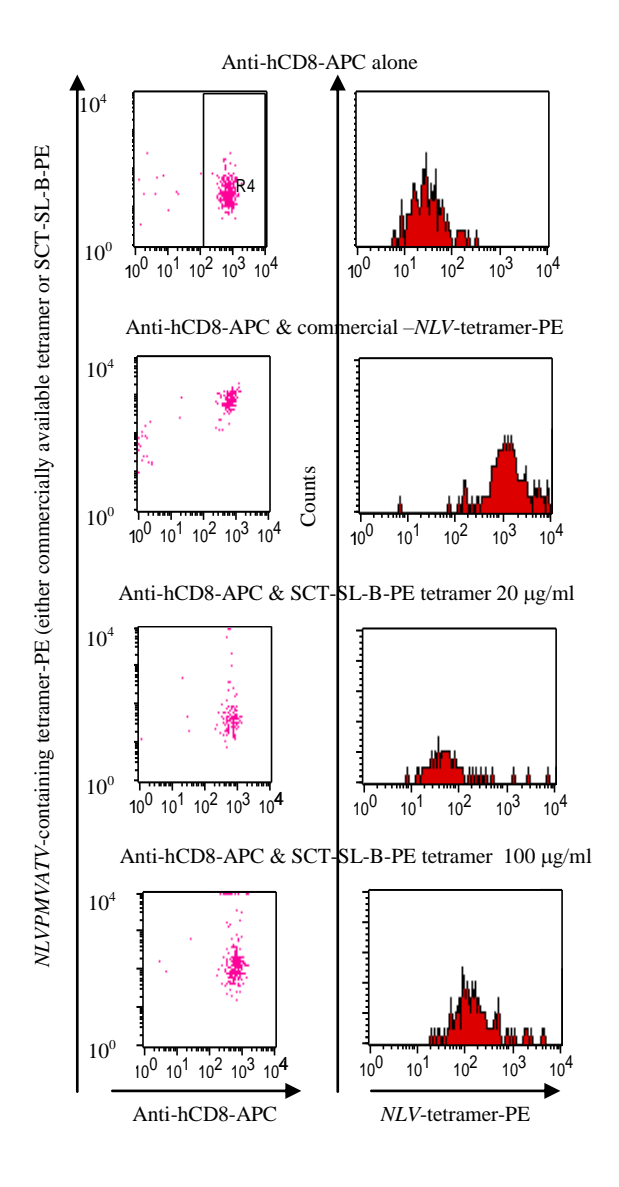
163

Figure 3.21 shows that very little monomer is left unconjugated after the tetramerisation reaction. The larger protein species appears to be composed of two distinct peaks which are difficult to accurately size on this system. The predicted size of the proteins from the tetramerisation reaction range from 300 kDa increasing in 50 kDa increments to 500 kDa; i.e. the expected size of unconjugated streptavidin-PE and the various oligomers increasing in size to that of the tetramer. The addition of streptavidin-PE to the biotinylated monomer in aliquots should favour the formation of complete tetramers rather than other oligomers as the monomer is always present in excess.

The quantity of streptavidin-PE necessary for complete tetramerisation of the monomers was calculated based on the assumption that all SCT protein was biotinylated and therefore would take part in the reaction. If a significant proportion of SCT protein remains unbiotinylated then after the latter aliquots of streptavidin-PE are added, monomer capable of taking part in the tetramerisation reaction (i.e. biotinylated monomer) is no longer in excess, favouring the formation of oligomers rather than tetramers. Although the western blot data shown in Figure 3.20 demonstrates that some SCT protein is biotinylated after the biotinylation reaction this data is only qualitative and gives no indication of the proportion of protein molecules successfully biotinylated.

Tetramers formed from SCT-B, SCT-SL-B and SCT-SL-C were used to stain *NLVPMVATV*-specific CTL (generated as described in section 2.1.1) which were then analysed by flow cytometry. The FACS profiles shown in Figure 3.22 demonstrate that compared with the commercial tetramers, even at a high concentration our SCT-SL-B-PE tetramers are very inefficient at recognizing their cognate TCR expressed on CTLs. Even though there was some shift at $100 \, \mu \text{g/ml}$, this was also observed with unstimulated PBMCs and so is likely to be non-specific (data not shown).

It may be that all of the tetramers consistently failed to recognise their cognate TCR because tetramer formation was incomplete as discussed previously. However, although the ELISA results suggested that active, correctly folded protein was present, the most likely explanation for tetramer failure is that there were too few correctly folded monomers in each tetramer for it to be able to bind its cognate TCR. In an attempt to improve the conformational integrity of the purified SCT proteins refolded SCT-SL-B was also purified using immunoaffinity chromatography (data not shown). However, in addition to a very poor yield, HPLC analysis of the purified protein showed a heterogeneous population of protein species.



Binding of tetramers to NLVPMVATV-specific CTLs compared with commercial tetramer.
NLVPMVATV-specific CTLs were labelled with tetramer and anti-hCD8-APC. Plots are gated on live cells as identified by FSC/SSC.
Histograms gated on CD8+ cells.

Figure 3.22: FACS profiles of NLVPMVATV peptide-specific CTLs labelled with SCT-SL-B-PE tetramer

An alternative purification method which could be investigated is anion exchange. Although this method has the advantage of both concentrating and purifying a particular protein, due to the high ionic strength of the refold buffers used in these studies it would require dialysis of the protein into a more appropriate buffer, a step which would have to be preceded by significant protein concentration, thus removing the advantage of being able to concentrate the protein whilst purifying it. An alternative strategy is to use two methods of purification; SCT protein could be initially purified using size exclusion chromatography, biotinylated, and then purified for a second time using immunoaffinity chromatography. The likely disadvantage of this approach is that yields would be significantly reduced as each manipulation results in the loss of protein.

The fact that murine SCT-B (SIINFEKL- β_2 m-K^b) purified using size exclusion chromatography alone could be biotinylated and made into tetramers which efficiently recognised CTLs expressing the cognate TCR at a concentration of 5 μ g/ml (see Figure 5.4), suggests that if a protein is sufficiently well folded the method of purification used in these studies is adequate. This leads to the conclusion that improving the SCT refolding method is likely to be key to producing tetramers which can recognise their cognate TCR.

The only difference between SCT-SL-B and the constructs refolded by Oved *et al* (whose methods were used throughout this study) is the choice of peptide: This study uses an HLA-A2 restricted CMV-derived peptide whilst their work used HLA-A2 restricted peptides derived from EBV and the melanoma Ags gp100 and MART1. Given that they were able to refold their SCT proteins sufficiently well to make functional tetramers it appears that the choice of peptide within an SCT determines the efficiency of refolding using a particular buffer. To my knowledge there are no reports of an *NLVPMVATV*-containing HLA-A2 SCT protein produced in bacteria in the literature. The only published report of production of a soluble construct composed of an *NLV*-peptide containing SCT protein is by Greten *et al* who used mammalian cells to produce an SCT covalently linked to the heavy chain of a mouse IgG₁.⁴⁸⁰

As discussed earlier, unfortunately determining the appropriate refolding conditions for a particular protein is largely empirical and the starting point is usually those published as being successful with similar proteins. ^{397,405} In this study both of the published refolding methods for SCT proteins have been extensively tried with ultimately little success. The modifications which can be made to the refolding buffers used are virtually infinite, meaning a large scale screen evaluating multiple sets of different conditions is likely to be required. Although commercial kits are available which allow aliquots of protein to be refolded on a small scale using ~100 different sets of conditions, these rely on the availability of a way of evaluating the efficiency of the refolding process using tiny amounts of protein.

Although the ELISA used to determine the conformational integrity of the refolded SCT protein (data shown in Figure 3.19) would be a suitable assay and is described throughout the published literature as a method for assessing the structure of MHC class I proteins, in this study recognition of SCT protein using this assay did not correlate with the formation of functional tetramers. In order to produce sufficient refolded SCT protein for biotinylation and tetramerisation post purification, it is necessary to refold at least 100 mg of denatured SCT, a process which uses several litres of refolding buffer. It is therefore not practical to test

multiple sets of refolding conditions using recognition of the cognate TCR by SCT tetramers as the method of evaluation. Before multiple refolding conditions can be investigated either the ELISA needs to be optimised or an alternative assay to assess the efficiency of protein refolding needs to be developed.

Therefore in summary, a number of different SCT constructs have been produced and expressed in bacteria. These SCT proteins have been refolded using both of the published methods, and size exclusion and immunoaffinity chromatography have been used to attempt to purify the resulting proteins. The purified SCT proteins have been analysed using HPLC, SDS-PAGE and ELISA in addition to being made into tetramers to investigate whether they are able to recognise cognate TCRs. Unfortunately, despite promising results during the production and purification process, none of the SCT proteins produced were able to form successful tetramers which is the ultimate functional assessment necessary if the SCT protein is to be used in a retargeting protein. These studies suggest that further optimisation of mammalian expression of SCT protein may be a more successful production strategy rather than using a bacterial expression system.

Chapter 4: Discussion (1) Human Constructs

4.1 Summary of Human Construct Data

The initial proof-of-principle experiments conducted as part of this study demonstrated that *NLVPMVATV*-specific CTL lines could be generated from circulating PBMCs from healthy HLA-A2⁺/CMV⁺ donors which had similar proliferative potential to non-transformed CTL lines described in the literature. ⁴³⁵ The effector phenotype of these lines was confirmed by their ability to lyse target cells in a two-step retargeting assay (after Savage)³⁸⁷ even at very low effector:target ratios.

The next stage of the investigation was to produce a single-molecule retargeting construct which consisted of a recombinant HLA-A2/NLVPMVATV pMHC molecule joined to an anti-hCD20 moiety. Initially (p)MHC expression in mammalian cells was explored in order to allow the addition of an Fc region to the molecule. Several genetic constructs were made which encoded for different combinations of components of the (p)MHC-Fc molecule. After transfection of 293F or CHO-K1 cells, production of the desired species could be detected by both Western blotting and ELISA, but very low yields limited further manipulation of the proteins. Owing to these low yields of MHC-Fc fusion proteins, a standard SCT was expressed in mammalian cells. This had an improved yield (although still very low in comparison to antibodies), but the absence of an Fc region meant purification was more problematic. The protein could be modified to include a selection tag (e.g. His or glutathione-S-transferase), although this would need to be cleaved from the molecule prior to use *in vivo* due to their potential immunogenicity.

Owing to the disappointing yields using mammalian expression systems, bacterial expression of the pMHC component of the single-step retargeting construct was pursued. To avoid the theoretical problems of peptide dissociation, the SCT format was chosen for the pMHC molecule and a number of genetic constructs encoding slightly modified versions of the same HLA-A2/NLVPMVATV SCT were produced. These were all expressed in *E. coli* and the induced protein was extracted from inclusion bodies and refolded using the two different methods described in the literature. Size exclusion and immunoaffinity chromatography were explored as methods of purification of the refolded SCTs and the success or otherwise of the process was evaluated using SDS-PAGE, Western blotting, ELISA, HPLC and tetramer formation. Unfortunately, although SDS-PAGE, Western blotting, ELISA and HPLC analysis all suggested that an SCT protein of the predicted size with the appropriate tertiary structure had been produced and purified, when conformational integrity was evaluated, via its ability to recognise its cognate TCR upon tetramerisation, this was found not to be the case: Tetramers of several different versions of the HLA-A2/NLVPMVATV SCT were unable to

recognise *NLVPMVATV*-specific CTL suggesting that an insufficient proportion of the SCT protein had refolded correctly.

Given that the refolding method of Oved used in this study has been shown to produce correct refolding of an SCT whose only difference is the identity of the peptide (EBV, Melan-A/MART-1 or gp100-derived),³⁹⁷ it is likely that the sequence of the peptide is the critical factor in determining the exact conditions necessary for successful refolding. As discussed above, the absence of a reliable assay which both detects successful refolding using very small quantities of protein, and correlates with functional tetramer formation, limits the number of different refolding conditions which can be evaluated (producing sufficient protein for subsequent tetramer formation can require several litres of refolding buffer).

4.2 Potential Future Studies: Human construct

One aspect of bacterial HLA-A2/*NLVPMVATV* SCT production which warrants further investigation is purification of the refolded protein; the failure to produce functional tetramers despite the apparent production of some conformationally correct protein of the predicted size (as shown by ELISA and SDS-PAGE respectively) may be a result of poor purification using size exclusion chromatography alone. An alternative purification strategy utilised by some investigators is anion exchange chromatography.³⁹⁷ A combination of anion exchange chromatography followed by size exclusion chromatography may provide better purification of conformationally correct protein. Although the SCT protein cannot be applied to the column in its refolding buffer due to its high ionic strength, if it is partially concentrated it can be dialysed against a buffer with a lower pH and L-arginine content and then loaded onto the column.

Amongst the (p)MHC constructs expressed in mammalian cells, the SCT format consistently produced the highest yields. Gould *et al* (personal communication) have developed a method of producing soluble recombinant SCTs in mammalian cells (293T) using a bicistronic retroviral vector which encodes both an SCT and green fluorescent protein (GFP). Successful transduction of a cell with this vector results in both secretion of the SCT and production of GFP, allowing transduced cells to be sorted by FACS. Cells strongly positive for GFP are repeatedly transduced with the same vector to increase the copy number of the SCT fusion gene within the cell and hence SCT protein secretion. Using this method they have produced SCT yields of up to 2.5 mg/l. Yield varies with the identity of the peptide in the SCT and some SCT constructs are retained within the cell rather than secreted.

Given the promise of this approach with certain SCTs we put the SCT-SL-B and SCT-SL-B-DST fusion genes into the MSCV 2.2 IRES GFP vector which is a bicistronic retroviral vector which can be used to transduce 293T cells. Despite multiple rounds of transduction which produced cells which had an MFI up to 10^4 in the FL1 channel on FACS analysis (represents intense expression of GFP suggesting multiple copies of the transgene within the cells) the desired SCT protein could not be detected in the cell supernatant by either ELISA or Western blotting. Instead, on lysis of the 293T cells, an appropriately sized protein recognised by anticlass I and anti- β_2 microglobulin antibodies could be detected by Western blotting suggesting that there is at least some production of the desired SCT protein albeit retained with the cell (data not shown). The lack of secretion of the desired protein despite evidence that multiple copies of the fusion gene were in the cell meant this strategy was not pursued any further.

4.3 Future Studies: Murine Construct

The significant difficulties encountered with production of the pMHC component of the human retargeting construct have meant that functional assessment of a retargeting molecule has been impossible. We have therefore decided to investigate the *in vivo* function of a murine retargeting construct which has been developed within our laboratory as discussed in the following chapter.

Chapter 5: Results - Murine Retargeting Constructs

$\underline{\textbf{5.1 Production of Murine } \textit{SHNFEKL-} \beta_2 \textbf{microglobulin-} \textbf{K}^b\textbf{-biotin-AviTag (mSCT-B)} } \\ \textbf{Protein}$

Owing to the difficulties producing a human SCT for conjugation to a Fab' to obtain a single-step retargeting construct, it was decided to concentrate on evaluating murine SCT-Fab' conjugates in order to assess the potential of this strategy. The murine SCT contained within these conjugates was *SIINFEKL*-β₂microglobulin-K^b-biotin-AviTag (mSCT-B) for which reliable bacterial expression and refolding techniques have previously been developed by Lybarger *et al*⁴⁰⁵, and for which there is a transgenic (Tg) mouse with a cognate TCR: CTLs in OT-1 mice⁴²⁸ specifically recognise *SIINFEKL* peptide in the context of K^b. Figure 5.1 illustrates the structure of mSCT-B which includes the Y84A substitution to enhance peptide binding within the peptide binding groove.

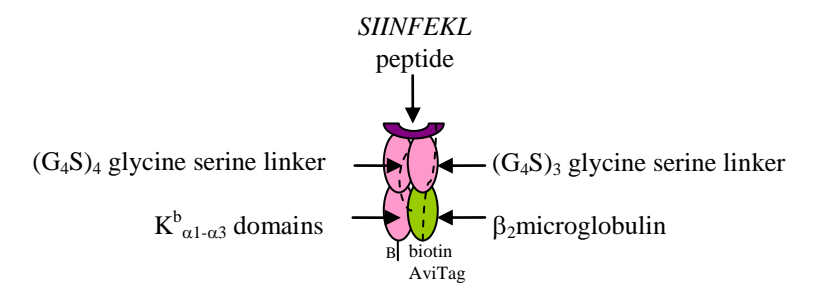


Figure 5.1: Structure of $\textit{SIINFEKL-}\beta_2 microglobulin-K^b$ -biotin-AviTag (mSCT-B) protein

As with human SCT proteins, mSCT-B was expressed in KRX *E. coli* using IPTG and L-rhamnose induction. Prior to extraction of mSCT-B protein from insoluble inclusion bodies, transformed uninduced and induced bacteria were analysed using SDS-PAGE to ensure over-expression of an appropriately sized protein; ~50 kDa (Figure 5.2 A lanes 2 & 3). Once protein expression was confirmed, inclusion bodies were extracted (section 2.3.2.3), solubilised and denatured and recovery of an appropriately sized protein confirmed by SDS-PAGE (Figure 5.2 A lane 4). The denatured protein was then refolded by dilution with a redox shuffling system, using the method of Lybarger before being concentrated, filtered and analysed by HPLC to assess the relative size and purity of the refolded protein (Figure 5.2 B). Purification of the refolded protein was achieved using size exclusion chromatography (Figure 5.2 C) while the size and purity were assessed using HPLC (Figure 5.2 D) and SDS-PAGE (Figure 5.2 A lane 5).

Figure 5.2 demonstrates that an appropriately sized protein is produced in pET21a-mSCT-B transformed KRX *E. coli* cells upon IPTG/L-Rhamnose induction that appears concentrated in inclusion bodies which can be extracted form the bacteria. Upon refolding, the predominant

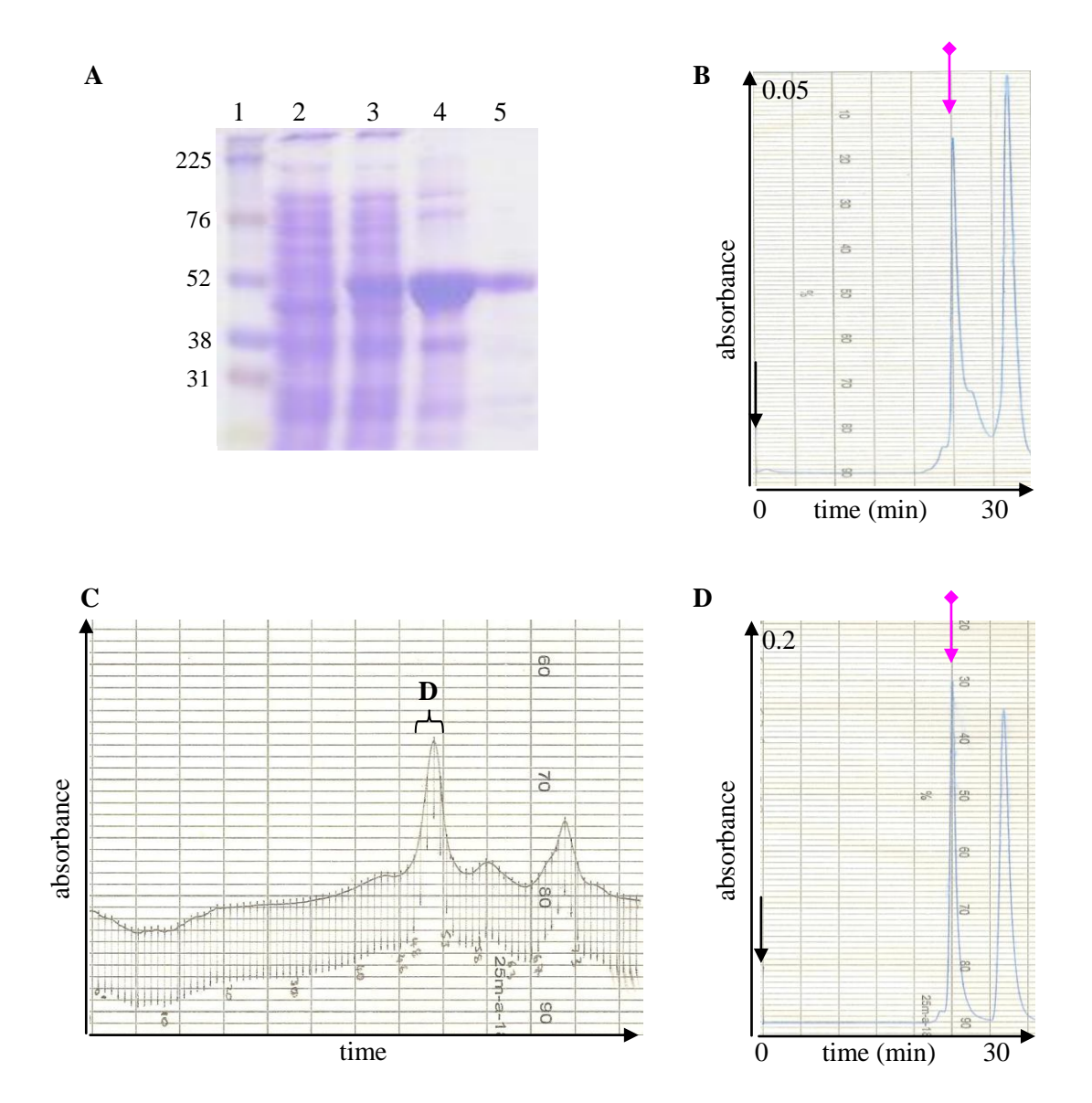


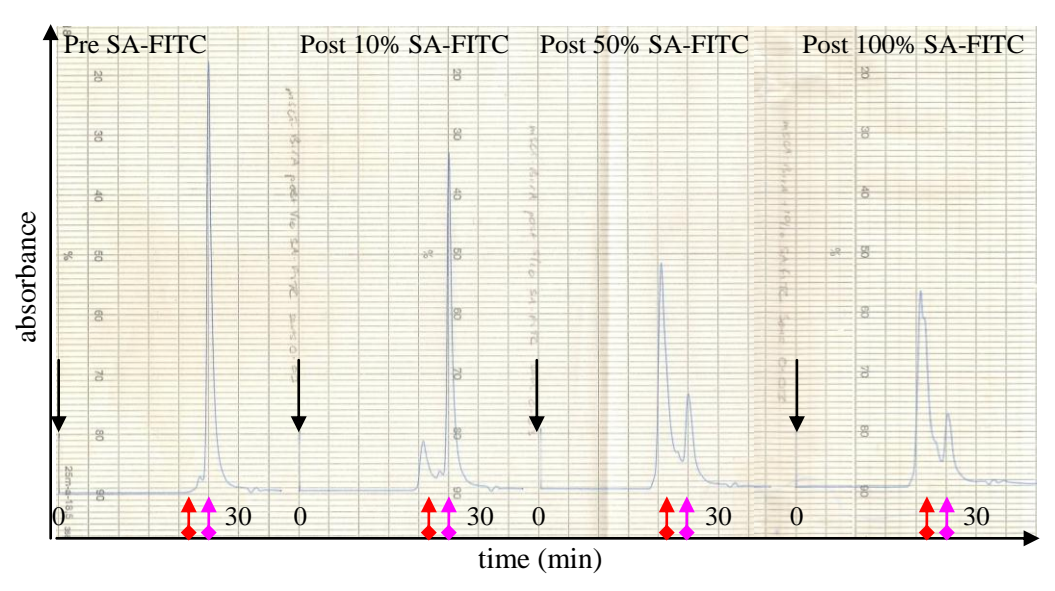
Figure 5.2: Expression and purification of mSCT-B protein

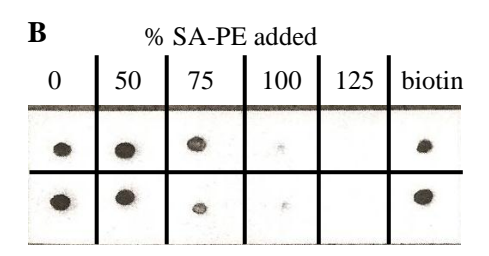
A 12.5% SDS-PAGE gel (reducing conditions) of the expression and purification of mSCT-B. Lanes: 1 markers; 2 uninduced and 3 induced KRX E. coli cells transformed with pET21a-mSCT-B; 4 denatured solubilised inclusion bodies; 5 refolded mSCT-B protein purified by size exclusion chromatography. B analysis of refolded, unpurified mSCT-B. Annotation on all HPLC chromatograms is as described in the legend of Figure 3.12 unless otherwise stated. C separation of the refolded mSCT-B by size exclusion chromatography. The fractions corresponding to the peak marked D were combined and analysed by HPLC as shown in D. This peak corresponds to a species of the expected size ~ 50 kDa and was assumed to represent mSCT-B.

product is a protein of the expected size (as shown on HPLC) which is considerably purer than anything produced when human SCTs were refolded (chapter 3). This protein can be further purified using size exclusion chromatography and both HPLC and SDS-PAGE confirm the resulting species is of the expected size (~50 kDa) and relatively free of contaminants. The yield of inclusion bodies per litre of transformed bacteria is approximately twice that seen for the human SCTs (chapter 3; i.e. 100 mg/l versus 50 mg/l), while the

refolding efficiency was in the region of 3-5% which is similar to that reported by many for conventional pMHC monomer refolding.⁴⁸¹

The conformational integrity of the mSCT-B molecules post-refolding was assessed by enzymatically biotinylating a sample from each refold, and using this as the substrate to make tetramers which could then be used to stain OT-1 CTLs. Successful biotinylation of mSCT-B and subsequent tetramerisation was confirmed using either HPLC analysis, when tetramerisation was performed using SA-FITC (Figure 5.3 **A**), or a dot blot (Figure 5.3 **B**) when SA-PE was used. In **A** the tetramerisation of mSCT-B-biotin with SA-FITC is followed by HPLC analysis: with each addition of SA-FITC the size of the starting monomer peak diminished and there was a progressive increase in the size of a peak representing a protein species > 150 kDa, presumed to be tetramers. Similarly in **B** the dot blot shows a progressive decline in the biotinylated monomer until when >100% of the theoretical amount of SA-PE necessary for complete tetramerisation has been added there is no biotinylated monomer detectable on the blot. These results confirm that the biotinylation and tetramerisation processes were successful.





A HPLC following tetramerisation of mSCT-B-biotin with SA-FITC. The black arrows indicate loading. The pink and red arrows indicate the elution positions of Fc (50 kDa) and IgG (150 kDa) respectively. B Dot blot (probed with SA-HRP) monitoring the tetramerisation reaction following the addition of SA-PE to mSCT-B-biotin. Samples were added in duplicate and biotin was used as a positive control Blot courtesy of Leon Douglas, Cancer Research UK Protein Core Facility, Southampton General Hospital, Southampton.

Figure 5.3: Tetramerisation of mSCT-B

mSCT-B-PE tetramers were then used to label splenocytes from OT-1 Tg mice and C57BL/6 wild type (WT) mice. Figure 5.4 demonstrates that the mSCT-B tetramers were able to bind specifically to CD8 $^+$ cells from OT-1 mice. Similar MFI values were seen when using 5 μ g/ml of the mSCT-B tetramers and the recommended amount of a commercially available tetramer. These results indicate that the mSCT-B has refolded sufficiently to recognise its target TCR and is therefore suitable for use in a retargeting construct.

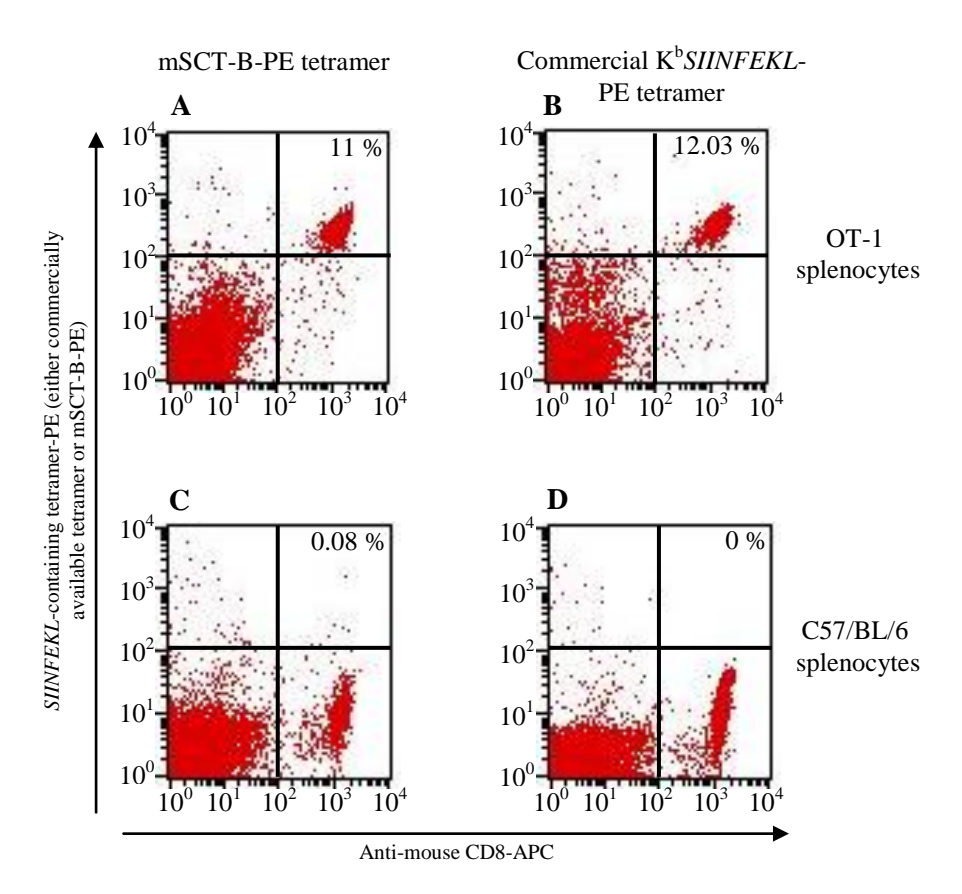


Figure 5.4: mSCT-B tetramer staining of splenocytes from OT-1 Tg and C57BL/6 mice Splenocytes from OT-1 Tg (A & B) and WT C57BL/6 (C & D) mice were labelled with anti-mCD8-APC and either mSCT-B-PE tetramer ($5 \mu g/ml$) (A & C) or commercial K^b SIINFEKL-PE tetramer (B & D). The %s indicate the level of OT-1 cells.

5.3 Production of mSCT-B x anti-hCD20 Fab' Conjugates

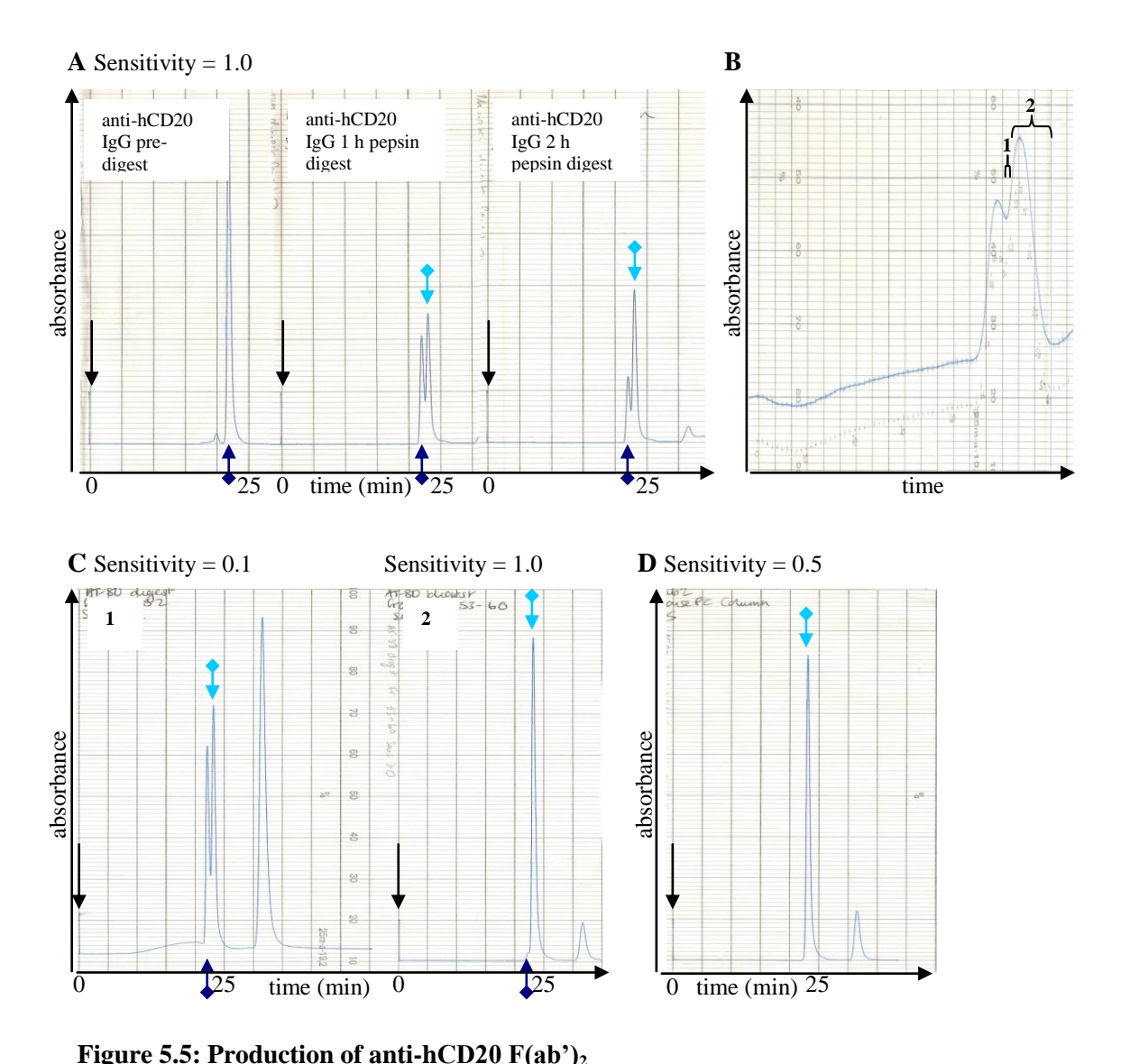
In order to retarget CTLs, in addition to a construct possessing a pMHC which can bind to CD8⁺ T cells, it is necessary for it to have an Ab moiety which can target a tumour Ag. As discussed in the introduction, due to the availability of both antibodies and tumour models (both *in vitro* and *in vivo*) within our laboratory, the target tumour Ag throughout this project was the B cell Ag hCD20 which is already exploited clinically with the mAb rituximab. Having demonstrated that functional mSCT-B protein was produced, the next stage was to conjugate it to an anti-hCD20 mAb derivative.

Figure 1.10 illustrates that, at least within BsAb, there are a variety of formats possible for the anti-tumour Ag moiety. The chosen format for our retargeting construct was Fab' due to the ease of its generation and its suitability for chemical conjugation due to the presence of sulfhydryl groups in the hinge region. The next stage therefore in the production of the retargeting constructs was the generation of anti-hCD20 Fab'.

The anti-hCD20 Ab chosen was the in-house produced AT80. In addition to its availability, being a murine IgG_1 Ab it has an odd number (3) of sulfhydryl groups in its hinge region: this means it can be easily conjugated to the rat anti-mouse CD3 Ab KT3 to produce an anti-mouse CD3 x anti-human hCD20 bispecific $F(ab')_2$ (henceforth known as [anti-hCD20 x anti-mCD3] BsAb) which can be used as a positive control for the functional evaluation of pMHC x Fab' retargeting constructs. To generate Fab', the parental IgG first underwent digestion with pepsin to produce $F(ab')_2$. The digestion was monitored by HPLC. Once greater than 50% of the IgG had been digested the reaction was stopped and the different species separated using size exclusion chromatography. Figure 5.5 shows the digestion and purification of the $F(ab')_2$ generated.

The next stage was to reduce the $F(ab')_2$ to Fab' and conjugate it to mSCT-B. A large number of different cross-linkers are commercially available for performing chemical conjugations: a number of variables can impact choice of cross-linker including the chemical composition of the molecules and the end structure and function of the conjugate. Conventionally linkers containing thiol-reactive groups such as maleimide have been used in the production of bispecific $F(ab')_2$ owing to the availability of sulfhydryl groups within the cysteine residues in the Fab' hinge regions (Figure 1.10 **B**).

The choice of mSCT-B as the pMHC component of the retargeting molecule prevents this approach to cross-linking as there are no free cysteine residues in the hinge region. The reason for this, perhaps counterintuitive, choice of pMHC conjugation partner comes from disappointing results from preliminary work within our lab (B King, personal communication) with a conjugate consisting of anti-hCD20 Fab' x mSCT-SH (i.e. *SIINFEKL*-β₂microglobulin-K^b engineered to contain a cysteine residue at the carboxy terminus of the protein), joined by a bismaleimide containing linker: In addition to both a lower yield of inclusion bodies and reduced refolding efficiency for mSCT-SH in comparison to mSCT-B, initial *in vitro* analyses of the conjugate suggest it is not particularly efficacious as a retargeting construct despite appearing to be conformationally intact.



A HPLC analysis of pepsin digestion of anti-hCD20 IgG to F(ab')₂. Black arrows indicate loading

points, dark blue and light blue arrows indicate the expected elution points of IgG and F(ab')2 respectively. B Size exclusion chromatography of 2 h digest. The small and large peaks represent antihCD20 IgG and F(ab)₂ respectively. C 1. HPLC of fraction 1 from B, showing significant IgG contamination. 2. Pooled $F(ab')_2$ fractions (2 in B), showing a slight shoulder (dark blue arrow) indicating low level IgG contamination. **D** HPLC of F(ab')₂ after passing through an anti-mouse Fc column to remove contaminating IgG.

The lack of free sulfhydryl groups within mSCT-B meant the heterobifunctional linker Succinimidyl-4-(N-maleimidomethyl) cyclohexane-1-carboxylate (SMCC) was used to effect conjugation. This is able to react with any amine group on mSCT-B via its NHS ester leaving its maleimide group free to interact with a sulfhydryl group in the hinge region of the Fab'. This has two implications for the structure of the resulting conjugates. First as any amine group within mSCT-B can be the target of SMCC the product is heterogeneous with the conjugates having a range of geometries. Second the presence of multiple amine groups within mSCT-B means >1 SMCC molecule can link to each mSCT-B molecule resulting in >1 Fab' molecule being attached to each mSCT-B. The conjugates chosen for further

evaluation were those whose molecular mass suggested they had a Fab':mSCT-B ratio of 1:1 or 2:1. Purification of these two species was achieved using size exclusion chromatography. Figure 5.6 shows analysis at various stages in the conjugation and subsequent purification. The starting materials and products were also evaluated on SDS-PAGE under reducing and non-reducing conditions (Figure 5.7).

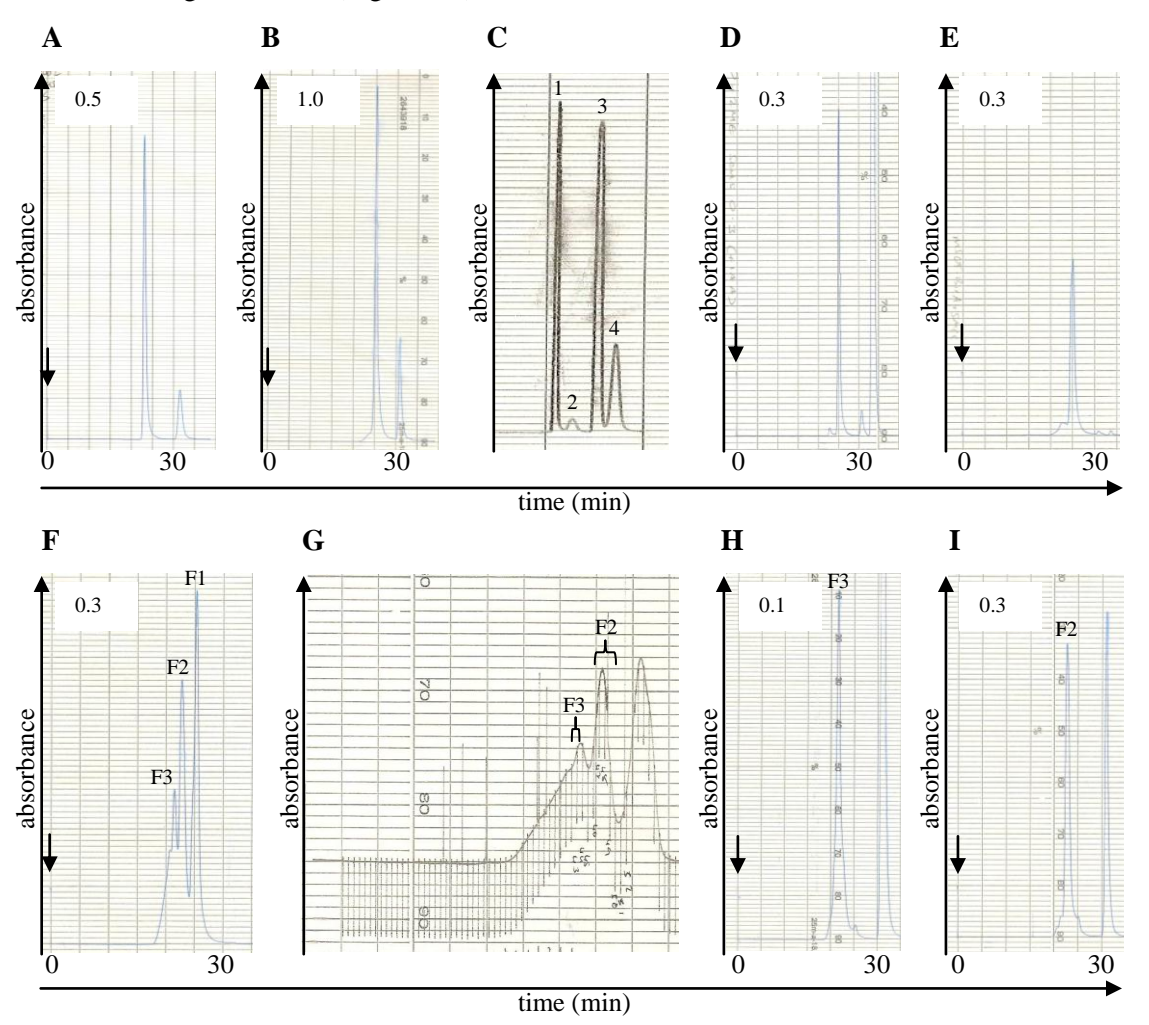


Figure 5.6: Conjugation of mSCT-B to anti-hCD20 Fab' using SMCC

A and B; HPLC of anti-hCD20 F(ab')₂ and mSCT-B respectively. C; reduced anti-hCD20 Fab' (peak 1) separated from 2-ME (peak 2) and mSCT-B_{mal} (peak 3) separated from DMF containing excess SMCC (peak 4) on a G25 column. D; HPLC of reduced anti-hCD20 Fab' after alkylation with iodoacetamide to prevent re-dimerisation. E HPLC of mSCT-B_{mal}. F HPLC of conjugation mixture after overnight incubation at 4 °C. Based on the mechanism of conjugation peaks probably represent: F1, mixture of starting materials (reduced anti-hCD20 Fab' and mSCT-B); F2, mSCT-B x anti-hCD20 Fab'; and F3, mSCT-B x (anti-hCD20 Fab')₂. A similar profile was obtained when the mixture was reduced and alkylated suggesting that the F2 peak is mSCT-B x anti-hCD20 Fab' rather than anti-hCD20 F(ab')₂. G size exclusion chromatography of reaction mixture. Fractions corresponding to F2 & F3 were analysed by HPLC (I and H respectively).

Figure 5.6 **F** and **G** show the distribution of the starting materials, reduced anti-hCD20 Fab' and mSCT-B, and the conjugation products, thought to be mSCT-B x (anti-hCD20 Fab')₂ (F3) and mSCT-B x anti-hCD20 Fab' (F2), after overnight incubation. **H** & **I** show HPLC analysis of F3 and F2 conjugates which elute at points corresponding to IgG and F(ab')₂

which correlates with their predicted masses based on their presumed structure. Lane 3 in the SDS-PAGE gel in Figure 5.7 confirms that the position of F2 was similar to that of anti-hCD20 F(ab')₂, consistent with its predicted size. Under reducing conditions (lane 7), this species resolves to show a band at the position of the light chain of anti-hCD20 Fab' and another band corresponding to approximately 75 kDa.

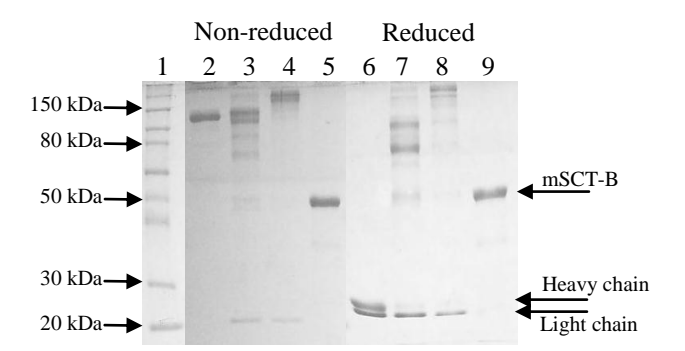


Figure 5.7: SDS-PAGE of mSCT-B x anti-hCD20 Fab' conjugation products SDS-PAGE of non-reduced (lanes 2-5) and reduced (lanes 6-9) substrates and conjugates. Lanes: 1 markers; 2 & 6 anti-hCD20 F(ab')₂; 3 & 7 mSCT-B x anti-hCD20 Fab'; 4 & 8 mSCT-B x (anti-hCD20 Fab')₂; 5 & 9 mSCT-B.

This is consistent with the predicted reaction whereby the maleimide group of SMCC attached to mSCT-B molecules reacts with the free sulfhydryl group on the hinge region of the heavy chain of reduced anti-hCD20 Fab' molecules to produce an irreducible thioether bond. In contrast, the light chain remains attached to the heavy chain via a disulphide bond which is susceptible to reduction. The presence of a species larger that 25 kDa upon reduction also illustrates that the F2 peak is not anti-hCD20 (Fab')₂ which has redimerised during the conjugation process. Lane 4 Figure 5.7 shows that F3 migrates slower than F2 consistent with its predicted larger size.

Despite both F2 and F3 looking relatively pure by HPLC (Figure 5.6 **H** & **I**), when analysed by SDS-PAGE both species have produced more of a smear with several distinct bands. Although these may represent poor protein separation, contamination or protease-mediated degradation, at least some of the 'smear' may be secondary to structural isomerism. Naturally occurring proteins are usually composed of single polypeptides folded into a tertiary structure stabilised by hydrophobic interactions, hydrogen, ionic and disulfide bonds, or are composed of several polypeptides folded together in a quaternary structure maintained by the same interactions and bonds. Branched proteins (similar to our conjugates) where a second polypeptide is attached by a non-reducible bond midway along the first polypeptide do not readily occur naturally.

With a natural protein, SDS with its multiple negative charges, in addition to destroying much of the higher structure, 'coats' the polypeptide with negative charges effectively linearising it. The SDS-coated linear polypeptides move towards the anode at a rate approximately proportional to their length and hence size with smaller polypeptides migrating faster. Modifications to the polypeptide such as phosphorylation or glycosylation can however affect its migration so there can be a slight discrepancy between the predicted and apparent molecular mass.

As discussed previously, SMCC can react with any primary amine group within the mSCT-B molecule. Although several amino acids contain primary amine groups, it is suggested that lysine is most reactive with SMCC. mSCT-B contains 22 lysine residues meaning there is the potential for anti-hCD20 Fab' to be attached as a branch (or branches) at several different sites. This would produce a heterogeneous end product which, although having the same size for any fixed ratio of anti-hCD20 Fab':mSCT-B, would contain conjugates with a number of different geometries: hence structural isomers.

Unless the Fab' is attached as a branch towards the end of the mSCT-B polypeptide, upon SDS denaturation and 2–ME reduction, the conjugate cannot form a truly linear polypeptide as the Fab' branch is also coated in negatively charged SDS molecules which are repelled from the SDS-coated mSCT-B 'stem'. The conjugate therefore has some geometric structure as it migrates and is likely be slower than a truly linear polypeptide of the same mass. The geometries of the conjugates are likely to vary depending on which lysine residues are conjugated meaning the species may migrate differentially despite having the same size and charge. This phenomenon has been observed when SMCC conjugation was used to link horse radish peroxidase enzyme to bovine serum albumin. 482

The typical yields of the F2 and F3 conjugates from a reaction with 10 mg of the two starting substrates (mSCT-B and anti-hCD20 Fab') are ~2 mg and ~1 mg respectively giving a conjugation efficiency of ~15%.

5.4 Production of anti-hCD20 x anti-mCD3 F(ab')₂ Conjugate: BsAb

Retargeting T cells has historically involved the use of anti-CD3-containing BsAb (section 1.5.2). In order to compare the efficacy and tolerability of our retargeting molecules with the traditional approach, a bispecific F(ab')₂ was produced by o-PDM mediated conjugation of anti-hCD20 to anti-mCD3 Fab' (derived from anti-mouse CD3 mAb KT3); this procedure has previously been used extensively in this laboratory. Unlike SMCC, o-PDM is able to produce a largely uniform conjugate as it reacts with the free sulfhydryl groups in the hinge region of

reduced Fab' molecules. It could be argued that it is unfair to compare the heterogeneous SMCC-conjugated F2 and F3 molecules with the homogeneous o-PDM-conjugated bispecific $F(ab')_2$, but any new retargeting molecule needs to be evaluated against the 'best' existing product.

Briefly, the [anti-hCD20 x anti-mCD3] BsAb is produced by reducing the parent F(ab')₂ molecules using 2-ME, conjugating one of the Fab' molecules using o-PDM, and then combining the two species to obtain the BsAb product; the reaction mixture and the isolated products are shown in Figure 5.8.

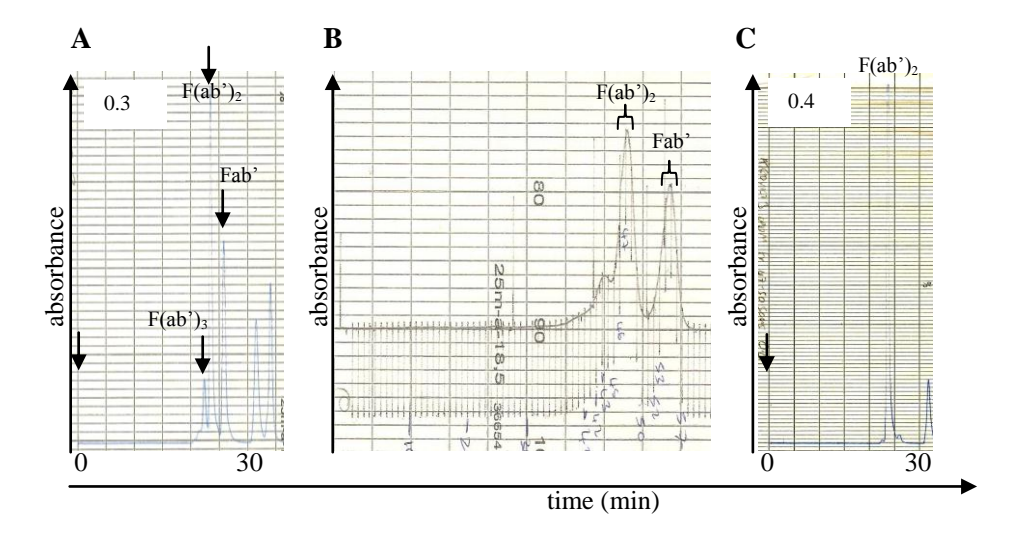


Figure 5.8: Conjugation of anti-hCD20 Fab' to anti-mCD3 Fab'

A HPLC of the conjugation reaction, anti-hCD20 Fab'_{mal} and anti-mCD3 Fab' after overnight incubation and reduction and alkylation to remove any reformed $F(ab')_2$ dimers. Fab' is a mixture of the starting materials, $F(ab')_2$ is [anti-hCD20 x anti-mCD3] BsAb, and $F(ab')_3$ is anti-hCD20 Fab' x anti-mCD3 (Fab')₂; Anti-hCD20 Fab' has 3 sulfhydryl groups in its hinge region and 2 of these should be joined together by the cross linker eliminating them from the conjugation reaction meaning the majority of the conjugate produced has an anti-hCD20 Fab': anti-mCD3 Fab' ratio of 1:1 **B** Size exclusion chromatography of the reaction products . **C** HPLC analysis of the $F(ab')_2$ product.

5.5 In Vitro Functional Characterisation of mSCT-B x anti-hCD20 Fab' Conjugates 5.5.1 Staining hCD20⁺ cells

The first stage of evaluating the functionality of the mSCT-B x anti-hCD20 Fab' conjugates was to confirm that the tertiary structure of each arm of the molecule was intact and able to bind to its target Ag (i.e. hCD20 in the case of the Fab' arm(s) and its cognate TCR in the case of the mSCT-B arm). This was performed using an indirect FACS assay: hCD20⁺ Daudi cells were incubated with the mSCT-B x anti-hCD20 Fab' conjugates and the binding of conformationally correct mSCT-B on the cell surface detected by labelling with 25D1-FITC; a TCR-like mAb specific for K^bSIINFEKL (Figure 5.9).

Figure 5.9 **A** and **B** confirm that the Daudi cells express hCD20 (positive for rituximab-FITC) but not K^bSIINFEKL (negative for 25D1-FITC) on their surface. With both F2 and F3 conjugates, K^bSIINFEKL can be detected on the cell surface indicating that both elements within the constructs have retained their structural integrity (**C** and **D**). Plots **E** and **F** in Figure 5.9 demonstrate that both retargeting constructs are binding specifically via the hCD20 on their surface as pre-incubation with anti-hCD20 F(ab')₂ substantially reduces the subsequent binding of both F2 and F3 conjugates.

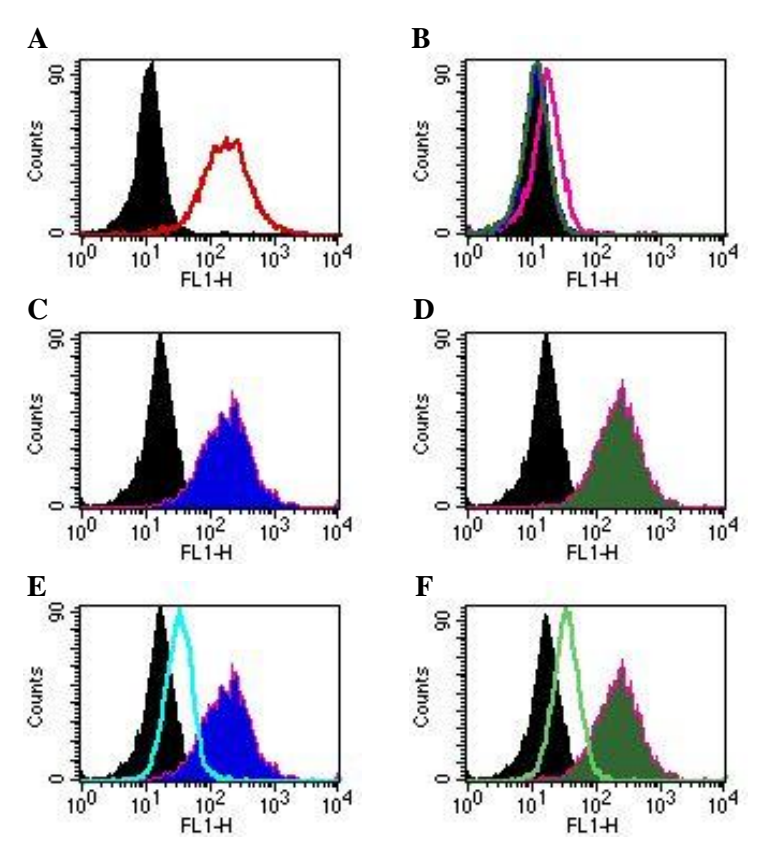


Figure 5.9: Labelling of hCD20⁺ Daudi cells with mSCT-B x anti-hCD20 Fab' retargeting constructs and 25D1

In all plots filled black histograms represent unstained cells. Daudi cells were labelled with: **A** rituximab-FITC; **B** 25D1-FITC (pink), F2 (blue), F3 (green) **C** F2 conjugate (30 μ g/ml) followed by 25D1-FITC: **D** F3 conjugate (30 μ g/ml)followed by 25D1-FITC. In **E** & **F** Daudi cells were preincubated (open histograms) or not (filled histograms) with 100 μ g/ml anti-hCD20 F(ab')₂ before being labelled with F2 (**E**) and F3 (**F**) and 25D1-FITC.

The binding of the F2 and F3 conjugates to Daudi cells was then compared over a range of concentrations as shown in Figure 5.10. The shape of the curves indicates that the binding of the F3 conjugate has a higher functional affinity, or avidity, than that of the F2 construct; this is consistent with its ability to bind to the target cell bivalently by virtue of its two anti-hCD20 Fab' arms.

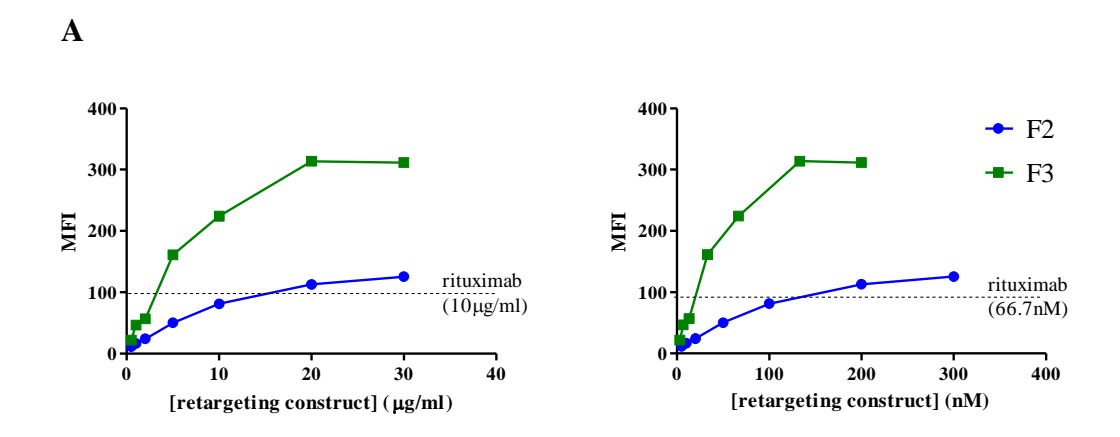


Figure 5.10: Binding of mSCT-B x anti-hCD20 Fab' conjugates to Daudi cells The graphs show the binding of the F2 (blue) and F3(green) conjugates to Daudi cells with the concentration of the construct expressed in terms of μ g/ml (A) and molarity (B). The binding of the constructs was detected with 25D1-FITC (10 μ g/ml). For comparison, the MFI observed when Daudi cells were labelled with rituximab-FITC (10 μ g/ml) is shown.

5.5.2 *In vitro* cytotoxicity assay

Having demonstrated that at least a proportion of the conjugates retained conformationally intact anti-hCD20 Fab' and mSCT-B moieties, the next stage of their *in vitro* evaluation was to use them to retarget non-cognate CTLs in a cytotoxicity assay. The assay chosen was a 4 h ⁵¹Cr assay (similar to that used for two-step retargeting of human HLA-A2 *NLVPMVATV* CTLs as described in section 2.1.2.2). The effector cells used were splenocytes from C57BL/6 mice adoptively transferred with 1 x 10⁶ OT-1 CTLs 6 days previously and activated with OVA and an agonistic anti-mouse CD40 Ab 5 days previously. The percentage of OT-1 CTLs was determined and the total number of splenocytes used adjusted to 5 x 10⁴ activated OT-1 cells per well giving an effector:target ratio of 10:1. An equal number of splenocytes from wild type C57BL/6 mice were used as irrelevant effectors.

The target cells were hCD20⁺ Daudi cells as before. Varying concentrations of the F2 and F3 retargeting constructs were used as shown in Figure 5.11. [anti-hCD20 x anti-mCD3] BsAb was used as a positive control as this should theoretically be able to retarget all mCD3⁺ T cells. The graphs in Figure 5.11 demonstrate that both the F2 and F3 retargeting constructs are able to redirect OT-1 CTLs to lyse hCD20⁺ cells, however neither retargeting construct is able to achieve a maximum level of lysis that matched that of the control BsAb. This is probably because the BsAb has a larger population of cells to retarget than the mSCT-B-containing constructs as it will retarget all mCD3⁺ cells rather than just OT-1 cells. Alternatively the percentage of the mSCT-B-containing retargeting constructs which are conformationally correct and therefore actually active in comparison to the bispecific F(ab')₂ may be significantly lower meaning the 'functional' concentration is much lower than the physical

concentration. Comparing the two retargeting constructs F3 is more potent than F2 which is likely to reflect the higher avidity of F3 for target cells than F2 owing to the presence of two anti-hCD20 Fab' moieties.

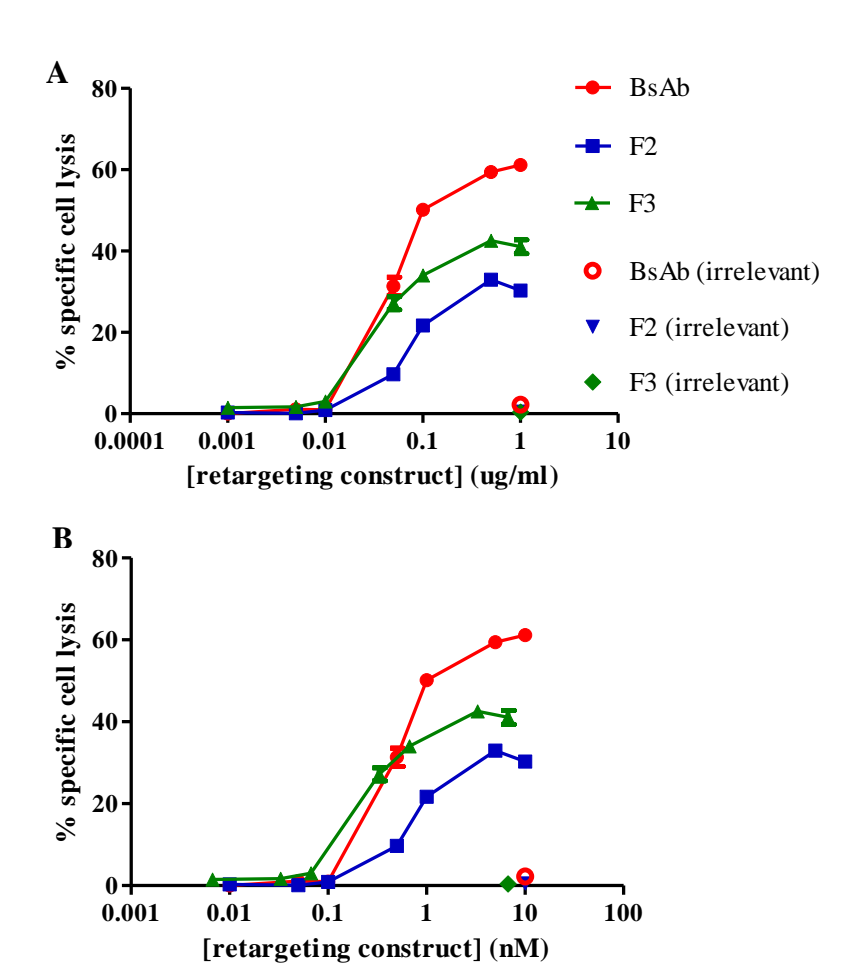


Figure 5.11: Retargeting construct mediated lysis of hCD20⁺ target cells by OT-1 CTLs A Daudi cell lysis with the different retargeting constructs. B The data was replotted in terms of molarity of the constructs. Each point is the mean of triplicate measurements and error bars represent the SEM. The data is representative of several cytotoxicity assays performed with this batch of retargeting constructs; similar trends were seen with other preparations.

It is surprising that the [anti-hCD20 x anti-mCD3] BsAb did not retarget T cells from within the naïve splenocytes to lyse the targets, particularly given the data obtained in subsequent experiments (proliferation in Figure 5.14 **B** and B cell depletion in Figure 5.18 **B**) and published data with bispecific anti-mouse-CD3 x anti-human CD19 molecules. One explanation may be that as similar numbers of splenocytes from naïve and adoptively transferred C57BL/6 mice were used rather than similar numbers of CD8 T cells or CD3 T cells, there may have been fewer retargetable cells in the naïve splenocytes. Alternatively it is possible that the structure of our BsAb meant that T cell activation and lysis took longer than the 4 h timescale of the assay.

In order to demonstrate that the F2 and F3 constructs are redirecting OT-1 CTLs to lyse hCD20⁺ cells in a specific manner dependent on the retargeting constructs interacting with both hCD20 and the OT-1 TCR, the cytotoxicity assays were repeated in the presence of an excess of either anti-hCD20 F(ab')₂ or 25D1 IgG. Figure 5.12 demonstrates that blocking either hCD20 Ag sites on the target cells or mSCT-B on the retargeting molecules with 25D1 IgG prevents most of the specific lysis showing that the F2 and F3-mediated killing is specific.

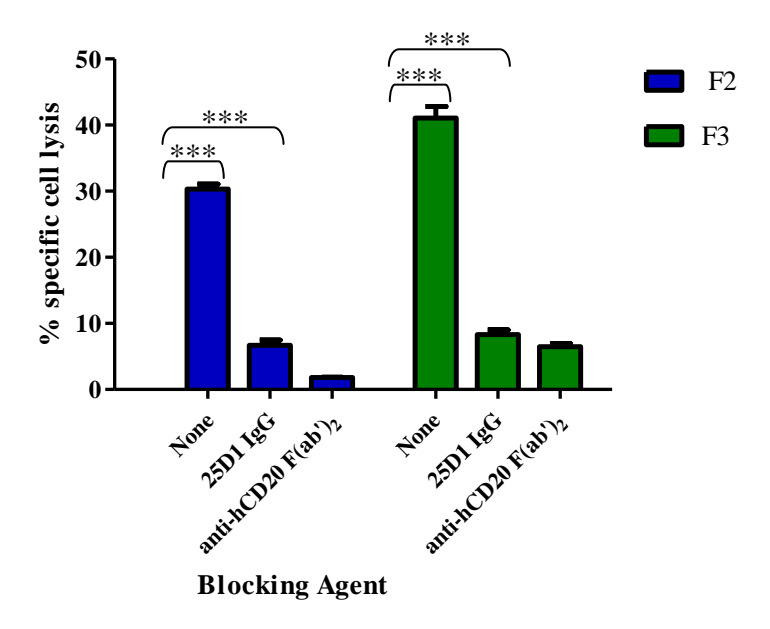


Figure 5.12: Blocking of F2 and F3 mediated cytotoxicity with anti-hCD20 $F(ab')_2$ and 25D1 IgG

The specific lysis shown is representative data from multiple experiments. The bars are plots of the mean with error bars showing standard error of the mean. Each point is the mean +/- SEM of triplicates. Blocking agents were added at $100\mu g/ml$. *** = p value <0.001 from an unpaired T test.

5.5.3 In vitro proliferation assays

Having established that the retargeting constructs were able to induce lysis of target tumour cells *in vitro* by non-cognate CTLs the next line of investigation was whether they were able to cause proliferation of their target CTL population. A conjugate which is able to cause expansion (and activation) of its target CTL has a potential advantage over one that requires an existing large population of primed cytotoxic T cells *in situ*. Given the F2 and F3 constructs contain only one pMHC arm, soluble retargeting constructs should not be able to cross link TCRs and induce proliferation. In contrast in the presence of target cells, immobilisation of multiple retargeting molecules in close proximity may be able to effect proliferation.

Purified OT-1 CTLs (shown in Figure 5.13 **B**) were used in ³H-thymidine incorporation and CFSE dilution assays to evaluate whether the retargeting constructs (in the presence of

appropriate target cells) could stimulate proliferation of appropriately restricted effectors (proliferation was also taken as a surrogate marker for activation). Figure 5.14 shows ³H-thymidine incorporation observed when OT-1 CTLs or equivalent numbers of CD8⁺ T cells from WT C57BL/6 mice were incubated in the presence of various cell lines +/- 1 μg/ml of the retargeting constructs (or *SIINFEKL* peptide).

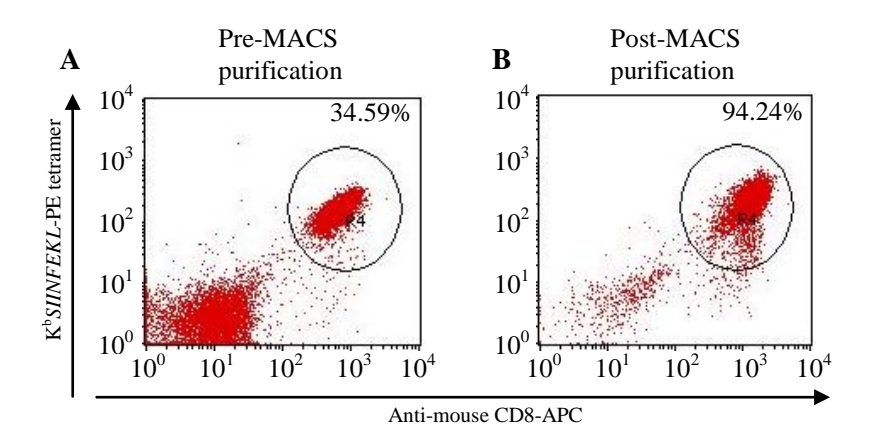
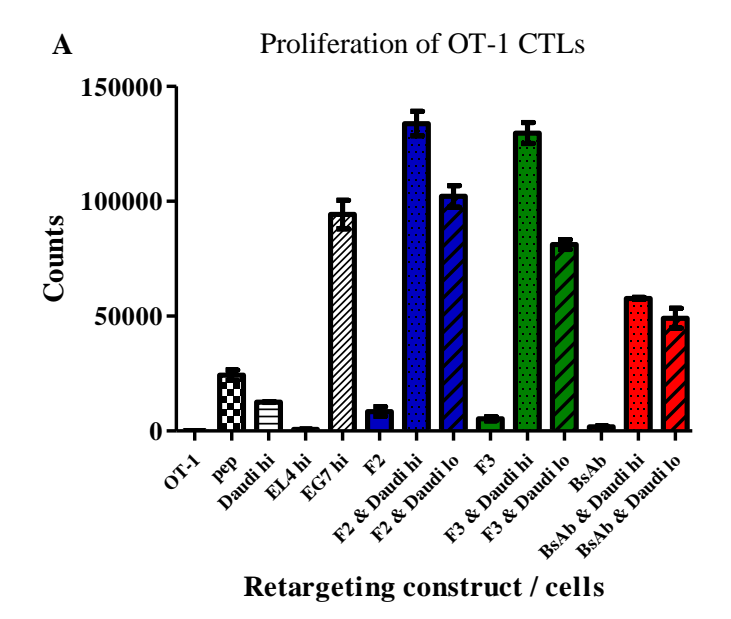


Figure 5.13: FACS staining of OT-1 CTLs pre and post MACS column purification CD8 T cells from spleen and lymph nodes of OT-1 Tg mice were purified by negative selection using a MACS CD8a⁺ T cell Isolation Kit. Cells were then labelled with anti-mouse CD8-APC and $K^bSIINFEKL$ -PE tetramers. A Pre- & B post-purification.

Figure 5.14 graph A demonstrates that when incubated alone OT-1 CTLs do not appear to undergo any homeostatic proliferation, whereas when specific peptide is added they divide, most likely secondary to peptide presentation from APCs contaminating the MACS purified OT-1 cells. EG7 cells which express K^bSIINFEKL on their surface were used as a positive control. In the presence of irradiated Daudi cells, F2, F3 and [anti-hCD20 x anti-mCD3] BsAb were all able to cause OT-1 proliferation with more division seen when a higher number of Daudi cells (and presumably therefore more immobilised pMHC or anti-CD3 Fab') were available to provide stimulation. In the absence of Daudi cells very low levels of proliferation are seen, most likely secondary to aggregation within the retargeting constructs effectively crosslinking TCRs and activating the CTLs. Have died concentration at a single time point was evaluated. The data presented could be anywhere on a dose response curve and it is possible that by the time point evaluated, many CTLs have died secondary to overstimulation.

Figure 5.14 **B** suggests that F2 and F3 mediated proliferation of OT-1 cells is produced via engagement of the TCR as when CD8⁺ T cells derived from C57BL/6 mice are substituted for OT-1 cells, no proliferation is observed. As expected, [anti-hCD20 x anti-mCD3] BsAb is

able to produce proliferation of the wild type CD8⁺ T cells as activation is through engagement of CD3 rather than the TCR.



B Proliferation of CD8⁺ T cells from C57BL/6 mice

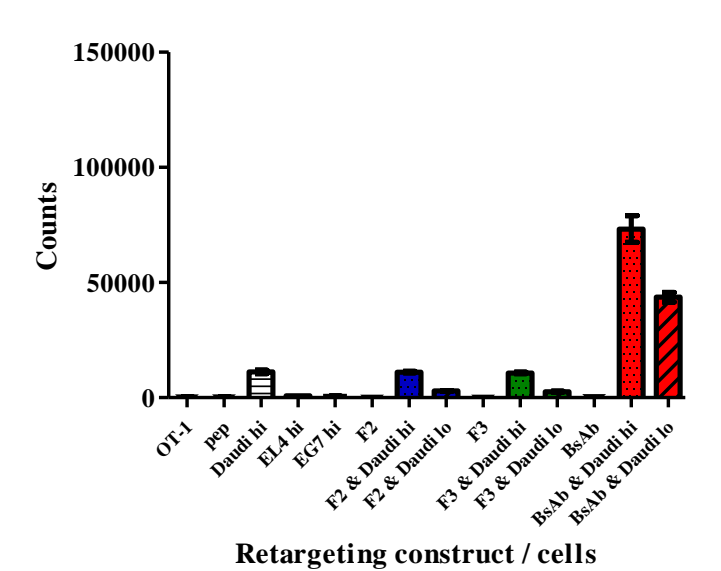


Figure 5.14: ³H-thymidine incorporation by OT-1 (A) and WT (B) CD8⁺ T cells induced by retargeting constructs

A OT-1 CTLs (5 x 10^4) were incubated in the presence of retargeting constructs (1 μ g/ml) and irradiated feeder cells at 1 x 10^5 (hi) or 1 x 10^4 (lo) per well for 72 h, with 1 μ Ci 3 H-thymidine added for the final 18 h of the assay. **B** As **A** but with OT-1 CTLs replaced with CD8⁺ T cells from WT C57BL/6 mice. Results show the mean of triplicates +/- SEM. The data in **A** is representative of two experiments and that in **B** is from one experiment.

Similar results were obtained using CFSE dilution as a measure of proliferation (Figure 5.15). The CFSE dilution profiles for OT-1 CTLs cultured with F2 or F3 alone are very similar; as with *SIINFEKL* peptide, a small number of cells are able to undergo a considerable number of

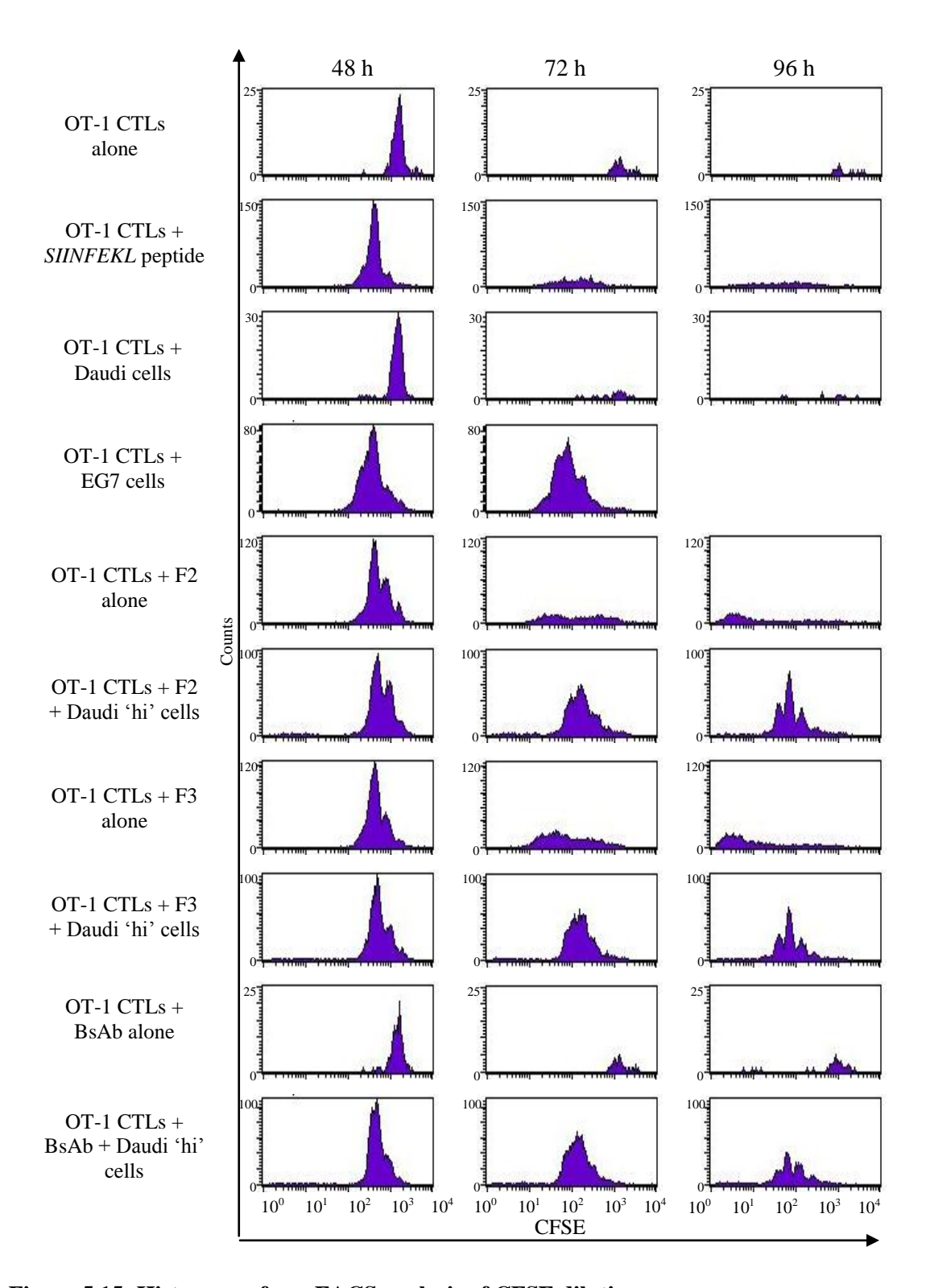


Figure 5.15: Histograms from FACS analysis of CFSE dilution assay

Histograms indicate strength of CFSE signal in FL1 (x axis) amongst the anti-mouse CD8-APC positive cells (i.e. OT-1 CTLs). Counts are shown on the y axis: NB these vary widely from well to well, with lower numbers suggesting very few intact (i.e. live) cells present in the culture. Cells were harvested at 48, 72 and 96 hours as indicated in the top legend. The culture conditions of each well are described in the left hand column. All wells had 5 x 10^4 OT-1 CTLs at the initiation of the culture, 1 x 10^5 irradiated feeder cells if appropriate and 1 μ g/ml of peptide or retargeting construct. Each histogram is from an individual well of cultures set up in triplicate and the data shown is representative of at least two experiments.

cell divisions. As discussed earlier this is assumed to be due to aggregation of the retargeting conjugates on storage which would allow multimeric engagement of the OT-1 TCRs. In contrast when OT-1 CTLs are cultured with F2 or F3 and irradiated Daudi cells, a similar dilution profile is obtained as when OT-1 CTLs are cocultured with irradiated EG7 cells: most of the OT-1 CTLs have appeared to have undergone several rounds of cell division.

When OT-1 CTLs are cultured with [anti-hCD20 x anti-mCD3] BsAb alone no proliferation is seen by CFSE dilution and even at 48 h the majority of the OT-1 CTLs have died. In contrast when OT-1 CTLs are cultured with [anti-hCD20 x anti-mCD3] BsAb in the presence of irradiated Daudi cells, significant proliferation is seen although it is interesting to note that compared to the wells with F2 or F3 and irradiated Daudi cells, by 96 h fewer OT-1 CTLs appear to be intact. As postulated before this may be due to premature death of the CTLs secondary to excessive stimulation by the [anti-hCD20 x anti-mCD3] BsAb.

Taken together, the results of the ³H-thymidine incorporation and CFSE dilution assays show that at least *in vitro*, the F2 and F3 retargeting constructs are able to cause proliferation of appropriately TCR restricted CTLs providing hCD20⁺ cells are available to immobilise the construct on their surface. Therefore it is possible that *in vivo* the constructs may be able to induce the expansion their target CTL population in addition to re-directing them to lyse the tumour cells.

5.6 In Vivo Functional Characterisation of mSCT-B x anti-hCD20 Fab' Conjugates 5.6.1 B cell depletion assay

Having established that the mSCT-B x anti-hCD20 Fab' conjugates (F2 and F3) were able to redirect non-cognate CTLs to lyse tumour cells expressing the appropriate Ag (hCD20) *in vitro*, the next stage of investigation was to evaluate their efficacy in an *in vivo* model. This was done using a hCD20 Tg mouse model which is frequently used for investigating the effect of anti-hCD20 therapies. These mice express hCD20 on all of their B cells, so depletion of circulating B cells can be used as measure of target cell killing. This model circumvents many of the problems of hCD20 transfected murine tumour models; the B cells consistently express hCD20 at a constant level, there are no concerns about tumour engraftment, and as hCD20 is expressed on the B cells throughout the development of the mouse's immune system, the animal is tolerant of hCD20, more accurately mimicking the situation in human cancers, particularly B cell malignancies.

We therefore used this hCD20 Tg mouse model as our *in vivo* tumour model. In order to have a ready supply of effector CTLs *in situ* in these animals they were adoptively transferred with naïve OT-1 splenocytes which were activated *in situ* via the administration of OVA and an agonistic anti-CD40 Ab. In order to establish the appropriate number of OT-1 CTLs to transfer and the kinetics of CTL expansion so retargeting could be attempted at the peak of the response, a number of trial OT-1 transfers were undertaken. Figure 5.16 shows the OT-1 expansion measured *in vivo* following the transfer of varying numbers of OT-1 CTLs into C57/Bl6 mice.

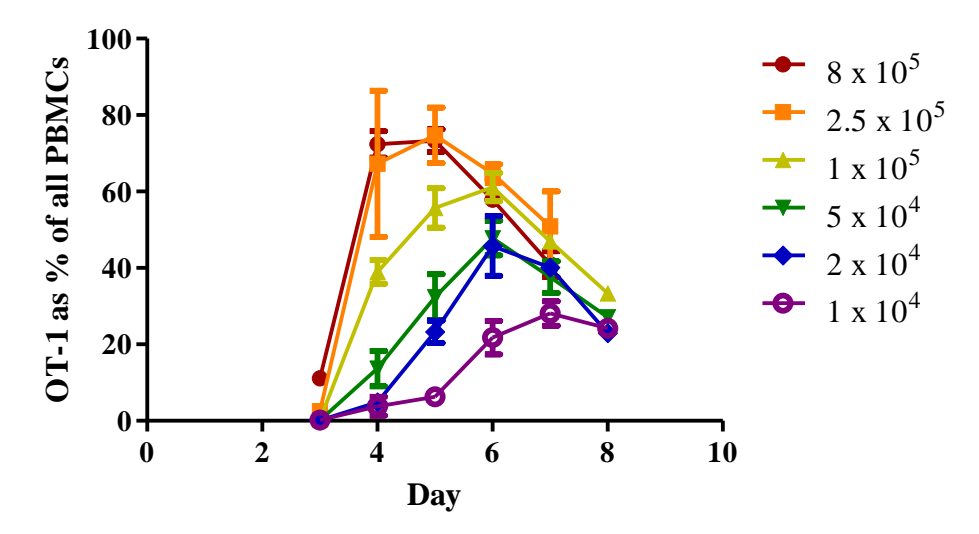


Figure 5.16: Graph of OT-1 expansion in vivo OT-1 CTLs (number shown in legend) were transferred int

OT-1 CTLs (number shown in legend) were transferred into wild type C57BL/6 mice on D -1 and were activated on D 0 by OVA (5 mg) and agonistic anti-murine CD40 mAb (3/23, 0.5 mg). Blood samples were taken from D3 to D8 and the proportion of OT-1 CTLs as a percentage of the total PBMCs determined by using anti-mCD8-APC and K^bSIINFEKL tetramer-PE. Points are the mean of two mice and the error bars represent the range.

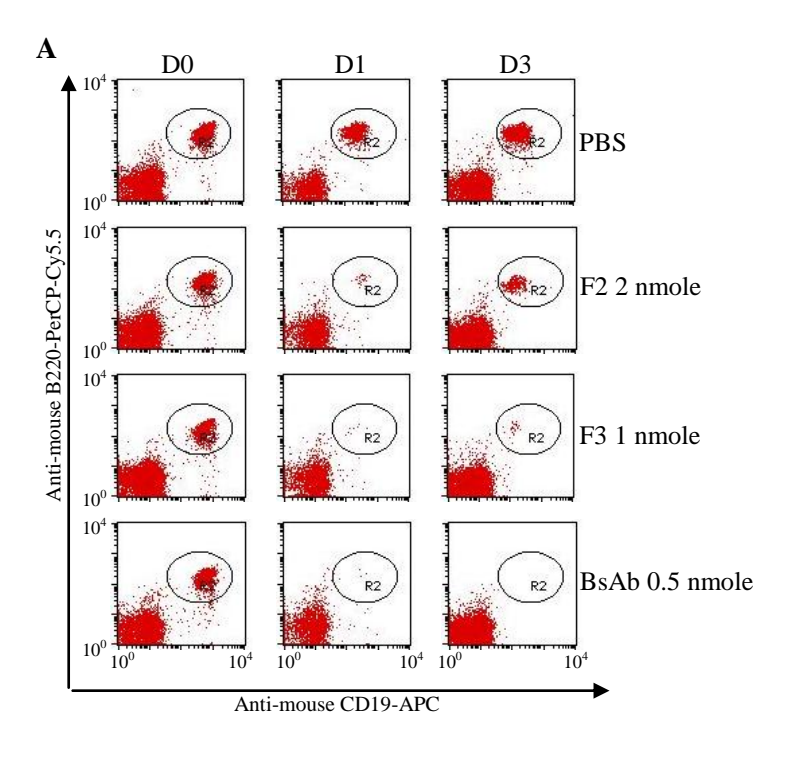
Based on these results, 1 x 10⁵ OT-1 CTLs, were transferred into the hCD20 Tg for the retargeting experiments. This resulted in OT-1 cells expanding to constitute 40-60% of PBMCs. Although there are reports that particularly the elderly can have up to 50% of their CD8⁺ T cell population directed against a single viral Ag (e.g. derived from CMV), ⁴¹⁹ CD8⁺ T cells only usually constitute approximately 20% of PBMCs; thus the pool of specific CTLs being retargeted in these experiments was clearly supra-physiological. However, for initial evaluations of the strategy *in vivo* we wanted to ensure that the availability of appropriately restricted CTLs for retargeting was not a limiting factor.

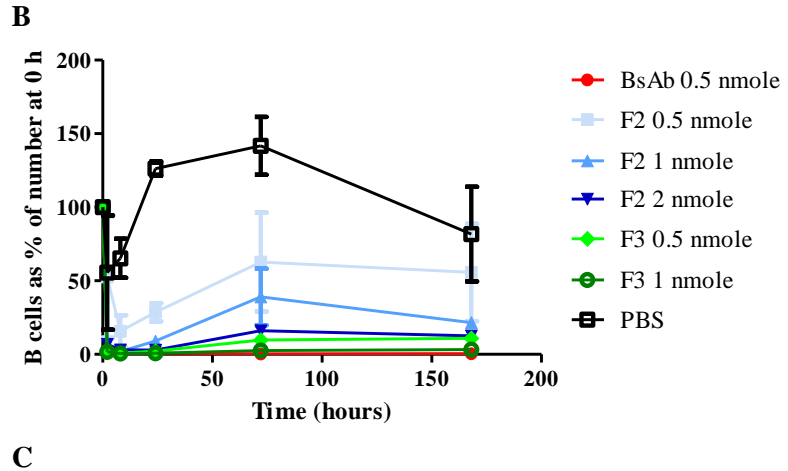
Owing to the clear peak in the OT-1 response it was decided to administer a single dose of retargeting construct rather than repeated smaller doses. Preliminary data (not shown) obtained with 50 μ g (0.5) nmole of the [anti-hCD20 x anti-mCD3] BsAb suggested that this produced a significant depletion of B cells and would be a suitable positive control.

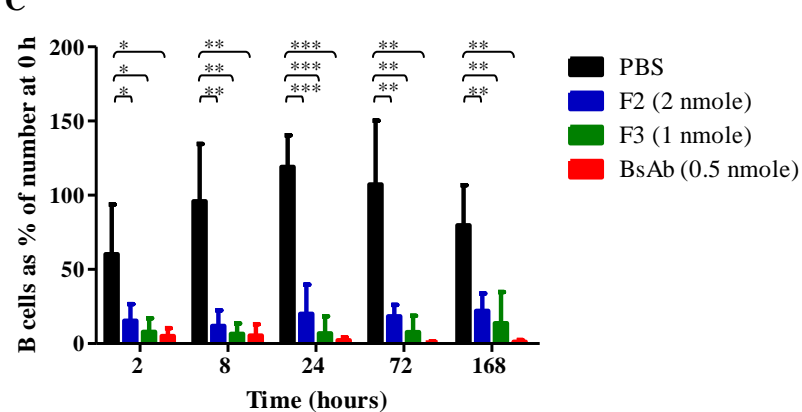
Equivalent molar quantities of F2 and F3 were chosen as a starting point for efficacy evaluation and higher doses were evaluated as availability of the constructs permitted. PBS was injected as a negative control. B cell depletion was determined by measuring absolute numbers of B cells (as described in section 2.4.5.1) rather than B cells as a percentage of PBMCs as the latter will vary independently of the administration of any retargeting construct as a result of the kinetics of the OT-1 response: the significant expansion of OT-1 CTLs observed on D6 i.e. the day of administration of the retargeting construct means B cells as a percentage of PBMCs is relatively low. As the OT-1 CTLs decline, the total number of PBMCs decreases, thus the same number of B cells will constitute a higher percentage of PBMCs.

Figure 5.17 **A** shows FACS plots of peripheral blood labelled with anti-mCD19-APC and anti-mB220-PerCP-Cy5.5 from sequential bleeds from individual animals treated with the different retargeting constructs. This data in conjunction with peripheral blood PBMC counts were used to calculate absolute numbers of B cells which were then plotted as a percentage of the number of B cells at time = 0 h as shown in Figures 5.17 **B** and 5.17 **C**. These results show that the BsAb and both retargeting constructs are able to cause depletion of B cells. Figure 5.17 **B** demonstrates that when equal doses of the constructs are used (0.5 nmole) the order of efficacy is [anti-hCD20 x anti-mCD3] BsAb > F3 > F2 which is what would be predicted from the *in vitro* studies. There appears to be a dose response relationship for both of the retargeting constructs but this could not be investigated fully due to the limited supply of construct. Figure 5.17 **C** shows that the order of efficacy is maintained even when comparing the depletion caused by the highest dose: 0.5 nmole [anti-hCD20 x anti-mCD3] BsAb > 1 nmole F3 > 2 nmole F2.

Peripheral B cell numbers recover to D0 levels by D14 for the F2 and F3 retargeting constructs and by ~D63 for the [anti-hCD20 x anti-mCD3] BsAb (data not shown) suggesting the B cell depletion produced by the BsAb is more profound than that produced by the mSCT-B-containing constructs. It is possible that the B cell depletion seen, particularly with the F2 and F3 retargeting constructs does not represent B cell death, but rather redistribution to the spleen or other tissues. Without doing further experiments to analyse B cell numbers within the peripheral tissues it is not possible to discount this possibility, but it might be expected that if B cells merely underwent a redistribution as a result of the retargeting construct they would have re-equilibrated back into peripheral blood rather quicker than that observed (i.e. before D14) particularly given that preliminary work by B King suggested the half lives of F2 and F3 were in the region of 8-9 h (personal communication).







A. FACS profiles of blood samples labelled with anti-mCD19-APC and anti-mB220-PerCP-Cy5.5; R2 represents B cells. Animals treated with F2 and F3 conjugates and BsAb.

B B cell number (as a percentage of the starting number) over time for each of the different retargeting constructs and doses evaluated. Results are from one experiment (n=2) with mean and range plotted. C. B cells (as a percentage of the starting number) at each time point for the highest dose of each of the retargeting constructs. Each bar is the mean of n=4 (i.e. combined data from two experiments) while error bars represent the standard deviation. An unpaired T test was performed comparing the depletion observed with each of the retargeting constructs with PBS at each of the time points and statistical significance is indicated by *. P values denoted by *s are as follow: * = p < 0.05, ** = p < 0.01, *** = p < 0.001.

Figure 5.17: Retargeting construct-mediated B cell depletion observed in hCD20 Tg mice

To demonstrate that these B cell depletion results were due to the conjugates specifically redirecting OT-1 CTLs against hCD20, the experiments were repeated with wild type mice adoptively transferred with OT-1 CTLs (i.e. no hCD20 on target B cells), and in hCD20 Tg mice that did not receive OT-1 CTLs (i.e. no specific effector). The results are shown in Figure 5.18 and confirm that both hCD20 Tg targets (**A**) and specific OT-1 effectors (**B**) are necessary for B-cell depletion with the F2 and F3 conjugates.

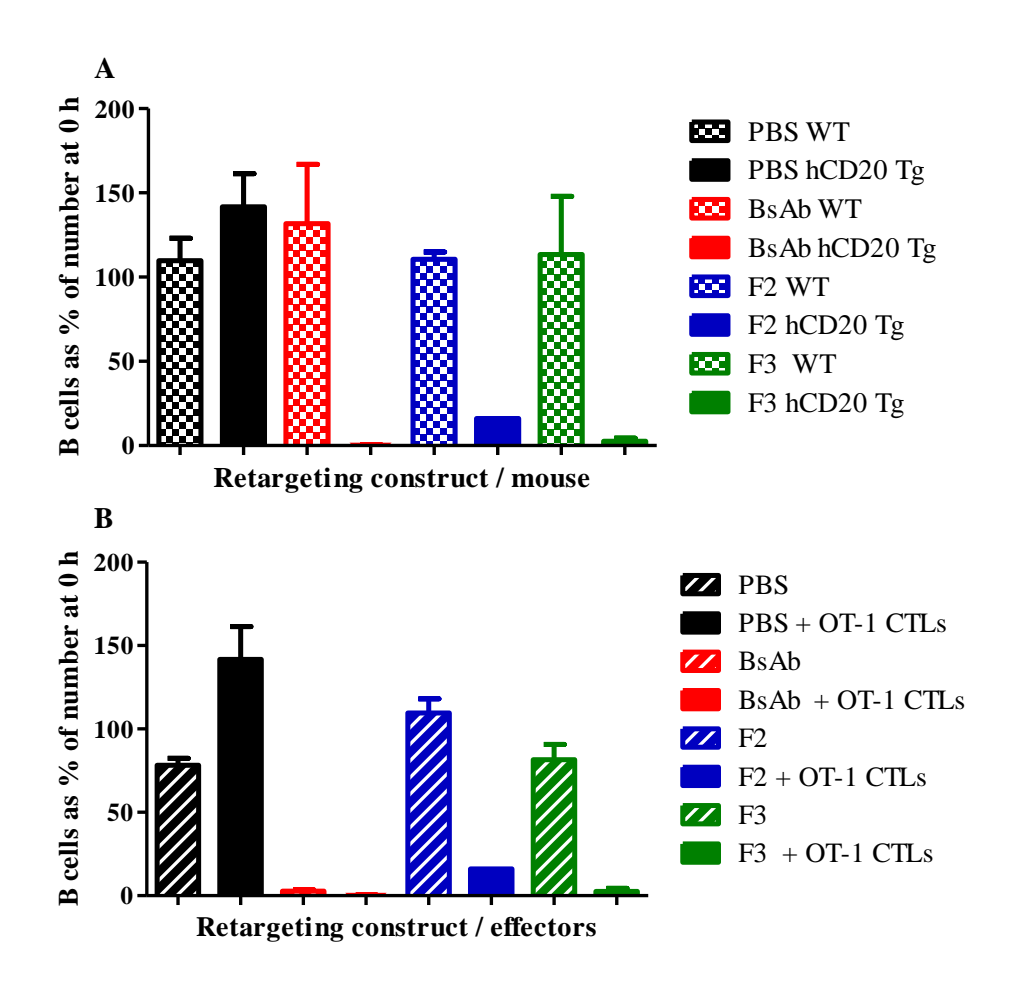


Figure 5.18: B cell depletion observed by retargeting constructs in the absence of hCD20 on target cells or OT-1 effector CTLs

A B cell depletion (D3) in C57BL/6 wild type mice which lack hCD20 on the surface of their B cells (checked bars). For comparison the solid bars of matching colour represent peripheral blood B cell depletion observed in hCD20 Tg mice at 72 h after treatment with the same dose of each retargeting construct. B shows peripheral blood B cell depletion seen at 72 h (D3) in hCD20 Tg mice which have not been adoptively transferred with OT-1 CTLs (striped bars). For comparison the solid bars of matching colour represent peripheral blood B cell depletion observed in hCD20 Tg mice at 72 h which have been adoptively transferred with OT-1 CTLs after treatment with the same dose of each retargeting construct. In both bar charts the bars represent the mean of n=2 and the error bars indicate the range.

Similarly hCD20 must be present on the surface of the B cells in order for [anti-hCD20 x anti-mCD3] BsAb to mediate depletion (**A**) although the BsAb does not require OT-1 CTL to effect killing consistent with its ability to recruit from the total CD3 population.

Given that the F3 retargeting molecule contains two anti-hCD20 Fab' fragments, it could be argued that its superior B cell depletion compared to the F2 molecule are due to it effectively containing a F(ab')₂ which may have some intrinsic cytotoxic activity of its own. There are reports that some anti-hCD20 F(ab')₂ (e.g. tositumomab (B1) and GA101) are able to produce direct B cell apoptosis via the activation of appropriate intracellular signalling pathways. ^{484,485} The results shown in Figure 5.12 suggest that high concentrations of anti-hCD20 F(ab')₂ acts as a blocking agent rather than an apoptosis inducer in cytotoxicity assays. This was confirmed in vivo (Fig 5.19) where we showed that anti-hCD20 F(ab')₂ was unable to mediate B-cell depletion in contrast to parental anti-hCD20 IgG.

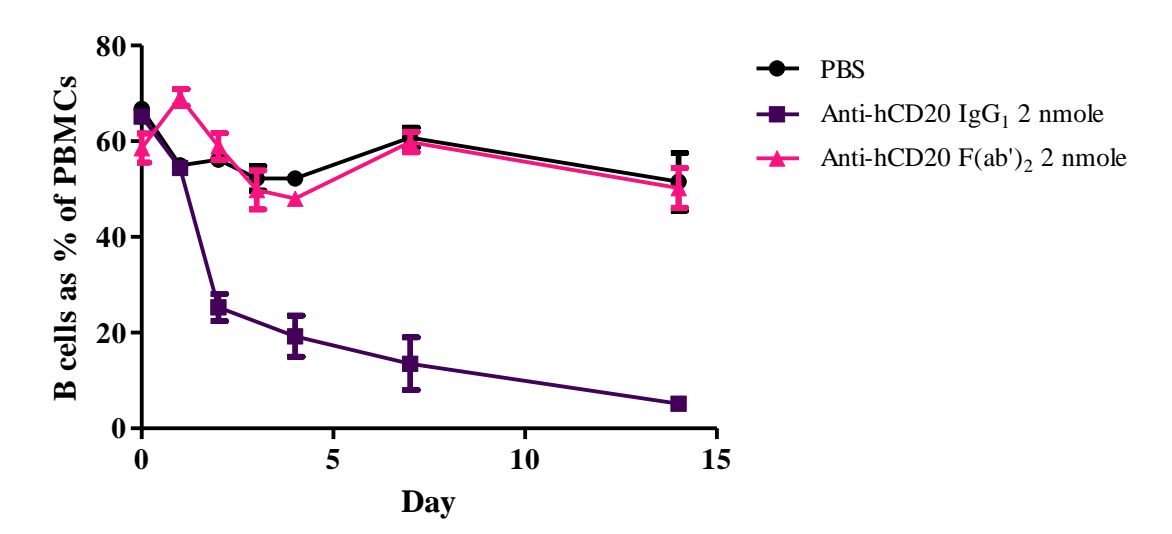


Figure 5.19: B cell depletion produced with single doses of parental anti-hCD20 IgG and its derivative $F(ab')_2$

hCD20 Tg mice received a single intravenous injection into the tail vein (as indicated in the legend) of either the parental anti-hCD20 IgG (with its original isotype IgG_1) or its derivative $F(ab')_2$ (produced by pepsin digestion), diluted in 200 μ l PBS. As a negative control 200 μ l of the diluent was administered via the same route. Mice were then bled from the tail vein at regular intervals and the percentage of B cells amongst the peripheral blood PBMCs determined by FACS using anti-mouse CD19-APC and anti-mouse B220-PerCP-Cy5.5 antibodies. For each experimental group n=2. It should be noted that more impressive depletion is seen with this anti-hCD20 IgG when the isotype is switched to mouse IgG_{2a} , but insufficient quantities of this isotype of the Ab were available at the time these experiments were conducted.

5.6.2 Measurement of cytokine release accompanying B cell depletion

So far our data demonstrate that the mSCT-B x anti-hCD20 Fab' conjugates are able to retarget non-cognate CTLs to eliminate targets both *in vitro* and *in vivo*, but their efficacy does not match that of the BsAb. However, as discussed in the introduction, bispecific antibodies and their derivatives have been undergoing clinical evaluation for more than two decades but excessive toxicity has rather limited their clinical utility. Previously the indiscriminate polyclonal activation of all subsets of T cells has meant the dose limiting toxicity was reached before a therapeutic effect was observed resulting in disappointing clinical responses. However, more recently the enhanced efficacy of the BiTE class of

bispecific antibodies⁴⁸⁶ has meant some of the not insignificant toxicity is more tolerable and has re-excited interest in this field.

The toxicity of bispecific antibodies is related to cytokine release and significant inflammatory cytokine release has been demonstrated, at least in the early stages, during treatment with BiTE antibodies. 487,488 It can be postulated that the cytokine release (and therefore toxicity) associated with the indiscriminate activation of any and potentially every T cell (with anti-CD3-containing retargeting constructs) is likely to be higher than that observed when retargeting CTLs alone, particularly of those cytokines associated with the activation of CD4⁺ T cells. If the pMHC-containing retargeting constructs are associated with reduced cytokine release then further studies to optimise the structure and production process of the conjugates could be worthwhile.

Cytokine levels were therefore measured in serum samples from the mice that received F3 retargeting constructs (1 nmole) and [anti-hCD20 x anti-mCD3] BsAb (0.5 nmole) in the B-cell depletion experiments shown in Figure 5.17 using the Meso Scale Discovery Mouse TH1/TH2 9-plex Assay (IL-2, IFN γ , TNF α , IL-1 β , IL-12 (total), IL-4, IL-5, IL-10 and KC). Figure 5.20 shows the change in the level of each of the cytokines from a single B cell depletion assay while Figure 5.21 shows the peak response (2 h) of each cytokine from both B cell depletion assays: as the data from 2 experiments was combined for this analysis, values are expressed as fold increase rather than absolute concentration.

Figure 5.20 shows that the peak cytokine concentration for both retargeting constructs (F3 and [anti-hCD20 x anti-mCD3] BsAb) for all cytokines is 2 h and that by 24 h the cytokine levels have returned to baseline. With the exception of IL-1β and IL-12, in this individual experiment, the administration of BsAb resulted in a higher cytokine peak concentration than the F3 construct. Together Figures 5.20 & 5.21 suggest that at least part of the starting hypothesis is largely confirmed by the data. Cytokines produced predominantly by CD4⁺ T cells i.e. IL-2, IL-4, IL-5 and IL-10 are present in the serum at higher concentrations after administration of [anti-hCD20 x anti-mCD3] BsAb compared to the F3 construct: This correlates with the fact that the BsAb is able to activate helper T cells while the F3 construct can activate only OT-1 CTLs directly. A small increase in these CD4⁺ T cell-produced cytokines is seen after administration of the F3 conjugate as cytokines produced by the OT-1 CTLs themselves (e.g. IL-2, IFNγ and TNFα) feed back to activate macrophages and helper T cells causing them to release their characteristic cytokines.

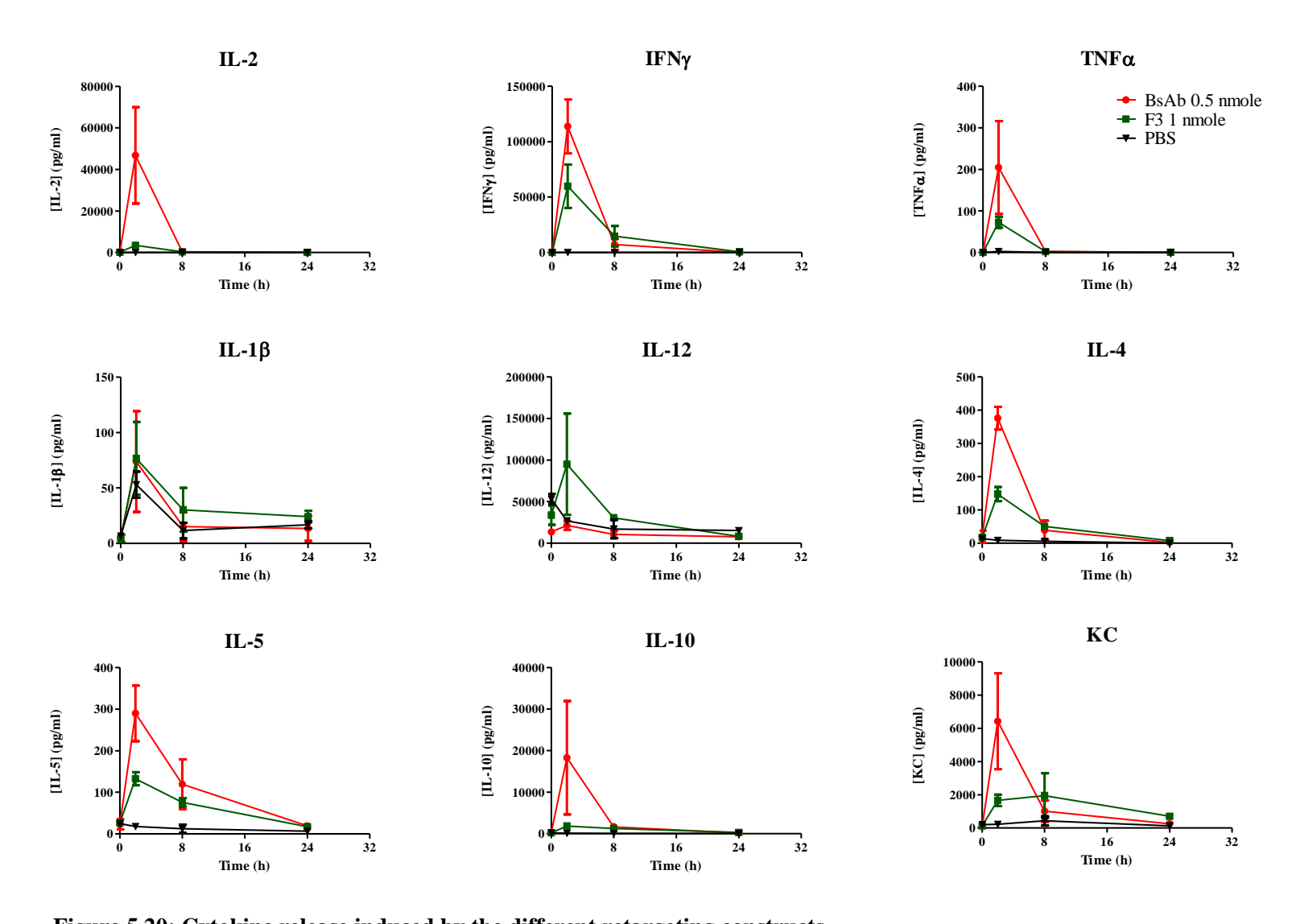


Figure 5.20: Cytokine release induced by the different retargeting constructs

Concentration of cytokines in mice from the B cell depletion experiment shown in Figure 5.17 B was measured after administration of the various retargeting constructs using the Meso Scale Discovery Mouse TH1/TH2 9-plex Assay. Each serum sample was analysed in duplicate and the data plotted shows the mean and range for n=2 mice for each retargeting construct.

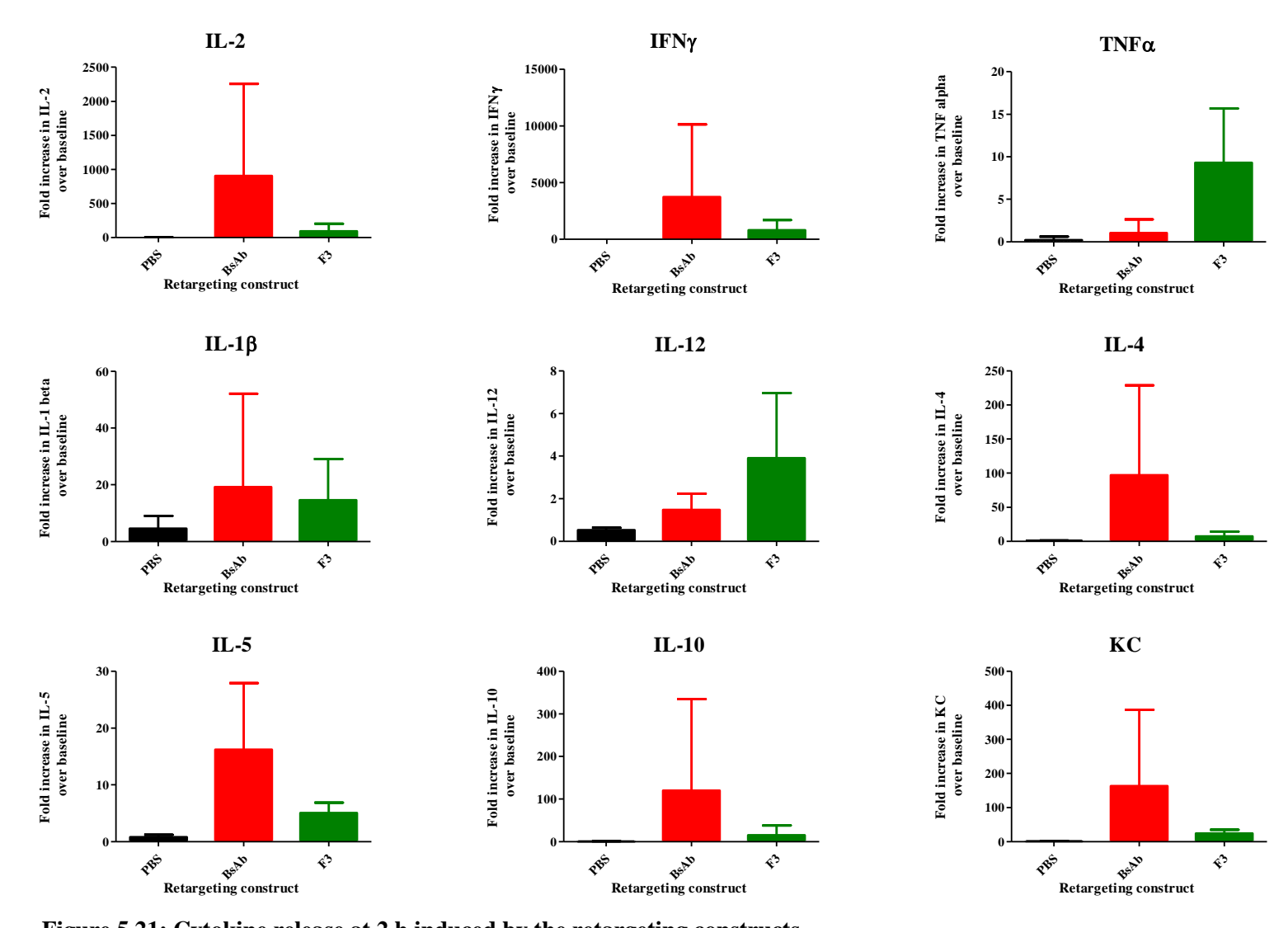


Figure 5.21: Cytokine release at 2 h induced by the retargeting constructs

Data plotted shows fold increase of each cytokine over baseline (t=0 h) at 2 h (maximal cytokine response) measured using the Meso Scale Discovery Mouse TH1/TH2

9-plex Assay. Each serum sample was analysed in duplicate and each bar is the mean of n=4 and error bars represent the SD. Data from two separate experiments was combined so 'fold increase' is plotted rather than absolute concentration.

IFN γ can be produced by both cytotoxic and helper T cells and therefore it is not unexpected that the [anti-hCD20 x anti-mCD3] BsAb induces more production that the F3 retargeting construct. The TNF α result is however rather unexpected; this cytokine can be produced by both CD4⁺ and CD8⁺ T cells in addition to cells of the innate immune system (such as macrophages) but, at least in humans, helper T cell production would usually far exceed cytotoxic T cell production. However, examination of the raw data suggests the increased TNF α production seen with the F3 construct is an artefact of plotting 'fold increase' increase over time zero.

The increased production of both IFN γ and TNF α in mice treated with the BsAb explains why these mice have higher levels of the chemokine KC circulating as both these cytokines can induce production of this chemokine. IL-1 β production appears fairly similar after administration of both retargeting constructs reflecting the fact that neither retargeting strategy should preferentially activate the inflammasome.

The one cytokine which does appear to be produced in greater quantity after administration of the F3 retargeting construct is IL-12. IL-12 is a 'type 1' cytokine associated with a CTL response which is produced by DCs in response to TLR ligation and inflammatory cytokines such as IFN γ and TNF α . In turn, IL-12 induces the production of these cytokines from cytotoxic T cells and NK cells and enhances the proliferation of CTLs. Given that [anti-hCD20 x anti-mCD3] BsAb appears to induce more IFN γ and TNF α than the F3 construct, it might be expected that it would engender more IL-12 production than the pMHC-containing construct. However, IL-12 production is negatively regulated by IL-4 and IL-10, ⁴⁹² both of which are produced in significant quantities when CD4⁺ T cells are activated via [anti-hCD20 x anti-mCD3] BsAb. These cytokines are therefore inhibiting DC production of IL-12 after administration of the BsAb whereas the relative absence of these type 2 cytokines after administration of the F3 conjugate allows IFN γ and TNF α -induced unopposed IL-12 production by DCs.

It therefore appears that with the exception IL-12, the F3 retargeting construct is associated with generally less cytokine release compared to the [anti-hCD20 x anti-mCD3] BsAb. Given that clinical trials of IL-2, IL-4, ⁴⁹³ IFN γ^{494} and TNF α^{495} have all been associated with toxicity, this should equate to less toxicity associated with the pMHC-retargeting construct approach compared with anti-CD3 containing constructs. Equating any given level of cytokine release to intolerable toxicity, particularly in a mouse, is not easy. Although in humans global assessments of toxicity can be performed using quality of life questionnaires, in a mouse it is

necessary to rely on behavioural observations. Although none of the mice given any of the retargeting constructs in the B cell depletion assays were cowering in the corner of the cage or appeared acutely unwell, more subtle markers of toxicity may have been overlooked. There are validated murine behavioural experiments such as assessing burrowing which can be used to evaluate more subtle toxicity in greater detail, 496 and if this strategy is pursued further these could be employed to try and more comprehensively assess toxicity.

The cytokine data obtained for the F3 construct is therefore promising as it suggests the retargeting strategy may be associated with less toxicity than that associated with anti-CD3-containing bispecific antibodies and their derivatives. It is therefore worthwhile to consider how the pMHC retargeting constructs could be optimised to try and improve both their production and structural integrity.

Several steps in the synthesis of mSCT-B x anti-hCD20 Fab' conjugates render the process intrinsically inefficient: The efficiency of the refolding strategy used is only 3-5% meaning the majority of the bacterially expressed mSCT-B polypeptide is misfolded, subsequently aggregates and is therefore unsuitable for conjugation. The efficiency of the conjugation reaction is at best 15-20% meaning that much of the correctly refolded mSCT-B polypeptide is wasted during the reaction because as yet there is no recovery step for unconjugated material.

These inefficiencies mean there was a very limited supply of the mSCT-B x anti-hCD20 Fab' constructs available for functional evaluation which limited the scope of the experiments which could be performed. In addition owing to doubts about the stability of refolded mSCT-B upon storage for any length of time and the requirement for very large volumes of refolding buffer which subsequently had to be concentrated the constructs could only be produced in relatively small quantities. As each individual batch of mSCT-B had to be tested for its ability to form tetramers which could stain OT-1 CTLs and each batch of F2 and F3 conjugates had to be tested as a minimum for its ability to bind to and be detected on the surface of hCD20⁺ cells, and retarget OT-1 CTLs to lyse hCD20⁺ cells in a cytotoxicity assay, this further limited the availability of retargeting conjugates for more in depth *in vitro* and *in vivo* evaluation

The conjugation reaction requires relatively harsh conditions such as exposure to reducing agents, organic solvents and column separations which can potentially alter the tertiary structure of the refolded proteins. This means a percentage of the conjugates produced may not actually possess the desired conformation and therefore not be functionally active. From our data it is impossible to estimate what percentage of the conjugates produced had the

required functional integrity but it is likely that it is considerably less than 100%; therefore in all of the experiments evaluating the functional integrity of the conjugates it is likely that the nanodrop determined concentration is an overestimation of the functionally active conjugate used. If this is the case the performance of the pMHC-containing constructs may not be so inferior to the [anti-hCD20 x anti-mCD3] BsAb as the results suggest.

This may explain why rather higher concentrations of the conjugates than perhaps would be expected are necessary in order to see binding saturation when they are used to stain hCD20⁺ cells in section 5.5. Another variable when considering the issue of what percentage of the retargeting construct is functionally active is the heterogeneity of the conjugation product suggested both theoretically and by the SDS-PAGE gel shown in Figure 5.7. It is possible that the functional abilities of the retargeting conjugates is influenced by the exact location of the lysine(s) to which the SMCC crosslinker joins and hence location of the anti-hCD20 Fab'(s) in relation to the peptide presented by mSCT-B.

It should be possible to use a Biacore to determine what percentage of each of the conjugate species have conformationally correct anti-hCD20 Fab' or mSCT-B moieties although it may be harder to devise an assay which assesses both moieties simultaneously on a single molecule. Although conformational integrity of both moieties within the conjugates could be assessed using a sandwich ELISA (e.g. coating with anti-mouse Fab' IgG and detecting with 25D1 IgG) at present there is no 'standard' molecule known to be 100% conformationally correct against which the conjugates could be compared.

The data presented in this chapter shows that we have produced a biologically active conjugate which is able to retarget non-cognate CTLs against cells bearing a tumour Ag. However, the inefficiency and labour intensiveness of the production process combined with the apparent variability in the percentage of the construct which is functionally active mean a number of refinements to both the production process and possibly the structure of the molecule are likely to be necessary in order to progress this strategy. Chapter 6 shows one group of modifications to the retargeting molecule which can potentially overcome a number of these issues.

Chapter 6: Results - 'Dock and Lock' Construct

6.1 Introduction

As discussed in chapter 5, modifications are required to both the structure and method of conjugation of the retargeting constructs in order that larger quantities of a more consistent product can be produced, allowing more detailed functional assessments. We were provided with a small quantity of a retargeting construct (courtesy of Immuomedics via Phil Savage) consisting of anti-hCD20 Fab and mSCT moieties whose method of production and conjugation could potentially solve some of the problems associated with the F2 and F3 conjugates: [mSCT x (anti-hCD20 Fab)₂] DnL consists of two anti-hCD20 Fab moieties conjugated to murine *SIINFEKL*-β₂microglobulin-K^b (mSCT) using the dock and lock platform (DnL).⁴³⁴ This technology exploits the naturally occurring specific protein:protein interaction between the dimerisation docking domain (DDD) in protein kinase A and the anchoring domain (AD) in a reactive A-kinase anchoring protein.

Figure 6.1 demonstrates that polypeptides engineered to contain a DDD will naturally dimerise and create a docking site for a polypeptide containing the AD domain: Therefore if anti-hCD20 Fab is engineered to express a DDD at its carboxy termini while mSCT is engineered to express an AD at its carboxy terminus, upon incubation they should naturally combine to form a trimeric protein with a stoichiometry of Fab:mSCT of 2:1 (i.e. similar to F3). In order to stabilise the non-covalent interactions between DDD₂:AD, cysteine residues can be inserted at the amino termini of the DDD and at both the amino and carboxy termini of the AD meaning, upon reduction, disulfide bonds are formed between the three polypeptides.

In addition to using a different method to couple the Fab and mSCT moieties to one another compared to our conjugates, [mSCT x (anti-hCD20 Fab)₂] DnL contains murine *SIINFEKL*- β_2 microglobulin- K^b produced using retroviral transduction of mammalian cells rather than transformed bacterial cells. As mammalian cells are able to fold proteins themselves and any misfolded protein should not be able to exit the ER, theoretically only correctly folded mSCT protein should be secreted from the cells abrogating the need for a laborious and inefficient refolding process. This, in turn, should reduce the probability that misfolded inactive protein is conjugated to anti-hCD20 Fab, therefore increasing the proportion of the conjugate which is biologically active.

The sequence of mSCT contained within [mSCT x (anti-hCD20 Fab)₂] DnL was similar to that of mSCT-B (found in F2 & F3 conjugates) other than the biotin AviTag being replaced with the AD of an A kinase anchor protein. The Fab however was derived from a different parental Ab: veltuzumab⁴⁹⁷ (a humanised anti-hCD20 IgG available in-house at Immunomedics).

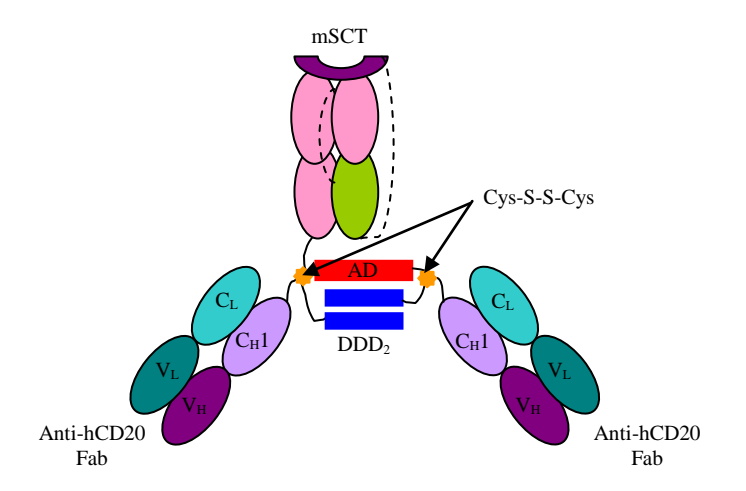


Figure 6.1: Structure of [mSCT x (anti-hCD20 Fab)₂] DnL

Two identical anti-hCD20 Fab moieties engineered to contain a dimerisation docking domain (DDD) should form a non-covalent interaction with an mSCT moiety engineered to contain an anchoring domain (AD). The locations of the interchain disulfide bonds are indicated.

6.2 Evaluation of [mSCT x (anti-hCD20 Fab)₂] DnL

6.2.1 Staining hCD20⁺ cells

As with the F2 & F3 retargeting constructs, in order to determine whether the DnL construct was conformationally intact with two types of functional moiety (i.e. anti-hCD20 Fab and mSCT components) it was incubated with hCD20⁺ cells and its presence on the cell surface detected with 25D1. Figure 6.2 demonstrates that [mSCT x (anti-hCD20 Fab)₂] DnL can be detected on the surface of hCD20⁺ cells by the K^bSIINFEKL-specific Ab suggesting that at least some of the construct contains two functional moieties. However, although maximal binding is seen at similar concentrations to the F3 construct, the MFI detected for any given concentration is significantly lower than that seen for F3 or even F2. Similar results were observed when hCD20⁺ Raji cells were used (data not shown).

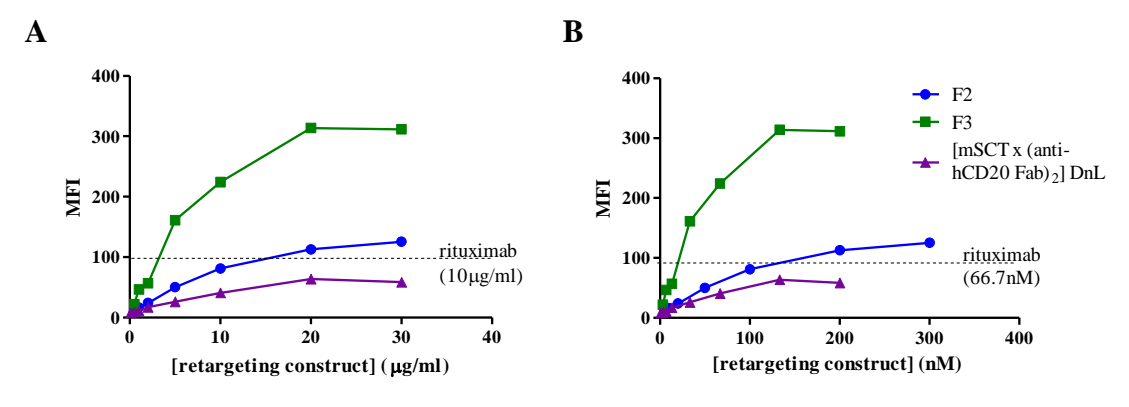


Figure 6.2: Binding of [mSCT x (anti-hCD20 Fab)₂] DnL construct to Daudi cells The graphs show binding of [mSCT x (anti-hCD20 Fab)₂] DnL (purple), F2 (blue) and F3(green) conjugates to Daudi cells with the concentration of the construct expressed in terms of μ g/ml (A) and molarity (B). The binding of the constructs was detected with 25D1-FITC (10 μ g/ml). For comparison, the MFI observed when Daudi cells were labelled with rituximab-FITC (10 μ g/ml) is shown.

One explanation for this poorer staining is differences in the intrinsic affinities of the hCD20 moieties contained within the constructs: Although there are no direct comparisons between veltuzumab and AT80 within the literature to determine their relative affinities, studies have suggested that veltuzumab binds to hCD20 with similar affinity to rituximab, 498 but has a lower off rate meaning differences in anti-hCD20 Fab affinity are unlikely to account for much of the difference in staining observed. Alternatively it could be that the structure assumed by the DnL molecule once mSCT has been conjugated to the two Fab moieties somehow sterically hinders the interaction between the Fab fragments and hCD20 on the surface of the cell or mSCT and soluble 25D1. As yet there is no information on the tertiary structure of [mSCT x (anti-hCD20 Fab)₂] DnL although work using a DnL construct consisting of two veltuzumab moieties coupled to an anti-histamine-succinyl-glycine (HSG) Fab showed it was able to more efficiently target a ⁹⁰Y hapten-peptide (⁹⁰Y-DOTA-HSG) to eliminate the hCD20⁺ B cell lymphoma cell line RAMOS in nude mice than whole veltuzumab IgG directly conjugated to 90 Y. 499 Although in this construct the third arm was a Fab rather than MHC class I, given they are both members of the immunoglobulin superfamily, it would seem unlikely that the presence of mSCT is able to significantly disrupt the interaction between the veltuzumab Fabs and hCD20.

A third explanation is that the conformational integrity of one or more of the components of the DnL molecule is inferior to that seen in the F2 & F3 constructs. As discussed previously, producing mSCT with the correct conformation has been extremely problematic although it had been hoped that the use of retroviral transduction of mammalian cells would avoid the difficulties associated with refolding protein. As we received the DnL construct as a conjugated bispecific molecule from Immunomedics we were not party to any initial testing it went through to ensure conformational integrity of the mSCT moiety. The construct is produced in two separate cells lines (one secretes the Fab fragment while the other produces the mSCT) and purified products are then mixed to enable the formation of non-covalent interactions between the DDD₂ and AD domains before being reduced to produce permanent disulfide bonds between the three chains. ⁴³⁴ It is possible that the purification and reduction process alters the tertiary structure of the refolded protein, or alternatively the mammalian cells may be partially misfolding the mSCT protein.

If the protein is misfolded or has a structure such that it cannot interact efficiently with either of its target cell populations (e.g. tumour cells or specific CTLs) then the poorer staining in this assay will translate into reduced killing in a cytotoxicity assay. If the poor staining is a function of this assay e.g. the structure of the DnL molecule limits access of 25D1 but does

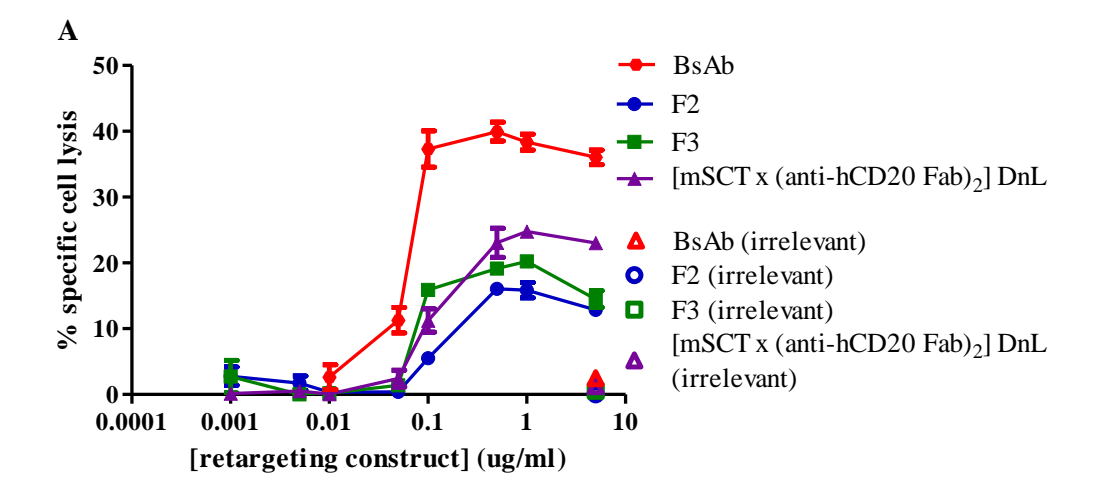
not impede interaction with the cognate TCR then the results of this FACS assay may not be reflected in its cytotoxic potential.

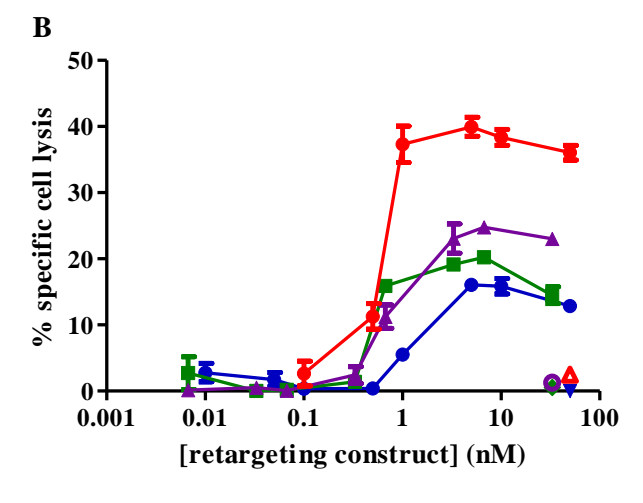
6.2.2 In vitro cytotoxicity assay

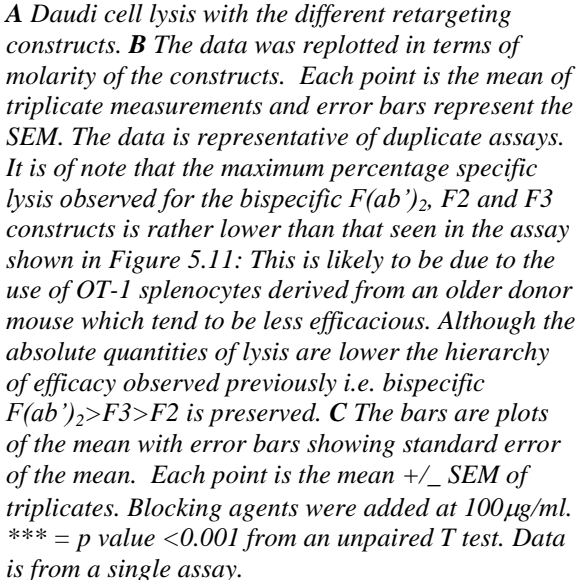
Having established that the DnL retargeting construct had some ability to bind to hCD20⁺ cells and be recognised by the K^bSIINFEKL specific Ab 25D1, it was then used to retarget non-cognate CTLs in a cytotoxicity assay. As with the F2 & F3 constructs, a 4 h ⁵¹Cr assay in which OT-1 CTLs were redirected against Daudi cells was used. Methodology and controls were as before and anti-hCD20 F(ab')₂ and 25D1 IgG were used as blocking agents to ensure any observed lysis was a function of interactions involving hCD20 on the Daudi cells and the OT-1 TCR. Figure 6.3 demonstrates the specific lysis mediated by the DnL construct and the results of the blocking experiments.

The graphs in figure 6.3 **A** & **B** demonstrate that [mSCT x (anti-hCD20 Fab)₂] DnL is able to retarget OT-1 CTLs to lyse Daudi cells. The lysis observed is at least equivalent to that seen with the F3 construct for any equivalent weight or molarity. The DnL construct appears more efficient at lysing Daudi cells than the F2 construct which is expected given that the DnL construct, like the F3 construct, has two anti-hCD20 moieties and therefore is likely to have a higher avidity for the target cells. As with the F3 conjugate, the DnL construct appears inferior to the control [anti-hCD20 x anti-mCD3] BsAb, presumably due to its inability to retarget *all* T cells. **C** demonstrates that blocking either hCD20 Ag sites on the target cells or mSCT-B on [mSCT x (anti-hCD20 Fab)₂] DnL with 25D1 IgG prevents most of the specific lysis showing that killing is specific.

Although not statistically significant, it appears that the DnL construct may be slightly more efficacious than the F3 conjugate which has an equivalent stoichiometry. This functional data is perhaps unexpected given the results of the indirect FACS assay shown in Figure 6.2: If the DnL was poorly folded it would not be expected to mediate target cell lysis while if the FACS results are an artefact of steric hindrance preventing access of 25D1 IgG it would not be expected that this could block lysis as shown in Figure 6.3 C. One explanation that could reconcile these differences is that amongst the F3 (and F2) constructs is a medium population of molecules with moderately well-folded mSCT-B which can be recognised by 25D1 IgG and form transient interactions with OT-1 CTL TCRs. This allows these molecules to be detected in a reasonable quantity on the surface of hCD20⁺ cells during the indirect FACS assay and retarget OT-1 CTLs, perhaps in a rather 'hit and miss' fashion owing to the less than optimal affinity of the mSCT-B:OT-1 CTL TCR interaction. In contrast, amongst the DnL construct there is a much smaller population of molecules with very well-folded mSCT which has assumed a more 'correct' conformation than that found in the F2 and F3 constructs.







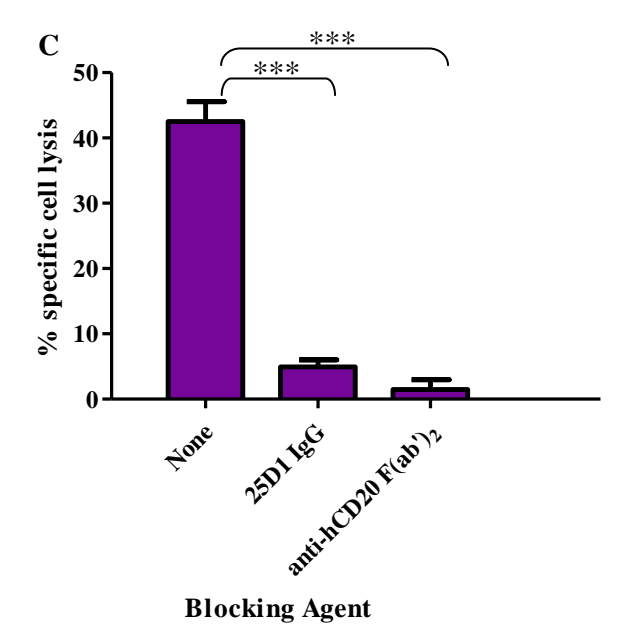


Figure 6.3: [mSCT x (anti-hCD20 Fab)₂] DnL mediated lysis of hCD20⁺ target cells by OT-1 CTLs.

These 'correctly' folded mSCT can be detected on the surface of hCD20⁺ cells using the indirect FACS assay, but as they are small in number the intensity of staining is low.

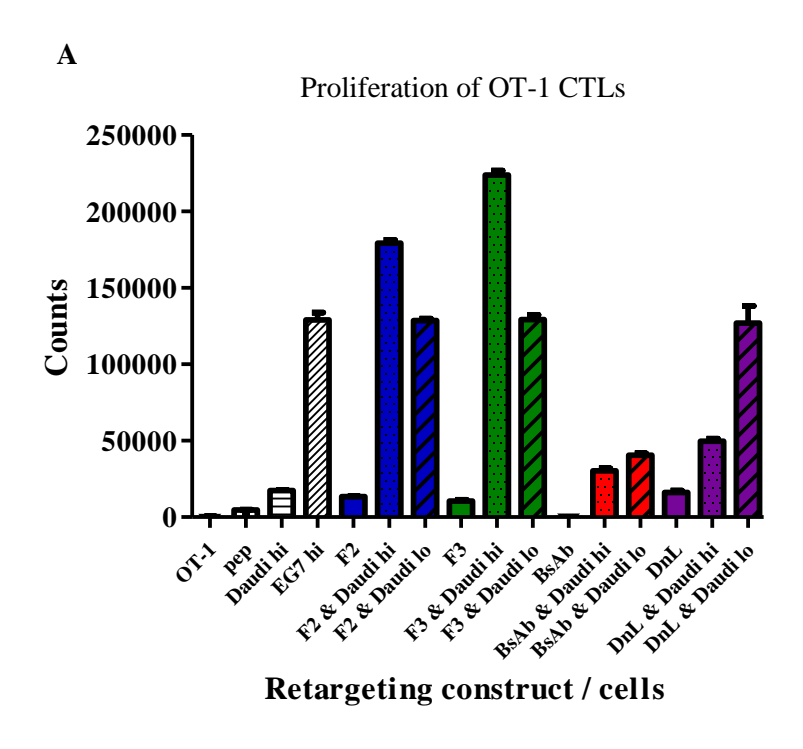
However, the improved conformation of the mSCT moiety in these DnL molecules means the constructs are able to form higher affinity interactions with the OT-1 CTL TCR resulting in an increased chance of activating and retargeting the cell. Therefore a smaller quantity of a very efficacious molecule is able to effect more killing than a larger quantity of less active construct. Interestingly when a sample of the DnL construct was subject to analytical HPLC (data not shown) the peak obtained was much broader than that observed for either the F2 or F3 conjugates suggesting it is less pure and perhaps more heterogeneous than expected.

In order to test this hypothesis it would be necessary to evaluate the structure of mSCT-B within both types of retargeting molecule in some detail. Circular dichroism could be used to assess secondary structure while higher levels of structure could be evaluated with X-ray crystallography or NMR, although the latter has size limitations. The most informative assays would be functional assessments and it may be possible to use a BIAcore based assay to assess the strength of interaction between mSCT and either 25D1 IgG or the OT-1 CTL TCR⁵⁰⁰ which would give the most accurate assessment of the conformational integrity of the mSCT moiety. The BIAcore could also be used to determine the 'functional' concentration (using competition assays) of the mSCT moiety which would allow an accurate calculation of the percentage of the protein which is biologically active.

6.2.3 In vitro proliferation assays

As discussed previously, the ability of a construct to cause proliferation of the target CTL population is a desirable attribute of any retargeting conjugate as it removes the need for prior vaccination or adoptive transfer. A thymidine incorporation assay was used to investigate whether the DnL retargeting construct possessed this ability with methodology and controls as before. Figure 6.4 **A** demonstrates that the DnL construct is able to induce OT-1 CTLs to proliferate in the presence of hCD20⁺ cells. In the absence of hCD20⁺ cells the construct is able to produce only low level OT-1 CTL proliferation (equivalent to that seen with the F2 and F3 constructs) which given the lack of similar proliferation with WT C57BL/6 CD8⁺ cells is likely to be due to aggregation of the construct producing mSCT multimers⁴⁸³ rather than a contaminating mitogen.

More proliferation was seen with 10⁴ rather than 10⁵ Daudi cells per well which is counterintuitive given that the more hCD20⁺ cells present the more mSCT can be immobilised on the cell surface and presented to the OT-1 TCR, the interaction critical for OT-1 CTL proliferation. As discussed previously however, the data shown represents only a single concentration of retargeting construct at a single time point: It is not possible to predict



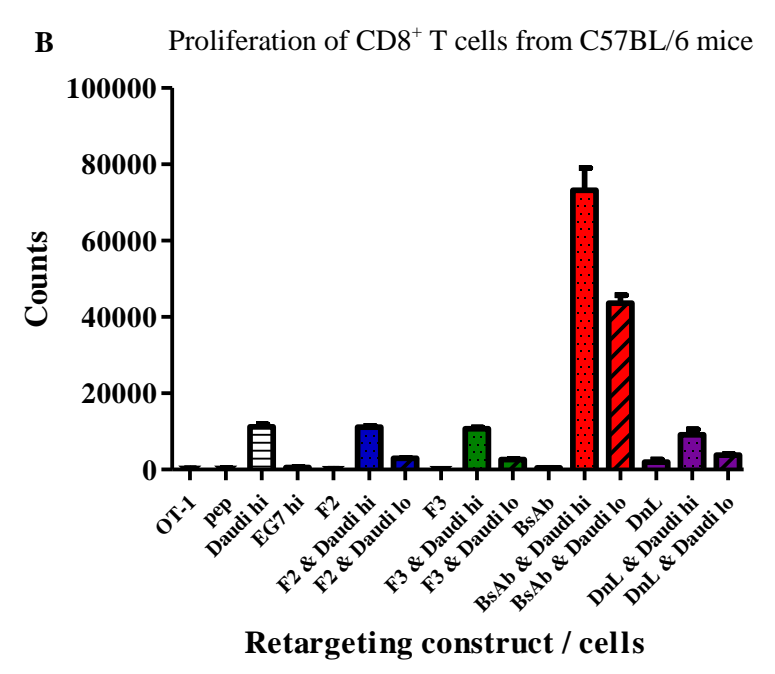


Figure 6.4: 3 H-thymidine incorporation by OT-1 / WT C57BL/6 T cells induced by [mSCT x (anti-hCD20 Fab)₂] DnL

A OT-1 CTLs (5 x 10^4) were incubated in the presence of retargeting constructs (1 μ g/ml) and irradiated feeder cells at 1 x 10^5 (hi) or 1 x 10^4 (lo) per well for 72 h, with 1 μ Ci 3 H-thymidine added for the final 18 h of the assay. **B** As **A** but with OT-1 CTLs replaced with CD8 $^+$ T cells from WT C57BL/6 mice. Results show the mean of triplicates +/- SEM. The data in **A** is representative of two experiments and that in **B** is from one experiment; however correlating data for this experiment was observed in CFSE dilution assays (data not shown).

where on the expansion/contraction curve the single data point is meaning it is possible that in the presence of higher numbers of Daudi cells the DnL construct has already caused maximal proliferation of the OT-1 CTLs present and the apparent reduced proliferation of OT-1 CTLS is due to over stimulation resulting in early apoptosis,⁵⁰¹ or starvation due to depletion of nutrients from the medium. For this reason it is also not possible to make comparisons between the proliferation seen with the different retargeting constructs.

The initial experiments using [mSCT x (anti-hCD20 Fab)₂] DnL have demonstrated that the molecule has some potential as a retargeting construct although a more thorough evaluation of the molecule is required if it is to be developed further as a possible viable therapy. It is necessary to look in detail at the conformation of ready-folded mSCT produced by retrovirally transduced mammalian cells both before and after the conjugation process. The construct also needs to be evaluated *in vivo* and as an initial investigation it could be used in the hCD20 Tg mouse model adoptively transferred with OT-1 CTLs (section 5.6.1) and accompanying cytokine release could be measured (section 5.6.2).

As with the F2 and F3 retargeting constructs, the DnL construct's natural competitors are also anti-CD3-containing bispecific antibodies: If DnL-mediated B cell elimination is accompanied by significant cytokine release there seems little advantage in pursuing this retargeting strategy. However if retargeting CTLs using a DnL pMHC-containing construct results in substantially reduced levels of cytokine release it has an advantage over the more easily produced anti-CD3-containing bispecific antibodies and therefore warrants further investigation. As discussed in the introduction to this chapter, the potential advantage of the DnL construct over the F2 and F3 constructs is its simpler, and theoretically more efficient, method of production in mammalian cells which should produce a consistent, correctly folded protein in sufficient quantities to allow more detailed evaluation of function. Assuming this is borne out in the studies suggested above it should provide sufficient material for a number of further evaluations, particularly in *in vivo* murine models. The following chapter outlines some of the lines of investigation which could be pursued providing sufficient material was available.

Chapter 7: Discussion (2) Murine <u>Constructs</u>

7.1 Summary of Mouse Construct Data

The preceding chapters have described the production of two pMHC x Fab' constructs (F2 & F3) whose structure confers on them at least some ability to interact with both hCD20-bearing cells and the K^bSIINFEKL cognate TCR. *In vitro* they are able to retarget OT-1 CTLs to lyse cells bearing the non-cognate Ag hCD20 and induce proliferation of OT-1 CTLs in the presence hCD20. Their ability to retarget OT-1 CTLs has also been demonstrated *in vivo* in a hCD20 Tg mouse model where a single dose of each of the retargeting constructs can produce significant B cell depletion from the peripheral blood. Although both *in vitro* and *in vivo* the pMHC x Fab' constructs have inferior cytotoxic abilities compared to the positive control [anti-hCD20 x anti-mCD3] BsAb, F3 is associated with reduced levels of inflammatory cytokine release suggesting toxicity may be lower.

As discussed there are a number of technical challenges in the synthesis of F2 & F3 meaning that supplies are always limited, hampering the scope of the evaluations possible. The interbatch variability observed with identical experiments illustrates that it is very unlikely that all the molecules within a batch are active, and the proportion of a batch which is functionally active can vary widely from one preparation to the next. Although assays may be devised (e.g. using the Biacore) which can more accurately measure the percentage of any batch with the correct conformation for each of the two components (Fab' and pMHC), ascertaining what proportion of the molecules within a preparation have two (or three) functional moieties is likely to remain very difficult.

The preliminary *in vitro* data for the [mSCT x (anti-hCD20 Fab)₂] DnL construct shows that as with F2 & F3 it is able to effect proliferation of OT-1 cells and retarget them to lyse hCD20-expressing target cells. The data also suggest that it is at least equivalent in efficacy to the SMCC-conjugated retargeting constructs, if not slightly more efficacious. This is encouraging given that the mechanism of production of the DnL construct (via retroviral transduction of mammalian cells) and its consistent method of conjugation (between DDD in protein kinase A and AD in reactive A-kinase anchoring domain) mean it should be possible to produce much larger quantities of a consistent, functionally invariant product. This is essential if this strategy of non-cognate CTL retargeting is to be taken further forward as the experiments outlined in section 7.4 need a reliable product with predictable behaviour.

7.2. Principles of a Retargeting Strategy

In order to evaluate whether there is any potential in any of the retargeting constructs evaluated in this study it is necessary to consider what the ideal characteristics of a T cell retargeting strategy are: Ideally a molecule is produced which is able to redirect a successful

immune response (e.g. against an infectious pathogen) against a tumour Ag. This should be achieved without excessive toxicity and preferably by expanding an existing pool of memory T cells avoiding the need for either vaccination or *ex vivo* expansion of autologous or allogeneic CTLs before reinfusion. Owing to the risk of down-regulation of the target cell Ag, ideally epitope spreading⁵⁰² will be observed with the production of endogenous tumour Agspecific CTLs. The construct should also create the appropriate inflammatory microenvironment for an anti-tumour rather than pro-tumour immune response.⁵⁰³

It is also important the retargeted immune response does not escape normal physiological control and in particular is down-regulated when appropriate without collateral damage to the host. An additional consideration is whether the retargeting strategy is likely to induce T cell exhaustion and whether the immune response intended to be retargeted is already showing features of this; the original plan for this study was to retarget CMV-specific CTLs owing to the prevalence of infection throughout the adult population, the limited repertoire of immunodominant peptides and the large number of specific CTLs found in the blood of particularly the elderly who are most likely to develop a malignancy. Given the increasing evidence that the accumulations of CTLs in latent CMV infection are dysfunctional and show features of exhaustion, it may be that attempts to retarget this population of cells are misguided as they lack the full repertoire of effector functions and are not going to be able to produce a robust anti-tumour response, even if they can be effectively redirected.

7.3 Current Retargeting Strategies

The approaches currently being tried to redirect cellular immune responses can be divided into those that alter the specificity of the T cell by introducing a 'new' Ag receptor, and those that effectively alter the surface of the target cell by placing a new Ag (pMHC) or effector molecule (anti-CD3 Fab^(*)) on its surface. Examples of the former are CARs, Tg TCRs and Immunocore's anti-CD3 x mTCR constructs while examples of the latter are bispecific antibodies and pMHC x Fab' conjugates.

As discussed in section 1.4.3 CARs are artificial Ag receptors introduced into CTLs which combine the specificity of an Ab with the intracellular signalling machinery of the TCR/CD3 complex. They can be improved by the addition of various costimulatory domains to enhance the signal received by the CTL once the Ab moiety is engaged. A number of small clinical trials have shown promising results: The latest data from the GD2-CAR trial in neuroblastoma has shown that CTLs expressing this CAR can be detected up to 4 years later and the persistence of these cells is associated with a continuing remission. ⁵⁰⁸ A recent trial in CLL of an anti-CD19 CAR containing a CD137 costimulatory domain showed clinical

efficacy in that 2/3 patients achieved a remission and there was evidence that CAR-expressing CTLs tracked to the bone marrow where they eliminated CD19⁺ cells. Additionally some of the CAR-expressing CTLs had a memory phenotype suggesting that the anti-CLL response would persist. ⁵⁰⁹

Although all CAR-CTL trials to date have considered the persistence of CAR-expressing CTLs as a desirable end point, it can be imagined that this could also be problematic. Such CTLs are effectively outside the normal mechanisms which would control the immune response and therefore could potentially cause excessive damage: 1/3 patients treated with the anti-CD19 CAR developed tumour lysis syndrome due to the brisk nature of the initial immune response. One mechanism for avoiding this problem is to insert a suicide gene into the construct containing the CAR such as thymidine kinase; administration of ganciclovir will cause all cells expressing the enzyme (i.e. those with the CAR) to die.

As discussed in section 1.4.3, the first clinical trial of adoptive transfer of T cells with a Tg TCR resulted in some unexpected toxicities due to the widespread expression of melanocyte Ags, particularly in the CNS. A subsequent trial of CTLs expressing a Tg TCR specific for CEA peptides in patients with metastatic colorectal cancer, although demonstrating some clinical efficacy, was also complicated by significant toxicity: 3/3 patients had a transient but severe inflammatory colitis which represented a dose limiting toxicity. ⁵¹⁰ This trial illustrates the potential autoimmune complications when tolerance is artificially broken via the introduction of a Tg Ag receptor. Again a suicide gene can be inserted into the construct as a way to terminate immune overstimulation, but once this is invoked the strategy is rendered useless as all cells expressing the Tg TCR should be killed.

Both CARs and Tg TCRs involve the insertion of a genetic construct into a T cell which is an *ex vivo* manipulation subject to all the normal constraints of good manufacturing practice and in addition to being time consuming is very expensive and therefore unlikely to be widely applicable. Although CARs bypass MHC restriction, this is a consideration of Tg TCRs as they need to be generated in a subject (usually a human MHC class I Tg mouse) with similar class I alleles, otherwise the resulting TCR will not be able to recognise any pMHC in the recipient.

A modification to this approach is the bivalent anti-CD3 scFv x TCR constructs which Immunocore are developing. The high affinity TCR recognises tumour Ag in the context of MHC, but rather than having to insert the Tg TCR into the cell to ensure surface expression, it is effectively placed on the surface of the T cell by linking it to anti-CD3 scFv which can

engage the CD3 molecule of the T cell's endogenous TCR. This can effect polyclonal activation of T cells, redirecting them against target cells expressing the cognate pMHC. IMCgp100, which consists of an optimized high affinity TCR against an HLA-A2 restricted peptide derived from the melanoma Ag gp100 coupled to an anti-CD3 scFv, is currently in phase I clinical trials.⁵¹¹

Although this approach avoids the problems of having to transfect or transduce T cells so they express the desired TCR it is still a relatively labour intensive approach in that it requires production of a range of high affinity TCRs specific for various pMHC combinations. Owing to the presence of an anti-CD3 moiety it also encounters the same problems as anti-CD3-containing bispecific retargeting molecules in that it can potentially activate any and every T cell with associated toxicity and can activate immunosuppressive T cells such as T_{regs} .

The retargeting strategy which is currently enjoying a resurgence is bispecific antibodies, mostly due to the superior efficacy of BiTEs which makes some of their toxicity more tolerable. In addition to the studies described in the introduction, blinatumomab has had some success in eliminating minimal residual disease in acute lymphoblastic leukaemia, while *in vitro* anti-melanoma Ag (MCSP) x anti-CD3⁵¹³ and anti-EpCAM x antiCD3⁵¹⁴ BiTEs have been able to eliminate melanoma cells and pancreatic carcinoma stem cells respectively. However, in addition to the toxicity described previously, there is now *in vitro* evidence that the indiscriminate retargeting of CD3⁺ cells can include redirecting T_{regs} to the tumour cell, a deleterious event. Therefore although currently very promising there are still some problems with bispecific antibodies and potentially room for other retargeting approaches.

7.4 Developing the pMHC x Fab^(*) Retargeting Strategy

In vitro and *in vivo* studies involving the different permutations of the pMHC x Fab' retargeting approach prior to our study are described in section 1.6.2. Essentially these have all involved a bivalent molecule with one pMHC molecule and one Fab' molecule. A variety of mouse models including OT-1 Tg, adoptively transferred and actively infected mice have been used to provide CTLs for retargeting, all with some success. In order to advance this approach further it is necessary to try and create experimental conditions which are closer to those which might be physiologically encountered.

As discussed in chapter 5, although showing promising efficacy, the F2 & F3 constructs are too labour intensive to make in the required quantities for thorough evaluation. The heterogeneity of the product coupled with the likely variable functional activity mean without major modifications to the production methodology and improved assays for measuring

functional activity, it is unlikely that further evaluation beyond the proof of principle assays presented in this study is going to be feasible or helpful. Equally promising in the assays undertaken was the [mSCT x (anti-hCD20 Fab)₂] DnL construct which potentially can be evaluated further. Its production in mammalian cells means it should be correctly folded and given that it is being produced by a pharmaceutical company it is likely that they have the facilities for producing the required quantities for systematic evaluation. Assuming sufficient quantities of this product can be produced a thorough assessment of its *in vitro* and *in vivo* activity needs to be undertaken. Alternatively the experiments outlined below could equally be used to evaluate any candidate retargeting molecule.

In vitro the mechanism of cytotoxicity can be investigated by using inhibitors of the perforin and Fas pathways to evaluate whether the mechanism of cytotoxicity is similar to that seen with blinatumomab. Additionally both dose:response and time:response curves for proliferation can be determined in order to understand the kinetics of the proliferative response produced by the construct. [mSCT x (anti-hCD20 Fab)₂] DnL induced activation can be measured by FACS by staining for upregulated cell surface proteins such as CD25 and CD69 and the adhesion molecules CD2 and LFA-1. FACS can also be used to look for increased production of intracellular cytokines such as IFNγ or TNFα.

In addition to demonstrating that [mSCT x (anti-hCD20 Fab)₂] DnL has equivalent, if not better, *in vivo* activity as F3 by repeating the B cell depletion experiments described in chapter 5, it is important that it is evaluated in some more physiological models: The number of specific CTLs available for retargeting was far in excess of what is likely to be encountered in most human experience; therefore it is necessary to try retargeting a smaller more physiological population (e.g. 1-5%) which is likely to necessitate repeated doses of the construct. If the DnL construct is more consistent with a fixed (high) percentage with the correct conformation, it may be that smaller doses can be used. To determine an optimal dosing schedule it is necessary to measure the half life of the molecule *in vivo* and look at tissue distribution of the construct. It would also be useful to look in different tissue compartments for B cell redistribution after administration of the DnL construct as it is important to determine that B cells are actually dying rather than, for example, all being sequestered in the spleen.

Although adoptive transfer provides a ready supply of easily activated specific CTLs for retargeting, in the human situation it is far more likely it would be necessary to retarget an endogenous population of cells. These are also most likely to be memory cells so it would be useful to see whether administration of the DnL construct to a mouse, which has previously

had an endogenously generated OT-1 response (through immunization with OVA and agonistic anti-CD40 mAb), causes generation of a secondary immune response. The ability to both activate/expand and retarget the same population would broaden the potential clinical use of the DnL construct. Repeated administration of the DnL construct would also allow evaluation as to whether this approach is able to induce clonal exhaustion which would have implications for adopting the strategy in humans.

Further evaluation of cytokine secretion would be useful, particularly in comparison to that seen with the [anti-hCD20 x anti-mCD3] BsAb: both overall cytokine release and the effect this is likely to have on skewing macrophages⁵¹⁶ towards making a pro-tumour response within the tumour microenvironment. Although, as discussed previously, B cell depletion experiments in hCD20 Tg mice have become the assay of choice when evaluating anti-hCD20 therapies, there are other hCD20⁺ tumour models available such as EL4⁵¹⁷ retrovirally (hence more stably) transduced with hCD20 which can be used *in vivo*.

Ultimately, if this strategy is aiming for use in humans it will be necessary to return to the production of human rather than murine retargeting constructs. If murine experiments with the DnL conjugate prove successful, it would be reasonable to have some human [HLA-A2peptide SCT x (anti-hCD20 Fab)₂] made (such a conjugate containing an HLA-A2 restricted peptide derived from melan A has already been produced, Phil Savage, personal communication). These could contain SCTs composed of HLA-A2 and appropriately restricted peptides derived from viruses e.g. influenza, CMV, EBV. Initial in vitro work could follow the same scheme as with the murine constructs using human CTL lines generated as described in section 2.1.1. Generating a mouse model is slightly more difficult: The traditional approach of using a severely immunosuppressed mouse (e.g. SCID or nude) adoptively transferred with human CTLs and subcutaneously engrafted with a hCD20⁺ tumour is one option. Alternatively, HHD mice could be crossed with hCD20 Tg creating a double Tg which expressed both hCD20 on its B cells and HLA-A2 on all its nucleated cells. A vaccination strategy e.g. DNA vaccine encoding a membrane-expressed SCT⁵¹⁸ could be used to generate an endogenous population of HLA-A2-restricted peptide-specific CTLs which could then be retargeted.

If promising data is obtained with [HLA-A2-peptide x (anti-hCD20 Fab)₂] DnL, altering the specificity of the Fab fragment to another tumour Ag (e.g. CEA or HER2) could be considered. This will extend this technique to non-B cell derived tumours. *In vitro* work could follow a similar scheme to that suggested for the anti-hCD20 Fab-containing DnL with hCD20⁺ cell lines substituted with alternative lines expressing the appropriate Ags. A

CEA/HLA-A2 double Tg mouse exists⁵¹⁹ which could be used for evaluation of anti-CEA Fab-containing DnL constructs. As yet, no double HER2/HLA-A2 Tg mouse exists, although this could be bred by crossing the single Tgs. It would be interesting to see whether equivalent results are obtained when CTLs are retargeted against cells lines which are not of B cell origin (i.e. bowel or breast cell lines) as these will lack the costimulatory molecules usually found on B cells which it could be argued are contributing to the activation of retargeted CTLs.

Since this current study retargeting non-cognate CTLs to tumour Ags using pMHC x Fab' construct began, new clinical data about the improved efficacy of bispecific antibodies (specific BiTEs) has emerged. It could therefore be argued that their apparent success and improved toxicity profile removes some of the need for alternative retargeting approaches. However, there are theoretical advantages to retargeting a limited population of cells (such as those specific for a particular peptide Ag) as discussed throughout the text, not least the potential for reduced toxicity. Just as it has taken several decades of intensive research and development throughout the world to design an improved BsAb format, it is likely that there will need to be extensive further development of the design and manufacturing process of pMHC-containing conjugates before they are at a stage where use in humans can be contemplated.

Appendices

Appendix 1: Reagent Recipes

TAE

40 mM tris acetate

1 mM EDTA

(to prepare 50 x stock use 242 g tris base, 57.1 ml glacial acetic acid, 100 ml 0.5 M EDTA pH 8, make up to final volume of 1 l with dH_2O)

TE buffer (for DNA)

10 mM TrisHCl 1 mM EDTA pH 8

PBS

35.05 g NaCl 17.2 g Na₂HPO₄ 3.95 g KH₂PO₄ Make up to final volume of 5 l with dH₂O

PBS-tween

PBS as above 0.05% v/v Tween-20

PBS-BSA

PBS as above 1% w/v bovine serum albumin

ELISA coating buffer

15 mM Na₂CO₃ 28.5 mM NaHCO₃

ELISA citrate buffer

19.2 g citric acid 1 l dH₂O

ELISA phosphate buffer

28.4 g Na₂HPO₄ 1 l dH₂O

ELISA OPD substrate buffer

24 ml ELISA citrate buffer 26 ml ELISA phosphate buffer 50 ml d H_2O 20 mg o-PhenylDiamine free base (o-PD) 100 μ l 30% w/v H_2O_2

Reducing SDS-PAGE loading buffer

0.1875 M TrisHCl pH 6.8 9% (w/v) sodium dodecyl sulfate 30% (v/v) glycerol 0.03% (w/v) bromophenol blue 10% (v/v) β_2 mercaptoethanol

Non-reducing SDS-PAGE loading buffer

0.1875 M TrisHCl pH 6.8 9% (w/v) sodium dodecyl sulfate 30% (v/v) glycerol 0.03% (w/v) bromophenol blue

12.5% SDS-PAGE resolving gel

5.2 ml 30% acrylamide (National Diagnostics) 3.96 ml dH₂O 3.25 ml resolving buffer (1.5 M TrisHCl, pH 8.7) 61 μl sodium dodecyl sulfate 41.25 μl 10% w/v ammonium persulfate 6.1 μl N,N,N,N-tetramethyl-ethane-1,2-diamine

3% SDS-PAGE stacking gel

0.5 ml 30% acrylamide 3 ml d H_2O 1.25 ml stacking buffer (0.5 M TrisHCl, pH 6.9) 25 μ l sodium dodecyl sulfate 50 μ l 10% w/v ammonium persulfate 5 μ l N,N,N,N-tetramethyl-ethane-1,2-diamine

SDS-PAGE electrode running buffer

192 mM glycine 25 mM TrisHCl 0.1% w/v sodium dodecyl sulfate pH 8

SDS-PAGE stain

40 ml methanol 7 ml glacial acetic acid 53 ml dH₂O 25 mg Coomassie blue

SDS-PAGE destain

250 ml methanol 350 ml glacial acetic acid Made up to 51 with dH₂O

Western blot transfer buffer

192 mM glycine 25 mM TrisHCl 20% v/v methanol

TBS-T

150 mM NaCl 50 mM Tris 0.05% Tween 20 pH 7.4

Sonication buffer

20 mM TrisHCl 5 mM EDTA pH 8

immediately before use add 1 mM PSMF & 1 mg/ml lysozyme

Wash Buffer 1

50 mM TrisHCl 5 mM EDTA 100 mM NaCl 0.5% Triton-X pH 8 immediately before use add 1 mM DTT

Wash Buffer 2

50 mM TrisHCl 100 mM NaCl pH 8

Urea solubilisation buffer

8 M urea 20 mM 2ME 50 mM TrisHCl 50 mM NaCl 1 mM EDTA pH 8

Guanidine solubilisation buffer

6 M guanidineHCl pH 7.4

TrisNaCl buffer (10x stock)

 $\begin{array}{c} 467.5 \text{ g NaCl} \\ 193.6 \text{ g Tris} \\ 29.76 \text{ g EDTA} \\ 160 \text{ ml 5M HCl} \\ 8 \text{ l } dH_2O \end{array}$

Used at a 1/2, 1/5, of 1/10 dilution according to indication

0.2M citrate buffer

210g citric acid 116.5 g NaOH Make up to 5l with dH₂O pH 6.5

0.2M TE8 buffer

121 g TrisHCl 18.64 g EDTA 100 ml 5M HCl 5 l dH₂O

$\frac{\textbf{Bicarbonate buffer}}{3.7 \text{ g NaHCO}_3} \text{ (for FITC labelling antibodies)}$

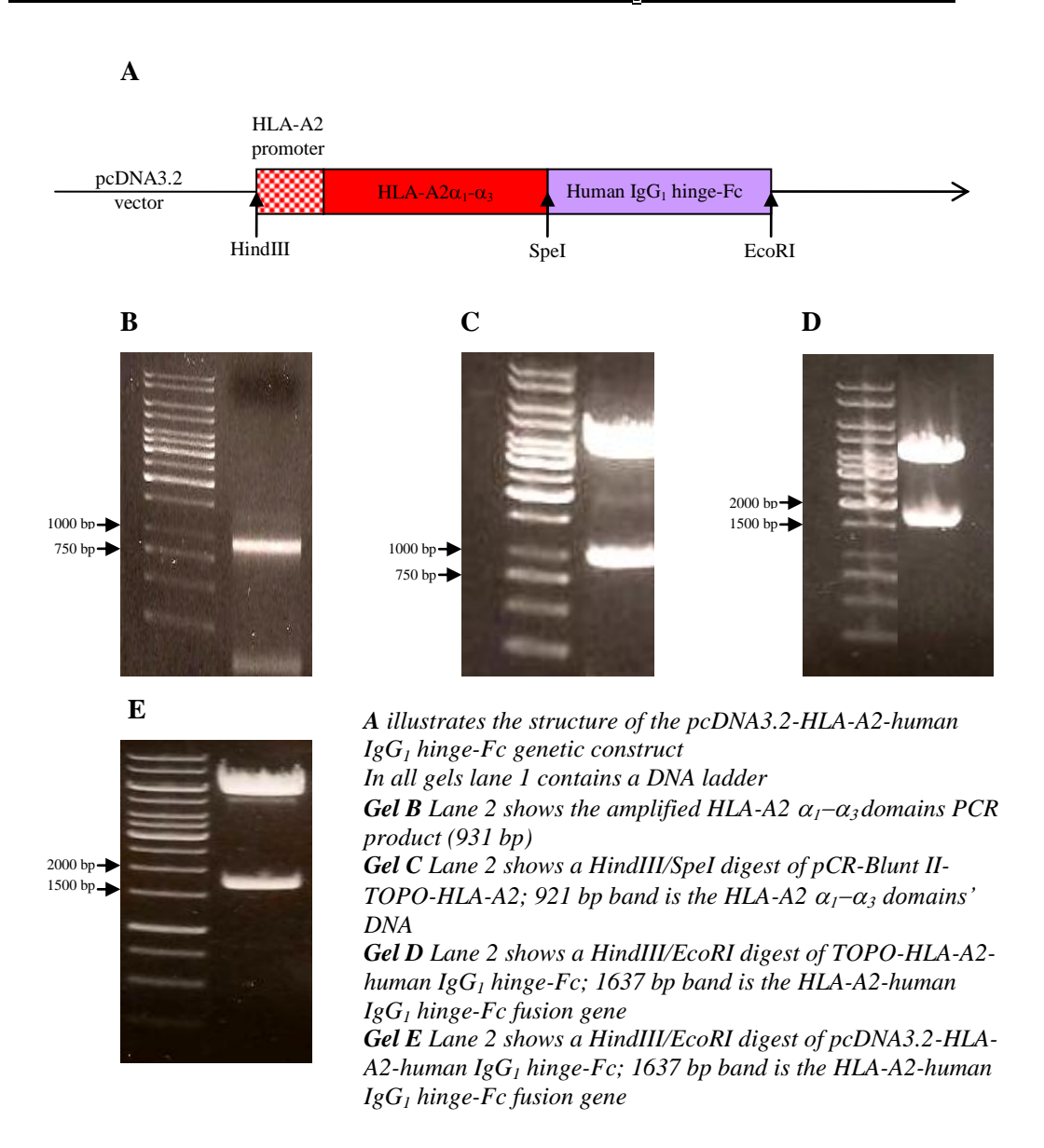
3.7 g NaHCO₃ 1.02 g Na₂CO₃ 100 ml dH₂O pH 9.5

<u>0.0175M Phosphate buffer</u> (for FITC labelling antibodies)

0.56 g Na₂HPO₄ 1.85 g KH₂PO₄ 1 l dH₂O pH 6.3

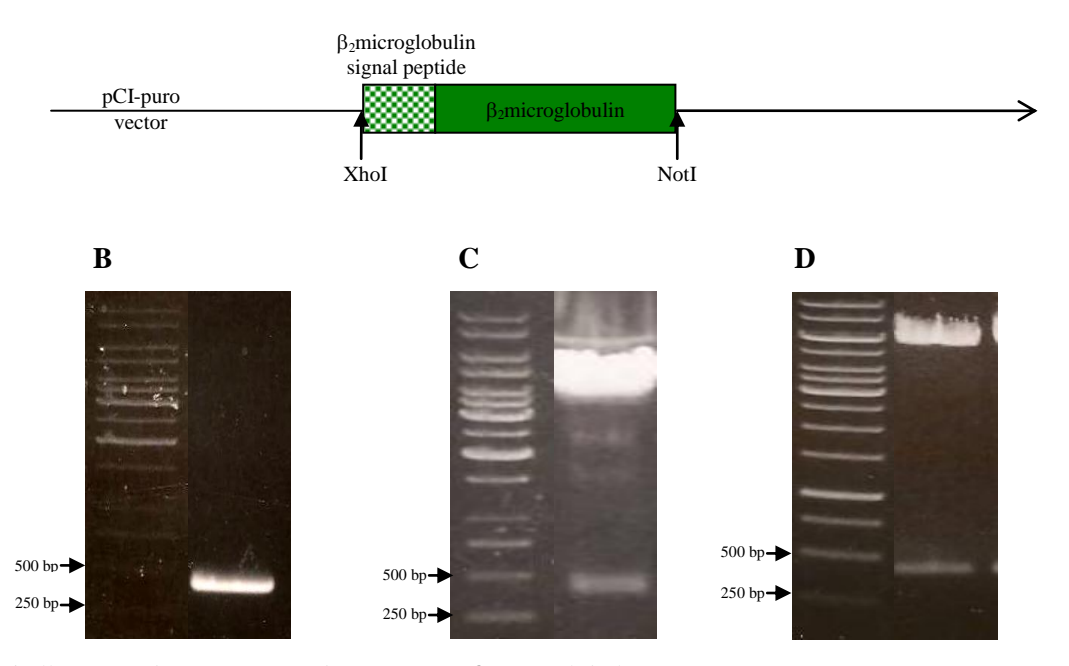
Appendix 2: Supplementary Data

A2 1.1 Production of pcDNA3.2-HLA-A2-human IgG₁ hinge-Fc genetic construct



A2 1.2 Production of pCI-puro-β₂microglobulin genetic construct

A



A illustrates the structure of the pCI-puro- β_2 microglobulin genetic construct In all gels lane 1 contains a DNA ladder

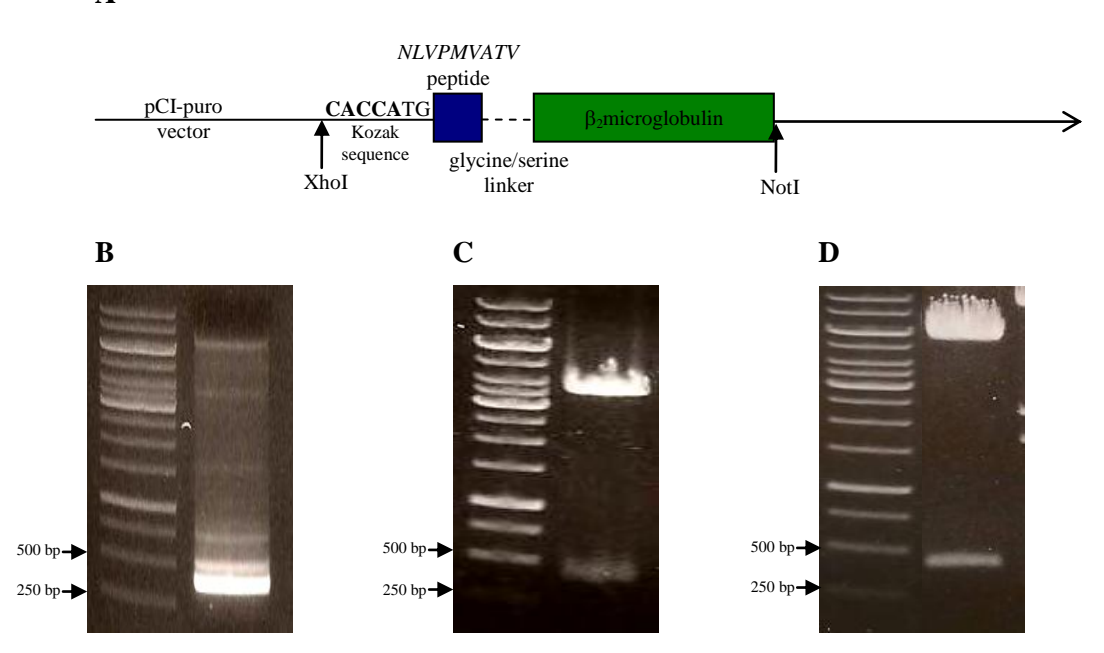
Gel B Lane 2 shows the amplified β_2 microglobulin gene PCR product (419 bp)

Gel C Lane 2 shows a XhoI/NotI digest of pCR-Blunt II-TOPO $-\beta_2$ microglobulin; 408 bp band is the β_2 microglobulin gene

Gel D Lane 2 shows a XhoI/NotI digest of pCI-puro- β_2 microglobulin; 408 bp band is the β_2 microglobulin gene

A2 1.3 Production of pCI-puro-CMV-(G₄S)₄-β₂microglobulin genetic construct

A



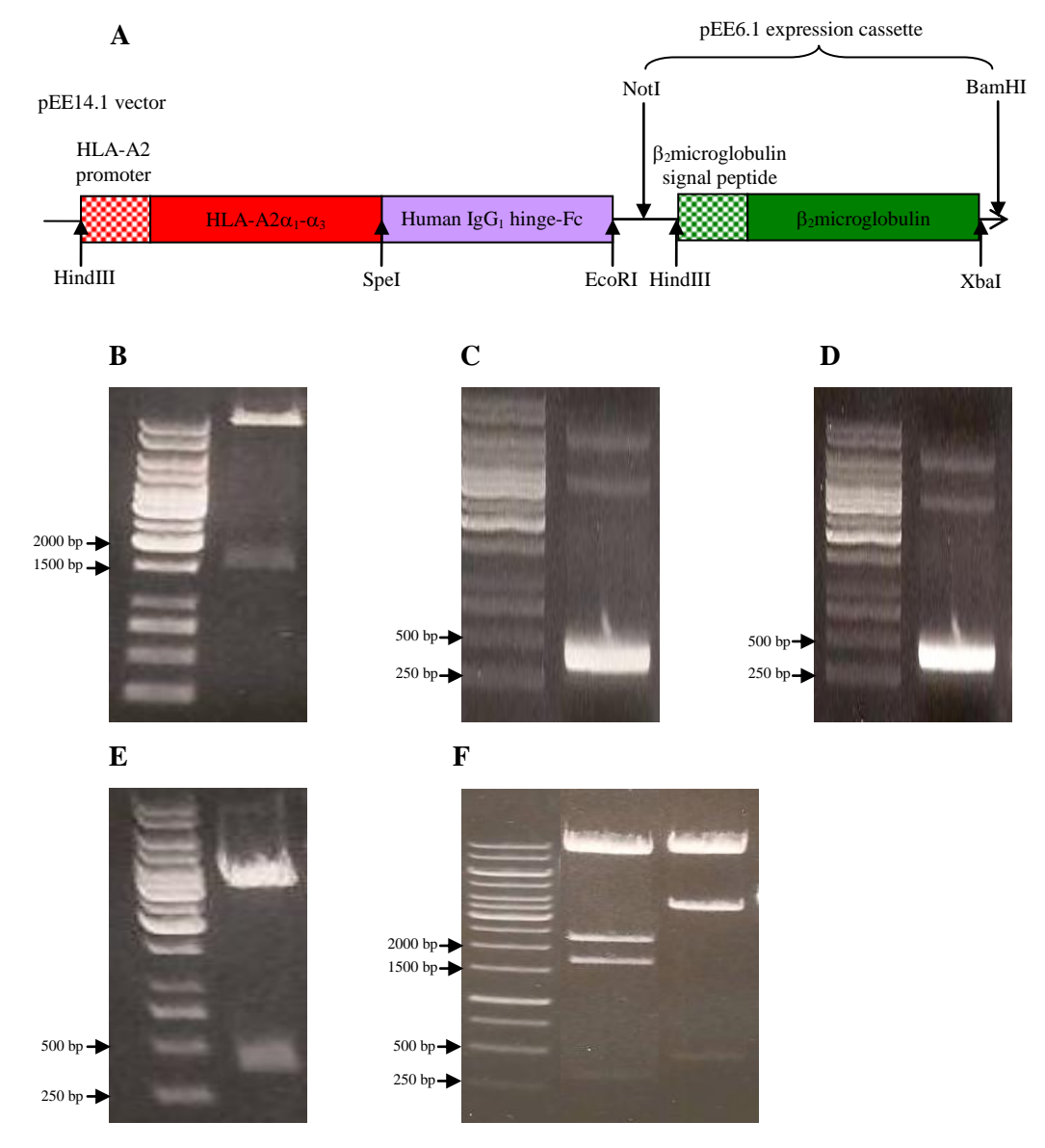
A illustrates the structure of the pCI-puro CMV- $(G_4S)_4$ - β_2 microglobulin genetic construct In all gels lane 1 contains a DNA ladder

Gel B Lane 2 shows the amplified CMV- $(G_4S)_4$ - β_2 microglobulin gene PCR product (397 bp)

Gel C Lane 2 shows a Xhol/NotI digest of pCR-Blunt II-TOPO CMV- $(G_4S)_4$ - β_2 microglobulin; 388 bp band is the CMV- $(G_4S)_4$ - β_2 microglobulin gene

Gel D Lane 2 shows a XhoI/NotI digest of pCI-puro CMV- $(G_4S)_4$ - β_2 microglobulin; 388 bp band is the CMV- $(G_4S)_4$ - β_2 microglobulin gene

A2 1.4 Production of pEE14.1-HLA-A2-human Ig G_1 hinge-Fc/pEE6.1- β_2 microglobulin genetic construct



A illustrates the structure of the pEE14.1--HLA-A2-human IgG_1 hinge-Fc/pEE6.1- β_2 microglobulin genetic construct

In all gels lane 1 contains a DNA ladder

Gel B Lane 2 shows HindIII/EcoRI digest of pEE14.1-HLA-A2-human IgG_1 hinge-Fc; 1637 bp band is the HLA-A2-human IgG_1 hinge-Fc fusion gene

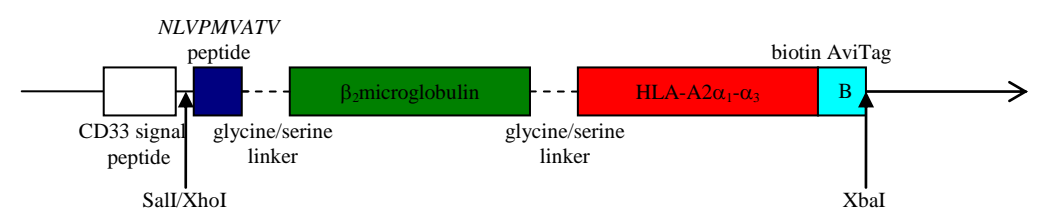
Gel C Lane 2 shows the amplified $\beta_2 m$ gene PCR product (399 bp) for sub-cloning into pEE6 Gel D Lane 2 shows a HindIII/XbaI digest of pCR-Blunt II-TOPO- $\beta_2 m$ gene

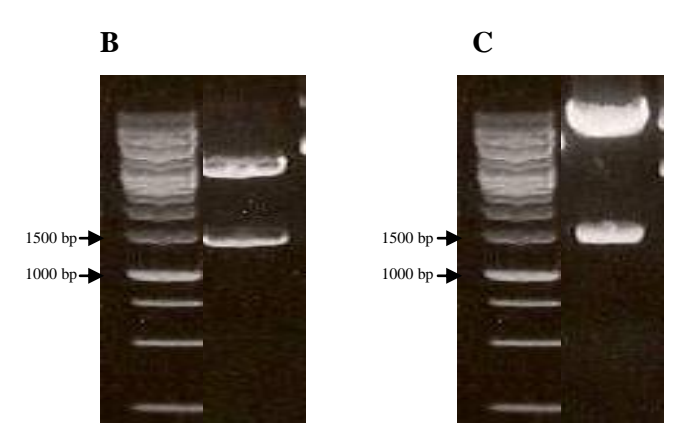
Gel E Lane 2 shows a HindIII/XbaI digest of pEE6.1- β_2 microglobulin; 389 bp band is β_2 m gene Gel F Lane 2 shows a HindIII/EcoRI digest of pEE14.1--HLA-A2-human Ig G_1 hinge-Fc/pEE6.1- β_2 microglobulin; 1637 bp band is HLA-A2-human Ig G_1 hinge-Fc fusion gene. Lane 3 shows a HindIII/XbaI digest of pEE14.1-HLA-A2-human Ig G_1 hinge-Fc/pEE6.1- β_2 microglobulin; 389 bp band is β_2 microglobulin gene

A2 1.5 Production of Signal pIg plus-CMV-short linker- β_2 microglobulin-HLA-A2-biotin-AviTag genetic construct

A

Signal pIg plus vector





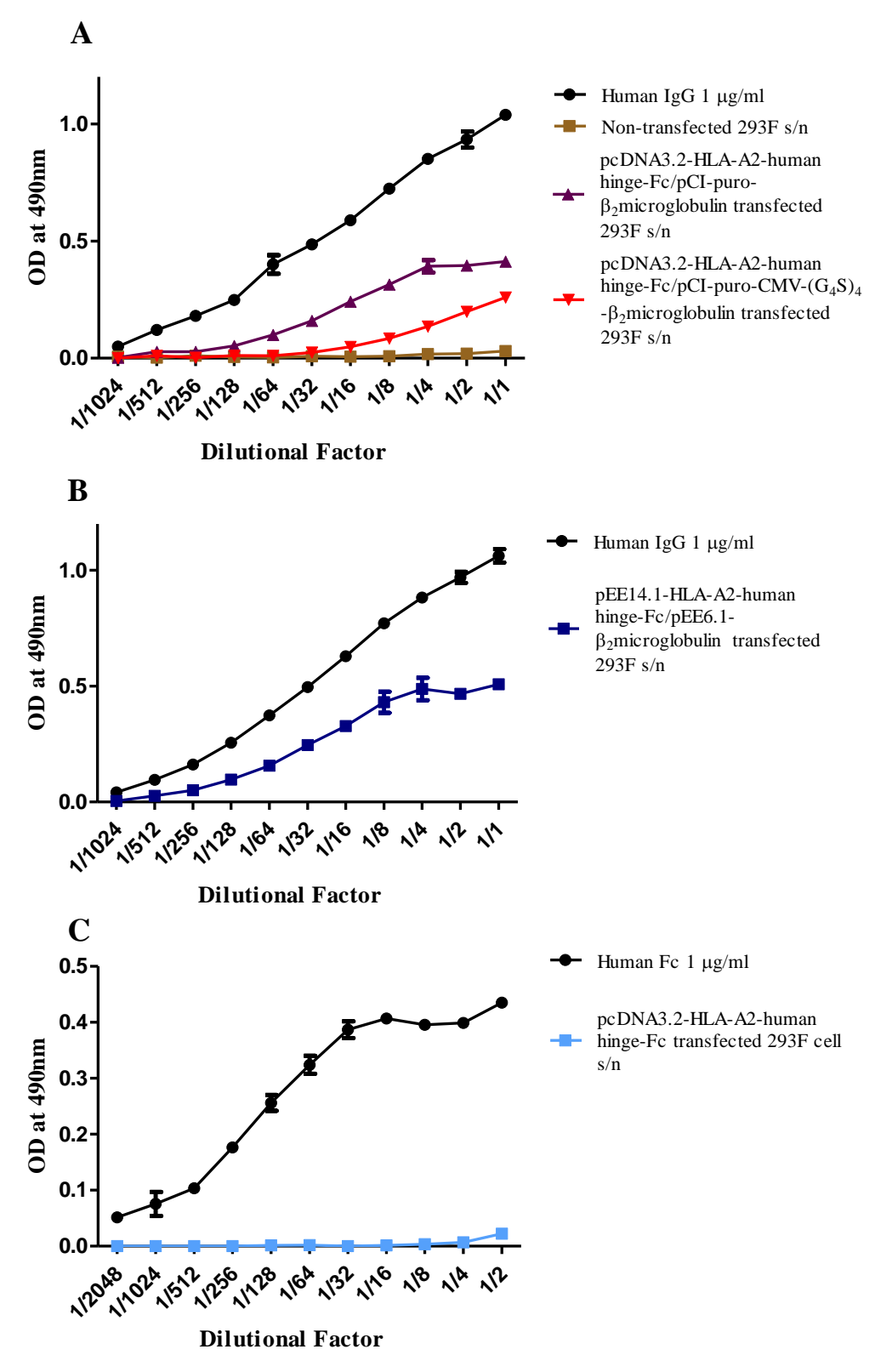
A illustrates the structure of the pIg plus CMV-short linker- β_2 microglobulin-HLA-A2-biotin-AviTag genetic construct

In all gels lane 1 contains a DNA ladder

Gel B Lane 2 shows Sall/XbaI digest of pCR-Blunt II-TOPO- CMV-short linker- β_2 microglobulin-HLA-A2-biotin-AviTag Sall/XbaI mutant; 1391 bp band is CMV-short linker- β_2 microglobulin-HLA-A2-biotin-AviTag fusion gene

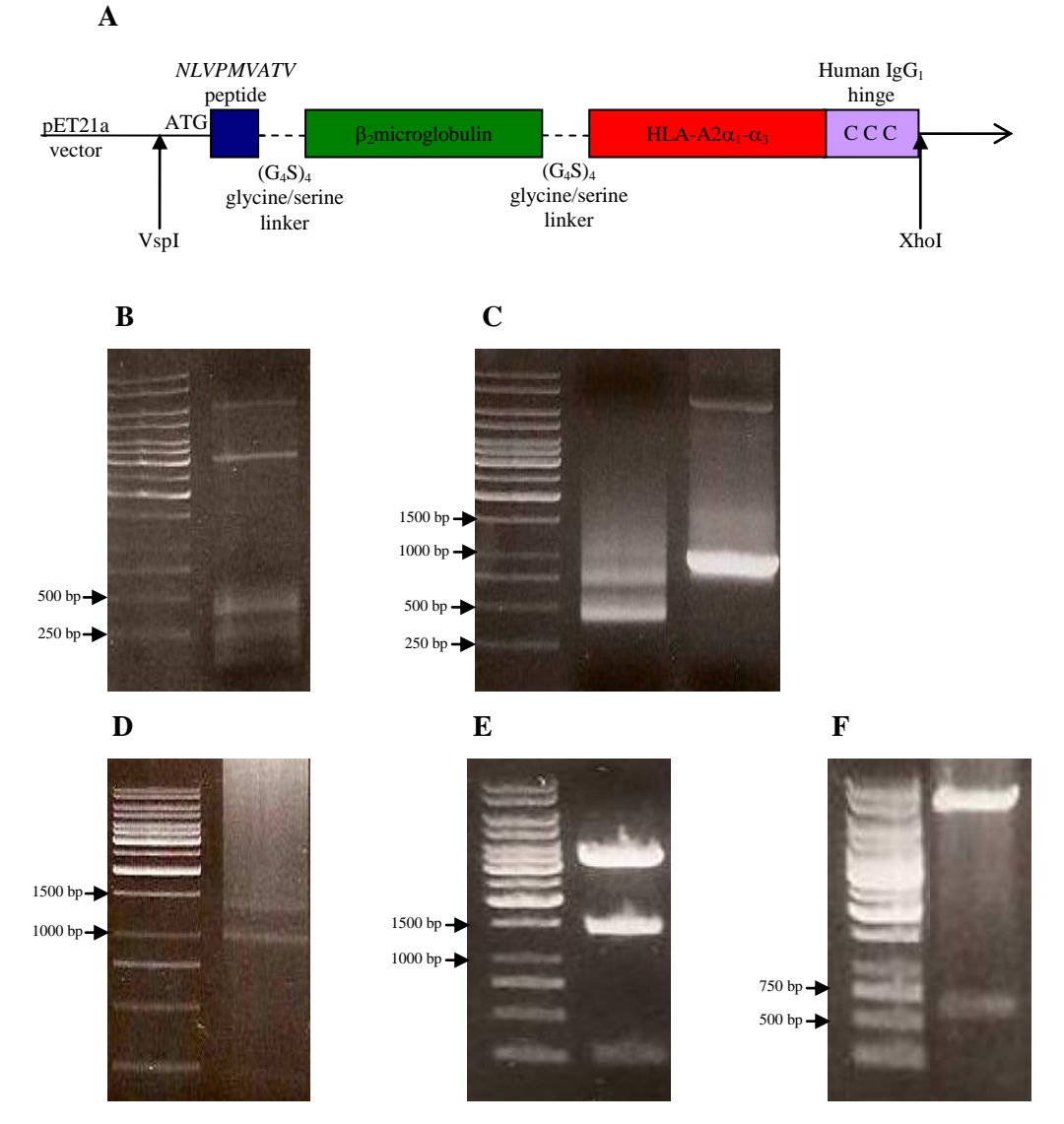
Gel C Lane 2 shows HindIII digest of pig plus CMV-short linker- β_2 microglobulin-HLA-A2-biotin-AviTag; HindIII digest generates 1300 bp fragment

A2 2.1: ELISA analysis of HLA-A2-human hinge-Fc protein secretion from 293F cells (co-)transfected with HLA-A2-human hinge-Fc/β₂m-containing vectors



Non-concentrated transfected 293F cell supernatants were used. The capture and detection antibodies were anti-human Fc and anti-human IgG-HRP respectively. Points represent mean +/- range of duplicate determinations. Data presented is representative of at least two experiments.

A2 3.1 Production of pET21a-CMV- β_2 microglobulin-HLA-A2-human IgG₁ hinge (SCT-3xCys) genetic construct



A illustrates the structure of the pET21a-CM- β_2 microglobulin-HLA-A2-human Ig G_1 hinge genetic construct

In all gels lane 1 contains a DNA ladder

Gel B Lane 2 shows the amplified $(G_4S)_3$ - β_2 microglobulin- $(G_4S)_3$ PCR product (399 bp)

Gel C Lane 2 shows the amplified NLVPMVATV- $(G_4S)_4$ - β_2 microglobulin- $(G_4S)_3$ PCR product (435 bp)

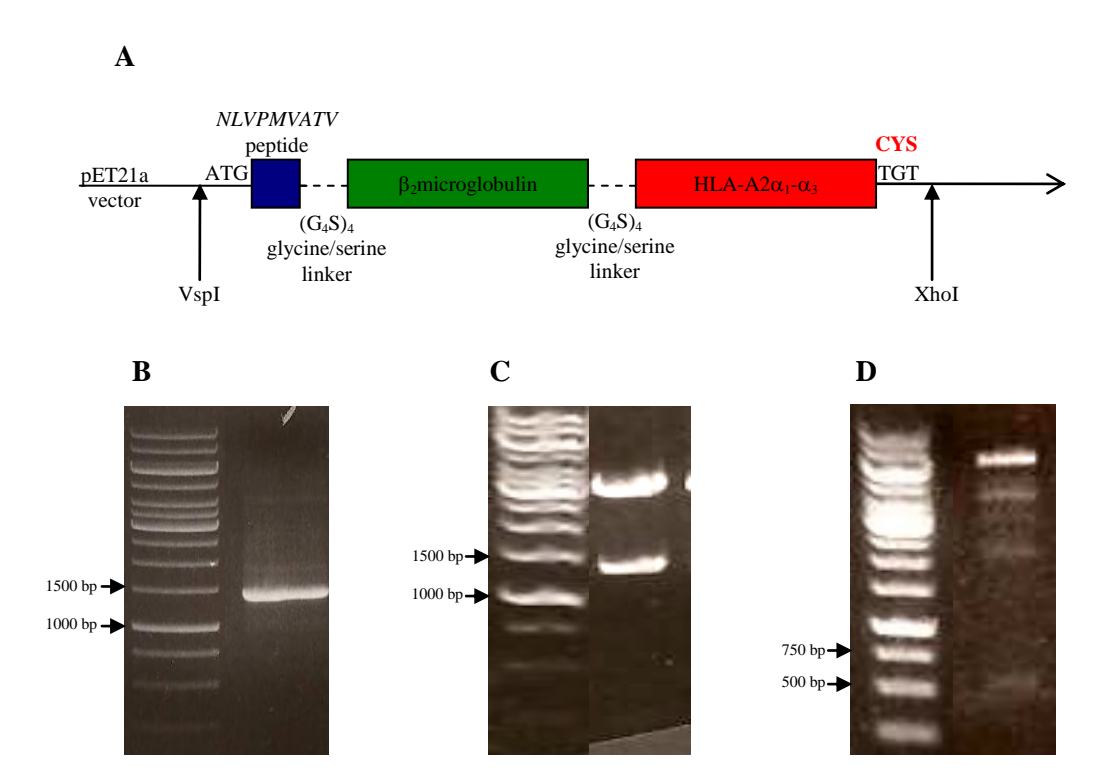
Lane 3 shows the amplified $(G_4S)_2$ -HLA-A2 α_1 - α_3 domains-human IgG_1 hinge PCR product (948 bp)

Gel D Lane 2 shows the amplified NLVPMVATV- $(G_4S)_4$ - β_2 microglobulin- $(G_4S)_3$ -HLA-A2 α_1 - α_3 domains-human IgG_1 hinge PCR product (1368 bp)

Gel E Lane 2 shows a VspI/XhoI digest of pCR-Blunt II-TOPO- NLVPMVATV- $(G_4S)_4$ - β_2 microglobulin- $(G_4S)_3$ -HLA-A2 α_1 - α_3 domains-human Ig G_1 hinge: 1363 bp band is NLVPMVATV- $(G_4S)_4$ - β_2 microglobulin- $(G_4S)_3$ -HLA-A2 α_1 - α_3 domains-human Ig G_1 -hinge fusion gene; i.e. CMV- β_2 microglobulin-HLA-A2-human Ig G_1 hinge fusion gene

Gel F Lane 2 shows a XhoI/KpnI digest of pET21a- CMV- β_2 microglobulin-HLA-A2-human Ig G_1 hinge yielding a 572 bp band

$\underline{A2~3.2~Production~of~pET21a\text{-}CMV-} \underline{\beta_2 microglobulin\text{-}HLA\text{-}A2\text{-}Cysteine~(SCT-C)~genetic}$



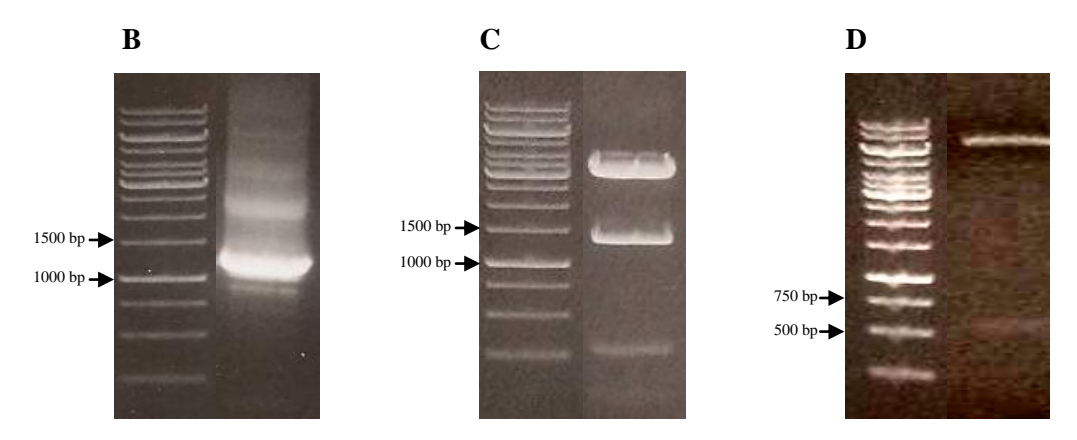
A illustrates the structure of the pET21a-CMV- β_2 microglobulin-HLA-A2-cysteine genetic construct In all gels lane 1 contains a DNA ladder

Gel B Lane 2 shows the amplified CMV- β_2 microglobulin-HLA-A2-cysteine fusion gene PCR product (1317 bp)

Gel C Lane 2 shows a VspI/XhoI digest of pCR-Blunt II-TOPO CMV- β_2 microglobulin-HLA-A2-cysteine: 1308 bp band is the CMV- β_2 microglobulin-HLA-A2-cysteine fusion gene

Gel D Lane 2 shows a XhoI/KpnI digest of pET21a- CMV- β_2 microglobulin-HLA-A2-cysteine yielding a 517 bp band

A2 3.3 Production of pET21a-CMV- β_2 microglobulin-HLA-A2 (SCT-X) genetic construct

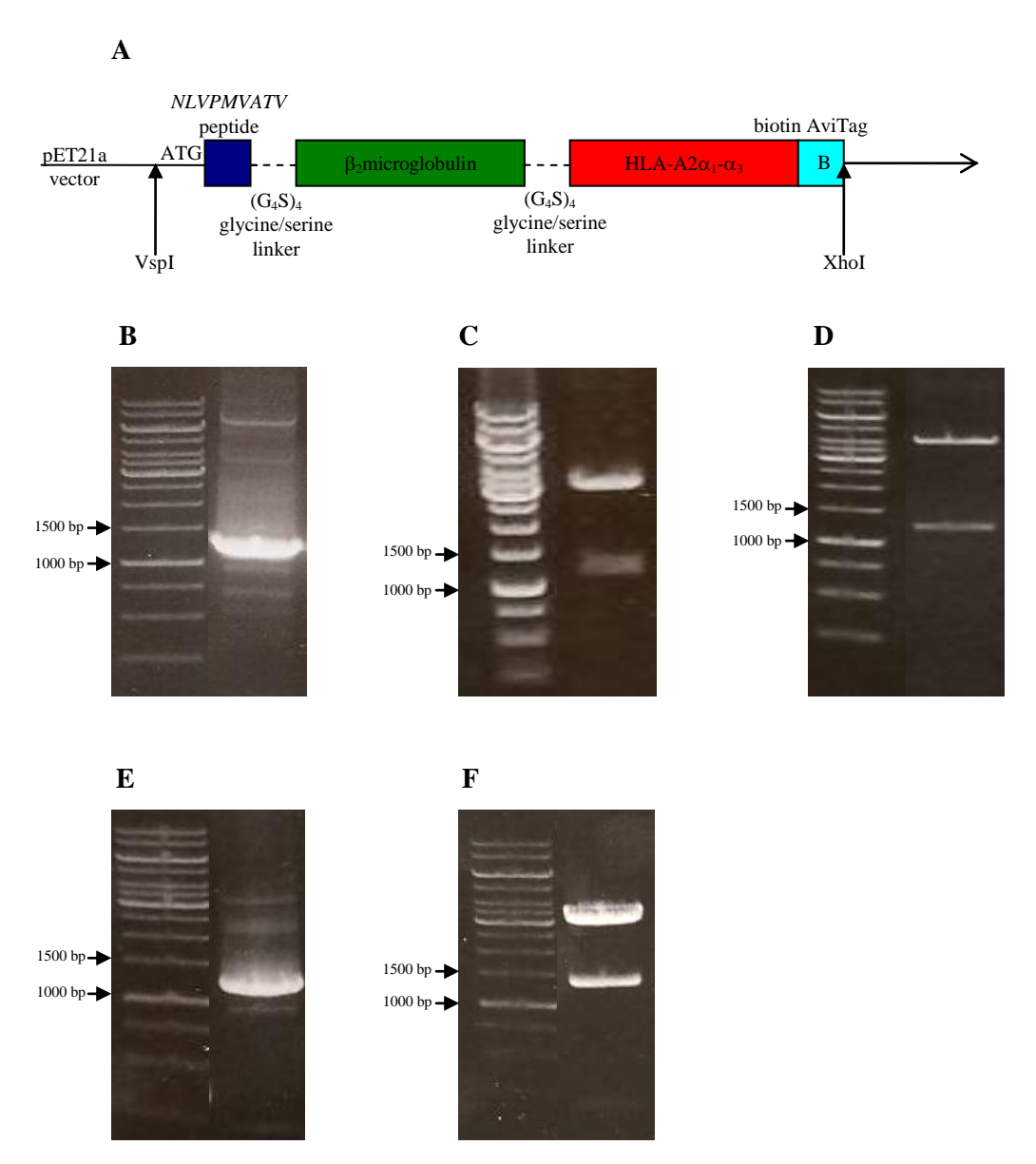


A illustrates the structure of the pET21a-CMV- β_2 microglobulin-HLA-A2 genetic construct In all gels lane 1 contains a DNA ladder

Gel B Lane 2 shows the amplified CMV- β_2 microglobulin-HLA-A2 fusion gene PCR product (1314 bp) Gel C Lane 2 shows a VspI/XhoI digest of pCR-Blunt II-TOPO CMV- β_2 microglobulin-HLA-A2:1305 bp band is the CMV- β_2 microglobulin-HLA-A2 fusion gene

Gel D Lane 2 shows a XhoI/KpnI digest of pET21a- CMV- β_2 microglobulin-HLA-A2 yielding a 514 bp band

A2 3.4 Production of pET21a-CMV-β₂microglobulin-HLA-A2-biotin-AviTag (SCT-B) genetic construct



A illustrates the structure of pET21a-CMV- β_2 microglobulin-HLA-A2 AviTag genetic construct In all gels lane 1 contains a DNA ladder

Gel B Lane 2 shows the amplified CMV- β_2 microglobulin-HLA-A2 fusion gene PCR product for subcloning into pAC-4 vector (1308 bp)

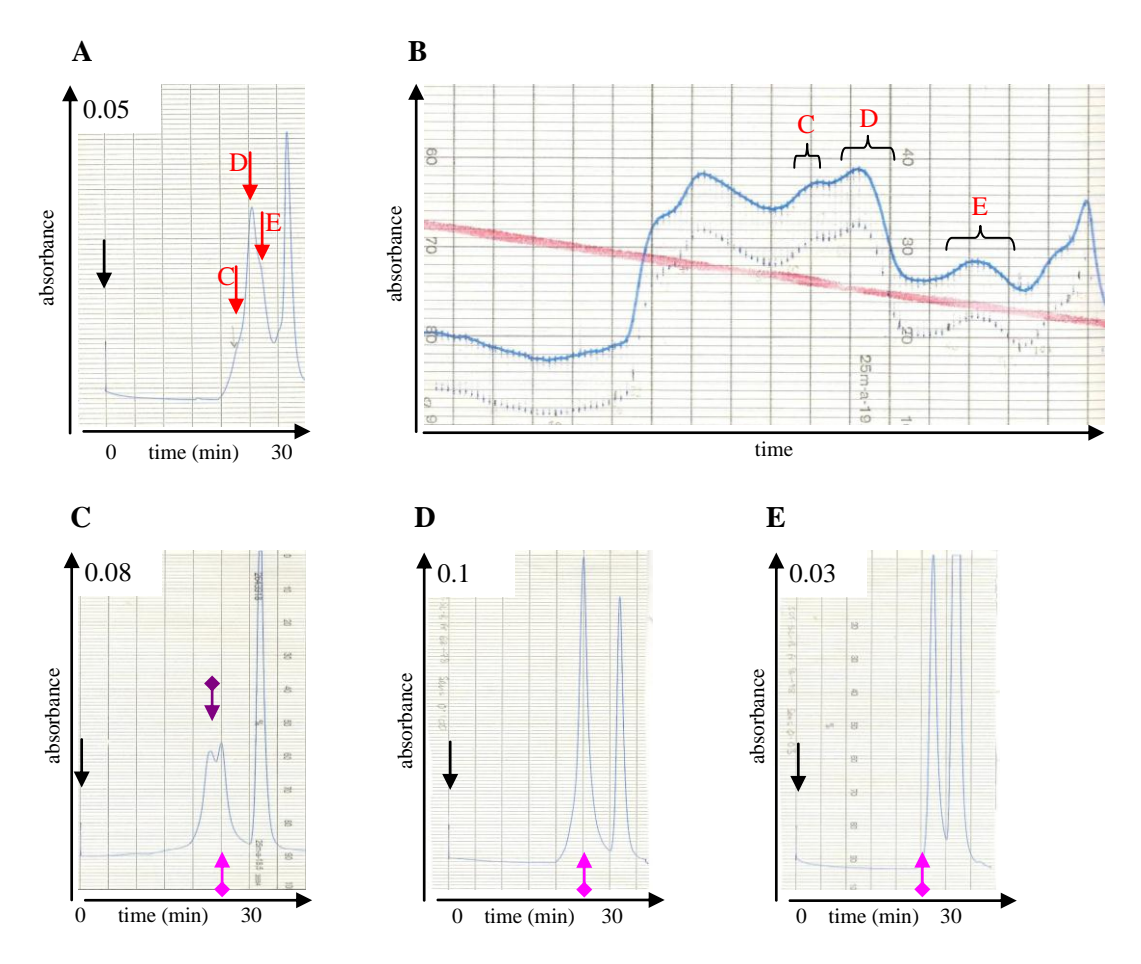
Gel C Lane 2 shows a XhoI/HindIII digest of pCR-Blunt II-TOPO CMV- β_2 microglobulin-HLA-A2:1298 bp band is the CMV- β_2 microglobulin-HLA-A2 fusion gene

Gel D Lane 2 shows a XhoI/HindIII digest of pAC-4-CMV- β_2 microglobulin-HLA-A2 yielding a 1298 bp band

Gel E Lane 2 shows the amplified CMV- β_2 microglobulin-HLA-A2-biotin-Avitag fusion gene PCR product (1379 bp)

Gel F Lane 2 shows a VspI/XhoI digest of pCR-Blunt II-TOPO CMV- β_2 microglobulin-HLA-A2-biotin-Avitag: 1369 bp band is CMV- β_2 microglobulin-HLA-A2-biotin-Avitag fusion gene

A2 4.1 Purification of SCT-SL-B using size exclusion chromatography



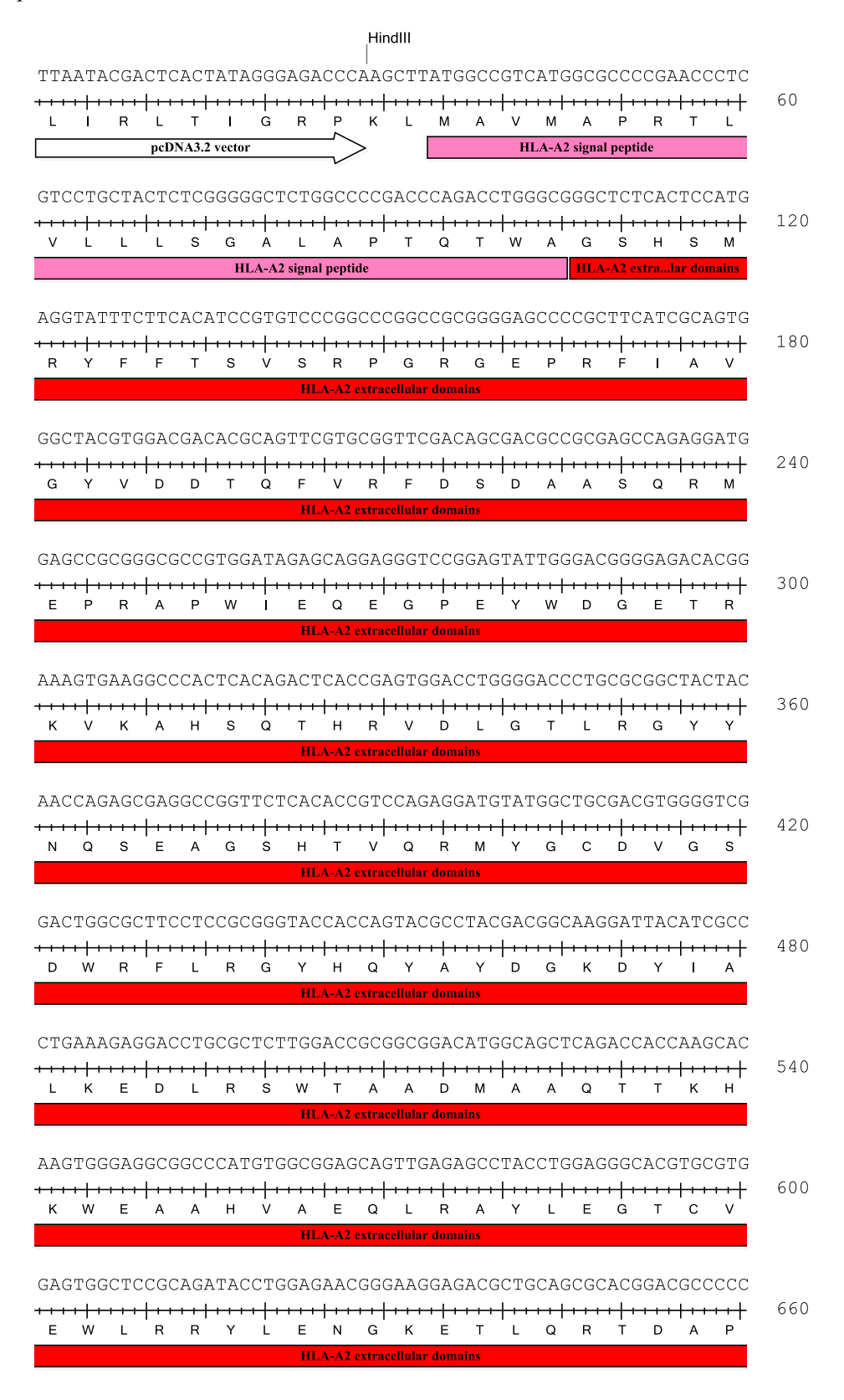
A demonstrates the HPLC chromatogram for SCT-SL-B (as shown in figure 3.13 I) refolded using the method of Oved et al. The arrows, peaks and fractions collected correspond to those described in the figure legend of figure 3.15 for SCT-SL-C.

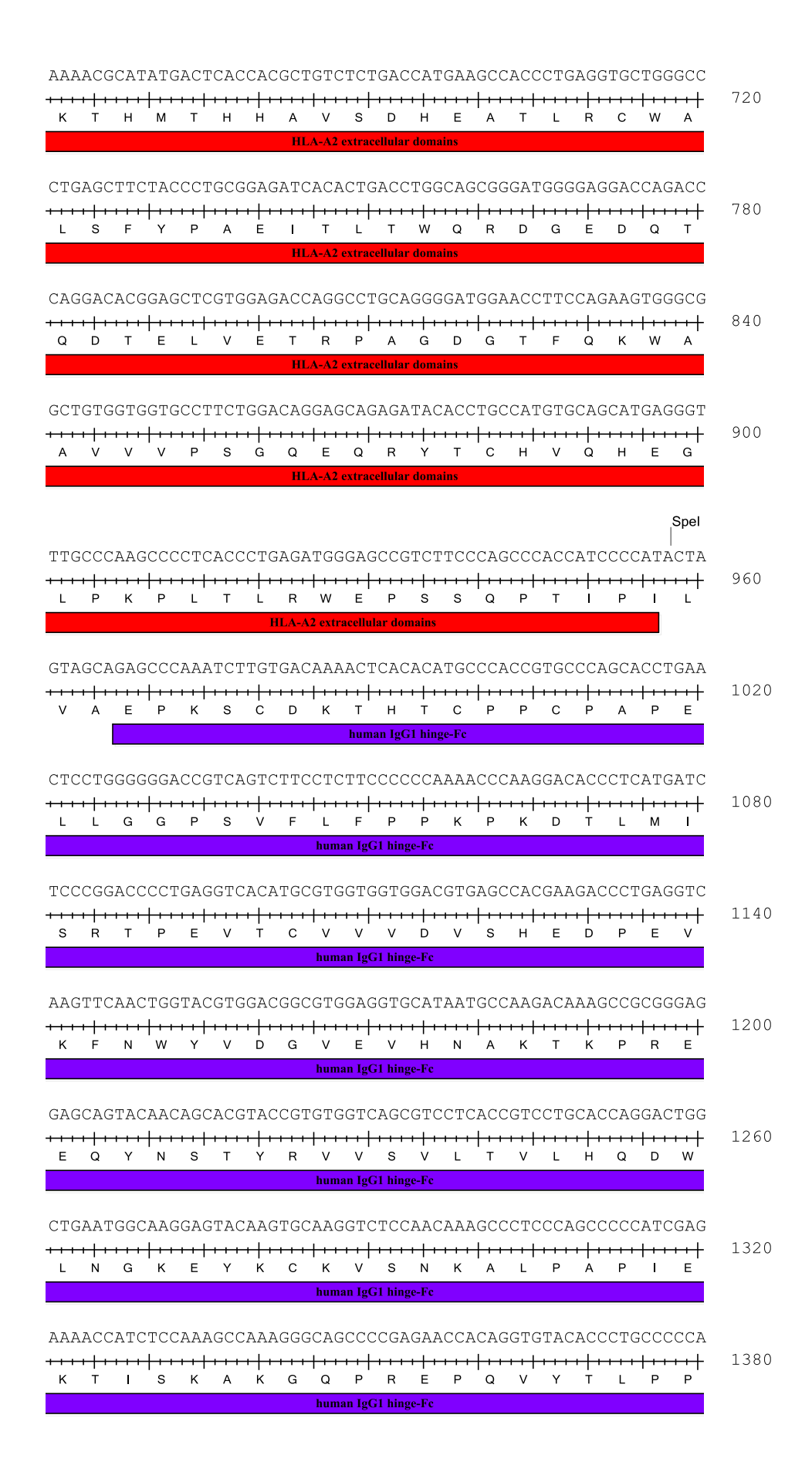
Appendix 3: Sequences

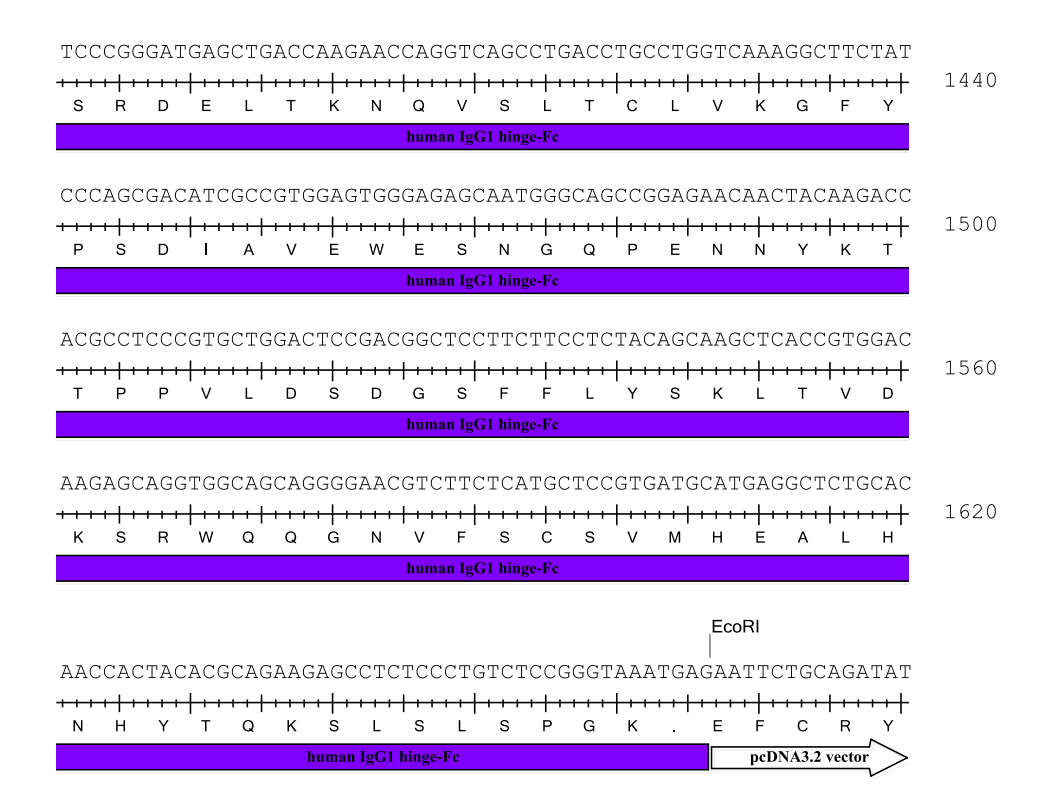
A3 1 Sequences of human constructs produced in mammalian cells

A3 1.1 pcDNA3.2-HLA-A2-human IgG₁ hinge-Fc

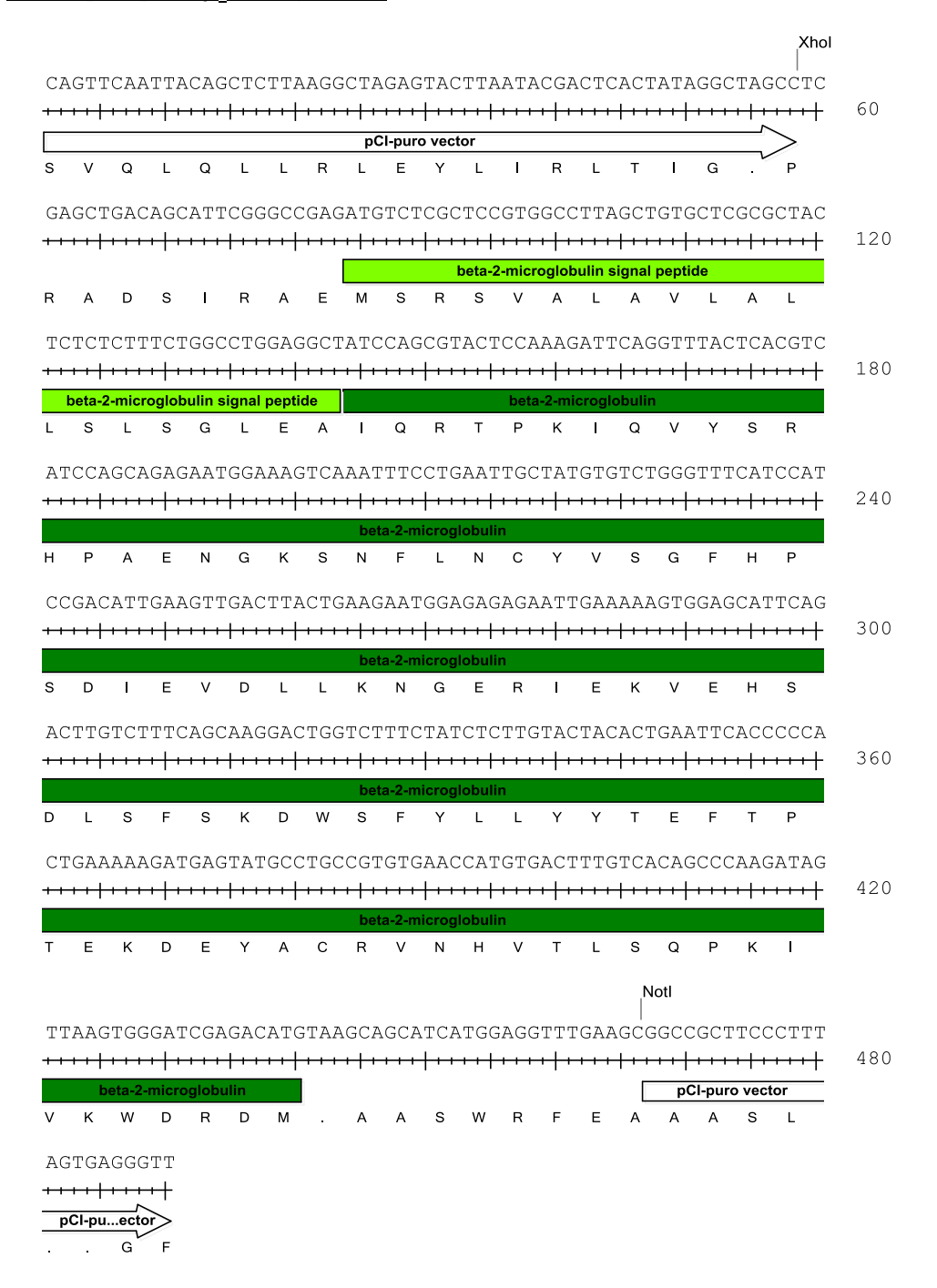
Mammalian sequences all presented using the SeqBuilder application of the DNASTAR Lasergene software suite. Restriction enzyme sites relevant to the production of a construct are indicated on the sequences.



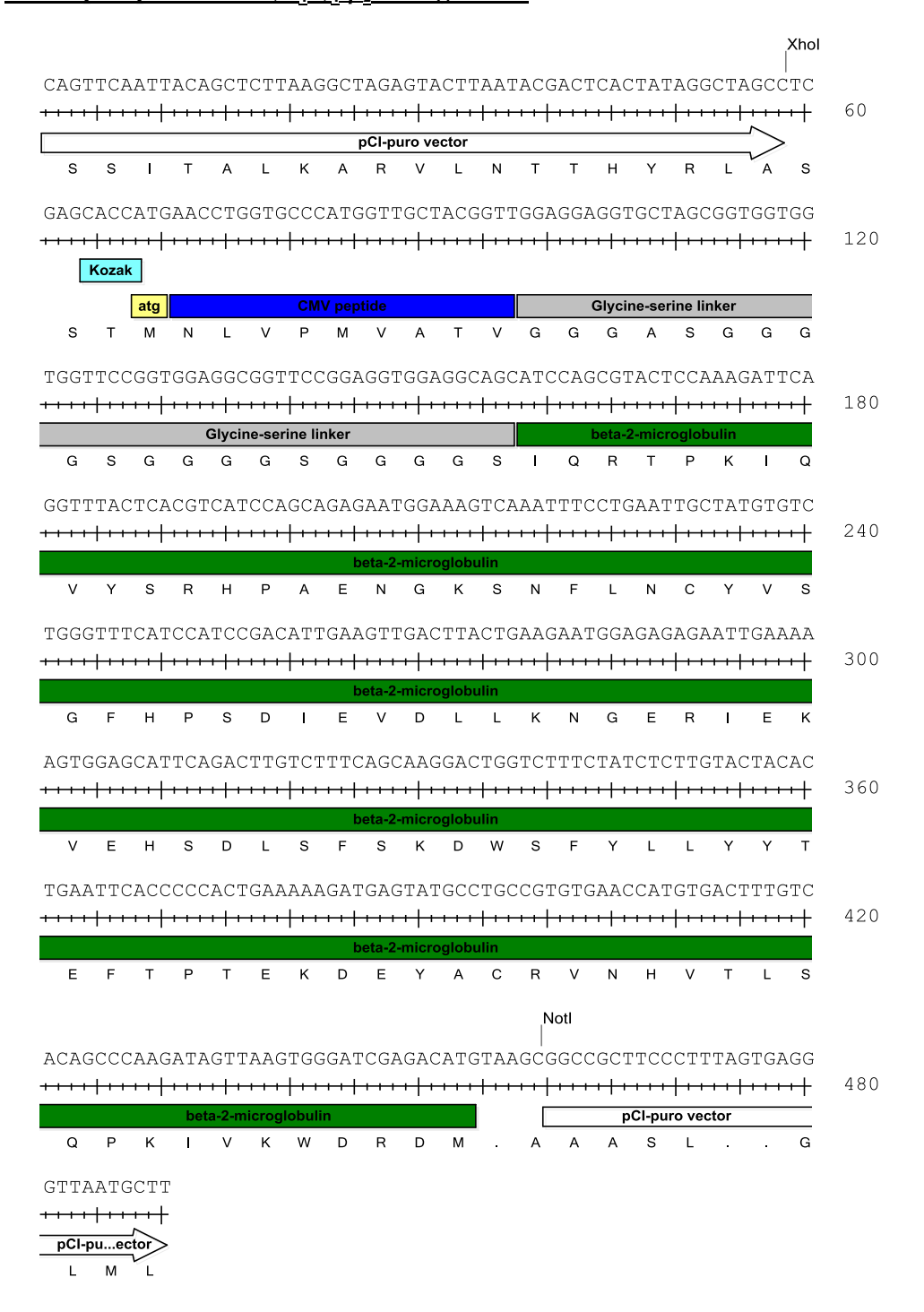




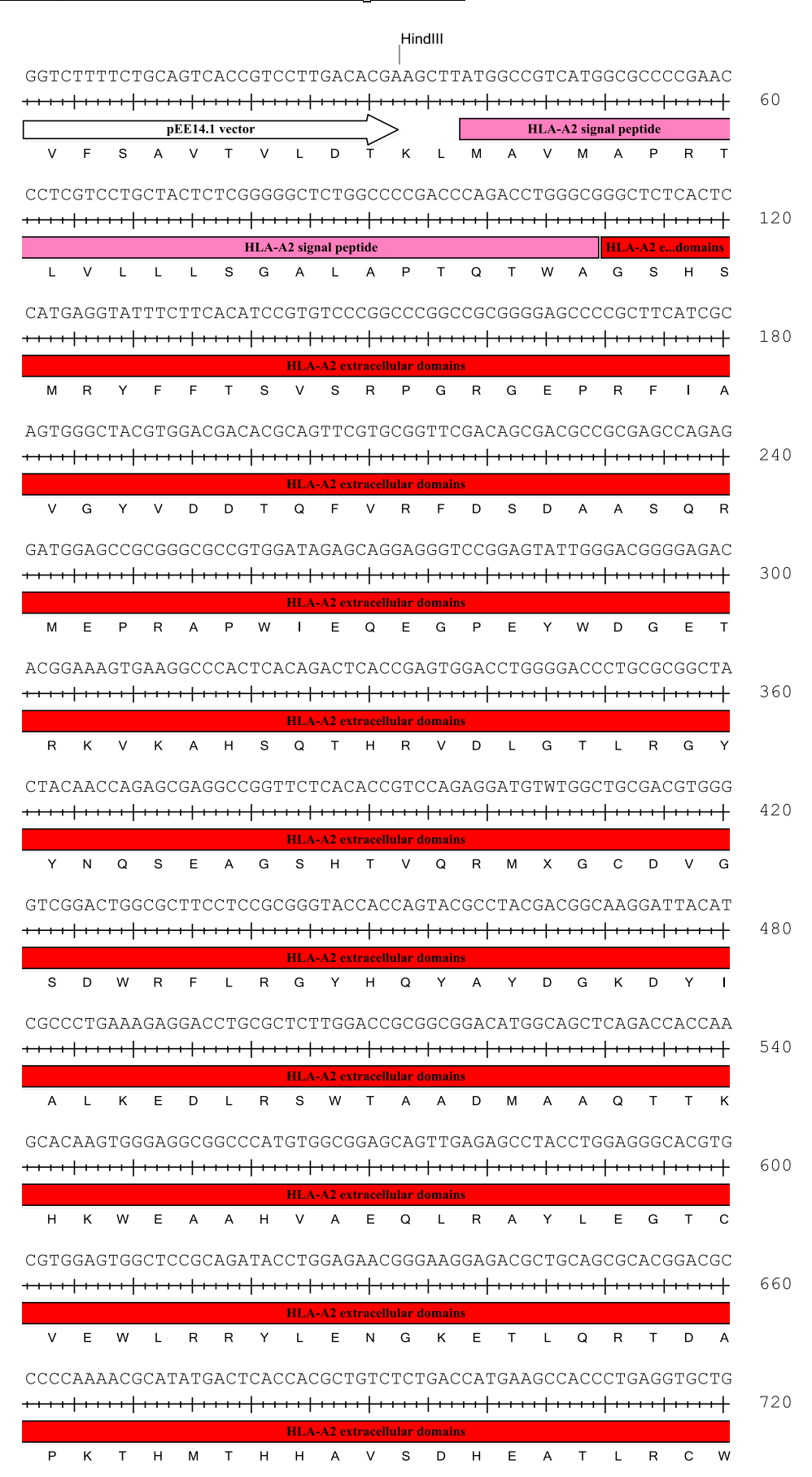
A3 1.2 pCI-puro-β₂microglobulin

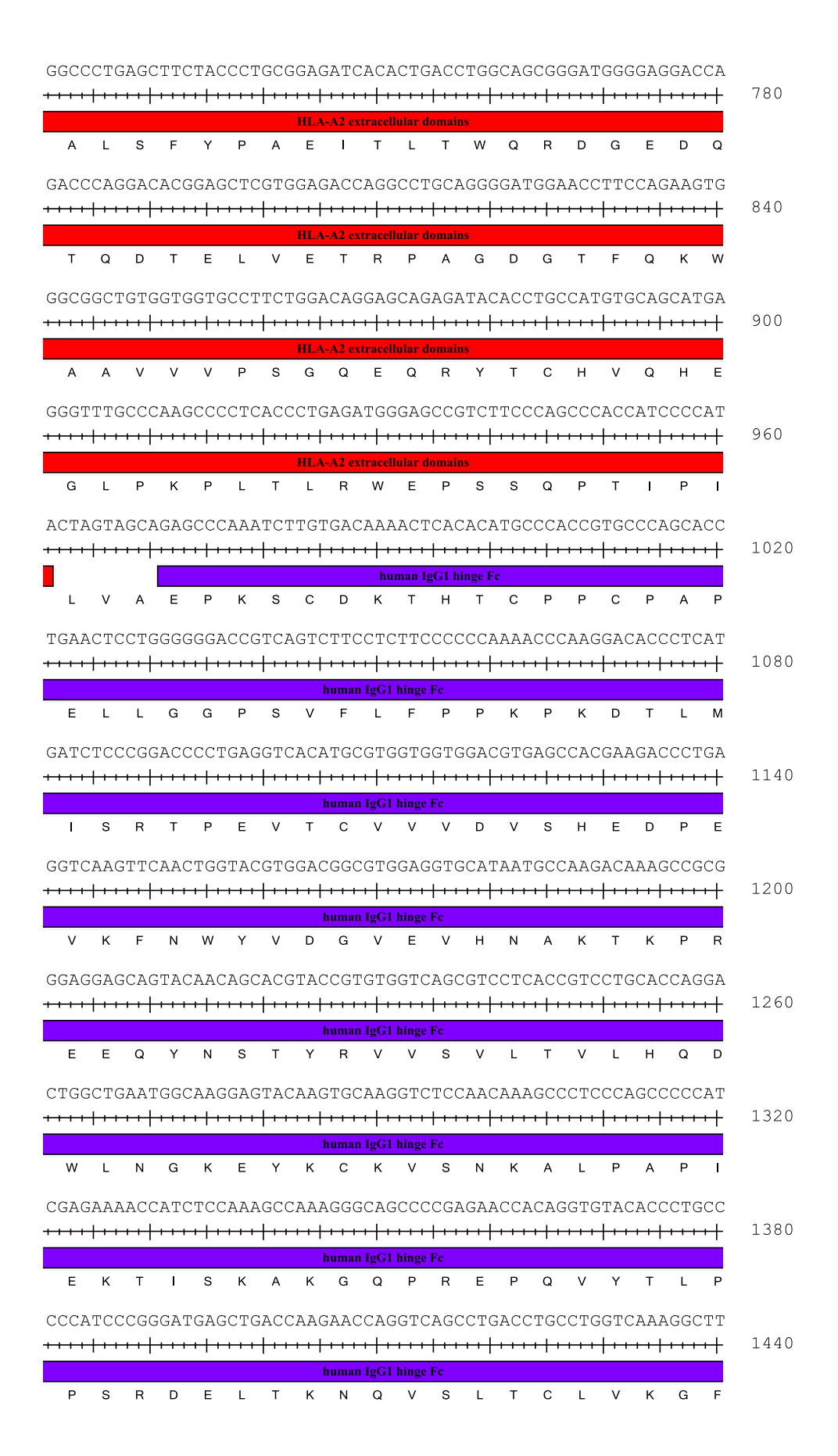


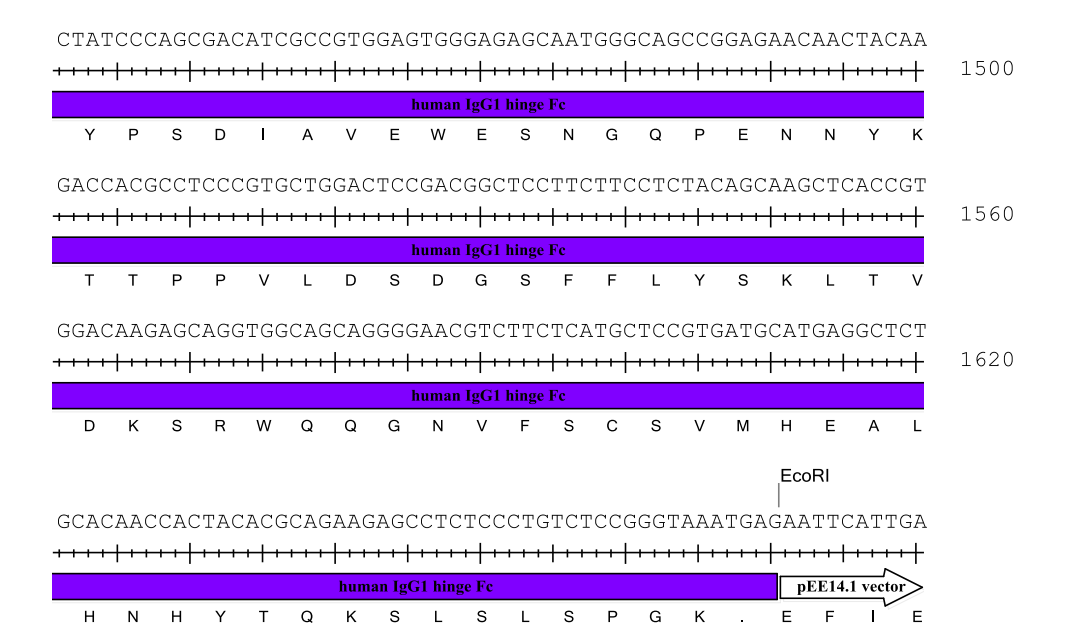
A3 1.3 pCI-puro-CMV-(G₄S)₄-β₂microglobulin



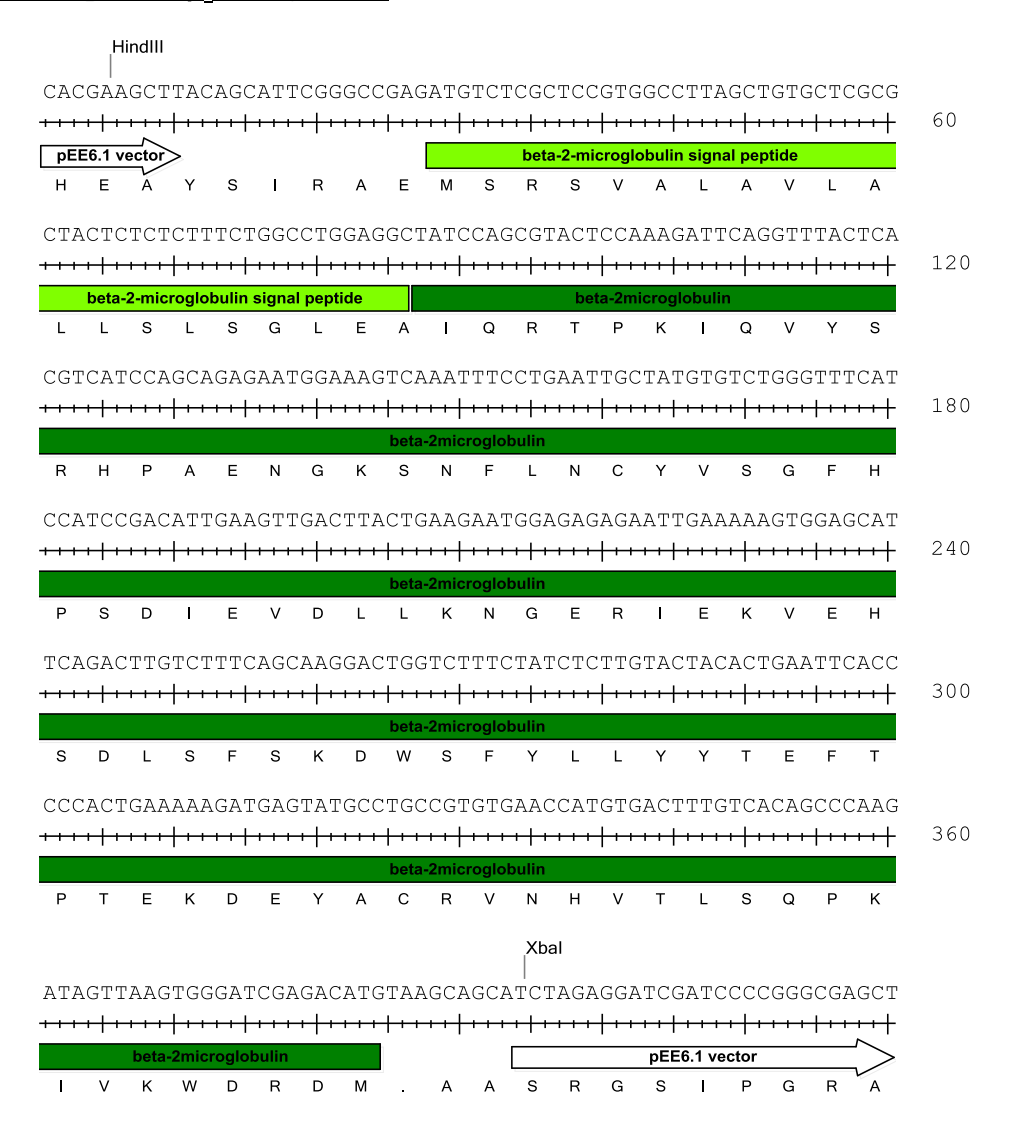
A3 3.4 pEE14.1-HLA-A2-human IgG₁ hinge-Fc



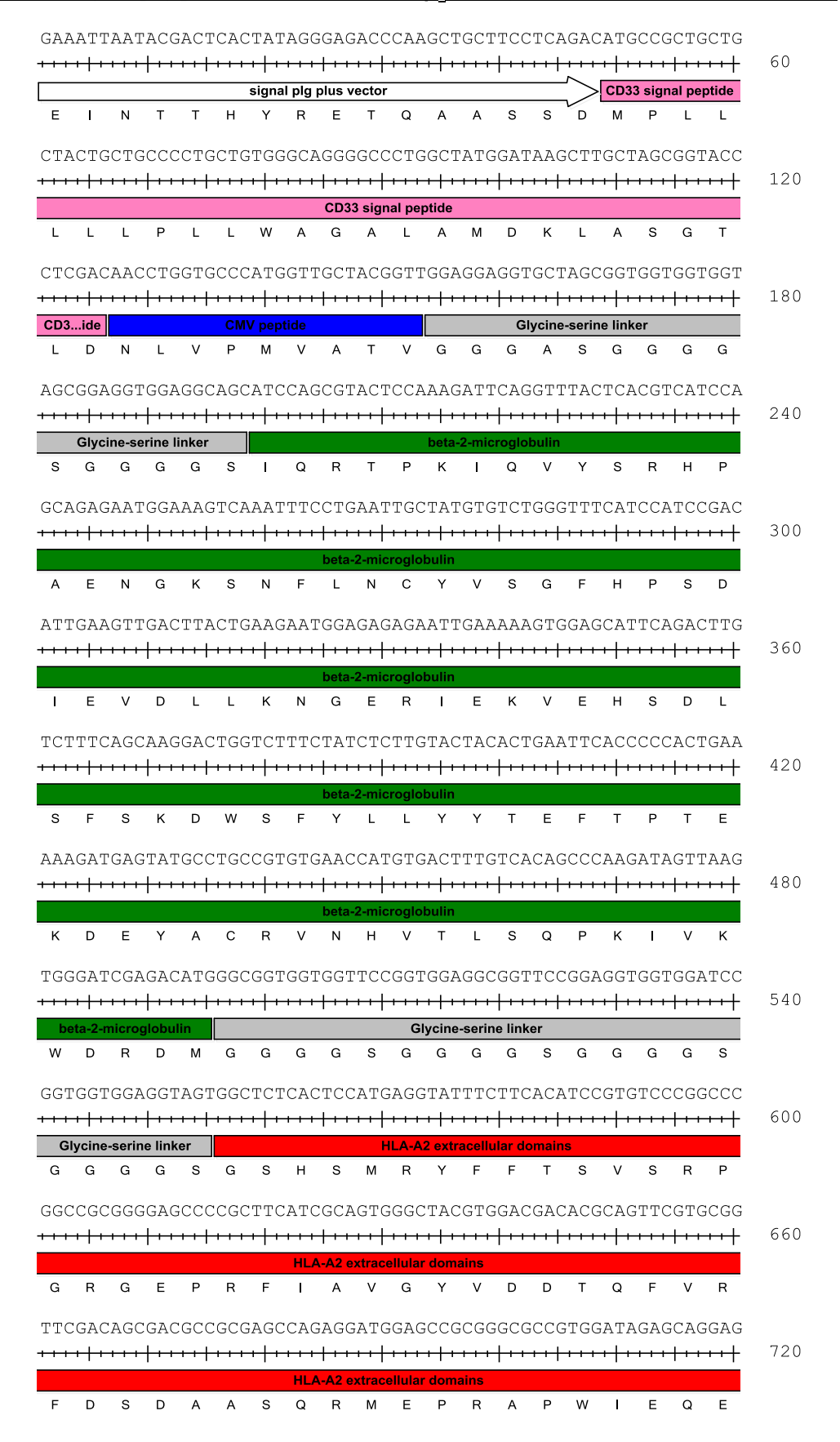


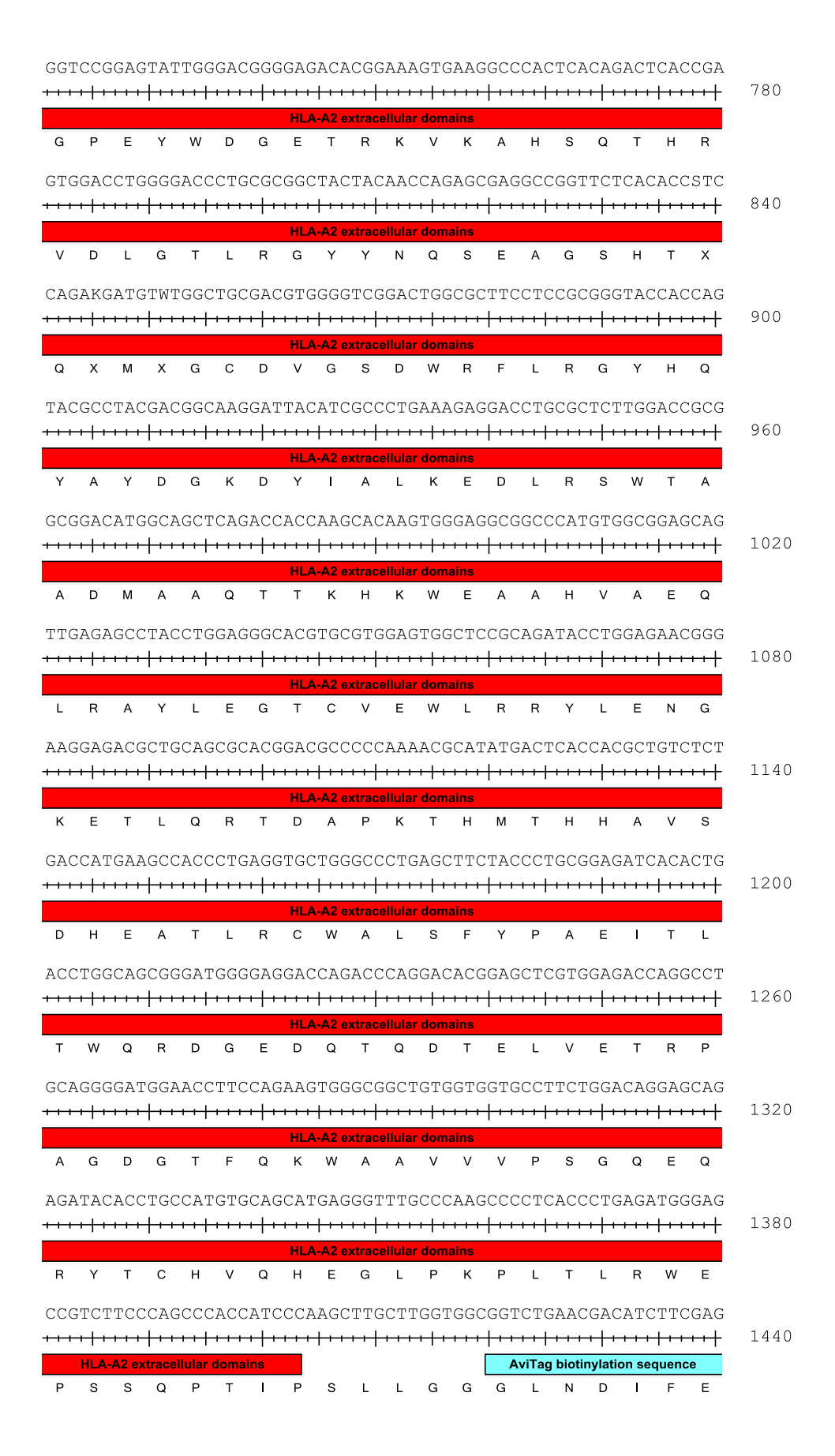


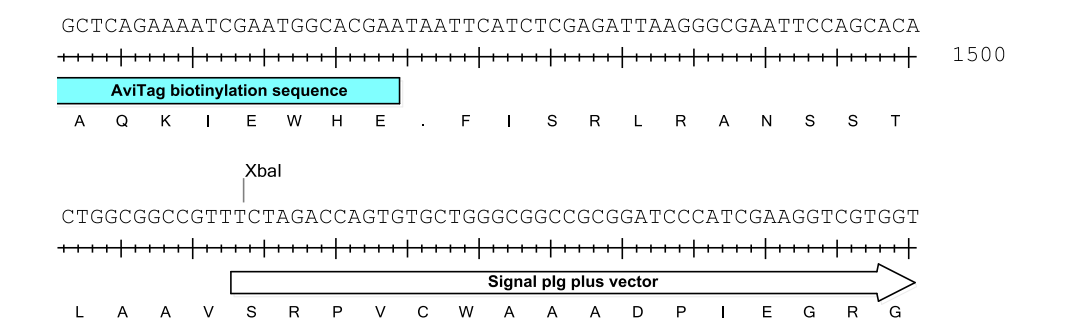
A3 3.5 pEE6.1-β₂microglobulin



A3 3.6 Signal pIg plus-CMV-short linker-β₂microglobulin-HLA-A2-biotin-AviTag







A3 2 Sequences of human constructs produced in bacterial cells

Bacterial sequences presented using the MegAlign application of the DNASTAR Lasergene software suite.

10	Majority	CATAAT <mark>AT</mark>								
SCT-B CATAATATGAACCTGGTGCCCATGGTTGCTACGGTTGGAGGAGGTGCTAGCGGTGGTGGTTCCGGTGGAGGCGGTT SCT-Cys-I CATAATATGAACCTGGTGCCCATGGTTGCTACGGTTGGAGGAGGTGCTAGCGGTGGTGGTGTTCCGGTGGAGGCGGTT SCT-Cys-II CATAATATGAACCTGGTGCCCATGGTTGCTACGGTTGGAGGAGGTGCTAGCGGTGGTGGTGGTTCCGGTGGAGGCGGTT SCT-Cys-III CATAATATGAACCTGGTGCCCATGGTTGCTACGGTTGGAGGAGGTGCTAGCGGTGGTGGTGGTGCTCCGGTGGAGGCGGTT SCT-Cys-III CATAATATGAACCTGGTGCCCATGGTTGCTACGGTTGGAGGAGGTGCTAGCGGTGGTGGTGCTCCGGTGAGGCCGGTT SCT-SL-B DST CATAATATGAACCTGGTGCCCATGGTTGCTACGGTTGGAGGAGGTGCTAGCGGTGGTGGTGTTCCGGTGAGGCGGTT SCT-SL-B CATAATATGAACCTGGTGCCCATGGTTGCTACGGTTGGAGGAGGTGCTAGCGGTGGTGGTGTGTAG SCT-SL-C CATAATATGAACCTGGTGCCCATGGTTGCTACGGTTGGAGGAGGTGCTAGCGGTGGTGGTGGTGTAG SCT-SL-C CATAATATGAACCTGGTGCCCATGGTTGCTACGGTTGGAGGAGGTGCTAGCGGTGGTGGTGTGTAG SCT-SL-C SCT-SL-C CATAATATGAACCTGGTGCCCATGGTTGCTACGGTTGGAGGAGGTGCTAGCGGTGGTGGTGT			10	20	30	40	50	60	70	80
SCT-C SCT-Cys-I SCT-Cys-II CATAATATGAACCTGGTGCCCATGGTTGCTACGGTTGGAGGAGGTGCTAGCGGTGGTGGTGTTCCGGTGAGGCGGTT SCT-Cys-II CATAATATGAACCTGGTGCCCATGGTTGCTACGGTTGCAGGAGGAGGTGCTAGCGGTGGTGTTCCGGTGGAGGCGGTT SCT-Cys-III SCT-Cys-III CATAATATGAACCTGGTGCCCATGGTTGCTACGGTTGGAGGAGGTGCTAGCGGTTGGTGTGCTTCCGGTGGAGGCGGTT SCT-SL-B DST SCT-SL-B DST SCT-SL-B SCT-SL-C CATAATATGAACCTGGTGCCCATGGTTGCTACGGTTGGAGGAGGTGCTAGCGGTGGTGGTGGTGCTTCCGGTGGAGGCGGTT SCT-SL-B SCT-SL-C CATAATATGAACCTGGTGCCCATGGTTGCTACGGTTGGAGGAGGTGCTAGCGGTGGTGGTGGTGTGCTACGGTTGGAGGAGGAGGTGCTAGCGGTGGTGGTGGTGGTGCTACGGTTGCTACCGGTTGGAGGAGGAGGTGCTAGCGGTGGTGGTGGTGCTAG SCT-SL-C SCT-X CATAATATGAACCTGGTGCCCATGGTTGCTACGGTTGGAGGAGGAGGTGCTAGCGGTGGTGGTGGTGTAG SCT-SL-C SCT-X CATAATATGAACCTGGTGCCCATGGTTGCTACGGTTGGAGGAGGAGGTGCTAGCGGTGGTGGTGGTGTAG SCT-X CATAATATGAACCTGGTGCCCATGGTTGCTACGGTTGGAGGAGGTGCTAGCGGTGGTGGTGGTGTTCCGGTGGAGGCGGTT Majority CGGAGGTGGAGGCAGCATCCAGCGTACTCCAAAGATTCAGGTTTACTCACGTCATCCAGCAGAGAATGGAAAGTCAAAT	SCT-3xCys	CATAAT <mark>AT</mark>	GAACCTGG:	GCCCATGGT	TGCTACGGTT	GGAGGAGGTG	CTAGCGGTG	GTGGTGGTTC	CGGTGGAGGC	GGTTC
SCT-Cys-I SCT-Cys-II SCT-SL-B SCT-SL-B SCT-SL-B SCT-SL-B SCT-SL-B SCT-SL-B SCT-SL-B SCT-SL-C SCT-SL-B SCT-SL-C SCT-SL-B SCT-SL-C SCGAGGTGGAGGCAGCATCCAGCGTACTCCAAAGATTCAGGTTTACTCACGTCATCCAGCAGAGAAATGGAAAGTCAAAT SCT-Cys-II CGGAGGTGGAGGCAGCATCCAGCGTACTCCAAAGATTCAGGTTTACTCACGTCATCCAGCAGAGAATGGAAAGTCAAAT SCT-Cys-II CGGAGGTGGAGGCAGCATCCAGCGTACTCCAAAGATTCAGGTTTACTCACGTCATCCAGCAGAGAATGGAAAGTCAAAT SCT-Cys-II CGGAGGTGGAGGCAGCATCCAGCGTACTCCAAAGATTCAGGTTTACTCACGTCATCCAGCAGAGAATGGAAAGTCAAAT SCT-Cys-II CGGAGGTGGAGGCAGCATCCAGCGTACTCCAAAGATTCAGGTTTACTCACGTCATCCAGCAGAGAATGGAAAGTCAAAT SCT-SL-B SCGAGGTGGAGGCAGCATCCAGCGTACTCCAAAGATTCAGGTTTACTCACGTCATCCAGCAGAGAATGGAAAGTCAAAT SCT-SL-B SCGAGGTGGAGGCAGCATCCAGCGTACTCCAAAGATTCAGGTTTACTCACGTCATCCAGCAGAGAATGGAAAGTCAAAT SCT-SL-B CGGAGGTGAGGCAGCATCCAGCGTACTCCAAAGATTCAGGTTTACTCACGTCATCCAGCAGAGAATGGAAAGTCAAAT SCT-SL-B CGGAGGTGGAGGCAGCATCCAGCGTACTCCAAAGATTCAGGTTTACTCACGTCATCCAGCAGAGAATGGAAAGTCAAAT SCT-SL-B CGGAGGTGGAGGCAGCATCCAGCGTACTCCAAAGATTCAGGTTTACTCACGTCATCCAGCAGAGAATGGAAAGTCAAAT SCT-SL-B CGGAGGTGGAGGCAGCATCCAGCGTACTCCAAAGATTCAGGTTTACTCACGTCATCCAGCAGAGAATGGAAAGTCAAAT SCT-SL-B CGGAGGTGGAGGCAGCATCCAGCGTACTCCAAAGATTCAGGTTTACTCACGTCATCCAGCAGAGAATGGAAAGTCAAAT SCT-SL-C CGGAGGTGGAGGCAGCATCCAGCGTACTCCAAAGATTCAGGTTTACTCACGTCATCCAGCAGAGAATGGAAAGTCAA	SCT-B	CATAAT <mark>AT</mark>	G <mark>AACCTGG</mark>	GCCCATGGT	TGCTACGGTT	GGAGGAGGTG	GCTAGCGGTG	GTGGTGGTTC	CGGTGGAGGC	GGTTC
SCT-Cys-II CATAATATGAACCTGGTGCCCATGGTTGCTACGGTTGGAGGAGGTGCTAGCGGTGGTGGTGGTGGAGGGGGTTGCTCYs-III CATAATATGAACCTGGTGCCCATGGTTGCTACGGTTGGAGGAGGTGCTAGCGGTGGTGGTGGTGTTCCGGTGGAGGCGGTTGCTSCT-SL-B DST CATAATATGAACCTGGTGCCCATGGTTGCTACGGTTGGATGGTGCTAGCGGTGGTGGTGGTGGTGTGTGGAGGCGGTTGCTSL-B CATAATATGAACCTGGTGCCCATGGTTGCTACGGTTGGATGGTGCTAGCGGTGGTGGTGGTGTGTAG SCT-SL-B CATAATATGAACCTGGTGCCCATGGTTGCTACGGTTGGAGGAGGTGCTAGCGGTGGTGGTGGTGAG	SCT-C	CATAAT <mark>AT(</mark>	GAACCTGG:	GCCCATGGT	TGCTACGGTT	GGAGGAGGTG	GCTAGCGGTG	GTGGTGGTTC	CGGTGGAGGC	GGTTC
SCT-Cys-III CATAATATGAACCTGGTGCCCATGGTTGCTACGGTTGGAGGAGGTGCTAGCGGTGGTGGTGGTGGTGGAGGGGGTT SCT-SL-B DST CATAATATGAACCTGGTGCCCATGGTTGCTACGGTTGGAGGAGGTGCTAGCGGTGGTGGTGGTGGTAG SCT-SL-C CATAATATGAACCTGGTGCCCATGGTTGCTACGGTTGGAGGAGGTGCTAGCGGTGGTGGTGGTGAG SCT-X CATAATATGAACCTGGTGCCCATGGTTGCTACGGTTGGAGGAGGTGCTAGCGGTGGTGGTGGTGAG SCT-X CATAATATGAACCTGGTGCCCATGGTTGCTACGGTTGGAGGAGGTGCTAGCGGTGGTGGTGGTGGTG	SCT-Cys-I	CATAAT <mark>AT</mark>	GAACCTGG:	GCCCATGGT	TGCTACGGTT	GGAGGAGGTG	GCTAGCGGTG	GTGGTGGTTC	CGGTGGAGGC	GGTTC
SCT-SL-B DST CATAATATGAACCTGGTGCCCATGGTTGCTACGGTTGGA SCT-SL-B CATAATATGAACCTGGTGCCCATGGTTGCTACGGTTGGAGGAGGTGGTGGTGGTGGTGGT	SCT-Cys-II	CATAAT <mark>AT(</mark>	GAACCTGG:	GCCCATGGT	TGCTACGGTT	GGAGGAGGTG	GCTAGCGGTG	GTGGTGGTTC	CGGTGGAGGC	GGTTC
SCT-SL-B SCT-SL-C CATAATATGAACCTGGTGCCCATGGTTGCTACGGTTGGAGGAGGTGGTGGTGGTGGTAG SCT-X CATAATATGAACCTGGTGCCCATGGTTGCTACGGTTGGAGGAGGTGCTAGCGGTGGTGGTGGTAG SCT-X CATAATATGAACCTGGTGCCCATGGTTGCTACGGTTGGAGGAGGTGCTAGCGGTGGTGGTGGTGCTCCGGTGGAGGGGGTGT Majority CGGAGGTGGAGGCAGCATCCAGCGTACTCCAAAGATTCAGGTTTACTCACGTCATCCAGCAGAGAATGGAAAGTCAAAT 90 100 110 120 130 140 150 SCT-3xCys SCT-B CGGAGGTGGAGGCAGCATCCAGCGTACTCCAAAGATTCAGGTTTACTCACGTCATCCAGCAGAGAATGGAAAGTCAAAT SCT-C CGGAGGTGGAGGCAGCATCCAGCGTACTCCAAAGATTCAGGTTTACTCACGTCATCCAGCAGAGAATGGAAAGTCAAAT SCT-Cys-I CGGAGGTGGAGGCAGCATCCAGCGTACTCCAAAGATTCAGGTTTACTCACGTCATCCAGCAGAGAATGGAAAGTCAAAT SCT-Cys-II CGGAGGTGGAGGCAGCATCCAGCGTACTCCAAAGATTCAGGTTTACTCACGTCATCCAGCAGAGAATGGAAAGTCAAAT SCT-Cys-III CGGAGGTGGAGGCAGCATCCAGCGTACTCCAAAGATTCAGGTTTACTCACGTCATCCAGCAGAGAATGGAAAGTCAAAT SCT-SL-B DST CGGAGGTGGAGGCAGCATCCAGCGTACTCCAAAGATTCAGGTTTACTCACGTCATCCAGCAGAGAATGGAAAGTCAAAT SCT-SL-B CGGAGGTGGAGGCAGCATCCAGCGTACTCCAAAAGATTCAGGTTTACTCACGTCATCCAGCAGAGAATGGAAAGTCAAAT SCT-SL-B CGGAGGTGGAGGCAGCATCCAGCGTACTCCAAAAGATTCAGGTTTACTCACGTCATCCAGCAGAGAATGGAAAGTCAAAT SCT-SL-B CGGAGGTGGAGGCAGCATCCAGCGTACTCCAAAAGATTCAGGTTTACTCACGTCATCCAGCAGAAATGGAAAGTCAAAT CGGAGGTGGAGGCAGCATCCAGCGTACTCCAAAAGATTCAGGTTTACTCACGTCATCCAGCAGAGAATGGAAAGTCAAAT CGGAGGTGGAGGCAGCATCCAGCGTACTCCAAAAGATTCAGGTTTACTCACGTCATCCAGCAGAGAATGGAAAGTCAAAT CGGAGGTGGAGGCAGCATCCAGCGTACTCCAAAAGATTCAGGTTTACTCACGTCATCCAGCAGAAATGGAAATGAAAT CGGAGGTGGAGGCAGCATCCAGCGTACTCCAAAAGATTCAGGTTTACTCACGTCA	SCT-Cys-III	CATAAT <mark>AT(</mark>	GAACCTGG:	GCCCATGGT	TGCTACGGTT	GGAGGAGGTG	GCTAGCGGTG	GTGGTGGTTC	CGGTGGAGGC	GGTTC
SCT-SL-C SCT-X CATAATATGAACCTGGTGCCCATGGTTGCTACGGTTGGAGGAGGTGCTAGCGGTGGTGGTGGTGGTAG SCT-X CATAATATGAACCTGGTGCCCATGGTTGCTACGGTTGGAGGAGGTGCTAGCGGTGGTGGTGGTGGTGGAGGCGGTT Majority CGGAGGTGGAGGCAGCATCCAGCGTACTCCAAAGATTCAGGTTTACTCACGTCATCCAGCAGAGAATGGAAAGTCAAAAT	SCT-SL-B DST	CATAAT <mark>AT(</mark>	GAACCTGG:	GCCCATGGT	TGCTACGGTT	GGA <mark>TGT</mark> GGTG	GCTAGCGGTG	GTGGTGGT	AG	
SCT-X CATAATATGAACCTGGTGCCCATGGTTGCTACGGTTGGAGGGGGTGCTAGCGGTGGTGGTGCTCCGGTGGAGGCGGTT Majority CGGAGGTGGAGGCAGCATCCAGCGTACTCCAAAGATTCAGGTTTACTCACGTCATCCAGCAGAGAATGGAAAGTCAAAT 90 100 110 120 130 140 150 SCT-3xCys CGGAGGTGGAGGCAGCATCCAGCGTACTCCAAAGATTCAGGTTTACTCACGTCATCCAGCAGAGAATGGAAAGTCAAAT SCT-B CGGAGGTGGAGGCAGCATCCAGCGTACTCCAAAGATTCAGGTTTACTCACGTCATCCAGCAGAGAATGGAAAGTCAAAT SCT-C CGGAGGTGGAGGCAGCATCCAGCGTACTCCAAAGATTCAGGTTTACTCACGTCATCCAGCAGAGAATGGAAAGTCAAAT SCT-Cys-I CGGAGGTGGAGGCAGCATCCAGCGTACTCCAAAGATTCAGGTTTACTCACGTCATCCAGCAGAGAATGGAAAGTCAAAT SCT-Cys-II CGGAGGTGGAGGCAGCATCCAGCGTACTCCAAAGATTCAGGTTTACTCACGTCATCCAGCAGAGAATGGAAAGTCAAAT SCT-Cys-III CGGAGGTGGAGGCAGCATCCAGCGTACTCCAAAGATTCAGGTTTACTCACGTCATCCAGCAGAGAATGGAAAGTCAAAT SCT-SL-B DST CGGAGGTGGAGGCAGCATCCAGCGTACTCCAAAGATTCAGGTTTACTCACGTCATCCAGCAGAGAATGGAAAGTCAAAT SCT-SL-B CGGAGGTGGAGGCAGCATCCAGCGTACTCCAAAGATTCAGGTTTACTCACGTCATCCAGCAGAGAATGGAAAGTCAAAT SCT-SL-B CGGAGGTGGAGGCAGCATCCAGCGTACTCCAAAGATTCAGGTTTACTCACGTCATCCAGCAGAGAATGGAAAGTCAAAT SCT-SL-B CGGAGGTGGAGGCAGCATCCAGCGTACTCCAAAGATTCAGGTTTACTCACGTCATCCAGCAGAGAATGGAAAGTCAAAT SCT-SL-B CGGAGGTGGAGGCAGCATCCAGCGTACTCCAAAGATTCAGGTTTACTCACGTCATCCAGCAGAGAATGGAAAGTCAAAT CCT-SL-B CGGAGGTGGAGGCAGCATCCAGCGTACTCCAAAGATTCAGGTTTACTCACGTCATCCAGCAGAGAATGGAAAGTCAAAT CCT-SL-B CGGAGGTGGAGGCAGCATCCAGCGTACTCCAAAGATTCAGGTTTACTCACGTCATCCAGCAGAGAATGGAAAGTCAAAT CCGAGGTGGAGGCAGCATCCAGCGTACTCCAAAAGATTCAGGTTTACTCACGTCATCCAGCAGAGAATGGAAAGTCAAAT CCGAGGTGGAGGCAGCATCCAGCGTACTCCAAAAGATTCAGGTTTACTCACGTCATCCAGCAGAGAATGGAAAGTCAAAT CCGAGGTGGAGGCAGCATCCAGCGTACTCCAAAAGATTCAGGTTTACTCACGTCATCCAGCAGAGAATGGAAAAGTCAAAT CCGAGGTGGAGGCAGCATCCAGCGTACTCCAAAAGATTCAGGTTTACTCACGTCATCCAGCAGAGAATGGAAAAGTCAAAT CCT-SL-B CGGAGGTGGAGGCAGCATCCAGCGTACTCCAAAAGATTCAGGTTTACTCACGGTCATCCAGCAGAGAATGGAAAAGTCAAAT CCGAGGTGGAGGAGCAGCATCCAGCGTACTCCAAAAGATTCAGGTTTACTCACGGTCATCCAGCAGAGAATGGAAAATCAAAT CCGAGGTGGAGGAGCAGCATCCAGCGTACTCCAAAAGATTCAGGTTTACTCACGGTCATCCAGCAGAGAAAGTCAAAT CCGAGGTGAGCAGCATCCAGCGTACTCCAAAAGATTCAGGTTTACTCACGGTCATCCAGCGAG	SCT-SL-B	CATAAT <mark>AT(</mark>	GAACCTGG:	GCCCATGGT	TGCTACGGTI	GGAGGAGGT	CTAGCGGTG	GTGGTGGT	AG	
Majority CGGAGGTGGAGGCAGCATCCAGCGTACTCCAAAGATTCAGGTTTACTCACGTCATCCAGCAGAGAATGGAAAGTCAAAT 90 100 110 120 130 140 150 SCT-3xCys CGGAGGTGGAGGCAGCATCCAGCGTACTCCAAAGATTCAGGTTTACTCACGTCATCCAGCAGAGAATGGAAAGTCAAAT SCT-B CGGAGGTGGAGGCAGCATCCAGCGTACTCCAAAGATTCAGGTTTACTCACGTCATCCAGCAGAGAATGGAAAGTCAAAT SCT-C CGGAGGTGGAGGCAGCATCCAGCGTACTCCAAAGATTCAGGTTTACTCACGTCATCCAGCAGAGAATGGAAAGTCAAAT SCT-Cys-I CGGAGGTGGAGGCAGCATCCAGCGTACTCCAAAGATTCAGGTTTACTCACGTCATCCAGCAGAGAATGGAAAGTCAAAT SCT-Cys-II CGGAGGTGGAGGCAGCATCCAGCGTACTCCAAAGATTCAGGTTTACTCACGTCATCCAGCAGAGAATGGAAAGTCAAAT SCT-Cys-III CGGAGGTGGAGGCAGCATCCAGCGTACTCCAAAGATTCAGGTTTACTCACGTCATCCAGCAGAGAATGGAAAGTCAAAT SCT-SL-B DST CGGAGGTGGAGGCAGCATCCAGCGTACTCCAAAGATTCAGGTTTACTCACGTCATCCAGCAGAGAATGGAAAGTCAAAT SCT-SL-B CGGAGGTGGAGGCAGCATCCAGCGTACTCCAAAGATTCAGGTTTACTCACGTCATCCAGCAGAGAATGGAAAGTCAAAT SCT-SL-B CGGAGGTGGAGGCAGCATCCAGCGTACTCCAAAGATTCAGGTTTACTCACGTCATCCAGCAGAGAATGGAAAGTCAAAT SCT-SL-B CGGAGGTGGAGGCAGCATCCAGCGTACTCCAAAGATTCAGGTTTACTCACGTCATCCAGCAGAGAATGGAAAGTCAAAT SCT-SL-B CGGAGGTGGAGGCAGCATCCAGCGTACTCCAAAGATTCAGGTTTACTCACGTCATCCAGCAGAGAATGGAAAGTCAAAT SCT-SL-B CGGAGGTGGAGGCAGCATCCAGCGTACTCCAAAGATTCAGGTTTACTCACGTCATCCAGCAGAGAATGGAAAGTCAAAT SCT-SL-B CGGAGGTGGAGGCAGCATCCAGCGTACTCCAAAGATTCAGGTTTACTCACGTCATCCAGCAGAGAATGGAAAGTCAAAT SCT-SL-C CGGAGGTGGAGGCAGCATCCAGCGTACTCCAAAGATTCAGGTTTACTCACGTCATCCAGCAGAGAATGGAAAGTCAAAT SCT-SL-C CGGAGGTGGAGGCAGCATCCAGCGTACTCCAAAGATTCAGGTTTACTCACGTCATCCAGCAGAGAATGGAAAGTCAAAT	SCT-SI-C	C A M A A M A M A	<mark>3</mark> 3300000					атаатаат	7. (
90 100 110 120 130 140 150 SCT-3xCys SCT-B SCT-C SCT-	DCI DI C	CAIAAIAI	JAACCTGG.	IGCCCATGGT	TGCTACGGTT	'GGAGGAGGT'	CTAGCGGTG	JTGGTGGT	AG	
SCT-B CGGAGGTGGAGGCAGCATCCAGCGTACTCCAAAGATTCAGGTTTACTCACGTCATCCAGCAGAAATGGAAAGTCAAAT SCT-C CGGAGGTGGAGGCAGCATCCAGCGTACTCCAAAGATTCAGGTTTACTCACGTCATCCAGCAGAAATGGAAAGTCAAAT SCT-Cys-I CGGAGGTGGAGGCAGCATCCAGCGTACTCCAAAGATTCAGGTTTACTCACGTCATCCAGCAGAAATGGAAAGTCAAAT SCT-Cys-II CGGAGGTGGAGGCAGCATCCAGCGTACTCCAAAGATTCAGGTTTACTCACGTCATCCAGCAGAAATGGAAAGTCAAAT SCT-SL-B DST CGGAGGTGGAGGCAGCATCCAGCGTACTCCAAAGATTCAGGTTTACTCACGTCATCCAGCAGAAAATGGAAAGTCAAAT SCT-SL-B CGGAGGTGGAGGCAGCATCCAGCGTACTCCAAAGATTCAGGTTTACTCACGTCATCCAGCAGAAAATGGAAAGTCAAAT SCT-SL-B CGGAGGTGGAGGCAGCATCCAGCGTACTCCAAAGATTCAGGTTTACTCACGTCATCCAGCAGAAGAATGGAAAGTCAAAT SCT-SL-C CGGAGGTGGAGGCAGCATCCAGCGTACTCCAAAGATTCAGGTTTACTCACGTCATCCAGCAGAGAATGGAAAGTCAAAT										GGTTC
SCT-B CGGAGGTGGAGGCAGCATCCAGCGTACTCCAAAGATTCAGGTTTACTCACGTCATCCAGCAGAGAATGGAAAGTCAAAT SCT-C CGGAGGTGGAGGCAGCATCCAGCGTACTCCAAAGATTCAGGTTTACTCACGTCATCCAGCAGAGAATGGAAAGTCAAAT SCT-Cys-I CGGAGGTGGAGGCAGCATCCAGCGTACTCCAAAGATTCAGGTTTACTCACGTCATCCAGCAGAGAATGGAAAGTCAAAT SCT-Cys-II CGGAGGTGGAGGCAGCATCCAGCGTACTCCAAAGATTCAGGTTTACTCACGTCATCCAGCAGAGAATGGAAAGTCAAAT SCT-SL-B DST CGGAGGTGGAGGCAGCATCCAGCGTACTCCAAAGATTCAGGTTTACTCACGTCATCCAGCAGAGAATGGAAAGTCAAAT SCT-SL-B CGGAGGTGGAGGCAGCATCCAGCGTACTCCAAAGATTCAGGTTTACTCACGTCATCCAGCAGAGAATGGAAAGTCAAAT SCT-SL-B CGGAGGTGGAGGCAGCATCCAGCGTACTCCAAAGATTCAGGTTTACTCACGTCATCCAGCAGAGAATGGAAAGTCAAAT SCT-SL-C CGGAGGTGGAGGCAGCATCCAGCGTACTCCAAAGATTCAGGTTTACTCACGTCATCCAGCAGAGAATGGAAAGTCAAAT	SCT-X	CATAAT <mark>AT</mark>	GAACCTGG GAGGCAGCA -+	GCCCATGGT ATCCAGCGTA	TGCTACGGTT	GGAGGAGGTG TCAGGTTTAC	CTAGCGGTG	GTGGTGGTTC(CCAGCAGAGA)	CGGTGGAGGCC	AAATT +
SCT-C CGGAGGTGGAGGCAGCATCCAGCGTACTCCAAAGATTCAGGTTTACTCACGTCATCCAGCAGAGAATGGAAAGTCAAAT SCT-Cys-I CGGAGGTGGAGGCAGCATCCAGCGTACTCCAAAGATTCAGGTTTACTCACGTCATCCAGCAGAGAATGGAAAGTCAAAT SCT-Cys-II CGGAGGTGGAGGCAGCATCCAGCGTACTCCAAAGATTCAGGTTTACTCACGTCATCCAGCAGAAATGGAAAGTCAAAT SCT-Cys-III CGGAGGTGGAGGCAGCATCCAGCGTACTCCAAAGATTCAGGTTTACTCACGTCATCCAGCAGAAAATGGAAAGTCAAAT SCT-SL-B DST CGGAGGTGGAGGCAGCATCCAGCGTACTCCAAAGATTCAGGTTTACTCACGTCATCCAGCAGAAAATGGAAAGTCAAAT SCT-SL-B CGGAGGTGGAGGCAGCATCCAGCGTACTCCAAAGATTCAGGTTTACTCACGTCATCCAGCAGAAAATGGAAAGTCAAAT SCT-SL-C CGGAGGTGGAGGCAGCATCCAGCGTACTCCAAAGATTCAGGTTTACTCACGTCATCCAGCAGAAAATGGAAAGTCAAAT	SCT-X Majority	CATAAT <mark>AT</mark>	GAACCTGG GAGGCAGCA -+ 90 -+	TGCCCATGGT ATCCAGCGTA 100	CTCCAAAGAT CTCCAAAGAT 110	GGAGGAGGTG TCAGGTTTAC + 120 +	CTAGCGGTG CTCACGTCAT + 130 +	GTGGTGGTTC CCAGCAGAGA + 140 +	CGGTGGAGGCC ATGGAAAGTCA 150 +	AAATT + 160
SCT-Cys-I CGGAGGTGGAGGCATCCAGCGTACTCCAAAGATTCAGGTTTACTCACGTCATCCAGCAGAGAATGGAAAGTCAAAT SCT-Cys-II CGGAGGTGGAGGCAGCATCCAGCGTACTCCAAAGATTCAGGTTTACTCACGTCATCCAGCAGAGAATGGAAAGTCAAAT SCT-Cys-III CGGAGGTGGAGGCAGCATCCAGCGTACTCCAAAGATTCAGGTTTACTCACGTCATCCAGCAGAGAATGGAAAGTCAAAT SCT-SL-B DST CGGAGGTGGAGGCAGCATCCAGCGTACTCCAAAGATTCAGGTTTACTCACGTCATCCAGCAGAGAATGGAAAGTCAAAT SCT-SL-B CGGAGGTGGAGGCAGCATCCAGCGTACTCCAAAGATTCAGGTTTACTCACGTCATCCAGCAGAGAATGGAAAGTCAAAT SCT-SL-C CGGAGGTGGAGGCAGCATCCAGCGTACTCCAAAGATTCAGGTTTACTCACGTCATCCAGCAGAGAATGGAAAGTCAAAT	SCT-X Majority SCT-3xCys	CATAATATO CGGAGGTGO CGGAGGTGO	GAACCTGG GAGGCAGCA -+ 90 -+ GAGGCAGCA	TGCCCATGGT ATCCAGCGTA+ 100+ ATCCAGCGTA	CTCCAAAGAT 110 CTCCAAAGAT 110 CTCCAAAGAT	GGAGGAGGTG TCAGGTTTAC+ 120+ TCAGGTTTAC	CTAGCGGTGCTCATCACGTCATCACGTCATCACGTCATCACGTCATCACGTCATCACGTCATCACGTCATCACGTCATCACGTCATCACGTCATCACGTCATCACGTCATCACGTCATCACGTCATCACGTCATCACGTCATCACGTCATCACGTCATCACGTCATCACGTCATCACGTCATCACGTCATCACGTCATCACGTCATCACGTCATCACGTCATCACGTCATCACGTCATCACGTCATCACGTCATCACGTCATCACGTCATCACGTCATCACGTCATCACGTCATCACGTCATCACGTCATCACGTCATCACACACA	CCAGCAGAGA + 140 + CCAGCAGAGAGA	CGGTGGAGGCC ATGGAAAGTCA+ 150+ ATGGAAAGTCA	AAATT + 160 + AAATT
SCT-Cys-II CGGAGGTGGAGGCATCCAGCGTACTCCAAAGATTCAGGTTTACTCACGTCATCCAGCAGAAATGGAAAGTCAAAT SCT-Cys-III CGGAGGTGGAGGCAGCATCCAGCGTACTCCAAAGATTCAGGTTTACTCACGTCATCCAGCAGAAATGGAAAGTCAAAT SCT-SL-B DST CGGAGGTGGAGGCAGCATCCAGCGTACTCCAAAGATTCAGGTTTACTCACGTCATCCAGCAGAAATGGAAAGTCAAAT SCT-SL-B CGGAGGTGGAGGCAGCATCCAGCGTACTCCAAAGATTCAGGTTTACTCACGTCATCCAGCAGAAAATGGAAAGTCAAAT SCT-SL-C CGGAGGTGGAGGCAGCATCCAGCGTACTCCAAAGATTCAGGTTTACTCACGTCATCCAGCAGAGAATGGAAAGTCAAAT	SCT-X Majority SCT-3xCys SCT-B	CATAATATO CGGAGGTGO CGGAGGTGO CGGAGGTGO	GAACCTGG GAGGCAGCA -+ 90 -+ GAGGCAGCA GAGGCAGCA	TGCCCATGGT ATCCAGCGTA+ 100+ ATCCAGCGTA ATCCAGCGTA	CTCCAAAGAT 110 CTCCAAAGAT CTCCAAAGAT	TGGAGGAGGTG TCAGGTTTAC 120 TCAGGTTTAC TCAGGTTTAC	CTAGCGGTG CTCACGTCAT 130 CTCACGTCAT CTCACGTCAT	CCAGCAGAGA 140 CCAGCAGAGA CCAGCAGAGA CCAGCAGAGA	CGGTGGAGGCC ATGGAAAGTCA 150 ATGGAAAGTCA ATGGAAAGTCA	AAATT + 160 + AAATT AAATT
SCT-Cys-III CGGAGGTGGAGGCATCCAGCGTACTCCAAAGATTCAGGTTTACTCACGTCATCCAGCAGAAATGGAAAGTCAAAT SCT-SL-B DST CGGAGGTGGAGGCAGCATCCAGCGTACTCCAAAGATTCAGGTTTACTCACGTCATCCAGCAGAAATGGAAAGTCAAAT SCT-SL-B CGGAGGTGGAGGCAGCATCCAGCGTACTCCAAAGATTCAGGTTTACTCACGTCATCCAGCAGAAAATGGAAAGTCAAAT SCT-SL-C CGGAGGTGGAGGCAGCATCCAGCGTACTCCAAAGATTCAGGTTTACTCACGTCATCCAGCAGAGAATGGAAAGTCAAAT	SCT-X Majority SCT-3xCys SCT-B SCT-C	CATAATATO CGGAGGTGO CGGAGGTGO CGGAGGTGO CGGAGGTGO	GAGCAGCAGCAGCAGCAGCAGCAGCAGCAGCAGCAGCAGC	TGCCCATGGT ATCCAGCGTA 100+ ATCCAGCGTA ATCCAGCGTA ATCCAGCGTA	CTCCAAAGAT 110 CTCCAAAGAT CTCCAAAGAT CTCCAAAGAT	TCAGGTTTAC TCAGGTTTAC 120 TCAGGTTTAC TCAGGTTTAC TCAGGTTTAC	CTAGCGGTG CTCACGTCAT 130 CTCACGTCAT CTCACGTCAT CTCACGTCAT	CCAGCAGAGA 140 CCAGCAGAGA CCAGCAGAGA CCAGCAGAGA CCAGCAGAGA	CGGTGGAGGCC ATGGAAAGTCA 150 ATGGAAAGTCA ATGGAAAGTCA ATGGAAAGTCA	AAATT+ 160+ AAATT AAATT
SCT-SL-B DST CGGAGGTGGAGGCATCCAGCGTACTCCAAAGATTCAGGTTTACTCACGTCATCCAGCAGAAATGGAAAGTCAAAT SCT-SL-B CGGAGGTGGAGGCAGCATCCAGCGTACTCCAAAGATTCAGGTTTACTCACGTCATCCAGCAGAAATGGAAAGTCAAAT SCT-SL-C CGGAGGTGGAGGCAGCATCCAGCGTACTCCAAAGATTCAGGTTTACTCACGTCATCCAGCAGAGAATGGAAAGTCAAAT	SCT-X Majority SCT-3xCys SCT-B SCT-C SCT-Cys-I	CATAATATO CGGAGGTGO CGGAGGTGO CGGAGGTGO CGGAGGTGO CGGAGGTGO	GAGCAGCAGCAGCAGCAGCAGCAGCAGCAGCAGCAGCAGC	TGCCCATGGT ATCCAGCGTA 100+ ATCCAGCGTA ATCCAGCGTA ATCCAGCGTA ATCCAGCGTA	CTCCAAAGAT 110 CTCCAAAGAT CTCCAAAGAT CTCCAAAGAT CTCCAAAGAT	TCAGGTTTAC TCAGGTTTAC 120 TCAGGTTTAC TCAGGTTTAC TCAGGTTTAC TCAGGTTTAC	CTACCTCAT 130 TCACCTCAT CTCACCTCAT CTCACCTCAT CTCACCTCAT CTCACCTCAT	CCAGCAGAGA 140 CCAGCAGAGA CCAGCAGAGA CCAGCAGAGA CCAGCAGAGA CCAGCAGAGA CCAGCAGAGA	CGGTGGAGGCC ATGGAAAGTCA 150 ATGGAAAGTCA ATGGAAAGTCA ATGGAAAGTCA ATGGAAAGTCA ATGGAAAGTCA	AAATT+ 160+ AAATT AAATT AAATT
SCT-SL-B CGGAGGTGGAGGCAGCATCCAGCGTACTCCAAAGATTCAGGTTTACTCACGTCATCCAGCAGAAATGGAAAGTCAAAT SCT-SL-C CGGAGGTGGAGGCAGCATCCAGCGTACTCCAAAGATTCAGGTTTACTCACGTCATCCAGCAGAAAATGGAAAGTCAAAT	SCT-X Majority SCT-3xCys SCT-B SCT-C SCT-C	CATAATATO CGGAGGTGO	GAGCAGCAGCAGCAGCAGCAGCAGCAGCAGCAGCAGCAGC	ATCCAGCGTA ATCCAGCGTA ATCCAGCGTA ATCCAGCGTA ATCCAGCGTA ATCCAGCGTA ATCCAGCGTA ATCCAGCGTA	CTCCAAAGAT 110 CTCCAAAGAT CTCCAAAGAT CTCCAAAGAT CTCCAAAGAT CTCCAAAGAT CTCCAAAGAT	TCAGGTTTAC TCAGGTTTAC 120 TCAGGTTTAC TCAGGTTTAC TCAGGTTTAC TCAGGTTTAC TCAGGTTTAC	CTACCTCATC 130 CTCACCTCATC CTCACCTCATC CTCACCTCATC CTCACCTCATC CTCACCTCATC CTCACCTCATC CTCACCTCATC	CCAGCAGAGAI 140 CCAGCAGAGAI CCAGCAGAGAI CCAGCAGAGAI CCAGCAGAGAI CCAGCAGAGAI CCAGCAGAGAI	CGGTGGAGGCC ATGGAAAGTCA 150 ATGGAAAGTCA ATGGAAAGTCA ATGGAAAGTCA ATGGAAAGTCA ATGGAAAGTCA ATGGAAAGTCA	AAATT+ 160+ AAATT AAATT AAATT AAATT
SCT-SL-C CGGAGGTGGAGGCAGCATCCAGCGTACTCCAAAGATTCAGGTTTACTCACGTCATCCAGCAGAAAATGGAAAGTCAAAT	SCT-X Majority SCT-3xCys SCT-B SCT-C SCT-Cys-I SCT-Cys-II SCT-Cys-III	CATAATATO CGGAGGTGO CGGAGGTGO CGGAGGTGO CGGAGGTGO CGGAGGTGO CGGAGGTGO CGGAGGTGO	GAGCAGCA GAGGCAGCA	ATCCAGCGTA ATCCAGCGTA ATCCAGCGTA ATCCAGCGTA ATCCAGCGTA ATCCAGCGTA ATCCAGCGTA ATCCAGCGTA ATCCAGCGTA	CTCCAAAGAT CTCCAAAGAT 110 CTCCAAAGAT CTCCAAAGAT CTCCAAAGAT CTCCAAAGAT CTCCAAAGAT CTCCAAAGAT	TCAGGTTTAC TCAGGTTTAC TCAGGTTTAC TCAGGTTTAC TCAGGTTTAC TCAGGTTTAC TCAGGTTTAC TCAGGTTTAC	CTACCTCAT 130 TCACCTCAT TCACCTCAT CTCACCTCAT CTCACCTCAT CTCACCTCAT CTCACCTCAT CTCACCTCAT	CCAGCAGAGAI 140 CCAGCAGAGAI CCAGCAGAGAI CCAGCAGAGAI CCAGCAGAGAI CCAGCAGAGAI CCAGCAGAGAI CCAGCAGAGAI CCAGCAGAGAI	CGGTGGAGGCC ATGGAAAGTCA 150 ATGGAAAGTCA ATGGAAAGTCA ATGGAAAGTCA ATGGAAAGTCA ATGGAAAGTCA ATGGAAAGTCA ATGGAAAGTCA ATGGAAAGTCA	AAATT+ 160+ AAATT AAATT AAATT AAATT AAATT AAATT
	SCT-X Majority SCT-3xCys SCT-B SCT-C SCT-Cys-I SCT-Cys-II SCT-Cys-III SCT-Cys-III	CATAATATO CGGAGGTGO	GAGCAGCA GAGGCAGCA	ATCCAGCGTA	CTCCAAAGAT CTCCAAAGAT 110 CTCCAAAGAT CTCCAAAGAT CTCCAAAGAT CTCCAAAGAT CTCCAAAGAT CTCCAAAGAT CTCCAAAGAT CTCCAAAGAT CTCCAAAGAT	TCAGGTTTAC TCAGGTTTAC TCAGGTTTAC TCAGGTTTAC TCAGGTTTAC TCAGGTTTAC TCAGGTTTAC TCAGGTTTAC TCAGGTTTAC	CTACCTCAT 130 CTCACCTCAT CTCACCTCAT CTCACCTCAT CTCACCTCAT CTCACCTCAT CTCACCTCAT CTCACCTCAT CTCACCTCAT	CCAGCAGAGAI CCAGCAGAGAI	CGGTGGAGGCC ATGGAAAGTCA 150 ATGGAAAGTCA ATGGAAAGTCA ATGGAAAGTCA ATGGAAAGTCA ATGGAAAGTCA ATGGAAAGTCA ATGGAAAGTCA ATGGAAAGTCA	AAATT+ 160+ AAATT AAATT AAATT AAATT AAATT AAATT AAATT
SCT-X CGGAGGTGGAGGCAGCATCCAGCGTACTCCAAAGATTCAGGTTTACTCACGTCATCCAGCAGAGAATGGAAAGTCAAAT	SCT-X Majority SCT-3xCys SCT-B SCT-C SCT-Cys-I SCT-Cys-II SCT-Cys-III SCT-SL-B DST SCT-SL-B	CATAATATO CGGAGGTGO	GAGCAGCA GAGGCAGCA	ATCCAGCGTA	CTCCAAAGAT	TCAGGTTTAC	CTACGTCAT 130 TCACGTCAT TCACGTCAT CTCACGTCAT CTCACGTCAT CTCACGTCAT CTCACGTCAT CTCACGTCAT CTCACGTCAT CTCACGTCAT	CCAGCAGAGAI	CGGTGGAGGCC ATGGAAAGTCA 150 ATGGAAAGTCA ATGGAAAGTCA ATGGAAAGTCA ATGGAAAGTCA ATGGAAAGTCA ATGGAAAGTCA ATGGAAAGTCA ATGGAAAGTCA ATGGAAAGTCA ATGGAAAGTCA	AAATT 160 AAATT

Majority	TCCTGAAT	TGCTATGT	3TCTGGGTT1	1	1	1	1	1	1
		170	180	190	200	210	220	230	240
SCT-3xCys	TCCTGAAT	TGCTATGT(GTCTGGGTTI	CATCCATCCG	•	•	'	GAGAGAATTG	AAAAA
SCT-B	TCCTGAAT	TGCTATGT	GTCTGGGTTI	CATCCATCCG	ACATTGAAGI	TGACTTACT(GAAGAATGGA	GAGAGAATTG	AAAAA
SCT-C	TCCTGAAT	TGCTATGT	GTCTGGGTTT	CATCCATCCG	ACATTGAAGT	TGACTTACT	GAAGAATGGA	GAGAGAATTG	AAAAA
SCT-Cys-I	TCCTGAAT	TGCTATGT	GTCTGGGTTT	CATCCATCCG	ACATTGAAGT	TGACTTACT	GAAGAATGGA	GAGAGAATTG	AAAAA
SCT-Cys-II	TCCTGAAT	TGCTATGT	GTCTGGGTTT	CATCCATCCG	ACATTGAAGT	TGACTTACT	GAAGAATGGA	GAGAGAATTG	AAAA
SCT-Cys-III	TCCTGAAT	TGCTATGT	GTCTGGGTTT	CATCCATCCG	ACATTGAAGT	TGACTTACT	GAAGAATGGA	GAGAGAATTG	AAAAA
SCT-SL-B DST	TCCTGAAT	TGCTATGT	GTCTGGGTTI	CATCCATCCG	ACATTGAAGI	TGACTTACT(GAAGAATGGA	GAGAGAATTG	AAAAA
SCT-SL-B	TCCTGAAT	TGCTATGT	GTCTGGGTTI	CATCCATCCG	ACATTGAAGI	TGACTTACT(GAAGAATGGA	GAGAGAATTG	AAAAA
				CATCCATCCG	ACATTGAAGT	TGACTTACT	GAAGAATGGAG	GAGAGAATTG	AAAA
SCT-SL-C	TCCTGAAT	TGCTATGT(3101666111	011100111000					
SCT-SL-C SCT-X Majority	TCCTGAAT	TGCTATGT	GTCTGGGTTI	CATCCATCCG	ACATTGAAGT		GAAGAATGGA		AAAAA
SCT-X	TCCTGAAT	TGCTATGT	GTCTGGGTTI	CATCCATCCG CAAGGACTGG 270	ACATTGAAGT TCTTTCTATC+ 280	TCTTGTACTA + 290	GAAGAATGGAGACACTGAATTC		AAAAA
SCT-X Majority	TCCTGAAT GTGGAGCA	TGCTATGT(TTCAGACTT -+ 250 -+	GTCTGGGTTT FGTCTTTCAG + 260 +	CATCCATCCG CAAGGACTGG+ 270	ACATTGAAGT TCTTTCTATC+ 280+	TCTTGTACTA + 290	GAAGAATGGA(ACACTGAATT(+ 300 +	CACCCCCACT(+ 310 +	AAAAA GAAAA + 320 +
SCT-X Majority SCT-3xCys	TCCTGAAT GTGGAGCA GTGGAGCA	TGCTATGT(TTCAGACTT -+ 250 -+ TTCAGACTT	GTCTGGGTTT IGTCTTTCAG + 260 + IGTCTTTCAG	CATCCATCCG CAAGGACTGG+ 270+ CCAAGGACTGG	ACATTGAAGT TCTTTCTATC+ 280 TCTTTCTATC	TCTTGTACTA + 290 +	GAAGAATGGAGACACCTGAATTC 300 ACACTGAATTC	CACCCCACT 310 CACCCCCACT	AAAAA GAAAA + 320 + GAAAA
SCT-X Majority SCT-3xCys SCT-B	TCCTGAAT GTGGAGCA GTGGAGCA GTGGAGCA	TGCTATGT(TTCAGACTT -+ 250 -+ TTCAGACTT TTCAGACTT	GTCTGGGTTT FGTCTTTCAG 260 FGTCTTTCAG FGTCTTTCAG	CATCCATCCG CAAGGACTGG 270+ GCAAGGACTGG CAAGGACTGG	ACATTGAAGT TCTTTCTATC 280 TCTTTCTATC TCTTTCTATC	TCTTGTACTA 290 TCTTGTACTA TCTTGTACTA	GAAGAATGGACACACTGAATTCACACTGAATTCACACTGAATTCACACTGAATTCACACTGAATTCACACTGAATTCACACTGAATTCACACTGAATTCACACTGAATTCACACTGAATTCACACTGAATTCACACTGAATTCACACTGAATTCACACTGAATTCACACTGAATTCACACTGAATTCACACTGAATTCACACTGAATTCACACTGAATTCACACTGAATTCACACTGAATTCACACTGAATTCACTGAATTCACACTGAATTCACACTGAATTCACACTGAATTCACACTGAATTCACACTGAATTCACTGAATTCACACTGAATTCACACTGAATTCACACTGAATTCACACTGAATTCACACTGAATTCACACTGAATTCACACTGAATTCACACTGAATTCACACTGAATTCACACTGAATTCACACTGAATTCACACTGAATTCACACTGAATTCACACTGAATTCACACTGAATTCACACTGAATTCACACTGAATTCACACTGAATTCACACTGAATTCACACTGAATTCACACTGAATTCACACTGAATTCACACTGAATTCACACTGAATTCACACTGAATTCACACTGAATTCACACTGAATTCACACTGAATTCACACTGAATTCACACTGAATTCACACTGAATTCACACTGAATTCACACTGAATTCACACTGAATTCACACTGAATTCACACTGAATTCACACTGAATTCACACTGAATTCACACTGAATTCACACTGAATTCACACTGAATTCACACTGAATTCACACTGAATTCACACTGAATTCACACTGAATTCACACTGAATTCACACTGAATTCACACTGAATTCACACTGAATTCACACTGAATTCACACTGAATTCACACTGAATTCACACTGAATTCACACTGAATTCACACTGAATTCACACTGAATTCACACTGAATTCACACTGAATTCACACTGAATTCACACTGAATTCACACTGAATTCACACTGAATTCACACTGAATTCACACTGAATTCACACTGAATTCACACTGAATTCACACTGAATTCACACTGAATTCACACTGAATTCACACTGAATTCACACTGAATTCACACTGAATTCACACTGAATTCACACTGAATTCACACTGAATTCACACTGAATTCACACTGAATTCACACTGAATTCACACTGAATTCACACTGAATTCACACTGAATTCACACTGAATTCACACTGAATTCACACTGAATTCACACACTGAATTCACACACTGAATTCACACTACACACAC	CACCCCACT 310 + CACCCCCACT CACCCCCACT	AAAAA GAAAA 320+ GAAAA GAAAA
SCT-X Majority SCT-3xCys SCT-B SCT-C	TCCTGAAT GTGGAGCA GTGGAGCA GTGGAGCA GTGGAGCA	TGCTATGT(TTCAGACTT -+ 250 -+ TTCAGACTT TTCAGACTT TTCAGACTT	GTCTGGGTTT GTCTTTCAG 260 GTCTTTCAG GTCTTTCAG GTCTTTCAG	CATCCATCCG CAAGGACTGG 270 CAAGGACTGG CAAGGACTGG CAAGGACTGG	ACATTGAAGT TCTTTCTATC 280 TCTTTCTATC TCTTTCTATC	TCTTGTACTA 290+ TCTTGTACTA TCTTGTACTA TCTTGTACTA	GAAGAATGGAGACACACTGAATTGACACTGAATTGACACTGAATTGACACTGAATTGACACTGAATTGACACTGAATTGACACTGAATTGACACTGAATTGACACTGAATTGACACTGAATTGACACTGAATTGACACTGAATTGACACTGAATTGA	CACCCCACTO 310+ CACCCCCACTO CACCCCCACTO CACCCCCACTO	AAAAA GAAAA 320+ GAAAA GAAAA GAAAA
SCT-X Majority SCT-3xCys SCT-B SCT-C	TCCTGAAT GTGGAGCA GTGGAGCA GTGGAGCA GTGGAGCA GTGGAGCA	TGCTATGT(TTCAGACTT 250 -+ TTCAGACTT TTCAGACTT TTCAGACTT TTCAGACTT	GTCTGGGTTT GTCTTTCAG 260 GTCTTTCAG GTCTTTCAG GTCTTTCAG GTCTTTCAG	CATCCATCCG CAAGGACTGG 270 CAAGGACTGG CAAGGACTGG CAAGGACTGG CAAGGACTGG	ACATTGAAGT TCTTTCTATC 280 TCTTTCTATC TCTTTCTATC TCTTTCTATC TCTTTCTATC	TCTTGTACTA 290 TCTTGTACTA TCTTGTACTA TCTTGTACTA TCTTGTACTA TCTTGTACTA TCTTGTACTA	GAAGAATGGAGACACACTGAATTGACACTGAATTGACACTGAATTGACACTGAATTGACACTGAATTGACACTGAATTGACACTGAATTGACACTGAATTGACACTGAATTGACACTGAATTGACACTGAATTGACACTGAATTGACACTGAATTGACACTGAATTGACACTGAATTGACACTGAATTGACACTGAATTGACACTGAATTGACACTGAATTGACACTGAATTGACACTGAATTGACACTGAATTGACACTGAATTGACACTGAATTGACACTGAATTGACACTGAATTGACACTGAATTGACACTGAATTGACACTGAATTGACACTGAATTGACACTGAATTGACACTGAATTGACACTGAATTGACACTGAATTGACACTGAATTGACACTGAATTGACACTGAATTGACACTGAATTGACACTGAATTGACACTGAATTGACACTGAATTGACACTGAATTGACACTGAATTGACACTGAATTGACACTGAATTGACACTGAATTGACACTGAATTGACACTGAATTGACACTGAATTGACACTGAATTGACACTGAATTGACACTGAATTGACACTGAATTGACACTGAATTGACACTGAATTGACACTGAATTGACACTGAATTGACACTGAATTGACACTGAATTGACACTGAATTGACACTGAATTGACACTGAATTGACACTGAATTGACACTGAATTGACACTGAATTGACACTGAATTGACACTGAATTGACACTGAATTGACACTGAATTGACACTGAATTGACACTGAATTGACACTGAATTGACACTGAATTGACACTGAATTGACACTGAATTGACACTGAATTGACACTGAATTGACACTGAATTGACACTGAATTGACACTGAATTGACACTGAATTGACACTGAATTGACACTGAATTGACACTGAATTGACACTGAATTGACACTGAATTGACACTGAATTGACACTGAATTGACACTGAATTGACACTGAATTGACACTGAATTGACACTGAATTGACACTGAATTGACACTGAATTGACACTGAATTGACACTGAATTGACACTGAATTGACACTGAATTGACACTGAATTGACACTGAATTGACACTGAATTGACACTGAATTGACACTGAATTGACACTGAATTGACACTGAATTGACACTGAATTGACACTGAATTGACACTGAATTGACACTGAATTGACACTGAATTGACACTGAATTGACACTGAATTGACACTGAATTGACACTGAATTGACACTGAATTGACACTGAATTGACACTGAATTGACACTGAATTGACACTGAATTGACACTGAATTGACACTGAATTGACACTGAATTGACACTGAATTGACACTGAATTGACACTGAATTGACACTGAATTGACACTGAATTGACACTGAATTGAATTGAATTGAATTGAATTGAATTGAATTGAATTGAATTGAATTGAATTGAATTGAATTGAATTGAATTGAATTGAATTGAATTGAATTGAATTGAATTGAATTGAATTGAATTGAATTGAATTGAATTGAATTGAATTGAATTGAATTGAATTGAATTGAATTGAATTGAATTGAATTGAATTGAATTGAATTGAATTGAATTGAATTGAATTGAATTGAATTGAATTGAATTGAATTGAATTGAATTGAATTGAATTGAATTGAATTGAATTGAATTGAATTGAATTGAATTGAATTGAATTGAATTGAATTGAATTGAATTGAATTGAATTGAATTGAATTGAATTGAATTGAATTGAATTGAATTGAATTGAATTGAATTGAATTGAATTGAATTGAATTGAATTGAATTGAATTGAATTGAATTGAATTGAATTGAATTGAATTGAATTGAATTGAATTGAATTGAATTGAATTGAATTGAATTGAATTGAATTGAATTGAATTGAATTGAATTGAATTGAATTGAATTGAATTGAATTGAATTGAATTGAATTGAATTGAATTGAATTGAATTGAATTGAATTGAATTGAATTGAATTGAATTGAATTGAATTGAATTG	CACCCCCACTO 310 CACCCCCCACTO CACCCCCACTO CACCCCCACTO CACCCCCACTO CACCCCCACTO	GAAAA GAAAA 320+ GAAAA GAAAA GAAAA
SCT-X Majority SCT-3xCys SCT-B SCT-C SCT-C	TCCTGAAT GTGGAGCA GTGGAGCA GTGGAGCA GTGGAGCA GTGGAGCA GTGGAGCA	TGCTATGT(TTCAGACTT 250 -+ TTCAGACTT TTCAGACTT TTCAGACTT TTCAGACTT TTCAGACTT TTCAGACTT	GTCTGGGTTT GTCTTTCAG 260 GTCTTTCAG GTCTTTCAG GTCTTTCAG GTCTTTCAG GTCTTTCAG	CATCCATCCG CAAGGACTGG 270 CAAGGACTGG CAAGGACTGG CAAGGACTGG CAAGGACTGG CAAGGACTGG	ACATTGAAGT TCTTTCTATC 280 TCTTTCTATC TCTTTCTATC TCTTTCTATC TCTTTCTATC	TCTTGTACTA 290 TCTTGTACTA TCTTGTACTA TCTTGTACTA TCTTGTACTA TCTTGTACTA TCTTGTACTA TCTTGTACTA TCTTGTACTA	ACACTGAATTO ACACTGAATTO ACACTGAATTO ACACTGAATTO ACACTGAATTO ACACTGAATTO ACACTGAATTO ACACTGAATTO ACACTGAATTO	CACCCCCACTO 310 CACCCCCACTO CACCCCCACTO CACCCCCACTO CACCCCCACTO CACCCCCACTO CACCCCCACTO CACCCCCACTO	GAAAA GAAAA GAAAA GAAAA GAAAA GAAAA GAAAA
SCT-X Majority SCT-3xCys SCT-B SCT-C SCT-C SCT-Cys-I SCT-Cys-II SCT-Cys-III	TCCTGAAT GTGGAGCA GTGGAGCA GTGGAGCA GTGGAGCA GTGGAGCA GTGGAGCA GTGGAGCA	TGCTATGT(TTCAGACTT 250 -+ TTCAGACTT TTCAGACTT TTCAGACTT TTCAGACTT TTCAGACTT TTCAGACTT TTCAGACTT	GTCTGGGTTT GTCTTTCAG 260 GTCTTTCAG GTCTTTCAG GTCTTTCAG GTCTTTCAG GTCTTTCAG GTCTTTCAG	CATCCATCCG CAAGGACTGG 270 CAAGGACTGG CAAGGACTGG CAAGGACTGG CAAGGACTGG CAAGGACTGG	ACATTGAAGT TCTTTCTATC 280 TCTTTCTATC TCTTTCTATC TCTTTCTATC TCTTTCTATC TCTTTCTATC	TCTTGTACTA 290 TCTTGTACTA	ACACTGAATTO	CACCCCCACTO 310 CACCCCCACTO	GAAAA GAAAA GAAAA GAAAA GAAAA GAAAA GAAAA GAAAA GAAAA
SCT-X Majority SCT-3xCys SCT-B SCT-C SCT-Cys-I SCT-Cys-II SCT-Cys-IIIS	TCCTGAAT GTGGAGCA GTGGAGCA GTGGAGCA GTGGAGCA GTGGAGCA GTGGAGCA GTGGAGCA GTGGAGCA	TGCTATGT(TTCAGACT: 250 -+ TTCAGACT: TTCAGACT: TTCAGACT: TTCAGACT: TTCAGACT: TTCAGACT: TTCAGACT: TTCAGACT: TTCAGACT:	GTCTGGGTTT GTCTTTCAG 260 GTCTTTCAG GTCTTTCAG GTCTTTCAG GTCTTTCAG GTCTTTCAG GTCTTTCAG GTCTTTCAG	CATCCATCCG CAAGGACTGG 270 CAAGGACTGG CAAGGACTGG CAAGGACTGG CAAGGACTGG CAAGGACTGG CAAGGACTGG CAAGGACTGG	ACATTGAAGT TCTTTCTATC 280 TCTTTCTATC TCTTTCTATC TCTTTCTATC TCTTTCTATC TCTTTCTATC TCTTTCTATC	TCTTGTACTA 290 TCTTGTACTA TCTTGTACTA	ACACTGAATTO	CACCCCCACTO 310 CACCCCCACTO CACCCCCCACTO	GAAAA
SCT-X	TCCTGAAT GTGGAGCA GTGGAGCA GTGGAGCA GTGGAGCA GTGGAGCA GTGGAGCA GTGGAGCA GTGGAGCA GTGGAGCA	TGCTATGT(TTCAGACT: 250 -+ TTCAGACT: TTCAGACT:	GTCTGGGTTT GTCTTTCAG 260 GTCTTTCAG GTCTTTCAG GTCTTTCAG GTCTTTCAG GTCTTTCAG GTCTTTCAG GTCTTTCAG GTCTTTCAG	CATCCATCCG CAAGGACTGG 270 CAAGGACTGG CAAGGACTGG CAAGGACTGG CAAGGACTGG CAAGGACTGG	ACATTGAAGT TCTTTCTATC 280 TCTTTCTATC TCTTTCTATC TCTTTCTATC TCTTTCTATC TCTTTCTATC TCTTTCTATC TCTTTCTATC	TCTTGTACTA 290 TCTTGTACTA	ACACTGAATTO	CACCCCACTO 310 CACCCCCACTO	GAAAA

Majority	AGATGAGTATGCCTG	CCGTGTGAACC			CAAGATAGTTA			CGGTG	
	330	340	350	360	370 +	380	390	400	
SCT-3xCys	AGATGAGTATGCCTG	CCGTGTGAACC	•			·	GAGACATGGGC	GGTG 400	0
SCT-B	AGATGAGTATGCCTG(CCGTGTGAACC	CATGTGACTTT	GTCACAGCCC	CAAGATAGTTA	AGTGGGATCG	GAGACATGGGC	CGGTG 400	0
SCT-C	AGATGAGTATGCCTG(CCGTGTGAACC	CATGTGACTTT	GTCACAGCCC	CAAGATAGTTA	AGTGGGATCG	GAGACATGGGC	CGGTG 400	0
SCT-Cys-I	AGATGAGTATGCCTG(CCGTGTGAACC	CATGTGACTTT	GTCACAGCCC	CAAGATAGTTA	AGTGGGATCG	GAGACATGGGC	CGGTG 400	0
SCT-Cys-II	AGATGAGTATGCCTG	CCGTGTGAACC	CATGTGACTTT	GTCACAGCCC	CAAGATAGTTA	AGTGGGATCG	GAGACATGGGC	GGTG 400	0
SCT-Cys-III	AGATGAGTATGCCTG	CCGTGTGAACC	CATGTGACTTT	GTCACAGCCC	CAAGATAGTTA	AGTGGGATCG	GAGACATGGGC	GGTG 400	0
SCT-SL-B DST	AGATGAGTATGCCTG	CCGTGTGAACC	CATGTGACTTT	GTCACAGCCC	CAAGATAGTTA	AGTGGGATCG	GAGACATGGGC	GGTG 385	5
SCT-SL-B	AGATGAGTATGCCTG	CCGTGTGAACC	CATGTGACTTT	GTCACAGCCC	CAAGATAGTTA	AGTGGGATCG	GAGACATGGGC	GGTG 385	5
SCT-SL-C	AGATGAGTATGCCTG	CCGTGTGAACC	CATGTGACTTT	GTCACAGCCC	CAAGATAGTTA	AGTGGGATCG	GAGACATGGGC	GGTG 385	5
SCT-X	AGATGAGTATGCCTG	CCGTGTGAACC	CATGTGACTTT	GTCACAGCCC	CAAGATAGTTA	AGTGGGATCG	GAGACATGGGC	CGGTG 400	0
Majority	GTGGTTCCGGTGGAG	GCGGTTCCGGA					ATGAGGTATTI	CCTTC	
Majority	GTGGTTCCGGTGGAGG	GCGGTTCCGGA + 420			GAGGTAGT <mark>GGC</mark> + 450		ATGAGGTATTT + 470	CCTTC + 480	
	410	420	430	440	450 +	460 +	470 +	480 +	0
Majority SCT-3xCys SCT-B		+ 420 + GCGGTTCCGGA	430 + AGGTGGTGGAT	+ 440 +	450 450 AGGTAGT <mark>GG</mark> C	460 +	470 + ATGAGGTATTI	480 + 2CTTC 480	
SCT-3xCys	410 	420 + GCGGTTCCGGA GCGGTTCCGGA	430 + AGGTGGTGGAT	440 + CCGGTGGTGG	450 450 GAGGTAGT <mark>GG</mark> C	460 + ETCTCACTCCA	470 470 + ATGAGGTATTI	480 + CCTTC 480 CCTTC 480	0
SCT-3xCys SCT-B SCT-C	410 	420 +GCGGTTCCGGA GCGGTTCCGGA GCGGTTCCGGA	430 +AGGTGGTGGAT AGGTGGTGGAT AGGTGGTGGAT	440 + CCGGTGGTGG CCGGTGGTGG	450 + GAGGTAGTGGC GAGGTAGTGGC	460+ TTCTCACTCCA TCTCACTCCA	470 + ATGAGGTATTT ATGAGGTATTT	480 + CCTTC 480 CCTTC 480 CCTTC 480	0
SCT-3xCys SCT-B SCT-C SCT-Cys-I	410	420+GCGGTTCCGGAGCGGTTCCGGAGCGGTTCCGGAGCGGGGGGGG	430 430 AGGTGGTGGAT AGGTGGTGGAT AGGTGGTGGAT	440+ CCGGTGGTGG CCGGTGGTGG CCGGTGGTGG	450 AGGTAGTGGC AGGTAGTGGC AGGTAGTGGC AGGTAGTGGC AGGTAGTGGC	460+ TTCTCACTCCA TTCTCACTCCA TTCTCACTCCA	470 470 ATGAGGTATTT ATGAGGTATTT ATGAGGTATTT	480 + CCTTC 480 CCTTC 480 CCTTC 480	0 0
SCT-3xCys SCT-B SCT-C SCT-Cys-I SCT-Cys-II	410	420 GCGGTTCCGGA GCGGTTCCGGA GCGGTTCCGGA GCGGTTCCGGA	430 + .GGTGGTGGAT .GGTGGTGGAT .GGTGGTGGAT	440+ CCGGTGGTGG CCGGTGGTGG CCGGTGGTGG	450 A50 AGGTAGTGGC AGGTAGTGGC AGGTAGTGGC AGGTAGTGGC AGGTAGTGGC	460+ TCTCACTCCA TCTCACTCCA TCTCACTCCA TCTCACTCCA	470 470 ATGAGGTATTT ATGAGGTATTT ATGAGGTATTT ATGAGGTATTT	480+ 480+ CCTTC 480 CCTTC 480 CCTTC 480 CCTTC 480 CCTTC 480	0 0 0 0
SCT-3xCys SCT-B SCT-C SCT-Cys-I	410	420 GCGGTTCCGGA GCGGTTCCGGA GCGGTTCCGGA GCGGTTCCGGA GCGGTTCCGGA	430 + .GGTGGTGGAT .GGTGGTGGAT .GGTGGTGGAT .GGTGGTGGAT	440+ CCGGTGGTGG CCGGTGGTGG CCGGTGGTGG CCGGTGGTGG	450 A50 AGGTAGTGGC AGGTAGTGGC AGGTAGTGGC AGGTAGTGGC AGGTAGTGGC AGGTAGTGGC	460 TCTCACTCA TCTCACTCA TCTCACTCA TCTCACTCA	470 ATGAGGTATTT ATGAGGTATTT ATGAGGTATTT ATGAGGTATTT ATGAGGTATTT	480+ 480+ 2CTTC 480	0 0 0 0 0
SCT-3xCys SCT-B SCT-C SCT-Cys-I SCT-Cys-II SCT-Cys-III	410	420 GCGGTTCCGGA GCGGTTCCGGA GCGGTTCCGGA GCGGTTCCGGA GCGGTTCCGGA GCGGTTCCGGA	430 + .GGTGGTGGAT .GGTGGTGGAT .GGTGGTGGAT .GGTGGTGGAT .GGTGGTGGAT	440+ CCGGTGGTGG CCGGTGGTGG CCGGTGGTGG CCGGTGGTGG CCGGTGGTGG	450 AGGTAGTGGC AGGTAGTGGC AGGTAGTGGC AGGTAGTGGC AGGTAGTGGC AGGTAGTGGC AGGTAGTGGC AGGTAGTGGC	460 TCTCACTCA TCTCACTCA TCTCACTCA TCTCACTCA	470 ATGAGGTATTI ATGAGGTATTI ATGAGGTATTI ATGAGGTATTI ATGAGGTATTI ATGAGGTATTI ATGAGGTATTI	480+ 480+ 2CTTC 480	0 0 0 0 0
SCT-3xCys SCT-B SCT-C SCT-Cys-I SCT-Cys-II SCT-Cys-III	410	420+ GCGGTTCCGGA GCGGTTCCGGA GCGGTTCCGGA GCGGTTCCGGA GCGGTTCCGGA GCGGTTCCGGA	430+	440	450 AGGTAGTGGC AGGTAGTGGC AGGTAGTGGC AGGTAGTGGC AGGTAGTGGC AGGTAGTGGC AGGTAGTGGC AGGTAGTGGC AGGTAGTGGC	460 TCTCACTCA TCTCACTCA TCTCACTCA TCTCACTCA	470 ATGAGGTATTI ATGAGGTATTI ATGAGGTATTI ATGAGGTATTI ATGAGGTATTI ATGAGGTATTI ATGAGGTATTI	480+ 480+ 2CTTC 480 2CTTC 465 2CTTC 465	0 0 0 0 0 5 5

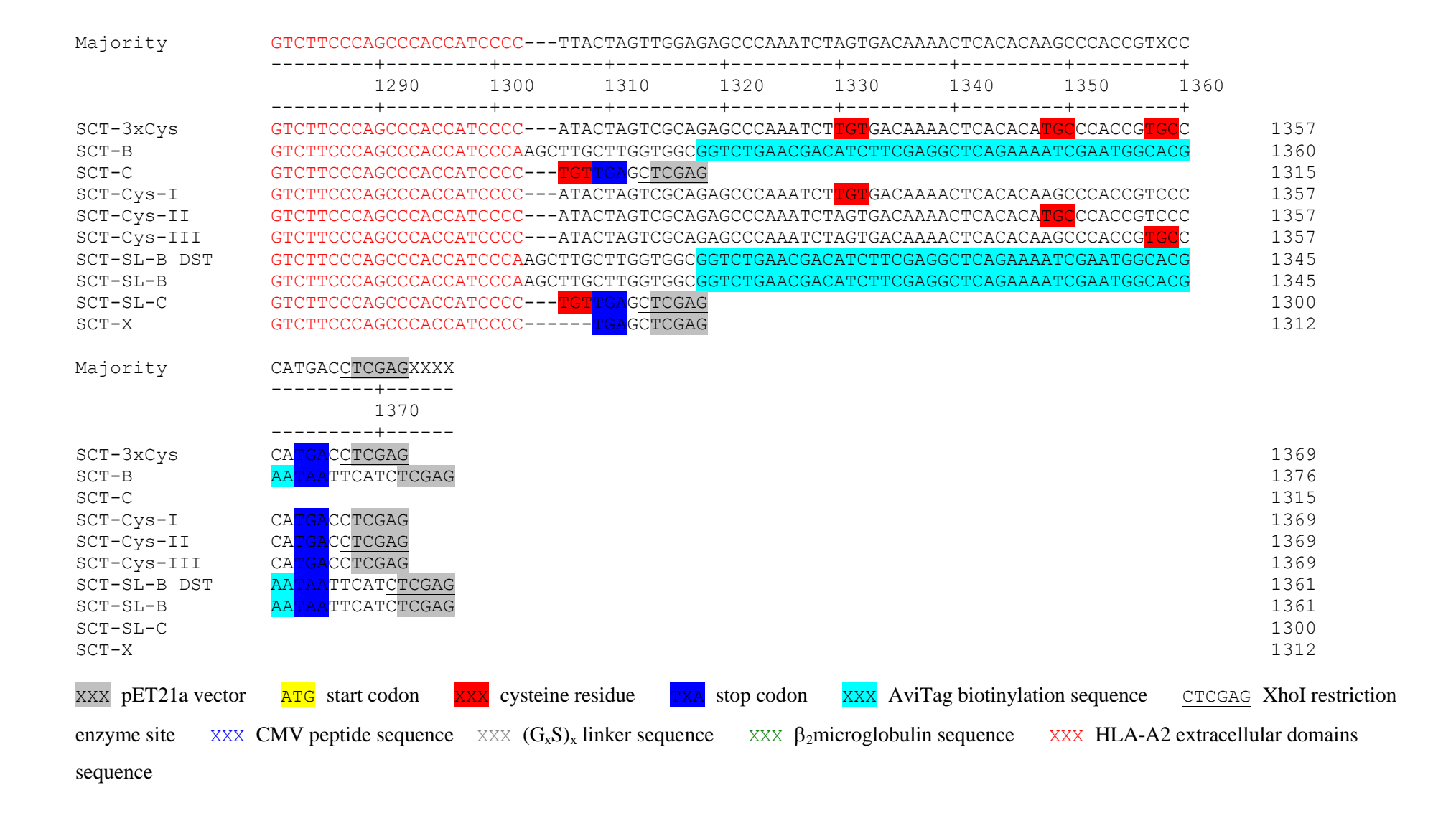
Majority	ACATCCGTGTC			1	1	1			1
	49	0	500	510	520	530	540	550	+ 560
SCT-3xCys	ACATCCGTGTC	CCGGCC	'	•		'	'	GCAGTTCGTG	CGGTT
SCT-B	ACATCCGTGTC	CCGGCC	CGGCCGCGG	GGAGCCCCGC	CTTCATCGCAC	GTGGGCTACG	rggacgacac	GCAGTTCGTG	CGGTT
SCT-C	ACATCCGTGTC	CCGGCC	CGGCCGCGG	GGAGCCCCGC	CTTCATCGCAC	GTGGGCTACG	rggacgacac	GCAGTTCGTG	CGGTT
CT-Cys-I	ACATCCGTGTC	CCGGCC	CGGCCGCGG	GGAGCCCCGC	CTTCATCGCAC	GTGGGCTACG	rggacgacac	GCAGTTCGTG	CGGTT
SCT-Cys-II	ACATCCGTGTC	CCGGCC	CGGCCGCGG	GGAGCCCCGC	CTTCATCGCAC	GTGGGCTACG	rggacgacac(GCAGTTCGTG	CGGTT
CT-Cys-III	ACATCCGTGTC	CCGGCC	CGGCCGCGG	GGAGCCCCGC	CTTCATCGCAC	GTGGGCTACG	rggacgacac	GCAGTTCGTG	CGGTT
SCT-SL-B DST	ACATCCGTGTC	CCGGCC	CGGCCGCGG	GGAGCCCCGC	CTTCATCGCAC	GTGGGCTACG	rggacgacac	GCAGTTCGTG	CGGTT
SCT-SL-B	ACATCCGTGTC	CCGGCC	CGGCCGCGG	GGAGCCCCGC	CTTCATCGCAC	GTGGGCTACG	rggacgacac	GCAGTTCGTG	CGGTT
									a c c m m
SCT-SL-C	ACATCCGTGTC	CCGGCC	CGGCCGCGC	GGAGCCCCGC	TTCATCGCAC	TGGGCTACG:	LGGACGACAC	JCAGIICGIG	CGGTT
SCT-SL-C SCT-X Majority	ACATCCGTGTC ACATCCGTGTC CGACAGCGACG	CCGGCC	CGGCCGCGG	GGAGCCCCGC	CTTCATCGCA(GTGGGCTACG' GATAGAGCAG	rggacgacaco gagggtccgg <i>i</i>	GCAGTTCGTG(CGGTT
SCT-X	ACATCCGTGTC	CCGCGA	CCGGCCGCGG CCCAGAGGA + 580	GGGAGCCCGC TGGAGCCGCG + 590	CTTCATCGCAC GGGCGCCGTGC + 600	GTGGGCTACG GATAGAGCAG + 610	rggacgacaco gagggtccgga + 620	GCAGTTCGTG AGTATTGGGA + 630	CGGTT CGGGG +
SCT-X Majority	ACATCCGTGTC CGACAGCGACG	CCGGCGA	CCGGCCGCGG AGCCAGAGGA + 580 +	GGGAGCCCCGC TGGAGCCGCG + 590 +	GGGCGCCGTGC 600	GTGGGCTACG GATAGAGCAG 610	FGGACGACACC GAGGGTCCGGA 620	GCAGTTCGTG AGTATTGGGA + 630 +	CGGTT CGGGG+ 640
SCT-X Majority SCT-3xCys	ACATCCGTGTC CGACAGCGACG	CCGCGA	CGGCCGCGG CGCCAGAGGA + 580 + CGCCAGAGGA	GGAGCCCCGC ATGGAGCCGCG 590 ATGGAGCCGCG	GGCGCCGTGC 600 GGGCGCCGTGC 600 GGCGCGCGTGC	GTGGGCTACG GATAGAGCAG + 610 + GATAGAGCAG	GGACGACACC GAGGGTCCGGA 620 GAGGGTCCGGA	AGTATTGGGA + 630 + AGTATTGGGA	CGGTT CGGGG+ 640+ CGGGG
SCT-X Majority	ACATCCGTGTC CGACAGCGACG 57 +- CGACAGCGACG	CCGCGA CCGCGA CCGCGA	CGGCCGCGCGCGCGCGCGCGCAGAGGAGGAGGAGGAGGAG	GGAGCCCCGC ATGGAGCCGCG 590+ ATGGAGCCGCG	GGCGCCGTGC GGGCGCCGTGC GGGCGCCGTGC	GTGGGCTACG GATAGAGCAG 610 GATAGAGCAG GATAGAGCAG	GGACGACACC GAGGGTCCGGA 620 GAGGGTCCGGA GAGGGTCCGGA	GCAGTTCGTG AGTATTGGGA + 630 + AGTATTGGGA AGTATTGGGA	CGGTT CGGGG+ 640+ CGGGG CGGGG
SCT-X Majority SCT-3xCys SCT-B	ACATCCGTGTC CGACAGCGACG 57 CGACAGCGACG CGACAGCGACG CGACAGCGACG	CCGCGA CCGCGA CCGCGA CCGCGA	CGGCCGCGCGCGCGCGCGCGCAGAGGAGGAGGAGGAGGAG	GGGAGCCCCGC TGGAGCCGCG 590 TGGAGCCGCG TGGAGCCGCG	GGCGCCGTGC GGGCGCCGTGC GGGCGCCGTGC	GTGGGCTACG GATAGAGCAG 610 GATAGAGCAG GATAGAGCAG GATAGAGCAG	GGACGACACC GAGGGTCCGGA G20 GAGGGTCCGGA GAGGGTCCGGA GAGGGTCCGGA	AGTATTGGGA 630 AGTATTGGGA AGTATTGGGA AGTATTGGGA AGTATTGGGA	CGGTT CGGGG+ 640+ CGGGG CGGGG
SCT-X Majority SCT-3xCys SCT-B SCT-C	ACATCCGTGTC CGACAGCGACG 57 CGACAGCGACG CGACAGCGACG	CCGCGA CCGCGA CCGCGA CCGCGA	CGGCCGCGCGCGCGCGCGCGCAGAGGAGGAGGAGGAGGAG	GGAGCCCGC TGGAGCCGCG 590 TGGAGCCGCG TGGAGCCGCG TGGAGCCGCG	GGCGCCGTGC GGGCGCCGTGC GGGCGCCGTGC	GATAGAGCAG GATAGAGCAG 610 GATAGAGCAG GATAGAGCAG GATAGAGCAG GATAGAGCAG	GGACGACACC GAGGGTCCGGA GAGGGTCCGGA GAGGGTCCGGA GAGGGTCCGGA GAGGGTCCGGA	AGTATTGGGA 630 AGTATTGGGA AGTATTGGGA AGTATTGGGA AGTATTGGGA AGTATTGGGA	CGGTT CGGGG+ 640+ CGGGG CGGGG CGGGG
SCT-X Majority SCT-3xCys SCT-B SCT-C SCT-Cys-I	CGACAGCGACG CGACAGCGACG CGACAGCGACG CGACAGCGACG CGACAGCGACG CGACAGCGACG	CCGCGA CCGCGA CCGCGA CCGCGA CCGCGA	CCGGCCGCGCGCGCGCGCGCGCAGAGGAGGAGGAGGAGGA	GGGAGCCCCGC TGGAGCCGCG TGGAGCCGCG TGGAGCCGCG TGGAGCCGCG TGGAGCCGCG	GGCGCCGTGC GGCGCCGTGC GGGCGCCGTGC GGGCGCCGTGC GGGCGCCGTGC	GATAGAGCAG GATAGAGCAG GATAGAGCAG GATAGAGCAG GATAGAGCAG GATAGAGCAG GATAGAGCAG	GGACGACACC GAGGGTCCGGA GAGGGTCCGGA GAGGGTCCGGA GAGGGTCCGGA GAGGGTCCGGA GAGGGTCCGGA	AGTATTGGGA 630 AGTATTGGGA AGTATTGGGA AGTATTGGGA AGTATTGGGA AGTATTGGGA AGTATTGGGA AGTATTGGGA	CGGTT CGGGG+ 640+ CGGGG CGGGG CGGGG CGGGG
SCT-X Majority SCT-3xCys SCT-B	CGACAGCGACG	CCGCGA CCGCGA CCGCGA CCGCGA CCGCGA CCGCGA	CCGGCCGCGCGCGCGCGCGCGCAGAGGAGGAGGAGGAGGA	GGGAGCCCCGC TGGAGCCGCG TGGAGCCGCG TGGAGCCGCG TGGAGCCGCG TGGAGCCGCG TGGAGCCGCG	GGCGCCGTGC GGGCGCCGTGC GGGCGCCGTGC GGGCGCCGTGC GGGCGCCGTGC GGGCGCCGTGC	GATAGAGCAG GATAGAGCAG GATAGAGCAG GATAGAGCAG GATAGAGCAG GATAGAGCAG GATAGAGCAG GATAGAGCAG	GGACGACACC GAGGGTCCGGA GAGGGTCCGGA GAGGGTCCGGA GAGGGTCCGGA GAGGGTCCGGA GAGGGTCCGGA GAGGGTCCGGA GAGGGTCCGGA GAGGGTCCGGA	AGTATTGGGA 630 AGTATTGGGA AGTATTGGGA AGTATTGGGA AGTATTGGGA AGTATTGGGA AGTATTGGGA AGTATTGGGA AGTATTGGGA	CGGTT CGGGG+ 640+ CGGGG CGGGG CGGGG CGGGG CGGGG
GCT-X Majority GCT-3xCys GCT-B GCT-C GCT-Cys-I GCT-Cys-II GCT-Cys-III	ACATCCGTGTC CGACAGCGACG 57 CGACAGCGACG CGACAGCGACG CGACAGCGACG CGACAGCGACG CGACAGCGACG CGACAGCGACG CGACAGCGACG CGACAGCGACG	CCGCGA CCGCGA CCGCGA CCGCGA CCGCGA CCGCGA CCGCGA	CCGGCCGCGCGCGCGCGCGCGCAGAGGAGGAGGAGGAGGA	TGGAGCCCCGC TGGAGCCGCG TGGAGCCGCG TGGAGCCGCG TGGAGCCGCG TGGAGCCGCG	GGCGCCGTGC GGGCGCCGTGC GGGCGCCGTGC GGGCGCCGTGC GGGCGCCGTGC GGGCGCCGTGC GGGCGCCGTGC	GATAGAGCAG GATAGAGCAG GATAGAGCAG GATAGAGCAG GATAGAGCAG GATAGAGCAG GATAGAGCAG GATAGAGCAG GATAGAGCAG	GGACGACACC GAGGGTCCGGA GAGGGTCCGGA	AGTATTGGGA 630 AGTATTGGGA AGTATTGGGA AGTATTGGGA AGTATTGGGA AGTATTGGGA AGTATTGGGA AGTATTGGGA AGTATTGGGA AGTATTGGGA	CGGTT CGGGG+ 640+ CGGGG CGGGG CGGGG CGGGG CGGGG CGGGG CGGGG
GCT-X Majority GCT-3xCys GCT-B GCT-C GCT-Cys-I GCT-Cys-II GCT-Cys-III GCT-SL-B DST	CGACAGCGACG	CCGGCGA CCGCGA CCGCGA CCGCGA CCGCGA CCGCGA CCGCGA CCGCGA	CCGGCCGCGCGCGCGCGCGCGCAGAGGAGGAGGAGGAGGA	TGGAGCCCCGC TGGAGCCGCG TGGAGCCGCG TGGAGCCGCG TGGAGCCGCG TGGAGCCGCG TGGAGCCGCG	GGCGCCGTGC GGGCGCCGTGC GGGCGCCGTGC GGGCGCCGTGC GGGCGCCGTGC GGGCGCCGTGC GGGCGCCGTGC GGGCGCCGTGC GGGCGCCGTGC	GATAGAGCAG GATAGAGCAG GATAGAGCAG GATAGAGCAG GATAGAGCAG GATAGAGCAG GATAGAGCAG GATAGAGCAG GATAGAGCAG GATAGAGCAG	GGACGACACC GAGGGTCCGGA	AGTATTGGGA 630 AGTATTGGGA AGTATTGGGA AGTATTGGGA AGTATTGGGA AGTATTGGGA AGTATTGGGA AGTATTGGGA AGTATTGGGA AGTATTGGGA	CGGTT CGGGG+ 640+ CGGGG CGGGG CGGGG CGGGG CGGGG CGGGG CGGGG CGGGG CGGGG

Majority	AGACACG	JAAAGTGAA	1	1	+	1	1	1	1
		650	660	670	680	690	700	710	720
SCT-3xCys	AGACACG(+ GAAAGTGAA	•	.CAGACTCACC	•		•	•	+ GCGAG
SCT-B	AGACACG	GAAAGTGAA	GGCCCACTCA	CAGACTCACC	GAGTGGACCT	GGGGACCCT	GCGCGGCTAC	racaaccaga(GCGAG
SCT-C	AGACACG	GAAAGTGAA	GGCCCACTCA	CAGACTCACC	GAGTGGACCT	GGGGACCCT	GCGCGGCTAC	racaaccaga(GCGAG
SCT-Cys-I	AGACACG	GAAAGTGAA	GGCCCACTCA	CAGACTCACC	GAGTGGACCT	GGGGACCCT	GCGCGGCTAC	racaaccaga(GCGAG
SCT-Cys-II	AGACACG	GAAAGTGAA	GGCCCACTCA	CAGACTCACC	GAGTGGACCT	GGGGACCCT	GCGCGGCTAC	racaaccaga(GCGAG
SCT-Cys-III	AGACACG	GAAAGTGAA	GGCCCACTCA	CAGACTCACC	GAGTGGACCT	GGGGACCCT	GCGCGGCTAC:	TACAACCAGA(GCGAG
SCT-SL-B DST	AGACACG	GAAAGTGAA	GGCCCACTCA	CAGACTCACC	GAGTGGACCT	GGGGACCCT	GCGCGGC <mark>TGC</mark>	racaaccaga(GCGAG
SCT-SL-B	AGACACG	GAAAGTGAA	GGCCCACTCA	CAGACTCACC	GAGTGGACCT	GGGGACCCT	GCGCGGCTAC	racaaccaga(GCGAG
COM OT C	AGACACGO	GAAAGTGAA	GGCCCACTCA	CAGACTCACC	GAGTGGACCT	GGGGACCCT	GCGCGGCTACT	racaaccaga(GCGAG
SCT-SL-C									
SCT-SL-C SCT-X Majority				CAGACTCACC					
SCT-X			TCCAGAGGAT + 740	'GTATGGCTGC + 750	GACGTGGGGT + 760	CGGACTGGC0	GCTTCCTCCG(+ 780	CGGGTACCAC + 790	
SCT-X Majority	GCCGGTT	CTCACACCG' + 730 +	TCCAGAGGAT + 740 +	CGTATGGCTGC + 750 +	CGACGTGGGGT + 760 +	CGGACTGGCC + 770 +	GCTTCCTCCG(+ 780 +	CGGGTACCAC + 790 +	CAGTA + 800
SCT-X Majority SCT-3xCys	GCCGGTT(CTCACACCG'+ 730+ CTCACACCG'	TCCAGAGGAT+ 740+ TCCAGAGGAT	'GTATGGCTGC + 750	GACGTGGGGT 760 +	CGGACTGGCC 770 +	GCTTCCTCCGC 780 +	CGGGTACCAC 790 +	CAGTA + 800 + CAGTA
SCT-X Majority	GCCGGTT(GCCGGTT(CTCACACCG'+ 730+ CTCACACCG' CTCACACCG	TCCAGAGGAT+ 740+ TCCAGAGGAT TCCAGAGGAT	GTATGGCTGC + 750 +	GACGTGGGGT 760 GACGTGGGGT	CGGACTGGCC 770 + 7CGGACTGGCC	GCTTCCTCCGC 780+ GCTTCCTCCGC	CGGGTACCAC 790 + CGGGTACCAC	CAGTA + 800 + CAGTA
SCT-X Majority SCT-3xCys SCT-B SCT-C	GCCGGTT(GCCGGTT(GCCGGTT(CTCACACCG' 730+ CTCACACCG' CTCACACCG'	TCCAGAGGAT+ 740+ TCCAGAGGAT TCCAGAGGAT TCCAGAGGAT	GTATGGCTGC 750+ GTATGGCTGC	GACGTGGGGT 760 + GACGTGGGGT GACGTGGGGT	CGGACTGGCC 770 CGGACTGGCCCCGGACTGGCCCCCGGACTGGCCCCCCGACTGGCCCCCCGACTGGCCCCCCGACTGGCCCCCCGACTGGCCCCCCGACTGGCCCCCCGACTGGCCCCCCGACTGGCCCCCCCC	GCTTCCTCCGC 780+ GCTTCCTCCGC GCTTCCTCCGC	CGGGTACCACC 790+ CGGGTACCACCCGGGTACCACC	CAGTA 800+ CAGTA CAGTA CAGTA
SCT-X Majority SCT-3xCys SCT-B SCT-C SCT-Cys-I	GCCGGTT(GCCGGTT(GCCGGTT(GCCGGTT(CTCACACCG' 730+ CTCACACCG' CTCACACCG' CTCACACCG'	TCCAGAGGAT+ 740+ TCCAGAGGAT TCCAGAGGAT TCCAGAGGAT	GTATGGCTGC 750+ GTATGGCTGC GTATGGCTGC	GACGTGGGGT 760 GACGTGGGGT GACGTGGGGT GACGTGGGGT	CGGACTGGCC 770 CGGACTGGCCCGGACTGGCCCCGGACTGGCCCCCGGACTGGCCCCCCGACTGGCCCCCGGACTGGCCCCCGGACTGGCCCCCGGACTGGCCCCCGGACTGGCCCCCGGACTGGCCCCCGGACTGGCCCCCCGACTGGCCC	GCTTCCTCCGC 780+ GCTTCCTCCGC GCTTCCTCCGC GCTTCCTCCGC	CGGGTACCAC 790 + CGGGTACCAC CGGGTACCAC CGGGTACCAC	CAGTA 800+ CAGTA CAGTA CAGTA CAGTA
SCT-X Majority SCT-3xCys SCT-B SCT-C SCT-Cys-I SCT-Cys-II	GCCGGTT(GCCGGTT(GCCGGTT(GCCGGTT(GCCGGTT(CTCACACCG' 730+ CTCACACCG' CTCACACCG' CTCACACCG' CTCACACCG'	TCCAGAGGAT 740 + TCCAGAGGAT TCCAGAGGAT TCCAGAGGAT TCCAGAGGAT	GTATGGCTGC 750 GTATGGCTGC GTATGGCTGC	GACGTGGGGT 760 GACGTGGGGT GACGTGGGGT GACGTGGGGT GACGTGGGGT	CGGACTGGCC 770 CGGACTGGCCCCGGACTGGCCCCGGACTGGCCCCCGACTGGCCCCCCGACTGGCCCCCCGACTGGCCCCCGGACTGGCCCCCGGACTGGCCCCCGGACTGGCCCCCGGACTGGCCCCCGACTGGCCCCCCGACTGGCCCCCC	GCTTCCTCCGC 780+ GCTTCCTCCGC GCTTCCTCCGC GCTTCCTCCGC	CGGGTACCACC 790+ CGGGTACCACCCGGGTACCACCCCGGGTACCACCCCGGGTACCACCCCGGGTACCACC	CAGTA 800+ CAGTA CAGTA CAGTA CAGTA CAGTA CAGTA
SCT-X Majority SCT-3xCys SCT-B SCT-C	GCCGGTTO GCCGGTTO GCCGGTTO GCCGGTTO GCCGGTTO	CTCACACCG' 730+ CTCACACCG' CTCACACCG' CTCACACCG' CTCACACCG' CTCACACCG'	TCCAGAGGAT 740 + TCCAGAGGAT TCCAGAGGAT TCCAGAGGAT TCCAGAGGAT TCCAGAGGAT	GTATGGCTGC 750 GTATGGCTGC GTATGGCTGC GTATGGCTGC	GACGTGGGGT 760 GACGTGGGGT GACGTGGGGT GACGTGGGGT GACGTGGGGT GACGTGGGGT	CGGACTGGCC 770 CGGACTGGCCCGGACTGGCCCCGGACTGGCCCCCGACTGGCCCCCCCGACTGGCCCCCCGACTGGCCCCCGACTGGCCCCCCGACTGGCCCCCCGACTGGCCCCCCGACTGGCCCCCCGACTGGCCCCCCGACTGGCCCCCCCC	GCTTCCTCCGC 780+ GCTTCCTCCGC GCTTCCTCCGC GCTTCCTCCGC GCTTCCTCCGC GCTTCCTCCGC	CGGGTACCACC 790+ CGGGTACCACCCGGGTACCACCCGGGTACCACCCCGGGTACCACCCCGGGTACCACCCCGGGTACCACCCCGGGTACCACCCCGGGTACCACCCCGGGTACCACCCCGGGTACCACC	CAGTA 800+ CAGTA CAGTA CAGTA CAGTA CAGTA CAGTA CAGTA CAGTA
SCT-X Majority SCT-3xCys SCT-B SCT-C SCT-Cys-I SCT-Cys-II SCT-Cys-III	GCCGGTTO GCCGGTTO GCCGGTTO GCCGGTTO GCCGGTTO GCCGGTTO	CTCACACCG' 730+ CTCACACCG' CTCACACCG' CTCACACCG' CTCACACCG' CTCACACCG' CTCACACCG'	TCCAGAGGAT+ 740+ TCCAGAGGAT TCCAGAGGAT TCCAGAGGAT TCCAGAGGAT TCCAGAGGAT	GTATGGCTGC 750 GTATGGCTGC GTATGGCTGC GTATGGCTGC GTATGGCTGC	GACGTGGGGT 760 GACGTGGGGT GACGTGGGGT GACGTGGGGT GACGTGGGGT GACGTGGGGT GACGTGGGGT	CGGACTGGCC 770 CGGACTGGCCCCGGACTGGCCCCGGACTGGCCCCCGACTGGCCCCCCGACTGGCCCCCCGACTGGCCCCCGGACTGGCCCCCGGACTGGCCCCCGGACTGGCCCCCGGACTGGCCCCCGGACTGGCCCCCCGACTGGCCCCCCGACTGGCCCCCCGACTGGCCCCCCGACTGGCCCCCGACTGGCCCCCCGACTGGCCCCCCGACTGGCCCCCCCC	GCTTCCTCCGC 780+ GCTTCCTCCGC GCTTCCTCCGC GCTTCCTCCGC GCTTCCTCCGC GCTTCCTCCGC	CGGGTACCACC 790+ CGGGTACCACC CGGGTACCACC CGGGTACCACC CGGGTACCACC	CAGTA 800+ CAGTA CAGTA CAGTA CAGTA CAGTA CAGTA CAGTA CAGTA CAGTA
SCT-X Majority SCT-3xCys SCT-B SCT-C SCT-Cys-I SCT-Cys-II SCT-Cys-III SCT-Cys-III	GCCGGTTO GCCGGTTO GCCGGTTO GCCGGTTO GCCGGTTO GCCGGTTO GCCGGTTO	CTCACACCG' 730+ CTCACACCG' CTCACACCG' CTCACACCG' CTCACACCG' CTCACACCG' CTCACACCG' CTCACACCG'	TCCAGAGGAT+ 740+ TCCAGAGGAT TCCAGAGGAT TCCAGAGGAT TCCAGAGGAT TCCAGAGGAT TCCAGAGGAT	GTATGGCTGC 750+ GTATGGCTGC GTATGGCTGC GTATGGCTGC GTATGGCTGC	GACGTGGGGT 760 GACGTGGGGT GACGTGGGGT GACGTGGGGT GACGTGGGGT GACGTGGGGT GACGTGGGGT GACGTGGGGT	CGGACTGGCC CGGACTGGCCCCGGACTGGCCCCCGACTGGCCCCCCGACTGGCCCCCCCC	GCTTCCTCCGC 780+ GCTTCCTCCGC GCTTCCTCCGC GCTTCCTCCGC GCTTCCTCCGC GCTTCCTCCGC GCTTCCTCCGC	CGGGTACCACC 790+ CGGGTACCACC CGGGTACCACC CGGGTACCACC CGGGTACCACC CGGGTACCACC CGGGTACCACC	CAGTA 800+ CAGTA

Majority	CGCCTACGACGGCAA							
	810	820	830	840	850	860 +	870	880
SCT-3xCys	CGCCTACGACGGCAA	.GGATTACATC	·	·	•	•	•	GACCA
SCT-B	CGCCTACGACGGCAA	GGATTACATC	GCCTGAAAGA	GGACCTGCGC	CTCTTGGACC	GCGGCGGACA'	TGGCAGCTCAC	GACCA
SCT-C	CGCCTACGACGGCAA	GGATTACATC	GCCTGAAAGA	GGACCTGCGC	CTCTTGGACC	GCGGCGGACA!	rggcagctca(GACCA
SCT-Cys-I	CGCCTACGACGGCAA	GGATTACATC	GCCTGAAAGA	GGACCTGCGC	CTCTTGGACC	GCGGCGGACA!	rggcagctca(GACCA
SCT-Cys-II	CGCCTACGACGGCAA	GGATTACATC	GCCTGAAAGA	GGACCTGCGC	CTCTTGGACC	GCGGCGGACA!	rggcagctca(GACCA
SCT-Cys-III	CGCCTACGACGGCAA	GGATTACATC	GCCTGAAAGA	GGACCTGCGC	CTCTTGGACC	GCGGCGGACA!	rggcagctca(GACCA
SCT-SL-B DST	CGCCTACGACGGCAA	GGATTACATC	GCCTGAAAGA	GGACCTGCGC	CTCTTGGACC	GCGGCGGACA!	rggcagctca(GACCA
SCT-SL-B	CGCCTACGACGGCAA	GGATTACATC	GCCTGAAAGA	GGACCTGCGC	CTCTTGGACC	GCGGCGGACA!	rggcagctca(GACCA
	CCCCMACCACCCAA	CCATTACATC	CCCTGAAAGA	GGACCTGCGC	CTCTTGGACC	GCGGCGGACA	rggcagctca(GACCA
SCT-SL-C								
SCT-SL-C SCT-X	CGCCTACGACGGCAA				CTCTTGGACC	GCGGCGGACA!	TGGCAGCTCAG	GACCA
		GGATTACATCO	GCCTGAAAGA IGTGGCGGAGC	GGACCTGCGC	CCTACCTGGA	GGCACGTGC	GTGGAGTGGC	
SCT-X	CGCCTACGACGGCAA CCAAGCACAAGTGGG	GGATTACATCO AGGCGGCCCA! 900	GCCCTGAAAGA FGTGGCGGAGC + 910	GGACCTGCGC AGTTGAGAGC + 920	CCTACCTGGA(+ 930	GGGCACGTGC0	GTGGAGTGGCT	
SCT-X	CGCCTACGACGGCAA CCAAGCACAAGTGGG	GGATTACATCO AGGCGGCCCAT 900	GCCCTGAAAGA IGTGGCGGAGC + 910 +	GGACCTGCGC AGTTGAGAGC + 920 +	CCTACCTGGA(+ 930 +	GGGCACGTGC(+ 940 +	GTGGAGTGGCT + 950 +	FCCGC + 960 +
SCT-X Majority	CGCCTACGACGGCAA CCAAGCACAAGTGGG	AGGCGGCCA 900 AGGCGGCCA	GCCCTGAAAGA FGTGGCGGAGC + 910 + FGTGGCGGAGC	GGACCTGCGC AGTTGAGAGC 920 AGTTGAGAGAGC	CCTACCTGGA 930 +	GGGCACGTGCC + 940 + GGGCACGTGCC	GTGGAGTGGCT 950 + GTGGAGTGGCT	FCCGC + 960 + FCCGC
SCT-X Majority SCT-3xCys SCT-B	CCAAGCACAAGTGGG 890 CCAAGCACAAGTGGG	AGGCGGCCA: AGGCGGCCCA: AGGCGGCCCA: AGGCGGCCCA:	GCCCTGAAAGA IGTGGCGGAGC 910 IGTGGCGGAGC IGTGGCGGAGC	GGACCTGCGC AGTTGAGAGC 920+ AGTTGAGAGC	CCTACCTGGA(930+ CCTACCTGGA(CCTACCTGGA(GGGCACGTGCC 940 + GGGCACGTGCC GGGCACGTGCC	GTGGAGTGGCT 950 + GTGGAGTGGCT GTGGAGTGGCT	rccgc + 960 + rccgc
SCT-X Majority SCT-3xCys SCT-B SCT-C	CGCCTACGACGGCAA CCAAGCACAAGTGGG 890+ CCAAGCACAAGTGGG CCAAGCACAAGTGGG	AGGCGGCCA: AGGCGGCCCA: AGGCGGCCCA: AGGCGGCCCA:	GCCCTGAAAGA IGTGGCGGAGC 910 IGTGGCGGAGC IGTGGCGGAGC	AGTTGAGAGO PAGTTGAGAGO AGTTGAGAGO AGTTGAGAGO AGTTGAGAGO	CCTACCTGGA(930+ CCTACCTGGA(CCTACCTGGA(CCTACCTGGA(GGGCACGTGCC 940 + GGGCACGTGCC GGGCACGTGCC	GTGGAGTGGCT 950 + GTGGAGTGGCT GTGGAGTGGCT	FCCGC 960 + FCCGC FCCGC
SCT-X Majority SCT-3xCys SCT-B SCT-C	CCAAGCACAAGTGGG 890 CCAAGCACAAGTGGG CCAAGCACAAGTGGG CCAAGCACAAGTGGG CCAAGCACAAGTGGG	AGGCGGCCA AGGCGGCCCA AGGCGGCCCA AGGCGGCCCA AGGCGGCCCA	GCCCTGAAAGA IGTGGCGGAGC 910 IGTGGCGGAGC IGTGGCGGAGC IGTGGCGGAGC	AGTTGAGAGC AGTTGAGAGC AGTTGAGAGC AGTTGAGAGC AGTTGAGAGC	CCTACCTGGA(930 CCTACCTGGA(CCTACCTGGA(CCTACCTGGA(CCTACCTGGA(CCTACCTGGA(CCTACCTGGA(CCTACCTGGA(CCTACCTGGA(CCTACCTGGA(CCTACCTGGA(CCTACCTGGA(CCTACCTGGA(CCTACCTGGA(CCTACCTGGA(CCTACCTGGA(CCTACCTGGA(CCTACCTGGA(CCTACCTGGA(CCTACCTGGA(CCTACCTGGA(CCTACCTGGA(CCTACCTGGA(CCTACCTGGA(CCTACCTGGA(CCTACCTGGA(CCTACCTGGA(GGGCACGTGCC 940 + GGGCACGTGCC GGGCACGTGCC GGGCACGTGCC	GTGGAGTGGCT 950 + GTGGAGTGGCT GTGGAGTGGCT GTGGAGTGGCT	FCCGC 960+ FCCGC FCCGC FCCGC
SCT-X Majority SCT-3xCys SCT-B SCT-C SCT-Cys-I	CGCCTACGACGGCAA CCAAGCACAAGTGGG 890 CCAAGCACAAGTGGG CCAAGCACAAGTGGG CCAAGCACAAGTGGG CCAAGCACAAGTGGG	AGGCGGCCA: AGGCGGCCA: AGGCGGCCCA: AGGCGGCCCA: AGGCGGCCCA: AGGCGGCCCA:	GCCCTGAAAGA IGTGGCGGAGC 910+ IGTGGCGGAGC IGTGGCGGAGC IGTGGCGGAGC	AGTTGAGAGO AGTTGAGAGO AGTTGAGAGO AGTTGAGAGO AGTTGAGAGO AGTTGAGAGO AGTTGAGAGO	CCTACCTGGA(930 CCTACCTGGA(CCTACCTGGA(CCTACCTGGA(CCTACCTGGA(CCTACCTGGA(CCTACCTGGA(CCTACCTGGA(CCTACCTGGA(CCTACCTGGA(CCTACCTGGA(CCTACCTGGA(CCTACCTGGA(CCTACCTGGA(CCTACCTGGA(CCTACCTGGA(CCTACCTGGA(CCTACCTGGA(CCTACCTGGA(CCTACCTGGA(CCTACCTGGA(CCTACCTGGA(CCTACCTGGA(CCTACCTGGA(CCTACCTGGA(CCTACCTGGA(CCTACCTGGA(CCTACCTGGA(CCTACCTGGA(CCTACCTGGA(CCTACCTGGA(GGGCACGTGCC 940 + GGGCACGTGCC GGGCACGTGCC GGGCACGTGCC GGGCACGTGCC	GTGGAGTGGCT 950 GTGGAGTGGCT GTGGAGTGGCT GTGGAGTGGCT GTGGAGTGGCT	ICCGC 960+ ICCGC ICCGC ICCGC ICCGC
SCT-X Majority SCT-3xCys	CGCCTACGACGGCAA CCAAGCACAAGTGGG 890 CCAAGCACAAGTGGG CCAAGCACAAGTGGG CCAAGCACAAGTGGG CCAAGCACAAGTGGG CCAAGCACAAGTGGG CCAAGCACAAGTGGG CCAAGCACAAGTGGG	AGGCGGCCA: AGGCGGCCA: AGGCGGCCA: AGGCGGCCCA: AGGCGGCCCA: AGGCGGCCCA: AGGCGGCCCA:	GCCCTGAAAGA IGTGGCGGAGC 910 + IGTGGCGGAGC IGTGGCGGAGC IGTGGCGGAGC IGTGGCGGAGC	AGTTGAGAGO AGTTGAGAGO AGTTGAGAGO AGTTGAGAGO AGTTGAGAGO AGTTGAGAGO AGTTGAGAGO AGTTGAGAGO	CCTACCTGGA(930 CCTACCTGGA(CCTACCTGGA(CCTACCTGGA(CCTACCTGGA(CCTACCTGGA(CCTACCTGGA(CCTACCTGGA(CCTACCTGGA(CCTACCTGGA(CCTACCTGGA(CCTACCTGGA(CCTACCTGGA(CCTACCTGGA(CCTACCTGGA(CCTACCTGGA(CCTACCTGGA(CCTACCTGGA(CCTACCTGGA(CCTACCTGGA(CCTACCTGGA(CCTACCTGGA(CCTACCTGGA(CCTACCTGGA(CCTACCTGGA(CCTACCTGGA(CCTACCTGGA(CCTACCTGGA(CCTACCTGGA(GGGCACGTGCC 940+ GGGCACGTGCC GGGCACGTGCC GGGCACGTGCC GGGCACGTGCC GGGCACGTGCC	GTGGAGTGGCT 950 GTGGAGTGGCT GTGGAGTGGCT GTGGAGTGGCT GTGGAGTGGCT GTGGAGTGGCT	ICCGC 960 + ICCGC ICCGC ICCGC ICCGC ICCGC
SCT-X Majority SCT-3xCys SCT-B SCT-C SCT-C SCT-Cys-I SCT-Cys-II SCT-Cys-III	CGCCTACGACGGCAA CCAAGCACAAGTGGG 890 CCAAGCACAAGTGGG CCAAGCACAAGTGGG CCAAGCACAAGTGGG CCAAGCACAAGTGGG CCAAGCACAAGTGGG	AGGCGGCCA: AGGCGGCCA: AGGCGGCCA: AGGCGGCCA: AGGCGGCCA: AGGCGGCCA: AGGCGGCCCA: AGGCGGCCCA: AGGCGGCCCA:	GCCCTGAAAGA IGTGGCGGAGC 910 IGTGGCGGAGC IGTGGCGGAGC IGTGGCGGAGC IGTGGCGGAGC IGTGGCGGAGC	AGTTGAGAGO AGTTGAGAGO AGTTGAGAGO AGTTGAGAGO AGTTGAGAGO AGTTGAGAGO AGTTGAGAGO AGTTGAGAGO AGTTGAGAGO	CCTACCTGGA(930 CCTACCTGGA(CCTACCTGGA(CCTACCTGGA(CCTACCTGGA(CCTACCTGGA(CCTACCTGGA(CCTACCTGGA(CCTACCTGGA(CCTACCTGGA(CCTACCTGGA(CCTACCTGGA(CCTACCTGGA(CCTACCTGGA(CCTACCTGGA(CCTACCTGGA(CCTACCTGGA(CCTACCTGGA(CCTACCTGGA(CCTACCTGGA(CCTACCTGGA(CCTACCTGGA(CCTACCTGGA(CCTACCTGGA(CCTACCTGGA(CCTACCTGGA(CCTACCTGGA(CCTACCTGGA(GGGCACGTGCC 940 + GGGCACGTGCC GGGCACGTGCC GGGCACGTGCC GGGCACGTGCC GGGCACGTGCC GGGCACGTGCC	GTGGAGTGGCT 950 GTGGAGTGGCT GTGGAGTGGCT GTGGAGTGGCT GTGGAGTGGCT GTGGAGTGGCT GTGGAGTGGCT	TCCGC 960+ TCCGC TCCGC TCCGC TCCGC TCCGC TCCGC
SCT-X Majority SCT-3xCys SCT-B SCT-C SCT-Cys-I SCT-Cys-II SCT-Cys-III SCT-Cys-III	CGCCTACGACGGCAA CCAAGCACAAGTGGG 890 CCAAGCACAAGTGGG CCAAGCACAAGTGGG CCAAGCACAAGTGGG CCAAGCACAAGTGGG CCAAGCACAAGTGGG CCAAGCACAAGTGGG	AGGCGGCCA: AGGCGGCCA: AGGCGGCCA: AGGCGGCCA: AGGCGGCCA: AGGCGGCCA: AGGCGGCCA: AGGCGGCCCA: AGGCGGCCCA: AGGCGGCCCA:	GCCCTGAAAGA IGTGGCGGAGC 910 IGTGGCGGAGC IGTGGCGGAGC IGTGGCGGAGC IGTGGCGGAGC IGTGGCGGAGC IGTGGCGGAGC	AGTTGAGAGO	CCTACCTGGA 930 CCTACCTGGA CCTACCTGGA CCTACCTGGA CCTACCTGGA CCTACCTGGA CCTACCTGGA CCTACCTGGA CCTACCTGGA CCTACCTGGA	GGGCACGTGCO 940+ GGGCACGTGCO GGGCACGTGCO GGGCACGTGCO GGGCACGTGCO GGGCACGTGCO GGGCACGTGCO GGGCACGTGCO GGGCACGTGCO GGGCACGTGCO	GTGGAGTGGCT 950 GTGGAGTGGCT GTGGAGTGGCT GTGGAGTGGCT GTGGAGTGGCT GTGGAGTGGCT GTGGAGTGGCT	FCCGC 960+ FCCGC FCCGC FCCGC FCCGC FCCGC FCCGC

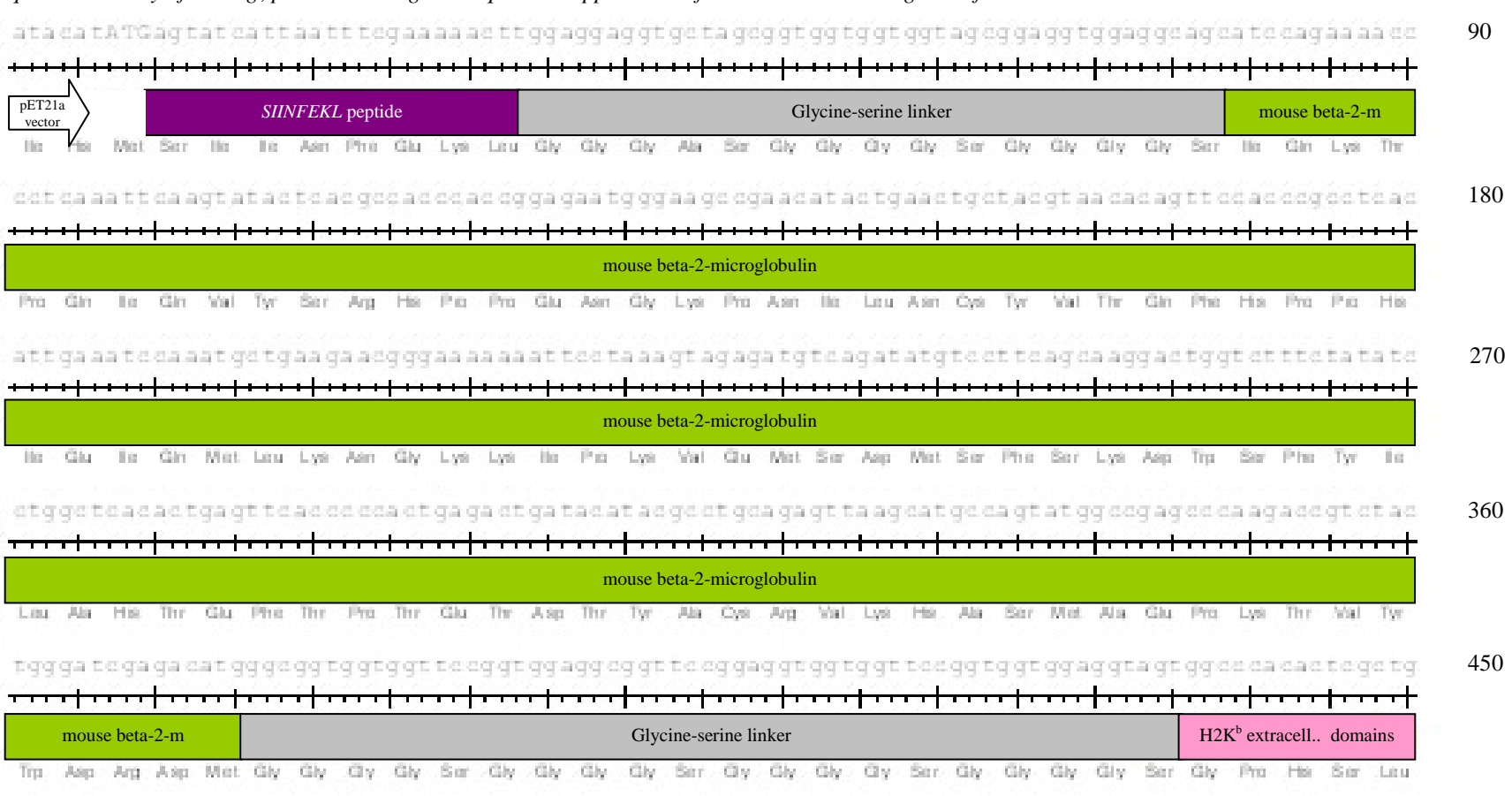
Majority	AGATACCTGGAG					AAACGCATAT			TGA
	970	9	80	990	1000		1020	1030	1040
SCT-3xCys	AGATACCTGGAG	•			•	·	·	•	·
SCT-B	AGATACCTGGAG	AACGGGAA	GGAGACGCT	GCAGCGCACG	GACGCCCC <i>R</i>	AAACGCATAT	GACTCACCA	CGCTGTCTC	TGA 1040
SCT-C	AGATACCTGGAG	AACGGGAA	GGAGACGCT	GCAGCGCACG	GACGCCCC <i>R</i>	AAACGCATAT	GACTCACCA	CGCTGTCTC	TGA 1040
SCT-Cys-I	AGATACCTGGAG	AACGGGAA	GGAGACGCT	GCAGCGCACG	GACGCCCC <i>R</i>	AAACGCATAT	GACTCACCA	CGCTGTCTC	TGA 1040
SCT-Cys-II	AGATACCTGGAG	AACGGGAA	GGAGACGCT	GCAGCGCACG	GACGCCCCC	AAACGCATAT	GACTCACCA	CGCTGTCTC	TGA 1040
SCT-Cys-III	AGATACCTGGAG	AACGGGAA	GGAGACGCT	GCAGCGCACG	GACGCCCCC	AAACGCATAT	GACTCACCA	CGCTGTCTC	TGA 1040
SCT-SL-B DST	AGATACCTGGAG	AACGGGAA	GGAGACGCT	GCAGCGCACG	GACGCCCC <i>R</i>	AAACGCATAT	GACTCACCA	CGCTGTCTC	TGA 1025
SCT-SL-B	AGATACCTGGAG	AACGGGAA	GGAGACGCT	GCAGCGCACG	GACGCCCCC	AAACGCATAT	GACTCACCA	CGCTGTCTC	TGA 1025
SCT-SL-C	AGATACCTGGAG	AACGGGAA	GGAGACGCT	GCAGCGCACG	GACGCCCCC	AAACGCATAT	GACTCACCA	CGCTGTCTC	TGA 1025
SCT-X	AGATACCTGGAG	AACGGGAA	GGAGACGCT	GCAGCGCACG	GACGCCCCC	AAACGCATAT	GACTCACCA	CGCTGTCTC	TGA 1040
Majority	CCATGAAGCCAC			FGAGCTTCTA				GGGATGGGG	AGG
							.+	-+	+
	105		060		1080	1090	1100	1110	1120
SCT-3xCvs	105	+	060	+	1080 +	1090	1100	-+	+
SCT-3xCys SCT-B	105	+ CCTGAGGT	060 : GCTGGGCCC	+ FGAGCTTCTA	1080 + CCCTGCGGA	1090 -+ ATCACACTGA	1100 -+ ACCTGGCAGC	-+ GGGATGGGG	AGG 1120
-	1050	+ CCTGAGGT CCTGAGGT	060 : GCTGGGCCC: GCTGGGCCC:	+ FGAGCTTCTA FGAGCTTCTA	1080 + CCCTGCGGAC CCCTGCGGAC	1090 GATCACACTGA	1100 ACCTGGCAGCO	-+ GGGATGGGG GGGATGGGG	AGG 1120 AGG 1120
SCT-B SCT-C	1050 	CCTGAGGT CCTGAGGT CCTGAGGT	060 GCTGGGCCC' GCTGGGCCC'	H FGAGCTTCTA FGAGCTTCTA FGAGCTTCTA	1080 +	1090 -+ GATCACACTGA GATCACACTGA	1100 -+ ACCTGGCAGCO ACCTGGCAGCO	-+GGGATGGGG GGGATGGGG GGGATGGGG	AGG 1120 AGG 1120 AGG 1120
SCT-B SCT-C SCT-Cys-I	1050 	CCTGAGGT CCTGAGGT CCTGAGGT CCTGAGGT	060 GCTGGGCCC' GCTGGGCCC' GCTGGGCCC'	H IGAGCTTCTA IGAGCTTCTA IGAGCTTCTA	1080 +	1090 SATCACACTGA SATCACACTGA SATCACACTGA SATCACACTGA	1100 ACCTGGCAGCO ACCTGGCAGCO ACCTGGCAGCO ACCTGGCAGCO	-+ GGGATGGGG GGGATGGGG GGGATGGGG	FAGG 1120 FAGG 1120 FAGG 1120 FAGG 1120
SCT-B SCT-C	1050	CCTGAGGT CCTGAGGT CCTGAGGT CCTGAGGT CCTGAGGT	060 GCTGGGCCC GCTGGGCCC GCTGGGCCC GCTGGGCCC	FOR CONTREMENT OF THE PROPERTY	1080 + CCCTGCGGAC CCCTGCGGAC CCCTGCGGAC	1090 HIDDO GATCACACTGA GATCACACTGA GATCACACTGA GATCACACTGA GATCACACTGA	1100 CCTGGCAGCO CCTGGCAGCO CCTGGCAGCO CCTGGCAGCO	-+ GGGATGGGG GGGATGGGG GGGATGGGG GGGATGGGG	AGG 1120 AGG 1120 AGG 1120 AGG 1120 AGG 1120
SCT-B SCT-C SCT-Cys-I SCT-Cys-II	1050 CCATGAAGCCACCCATGAAGCCACCCATGAAGCCACCCCATGAAGCCACCCCATGAAGCCACCCCATGAAGCCACCCCATGAAGCCACCCATGAAGCCACCCATGAAGCCACC	CCTGAGGT CCTGAGGT CCTGAGGT CCTGAGGT CCTGAGGT	060 GCTGGGCCC GCTGGGCCC GCTGGGCCC GCTGGGCCC	FORGETTCTA FGAGCTTCTA FGAGCTTCTA FGAGCTTCTA FGAGCTTCTA FGAGCTTCTA FGAGCTTCTA	1080 + CCCTGCGGAC CCCTGCGGAC CCCTGCGGAC CCCTGCGGAC	1090 HODGE TO THE TOTAL T	1100 ACCTGGCAGCO ACCTGGCAGCO ACCTGGCAGCO ACCTGGCAGCO ACCTGGCAGCO ACCTGGCAGCO	-+ GGGATGGGG GGGATGGGG GGGATGGGG GGGATGGGG	AGG 1120 AGG 1120 AGG 1120 AGG 1120 AGG 1120 AGG 1120
SCT-B SCT-C SCT-Cys-I SCT-Cys-II SCT-Cys-III	1050 CCATGAAGCCACCCATGAAGCCACCCATGAAGCCACCCCATGAAGCCACCCCATGAAGCCACCCCATGAAGCCACCCCATGAAGCCACCCCATGAAGCCACCCATGAAGCCACC	CCTGAGGT CCTGAGGT CCTGAGGT CCTGAGGT CCTGAGGT CCTGAGGT	060 GCTGGGCCC GCTGGGCCC GCTGGGCCC GCTGGGCCC GCTGGGCCC GCTGGGCCC	FORGETTCTA FGAGCTTCTA FGAGCTTCTA FGAGCTTCTA FGAGCTTCTA FGAGCTTCTA FGAGCTTCTA FGAGCTTCTA	1080 + CCCTGCGGAC CCCTGCGGAC CCCTGCGGAC CCCTGCGGAC CCCTGCGGAC	1090 HHTTP: GATCACACTGA GATCACACTGA GATCACACTGA GATCACACTGA GATCACACTGA GATCACACTGA GATCACACTGA GATCACACTGA	1100 ACCTGGCAGCO ACCTGGCAGCO ACCTGGCAGCO ACCTGGCAGCO ACCTGGCAGCO ACCTGGCAGCO ACCTGGCAGCO ACCTGGCAGCO	GGGATGGGGGGGGATGGGGGGATGGGGGGATGGGGGGGATGGGGGG	AGG 1120 AGG 1120 AGG 1120 AGG 1120 AGG 1120 AGG 1120 AGG 1120 AGG 1105
SCT-B SCT-C SCT-Cys-I SCT-Cys-II SCT-Cys-III SCT-Cys-III	1050 CCATGAAGCCACCCATGAAGCCACCCATGAAGCCACCCATGAAGCCACCCCATGAAGCCACCCCATGAAGCCACCCCATGAAGCCACCCCATGAAGCCACCCATGAAGCCACCCATGAAGCCACCCATGAAGCCACCCATGAAGCCACC	CCTGAGGT CCTGAGGT CCTGAGGT CCTGAGGT CCTGAGGT CCTGAGGT CCTGAGGT	060 GCTGGGCCC GCTGGGCCC GCTGGGCCC GCTGGGCCC GCTGGGCCC GCTGGGCCC GCTGGGCCC	FORGETTCTA FGAGCTTCTA FGAGCTTCTA FGAGCTTCTA FGAGCTTCTA FGAGCTTCTA FGAGCTTCTA FGAGCTTCTA FGAGCTTCTA	1080 + CCCTGCGGAC CCCTGCGGAC CCCTGCGGAC CCCTGCGGAC CCCTGCGGAC CCCTGCGGAC	TO90 ATCACACTGA GATCACACTGA	1100 ACCTGGCAGCO ACCTGGCAGCO ACCTGGCAGCO ACCTGGCAGCO ACCTGGCAGCO ACCTGGCAGCO ACCTGGCAGCO ACCTGGCAGCO	GGGATGGGGGGGGATGGGGGGATGGGGGGATGGGGGGGATGGGGGG	AGG 1120 AGG 1120 AGG 1120 AGG 1120 AGG 1120 AGG 1120 AGG 1120 AGG 1105 AGG 1105

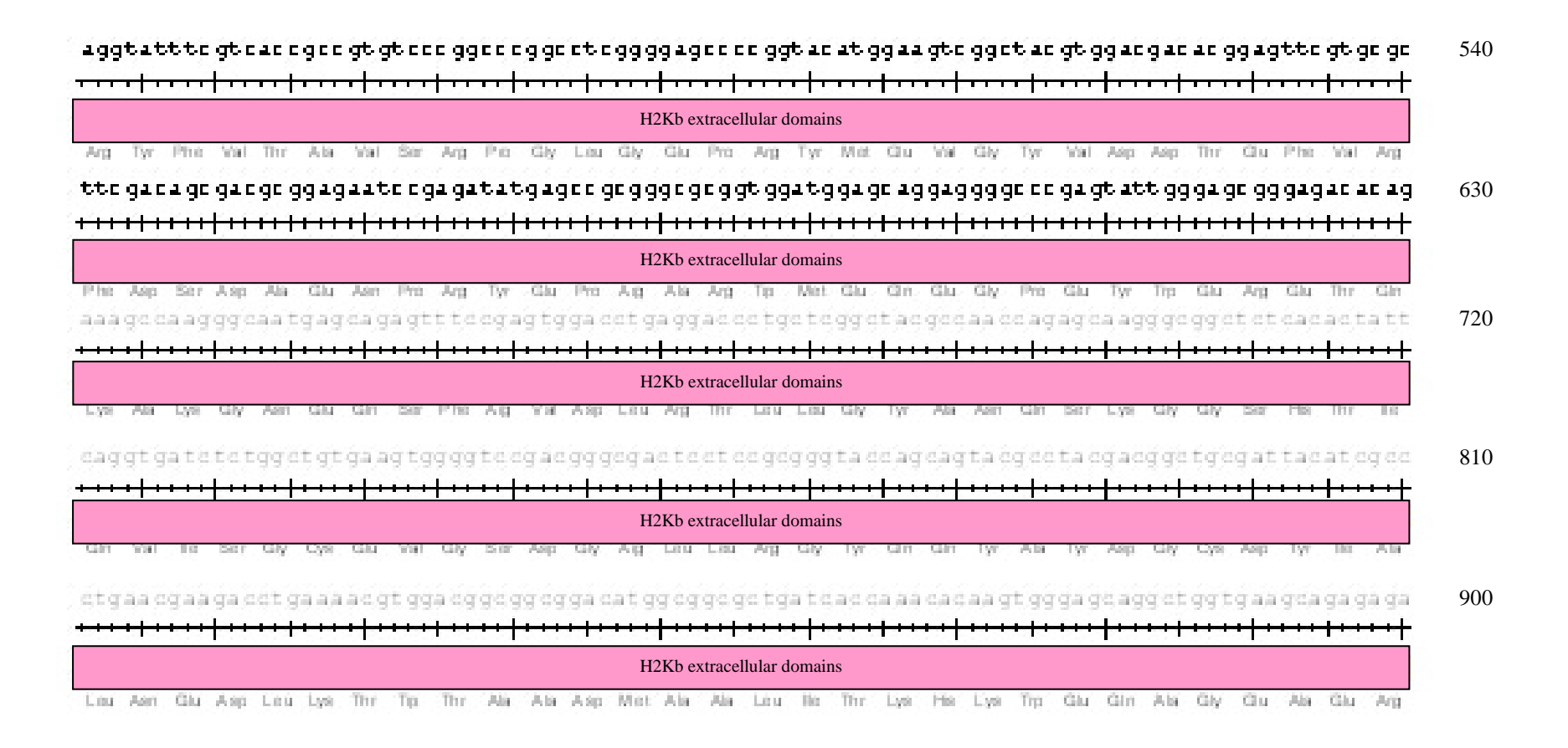
Majority	ACCAGAC	CAGGACAC		1	+	1	1	1	1
		1130	1140	1150	1160	1170	1180	1190	1200
SCT-3xCys	ACCAGAC	•	·	GAGACCAGGC(·	·	•	·	•
SCT-B	ACCAGAC	CCAGGACAC	GAGCTCGTG	GAGACCAGGC(CTGCAGGGGA	TGGAACCTTC	CAGAAGTGGG	CGGCTGTGGT	'GGTG
SCT-C	ACCAGAC	CCAGGACAC	GAGCTCGTG	GAGACCAGGC(CTGCAGGGGA	TGGAACCTTC	CAGAAGTGGG	CGGCTGTGGT	'GGTG
SCT-Cys-I	ACCAGAC	CCAGGACAC	GAGCTCGTG	GAGACCAGGC(CTGCAGGGGA	TGGAACCTTC	CAGAAGTGGG	CGGCTGTGGT	'GGTG
SCT-Cys-II	ACCAGAC	CCAGGACAC	GAGCTCGTG	GAGACCAGGC(CTGCAGGGGA	TGGAACCTTC	CAGAAGTGGG	CGGCTGTGGT	'GGTG
SCT-Cys-III	ACCAGAC	CCAGGACAC	GAGCTCGTG	GAGACCAGGC(CTGCAGGGGA	TGGAACCTTC	CAGAAGTGGG	CGGCTGTGGT	'GGTG
SCT-SL-B DST	ACCAGAC	CCAGGACAC	GAGCTCGTG	GAGACCAGGC(CTGCAGGGGA	TGGAACCTTC	CAGAAGTGGG	CGGCTGTGGT	'GGTG
SCT-SL-B	ACCAGAC	CCAGGACAC	GAGCTCGTG	GAGACCAGGC(CTGCAGGGGA	TGGAACCTTC	CAGAAGTGGG	CGGCTGTGGT	'GGTG
	$\lambda C C \lambda C \lambda C \lambda C C$	C	CACCTCCTC	SAGACCAGGC	CTGCAGGGGA	TGGAACCTTC	CAGAAGTGGG	CGGCTGTGGT	GGTG
SCT-SL-C	ACCAGAC	JUAUGACAC	001100100100	3110110011000					
SCT-X	ACCAGAC	CCAGGACAC	GGAGCTCGTG	GAGACCAGGC CTGCCATGTG	CTGCAGGGGA		CAGAAGTGGG		'GGTG
	ACCAGAC	CCAGGACACO GACAGGAGCA + 1210	GGAGCTCGTGC AGAGATACACC + 1220	GAGACCAGGCCCTGCCATGTGCCATGTGCCATGTGCCATGTGCCATGTGCCATGTGCCATGTGCCATGTGCCATGTGCATGTGCATGTGCATGTGCATGTGCATGTGCATGTGCATGTGCATGTGCATGTGCATGTGCATGTGCATGTGCATGTGCATGTGCATGTGCATGTGCATGTGCATGTGCATGTGCATGTGCATGTGCATGTGCATGTGCATGTGCATGTGCATGTGCATGTGCATGTGCATGTGCATGTGCATGTGCATGTGCATGTGCATGTGCATGTGCATGTGCATGTGCATGTGCATGTGCATGTGCATGTGCATGTGCATGTGCATGTGCATGTGCATGTGCATGTGCATGTGCATGTGCATGTGCATGTGCATGTGCATGTGCATGTGCATGTGCATGTGCATGTGCATGTGCATGTGCATGTGCATGTGCATGTGCATGTATGT	CTGCAGGGGA CAGCATGAGG + 1240	GTTTGCCCAA + 1250	CAGAAGTGGG GCCCCTCACC + 1260	CTGAGATGGG	GGTG AGCC 1280
SCT-X Majority	ACCAGAC	GACAGGAGCA GACAGGAGCA 1210	GGAGCTCGTGC AGAGATACACC + 1220 +	GAGACCAGGCCCTGCCATGTGCCATGTGCCATGTGCCATGTGCCATGTGCCATGTGCCATGTGCCATGTGCATGTGCATGTGCATGTGCATGTGCATGTGCATGTGCATGTGCATGTGCATGTGCATGTGCATGTGCATGTGCATGTGCATGTGCATGTGCATGTGCATGTGCATGTGCATGTGCATGTGCATGTGCATGTGCATGTGCATGTGCATGTGCATGTGCATGTGCATGTGCATGTGCATGTGCATGTGCATGTGCATGTGCATGTGCATGTGCATGTGCATGTGCATGTGCATGTGCATGTGCATGTGCATGTGCATGTGCATGTGCATGTGCATGTGCATGTGCATGTGCATGTGCATGTGCATGTGCATGTGCATGTGCATGTGCATGTGCATGTGCATGTGCATGTGCATGTGCATGTGCATGTGCATGTGCATGTGCATGTGCATGTGCATGTGCATGTGCATGTGCATGTGCATGTGCATGTGCATGTGCATGTGCATGTGCATGTGCATGTGCATGTGCATGTGCATGTGCATGTGCATGTGCATGTGCATGTGCATGTGCATGTGCATGTGCATGTGCATGTGCATGTGCATGTGCATGTGCATGTGCATGTGCATGTGCATGTGCATGTGCATGTGCATGTGCATGTGCATGTGCATGTGCATGTGCATGTGCATGTGCATGTGCATGTGCATGTGCATGTGCATGTGCATGTGCATGTGCATGTGCATGTGCATGTGCATGTGCATGTGCATGTGCATGTGCATGTGCATGTGCATGTGCATGTGCATGTGCATGTGCATGTGCATGTGCATGTGCATGTGCATGTGCATGTGCATGTGCATGTGCATGTGCATGTGCATGTGCATGTGCATGTGCATGTGCATGTGCATGTGCATGTGCATGTGCATGTGCATGTGCATGTGCATGTGCATGTGCATGTGCATGTGCATGTGCATGTGCATGTGCATGTGCATGTGCATGTGCATGTGCATGTGCATGTGCATGTGCATGTGCATGTGCATGTGCATGTGCATGTGCATGTGCATGTGCATGTGCATGTGCATGTGCATGTGCATGTGCATGTGCATGTGCATGTGCATGTGCATGTGCATGTGCATGTGCATGTGCATGTGCATGTGCATGTGCATGTGCATGTGCATGTGCATGTGCATGTGCATGTGCATGTGCATGTGCATGTGCATGTGCATGTGCATGTGCATGTGCATGTGCATGTGCATGTGCATGTGCATGTGCATGTGCATGTGCATGTGCATGTGCATGTGCATGTGCATGTGCATGTGCATGTGCATGTGCATGTGCATGTGCATGTGCATGTGCATGTGCATGTGCATGTGCATGTGCATGTGCATGTGCATGTGCATGTGCATGTGCATGTGCATGTGCATGTGCATGTGCATGTGCATGTGCATGTGCATGTGCATGTGCATGTGCATGTGCATGTGCATGTGCATGTGCATGTGCATGTGCATGTGCATGTGCATGTGCATGTGCATGTGCATGTGCATGTGCATGTGCATGTGCATGTGCATGTGCATGTGCATGTGCATGTGCATGTGCATGTGCATGTGCATGTGCATGTGCATGTGCATGTGCATGTGCATGTGCATGTGCATGTGCATGTGCATGTGCATGTGCATGTGCATGTGCATGTGCATGTGCATGTGCATGTGCATGTGCATGTGCATGTGCATGTGCATGTGCATGTGCATGTGCATGTGATGTGATGTGATGTGATGATGATGATGATGATGAT	CTGCAGGGA CAGCATGAGG + 1240 +	GTTTGCCCAA + 1250 +	CAGAAGTGGG GCCCCTCACC + 1260 +	CTGAGATGGG + 1270 +	GGTG AGCC+ 1280
SCT-X Majority SCT-3xCys	ACCAGAC	GACAGGACACC GACAGGAGCA+ 1210+ GACAGGAGCA	GGAGCTCGTGC AGAGATACACC + 1220 + AGAGATACACC	GAGACCAGGCCCTGCCATGTGCCATGTGCCATGTGCCATGTGCCATGTGCCATGTGCCATGTGCCATGTGCCATGTGCATGTGCATGTGCATGTGCATGTGCATGTGCATGTGCATGTGCATGTGCATGTGCATGTGCATGTGCATGTGCATGTGCATGTGCATGTGCATGTGCATGTGCATGTGCATGTGCATGTGCATGTGCATGTGCATGTGCATGTGCATGTGCATGTGCATGTGCATGTGCATGTGCATGTGCATGTGCATGTGCATGTGCATGTGCATGTGCATGTGCATGTGCATGTGCATGTGCATGTGCATGTGCATGTGCATGTGCATGTGCATGTGCATGTGCATGTGCATGTGCATGTGCATGTGCATGTGCATGTGCATGTGCATGTGCATGTGCATGTGCATGTGCATGTGCATGTGCATGTGCATGTGCATGTGCATGTATGT	CTGCAGGGA CAGCATGAGG+ 1240+CAGCATGAGG	GTTTGCCCAA 1250 + GTTTGCCCAA	CAGAAGTGGG GCCCCTCACC+ 1260+ GCCCCTCACC	CTGAGATGGG + 1270 + CTGAGATGGG	AGCC 1280 1280
SCT-X Majority	CCTTCTG	GACAGGACAC GACAGGAGCA 1210 + GACAGGAGCA GACAGGAGCA	GGAGCTCGTGC AGAGATACACC 1220+ AGAGATACACC	GAGACCAGGCC CTGCCATGTGC+ 1230+ CTGCCATGTGC	CTGCAGGGA CAGCATGAGG+ 1240+ CAGCATGAGG CAGCATGAGG	GTTTGCCCAA+ 1250+ GTTTGCCCAA GTTTGCCCAA	CAGAAGTGGG GCCCTCACC+ 1260+ GCCCCTCACC	CTGAGATGGG 1270+ CTGAGATGGG	AGCC AGCC AGCC AGCC AGCC
SCT-X Majority SCT-3xCys SCT-B SCT-C	CCTTCTGCCCTTCTGCCCTTCTGCCCTTCTGCCCTTCTGCCCTTCTGCCCTTCTGCCCTTCTGCCCTTCTGCCCTTCTGCCCTTCTGCCCTTCTGCCCTTCTGCCCTTCTGCCCTTCTGCCCTTCTGCCCTTCTGCCCTTCTGCCCTTCTGCCCTTCTGCCCTTCTGCCCTTCTGCCCTTCTGCCCTTCTGCCCTTCTGCCCTTCTGCCCTTCTGCCCTTCTGCCCTTCTGCCCTTCTGCCCTTCTGCCCTTCTGCCCTTCTGCCCTTCTGCCCTTCTGCCCTTCTGCCCTTCTGCCCTTCTGCCCTTCTGCCCTTCTGCCCTTCTGCCCTTCTGCCCTTCTGCCCTTCTGCCCTTCTGCCCTTCTGCCCTTCTGCCCTTCTGCCCTTCTGCCCTTCTGCCCTTCTGCCCTTCTGCCCTTCTGCCCTTCTGCCCTTCTGCCCTTCTGCCCTTCTGCCCTTCTGCCCTTCTGCCTTCTGCCCTTCTGCCCTTCTGCCCTTCTGCCCTTCTGCCCTTCTGCCCTTCTGCCCTTCTGCCCTTCTGCCCTTCTGCCCTTCTGCCCTTCTGCCCTTCTGCCCTTCTGCCCTTCTGCCCTTCTGCCTTCTGCCTTCTGCCTTCTGCCTTCTGCCTTCTGCCTTCTGCCTTCTGCCTTCTGCCTTCTGCCTTCTGCCTTCTT	GACAGGACACA 1210 + GACAGGAGCA GACAGGAGCA GACAGGAGCA GACAGGAGCA GACAGGAGCA GACAGGAGCA GACAGGAGCA	GGAGCTCGTGC AGAGATACACC 1220 AGAGATACACC AGAGATACACCA AGAGATACACCA	GAGACCAGGCC CTGCCATGTGC 1230+ CTGCCATGTGC CTGCCATGTGC CTGCCATGTGC	CTGCAGGGA CAGCATGAGG 1240 CAGCATGAGG CAGCATGAGG CAGCATGAGG CAGCATGAGG	GTTTGCCCAA+ 1250+ GTTTGCCCAA GTTTGCCCAA	CAGAAGTGGG GCCCTCACC+ 1260+ GCCCCTCACC GCCCCTCACC	CTGAGATGGG 1270+ CTGAGATGGG CTGAGATGGG	AGCC AGCC AGCC AGCC AGCC AGCC
SCT-X Majority SCT-3xCys SCT-B SCT-C SCT-Cys-I	CCTTCTG CCTTCTG CCTTCTG CCTTCTG	GACAGGACACA GACAGGAGCA 1210 GACAGGAGCA GACAGGAGCA GACAGGAGCA GACAGGAGCA GACAGGAGCA GACAGGAGCA GACAGGAGCA GACAGGAGCA	GGAGCTCGTGC AGAGATACACC 1220+ AGAGATACACC AGAGATACACC AGAGATACACC	GAGACCAGGCC CTGCCATGTGC+ 1230+ CTGCCATGTGC	CTGCAGGGA CAGCATGAGG 1240 + CAGCATGAGG CAGCATGAGG CAGCATGAGG CAGCATGAGG CAGCATGAGG	GTTTGCCCAA 1250 + GTTTGCCCAA GTTTGCCCAA GTTTGCCCAA GTTTGCCCAA	CAGAAGTGGG GCCCTCACC+ 1260+ GCCCCTCACC GCCCCTCACC GCCCCTCACC	CTGAGATGGG 1270+ CTGAGATGGG CTGAGATGGG	AGCC AGCC AGCC AGCC AGCC AGCC AGCC
SCT-X Majority SCT-3*Cys SCT-B SCT-C SCT-Cys-I SCT-Cys-II	CCTTCTGCCCTTCTGCCCTTCTGCCCTTCTGCCCTTCTGCCCTTCTGCCCTTCTGCCCTTCTGCCCCTTCTGCCCCTTCTGCCCCTTCTGCCCCTTCTGCCCTTCTGCCCTTCTGCCCTTCTGCCCTTCTGCCCTTCTGCCCTTCTGCCCTTCTGCCCTTCTGCCCTTCTGCCCTTCTGCCCTTCTGCCCTTCTGCCCTTCTGCCCTTCTGCCCTTCTGCCCTTCTGCCCTTCTGCCCTTCTGCCCTTCTGCCCTTCTGCCCTTCTGCCCTTCTGCCCTTCTGCCCTTCTGCCCTTCTGCCCTTCTGCCCTTCTGCCCTTCTGCCCTTCTGCCCTTCTGCCCTTCTGCCCTTCTGCCCTTCTGCCCTTCTGCCCTTCTGCCCTTCTGCCCTTCTGCCCTTCTGCCCTTCTGCCCTTCTGCCCTTCTGCCCTTCTGCCCTTCTGCCTTCTGCCCTTCTGCCCTTCTGCCCTTCTGCCCTTCTGCCCTTCTGCCCTTCTGCCCTTCTGCCCTTCTGCCCTTCTGCCCTTCTGCCCTTCTGCCCTTCTGCCCTTCTGCCCTTCTGCCCTTCTGCCCTTCTGCCCTTCTGCCCTTCTGCCCTTCTGCCCTTCTGCCCTTCTGCCCTTCTGCCCTTCTGCCCTTCTGCCCTTCTGCCCTTCTGCCCTTCTGCCCTTCTGCCCTTCTGCCCTTCTGCCCTTCTGCCCTTCTGCCCTTCTGCCCTTCTGCCCTTCTGCCCTTCTGCCCTTCTGCCCTTCTGCCCTTCTGCCCTTCTGCCCTTCTGCCCTTCTGCCCTTCTGCCCTTCTGCCTTCTGCCTTCTGCCTTCTGCCTTCTGCCCTTCTGCCTTCTGCCTTCTGCCTTCTGCCTTCTT	GACAGGACACA TABLE TO THE TRANSPORT TO T	GGAGCTCGTGC AGAGATACACC AGAGATACACC AGAGATACACC AGAGATACACC AGAGATACACC AGAGATACACC	GAGACCAGGCC CTGCCATGTGC 1230+ CTGCCATGTGC CTGCCATGTGC CTGCCATGTGC CTGCCATGTGC	CTGCAGGGA CAGCATGAGG 1240 CAGCATGAGG	GTTTGCCCAA 1250 TTTGCCCAA GTTTGCCCAA GTTTGCCCAA GTTTGCCCAA GTTTGCCCAA	CAGAAGTGGG GCCCTCACC 1260+ GCCCCTCACC GCCCCTCACC GCCCCTCACC GCCCCTCACC	CTGAGATGGG 1270+ CTGAGATGGG CTGAGATGGG CTGAGATGGG	AGCC AGCC AGCC AGCC AGCC AGCC AGCC AGCC
SCT-X Majority SCT-3xCys SCT-B SCT-C SCT-Cys-I	CCTTCTGCCCTTCTGCCCTTCTGCCCTTCTGCCCTTCTGCCCTTCTGCCCTTCTGCCCTTCTGCCCTTCTGCCCCTTCTGCCCCTTCTGCCCTTCTGCCCTTCTGCCCTTCTGCCCTTCTGCCCTTCTGCCCTTCTGCCCTTCTGCCCTTCTGCCCTTCTGCCCTTCTGCCCTTCTGCCCTTCTGCCCTTCTGCCCTTCTGCCCTTCTGCCCTTCTGCCCTTCTGCCCTTCTGCCCTTCTGCCCTTCTGCCCTTCTGCCCTTCTGCCCTTCTGCCCTTCTGCCCTTCTGCCCTTCTGCCCTTCTGCCCTTCTGCCCTTCTGCCCTTCTGCCCTTCTGCCCTTCTGCCCTTCTGCCCTTCTGCCCTTCTGCCCTTCTGCCCTTCTGCCCTTCTGCCCTTCTGCCCTTCTGCCCTTCTGCCCTTCTGCCCTTCTGCCCTTCTGCCCTTCTGCCCTTCTGCCCTTCTGCCCTTCTGCCCTTCTGCCCTTCTGCCCTTCTGCCCTTCTGCCCTTCTGCCCTTCTGCCCTTCTGCCCTTCTGCCCTTCTGCCCTTCTGCCCTTCTGCCCTTCTGCCCTTCTGCCCTTCTGCCCTTCTGCCCTTCTGCCCTTCTGCCCTTCTGCCCTTCTGCCCTTCTGCCCTTCTGCCCTTCTGCCCTTCTGCCCTTCTGCCCTTCTGCCCTTCTGCCCTTCTGCCCTTCTGCCCTTCTGCCCTTCTGCCCTTCTGCCCTTCTGCCCTTCTGCCCTTCTGCCCTTCTGCCCTTCTGCCCTTCTGCCCTTCTGCCCTTCTGCCCTTCTGCCCTTCTGCCCTTCTGCCCTTCTGCCCTTCTGCCCTTCTGCCCTTCTGCCCTTCTGCCCTTCTGCCCTTCTGCCCTTCTGCCCTTCTGCCCTTCTGCCCTTCTGCCCTTCTGCCCTTCTGCCCTTCTGCCCTTCTGCCCTTCTGCCCTTCTGCCCTTCTGCCCTTCTGCCCTTCTGCCCTTCTGCCCTTCTGCCCTTCTGCCCTTCTGCCCTTCTGCCCTTCTGCCCTTCTGCCCTTCTGCCCTTCTGCCCTTCTGCCCTTCTGCCTTCTGCCTTCTT	GACAGGACACA TABLE TO THE TOTAL TO THE TOTAL TO THE TOTAL TO THE TOTAL T	AGAGATACACO	GAGACCAGGCC CTGCCATGTGC 1230+ CTGCCATGTGC CTGCCATGTGC CTGCCATGTGC CTGCCATGTGC CTGCCATGTGC CTGCCATGTGC	CTGCAGGGA CAGCATGAGG 1240 CAGCATGAGG CAGCATGAGG CAGCATGAGG CAGCATGAGG CAGCATGAGG CAGCATGAGG CAGCATGAGG	GTTTGCCCAA 1250 + GTTTGCCCAA GTTTGCCCAA GTTTGCCCAA GTTTGCCCAA GTTTGCCCAA	CAGAAGTGGG GCCCTCACC 1260+ GCCCCTCACC GCCCCTCACC GCCCCTCACC GCCCCTCACC GCCCCTCACC	CTGAGATGGG 1270 CTGAGATGGGCCTGAGATGGGCCTGAGATGGGCCTGAGATGGGCCTGAGATGGGCCTGAGATGGGCCTGAGATGGGCCTGAGATGGG	AGCC AGCC AGCC AGCC AGCC AGCC AGCC AGCC
SCT-X Majority SCT-3xCys SCT-B SCT-C SCT-Cys-I SCT-Cys-II SCT-Cys-III	CCTTCTG CCTTCTG CCTTCTG CCTTCTG CCTTCTG CCTTCTG CCTTCTG	GACAGGACACA GACAGGAGCA	AGAGATACACO	GAGACCAGGCC CTGCCATGTGC 1230+ CTGCCATGTGC CTGCCATGTGC CTGCCATGTGC CTGCCATGTGC CTGCCATGTGC CTGCCATGTGC CTGCCATGTGC CTGCCATGTGC CTGCCATGTGC	CTGCAGGGA CAGCATGAGG 1240 CAGCATGAGG	GTTTGCCCAA 1250 GTTTGCCCAA GTTTGCCCAA GTTTGCCCAA GTTTGCCCAA GTTTGCCCAA GTTTGCCCAA GTTTGCCCAA	CAGAAGTGGG GCCCTCACC 1260+ GCCCCTCACC GCCCCTCACC GCCCCTCACC GCCCCTCACC GCCCCTCACC GCCCCTCACC GCCCCTCACC	CTGAGATGGG 1270+ CTGAGATGGG CTGAGATGGG CTGAGATGGG	AGCC AGCC AGCC AGCC AGCC AGCC AGCC AGCC
SCT-X Majority SCT-3xCys SCT-B SCT-C SCT-Cys-I SCT-Cys-II SCT-Cys-III SCT-Cys-III	CCTTCTG CCTTCTG CCTTCTG CCTTCTG CCTTCTG CCTTCTG CCTTCTG CCTTCTG	GACAGGAGA TABLE TO THE TOTAL TO	AGAGATACACO	GAGACCAGGCC CTGCCATGTGC 1230+ CTGCCATGTGCCATGTGCCATGTGCCATGTGCCATGTGCCATGTGCCATGTGCCATGTGCCATGTGCCATGTGCCATGTGCCATGTGCCATGTGCCATGTGCCATGTGCCATGTGCCATGTGCCATGTGCCATGTGCCATGTGCCATGTGCCATGTGCCATGTGCCATGTGCCATGTGCCATGTGCCATGTGCCATGTGCCATGTGCCATGTGCCATGTGCCATGTGCCATGTGCCATGTGCCATGTGCCATGTGCCATGTGCCATGTGCCATGTGCCATGTGCCATGTGCCATGTGCCATGTGCCATGTGCCATGTGCCATGTGCCATGTGCCATGTGCCATGTGCCATGTGCCATGTGCCATGTGCCATGTGCCATGTGCCATGTGCCATGTGCCATGTGCCATGTGCCATGTGCCATGTGCCATGTGCCATGTGCCATGTGCCATGTGCCATGTGCCATGTGCCATGTGCCATGTGCCATGTGCCATGTGCCATGTGCCATGTGCCATGTGCCATGTGCCATGTGCCATGTGCCATGTGCCATGTGCCATGTGCCATGTGCCATGTGCCATGTGCCATGTGCCATGTGCCATGTGCCATGTGCCATGTGCCATGTGCCATGTGCCATGTGCCATGTGCCATGTGCCATGTGCCATGTGCCATGTGCCATGTGCCATGTGCCATGTGCCATGTGCCATGTGCCATGTGCCATGTGCCATGTGCCATGTGCCATGTGCCATGTGCCATGTGCCATGTGCCATGTGCCATGTGCCATGTGCCATGTGCCATGTGCCATGTGCCATGTGCCATGTGCCATGTGCCATGTGCCATGTGCCATGTGCCATGTGCCATGTGCCATGTGCCATGTGCCATGTGCCATGTGCCATGTGCCATGTGCCATGTGCCATGTGCCATGTGCCATGTGCCATGTGCCATGTGCCATGTGCCATGTGCCATGTGCCATGTGCCATGTGCCATGTGCCATGTGCCATGTGCCATGTGCCATGTGCCATGTGCCATGTGCCATGTGCCATGTGCCATGTGCCATGTGCCATGTGCCATGTGCCATGTGCCATGTGCCATGTGCCATGTGCCATGTGCCATGTGCCATGTGCCATGTGCCATGTGCCATGTGCCATGTGCCATGTGCCATGTGCCATGTGCCATGTGCCATGTGCCATGTGCCATGTGCCATGTGCCATGTGCCATGTGCCATGTGCCATGTGCCATGTGCCATGTGCCATGTCATGTCATGCATG	CTGCAGGGA CAGCATGAGG 1240 CAGCATGAGG	GTTTGCCCAA 1250 GTTTGCCCAA GTTTGCCCAA GTTTGCCCAA GTTTGCCCAA GTTTGCCCAA GTTTGCCCAA GTTTGCCCAA	CAGAAGTGGG GCCCCTCACC 1260+ GCCCCTCACC GCCCCTCACC GCCCCTCACC GCCCCTCACC GCCCCTCACC GCCCCTCACC GCCCCTCACC GCCCCTCACC	CTGAGATGGG 1270 CTGAGATGGG CTGAGATGGG CTGAGATGGG CTGAGATGGG	AGCC AGCC AGCC AGCC AGCC AGCC AGCC AGCC

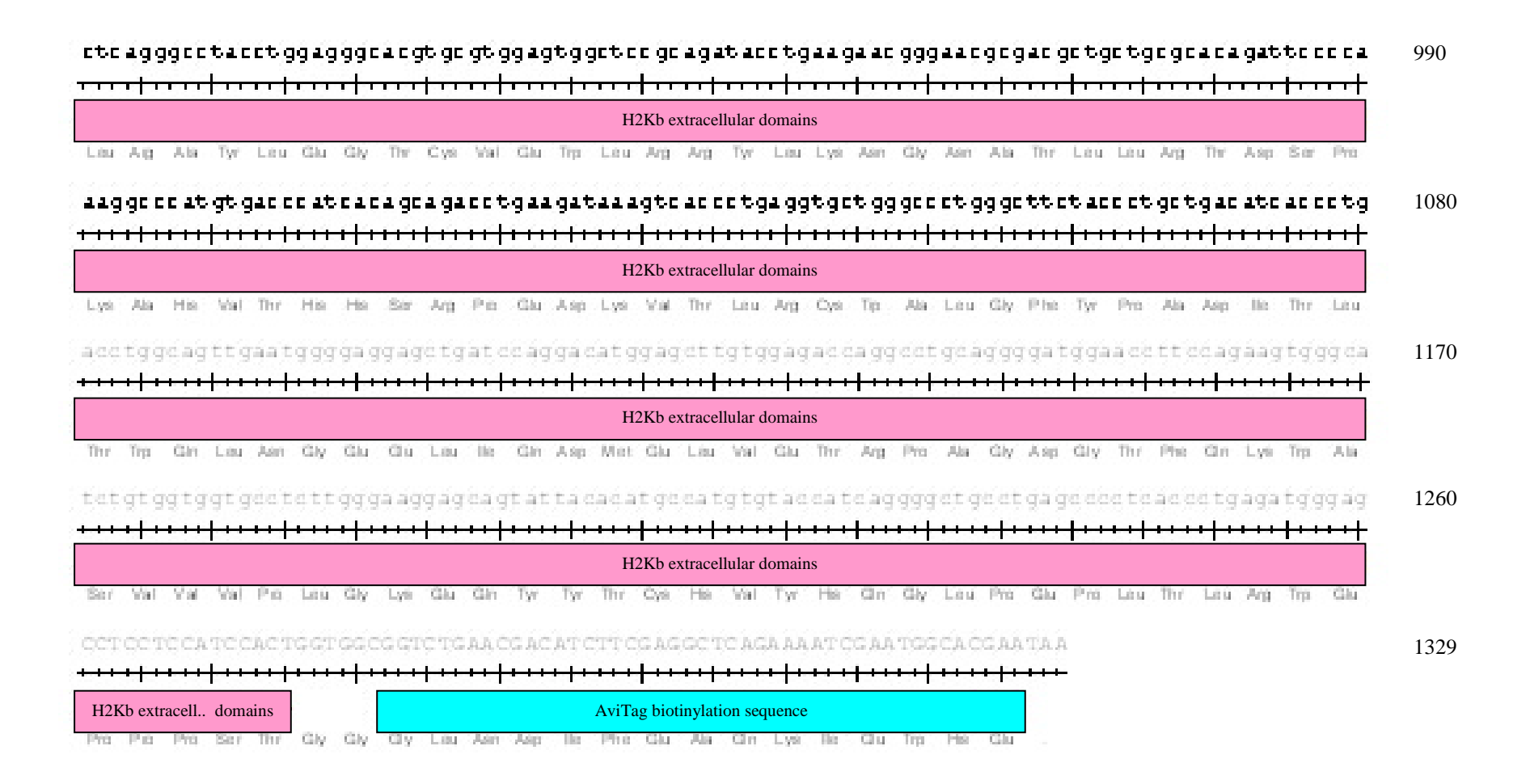


A3 2 Sequence of murine construct produced in bacterial cells murine SHNFEKL-β₂microglobulin-K^b-biotin-AviTag (mSCT-B)

Sequence courtesy of B King; presented using the SeqBuilder application of the DNASTAR Lasergene software suite.







References

References

1

¹ World Health Organisation Fact sheet on Cancer. Fact sheet No. 297. Feb 2012

² Karim-Kos, H., et al., *Recent trends of cancer in Europe: A combined approach of incidence, survival and mortality for 17 cancer sites since the 1990s.* Eur J Cancer, 2008. 44(10): p. 1345-1389.

³ Eiermann, W., *Trastuzumab combined with chemotherapy for the treatment of HER2-positive metastatic breast cancer: pivotal trial data.* Ann Oncol, 2001. 12 Suppl 1: p. S57-62.

⁴ McLaughlin, P., et al., *Rituximab chimeric anti-CD20 monoclonal antibody therapy for relapsed indolent lymphoma: half of patients respond to a four-dose treatment programme.* J Clin Oncol, 1998. 16(8): p. 2825-2833.

⁵ Erlich, P., *Ueber den jetzigen stand der Karzinomforschung*. Ned Tijdschr Geneeskd, 1909. 5: p. 273-290.

⁶ Burnet, F., *The concept of immunological surveillance*. Prog Exp Tumor Res, 1970. 13: p. 1-27.

⁷ Old, L., & Boyse E., *Immunology of experimental tumours*. Annu Rev Med, 1964. 15: p. 167-186.

⁸ Stutman, O., *Immunodepression and malignancy*. Adv Cancer Res, 1975. 22: p. 261-422.

⁹ Stutman, O., *Tumour development after 3-methylcholanthrene in immunologically deficient athymic nude mice*. Science, 1974. 183(4124): p. 534-536.

¹⁰ Stutman, O., In Fogh, J., & Giovanella, B., *The nude mouse in experimental and clinical research*. 1978. p. 411-435.

¹¹ Maleckar, J., & Sherman, L., *The composition of the T cell receptor repertoire in nude mice.* J Immunol, 1987. 138(11): p. 3873-3876.

¹² Shinkai, Y., et al., *RAG-2-deficient mice lack mature lymphocytes owing to inability to initiate V(D)J rearrangements.* Cell, 1992. 68(5): p. 855-867.

¹³ Shankaran, V., et al., *IFNgamma and lymphocytes prevent primary tumour development and shape tumour immunogenicity*. Nature, 2001. 410(6832): p. 1107-1111.

¹⁴ van den Broek, M., et al., *Decreased tumour surveillance in perforin deficient mice*. J Exp Med, 1996. 184(5): p. 1781-1790.

¹⁵ Qin, Z., & Blankenstein, T., *A cancer immunosurveillance controversy*. Nat Immunol, 2004. 5(1): p. 3-4.

¹⁶ Kammertoens, T., et al., *B-cells and IL-4 promote methylcholanthrene-induced carcinogenesis but there is no evidence for a role of T/NKT-cells and their effector molecules (Fas-ligand, TNF-\alpha, perforin).* Int J Cancer, 2011. [Epub ahead of print]

¹⁷ Schreiber, T., et al., *A cancer immunosurveillance controversy. Author reply.* Nat Immunol, 2004. 5(1): p. 4-5.

¹⁸ Schreiber, T., & Podack, E,. A critical analysis of the tumour immunosurveillance controversy for 3-MCA-induced sarcomas. Br J Cancer, 2009. 101(3): p. 381-386.

¹⁹ Gershwin, M., et al., *Anti-mu induces lymphoma in germfree congenitally athymic (nude) but not in heterozygous (nu/+) mice.* J Immunol, 1983. 131(4): p. 2069-2073.

 $^{^{20}}$ Smyth, M., et al., NK cells and NKT cells collaborate in host protection from methylcholanthrene-induced fibrosarcoma. Int Immunol, 2001. 13(4): p. 459-463.

²¹ Girardi, M., et al., *Regulation of cutaneous malignancy by gammadelta T cells*. Science, 2001. 294(5542); p. 605-609.

- ²³ Smyth, M., et al., *Differential tumor surveillance by natural killer (NK) and NKT cells*. J Exp Med, 2000. 191(4): p. 661-668.
- ²⁴ Tawara, I., et al., Sequential involvement of two distinct CD4+ regulatory T cells during the course of transplantable tumor growth and protection from 3-methylcholanthrene-induced tumorigenesis by CD25-depletion. Jpn J Cancer Res, 2002. 93(8): p. 911-916.
- ²⁵ Kaplan, D., et al., *Demonstration of an interferon gamma-dependent tumor surveillance system in immunocompetent mice*. Proc Natl Acad Sci U S A, 1998. 95(13): p. 7556-7561.
- ²⁶ Street, S., et al., *Perforin and interferon-gamma activities independently control tumor initiation, growth, and metastasis.* Blood, 2001. 97(1): p. 192-197.
- ²⁷ Street, S., et al., *Suppression of lymphoma and epithelial malignancies effected by interferon gamma*. J Exp Med, 2002. 196(1): p. 129-134.
- ²⁸ Mitra-Kaushik, S., et al., *Enhanced tumorigenesis in HTLV-1 tax-transgenic mice deficient in interferon-gamma*. Blood, 2004. 104(19): p. 3305-3311.
- ²⁹ Dunn, G., et al., *A critical function for type I interferons in cancer immunoediting*. Nat Immunol, 2005. 6(7): p. 722-729.
- ³⁰ Gresser, I., et al., *Injection of mice with antibody to interferon enhances the growth of transplantable murine tumors.* J Exp Med, 1983. 158(6): p. 2095-2107.
- ³¹ Smyth, M., et al., *Perforin-mediated cytotoxicity is critical for surveillance of spontaneous lymphoma*. J Exp Med, 2000. 192(5): p. 755-760.
- ³² Cretney, E., et al., *Increased susceptibility to tumor initiation and metastasis in TNF-related apoptosis-inducing ligand-deficient mice.* J Immunol, 2002. 168(3): p. 1356-1361.
- ³³ Takeda, K., et al., *Critical role for tumor necrosis factor-related apoptosis-inducing ligand in immune surveillance against tumor development.* J Exp Med, 2002. 195(2): p. 161-169.
- ³⁴ Hayashi, T., & Faustman, D., *Development of spontaneous uterine tumors in low molecular mass polypeptide-2 knockout mice*. Cancer Res, 2002. 62(1): p. 24-27.
- ³⁵ Smyth, M., et al., *Cancer immunosurveillance and immunoediting: the roles of immunity in suppressing tumor development and shaping tumor immunogenicity.* Adv Immunol, 2006. 90: p. 1-50.
- ³⁶ Kobayashi, N., *Malignant neoplasms in registered cases of primary immunodeficiency syndrome*. Jpn J Clin Oncol, 1985. 15 (Suppl 1): p. 307-312.
- ³⁷ Penn, I., *Posttransplant malignancies*. Transplant Proc, 1999. 31(1-2): p. 1260-1262.
- ³⁸ Birkeland, S., et al., *Cancer risk after renal transplantation in the Nordic countries. 1964-1986.* Int J Cancer, 1995. 60(2): p. 183-189.
- ³⁹ Clark, W. Jr., et al., *Model predicting survival in stage I melanoma based on tumour progression*. J Natl Cancer Inst, 1989. 81(24): p. 1893-1904.

²² Girardi, M,. et al., *The distinct contributions of murine T cell receptor (TCR)gammadelta+ and TCRalphabeta+ T cells to different stages of chemically induced skin cancer.* J Exp Med, 2003. 198(5): p. 747-755.

⁴⁰ Di Giorgio, A., et al., *The influence of tumor lymphocytic infiltration on long term survival of surgically treated colorectal cancer patients.* Int Surg, 1992. 77(4): p. 256-260.

⁴¹ Diederichsen, A., et al., *Prognostic value of the CD4+/CD8+ ratio of tumour infiltrating lymphocytes in colorectal cancer and HLA-DR expression on tumour cells*. Cancer Immunol Immunother, 2003. 52(7): p. 423–428.

⁴² Galon, J., et al., *Type, density, and location of immune cells within human colorectal tumous predict clinical outcome.* Science, 2006. 313(5795): p. 1960-1964.

⁴³ Clemente, C., et al., *Prognostic value of tumor infiltrating lymphocytes in the vertical growth phase of primary cutaneous melanoma*. Cancer, 1996. 77(7): p. 1303-1310.

 $^{^{44}}$ Zhang, L., et al., *Intratumoral T cells*, *recurrence*, and survival in epithelial ovarian cancer. N Engl J Med, 2003. 348(3): p. 203-213.

⁴⁵ Schumacher, K., et al., *Prognostic significance of activated CD8(+) T cell infiltrations within esophageal carcinomas.* Cancer Res, 2001. 61(10): p. 3932-3936.

⁴⁶ Vignali, D., et al., *How regulatory T cells work*. Nat Rev Immunol, 2008. 8(7): p. 523-532.

⁴⁷ Curiel, T., et al., *Specific recruitment of regulatory T cells in ovarian carcinoma fosters immune privilege and predicts reduced survival.* Nat Med, 2004. 10(9): p. 942-999.

⁴⁸ Hiraoka, N., et al., *Prevalence of FOXP3+ regulatory T cells increases during the progression of pancreatic ductal adenocarcinoma and its premalignant lesions.* Clin Cancer Res, 2006. 12(18): p. 5423-5434.

⁴⁹ Fu, J., et al., *Increased regulatory T cells correlate with CD8 T-cell impairment and poor survival in hepatocellular carcinoma patients*. Gastroenterology, 2007. 132(7): p. 2328-2339.

⁵⁰ Ling, K., et al., *Increased frequency of regulatory T cells in peripheral blood and tumour infiltrating lymphocytes in colorectal cancer patients.* Cancer Immun, 2007. 7: p. 7-13.

⁵¹ Salama, P., et al., *Tumor-infiltrating FOXP3+ T regulatory cells show strong prognostic significance in colorectal cancer.* J Clin Oncol, 2009. 27(2): p. 186-192.

⁵² Alvaro, T., et al., *Outcome in Hodgkin's lymphoma can be predicted from the presence of accompanying cytotoxic and regulatory T cells.* Clin Cancer Res, 2005. 11(4): p. 1467-1473.

⁵³ Carreras, J., et al., *High numbers of tumor-infiltrating FOXP3-positive regulatory T cells are associated with improved overall survival in follicular lymphoma*. Blood, 2006. 108(9): p. 2957-2964.

⁵⁴ Badoual, C., et al., *Prognostic value of tumor-infiltrating CD4+ T-cell subpopulations in head and neck cancers.* Clin Cancer Res, 2006. 12(2): p. 465-472.

⁵⁵ Badoual, C., et al., Revisiting the prognostic value of regulatory T cells in patients with cancer. J Clin Oncol, 2009. 27(19): e5-6.

⁵⁶ Roncador, G., et al., *Analysis of FOXP3 protein expression in human CD4+CD25+ regulatory T cells at the single-cell level.* Eur J Immunol, 2005. 35(6): p. 1681-1691.

⁵⁷ Kiniwa, Y., et al., *CD8+ Foxp3+ regulatory T cells mediate immunosuppression in prostate cancer*. Clin Cancer Res, 2007. 13(23): p. 6947-6958.

⁵⁸ Dunn, G., et al., *Cancer immunoediting: from immunosurveillance to tumor escape*. Nat Immunol, 2002. 3(11): p. 991-998.

⁵⁹ Srivastava, P., *Heat shock proteins and immune response: methods to madness*. Methods, 2004. 32(1): p. 1-2.

⁶⁰ Shi, Y.,et al., *Molecular identification of a danger signal that alerts the immune system to dying cells.* Nature, 2003. 425(6957): p. 516-521.

⁶¹ Matzinger, P., *Tolerance, danger, and the extended family*. Annu Rev Immunol, 1994. 12: p. 991-1045.

⁶² Groh, V., et al., *Broad tumor-associated expression and recognition by tumor-derived gamma delta T cells of MICA and MICB.* Proc Natl Acad Sci U S A, 1999. 96(12): p. 6879–6884.

⁶³ Gasser, S., et al., *The DNA damage pathway regulates innate immune system ligands of the NKG2D receptor.* Nature, 2005. 436(7054): p. 1186-1190.

⁶⁴ Hayakawa, Y., et al., *Cutting edge: tumor rejection mediated by NKG2D receptor-ligand interaction is dependent upon perforin.* J Immunol, 2002. 169(10): p. 5377-5381.

⁶⁵ Bromberg, J., et al., *Transcriptionally active Stat1 is required for the antiproliferative effects of both interferon alpha and interferon gamma.* Proc Natl Acad Sci U S A, 1996. 93(15): p. 7673-7678.

⁶⁶ Kumar, A., et al., *Defective TNF-alpha-induced apoptosis in STAT1-null cells due to low constitutive levels of caspases.* Science, 1997. 278(5343): p. 1630-1632.

⁶⁷ Qin, Z., & Blankenstein, T., *CD4+ T cell-mediated tumor rejection involves inhibition of angiogenesis that is dependent on IFN gamma receptor expression by nonhematopoietic cells.* Immunity, 2000. 12(6): p. 677-686.

⁶⁸ Espey, M., *Tumor macrophage redox and effector mechanisms associated with hypoxia*. Free Radic Biol Med, 2006. 41(11): p. 1621-1628.

⁶⁹ MacMicking, J., et al., *Nitric oxide and macrophage function*. Annu Rev Immunol, 1997. 15: p. 323-350.

⁷⁰ Ambrosino, E., et al., *Regulation of tumor immunity: the role of NKT cells*. Expert Opin Biol Ther, 2008. 8(6): p. 725-734.

⁷¹ Tsang, K., et al., Generation of human cytotoxic T cells specific for human carcinoembryonic antigen epitopes from patients immunized with recombinant vaccinia-CEA vaccine. J Natl Cancer Inst, 1995. 87(13): p. 982-990.

⁷² Kawakami, Y., et al., *Identification of the immunodominant peptides of the MART-1 human melanoma antigens recognized by the majority of HLA-A2-restricted tumor infiltrating lymphocytes.* J Exp Med, 1994. 180(1): p. 347-352.

⁷³ Yotnda, P., et al., *Cytotoxic T cell response against the chimeric p210 BCR-ABL protein in patients with chronic myelogenous leukemia.* J Clin Invest, 1998. 101(10): p. 2290-2296.

⁷⁴ Ito, D., et al., *Immunological characterization of missense mutations occurring within cytotoxic T cell-defined p53 epitopes in HLA-A*0201+ squamous cell carcinomas of the head and neck*. Int J Cancer, 2007. 120(12): p. 2618-2624.

⁷⁵ Fisk, B., et al., *Identification of an immunodominant peptide of HER-2/neu protooncogene recognized by ovarian tumor-specific cytotoxic T lymphocyte lines.* J Exp Med, 1995. 181(6): p. 2109-2117.

⁷⁶ Brossart, P., et al., *Identification of HLA-A2-restricted T-cell epitopes derived from the MUC1 tumor antigen for broadly applicable vaccine therapies.* Blood, 1999. 93(12): p. 4309-4317.

⁷⁷ Ottaviani, S., et al., *A MAGE-1 antigenic peptide recognized by human cytolytic T lymphocytes on HLA-A2 tumor cells.* Cancer Immunol Immunother, 2005. 54(12): p. 1214-1220.

- ⁷⁹ Straathof, K., et al., Treatment of nasopharyngeal carcinoma with Epstein-Barr virus--specific T lymphocytes. Blood, 2005, 105(5); p. 1898-1904.
- ⁸⁰ Oerke, S., et al., *Naturally processed and HLA-B8-presented HPV16 E7 epitope recognized by T cells from patients with cervical cancer.* Int J Cancer, 2005. 114(5): p. 766-778.
- ⁸¹ Uhr, J., et al., *Cancer dormancy: opportunities for new therapeutic approaches.* Nat Med, 1997. 3(5): p. 505-509.
- ⁸² Karrison, T., et al., *Dormancy of mammary carcinoma after mastectomy*. J Natl Cancer Inst, 1999. 91(1): p. 80-85.
- ⁸³ Meng, S., et al., *Circulating tumor cells in patients with breast cancer dormancy*. Clin Cancer Res. 2004. 10(24): p. 8152-8162.
- ⁸⁴ Stewart, T., et al., *Tumour dormancy: initiation, maintenance and termination in animals and humans.* Can J Surg, 1991. 34(4): p. 321-325.
- ⁸⁵ Myron Kauffman, H., et al., *Transplant tumor registry: donor related malignancies*. Transplantation, 2002. 74(3): p. 358-362.
- ⁸⁶ Shachaf, C., & Felsher, D., *Rehabilitation of cancer through oncogene inactivation*. Trends Mol Med, 2005. 11(7): p. 316-321.
- ⁸⁷ Montagna, D., et al., *Emergence of antitumor cytolytic T cells is associated with maintenance of hematologic remission in children with acute myeloid leukemia.* Blood, 2006. 108(12): p. 3843-3850.
- ⁸⁸ Dhodapkar, M., et al., *Vigorous Premalignancy-specific Effector T Cell Response in the Bone Marrow of Patients with Monoclonal Gammopathy*. J Exp Med, 2003. 198(11): p. 1753-1757.
- ⁸⁹ Farrar, J., et al., Cancer dormancy. VII. A regulatory role for CD8+ T cells and IFN-gamma in establishing and maintaining the tumor-dormant state. J Immunol, 1999. 162(5): p. 2842-2849.
- ⁹⁰ Koebel, C., et al., *Adaptive immunity maintains occult cancer in an equilibrium state*. Nature, 2007. 450(7171): p. 903-907.
- ⁹¹ Shi, B., et al., Differential expression of MHC class II molecules in highly metastatic breast cancer cells is mediated by the regulation of the CIITA transcription Implication of CIITA in tumor and metastasis development. Int J Biochem Cell Biol, 2006. 38(4): p. 544-562.
- ⁹² Fujiwara, K., et al., *Decreased expression of B7 costimulatory molecules and major histocompatibility complex class-I in human hepatocellular carcinoma*. J Gastroenterol Hepatol, 2004. 19(10): p. 1121-1127.
- ⁹³ Algarra, I., et al., *The HLA crossroad in tumor immunology*. Hum Immunol, 2000. 61(1): p. 65-73.
- ⁹⁴ Seliger, B., et al., Coordinate downregulation of multiple MHC class I antigen processing genes in chemical-induced murine tumor cell lines of distinct origin. Tissue Antigens, 2000. 56(4): p. 327-336.
- ⁹⁵ Spiotto, M., et al., *Bystander elimination of antigen loss variants in established tumors*. Nat Med, 2004. 10(3): p. 294-298.

⁷⁸ Jäger, E., et al., Simultaneous humoral and cellular immune response against cancer-testis antigen NY-ESO-1: definition of human histocompatibility leukocyte antigen (HLA)-A2-binding peptide epitopes. J Exp Med, 1998. 187(2): p. 265-270.

⁹⁶ Dunn, G., et al., *Interferons, immunity and cancer immunoediting*. Nat Rev Immunol, 2006. 6(11): p. 836-848.

- ⁹⁷ Ochsenbein, A., et al., *Roles of tumour localization, second signals and cross priming in cytotoxic T-cell induction.* Nature, 2001. 411(6841): p. 1058-1064.
- ⁹⁸ Ochsenbein, A., *Immunological ignorance of solid tumors*. Springer Semin Immunopathol, 2005. 27(1): p. 19-35.
- ⁹⁹ Shrikant, P., & Mescher, M., Control of syngeneic tumor growth by activation of CD8+ T cells: efficacy is limited by migration away from the site and induction of nonresponsiveness. J Immunol, 1999. 162(5): p. 2858-2866.
- ¹⁰⁰ Teicher, B., *Transforming growth factor-beta and the immune response to malignant disease*. Clin Cancer Res, 2007. 13(21): p. 6247-6251.
- ¹⁰¹ Groh, V., et al., *Tumour-derived soluble MIC ligands impair expression of NKG2D and T-cell activation*. Nature, 2002. 419(6908): p. 734-738.
- Wang, T., et al.. Regulation of the innate and adaptive immune responses by Stat-3 signaling in tumor cells. Nat Med, 2004. 10(1): p. 48-54.
- ¹⁰³ Watanabe, S., et al., *Tumor-induced CD11b+Gr-1+ myeloid cells suppress T cell sensitization in tumor-draining lymph nodes*. J Immunol, 2008. 181(5): p. 3291-3300.
- ¹⁰⁴ Piersma, S., et al., *Tumor-specific regulatory T cells in cancer patients*. Hum Immunol, 2008. 69 (4-5): p. 241-249.
- ¹⁰⁵ Willimsky, G., & Blankenstein, T., *Sporadic immunogenic tumours avoid destruction by inducing T-cell tolerance*. Nature, 2005. 437(7055): p. 141-146.
- ¹⁰⁶ Willimsky, G., et al., *Immunogenicity of premalignant lesions is the primary cause of general cytotoxic T lymphocyte unresponsiveness.* J Exp Med, 2008. 205(7): p. 1687-1700.
- ¹⁰⁷ Matsushita, H., et al., *Cancer exome analysis reveals a T-cell-dependent mechanism of cancer immunoediting*. Nature, 2012. 482(7385): p. 400-404.
- ¹⁰⁸ Balkwill, F., & Mantovani, A., *Inflammation and cancer: back to Virchow?* Lancet, 2001. 357(9255): p. 539-545.
- ¹⁰⁹ Flossmann, E., & Rothwell, P., *Effect of aspirin on long-term risk of colorectal cancer: consistent evidence from randomised and observational studies.* Lancet, 2007. 369(9573): p. 1603-1613.
- ¹¹⁰ Yano, S., et al., *Multifunctional interleukin-1beta promotes metastasis of human lung cancer cells in SCID mice via enhanced expression of adhesion-, invasion- and angiogenesis-related molecules.* Cancer Sci, 2003. 94(3): p. 244-252.
- ¹¹¹ Azad, N., et al., *Inflammation and lung cancer: roles of reactive oxygen/nitrogen species*. J Toxicol Environ Health B Crit Rev, 2008. 11(1): p. 1-15.
- ¹¹² Ono, M.. Molecular links between tumor angiogenesis and inflammation: inflammatory stimuli of macrophages and cancer cells as targets for therapeutic strategy. Cancer Sci, 2008. 99(8): p. 1501-1506.
- ¹¹³ Hojilla, C., et al., *Inflammation and breast cancer: metalloproteinases as common effectors of inflammation and extracellular matrix breakdown in breast cancer.* Breast Cancer Res, 2008. 10(2): p. 205.

¹¹⁴ Andreu, P., et al., *FcRgamma activation regulates inflammation-associated squamous carcinogenesis*. Cancer Cell, 2010. 17(2): p. 121-34.

- ¹¹⁵ Borrello, M., et al., *Induction of a proinflammatory program in normal human thyrocytes by the RET/PTC1 oncogene.* Proc Natl Acad Sci U S A, 2005. 102(41): p. 14825-14830.
- ¹¹⁶ Johansson, M., et al., Polarized immune responses differentially regulate cancer development. Immunol Rev, 2008. 222: p. 145-154.
- ¹¹⁷ Delves, P., & Roitt, I., *The immune system. Second of two parts.* N Engl J Med, 2000. 343(2): p. 108-117.
- ¹¹⁸ Xu, D., et al., *Direct and indirect role of Toll-like receptors in T cell mediated immunity*. Cell Mol Immunol. 2004. 1(4): p. 239-246.
- ¹¹⁹ Jin, M., & Lee, J., *Structures of the toll-like receptor family and its ligand complexes*. Immunity, 2008. 29(2): p. 182-191.
- ¹²⁰ Apetoh, L., et al., *Toll-like receptor 4-dependent contribution of the immune system to anticancer chemotherapy and radiotherapy*. Nat Med, 2007. 13(9): p. 1050-1059.
- Weighardt, H., et al., *Identification of a TLR4- and TRIF-dependent activation program of dendritic cells*. Eur J Immunol, 2004. 34(2): p. 558-564.
- ¹²² Janssens, S., & Beyaert, R., *A universal role for MyD88 in TLR/IL-1R-mediated signaling*. Trends Biochem Sci, 2002. 27(9): p. 474-482.
- ¹²³ Akira, S., et al., *Pathogen recognition and innate immunity*. Cell, 2006. 124(4): p. 783-801.
- ¹²⁴ Ellyard, J., et al., *Th2-mediated anti-tumour immunity: friend or foe?* Tissue Antigens, 2007. 70(1): p. 1-11.
- Gumus, E., et al., Association of positive serum anti-p53 antibodies with poor prognosis in bladder cancer patients. Int J Urol, 2004. 11(12): p. 1070-1077.
- ¹²⁶ Bettelli, E., et al., *Reciprocal developmental pathways for the generation of pathogenic effector TH17 and regulatory T cells.* Nature, 2006. 441(7090): p. 235-238.
- ¹²⁷ Tesmer, L., et al., *Th17 cells in human disease*. Immunol Rev, 2008. 223: p. 87-113.
- ¹²⁸ Curotto de Lafaille, M., & Lafaille, J., *Natural and adaptive foxp3+ regulatory T cells: more of the same or a division of labor?* Immunity, 2009. 30(5): p. 626-635.
- ¹²⁹ Cools, N., et al., Regulatory T cells and human disease. Clin Dev Immunol, 2007. 2007: p. 89195.
- ¹³⁰ Sica, A., et al., *Macrophage polarization in tumour progression*. Semin Cancer Biol, 2008. 18(5): p. 349-355.
- ¹³¹ Saccani, A., et al., p50 nuclear factor-kappaB overexpression in tumor-associated macrophages inhibits M1 inflammatory responses and antitumor resistance. Cancer Res, 2006. 66(23): p. 11432-11440.
- ¹³² Ostrand-Rosenberg, S., & Sinha, P., *Myeloid-derived suppressor cells: linking inflammation and cancer*. J Immunol, 2009. 182(8): p. 4499-4506.
- ¹³³ Almand, B., et al., *Increased production of immature myeloid cells in cancer patients: a mechanism of immunosuppression in cancer.* J Immunol, 2001. 166(1): p. 678-689.

¹³⁴ Marigo, I., et al., *Tumor-induced tolerance and immune suppression by myeloid derived suppressor cells.* Immunol Rev, 2008. 222: p. 162-179.

- ¹³⁵ Bunt, S., et al., Reduced inflammation in the tumor microenvironment delays the accumulation of myeloid-derived suppressor cells and limits tumor progression. Cancer Res, 2007. 67(20): p. 10019-10026.
- ¹³⁶ Sinha, P., et al., *Prostaglandin E2 promotes tumor progression by inducing myeloid-derived suppressor cells*. Cancer Res, 2007. 67(9): p. 4507–4513.
- ¹³⁷ Bronte, V., et al., *L-arginine metabolism in myeloid cells controls T-lymphocyte functions*. Trends Immunol, 2003. 24(6): p. 302-306.
- ¹³⁸ Nagaraj, S., et al., *Altered recognition of antigen is a mechanism of CD8+ T cell tolerance in cancer.* Nat Med, 2007. 13(7): p. 828-835.
- ¹³⁹ Serafini, P., et al., *Myeloid-derived suppressor cells promote cross-tolerance in B-cell lymphoma by expanding regulatory T cells.* Cancer Res, 2008. 68(13): p. 5439-5449.
- ¹⁴⁰ Sinha, P., et al., *Cross-talk between myeloid-derived suppressor cells and macrophages subverts tumor immunity toward a type 2 response.* J Immunol, 2007. 179(2): p. 977-983.
- ¹⁴¹ Borst, J., et al., *The delta- and epsilon-chains of the human T3/T-cell receptor complex are distinct polypeptides.* Nature, 1984. 312(5993): p. 455-458.
- ¹⁴² Yoshikai, Y., et al., *Organisation and sequences of the variable, joining and constant regions of the human T-cell receptor alpha-chain.* Nature, 1985. 316(6031): p. 837-840.
- ¹⁴³ Hayday, A., et al., *Structure, organisation and somatic rearrangement of T cell gamma genes*. Cell, 1985. 40(2): p. 259-269.
- ¹⁴⁴ Clark, S., et al., *Identification of a diversity segment of human T-cell receptor beta-chain, and comparison with the analogous murine element.* Nature, 1984. 311(5984): p. 387-389.
- 145 Chien, Y., et al., *T-cell receptor delta gene rearrangements in early thymocytes*. Nature, 1987. 330(6150): p. 722-727.
- 146 Entrez Gene: TRA@ T cell receptor alpha locus [$\it Homo\ sapiens$] GeneID: 6955 updated 4-Mar-2012
- $^{147}\,\mathrm{Entrez}$ Gene: TRD@ T cell receptor delta locus [$Homo\ sapiens$] GeneID: 6964 updated 5-Feb-2012
- ¹⁴⁸ Entrez Gene: TRB@ T cell receptor beta locus [*Homo sapiens*] GeneID: 6957 updated 4-Mar-2012
- ¹⁴⁹ Mombaerts, P., et al., *RAG-1-deficient mice have no mature B and T lymphocytes*. Cell, 1992. 68(5): p. 869-877.
- ¹⁵⁰ Lafaille, J., et al., *Junctional sequences of T cell receptor* $\gamma\delta T$ *cell lineages and for a novel intermediate of V-(D)-J joining.* Cell, 1989. 59(5): p. 850-870.
- ¹⁵¹ Komori, T., et al., *Lack of N regions in antigen receptor variable region genes of TdT-deficient lymphocytes*. Science, 1993. 261(5125): p. 1171-1175. Erratum in Science, 1993. 262(5142): p. 1957.
- 152 Kuhns, M., et al., *Deconstructing the form and function of the TCR/CD3 complex.* Immunity, 2006. 24(2): p. 133-139.
- ¹⁵³ Hayes, S., & Love, P., *Stoichiometry of the murine gammadelta T cell receptor.* J Exp Med, 2006. 203(1): p. 47-53.

¹⁵⁴ Doherty, P., & Zinkernagel, R., *H-2 compatibility is required for T-cell mediated lysis of target cells infected with lymphocytic choriomeningitis virus*. J Exp Med, 1975. 141(2): p. 502-507.

- ¹⁵⁵ Garboczi, D., et al., *Structure of the complex between human T-cell receptor*, *viral peptide and HLA-A2*. Nature, 1996. 384(6605): p. 134-141.
- ¹⁵⁶ Shastri, N., et al., *Producing nature's gene chips: the generation of peptides for display by MHC class I molecules*. Annu Rev Immunol, 2002. 20: p. 463-493.
- ¹⁵⁷ York, I., et al., *Tripeptidyl peptidase II is the major peptidase needed to trim long antigenic precursors, but is not required for most MHC class I antigen presentation*. J Immunol, 2006. 177(3): p. 1434-1443.
- ¹⁵⁸ Chang, S., et al., *The ER aminopeptidase, ERAP1, trims precursors to lengths of MHC class I peptides by a 'molecular ruler' mechanism.* Proc Natl Acad Sci U S A, 2007. 102(47): p. 17107-17122.
- ¹⁵⁹ Howarth, M., et al., *Tapasin enhances MHC class I peptide presentation according to peptide half-life.* Proc Natl Acad Sci U S A, 2004. 101(32): p. 11737-11742.
- ¹⁶⁰ Wearsch, P., & Cresswell, P., *Selective loading of high-affinity peptides onto major histocompatibility complex class I molecules by the tapasin-ERp57 heterodimer*. Nat Immunol, 2007. 8(8): p. 873-881.
- ¹⁶¹ Park, B., et al., *Redox regulation facilitates optimal peptide selection by MHC class I during antigen processing.* Cell, 2006. 127(2): p. 369-382.
- ¹⁶² Cresswell, P., *Invariant chain structure and MHC class II function*. Cell, 1996. 84(4): p. 505-507.
- ¹⁶³ Lazarski, C., et al., *The impact of DM on MHC class II-restricted antigen presentation can be altered by manipulation of MHC-peptide kinetic stability*. J Exp Med ,2006. 203(5): p.1319-1328.
- ¹⁶⁴ Denzin, L., et al., *Negative regulation by HLA-DO of MHC Class II-restricted antigen processing*. Science, 1997. 278(5335): p. 106-109.
- ¹⁶⁵ Liljedahl, M., et al., *Altered antigen presentation in mice lacking H2-O*. Immunity, 1998. 8(2): p. 233-243.
- ¹⁶⁶ Hornell, T., et al., *Human dendritic cell expression of HLA-DO is subset specific and regulated by maturation*. J Immunol, 2006. 176(6): p. 3536-3547.
- ¹⁶⁷ Menendez-Benito, V., & Neefjes, J., *Autophagy in MHC class II presentation: Sampling from within*. Immunity, 2007. 26(1): p. 1-3.
- ¹⁶⁸ Chicz, R., et al., Specificity and promiscuity among naturally processed peptides bound to HLA-DR alleles. J Exp Med, 1993. 178(1): p. 27-47.
- ¹⁶⁹ Sercarz, E., & Maverakis, E., *MHC-guided processing: binding of large antigen fragments*. Nat Rev Immunol, 2003. 3(8): p. 621-629. Erratum in Nat Rev Immunol, 2003. 3(10): p. 839.
- ¹⁷⁰ Mimura, Y., et al., Folding of an MHC class II-restricted tumor antigen controls its antigenicity via MHC-guided processing. Proc Natl Acad Sci U S A, 2007. 104(14): p. 5983-5988.
- ¹⁷¹ Bevan, M., Cross-priming for a secondary cytotoxic response to minor H antigens with H-2 congenic cells which do not cross-react in the cytotoxic assay. J Exp Med, 1976. 143(5): p. 1283-1288.
- ¹⁷² Shen, L., et al., *Important role of cathepsin S in generating peptides for TAP-independent MHC class I crosspresentation in vivo*. Immunity, 2004. 21(2): p. 155-165.

¹⁷³ Burgdorf, S., et al., *Distinct pathways of antigen uptake and intracellular routing in CD4 and CD8 T cell activation*. Science, 2007. 316(5824): p. 612-616.

- ¹⁷⁵ Zinkernagel, R., & Althage, A., On the role of thymic epithelium vs. bone marrow-derived cells in repertoire selection of T cells. Proc Natl Acad Sci U S A, 1999. 96(14): p. 8092-8097.
- ¹⁷⁶ Balciunaite, G., et al., *The earliest subpopulation of mouse thymocytes contains potent T, significant macrophage, and natural killer cell but no B-lymphocyte potential.* Blood, 2005. 105(5): p. 1930-1936.
- ¹⁷⁷ Radtke, F., et al., *Deficient T cell fate specification in mice with an induced inactivation of Notch1*. Immunity, 1999. 10(5): p. 547-558.
- ¹⁷⁸ Pui, J., et al., *Notch1 expression in early lymphopoiesis influences B versus T lineage determination.* Immunity, 1999. 11(3): p. 299-308.
- ¹⁷⁹ Von Boehmer, H., et al., *Pleiotropic changes controlled by the pre-T-cell receptor*. Curr Opin Immunol, 1999. 11(2): p. 135-142.
- 180 Dudley, E., et al., *Alpha beta and gamma delta T cells can share a late common precursor*. Curr Bio, 1995. 5(6): p. 659-669.
- Kang, J., et al., Evidence that productive rearrangements of TCR γ genes influence the commitment of progenitor cells to differentiate into $\alpha\beta$ or $\gamma\delta$ T cells. Eur J Immunol, 1995. 25(9): p. 2706-2709.
- ¹⁸² Livak, F., et al., *In-frame TCR* δ *gene rearrangements play a critical role in the* $\alpha\beta/\gamma\delta T$ *cell lineage decision.* Immunity, 1995. 2(6): p. 617-627.
- ¹⁸³ Kreslavsky, T., et al., T cell receptor-instructed $\alpha\beta$ versus $\gamma\delta$ lineage commitment revealed by single-cell analysis. J Exp Med, 2008. 205(5): p. 1173-1186.
- ¹⁸⁴ Ciofani, M., & Zuniga-Pflucker, J., *Notch promotes survival of pre-T cells at the* β -selection checkpoint by regulating cellular metabolism. Nat Immunol, 2005. 6(9): p. 881–888.
- 185 Van de Walle, I., et al., An early decrease in Notch activation is required for human TCR-{alpha}{beta} lineage differentiation at the expense of TCR-{gamma}{delta} T cells. Blood, 2009. 113(13): p. 2988-2998.
- ¹⁸⁶ Levelt, C., et al., Regulation of T cell receptor (TCR)-beta locus allelic exclusion and initiation of TCR-alpha locus rearrangement in immature thymocytes by signalling through the CD3 complex. Eur J Immunol, 1995. 25(5): p. 1257-1261.
- ¹⁸⁷ Yamasaki, S., & Saito, T., *Molecular basis for pre-TCR-mediated autonomous signalling*. Trends Immunol, 2007. 28(1): p. 39-43.
- ¹⁸⁸ Yannoutsos, N., et al., *The Role of Recombination Activating Gene (RAG) Reinduction in Thymocyte Development In Vivo.* J Exp Med, 2001. 194(4): p. 471-480.
- ¹⁸⁹ Takahama, Y., *Journey through the thymus: stromal guides for T-cell development and selection.* Nat Rev Immunol, 2006. 6(2): p. 127-135.
- ¹⁹⁰ Fink, P., & Bevan, M., *H-2 antigens of the thymus determine lymphocyte specificity*. J Exp Med, 1978. 148(3): p. 766-775.
- ¹⁹¹ Padovan, E., et al., *Expression of two T-cell receptor \alpha chains: Dual receptor T cells*. Science, 1993. 262(5132): p. 422-424.

¹⁷⁴ Shortman, K., et al., *The generation and fate of thymocytes*. Semin Immunol, 1990. 2(1): p. 3-12.

¹⁹² Hardardottir, F., et al., *T cells with two functional antigen-specific receptors*. Proc Natl Acad Sci U S A, 1995. 92(2): p. 354-358.

- ¹⁹³ Zal, T., et al., Expression of a second receptor rescues self-specific T cells from thymic deletion and allows activation of autoreactive effector function. Proc Natl Acad Sci U S A, 1996 93(17): p. 9102-9107.
- ¹⁹⁴ Singer, A., et al., *Lineage fate and intense debate: myths, models and mechanisms of CD4- versus CD8-lineage choice.* Nat Rev Immunol, 2008. 8(10): p. 788-801.
- ¹⁹⁵ Brugnera, E., et al., *Coreceptor reversal in the thymus: signalled CD4*⁺8⁺ thymocytes initially terminate CD8 transcription even when differentiating into CD8⁺ T cells. Immunity, 2000. 13(1): p. 59-71.
- ¹⁹⁶ Park, J., et al., 'Coreceptor tuning': cytokine signals transcriptionally tailor CD8 coreceptor expression to the self-specificity of the TCR. Nat Immunol, 2007. 8(10): p. 1049-1059.
- ¹⁹⁷ Yu, Q., et al., *In vitro evidence that cytokine receptor signals are required for differentiation of double positive thymocytes into functionally mature CD8*⁺ *T cells.* J Exp Med, 2003. 197(4): p. 475-487.
- ¹⁹⁸ Huang, F., et al., *Establishment of the major compatibility complex-dependent development of CD4*⁺ and CD8⁺ T cells by the Cbl family proteins. Immunity, 2006. 25(4): p. 571-581.
- ¹⁹⁹ Palmer, E., & Naeher, D., *Affinity threshold for thymic selection through a T-cell receptor-coreceptor zipper*. Nat Rev Imunol, 2009. 9(3): p. 207-213.
- ²⁰⁰ Shores, E., et al., *Role of the multiple T cell receptor (TCR)-zeta chain signalling motifs in the selection of the T cell repertoire.* J Exp Med, 1997. 185(5): p. 893-900.
- ²⁰¹ Murata, S., et al., *Regulation of CD8+ T cell development by thymus-specific proteasomes*. Science, 2007. 316(5829): p. 1349-1353.
- Honey, K., et al., Cathepsin L regulates CD4+ T cell selection independently of its effect on invariant chain: a role in the generation of positively selecting peptide ligands. J Exp Med, 2002. 195(10): p. 1349-1358.
- ²⁰³ Peterson, P., et al., *Transcriptional regulation by AIRE: molecular mechanisms of central tolerance*. Nat Rev Immunol, 2008. 8(12): p. 948-957.
- ²⁰⁴ Peterson, P., & Peltonen, L., *Autoimmune polyendocrinopathy syndrome type 1 (APS1) and AIRE gene: new views on molecular basis of autoimmunity*. J Autoimmun, 2005. 25 Suppl: p. 49-55.
- ²⁰⁵ Ramsey, C., et al., *Aire deficient mice develop multiple features of APECED phenotype and show altered immune response.* Hum Mol Genet, 2002. 11(4): p. 397-409.
- ²⁰⁶ Eberl, G., & Littman, D., *Thymic origin of intestinal alphabeta T cells revealed by fate mapping of RORgammat+ cells.* Science, 2004. 305(5681): p. 248-251.
- ²⁰⁷ Grusby, M., et al., *Mice lacking major histocompatibility complex class I and class II molecules*. Proc Natl Acad Sci U S A, 1993. 90(9): p. 3913-3917.
- ²⁰⁸ Holtmeier, W.,& Kabelitz, D., $\gamma\delta$ *T cells link innate and adaptive immune responses*. Chem Immunol Allergy, 2005. 86: p. 151-183
- Moon, J., et al., *Naive CD4(+) T cell frequency varies for different epitopes and predicts repertoire diversity and response magnitude.* Immunity. 2007. 27(2): p. 203-213.
- ²¹⁰ Marelli-Berg, F., et al., *The highway code of T cell trafficking*. J Pathol, 2008. 214(2): p. 179–189.

²¹¹ Bargatze, R., & Butcher, E., *Rapid G protein-regulated activation event involved in lymphocyte binding to high endothelial venules*. J Exp Med, 1993. 178(1): p. 367-372.

- ²¹² Denucci, C., et al., *Integrin function in T-cell homing to lymphoid and nonlymphoid sites: getting there and staying there*. Crit Rev Immunol, 2009. 29(2): p. 87-109.
- ²¹³ Vestweber, D., *Adhesion and signaling molecules controlling the transmigration of leukocytes through endothelium.* Immunol Rev, 2007. 218: p. 178-196.
- ²¹⁴ Castellino, F., et al., *Chemokines enhance immunity by guiding naive CD8*⁺ *T cells to sites of CD4*⁺ *T cell–dendritic cell interaction.* Nature, 2006. 440(7086): p. 890-895.
- ²¹⁵ Bajénoff, M., et al., *The strategy of T cell antigen-presenting cell encounter in antigen-draining lymph nodes revealed by imaging of initial T cell activation.* J Exp Med, 2003. 198(5): p. 715-724.
- ²¹⁶ Sato, K., & Fujita, S., *Dendritic cells: nature and classification*. Allergol Int, 2007. 56(3): p. 183-191.
- ²¹⁷ Joffre, O., et al., *Inflammatory signals in dendritic cell activation and the induction of adaptive immunity*. Immunol Rev, 2009. 227(1): p. 234-247.
- ²¹⁸ Banerjee, D., et al., *Expansion of FOXP3high regulatory T cells by human dendritic cells (DCs) in vitro and after injection of cytokine-matured DCs in myeloma patients*. Blood, 2006. 108(8): p. 2655-2661.
- ²¹⁹ Curtsinger, J., et al., Signal 3 determines tolerance versus full activation of naive CD8 T cells: dissociating proliferation and development of effector function. J Exp Med, 2003. 197(9): p. 1141-1151.
- ²²⁰ Keene, J., & Forman, J., *Helper activity is required for the in vivo generation of cytotoxic T lymphocytes*. J Exp Med, 1982. 155(3): p. 768-782.
- ²²¹ Schoenberger, S., et al., *T-cell help for cytotoxic T lymphocytes is mediated by CD40-CD40L interactions*. Nature, 1998. 393(6684): p. 480-483.
- ²²² Lanzavecchia, A., *Immunology: licence to kill.* 1998, Nature. 393(6684): p. 413-414.
- ²²³ Quezada, S., et al., *CD40/CD154 interactions at the interface of tolerance and immunity*. Annu Rev Immunol, 2004. 22: p. 307-328.
- ²²⁴ Jenkins, M., et al., *Inhibition of antigen-specific proliferation of type 1 murine T cell clones after stimulation with immobilized anti-CD3 monoclonal antibody*. J Immunol, 1990. 144(1): p. 16-22.
- ²²⁵ Yokosuka, T., & Saito, T., *Dynamic regulation of T-cell costimulation through TCR-CD28 microclusters*. Immunol Rev, 2009. 229(1): p. 27-40.
- ²²⁶ van der Merwe, P., et al., *CD80 (B7-1) binds both CD28 and CTLA-4 with a low affinity and very fast kinetics*. J Exp Med, 1997. 185(3) p. 393–403.
- ²²⁷ Rudd, C., et al., *CD28 and CTLA-4 coreceptor expression and signal transduction*. Immunol Rev, 2009. 229(1): p. 12-26.
- ²²⁸ Nurieva, R., et al., *Yin-Yang of costimulation: crucial controls of immune tolerance and function.* Immunol Rev, 2009. 229(1): p. 88-100.
- 229 Hendriks, J., et al., CD27 is required for generation and long-term maintenance of T cell immunity. Nat Immunol, 2000. 1(5): p. 433–440.

²³⁰ Nolte, M., et al., *Timing and tuning of CD27-CD70 interactions: the impact of signal strength in setting the balance between adaptive responses and immunopathology.* Immunol Rev, 2009. 229(1): p. 216-231.

- Wang, C., et al., *Immune regulation by 4-1BB and 4-1BBL: complexities and challenges*. Immunol Rev, 2009. 229(1): p. 192-215.
- ²³² Croft, M., et al.. *The significance of OX40 and OX40L to T-cell biology and immune disease*. Immunol Rev, 2009. 229(1): p. 173-191.
- ²³³ Weiss, A., & Stobo, J., Requirement for the coexpression of T3 and the T cell antigen receptor on a malignant human T cell line. J Exp Med, 1984. 160(5): p. 1284-1299.
- ²³⁴ Smith-Garvin, J., et al., *T cell activation*. Annu Rev Immunol, 2009. 27: p. 591-619.
- ²³⁵ Davis, S., & van der Merwe, P., The kinetic-segregation model: TCR triggering and beyond. Nat Immunol, 2006. 7(8): p. 803-809.
- ²³⁶ Choudhuri, K., et al., *T cell receptor triggering is critically dependent on the dimensions of its peptide-MHC ligand.* Nature, 2005. 436(7050): p. 578–582.
- ²³⁷ Burroughs, N., & van der Merwe, P., *Stochasticity and spatial heterogeneity in T-cell activation*. Immunol Rev, 2007. 216: p. 69-80.
- ²³⁸ Peters, P., et al., *Cytotoxic T lymphocyte granules are secretory lysosomes, containing both perforin and granzymes.* J Exp Med, 1991. 173(5): p. 1099-1109.
- ²³⁹ Sauer, H., et al., Functional size of complement and perforin pores compared by confocal laser scanning microscopy and fluorescence microphotolysis. Biochim Biophys Acta, 1991. 1063(1): p. 137-146.
- ²⁴⁰ Motyka, B., et al., *Mannose 6-phosphate/insulin-like growth factor II receptor is a death receptor for granzyme B during cytotoxic T cell-induced apoptosis*. Cell, 2000. 103(3): p. 491-500.
- ²⁴¹ Keefe, D., et al., *Perforin triggers a plasma membrane-repair response that facilitates CTL induction of apoptosis.* Immunity, 2005. 23(3): p. 249-262.
- ²⁴² Muralitharan, S., et al., *Novel spectrum of perforin gene mutations in familial hemophagocytic lymphohistiocytosis in ethnic Omani patients*. Am J Hematol, 2007. 82(12): p. 1099-1102.
- ²⁴³ Chávez-Galán, L., et al., *Cell death mechanisms induced by cytotoxic lymphocytes*. Cell Mol Immunol, 2009. 6(1): p. 15-25.
- ²⁴⁴ Sutton, V., et al., *Residual active granzyme B in cathepsin C-null lymphocytes is sufficient for perforin-dependent target cell apoptosis.* J Cell Biol, 2007. 176(4): p. 425-433.
- ²⁴⁵ Kaspar, A., et al., *A distinct pathway of cell-mediated apoptosis initiated by granulysin*. J Immunol, 2001. 167(1): p. 350-356.
- ²⁴⁶ Walch, M., et al., *Perforin enhances the granulysin-induced lysis of listeria innocua in human dendritic cells.* BCM Immunol, 2007. 8: p. 14.
- ²⁴⁷ Rogers, P., et al., *Qualitative changes accompany memory T cell generation: faster, more effective responses at lower doses of antigen.* J Immunol, 2000. 164(5): p. 2338–2346.
- ²⁴⁸ Dengler, T., &. Pober, J., *Human vascular endothelial cells stimulate memory but not naïve CD8+ T cells to differentiate into CTL retaining an early activation phenotype.* J Immunol, 2000. 164(10): p. 5146–5155.

²⁴⁹ Slifka, M., & Whitton, J., *Activated and memory CD8+ T cells can be distinguished by their cytokine profiles and phenotypic markers*. J Immunol, 2000. 164(1): p. 208-216.

- ²⁵⁰ Sallusto, F., et al., *Two subsets of memory T lymphocytes with distinct homing potentials and effector functions.* Nature, 1999. 401(6754): p. 708–712.
- ²⁵¹ Ravkov, E., et al., *Immediate early effector functions of virus-specific CD8+CCR7+ memory cells in humans defined by HLA and CC chemokine ligand 19 tetramers*. J. Immunol, 2003. 170(5): p. 2461–2468.
- ²⁵² Kaech, S., et al., *Molecular and functional profiling of memory CD8 T cell differentiation*. Cell, 2002. 111(6): p. 837-851.
- ²⁵³ Wherry, E,, et al., *Lineage relationship and protective immunity of memory CD8 T cell subsets*. Nat Immunol, 2003. 4(3): p. 225–234.
- ²⁵⁴ Chang, J., et al., *Asymmetric T lymphocyte division in the initiation of adaptive immune responses*. Science, 2007. 315(5819): p. 1687–1691.
- ²⁵⁵ Bannard, O., et al., Secondary replicative function of CD81 T cells that had developed an effector phenotype. Science, 2009. 323(5913): p. 505–509.
- ²⁵⁶ Bannard, O., et al., *Pathways of memory CD8+ T-cell development*. Eur J Immunol, 2009. 39(8): p. 2083-2087.
- ²⁵⁷ Janssen, E., et al., *CD4*⁺ *T-cell help controls CD8*⁺ *T-cell memory via TRAIL-mediated activation-induced cell death.* Nature, 2005. 434(7029): p. 88–93.
- ²⁵⁸ Williams, M., et al., Interleukin-2 signals during priming are required for secondary expansion of CD8⁺ memory T cells. Nature, 2006. 441(7095): p. 890–893.
- ²⁵⁹ Tan, J., et al., *Interleukin (IL)-15 and IL-7 jointly regulate homeostatic proliferation of memory phenotype CD81 cells but are not required for memory phenotype CD41 cells.* J Exp Med, 2002. 195(12): p. 1523–1532.
- ²⁶⁰ High, W., et al., Completely regressed primary cutaneous malignant melanoma with nodal and/or visceral metastases: a report of 5 cases and assessment of the literature and diagnostic criteria. J Am Acad Dermatol, 2005. 53(1): p. 89-100.
- ²⁶¹ Morton, D., et al., *Prolongation of survival in metastatic melanoma after active specific immunotherapy with a new polyvalent melanoma vaccine*. Ann Surg, 1992. 216(4): p. 463-482.
- ²⁶² Mitchell, M., et al., *Active specific immunotherapy for melanoma: phase I trial of allogeneic lysates and a novel adjuvant.* Cancer Res, 1988. 48(20): p. 5883-5893.
- ²⁶³ Sondak, V., et al., *Adjuvant immunotherapy of resected, intermediate-thickness, node-negative melanoma with an allogeneic tumor vaccine: overall results of a randomized trial of the Southwest Oncology Group.* J Clin Oncol, 2002. 20(8): p. 2058-2066.
- ²⁶⁴ Reynolds, S., et al., *Stimulation of CD8+ T cell responses to MAGE-3 and Melan A/MART-1 by immunization to a polyvalent melanoma vaccine*. Int J Cancer, 1997. 72(6): p. 972-976.
- ²⁶⁵ Slingluff C. Jr., et al., *Phase I trial of a melanoma vaccine with gp100(280-288) peptide and tetanus helper peptide in adjuvant: immunologic and clinical outcomes.* Clin Cancer Res,, 2001. 7(10): p. 3012-3024.
- ²⁶⁶ Rosenberg, S., et al., *Immunologicl and therapeutic evaluation of a synthetic peptide vaccine for the treatment of patients with metastatic melanoma*. Nat Med, 1998. 4(3): p. 321-327.

²⁶⁷ Lens, M., *The role of vaccine therapy in the treatment of melanoma*. Expert Opin Biol Ther, 2008. 8(3): p. 315-323.

- ²⁶⁸ Rosenberg, S., et al., *Tumor progression can occur despite the induction of very high levels of self/tumor antigen-specific CD8+ T cells in patients with melanoma*. J Immunol, 2005. 175(9): p. 6169-6176.
- ²⁶⁹ Kenter, G., et al., *Vaccination against HPV-16 oncoproteins for vulvar intraepithelial neoplasia.* N Engl J Med, 2009. 361(19): p. 1838-47.
- ²⁷⁰ Yuan, J., et al., Safety and immunogenicity of a human and mouse gp100 DNA vaccine in a phase I trial of patients with melanoma. Cancer Immun, 2009. 9: p. 5.
- ²⁷¹ Meyer, R., et al., *A phase I vaccination study with tyrosinase in patients with stage II melanoma using recombinant modified vaccinia virus Ankara (MVA-hTyr)*. Cancer Immunol Immunother. 2005. 54(5): p. 453-467.
- ²⁷² Zajac, P., et al., *Phase I/II clinical trial of a nonreplicative vaccinia virus expressing multiple HLA-A0201-restricted tumor-associated epitopes and costimulatory molecules in metastatic melanoma patients.* Hum Gene Ther, 2003. 14(16): p. 1497-1510.
- ²⁷³ Lindsey, K., et al., *Evaluation of prime/boost regimens using recombinant poxvirus/tyrosinase vaccines for the treatment of patients with metastatic melanoma*. Clin Cancer Res, 2006. 12(8): p. 2526-2537.
- ²⁷⁴ Caux, C., et al., *GM-CSF and TNF-alpha cooperate in the generation of dendritic Langerhans cells*. Nature, 1992. 360(6401): p. 258-261.
- ²⁷⁵ Gilboa, E., *DC-based cancer vaccines*. J Clin Invest, 2007. 117(5): p. 1195-1203.
- ²⁷⁶ Engell-Noerregaard, L., et al., *Review of clinical studies on dendritic cell-based vaccination of patients with malignant melanoma: assessment of correlation between clinical response and vaccine parameters.* Cancer Immunol Immunother, 2009. 58(1): p. 1-14.
- ²⁷⁷ Rosenberg, S., et al., *Cancer immunotherapy: moving beyond current vaccines.* Nat Med, 2004. 10(9): p. 909-915.
- ²⁷⁸ Rosenberg, S., et al., *Adoptive cell transfer: a clinical path to effective cancer immunotherapy*. Nat Rev Cancer, 2008. 8(4): p. 299-308.
- ²⁷⁹ Rosenberg, S., et al., *Treatment of patients with metastatic melanoma with autologous tumor-infiltrating lymphocytes and interleukin* 2. J Natl Cancer Inst, 1994. 86(15): p. 1159-1166.
- ²⁸⁰ Dudley, M., et al., *Adoptive cell transfer therapy following non-myeloablative but lymphodepleting chemotherapy for the treatment of patients with refractory metastatic melanoma*. J Clin Oncol, 2005. 23(10): p. 2346-2357.
- ²⁸¹ Gattinoni, L., et al., *Adoptive immunotherapy for cancer: building on success.* Nat Rev Immunol, 2006. 6(5): p. 383-393.
- ²⁸² Gattinoni, L., et al., Removal of homeostatic cytokine sinks by lymphodepletion enhances the efficacy of adoptively transferred tumor-specific CD8+ T cells. J Exp Med, 2005. 202(7): p. 907-912.
- ²⁸³ Gattinoni, L., et al., *Acquisition of full effector function in vitro paradoxically impairs the in vivo antitumor efficacy of adoptively transferred CD8+ T cells.* J Clin Invest, 2005. 115(6): p. 1616-1626.
- ²⁸⁴ Berger., et al., *Adoptive transfer of effector CD8+ T cells derived from central memory cells establishes persistent T cell memory in primates.* J Clin Invest, 2008. 18(1): p. 294-305.

²⁸⁵ Butler, M., et al., *Establishment of antitumor memory in humans using in vitro-educated CD8+T cells.* Sci Transl Med, 2011. 3(80): p. 80ra34.

- ²⁸⁶ Savoldo, B., et al. *Treatment of solid organ transplant recipients with autologous Epstein Barr virus-specific cytotoxic T lymphocytes (CTLs)*. Blood, 2006. 108(9): p. 2942-2949.
- ²⁸⁷ Bollard, C., et al., *Cytotoxic T lymphocyte therapy for Epstein-Barr virus+ Hodgkin's disease*. J Exp Med, 2004. 200(12): p. 1623-1633.
- ²⁸⁸ Straathof, K., et al., *Treatment of nasopharyngeal carcinoma with Epstein-Barr virus--specific T lymphocytes.* Blood, 2005. 105(5): p. 1898-1904.
- ²⁸⁹ Bollard, C., et al., *Immunotherapy targeting EBV-expressing lymphoproliferative diseases*. Best Pract Res Clin Haematol. 2008. 21(3): p. 405-420.
- ²⁹⁰ Lucas, K., et al., Adoptive immunotherapy with allogeneic Epstein-Barr virus (EBV)-specific cytotoxic T-lymphocytes for recurrent, EBV-positive Hodgkin disease. Cancer, 2004. 100(9): p. 1892-1901.
- ²⁹¹ Kolb, H., *Graft-versus-leukemia effects of transplantation and donor lymphocytes*. Blood, 2008. 112(12): p. 4371-4383.
- ²⁹² Alyea, E., *Modulating graft-versus-host disease to enhance the graft-versus-leukemia effect.* Best Pract Res Clin Haematol, 2008. 21(2): p. 239-250.
- ²⁹³ Demirer, T., et al., *Transplantation of allogeneic hematopoietic stem cells: an emerging treatment modality for solid tumors*. Nat Clin Pract Oncol, 2008. 5(5): p. 256-267.
- ²⁹⁴ Hunder, N., et al., *Treatment of metastatic melanoma with autologous CD4+ T cells against NY-ESO-1*. N Engl J Med, 2008. 358(25): p. 2698-2703.
- ²⁹⁵ Jorritsma, A., et al., *Selecting highly affine and well expressed TCRs for gene therapy of melanoma*. Blood, 2007. 110(10): p. 3564-3572
- ²⁹⁶ Dembic, Z., et al., *Transfer of specificity by murine alpha and beta T-cell receptor genes*. Nature, 1986. 320(6059): p. 232–238.
- ²⁹⁷ de Witte, M., et al., *Targeting self-antigens through allogeneic TCR gene transfer*. Blood, 2006. 108(3): p. 870-877.
- ²⁹⁸ Bendle, G., et al., *Preclinical development of T cell receptor gene therapy*. Curr Opin Immunol, 2009. 21(12): p. 209-214.
- ²⁹⁹ Kuball, J., et al., Facilitating matched pairing and expression of TCR chains introduced into human T cells. Blood, 2007. 109(6): p. 2331-2338.
- Morgan, R., et al., *Cancer regression in patients after transfer of genetically engineered lymphocytes*. Science, 2006. 314(5796): p.126-129.
- ³⁰¹ Johnson, L., et al., *Gene therapy with human and mouse T-cell receptors mediates cancer regression and targets normal tissues expressing cognate antigen.* Blood, 2009. 114(3): p. 535-546.
- ³⁰² Uckert, W., & Schumacher, T., *TCR transgenes and transgene cassettes for TCR gene therapy: status in 2008.* Cancer Immunol Immunother, 2009. 58(5): p. 809-822.
- 303 Dotti, G., & Heslop, H., Current status of genetic modification of T cells for cancer treatment. Cytotherapy, 2005. 7(3): p. 262-272.

Rossig, C., et al., Targeting of G(D2)-positive tumor cells by human T lymphocytes engineered to express chimeric T-cell receptor genes. Int J Cancer, 2001. 94(2): p. 228-236.

- ³⁰⁵ Savoldo, B., et al., *Epstein Barr virus specific cytotoxic T lymphocytes expressing the anti-CD30zeta artificial chimeric T-cell receptor for immunotherapy of Hodgkin disease*. Blood, 2007. 110(7): p. 2620-2630.
- ³⁰⁶ Shibaguchi, H., et al., *A fully human chimeric immune receptor for retargeting T-cells to CEA-expressing tumor cells*. Anticancer Res, 2006. 26(6A): p. 4067-4072.
- Wilkie, S., et al., Retargeting of human T cells to tumor-associated MUC1: the evolution of a chimeric antigen receptor. J Immunol, 2008. 180(7): p. 4901-4909.
- ³⁰⁸ Wang, J., et al., *Optimizing adoptive polyclonal T cell immunotherapy of lymphomas, using a chimeric T cell receptor possessing CD28 and CD137 costimulatory domains.* Hum Gene Ther, 2007. 18(8): p. 712-725.
- ³⁰⁹ Heslop, H., et al., *Long-term restoration of immunity against Epstein-Barr virus infection by adoptive transfer of gene-modified virus-specific T lymphocytes*. Nat Med, 1996. 2(5): p. 551-555.
- ³¹⁰ Pule, M., et al., *Virus-specific T cells engineered to coexpress tumor-specific receptors: persistence and antitumor activity in individuals with neuroblastoma*. Nat Med, 2008. 14(11): p. 1264-1270.
- Atkins, M., et al., *High-dose recombinant interleukin 2 therapy for patients with metastatic melanoma: analysis of 270 patients treated between 1985 and 1993*. J Clin Oncol, 1999. 17(7): p. 2105-2116.
- Wheatley, K., et al., *Does adjuvant interferon-alpha for high-risk melanoma provide a worthwhile benefit? A meta-analysis of the randomised trials.* Cancer Treat Rev, 2003. 29(4): p. 241-252.
- ³¹³ Ribas, A., et al., *Antitumor activity in melanoma and anti-self responses in a phase I trial with the anti-cytotoxic T lymphocyte-associated antigen 4 monoclonal antibody CP-675,206.* J Clin Oncol, 2005. 23(35): p. 8968-8977.
- ³¹⁴ Phan, G., et al., *Cancer regression and autoimmunity induced by cytotoxic T lymphocyte-associated antigen 4 blockade in patients with metastatic melanoma*. Proc Natl Acad Sci U S A, 2003. 100(14): p. 8372-8377.
- ³¹⁵ Robert, C., et al., *Ipilimumab plus dacarbazine for previously untreated metastatic melanoma*. N Engl J Med, 2011. 364(26): p. 2517-2526.
- ³¹⁶ Müller, K., et al., *The first constant domain (C(H)1 and C(L)) of an antibody used as heterodimerization domain for bispecific miniantibodies.* FEBS Lett, 1998. 422(2): p. 259-264.
- ³¹⁷ Kostelny, S., et al., Formation of a bispecific antibody by the use of leucine zippers. J Immunol, 1992. 148(5): p. 1547-1553.
- ³¹⁸ Holliger, P., et al., "Diabodies": small bivalent and bispecific antibody fragments. Proc Natl Acad Sci U S A, 1993. 90(14): p. 6444-6448.
- Mack, M., et al., A small bispecific antibody construct expressed as a functional single-chain molecule with high tumor cell cytotoxicity. Proc Natl Acad Sci U S A, 1995. 92(15): p. 7021-7025.
- 320 Kufer, P., et al., A revival of bispecific antibodies. Trends Biotechnol, 2004. 22(5): p. 238-244.
- ³²¹ Titus, J., et al., *Human K/natural killer cells targeted with hetero-cross-linked antibodies* specifically lyse tumor cells in vitro and prevent tumor growth in vivo. J Immunol, 1987. 139(9): 3153-3158.

Renner, C., et al., *Initiation of humoral and cellular immune responses in patients with refractory Hodgkin's disease by treatment with an anti-CD16/CD30 bispecific antibody.* Cancer Immunol Immunother, 2000. 49(3): p. 173-180.

- ³²⁵ Ball, E., et al., *Initial trial of bispecific antibody-mediated immunotherapy of CD15-bearing tumors: cytotoxicity of human tumor cells using a bispecific antibody comprised of anti-CD15 (MoAb PM81) and anti-CD64/Fc gamma RI (MoAb 32).* J Hematother, 1992. 1(1): p. 85-94.
- ³²⁶ Curnow, R., *Clinical experience with CD64-directed immunotherapy. An overview.* Cancer Immunol Immunother, 1997. 45(3-4): p. 210-215.
- ³²⁷ Repp, R., et al., *Phase I clinical trial of the bispecific antibody MDX-H210 (anti-FcgammaRI x anti-HER-2/neu) in combination with Filgrastim (G-CSF) for treatment of advanced breast cancer.* Br J Cancer, 2003. 89(12): p. 2234-2243.
- ³²⁸ Fury, M., et al., A phase-I trial of the epidermal growth factor receptor directed bispecific antibody MDX-447 without and with recombinant human granulocyte-colony stimulating factor in patients with advanced solid tumors. Cancer Immunol Immunother, 2008. 57(2): p. 155-163.
- ³²⁹ Kellner, C., et al., A novel CD19-directed recombinant bispecific antibody derivative with enhanced immune effector functions for human leukemic cells. J Immunother, 2008. 31(9): p. 871-884.
- Ranft, K., et al., Recombinant bispecific single chain antibody fragments induce Fc gamma-receptor-mediated elimination of CD30+ lymphoma cells. Cancer Lett, 2009. 282(2): p. 187-194.
- ³³¹ Früh, K., & Yang, Y., *Antigen presentation by MHC class I and its regulation by interferon gamma*. Curr Opin Immunol, 1999. 11(1): p. 76-81.
- ³³² Perez, P., et al., *Specific targeting of cytotoxic T cells by anti-T3 linked to anti-target cell antibody*. Nature, 1985. 316(6026): p. 354-356.
- Davico Bonino, L., et al., *Bispecific monoclonal antibody anti-CD3 x anti-tenascin: an immunotherapeutic agent for human glioma.* Int J Cancer, 1995. 61(4): p. 509-515.
- ³³⁴ Nitta, T., et al., Induction of cytotoxicity in human T cells coated with anti-glioma x anti-CD3 bispecific antibody against human glioma cells. J Neurosurg, 1990. 72(3): p. 476-481.
- ³³⁵ Nitta, T., et al., *Preliminary trial of specific targeting therapy against malignant glioma*. Lancet, 1990. 335(8686): p. 368-371.
- ³³⁶ Kaneko, T., et al., *A bispecific antibody enhances cytokine-induced killer-mediated cytolysis of autologous acute myeloid leukemia cells.* Blood, 1993. 81(5): p. 1333-1341.
- ³³⁷ Katayose, Y., et al., *MUC1-specific targeting immunotherapy with bispecific antibodies: inhibition of xenografted human bile duct carcinoma growth.* Cancer Res, 1996. 56(18): p. 4205-4212.
- ³³⁸ Riesenberg, R., et al., *Lysis of prostate carcinoma cells by trifunctional bispecific antibodies (alpha EpCAM x alpha CD3)*. J Histochem Cytochem, 2001. 49(7): p. 911-917.
- ³³⁹ Burges, A., et al., *Effective relief of malignant ascites in patients with advanced ovarian cancer by a trifunctional anti-EpCAM x anti-CD3 antibody: a phase I/II study.* Clin Cancer Res, 2007. 13(13): p. 3899-3905.

Hartmann, F., et al., *Anti-CD16/CD30 bispecific antibody treatment for Hodgkin's disease: role of infusion schedule and costimulation with cytokines.* Clin Cancer Res, 2001. 7(7): p. 1873-1881.

³²⁴ Ravetch, J., & Kinet, J., Fc Receptors. Annu Rev Immunol, 1991. 9: p. 457-492.

³⁴⁰ Sebastian, M., et al., *Treatment of non-small cell lung cancer patients with the trifunctional monoclonal antibody catumaxomab (anti-EpCAM x anti-CD3): a phase I study.* Cancer Immunol Immunother, 2007. 56(10): p. 1637-1644.

- Riechelmann, H., et al., Adoptive therapy of head and neck squamous cell carcinoma with antibody coated immune cells: a pilot clinical trial. Cancer Immunol Immunother, 2007. 56(10): p. 1397-1406.
- ³⁴² Sebastian, M., et al., *Treatment of malignant pleural effusion with the trifunctional antibody catumaxomab (Removab) (anti-EpCAM x Anti-CD3): results of a phase 1/2 study.* J Immunother, 2009. 32(2): p. 195-202.
- ³⁴³ Amann, M., et al., *Antitumor activity of an EpCAM/CD3-bispecific BiTE antibody during long-term treatment of mice in the absence of T-cell anergy and sustained cytokine release*. J Immunother, 2009. 32(5): p. 452-464.
- ³⁴⁴ Mezzanzanica, D., et al., *Human ovarian carcinoma lysis by cytotoxic T cells targeted by bispecific monoclonal antibodies: analysis of the antibody components.* Int J Cancer, 1988. 41(4): p. 609-615.
- ³⁴⁵ Bolhuis, R., et al., *Adoptive immunotherapy of ovarian carcinoma with bs-MAb-targeted lymphocytes: a multicenter study.* Int J Cancer Suppl, 1992. 7: p. 78-81.
- ³⁴⁶ Zhu, Z., et al., *Tumor localization and therapeutic potential of an antitumor-anti-CD3 heteroconjugate antibody in human renal cell carcinoma xenograft models.* Cancer Lett, 1994. 86(1): p. 127-134.
- ³⁴⁷ Luiten, R., et al., Generation of chimeric bispecific G250/anti-CD3 monoclonal antibody, a tool to combat renal cell carcinoma. Br J Cancer, 1996. 74(5): p. 735-744.
- ³⁴⁸ Danels, T., et al., *The transferrin receptor part I: Biology and targeting with cytotoxic antibodies for the treatment of cancer.* Clin Immunol, 2006. 121(2): p. 144-158.
- ³⁴⁹ Jost, C., et al., *A single-chain bispecific Fv2 molecule produced in mammalian cells redirects lysis by activated CTL*. Mol Immunol, 1996. 33(2): p. 211-219.
- ³⁵⁰ de Leij, L., et al., *Bispecific antibodies for treatment of cancer in experimental animal models and man.* Adv Drug Deliv Rev, 1998. 31(1-2): p. 105-129.
- ³⁵¹ Kroesen, B., et al., *Local antitumour treatment in carcinoma patients with bispecific-monoclonal-antibody-redirected T cells*. Cancer Immunol Immunother, 1993. 37(6): p. 400-407.
- ³⁵² Anderson, P., et al., *G19.4(alpha CD3) x B43(alpha CD19) monoclonal antibody heteroconjugate triggers CD19 antigen-specific lysis of t(4;11) acute lymphoblastic leukemia cells by activated CD3 antigen-positive cytotoxic T cells.* Blood, 1992. 80(11): p. 2826-2834.
- ³⁵³ de Gast, G., et al., *CD8 T cell activation after intravenous administration of CD3 x CD19 bispecific antibody in patients with non-Hodgkin lymphoma*. Cancer Immunol Immunother, 1995. 40(6): p. 390-396.
- ³⁵⁴ Bargou, R., et al., *Tumor regression in cancer patients by very low doses of a T cell-engaging antibody*. Science, 2008. 321(5891): p. 974-977.
- Kuwahara, M., et al., *A mouse/human-chimeric bispecific antibody reactive with human carcinoembryonic antigen-expressing cells and human T-lymphocytes*. Anticancer Res, 1996. 16(5A): p. 2661-2667.
- ³⁵⁶ Lutterbuese, R., et al., *Potent control of tumor growth by CEA/CD3-bispecific single-chain antibody constructs that are not competitively inhibited by soluble CEA.* J Immunother, 2009. 32(4): p. 341-352.

³⁵⁷ Sen, M., et al., *Use of anti-CD3 x anti-HER2/neu bispecific antibody for redirecting cytotoxicity of activated T cells toward HER2/neu+ tumors.* J Hematother Stem Cell Res, 2001. 10(2): p. 247-260.

- ³⁵⁹ Renner, C., et al., *Cure of xenografted human tumors by bispecific monoclonal antibodies and human T cells*. Science, 1994. 264(5160): p. 833-835.
- ³⁶⁰ Katzenwadel, A. et al., Construction and in vivo evaluation of an anti-PSA x anti-CD3 bispecific antibody for the immunotherapy of prostate cancer. Anticancer Res, 2000. 20(3A): p. 1551-1555.
- ³⁶¹ Hombach, A., et al., *Specific activation of resting T cells against CA19-9+ tumor cells by an anti-CD3/CA19-9 bispecific antibody in combination with a costimulatory anti-CD28 antibody.* J Immunother, 1997. 20(5):325-333.
- Negri, D., et al., In vitro and in vivo stability and anti-tumour efficacy of an anti-EGFR/anti-CD3 F(ab')2 bispecific monoclonal antibody. Br J Cancer, 1995. 72(4): p. 928-933.
- ³⁶³ Bühler, P., et al., *Target-dependent T-cell activation by coligation with a PSMA x CD3 diabody induces lysis of prostate cancer cells.* J Immunother, 2009. 32(6): p. 565-573.
- ³⁶⁴ Withoff, S., et al., *Characterization of BIS20x3*, a bi-specific antibody activating and retargeting *T-cells to CD20-positive B-cells*. Br J Cancer, 2001. 84(8): p. 1115-1121.
- ³⁶⁵ Stanglmaier, M., et al., *Bi20 (fBTA05)*, a novel trifunctional bispecific antibody (anti-CD20 x anti-CD3), mediates efficient killing of B-cell lymphoma cells even with very low CD20 expression levels. Int J Cancer, 2008. 123(5): p. 1181-1189.
- ³⁶⁶ Buhmann, R., et al., *Immunotherapy of recurrent B-cell malignancies after allo-SCT with Bi20 (FBTA05), a trifunctional anti-CD3 x anti-CD20 antibody and donor lymphocyte infusion.* Bone Marrow Transplant, 2009. 43(5): p. 383-397.
- ³⁶⁷ Cosimi, A.,et al., *Treatment of acute renal allograft rejection with OKT3 monoclonal antibody*. Transplantation, 1981. 32(6): p. 535-539.
- ³⁶⁸ Canevari, S., et al., *Regression of advanced ovarian carcinoma by intraperitoneal treatment with autologous T lymphocytes retargeted by a bispecific monoclonal antibody*. J Natl Cancer Inst, 1995. 87(19): p. 1463-1469.
- ³⁶⁹ Lamers, C., et al., *Local but no systemic immunomodulation by intraperitoneal treatment of advanced ovarian cancer with autologous T lymphocytes re-targeted by a bi-specific monoclonal antibody*. Int J Cancer, 1997. 73(2): p. 211-219.
- ³⁷⁰ Tibben, J., et al., *Pharmacokinetics, biodistribution and biological effects of intravenously administered bispecific monoclonal antibody OC/TR F(ab')2 in ovarian carcinoma patients*. Int J Cancer, 1996. 66(4): p. 477-483.
- ³⁷¹ Link, B., et al., *Anti-CD3-based bispecific antibody designed for therapy of human B-cell malignancy can induce T-cell activation by antigen-dependent and antigen-independent mechanisms.* Int J Cancer, 1998. 77(2): p. 251-256.
- ³⁷² Löffler, A., et al., A recombinant bispecific single-chain antibody, CD19 x CD3, induces rapid and high lymphoma-directed cytotoxicity by unstimulated T lymphocytes. Blood, 2000. 95(6): p. 2098-2103.
- ³⁷³ Mack, M., et al., A small bispecific antibody construct expressed as a functional single-chain molecule with high tumor cell cytotoxicity. Proc Natl Acad Sci U S A, 1995. 92(15): p. 7021-7025.

³⁵⁸ Kiewe, P., et al., *Phase I trial of the trifunctional anti-HER2 x anti-CD3 antibody ertumaxomab in metastatic breast cancer*. Clin Cancer Res, 2006. 12(10): p. 3085-3091.

³⁷⁴ Hoffmann, P., et al., *Serial killing of tumor cells by cytotoxic T cells redirected with a CD19-/CD3-bispecific single-chain antibody construct.* Int J Cancer, 2005. 115(1): p. 98-104.

- ³⁷⁵ Offner, S., et al., *Induction of regular cytolytic T cell synapses by bispecific single-chain antibody constructs on MHC class I-negative tumor cells.* Mol Immunol, 2006. 43(6): p. 763-771.
- ³⁷⁶ Gruen, M., et al., T-cell-mediated lysis of B cells induced by a CD19xCD3 bispecific single-chain antibody is perforin dependent and death receptor independent. Cancer Immunol Immunother, 2004. 53(7): p. 625-632.
- Wolf, E., et al., *BiTEs: bispecific antibody constructs with unique anti-tumor activity.* Drug Discov Today, 2005. 10(18): p. 1237-1244.
- ³⁷⁸ Saulquin, X., et al., A global appraisal of immunodominant CD8 T cell responses to Epstein-Barr virus and cytomegalovirus by bulk screening. Eur J Immunol, 2000. 30(9): p. 2531-2539.
- ³⁷⁹ Hu, N., et al., *Highly conserved pattern of recognition of influenza A wild-type and variant CD8+CTL epitopes in HLA-A2+ humans and transgenic HLA-A2+/H2 class I-deficient mice*. Vaccine, 2005. 23(45): p. 5231-5244.
- ³⁸⁰ Hislop, A., et al., *Epitope-specific evolution of human CD8(+) T cell responses from primary to persistent phases of Epstein-Barr virus infection.* J Exp Med, 2002. 195(7): p. 893-905.
- Almanzar, G., et al., Long-term cytomegalovirus infection leads to significant changes in the composition of the CD8+ T-cell repertoire, which may be the basis for an imbalance in the cytokine production profile in elderly persons. J Virol, 2005. 79(6): p. 3675-3683.
- ³⁸² Ogg, G., et al., Sensitization of tumour cells to lysis by virus-specific CTL using antib.ody-targeted MHC class I/peptide complexes. Br J Cancer, 2000. 82(5): p. 1058-1062.
- ³⁸³ Schultz, J., et al., *A tetravalent single-chain antibody-streptavidin fusion protein for pretargeted lymphoma therapy*. Cancer Res, 2000. 60(23): p. 6663-6669.
- ³⁸⁴ Savage, P., et al., *Induction of viral and tumour specific CTL responses using antibody targeted HLA class I peptide complexes*. Br J Cancer, 2002. 86(8): p. 1336-1342.
- Robert, B., et al., *Antibody-conjugated MHC class I tetramers can target tumour cells for lysis by T lymphocytes.* Eur J Immunol, 2000. 30(11): p. 3165-3170.
- ³⁸⁶ Mous, R., et al., *Redirection of CMV-specific CTL towards B-CLL via CD20-targeted HLA/CMV complexes*. Leukaemia, 2006. 20(6): p. 1096-1102.
- ³⁸⁷ Savage, P., et al., *Anti-viral cytotoxic T cells inhibit the growth of cancer cells with antibody targeted HLA class I / peptide complexes in SCID mice.* Int J Cancer, 2002. 98(4): p. 561-566.
- ³⁸⁸ Savage, P., et al., *Immunotherapy with antibody-targeted HLA class I complexes: Results of in vivo tumour cell killing and therapeutic vaccination.* Tumor Biol, 2007. 28(4): p. 205-211.
- ³⁸⁹ Forero, A., et al., *Phase I trial of a novel anti-CD20 fusion protein in pretargeted radioimmunotherapy for B cell non-Hodgkin lymphoma*. Blood, 2004. 104(1): p. 227-236.
- ³⁹⁰ Knox, S., et al., *Phase II trial of yttrium-90-DOTA-biotin pretargeted by NR-LU-10* antibody/streptavidin in patients with metastatic colon cancer. Clin Cancer Res, 2000. 6(2): p. 406-14.
- ³⁹¹ Robert, B., et al., *Redirecting anti-viral CTL against cancer cells by surface targeting monomeric MHC class I-viral peptide conjugated to antibody fragments.* Cancer Immun, 2001. 1: p. 2.

³⁹² Donda, A., et al., *In vivo targeting of an anti-tumour antibody coupled to antigenic MHC class I complexes induces specific growth inhibition and regression of established syngeneic tumour grafts.* Cancer Immunol, 2003. 3: p. 11.

- ³⁹³ Cesson, V., et al., *Active antiviral T-lymphocyte response can be redirected against tumour cells by antitumour antibody x MHC/viral peptide conjugates.* Clin Cancer Res, 2006. 12(24): p. 7422-7430.
- ³⁹⁴ Lev, A., et al., *Recruitment of CTL activity by tumour-specific antibody-mediated targeting of single-chain class I MHC-peptide complexes.* J Immunol, 2002. 169(6): p. 2988-2996.
- ³⁹⁵ Lev, A., et al., *Tumour-specific ab-mediated targeting of MHC-peptide complexes induces regression of human tumour xenografts in vivo*. Proc Natl Acad Sci U S A, 2004. 101(24): p. 9051-9056.
- ³⁹⁶ Novak, H., et al., Selective antibody-mediated targeting of class I MHC to EGFR-expressing tumour cells induces potent antitumour CTL activity in vitro and in vivo. Int J Cancer, 2006. 120(2): p. 329-336.
- ³⁹⁷ Oved, K., et al., *Antibody-mediated targeting of human single-chain class I MHC with covalently linked peptides induces efficient killing of tumor cells by tumor or viral-specific cytotoxic T lymphocytes.* Cancer Immunol Immunother, 2005. 54(9): p. 867-879.
- ³⁹⁸ Ge, Q., et al., Soluble peptide-MHC monomers cause activation of CD8+ T cells through transfer of the peptide to T cell MHC molecules. Proc Natl Acad Sci U S A, 2002. 99(21): p. 13729-13734.
- ³⁹⁹ Schott, E., et al., *Class I negative CD8 T cells reveal the confounding role of peptide-transfer onto CD8 T cells stimulated with soluble H2-K^b molecules.* Proc Natl Acad Sci U S A, 2002. 99(21): p. 13735-13740.
- ⁴⁰⁰ Su, M., et al., Cognate peptide-induced destruction of CD8+ cytotoxic T lymphocytes is due to fratricide. J Immunol, 1993. 151(2): p. 658-667.
- ⁴⁰¹ Su, M., et al., *Fratricide of CD8+ cytotoxic lymphocytes is dependent on cellular activation and perforin-mediated killing*. Eur J Immunol, 2004. 34(9): p. 2459-2470.
- ⁴⁰² Mottez, E., et al., *Cells expressing a Major Histocompatibility Complex class I molecule with a single covalently bound peptide are highly immunogenic*. J Exp Med, 1995. 181(2): p. 495-502.
- ⁴⁰³ Vest Hansen, N., et al., *Phage display of peptide / major histocompatibility class I complexes*. Eur J Immunol, 2001. 31(1): p. 32-38.
- ⁴⁰⁴ Yu, Y., et al., *Cutting edge: single-chain trimers of MHC class I molecules form stable structures that potently stimulate antigen-specific T cells and B cells.* J Immunol, 2002. 168(7): p. 3145-3149.
- ⁴⁰⁵ Lybarger, L., et al., *Enhanced immune presentation of a single-chain major histocompatibility complex class I molecule-engineered to optimize linkage of a C-terminally extended peptide*. J Biol Chem, 2003. 278(29): p. 27105-27111.
- ⁴⁰⁶ Truscott, S., et al., *Disulfide bond engineering to trap peptides in the MHC class I binding groove*. J Immunol, 2007. 178(10): p. 6280-6289.
- ⁴⁰⁷ Mitaksov, V., et al., *Structural engineering of pMHC reagents for T cell vaccines and diagnostics*. Chem Biol, 2007. 14(8): p. 909-922.
- ⁴⁰⁸ Truscott, S., et al., *Human MHC class I molecules with disulphide traps secure disease-related antigenic peptides and exclude competitor peptides.* J Biol Chem, 2008. 283(12): p. 7480-7490.
- ⁴⁰⁹ Jaramillo, A., et al., *Recognition of HLA-A2-restricted mammaglobin-A-derived epitopes by CD8+cytotoxic T lymphocytes from breast cancer patients*. Breast Cancer Res Treat, 2004. 88(1): p. 29-41.

⁴¹⁰ Huang, C., et al., Cancer immunotherapy using a DNA vaccine encoding a single-chain trimer of MHC class I linked to an HPV-16 E6 immunodominant CTL epitope. Gene Ther, 2005. 12(15): p. 1180-1186.

- ⁴¹¹ Hung, C., et al., A DNA vaccine encoding a single-chain trimer of HLA-A2 linked to human mesothelin peptide generates anti-tumour effects against human mesothelin-expressing tumours. Vaccine, 2007. 25(1): p. 127-135.
- ⁴¹² Zhang, Y., et al., *Hepatitis B virus core antigen epitopes presented by HLA-A2 single chain trimers induce functional epitope-specific CD8+ T-cell responses in HLA-A2.1/Kb transgenic mice.* Immunology, 2007. 121(1): p. 105-112.
- ⁴¹³ Palmowski, M., et al., *A single-chain H-2Db molecule presenting an influenza virus nucleoprotein epitope shows enhanced ability at stimulating CD8+ T cell responses in vivo*. J Immunol, 2009. 182(8): p. 4565-4571.
- ⁴¹⁴ Cheung, Y., et al., *Induction of T-cell response by a DNA vaccine encoding a novel HLA-A*0201 severe acute respiratory syndrome coronavirus epitope.* Vaccine, 2007. 25(32): p. 6070-6077.
- ⁴¹⁵ Pascolo, S., et al., *HLA-A2.1-restricted education and cytolytic activity of CD8(+) T lymphocytes* from beta2 microglobulin (beta2m) HLA-A2.1 monochain transgenic H-2Db beta2m double knockout mice. J Exp Med, 1997. 185(12): p. 2043-2051.
- ⁴¹⁶ Wang, Z., et al., *Attenuated poxviruses generate clinically relevant frequencies of CMV-specific T cells.* Blood, 2004. 104(3): p. 847-856.
- ⁴¹⁷ Brown, J., et al., *HLA-A*, *-B and -DR antigen frequencies of the London Cord Blood Bank units differ from those found in established bone marrow donor registries*. Bone Marrow Transplant, 2000. 25(5): p. 475-481.
- ⁴¹⁸ Khan, N., et al., *Cytomegalovirus seropositivity drives the CD8 T cell repertoire toward greater clonality in healthy elderly individuals.* J Immunol, 2002. 169(4): p. 1984-1992.
- 419 Moss, P., & Khan, N., CD8(+) T-cell immunity to cytomegalovirus. Hum Immunol, 2004. 65(5): p. 456-464.
- ⁴²⁰ Einfeld, D., et al., *Molecular cloning of the human B cell CD20 receptor predicts a hydrophobic protein with multiple transmembrane domains*. EMBO J, 1988. 7(3): p. 711-717.
- ⁴²¹ Roopenian, D., & Akailesh, S., *FcRn: the neonatal Fc receptor comes of age.* Nat Rev Immunol, 2007. 7(9): p. 715-725.
- ⁴²² Ghei, M., et al., *Analysis of memory T lymphocyte activity following stimulation with overlapping HLA-A*2402, A*0101 and Cw*0402 restricted CMV pp65 peptides.* J Transl Med, 2005. 3: p. 23.
- ⁴²³ Lee, H., et al., *Peptide-specific CTL induction in HBV-seropositive PBMC by stimulation with peptides in vitro: novel epitopes identified from chronic carriers.* Virus Res, 1997. 50(2): p. 185-194.
- ⁴²⁴ Millo, E., et al., *Purification and HPLC-MS analysis of a naturally processed HCMV-derived peptide isolated from the HEK-293T/HLA-E+/UI40+ cell transfectants and presented at the cell surface in the context of HLA-E.* J Immunol Methods, 2007. 322(1-2): p. 128-136.
- ⁴²⁵ Brekke, O., et al., *The structural requirements for complement activation by IgG: does it hinge on the hinge?* Immunol Today, 1995. 16(2): p. 85-90.
- 426 http://www.expasy.ch/cgi-bin/protparam
- ⁴²⁷ Warburg, O., & Christian W., *Isolation and crystallization of enolase*. Biochem Z, 1942. 310: p. 384-421.

⁴²⁸ Hogquist, K., et al., *T cell receptor antagonist peptides induce positive selection*. Cell, 1994. 76(1): p. 17-27.

- ⁴³⁰ French, R., *How to make bispecific antibodies*. Methods Mol Med, 2000. 40: p. 333-339.
- ⁴³¹ Porgador, A., et al., *Localization, quantitation, and in situ detection of specific peptide-MHC class I complexes using a monoclonal antibody*. Immunity, 1997. 6(6): p. 715-726.
- ⁴³² Hasbold, J., et al., *Properties of mouse CD40: cellular distribution of CD40 and B cell activation by monoclonal anti-mouse CD40 antibodies.* Eur J Immunol, 1994. 24(8): p. 1835-1842.
- ⁴³³ Ahuja, A., et al., *Depletion of B cells in murine lupus: efficacy and resistance*. J Immunol, 2007. 179(5): p. 3351-3361.
- ⁴³⁴ Rossi, E., et al., *Stably tethered multifunctional structures of defined composition made by the dock and lock method for use in cancer targeting.* Proc Natl Acad Sci U S A, 2006. 103(18): p. 6841-6846.
- ⁴³⁵ Effros, R., & Pawelec, G., Replicative senescence of T lymphocytes: does the hayflick limit lead to immune exhaustion? Immunol Today, 1997. 18(9): p. 450-454.
- ⁴³⁶ Campisi, J., et al., *Cellular senescence, cancer and aging: the telomere connection.* Exp Gerontol, 2001. 36(10): p. 1619-1637.
- ⁴³⁷ Valenzuela, H., & Effros, R., *Divergent telomerase and CD28 expression patterns in human CD4 and CD8 T cells following repeated encounters with the same antigenic stimulus.* Clin Immunol, 2002. 105(2): p. 117-125.
- ⁴³⁸ Rufer, N., et al., *Transfer of the human telomerase reverse transcriptase (TERT) gene into T lymphocytes results in extension of replicative potential.* Blood, 2001. 98(3): p. 597-603.
- ⁴³⁹ Perillo, N., et al., *Human T lymphocytes possess a limited in vitro lifespan*. Exp Gerontol, 1989. 24(3): p. 177–187.
- ⁴⁴⁰ Koch, S., et al., *Cytomegalovirus infection: a driving force in human T cell immunosenescence*. Ann N Y Acad Sci, 2007. 1114: p. 23-35.
- ⁴⁴¹ Oelke, M., & Schenck, J., *HLA-Ig-based artificial antigen-presenting cells: setting the terms of engagement.* Clin Immunol, 2004. 110(3): p. 243-251.
- ⁴⁴² Trill, J., et al., *Production of monoclonal antibodies in COS and CHO cells*. Curr Opin Biotechnol, 1995. 6(5): p. 553-560.
- ⁴⁴³ Lo, K., et al., *High level expression and secretion of Fc-X fusion proteins in mammalian cells.* Protein Engineering, 1998. 11(6): p. 495-450.
- ⁴⁴⁴ Buist, M., et al., *Kinetics and tissue distribution of the radiolabelled chimeric monoclonal antibody MOv18 IgG and F(ab')2 fragments in ovarian carcinoma patients.* Cancer Res, 1993. 53(22): p. 5413-5418.
- ⁴⁴⁵ Lane, D., et al., *Radioimmunotherapy of metastatic colorectal tumours with iodine-131-labelled antibody to carcinoembryonic antigen: phase I/II study with comparative biodistribution of intact and (Fab')2 antibodies.* Br J Cancer, 1994. 70(3): p. 521-525.
- ⁴⁴⁶ Kontermann, R., *Strategies for extended serum half-life of protein therapeutics*. Curr Opin Biotechnol, 2011. 22(6): p. 868-876.

⁴²⁹ Tomonari, K., *A rat antibody against a structure functionally related to the mouse T-cell receptor/T3 complex.* Immunogenetics, 1988. 28(6): p. 455-458.

⁴⁴⁷ Shields, R., et al., *High resolution mapping of the binding site on human IgG1 for FcγRI, FcγRII, FcγRIII, and FcRn and design of IgG1 variants with improved binding to the FcγR.* J Biol Chem, 2001. 276(9): p. 659-6604.

- ⁴⁴⁸ Zhang, J., et al., *Tolerance by selective in vivo expansion of foreign major histocompatibility complex-transduced bone marrow.* Transplantation, 2005. 80(3): p. 362-369.
- Seong, R., et al., Rescue of Daudi cell HLA expression by transfection of the mouse β_2 microglobulin gene. J Exp Med, 1988. 167(2): p. 288-299.
- ⁴⁵⁰ Uger, R., & Barber, B., Creating CTL targets with epitope-linked β_2 microglobulin constructs. J Immunol, 1998. 160(4): p. 1598-1605.
- ⁴⁵¹ Shen, C., et al., *Structural and functional characterization of peptide-beta2m fused HLA-A2/MART1(27-35) complexes*. Biochem Biophys Res Commun, 2006. 342(1): p. 57-65.
- ⁴⁵² Kozak, M., *An analysis of 5'-noncoding sequences from 699 vertebrate messenger RNAs.* Nucleic Acids Res, 1987. 15(20): p. 8125-8148.
- ⁴⁵³ Li, J.,et al., A comparative study of different vector designs for the mammalian expression of recombinant IgG antibodies. J Immunol Methods, 2007. 318(1-2): p. 113-124.
- ⁴⁵⁴ Leidhold, C., & Voos, W., *Chaperones and proteases-guardians of protein integrity in the eukaryotic organelles*. Ann N Y Acad Sci, 2007. 1113: p. 72-86.
- ⁴⁵⁵ Remes, K., et al., *Effects of alpha-interferon on serum beta-2-microglobulin*. Leuk lymphoma, 1996. 21(3-4): p. 233-238.
- ⁴⁵⁶ Parham, P., & Brodsky, F., *Partial purification and some properties of BB7.2. A cytotoxic monoclonal antibody with specificity for HLA-A2 and a variant of HLA-A28.* Hum Imunol, 1981. 3(4): p. 277-299.
- ⁴⁵⁷ Barnstable, C., et al., *Production of monoclonal antibodies to group A erythrocytes, HLA and other human cell surface antigens new tools for genetic analysis.* Cell, 1978. 14(1): p. 9-20.
- ⁴⁵⁸ Hengen, P., *Purification of His-Tag fusion proteins from Escherichia coli*. Trends Biochem Sci. 1995. 20(7): p. 285-286.
- ⁴⁵⁹ Carrió, M., et al., Fine architecture of bacterial inclusion bodies. FEBS Lett, 2000. 471(1): p. 7-11.
- 460 Raj, T., Terminal sugars of Fc glycans influence antibody effector functions of IgGs. Curr Opin Immunol, 2008. 20(4): p. 471-478.
- ⁴⁶¹ Abu-Qarn, M., et al., *Not just for Eukarya anymore: protein glycosylation in Bacteria and Archaea.* Curr Opin Struct Biol, 2008. 18(5): p. 544-550.
- ⁴⁶² Garboczi, D., et al., *HLA-A2-peptide complexes: Refolding and crystallization of molecules expressed in Escherichia coli and complexes with single antigenic peptides.* Proc Natl Acad Sci U S A, 1992. 89(8): p. 3429-3433.
- ⁴⁶³ Altman, J., et al., *Phenotypic analysis of antigen-specific T lymphocytes*. Science, 1996. 274(5284): p. 94-96. Erratum in Science, 1998. 280(5371): p. 1821.
- ⁴⁶⁴ Hashida, S., et al., *More useful maleimide compounds for the conjugation of Fab' to horseradish peroxidase through thiol groups in the hinge.* J Appl Biochem, 1984. 6(1-2): p. 56-63.
- ⁴⁶⁵ Simmons, L., et al., *Expression of full-length immunoglobulins in Escherichia coli: rapid and efficient production of aglycosylated antibodies.* J Immunol Methods, 2002. 263(1-2): p. 133-147.

⁴⁶⁶ Yagi, M., et al,. Reversible Unfolding of Bovine β -Lactoglobulin Mutants without a Free Thiol Group. J Biol Chem, 2003. 278(47): p. 47009-47015.

- ⁴⁶⁸ Beckealtt, D., et al,. *A minimal peptide substrate in biotin holoenzyme synthetase-catalyzed biotinylation.* Protein Sci, 1999. 8(4): p. 921-929.
- ⁴⁶⁹ Clark, E., Refolding of recombinant proteins. Curr Opin Biotechnol, 1998. 9(2): p. 157-163.
- ⁴⁷⁰ Ahmed, A., et al., *Nonenzymic reactivation of reduced bovine pancreatic ribonuclease by air oxidation and by glutathione oxidoreduction buffers*. J Biol Chem, 1975. 250(21): p. 8477-8482.
- ⁴⁷¹ Arakawa, T., et al., *Suppression of protein interactions by arginine: a proposed mechanism of the arginine effects.* Biophys Chem, 2007. 127(1-2): p. 1-8.
- ⁴⁷² Stöckel, J., et al., *Pathway of detergent-mediated and peptide ligand-mediated refolding of heterodimeric class II major histocompatibility complex (MHC) molecules*. Eur J Biochem, 1997. 248(3): p. 684-691.
- ⁴⁷³ Thomas, J., et al., *Molecular chaperones, folding catalysts, and the recovery of active recombinant proteins from E. coli. To fold or to refold.* Appl Biochem Biotechnol, 1997. 66(3): p. 197-238.
- ⁴⁷⁴ Jungbauer, A., & Kaar, W., *Current status of technical protein refolding*. J Biotechnol, 2007. 128(3): p. 587-596.
- ⁴⁷⁵ Gallimore, A., et al., *Induction and exhaustion of lymphocytic choriomeningitis virus-specific cytotoxic T lymphocytes visualized using soluble tetrameric major histocompatibility complex class I-peptide complexes.* J Exp Med, 1998. 187(9): p. 1383-1393.
- ⁴⁷⁶ Jefferies, W., & MacPherson, G., Expression of the W6/32 HLA epitope by cells of rat, mouse, human and other species: critical dependence on the interaction of specific MHC heavy chains with human or bovine beta 2-microglobulin. Eur J Immunol, 1987. 17(9): p. 1257-1263.
- ⁴⁷⁷ Shields, M., & Ribaudo, R., *Mapping of the monoclonal antibody W6/32: sensitivity to the amino terminus of beta2-microglobulin*. Tissue Antigens, 1998. 51(5): p. 567–570.
- ⁴⁷⁸ Hogan, K., & Brown, S., *Localization and Characterization of Serologic Epitopes on HLA-A2*. Hum Immunol, 1992. 33(3): p. 185-192.
- ⁴⁷⁹ Kotsiou, E., et al., *Dimerization of soluble disulfide trap single-chain major histocompatibility complex class I molecules dependent on peptide binding affinity.* Antioxid Redox Signal, 2011. 15(3): p. 635-44.
- ⁴⁸⁰ Greten, T., et al., *Peptide–β2-microglobulin–MHC fusion molecules bind antigen-specific T cells and can be used for multivalent MHC–Ig complexes.* J Immunol Methods, 2002. 271(1-2): p. 125-135.
- ⁴⁸¹ Shen, C., et al., *Characterization of MHC/peptide complexes refolded by a one-step ion-exchange chromatography.* J Immunol Methods, 2011. 369(1-2): p. 81-90.
- ⁴⁸² Tacal, O., & Ozer, I., A comparison between SDS-PAGE and size exclusion chromatography as analytical methods for determining product composition in protein conjugation reactions. J Biochem Biophys Methods, 2002. 52(3): p. 161-168.
- ⁴⁸³ Stone, J., & Stern, L., *CD8 T cells, like CD4 T cells, are triggered by multivalent engagement of TCRs by MHC-peptide ligands but not by monovalent engagement.* J Immunol, 2006. 176(3): p. 1498-1505.

⁴⁶⁷ Barker, D., & Campbell, A., *The birA gene of Escherichia coli encodes a biotin holoenzyme synthetase*. J Mol Biol, 1981. 146(4): p. 451-467.

⁴⁸⁴ Cardarelli, P., et al., *Binding to CD20 by anti-B1 antibody or F(ab')(2) is sufficient for induction of apoptosis in B-cell lines.* Cancer Immunol Immunother, 2002. 51(1): p. 15-24.

- ⁴⁸⁵ Alduaij, W., et al., *Novel type II anti-CD20 monoclonal antibody (GA101) evokes homotypic adhesion and actin-dependent, lysosome-mediated cell death in B-cell malignancies.* Blood, 2011. 117(17): p. 4519-4529.
- ⁴⁸⁶ Viardot, A., et al., *Treatment of Patients With Non-Hodgkin Lymphoma With CD19/CD3 Bispecific Antibody Blinatumomab (MT103): Double-Step Dose Increase to Continuous Infusion of 60 μg/m²/day is Tolerable and Highly Effective.* Blood (ASH Annual Meeting Abstracts), 2010. 116(21): 2880.
- ⁴⁸⁷ Choi, B., et al., *Bispecific antibodies engage T cells for antitumor immunotherapy*. Expert Opin Biol Ther, 2011. 11(7): p. 843-853.
- ⁴⁸⁸ Nagorsen, D., & Baeuerle, P., *Immunomodulatory therapy of cancer with T cell-engaging BiTE antibody blinatumomab*. Exp Cell Res, 2011. 317(9): p. 1255-1260.
- ⁴⁸⁹ North, M., et al., *Intracellular cytokine production by human CD4+ and CD8+ T cells from normal and immunodeficient donors using directly conjugated anti-cytokine antibodies and three-colour flow cytometry*. Clin Exp Immunol, 1996. 105(3): p. 517-522.
- ⁴⁹⁰ Amiri, K., & Richmond, A., *Fine tuning the transcriptional regulation of the CXCL1 chemokine*. Prog Nucleic Acid Res Mol Biol, 2003. 74: p. 1-36.
- ⁴⁹¹ Zhang, S., & Wang, Q., *Factors determining the formation and release of bioactive IL-12: regulatory mechanisms for IL-12p70 synthesis and inhibition.* Biochem Biophys Res Commun, 2008. 372(4): p. 509-512.
- ⁴⁹² Kang, B., et al., *Regulatory mechanisms and their therapeutic implications of interleukin-12 production in immune cells.* Cell Signal, 2005. 17(6): p. 665-673.
- ⁴⁹³ Dutcher, J., et al., *Kidney cancer: the Cytokine Working Group experience (1986-2001): part II. Management of IL-2 toxicity and studies with other cytokines.* Med Oncol, 2001. 18(3): p. 209-219.
- ⁴⁹⁴ Gleave, M., et al., *Interferon gamma-1b compared with placebo in metastatic renal-cell carcinoma. Canadian Urologic Oncology Group*. N Engl J Med, 1998. 338(18): p. 1265-1271.
- ⁴⁹⁵ Feldman, E., et al., *Phase II trial of recombinant tumor necrosis factor in disseminated malignant melanoma*. Am J Clin Oncol, 1992. 15(3): p. 256-259.
- ⁴⁹⁶ Teeling, J., et al., *Sub-pyrogenic systemic inflammation impacts on brain and behavior, independent of cytokines.* Brain Behav Immun, 2007. 21(6): p. 836-850.
- ⁴⁹⁷ Stein, R., et al., *Characterization of a new humanized anti-CD20 monoclonal antibody, IMMU-106, and Its use in combination with the humanized anti-CD22 antibody, epratuzumab, for the therapy of non-Hodgkin's lymphoma*. Clin Cancer Res, 2004. 10(8): p. 2868-2878.
- ⁴⁹⁸ Goldenberg, D., et al., *Properties and structure-function relationships of veltuzumab (hA20), a humanized anti-CD20 monoclonal antibody.* Blood, 2009. 113(5): p. 1062-1070.
- ⁴⁹⁹ Sharkey, R., et al., *Improved therapeutic results by pretargeted radioimmunotherapy of non-Hodgkin's lymphoma with a new recombinant, trivalent, anti-CD20, bispecific antibody.* Cancer Res, 2008. 68(13): p. 5282-5290.
- ⁵⁰⁰ Wu, L., et al., *Two-step binding mechanism for T-cell receptor recognition of peptide MHC*. Nature, 2002. 418(6897): p. 552-556.
- ⁵⁰¹ Kennedy, R., & Celis, E., *T helper lymphocytes rescue CTL from activation-induced cell death.* J Immunol, 2006. 177(5): p. 2862-2872.

⁵⁰² Hardwick, N., & Chain, B., *Epitope spreading contributes to effective immunotherapy in metastatic melanoma patients*. Immunotherapy, 2011. 3(6): p. 731-733.

- ⁵⁰³ Shiao, S., et al. *Immune microenvironments in solid tumors: new targets for therapy*. Genes Dev, 2011. 25(24): p. 2559-2572.
- ⁵⁰⁴ Pentcheva-Hoang, T., et al., *Negative regulators of T-cell activation: potential targets for therapeutic intervention in cancer, autoimmune disease, and persistent infections.* Immunol Rev, 2009. 229(1): p. 67-87.
- ⁵⁰⁵ Yi, J., et al., *T-cell exhaustion: characteristics, causes and conversion*. Immunology, 2010. 129(4): p. 474-481.
- ⁵⁰⁶ Ouyang, Q., et al., *Large numbers of dysfunctional CD8+ T lymphocytes bearing receptors for a single dominant CMV epitope in the very old.* J Clin Immunol, 2003. 23(4): p. 247-257.
- ⁵⁰⁷ Faist, B., et al., *Cytomegalovirus infection- and age-dependent changes in human CD8+ T-cell cytokine expression patterns*. Clin Vaccine Immunol, 2010. 17(6): p. 986-992.
- ⁵⁰⁸ Louis, C., et al., *Antitumor activity and long-term fate of chimeric antigen receptor-positive T cells in patients with neuroblastoma*. Blood, 2011. 118(23): p. 6050-6056.
- ⁵⁰⁹ Porter, D., et al., *Chimeric antigen receptor-modified T cells in chronic lymphoid leukemia*. N Engl J Med, 2011. 365(8): p. 725-733.
- ⁵¹⁰ Parkhurst, M., et al., *T cells targeting carcinoembryonic antigen can mediate regression of metastatic colorectal cancer but induce severe transient colitis.* Mol Ther, 2011. 19(3): p. 620-626.
- ⁵¹¹ Dhimolea, E., & Reichert, J., World Bispecific Antibody Summit, September 27-28, 2011, Boston, MA. MAbs, 2012. 4(1): p. 4-16.
- ⁵¹² Topp, M., et al., *Targeted therapy with the T-cell-engaging antibody blinatumomab of chemotherapy-refractory minimal residual disease in B-lineage acute lymphoblastic leukemia patients results in high response rate and prolonged leukemia-free survival.* J Clin Onco, 2011. 29(18): p. 2493-2498.
- ⁵¹³ Torisu-Itakura, H., et al., *Redirected lysis of human melanoma cells by a MCSP/CD3-bispecific BiTE antibody that engages patient-derived T cells.* J Immunother, 2011. 34(8): p. 597-605.
- ⁵¹⁴ Cioffi, M., et al., *EpCAM/CD3-Bispecific T-cell Engaging Antibody MT110 Eliminates Primary Human Pancreatic Cancer Stem Cells.* Clin Cancer Res, 2012. 18(2): p. 465-474.
- ⁵¹⁵ Koristka, S., et al., *Retargeting of Human Regulatory T cells by Single Chain Bispecific Antibodies*. J Immunol, 2012, 188(3): p. 1551-1558.
- ⁵¹⁶ Ruffell, B., et al., *Differential macrophage programming in the tumor microenvironment*. Trends Immunol, 2012. 33(3): p. 119-126.
- ⁵¹⁷ Di Gaetano, N., et al., *Complement activation determines the therapeutic activity of rituximab in vivo*. J Immunol, 2003. 171(3): p. 1581-1587.
- ⁵¹⁸ Cheung, Y., et al., *Two novel HLA-A*0201 T-cell epitopes in avian H5N1 viral nucleoprotein induced specific immune responses in HHD mice.* Vet Res, 2010. 41(2): p. 24.
- ⁵¹⁹ Saha, A., et al., *Therapy of established tumors in a novel murine model transgenic for human carcinoembryonic antigen and HLA-A2 with a combination of anti-idiotype vaccine and CTL peptides of carcinoembryonic antigen.* Cancer Res, 2007. 67(6): p. 2881–2892.